



GEOLOGICAL SURVEY OF CANADA
COMMISSION GÉOLOGIQUE DU CANADA

PAPER 76-1B

This document was produced
by scanning the original publication.

Ce document est le produit d'une
numérisation par balayage
de la publication originale.

REPORT OF ACTIVITIES PART B



Energy, Mines and
Resources Canada

Énergie, Mines et
Ressources Canada

1976

Technical editing and compilation

*P. J. Griffin
H. Dumych
E. J. W. Irish*

Production editing and layout

*Leona R. Mahoney
Angelica F. V. Koops
Richard Fix*

Typed and checked by

*Debbie Busby
Janet Gilliland
Sharon Parnham
W. E. Anderson*

GEOLOGICAL INFORMATION
DIVISION

JUN 2 1976
JUN 2 1976

DIVISION DE L'INFORMATION
GÉOLOGIQUE



GEOLOGICAL SURVEY
PAPER 76-1B

R 187
1976

REPORT OF ACTIVITIES PART B

© Minister of Supply and Services Canada 1976

Available by mail from

Printing and Publishing
Supply and Services Canada,
Ottawa, Canada K1A 0S9,

from the Geological Survey of Canada
601 Booth St., Ottawa, K1A 0E8

and at Canadian Government Bookstores:

HALIFAX
1683 Barrington Street

MONTREAL
640 St. Catherine Street West

OTTAWA
171 Slater Street

TORONTO
221 Yonge Street

WINNIPEG
393 Portage Avenue

VANCOUVER
800 Granville Street

or through your bookseller

Catalogue No. M44-76-1B

Price: Canada: \$5.00
Other countries: \$6.00

Price subject to change without notice

TABLE OF CONTENTS

	Page
INTRODUCTION	vii
ANALYTICAL CHEMISTRY	
J.-L. BOUVIER and SYDNEY ABBEY: Improvements in the "screw-rod" method for determination of lithium, rubidium and cesium	13
W.H. CHAMP and C.F. MEEDS: Application of spectrochemical methods to trace element determinations in geological materials	11
APPALACHIAN GEOLOGY	
W.H. POOLE: Plate tectonic evolution of the Canadian Appalachian region	113
CORDILLERAN GEOLOGY	
R.G. CURRIE and J.E. MULLER: Magnetic susceptibility as a diagnostic parameter of Vancouver Island volcanic rocks	97
P.R. FERMOR and R.A. PRICE: Imbricate structures in the Lewis thrust sheet around the Cate Creek and Haig Brook windows, southeastern British Columbia	7
J.K. GLOVER and R.A. PRICE: Stratigraphy and structure of the Windermere Supergroup, southern Kootenay Arc, British Columbia	21
S.P. GORDEY and D.J. TEMPELMAN-KLUIT: Stratigraphic and structural studies in the Pelly Mountains, Yukon Territory	1
GEOCHEMISTRY	
I.R. JONASSON: Trace metals in snow strata as indicators of silver-arsenide vein mineralization, Camsell River area, District of Mackenzie	71
GEOPHYSICS	
A. DICAIRE, T.R. FLINT, H.W.C. KNAPP, D. OLSON, and P. SAWATZKY: The Geological Survey of Canada aeromagnetic gradiometer system: A progress report	303
R.L. GRASTY: The circle of investigation of airborne gamma-ray spectrometers	77
R.L. GRASTY: The 'field of view' of gamma-ray detectors — a discussion	81
P.J. HOOD and E. READY: Federal-Provincial Aeromagnetic Survey Program of Canada: A progress report	267
T.J. KATSUBE: New requirements for electrical exploration methods and for laboratory R and D	229
A.K. SINHA: A technique for obtaining correct ground resistivity from airborne wave tilt measuring systems	281
D. SWAN, I. FRYDECKY, and R.G. CURRIE: A library of computer programs for the processing of hyperbolic and range-range navigation data	95

MARINE GEOSCIENCE

I. A. HARDY and D. C. UMPLEBY: Lithostratigraphy of the Labrador Shelf	31
L. F. JANSA: Lower Paleozoic Radiolaria-bearing limestones from the Baffin Island shelf	99
GEORGE PATTON: Estuarine sedimentary dynamics in the Minas Basin, Bay of Fundy, Nova Scotia	25

MINERAL DEPOSITS

L. D. AYRES and D. J. FINDLAY: Precambrian porphyry copper and molybdenum deposits in Ontario and Saskatchewan	39
J. L. JAMBOR and W. J. McMILLAN: Distribution and origin of the "Gypsum Line" in the Valley Copper porphyry deposit, Highland Valley, British Columbia	335
V. RUZICKA: Evaluation of uranium resources in the Elliot Lake-Blind River area, Ontario	127

MINERALOGY

H. G. ANSELL, G. J. PRINGLE, and A. C. ROBERTS: A hydrated neodymium-lanthanum carbonate from Curitiba, Parana, Brazil	353
J. L. JAMBOR: New occurrences of the hybrid sulphide tochilinite	65
J. L. JAMBOR, A. G. PLANT, and H. R. STEACY: A dawsonite-bearing silicocarbonatite sill from Montreal Island, Quebec	357
R. M. MacKay and M. Zentilli: Mineralogical observations on the copper-uranium occurrence at Black Brook, Nova Scotia	343
ANN P. SABINA: The Francon Quarry, a mineral locality	15

PALEOMAGNETISM

W. F. FAHRIG: Paleomagnetism and age of the Schefferville diabase dykes	153
E. J. SCHWARZ: Paleomagnetism of the Circum-Ungava Belt: East coast of Hudson Bay	37

PALEONTOLOGY

M. S. BARSS and B. CRILLEY: A mounting medium for palynological residues ..	131
W. W. BRIDEAUX: Taxonomic notes and illustrations of selected dinoflagellate cyst species from the Gulf Mobil Parsons N-10 well	251
M. J. COPELAND: Leperditicopid ostracodes as Silurian biostratigraphic indices	83
W. S. HOPKINS, JR. and A. R. SWEET: A microflora from a short section of the Paleogene Kishenehn Formation, southeastern British Columbia	307

	Page
R. A. McLEAN: Genera and stratigraphic distribution of the Silurian and Devonian rugose coral family Cystiphyllidae Edwards and Haime	295
A. E. H. PEDDER: Initial records of two unusual Late Silurian rugose coral genera from Yukon Territory	285
A. E. H. PEDDER: First records of five rugose coral genera from Upper Silurian rocks of the Canadian Arctic Islands	287
PRECAMBRIAN GEOLOGY	
ERICH DIMROTH: Physical volcanology and sedimentology of the Abitibi greenstone belt, Québec	107
QUATERNARY GEOLOGY: ENVIRONMENTAL AND ENGINEERING GEOLOGY STUDIES	
J. E. GALE, K. RAVEN, J. DUGAL, and P. BROWN: Subsurface containment of solid radioactive wastes	147
J. S. O. LAU and D. E. LAWRENCE: Winter ground-ice distribution for selected map-areas, Mackenzie Valley	161
R. N. YONG and P. B. FRANSHAM: Dynamic behaviour and response of sensitive clays of Champlain Sea deposits	371
QUATERNARY GEOLOGY: INVENTORY MAPPING AND STRATIGRAPHIC STUDIES	
J. E. ARMSTRONG and S. R. HICOCK: Quaternary multiple valley development of the lower Coquitlam Valley, Coquitlam, British Columbia (92 G/7c)	197
J. J. CLAGUE: Pleistocene sediments in the northern Strait of Georgia, British Columbia	157
J.-M. DUBOIS: Levé préliminaire du complexe morainique de Manitou-Matamek sur la Côte Nord de l'estuaire maritime du Saint-Laurent	89
D. R. GRANT: Reconnaissance of early and middle Wisconsinan deposits along the Yarmouth-Digby coast of Nova Scotia	363
C. TARNOCAI: Soils of Bathurst, Cornwallis, and adjacent islands, District of Franklin	137
S. C. ZOLTAI and V. WOO: Soils and vegetation of Somerset and Prince of Wales islands, District of Franklin	143
QUATERNARY GEOLOGY: PALEOECOLOGY AND GEOCHRONOLOGY	
W. BLAKE, JR: Sea and land relations during the last 15 000 years in the Queen Elizabeth Islands, Arctic Archipelago	201
D. C. FORD and H. P. SCHWARCZ: Radiometric age studies of speleothem	151
L. V. HILLS and R. M. BUSTIN: <i>Picea banksii</i> Hills & Ogilvie from Axel Heiberg Island, District of Franklin	61

	Page
D. M. JONES, W. W. SHILTS, and R. W. WEIR: Heavy metal content of tundra plant species	273
S. LICHTI-FEDEROVICH: A preliminary list of diatoms from sea floor sediments in Croker Bay, Devon Island, District of Franklin	133
JOHN V. MATTHEWS, JR: Insect fossils from the Beaufort Formation: geological and biological significance	217

QUATERNARY MARINE GEOLOGY

J. L. LUTERNAUER: Fraser Delta sedimentation, Vancouver, British Columbia ..	169
--	-----

QUATERNARY SEDIMENTOLOGY AND GEOMORPHOLOGY

T. J. DAY and J. C. ANDERSON: Observations on river ice, Thomsen River, Banks Island, District of Franklin	187
T. J. DAY and R. J. GALE: Geomorphology of some Arctic gullies, Banks Island, District of Franklin	173
A. S. DYKE: Tors and associated weathering phenomena, Somerset Island, District of Franklin	209
J. ROSS MACKAY: The age of the Ibyuk pingo, Tuktoyaktuk Peninsula, District of Mackenzie	59
R. B. TAYLOR: Nearshore observations along the east coast of Melville Island, District of Franklin	43

STRATIGRAPHY AND STRUCTURAL GEOLOGY

H. R. BALKWILL and W. S. HOPKINS, JR: Cretaceous stratigraphy, Hoodoo Dome, Ellef Ringnes Island, District of Franklin	329
W. W. BRIDEAUX and D. W. MYHR: Lithostratigraphy and dinoflagellate cyst succession in the Gulf Mobil Parsons N-10 well, District of Mackenzie	235
R. L. CHRISTIE: Tertiary rocks at Lake Hazen, northern Ellesmere Island	259
D. G. COOK and J. D. AITKEN: Two cross-sections across selected Franklin Mountain structures and their implications for hydrocarbon exploration	315
J. R. McLEAN: Cadomin Formation: eastern limit and depositional environment ..	323
D. W. MYHR and R. R. BAREFOOT: Geochemical properties of Cretaceous rocks and their use as a correlation tool, Mackenzie Delta and Yukon Coastal Plain areas	311
D. K. NORRIS: Geological time symbols used on Operation Porcupine	263
T. P. POULTON and J. H. CALLOMON: Major features of the Lower and Middle Jurassic stratigraphy of northern Richardson Mountains, northeastern Yukon Territory, and northwestern District of Mackenzie	345

INTRODUCTION

The basic reason for an organization like the Geological Survey is that most nations require a comprehensive inventory and understanding of the geological framework of their countries in order that all activities that depend on geology can be supplied with the requisite information. Resource depletion and degradation of the landmass are subjects of particular importance and many of the on-going projects reported on in this publication are designed to provide the data needed to lessen the impact of these problems.

In broad terms the Geological Survey of Canada is concerned with determining the mineral and energy resource potential available to Canada, carrying out land capability studies, studies on the geology of urban areas, and studies designed to assist in conserving our natural environment. These activities contribute to two programs of the Department of Energy, Mines and Resources – the Earth Sciences Service Program and the Mineral and Energy Resources Program.

The first program is concerned with obtaining information about the geological framework of Canada, its properties, evolution and development. Information on bedrock geology is obtained through systematic surveys, regional studies and national compilations and is used for identifying resources and for making appraisals of non-renewable resources. Similar studies are carried out to obtain information about the nature and evolution of the Canadian landscape, its surficial materials, terrain properties, processes, hazards and capability for use. Such information is essential when evaluating the effects of energy and mineral resource development.

The second program is concerned with resource identification and resource estimation. Attention is given to identifying areas likely to contain mineral and fossil fuel resources. Estimates of the amount and quality of energy resources are made each year but those for mineral commodities, because of the complex calculations involved, are made less frequently.

The two programs are of course interrelated – assessments of resource potential depend on bedrock geology data; environmental constraints may have a definite economic impact on the viability of mineral or energy resources.

It is only recently that a significant segment of the population including our elected representatives, have accepted the finite nature of many resources and have recognized the need to take this limitation into account in long-term planning. Studies carried out under the auspices of EMR indicate that the world's supply base of minerals is capable of meeting demand to 2000 AD and that the Canadian mineral industry will continue to meet domestic requirements and export opportunities well into the 1980's. Indeed in 1975 we exported more than half our 13.4 billion dollar mineral production, an important factor in Canada's economic well-being. We must continue a vigorous program of mineral resource identification for the long-term but we are not faced with immediate shortages.

The situation in the field of energy commodities is much more critical as all informed Canadians are aware and the Geological Survey is participating in major programs concerned with the identification and assessments of conventional energy sources.

During 1975 the Federal Cabinet indicated that priority would be given to government programs designed to meet certain fairly well defined objectives. Many of these programs involve the Geological Survey to a greater or lesser degree. For example meeting the objective of developing a greater balance in the distribution of people and wealth by encouraging regional development requires amongst other things information on likely areas where additional non-renewable resources may be found and how much there is; terrain studies to determine the capability of the landmass to withstand additional uses and to identify the necessary construction materials are also vital. In order to meet the government's aim of making more rational use of resources and of being sensitive to the natural and human environment we must establish the carrying capacity of Canada in terms of mineral and energy resources and assess the impact of resource development on the Canadian landmass.

The reports included in this publication reflect the Geological Survey's concern with the on-going improvement of the description and understanding of the geological framework of Canada. Emphasis continues to be given to the area north of 60°, an area in which the present level of information is low and where the need for regional information for resource exploration and for the assessment of the impact of exploitation are greatest. Regional studies, however, are being continued in the provinces in order to keep in close touch with the progress of provincial agencies and to be able to judge mineral and regional development proposals made by the provinces.

Stratigraphic and structural studies such as those described in Reports 1, 6 and 23 are basic to understanding the conditions under which mineral and hydrocarbon deposits may be formed. Such studies sometimes enable the preparation of major syntheses such as that presented in Report 24 in which the theory of plate tectonics is applied to the evolution of the Canadian Appalachian

region. This region, for some years neglected by the Survey due to other commitments, is the centre of renewed interest and this synthesis should be most useful to the development of exploration strategies.

Each year the Geological Survey carries out many studies in Economic Geology. Some of these involve the study of specific mineral commodities to determine how and why they are concentrated in the Earth's crust. Others involve regional metallogeny which relates the nature and distribution of the mineral deposits in a large area to the geological features. Reports 10, 59 and 60 describe different aspects of copper deposits, and Report 25 the uranium resources of the Elliot Lake-Blind River area. Reports 15 and 48 present the results of two different approaches to mineral exploration. The first describes the use of trace metals in snow layers as indicators of silver-arsenide deposits in the District of Mackenzie and the second the use of the trace element content of plants as a mineral resource indicator.

Terrain surveys and related studies although carried out on a national scale were concentrated for some years in the District of Mackenzie where the demand for data for a proposed transportation corridor has been high. Similar information is now needed to assist in evaluating a pipeline route from the Arctic Islands southward along the west side of Hudson Bay, a route that in addition to studies of terrain features also requires the investigation of bottom and coastal conditions of the ice-infested channels that would have to be crossed. Reports 28, 29 and 40 describe the geomorphology soils and vegetation of several of the islands that might be traversed by such a pipeline. Reports 11, 34, 36 and 37 describe the geomorphological phenomena from the western Arctic. The results of such studies are, of course, applicable far beyond the particular region studied.

The Geological Survey continues to lead in the development and application of geophysical techniques to the search for mineral deposits and in Reports 16 and 17 observations applicable to gamma-ray spectrometry surveys are given. The Geological Survey has been conducting aeromagnetic surveys since 1947 and in 1960 launched the Federal-Provincial Aeromagnetic Survey project. From time to time the "Report of Activities" has included progress reports on this project and Report 47 comprises the latest such review. The program has been completed for New Brunswick, Ontario, Manitoba, Saskatchewan and Alberta (Prince Edward Island and Nova Scotia were completed prior to 1960). The island of Newfoundland is now also complete as is 60 per cent of Labrador and 70 per cent of Quebec. The report also details the current phases of the project which has been widely acknowledged by the mineral exploration industry as the most valuable of recent government programs. The results are much used in planning mineral exploration programs and are credited with a prime role in the discovery of a number of Canadian mineral deposits.

At present the "Report of Activities" is published three times each year – early January, early June and mid-November. Material for this report was received and edited between April 1st and 27th; production editing, typing, proofreading and preparation of camera ready copy were carried out between April 5th and 30th and the manuscript was sent to the printer in early May. The individual contributions are arranged in the order in which they were received in order to expedite preparation but a separation by discipline is given in the Contents section.

April 30, 1976

R. G. Blackadar
Chief Scientific Editor

REPRINTS

A limited number of reprints of the papers that appear in this volume are available by direct request to the individual authors. The addresses of the Geological Survey of Canada offices follow:

601 Booth Street,
OTTAWA, Ontario
K1A 0E8

Institute of Sedimentary and Petroleum Geology,
3303-33rd St. N.W.,
CALGARY, Alberta
T2L 2A7

British Columbia Office,
100 West Pender Street,
VANCOUVER, B. C.
V6B 1R8

Atlantic Geoscience Centre,
Bedford Institute of Oceanography,
P. O. Box 1006,
DARTMOUTH, N. S.
B2Y 4A2

When no location accompanies an author's name in the title of a paper, the Ottawa address should be used.

Project 730037

S. P. Gordey¹ and D. J. Tempelman-Kluit
Regional and Economic Geology Division, Vancouver

Detailed mapping at 1:50 000 scale was carried out during 1975 in part of Finlayson Lake map-area (105 G) (see Fig. 1.1) as part of a broader study of stratigraphy and structure in the Pelly Mountains. A summary of this regional work by Tempelman-Kluit *et al.* (1976) provides a framework for the following discussion.

Stratigraphy

The general stratigraphy has been described elsewhere (Tempelman-Kluit *et al.*, 1976) and only a few refinements pertinent to the area of this report will be given here.

Adjacent to Tintina Trench, Mississippian black siliceous slate lies with marked disconformity on a Devonian carbonate sequence and, locally, on Silurian dolomitic siltstone. Abundant dolomite breccia distinguishes the Devonian carbonate sequence here from well-bedded dolomites to the southwest.

The Mississippian black siliceous slate, roughly 480 m thick, is overlain throughout the area by slate, greywacke, and chert pebble conglomerate, roughly 80 m thick. The greywacke and conglomerate occur, in part, as thin, sheet-like units within the slate. Rhythmically interbedded slate and graded greywacke occur locally. An overlying thin-bedded tuffaceous chert forms a widespread marker unit.

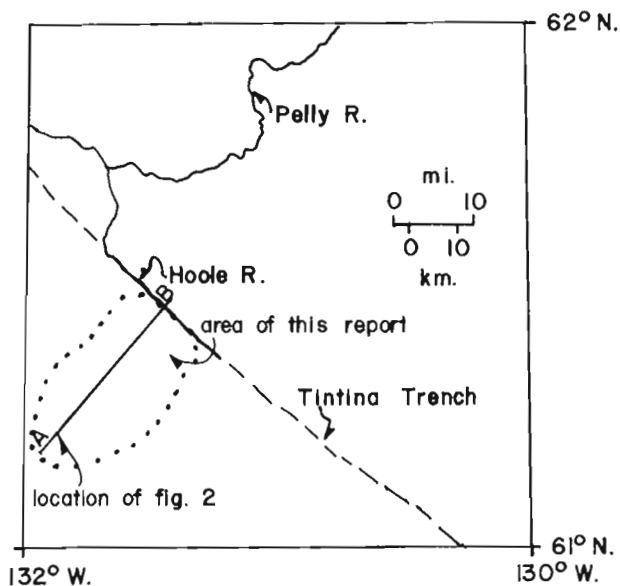


Figure 1.1. Index map of Finlayson Lake map-area (105G) showing area referred to in this report.

¹Queen's University, Kingston, Ontario

In the central part of the area the black slate changes facies, to a volcanic pile of acid flows and tuffs. There, the acid volcanics rest unconformably on the Devonian carbonate sequence.

Metamorphic Rocks

Highly deformed low-grade metamorphic rocks, part of the Big Salmon - Englishman's Allochthon (Tempelman-Kluit *et al.*, 1976) form a number of klippen in the southwestern part of the area (Fig. 1.2).

Very fine grained, poorly schistose, muscovite-chlorite-albite-quartz rock is dominant but non-schistose, very fine grained, quartz-chlorite-epidote-albite assemblages are abundant, and calc-silicate rocks occur at a few localities. The rocks weather grey or pale green and form good outcrops. Bedding is only apparent locally and is defined by subtle colour laminations a few millimetres thick, or by millimetre-scale alternations of pelite and quartzite. Other primary textures have been obscured by deformation and metamorphism.

The mineral assemblages indicate a lower greenschist facies of regional metamorphism (see Table 1.1).

Table 1.1

Mineral assemblages of the metamorphic rocks

Minerals	Mineral Assemblages						
quartz	x	x	x	x	x	x	x
muscovite	x	x	x	x	x	x	x
chlorite			x		x	x	
albite		x	x	x	x	x	
epidote					x		
zoisite							x
clinozoisite							x
sphene						x	
carbonate			x	x			x

Structure

The main structures are illustrated in a cross-section drawn normal to the northwest-southeast structural grain (see Fig. 1.2). The most conspicuous features are the allochthonous sheet of metamorphic rocks, and the steepening of bedding and cleavage within Tintina Fault Zone. Folding and thrusting involved rocks as young as Triassic.

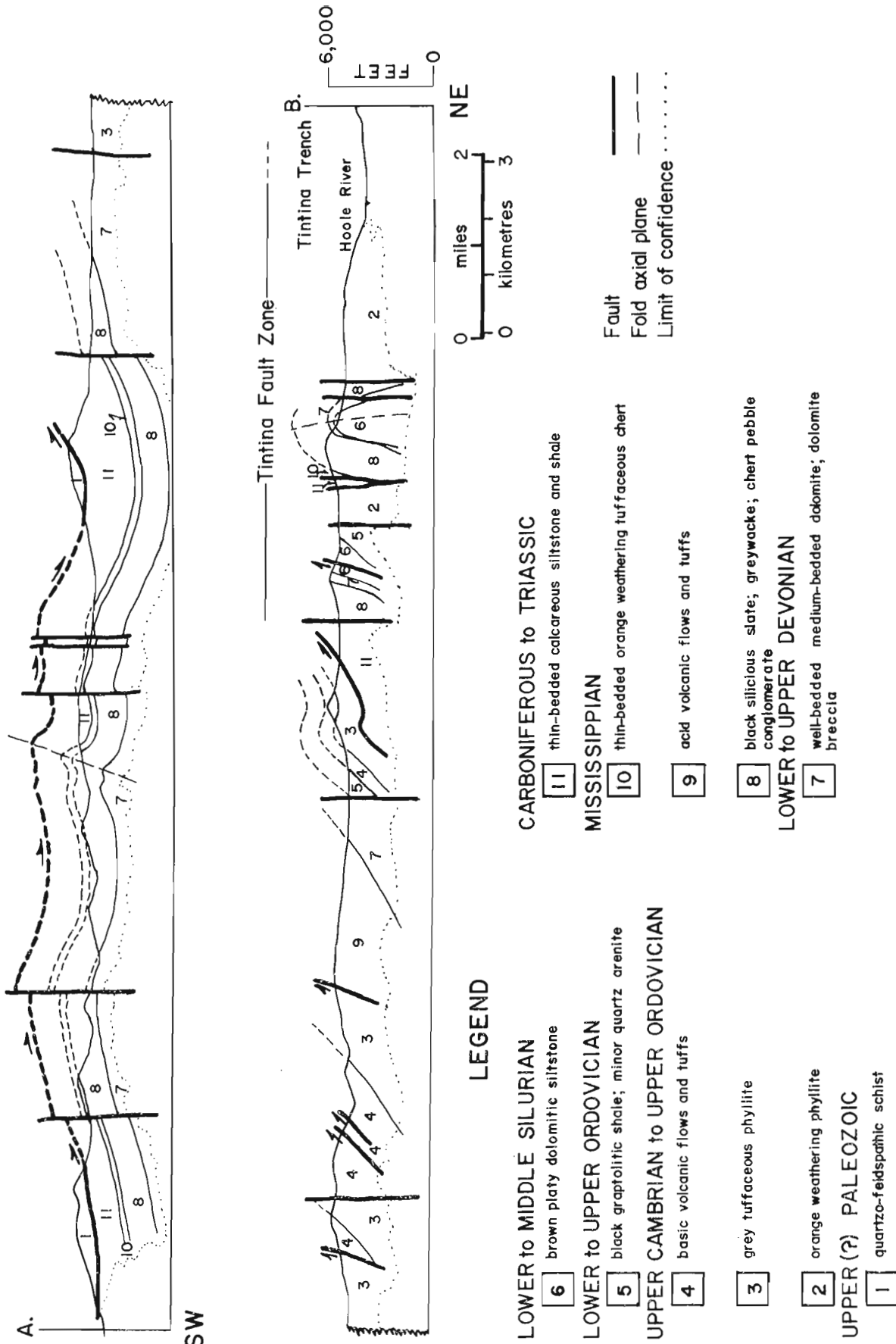


Figure 1.2. Cross-section across Pelly Mountains from 61°9'N; 131°55'W to 61°27'N; 131°23'W. The approximate location of the section is shown in figure 1.1.

Pre-Mississippian vertical faults, although not occurring along the line of cross-section, are found in the southwestern part of the area. These faults cut Devonian carbonates but do not cut the overlying Mississippian black slate.

Metamorphic Rocks

The metamorphic rocks are folded by isoclinal recumbent folds on which are superposed upright to

overturned folds that verge to the north-northeast (Figs. 1.3 - 1.5). The main fabric elements are:

S_1 — a penetrative schistosity defined by parallel alignment of muscovite and chlorite, and more or less parallel with bedding. This schistosity wraps around helicitic albite porphyroblasts that contain inclusion trains which are steeply inclined to S_1 have not been recognized.

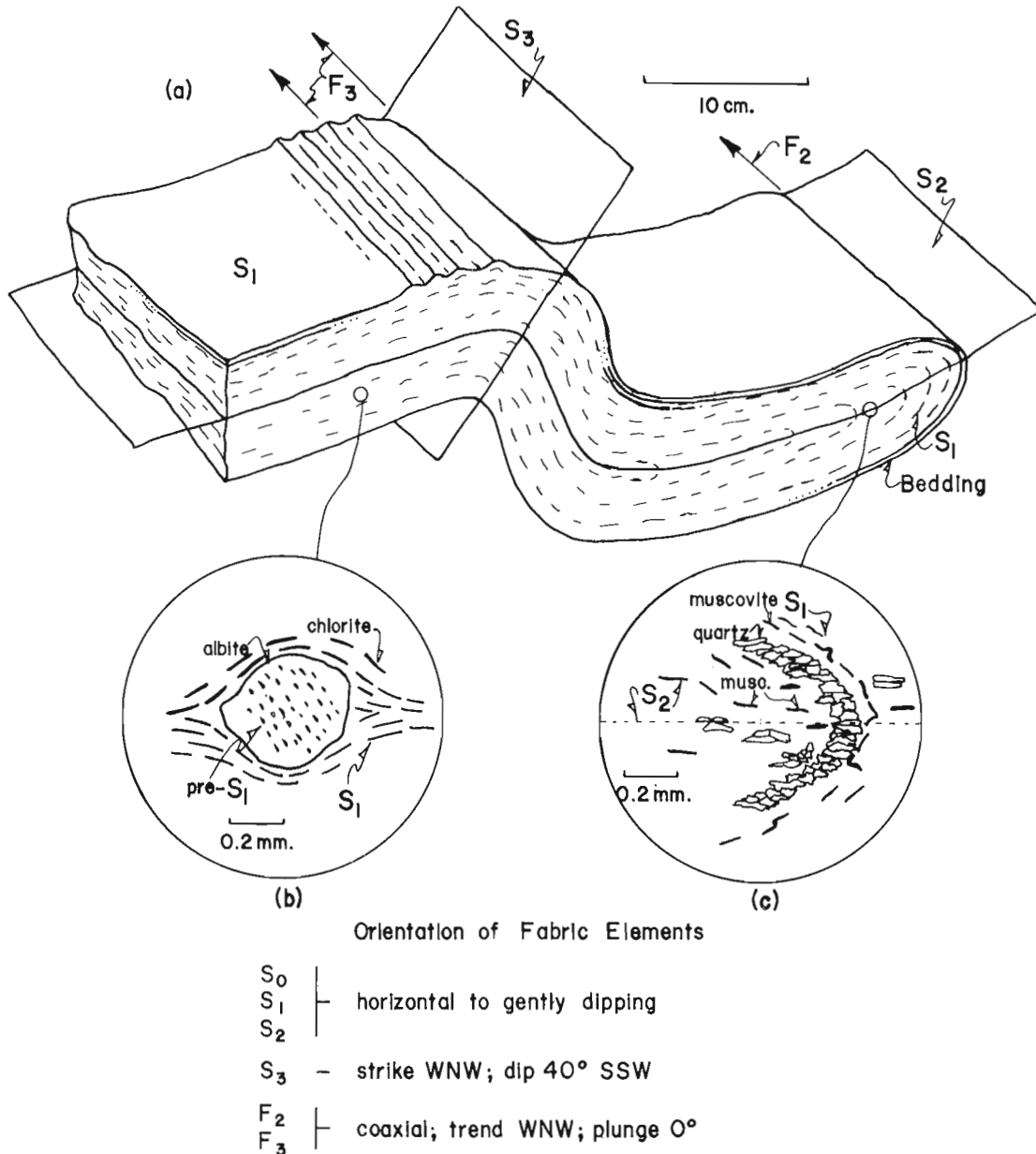


Figure 1.3. Diagrammatic sketch showing the style of folding and the fabric of the metamorphic rocks. The fabric elements are described in the text.

(b) — chlorite wrapping around an albite porphyroblast.

(c) — a dimensional preferred orientation of quartz parallel with S_2 within a folded relatively coarse-grained quartz layer. Some muscovite has grown parallel with S_2 .

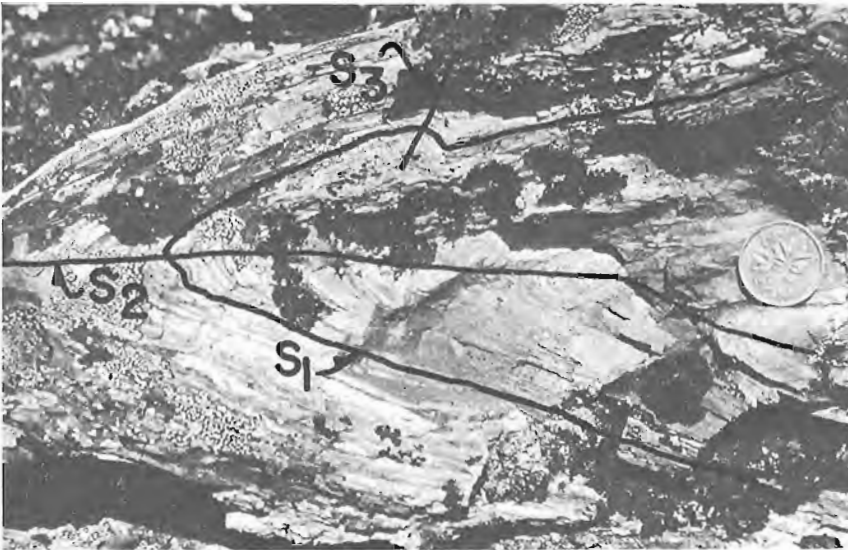
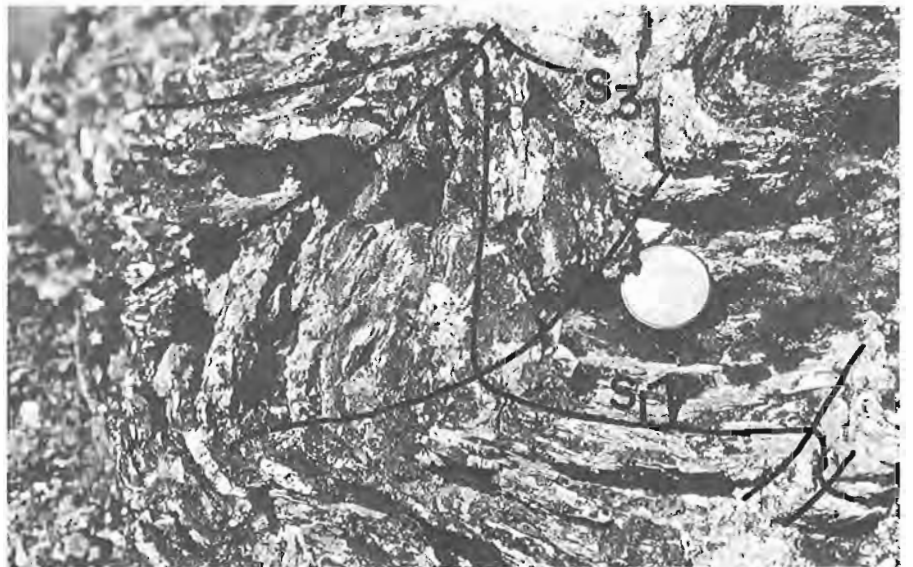


Figure 1. 4

Recumbent fold in the metamorphic rocks characteristic of folding about S_2 . One limb has been refolded about S_3 .

Figure 1. 5

Upright to overturned folds in the metamorphic rocks characteristic of folding about S_3 .



S_2 — defined by the axial planes of isoclinal recumbent folds in bedding and S_1 . A dimensional preferred orientation of tabular quartz grains and scattered muscovite flakes aligned parallel with S_2 occurs locally (Fig. 1. 3c) but does not define a mesoscopic fabric. The quartz may be highly deformed, showing extreme undulatory extinction and, more rarely, deformation lamellae. Folding about S_2 has kinked S_1 micas. S_2 is subparallel with the thrust surface marking the base of the allochthonous sheet.

S_3 — is defined by the axial planes of upright to slightly overturned folds in bedding, S_1 , and S_2 that verge to the north-northeast. It is not associated with new mineral growth. S_3 is subparallel with a cleavage developed locally in the rocks underlying the allochthonous sheet.

L_2 — defined by the hinge lines of folds in bedding and S_1 , and is associated with S_2 .

L_3 — defined by the hinge lines of folds in bedding, S_1 , and S_2 , and is associated with S_3 . It is locally expressed as a crenulation of S_1 and S_2 .

The lack of stratigraphic markers in the allochthonous mass makes it difficult to outline the larger structures within it. The largest folds that have been recognized are on the scale of one metre.

There is a pronounced contrast in intensity of deformation and metamorphic grade between the allochthonous mass and the rocks underlying it. The underlying rocks are unmetamorphosed siltstones and shales, in which primary sedimentary structures are well preserved. The folds are open, and associated slaty cleavage is only developed locally.

Tintina Fault Zone

Within Tintina Fault Zone (Fig. 1. 2), bedding dips steeply, locally being overturned to the southwest, and cleavage dips moderately to steeply to the northeast. The steep faults of this zone, which in plan view form a braided or anastomosing network trending northwest-southeast, have juxtaposed rocks of all parts of the autochthonous sedimentary sequence recognized elsewhere in the area. Individual fault blocks have been little deformed by movements on faults of the fault zone.

Faults of the Tintina Fault Zone cut rocks as young as Triassic, as well as folds and thrusts, and accordingly, displacements along these faults are post-Triassic and post-thrusting and folding. Although

some dip-slip movement is evident, the pattern of a bifurcating network of subparallel faults distributed over a wide zone is consistent with the strike-slip displacements postulated by Roddick (1967) and Tempelman-Kluit *et al.* (1976).

References

Roddick, J. A.

1967: Tintina Trench; *J. Geol.*, v. 75, p. 23-33.

Tempelman-Kluit, D. J., Gordey, S. P., and Read, B. C.

1976: Stratigraphic and structural studies in the Pelly Mountains, Yukon Territory; in Report of Activities, Part A, *Geol. Surv. Can.*, Paper 76-1A, p. 97-106.

IMBRICATE STRUCTURES IN THE LEWIS THRUST SHEET AROUND THE CATE CREEK
AND HAIG BROOK WINDOWS, SOUTHEASTERN BRITISH COLUMBIA

E. M. R. Research Agreement 1135-D-13-4-157/75

P. R. Fermor¹ and R. A. Price¹
Regional and Economic Geology Division

Upper Cretaceous strata exposed in windows through the Lewis thrust sheet at Cate Creek and Haig Brook in northern Clark Range of southeastern British Columbia (Olsson and Caster, 1935; Price, 1959, 1962 and 1965; Norris, 1959; Jones, 1969) are overlain by a discrete layer of imbricate, southwesterly facing sigmoidal thrust fault slices (Dahlstrom, 1970), comprising repetitions of a thin stratigraphic interval from the base of the Middle Proterozoic (Helikian) Belt-Purcell Supergroup (Fig. 2.1). The imbricate layer forms a zone up to 300 m thick that is bounded below by the Lewis thrust fault and above by another thrust fault, the Tombstone thrust, which is essentially a bedding glide fault within the Waterton Formation, the oldest formation known from the Belt-Purcell Supergroup within the Lewis thrust sheet in southeastern British Columbia and adjacent parts of Alberta and Montana. The nature and structural relationships of the imbricate zone provide some new insight on the mechanism and magnitude of the large northeastward relative translation of the Lewis thrust sheet.

The Lewis thrust is a major low-angle overthrust fault along which a sheet of Proterozoic to Lower Cretaceous rocks up to 7 km thick has been displaced more than 40 km northeast relative to Upper Cretaceous

clastic deposits of the Rocky Mountain exogeocline below the fault (Price, 1962 and 1965; Dahlstrom, *et al.*, 1962). The sole fault emerges along the eastern and northern slopes of Clark Range in southwestern Alberta, about 11 km east and northeast of the Cate Creek and Haig Brook windows. The sheet of Helikian strata above the fault is truncated to the southeast by the Flathead fault, a major southwesterly dipping normal fault which flattens with depth and may merge with the Lewis thrust beneath the Flathead Valley of southeastern British Columbia (Bally *et al.*, 1966).

The Cate Creek and Haig Brook windows occur along the crest of a northwest-trending anticlinal culmination that extends along the southwest side of Clark Range from near North Kootenay Pass into northern Montana. The Lewis thrust fault is folded along with the overlying strata in this anticlinal structure (Clark, 1954; Price, 1959, 1962 and 1965; Norris, 1959).

Although the Lewis thrust fault is rarely exposed in the Cate Creek and Haig Brook windows, its position can be fixed rather closely on the basis of extensive exposures of the imbrications of Purcell strata above it and a few critical exposures of Upper Cretaceous strata below the fault.

The Waterton Formation occurs along or near the base of the Lewis thrust sheet in the Waterton Lakes area (Douglas, 1950) and in the Pacific-Atlantic Flathead well (Clark, 1954; Price, 1962) at Sage Creek, 40 km west of Waterton Lakes, as well as in the vicinity of the Cate Creek and Haig Brook windows and along the north side of Clark Range. Accordingly, under most of the Clark Range, over an area of more than 2000 km², the Lewis thrust is essentially a bedding glide zone with respect to the allochthonous succession comprising the Lewis thrust sheet.

The zone of imbricate thrust faults that frames Cate Creek and Haig Brook windows varies in thickness from 150 to 300 m. It involves strata of the Waterton Formation, but over the eastern parts of the windows the zone includes some other strata of an uncertain stratigraphic position but probably comprise part of the thin, condensed eastern facies of the Helikian Belt-Purcell Supergroup. A zone of imbricate structures involving the Waterton Formation also occurs north of the Cate Creek window in the St. Eloi and Syncline Brooks valleys (Price, 1959, 1962 and 1965; Norris, 1959); and moreover, the strata in the hanging wall of the Lewis thrust along the mountain front in northern Clark Range, which are about 150 to 200 m thick and were assigned to the Waterton Formation by Norris (1959), may also include the imbricate zone.

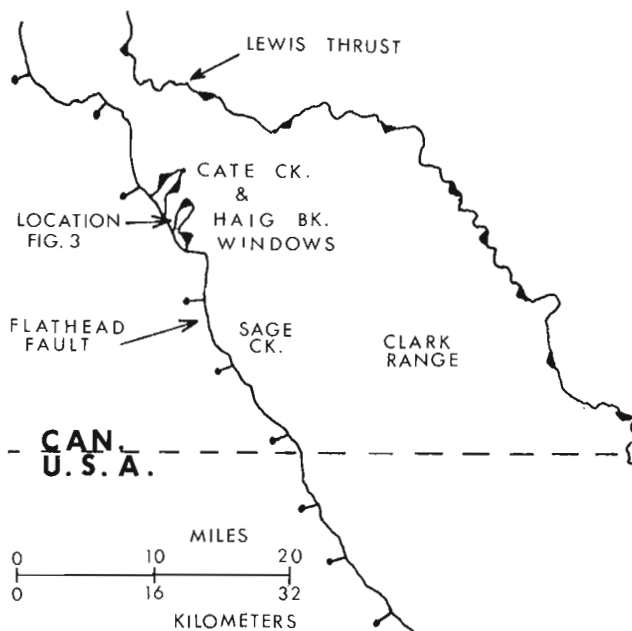


Figure 2.1. Index map.

¹Department of Geological Sciences, Queen's University, Kingston, Ontario.

In order to facilitate the structural analysis of the imbricate thrust faulting, the Waterton Formation near the windows has been subdivided into a number of distinctive stratigraphic units (Fig. 2. 2). Because completely unfaulted sections are not present in the imbricate zone, a composite section based on the stratigraphically overlapping partial sections in individual fault slices has been established. The subdivisions of the Waterton Formation established in this way can be correlated with those described from the upper part of the Waterton Formation near Waterton Lakes (Douglas, 1952) and from cuttings from the Pacific-Atlantic-Flathead no. 1 well (Price, 1964; and Douglas, unpublished descriptions, 1952) in southwestern Clark Range.

A cross-section through the Lewis thrust sheet along the cliffs on the northwest side of Haig Brook has been constructed from detailed structural and stratigraphic data obtained from traverses along the top and bottom of the cliffs, and from field sketches on enlarged oblique air and ground photographs of faults and marker beds that are exposed in the cliffs (Fig. 2. 3). Not all the area encompassed by the section is underlain by exposed bedrock. Where bedrock exposures do not occur the structure section has been drawn so as to ensure that it is balanced (Dahlstrom, 1969), and that the thicknesses of stratigraphic units and the angular relationships between the faults and beds do not change from one side of a fault to the other. The section has been drawn, almost perpendicular to the strike of the beds; and therefore, the true thicknesses of the beds and angular relationships between the faults and the beds are slightly distorted.

Along its hanging wall the Lewis thrust follows a zone of bedding glide that coincides with the base of unit A of the Waterton Formation. The Tombstone thrust, which marks the top of the imbricate zone, follows a zone of bedding glide high in unit B of the Waterton Formation along its hanging wall, except in the western part of the section where it steps down abruptly to a

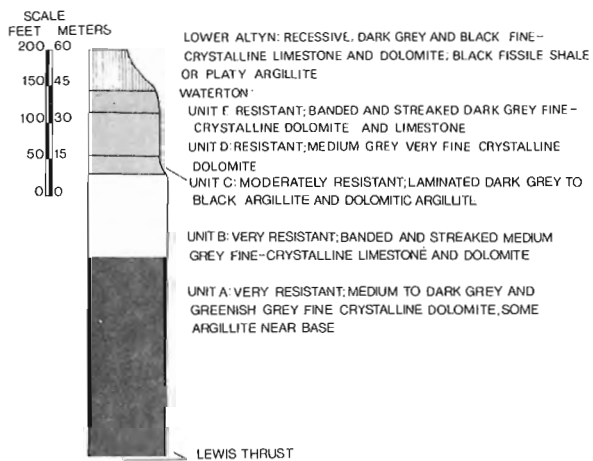


Figure 2. 2. Composite stratigraphic section of rocks overlying the Lewis thrust fault in the vicinity of Haig Brook and Cate Creek windows.

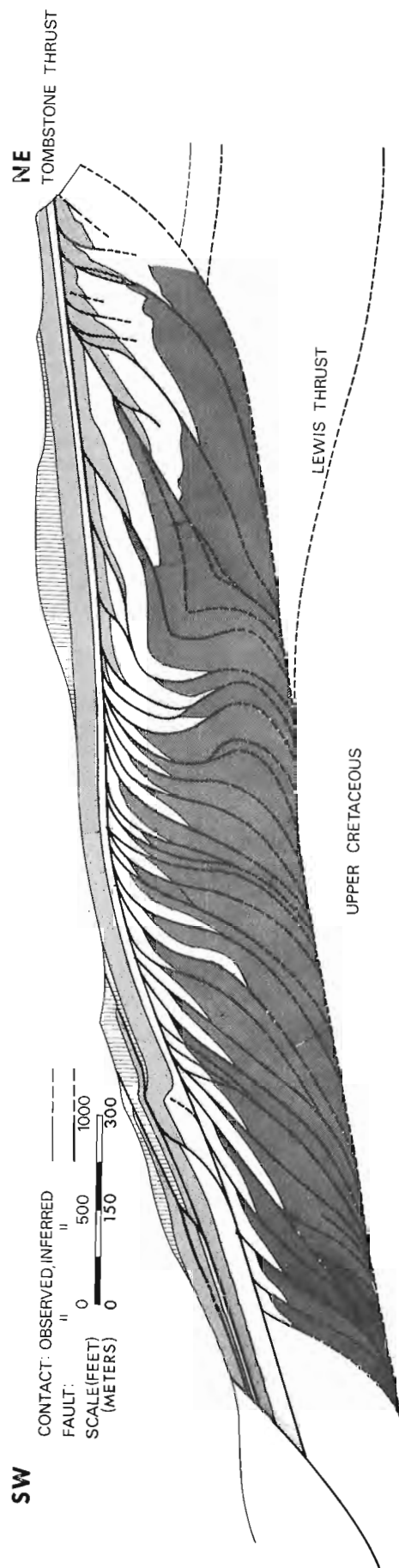


Figure 2. 3. Cross-section of geologic structure in the hanging wall of the Lewis thrust sheet along the northwest side of Haig Brook, Clark Range, British Columbia. Stratigraphic units are shown with the same patterns as in Figure 2. 2.

lower bedding glide zone in unit B. On the other hand, along the footwall, the Tombstone thrust rises along an abrupt step in the middle of the section from a bedding glide zone in unit B in the west of another bedding glide zone in unit D in the east. The entire imbricate zone and the Tombstone thrust have been offset, in the eastern part of the section, by a younger high-angle reverse fault which splays off from the Lewis thrust. All of the faults, including the Tombstone thrust, must merge with the Lewis thrust to the southwest. A normal fault in the southwestern part of the section with a stratigraphic separation of about 40 m appears to merge downward with the Lewis thrust. This normal fault is within 1 km of the Flathead normal fault, and is probably related to it.

The faults which form the imbricate zone splay off from the Lewis thrust and merge upward with the Tombstone thrust. The sigmoidal shape of the faults is primarily a reflection of the fact that they represent a transfer of northeasterly displacement from the Lewis thrust to the overlying Tombstone thrust. However, the steep southwesterly dip of the imbricate fault slices can be attributed to the external rotation that was imparted to them as movement occurred along sigmoidal fault surfaces and as the displacement along east successively lower fault rotated all the beds and faults that lay above it. The backfolding of some of the faults slices can be attributed to the adjustments that were necessary to accommodate the sudden change in thickness of the imbricated zone where the Tombstone thrust steps abruptly upward along its footwall, from unit B to unit D. The pattern of change in shape from northeast to southwest among the backfolded imbricate thrust fault slices, provides further evidence that the general sequence of development of the individual faults in the imbricate zone was from southwest to northeast.

The rocks within the imbricate zone show many fine details of their primary sedimentary structure and texture, and obviously have not been subjected to any large penetrative internal deformation. The internal deformation that is discernible as small-scale faulting and folding is mainly, if not entirely, a result of compression more or less parallel with the bedding. Accordingly, the present aggregate length of the folded segments of a stratigraphic marker in a balanced structure section drawn perpendicular to the folds and faults (and therefore parallel with the inferred direction of displacement on the faults) may be less than, but is certainly not more than, the length of the same marker between the same end points prior to the thrusting. On this basis, the minimum amount of northeasterly displacement of the highest (most southwesterly) slice in the imbricate zone relative to the lowest (most northeasterly) slice has been estimated, by subtracting the present distance between reference points on the contact between units A and B in these two slices from the cumulative length of the contact between units A and B between the same reference points, as about 2.2 km. This represents a minimum "horizontal shortening" (ratio of final to original length) of about 60 per cent.

This northeasterly translation of the main mass of the Lewis thrust sheet relative to the sole fault and the rocks below it must be added to previous estimates of about 25 miles (40 km) for the minimum horizontal translation of the Lewis thrust sheet (Clark, 1954; Price, 1962 and 1965; Dahlstrom *et al.*, 1962), because these previous estimates did not take into account translation related to deformation of this type within the Lewis thrust sheet. Moreover, this additional 2.2 km is the amount of translation represented by one short segment of a zone of imbrication that is obviously much more extensive; and therefore, the total amount of translation of the Lewis thrust sheet that is expressed as imbricate thrusting near the sole fault may well be many tens of kilometres.

References

- Bally, A.W., Gordy, P.L., and Stewart, G.A.
1966: Structure, seismic data and orogenic evolution of southern Canadian Rocky Mountains; Bull. Can. Pet. Geol. v. 14, p. 337-381.
- Clark, L.M.
1954: Cross section through the Clark Range of the Rocky Mountains of southern Alberta and British Columbia; Alta. Soc. Petrol. Geol., Guidebook 4th Ann. Field Conf., p. 105-109.
- Dahlstrom, C.D.A.
1969: Balanced cross sections; Can. J. Earth Sci., v. 6, p. 743-757.
1970: Structural geology in the eastern margin of the Canadian Rocky Mountains; Bull. Can. Pet. Geol., v. 18, p. 332-406.
- Dahlstrom, C.D.A., Daniels, R.E., and Henderson, G.G.L.
1962: The Lewis Thrust and Fording Mountain, British Columbia; J. Alta. Soc. Petrol. Geol., v. 10, p. 373-395.
- Douglas, R.J.W.
1950: Callum Creek, Langford Creek, and Gap map-areas, Alberta; Geol. Surv. Can., Mem. 255.
1952: Waterton, Alberta; Geol. Surv. Can., Paper 52-10.
- Jones, P.B.
1969: Tectonic windows in the Lewis Thrust, southeastern British Columbia; Bull. Can. Pet. Geol., v. 17, p. 247-251.
- Norris, D.K.
1959: Carbondale River, Alberta-British Columbia; Geol. Surv. Can., Map 5-1959.

Olsson, A. A. and Caster, K. E.

1935: Occurrence of *Baculites ovatus* zone of Upper Alberta Shales in southeastern British Columbia; Am. Assoc. Pet. Geol., Bull., v. 19, p. 295-299.

Price, R. A.

1959: Flathead, British Columbia and Alberta; Geol. Surv. Can., Map 1-1959.

1962: Fernie map-area, east half, Alberta and British Columbia; Geol. Surv. Can., Paper 61-24.

Price, R. A. (cont.)

1964: The Precambrian Purcell system in the Rocky Mountains of southern Alberta and British Columbia; Bull. Can. Pet. Geol., v. 12, p. 399-426.

1965: Flathead map-area, British Columbia and Alberta; Geol. Surv. Can., Mem. 336.

APPLICATION OF SPECTROCHEMICAL METHODS TO TRACE ELEMENT
DETERMINATIONS IN GEOLOGICAL MATERIALS

Project 690090

W.H. Champ, C.F. Meeds, and Laboratory Staff
Central Laboratories and Administrative Services Division

The re-modelling of our Jaco Direct Reading Spectrometer as described in a previous report (Champ, *et. al.*, 1975) was finished in November of 1975. Physical adjustments, re-alignment and checking of optical components and electronic testing, etc. of the 42-channel system were completed in late December.

Calibration of the instrument and overall system to provide a 30-element analytical method, using 35 channels, was then begun and it is now in operation for the following determinations:

<u>Element</u>	<u>Range in %</u>	<u>Element</u>	<u>Range in %</u>
Si	.05-30	Cr	.0005-7.0
Al	.03-25	Cu	.0007-12.5
Fe	.03-30	La	.01-2.0
Ca	.002-30	Mo	.007-1.0
Na	.005-2.0	Ni	.001-2.0
Mg	.05-30	Pb	.05-10
Ti	.007-3.0	Sb	.07-7.0
Mn	.003-1.75	Sn	.01-3.0
Ag	.0005-.45	Sr	.001-7.0
As	.10-10	V	.002-1.25
B	.005-2.0	W	-
Ba	.0005-4.0	Y	.002-1.5
Be	.0003-.20	Yb	.0002-.22
Ce	.01-3.5	Zn	.01-7.0
Co	.001-1.0	Zr	.002-1.75

The procedure is intended to provide reasonably rapid "routine" analyses over wide ranges of concentration without severe restrictions on sample type and with accuracy acceptable for most purposes. In order to accomplish this, some limitations in element sensitivities have to be accepted. Coverage cannot be extended beyond the elements listed.

This method ("12B-DR") is directly adapted from our general spectrographic method (QN12B) for silicates and results are expected to be comparable in both precision and accuracy. All results will be reported on the basis of a single exposure per sample and will be expected to lie within 15% of the value given.

This means that values for the major elements, i.e. above the 5% concentration level, should be regarded as useful only for preliminary screening and characterization of the sample matrix. This is primarily for laboratory purposes, to decide which analytical methods should be applied when samples received are not sufficiently well identified or described.

Values for the minor and trace elements, however, should be quite as accurate as those obtainable from most other methods for rapid quantitative analysis.

Corrections for varying backgrounds and spectral interferences are made in the controlling computer programs. This permits a wide variety of rock and mineral types to be analyzed. Any sample whose components fall within the concentration ranges listed will be acceptable to the system. Some samples of extremely complex composition, or having physical characteristics which prevent successful exposure, such as high water or organic content, may be rejected and would have to be done by alternate methods.

Refinements to the computer program may lead to slight changes in the sensitivities listed in future. Information on analytical capabilities and the submission of samples for analyses will be available on request.

Reference

- Champ, W.H., Church, K.A., and Jones, F.W.
1975: Application of spectrochemical methods to trace element determinations in geological materials; in Report of Activities, Part B, Geol. Surv. Can., Paper 75-1B, p. 3.

IMPROVEMENTS IN THE "SCREW-ROD" METHOD FOR
DETERMINATION OF LITHIUM, RUBIDIUM, AND CESIUM

Project 690090

J. -L. Bouvier and Sydney Abbey
Central Laboratories and Administrative Services

This method, originally developed by Govindaraju (1975), has been used in our laboratories for two years. It involves impregnation of a mixture of the finely-ground sample and a suitable salt in the grooves of the screw thread on a small iron rod. By heating the rod in an air-acetylene flame, it is possible to atomize the sample and to obtain atomic-absorption measurements for certain volatile elements, particularly the rarer alkali metals.

The major advantages of the method over those based on acid decomposition of the sample are increased speed and sensitivity. A disadvantage is the fact that the sample must be mixed with sodium chloride for lithium and rubidium determination, and with sodium carbonate for determination of cesium. An investigation was therefore undertaken to find a salt or combination of salts that would provide adequate sensitivity for all three elements in one mixture.

Various combinations of sodium salts were first tried. Certain organic salts (citrate, tartrate, oxalate) were found to give significant improvement for cesium, when compared to the carbonate, but lithium sensitivity was poor. Mixtures of sodium chloride and carbonate proved unsatisfactory. However, Poluektov *et al.* (1969) reported good sensitivity for alkali metals when the

flame was fed with pressed pellets of mixtures of sample, ammonium chloride and calcium carbonate, in proportions approaching those used in the classical J. Lawrence Smith sinter. Various combinations of chlorides and carbonates of cations other than sodium were then tried, and a combination of the chloride and carbonate of barium, mixed with pure silica, was found to produce satisfactory sensitivity for both lithium and cesium. Rubidium sensitivity was too high, but that was overcome by reducing the response of the integrator used in recording the atomic absorption signal.

Further work is underway to find the best proportions of flux constituents and sample, and to study the possible determination of other elements.

References

- Govindaraju, K.
1975: Iron screw rod powder techniques using flame for direct atomic absorption determination of rare alkali elements (Li, Rb, Cs) in silicate rock samples; *Analysis*, v. 3, p. 164-169.
- Poluektov, N.S., Meshkova, S.B., and Nikinova, M.P.
1969: Determination of sodium and potassium in aluminosilicates difficult to decompose; *Zav. Lab.*, v. 35, p. 166-169.

Project 640048

Ann P. Sabina

Central Laboratories and Administrative Services Division

A few years ago, two new minerals — welonganite and dresserite — were described from the Francon quarry, Montreal Island, as a result of a mineralogical investigation that began in 1966. The investigation was resumed in 1974, resulting in the identification of a number of minerals not previously reported. During the summers of 1974 and 1975, eight visits were made to the quarry and representative suites of minerals were collected. This progress report is based on the examination of these minerals as well as mineral specimens from the National Mineral Collection, and specimens collected by amateur mineral collectors.

The quarry, (Fig. 5.1) operated by Francon, Division of Canfarge Limited was originally worked by Arthur Dupré from 1924 to 1928, and subsequently by National Quarries Limited (1930-1962), Highway Paving

Company (1963-1965), and by the current operator since 1966. It produces crushed limestone for use in the manufacture of cement and for road metal.

The limestone exposed in the quarry is the St. Michel member of the Montreal Formation of Trenton (Ordovician) age. It is intruded by alkalic sills which have been encountered in quarry operations since about 1955 and are believed to be satellitic rocks related to the Monteregian intrusions. About 40 minerals have been identified from the sills, most of them occurring in vugs in the rock. The mineral-bearing sills are exposed in the upper and lower levels of the quarry, both of which are currently in operation. A list of these minerals with brief descriptions is given below; unless otherwise noted, the minerals are found in the vugs.



Figure 5.1. Mineral-bearing alkalic sills cutting Ordovician limestone, Upper level of Francon Quarry. (GSC-163133).

Analcime:

colourless to yellow and orange-red trapezohedral crystals averaging 5 mm in diameter; white globular aggregates, spheres, cubes (measuring 1 mm along the edge); white granular aggregates lining cavities. Analcime is a relatively common mineral, particularly in the lower level of the quarry.

Anatase:

dark ink-blue, opaque, finely granular aggregates associated with pyrite grains in pockets in sill rock.

Baddeleyite:

tan-coloured scaly to granular aggregates associated with crystals of calcite, fluorite, barite and strontianite; straw-yellow scaly aggregates forming fragile sheets on calcite crystals associated with purple fluorite and botryoidal hematite. This mineral is rare and was found only in the lower level. It is the second known occurrence of baddeleyite in Canada.

Barite:

white, grey, yellowish granular to powdery masses; chalk-white stacked plates; colourless, white, grey or reddish orange prisms, some with dome terminations. Tabular prisms measuring 2 to 3 cm were found in the lower level but are rare. Barite is relatively uncommon in the lower level and rare in the upper level.

Calcite:

colourless, white, yellowish, lilac, grey crystals or massive; colourless to light yellow cone-shaped crystal aggregates and globular forms. Calcite is one of the most common minerals lining vugs throughout the quarry.

Celestite:

colourless, white, grey tabular and divergent acicular crystal aggregates; pulverulent. Colourless transparent tabular prisms measuring up to 8 mm long were found in association with calcite and fluorite in the lower level. Celestite is relatively uncommon in the lower level and rare in the upper.

Chalcedony:

white to greyish white, associated with calcite, quartz and other minerals. Rare.

Clinopyroxene:

green acicular aggregates in analcime associated with unknown No. 9. Rare and noted only in the lower level.

Cryolite:

colourless, yellow crystals, massive; sugary masses in which crystals are embedded. Although cryolite is rare, transparent crystals were encountered in relative abundance in one area of the sill that was quarried in the lower level during a three-week period in 1975. At other known occurrences, cryolite in the crystal form is rare; at the Francon Quarry, however, the crystal form is more common than the massive. The individual crystals average 1 mm in diameter, are transparent yellow or grade from colourless to yellow, and commonly form aggregates (some with triangular outline) measuring up to 1½ cm in diameter. They occur in cavities with crystals of colourless calcite, colourless to slightly yellowish weloganite and dawsonite. This is the only known Canadian occurrence of cryolite.

Dawsonite:

Colourless transparent squat to elongated striated prisms measuring up to 2 mm long; acicular crystals forming rosettes, spheres, tufts, or in random array; white matted and radiating fibres; flaky, scaly, hair-like and botryoidal aggregates. Dawsonite is one of the most common minerals along with calcite and quartz. Spectacular specimens consisting of masses of radiating and randomly oriented acicular dawsonite were exposed in the upper level during a two-month period of operations in 1975; small cubes of lilac to purple fluorite and orange sphalerite occurred on the dawsonite crystals.

Dolomite-ankerite series:

colourless, white to yellowish and amber crystal and granular aggregates lining vugs; white rosettes.

Dresserite:

colourless to white spheres composed of radiating fibres or blade-like crystals tapering toward the centre of the sphere and with blunt terminations. The spheres measure up to 4 mm in diameter and are generally associated with weloganite. Found only in the upper level. Only known occurrence (Fig. 5.2).

Elpidite:

Colourless to white acicular to fibrous aggregates in parallel, divergent, radial or random arrangement. The crystals commonly measure 1 mm long. Elpidite was noted only in association with yellow cryolite and is rare, having been identified in about one-third of the cryolite specimens examined. This is the second known occurrence of elpidite in Canada.

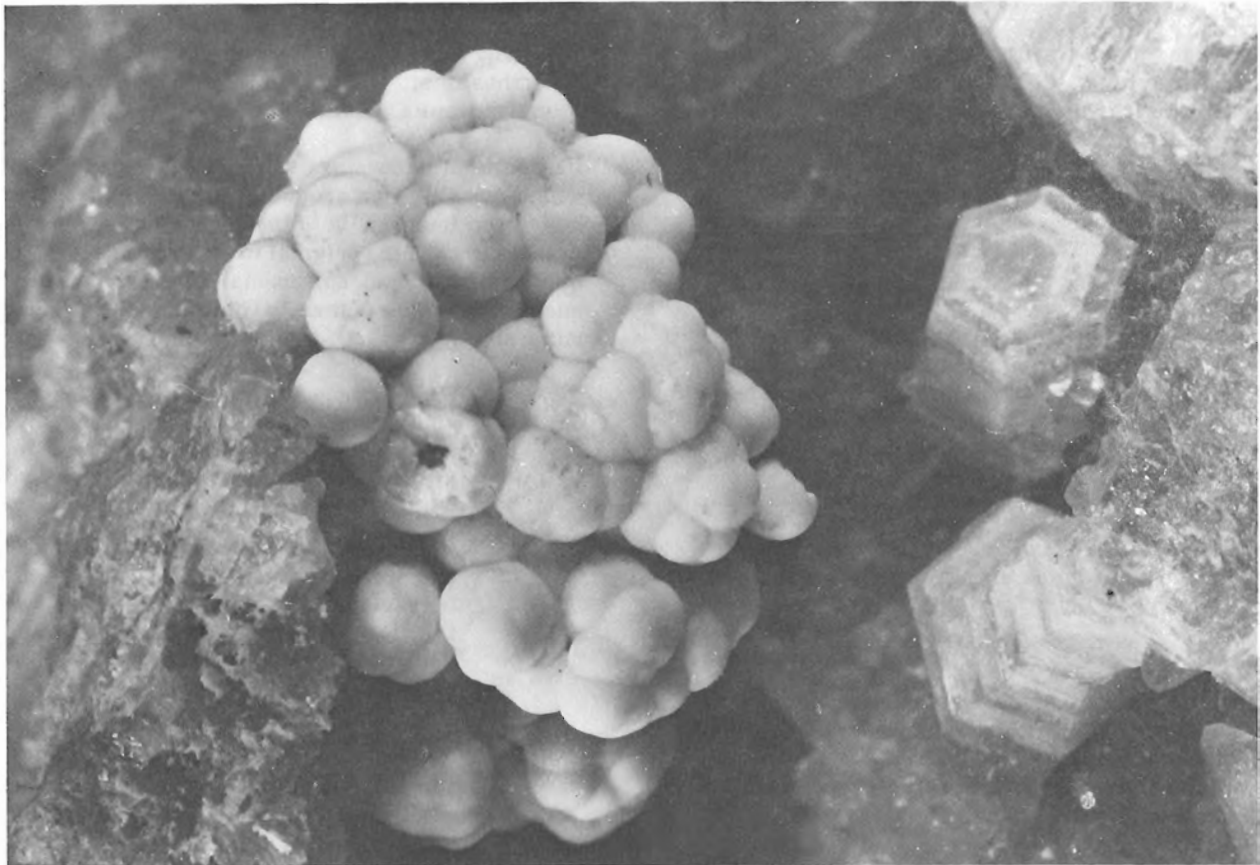


Figure 5. 2. Cluster of dresserite spheres with weloganite crystals (in cross-section) in quartz-lined vug. The individual dresserite spheres average 1 mm in diameter. (GSC 202820-H).

Fluorite:

clourless, white, lilac to deep purple cubes (less than 2 mm along the edge) and crystal aggregates; white platy, spherical, botryoidal and shell-like forms; granular massive. Also found as finely granular black patches in the sill rock. Uncommon in the upper level; common in the lower level as finely crystalline lilac to deep purple crystal aggregates coating dawsonite to form masses of flattened spheres.

Galena:

crystals (microscopic) and granular masses in vugs; granular masses in sill rock. Rare.

Graphite:

black patches in sill rock.

Gypsum:

Selenite variety, large sheets about 5 cm thick and tabular prisms (1-5 mm long) associated with yellow, pink and white massive dolomite. Rare.

Harmotome:

grey finely granular lining of cavity. Was noted in only one specimen obtained from the upper level.

Hematite:

dark brown finely botryoidal and powdery encrustations on crystals such as celestite, calcite and quartz occupying cavities in sills in the lower level. It is not common.

Marcasite:

various forms; commonly tarnished to blue, violet, green metallic.

Molybdenite:

a crystal was noted in a cavity with other minerals in one specimen found in the upper level.

Mordenite:

white matted very fine fibres forming thin sheets on crystals lining vugs. It is of rare occurrence and was observed in association with dolomite crystals and unknown No. 9 specimens from the lower level only.

Plagioclase:

white translucent upright plates forming a lattice-like lining in cavities. Common, particularly in the upper level where it is associated with welonganite, dresserite, quartz and some of the unknown minerals.

Pyrite:

common in various forms generally coating crystals.

Quartz:

colourless, transparent, frosty white and smoky crystals; colourless stacked plates curved slightly to produce somewhat artichoke-like and sheaf-like forms commonly lining vugs. Ranks with calcite as the most common mineral lining vugs in both levels.

Siderite:

light yellow, yellowish green and brown finely crystalline aggregates lining vugs; often intergrown with dolomite.

Sphalerite:

orange crystalline aggregates and microscopic crystals associated with acicular masses of dawsonite and less commonly with analcime; microscopic greenish brown crystals; orange-brown granular patches in sill rock. Rare.

Strontianite:

colourless to white spear-shaped acicular crystals commonly forming spheres resembling dresserite but distinguished from dresserite by its acutely pointed terminations; colourless white, light yellow, greenish yellow fibrous to columnar aggregates forming tufts, sheaves, hemi-spheres; colourless, yellow, amber, pink tabular crystal aggregates; white finely granular porcelain-like and compact fibrous masses in mammillary groups; white waxy globules. Strontianite is a very common mineral, particularly in the lower level.

Thenardite:

white powdery coating on the sill rock. It was noted in one area in the upper level where analcime is abundant.

Welonganite:

colourless, light yellow to orange-yellow, amber, white, transparent to translucent six-sided prisms (measuring up to 6 cm long) with pediton or pyramidal terminations and transverse grooves and striations; white stacked plates; white powdery to finely granular forming core of crystals or coating on crystals; colourless, yellow, olive green (rare) vitreous massive. Occurs in upper and lower levels but more abundant and larger-sized crystals in upper level. Only known occurrence.

Zircon:

yellow, amber, tan-coloured grains and granular patches in sill rock; yellow vitreous granular crust on welonganite. Rare.

Unidentified minerals: seven unknown minerals, of which possibly five are believed to be new species, have been found. Six of them were first encountered in the course of the original investigation of the Francon quarry; additional specimens collected recently enabled the study of them to continue. The unidentified minerals include:

- No. 2: White spheres identical to dresserite with similar composition but is a higher hydrate and has different crystal structure. Unstable, decomposes at room temperature. Associated with welonganite in the upper level.
- No. 3: Chalk-white powdery coatings; white translucent porcelain-like smooth and botryoidal crusts; white shells with hollow interior. Of common occurrence in upper and lower levels. Believed to be an aluminum hydroxide with X-ray diffraction pattern similar to gibbsite.
- No. 5: Cream-white compact aggregates of fine fibres or flakes with silky lustre. Qualitative electron microprobe analysis indicates the major elements to be Zr, Ti and Na. The mineral is associated with dresserite in the upper level. Uncommon.
- No. 6: White silky, flaky aggregates associated with quartz and strontianite in the upper level. Major elements as determined by qualitative microprobe analysis are Al and Sr. Uncommon.
- No. 7: White granular, botryoidal, flaky aggregates with silky or waxy lustre. Believed to be a clay mineral of the kaolinite group.
- No. 8: White soft waxy finely granular massive. Believed to be a clay mineral of the montmorillonite group. No. 7 and No. 8 are common in the lower level, quite rare in the upper level.
- No. 9: White acicular crystals forming parallel and divergent aggregates measuring 1 to 2 mm long. Its distinctive silky lustre distinguishes it from other Francon minerals of similar habit, notably celestite and strontianite. It is associated with hemispherical aggregates of light yellow calcite, yellowish white crystalline dolomite and colourless to light brown analcime. Major elements as determined by qualitative electron microprobe analysis, are Na, Al, K, Si. X-ray diffraction pattern is similar to that of dachiardite. Believed to be a zeolite. Found in lower level. Very rare.

A noteworthy feature of the sills is the consistent uniformity of the mineral assemblages characterizing each level of the quarry. In the upper level, the most common minerals formed in vugs are quartz, calcite, dawsonite and strontianite generally with weloganite and, less commonly, dresserite. Quartz, calcite and dawsonite are also common in the lower level sills but with consistently greater amounts of strontianite, fluorite and analcime. Where the mineralization has shown any variation, as in the case of the cryolite-calcite-dawsonite-weloganite or the dawsonite-fluorite-sphalerite assemblages, these concentrations were found to be in relatively small areas of particular sills which were exposed during operations of one to two month duration. Similarly localized are other minerals including dresserite and three of the unidentified minerals which have so far been found only in the upper level sills; others — mordenite, baddeleyite, elpidite and Unknown No. 9 — have been encountered only in the sills of the lower level. There are also areas in the sills of each level where vugs contain only crystals of quartz or calcite.

References

- Clark, T. H.
 1952: Montreal area, Laval and Lachine map, areas, Que. Dep. Mines, Geol. Rep. 46.
- Clark, T. H. (cont.)
 1972: Montreal area, Quebec Dep. Nat. Res., Geol. Rep. 152.
- Jambor, J. L., Fong, D. G., and Sabina, Ann P.
 1969: Dresserite, the new barium analogue of dundasite; Can. Mineral, v. 10, pt. 1, p. 84-89.
- Quebec
 1925: Report on mining operations in the Province of Quebec during the year 1924; Que. Dep. Colonization, Mines, Fisheries.
 1931: Report of the Minister of Mines of the Province of Quebec for the fiscal year 1930-31, Pt. A, Que. Bur. Mines.
 1967: The Mining Industry in Quebec in 1963 and 1964; Que. Dep. Nat. Res.
- Sabina, Ann P.
 1968: Rocks and Minerals for the Collector: Kingston, Ontario to Lac St. Jean, Quebec; Geol. Surv. Can., Paper 67-51.
- Sabina, Ann. P., Jambor, J. L., and Plant, A. G.
 1968: Weloganite, a new strontium, zirconium carbonate from Montreal Island, Canada; Can. Mineral, v. 9, pt. 4, p. 468-477.

E. M. R. Research Agreement 1135-D-13-4-157/75

J. K. Glover¹ and R. A. Price¹
Regional and Economic Geology Division

Rocks of the Windermere Supergroup form a thick section on the west flank of the Purcell Anticlinorium between Creston and Salmo, British Columbia (Rice, 1941; Little, 1960). Detailed field investigations of these rocks within an area of about 100 square miles (Fig. 6.1) during the 1974 and 1975 field seasons were focused upon their internal stratigraphy, geologic structure, metamorphism and regional tectonic significance. The preliminary results of geological mapping at a scale of 1:25 000 are summarized in a geologic sketch map (Fig. 6.2).

The Windermere Supergroup in this area has an aggregate thickness of at least 7.5 km comprising the Toby Formation, at the base, the Irene Volcanic Formation, the Monk Formation and the Three Sisters Formation. It lies with angular unconformity on the underlying Purcell Supergroup and is transitional into the Quartzite Range Formation of the Lower Cambrian or Late Proterozoic Hamill Group.

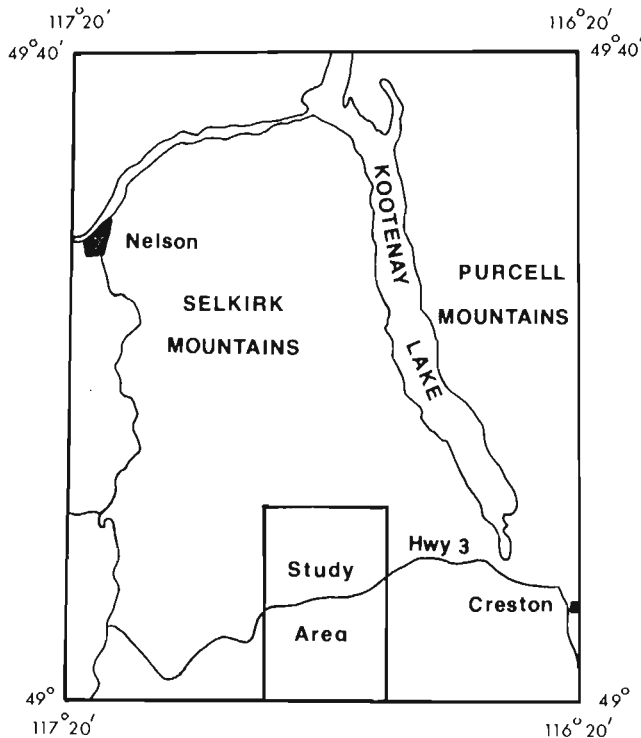


Figure 6.1. Location map.

Stratigraphy

The Toby Formation, which attains a maximum thickness of 2.5 km, consists of polymict conglomerate and conglomeratic sandstone and mudstone, and unconformably overlies both the Dutch Creek and Mount Nelson formations of the Purcell Supergroup. The majority of the boulders, cobbles and pebbles in the conglomerate consist of quartzite and dolomite so similar to that in the Dutch Creek and Mount Nelson Formations as to leave little doubt that most of the Toby Formation represents debris that was eroded from the underlying Purcell Supergroup. The conglomerates and conglomeratic mudstones occur in distinct beds and are intercalated with sandstone, but conspicuous lateral variations occur within the formation and no persistent marker units have been recognized. Although Aalto (1971) has argued that the Toby conglomerate is a glacial marine deposit, the coarse to medium grained clastics of the Toby Formation show widespread development of medium-scale cross-bedding and channel-fill structures that are suggestive of deposition in a fluvial environment. Moreover, slump structures associated with some of the conglomeratic mudstone units indicate that they are mass flow deposits. Basic tuff and agglomerate occur as minor intercalations throughout the sequence and provide evidence of intermittent volcanism while the Toby Formation was being deposited. Numerous basic sills and dykes, which occur in the Toby Formation and the upper part of the Purcell Supergroup, are thought to represent feeders for these pyroclastic deposits and for the overlying volcanic rocks of the Irene Volcanic Formation.

The Irene Volcanic Formation attains a maximum thickness of 2 km and consists of basic pillow lava with intercalations of basic agglomerate and tuff. Beds of finely laminated stromatolitic dolomite, which are a minor component of the formation, indicate that it is a shallow-water deposit. In the southern part of the area, where the formation is thickest, coarse grained basic intrusives occur with extensive hydrothermal alteration of the underlying conglomerate suggesting that a local eruptive centre was located nearby. Clasts of dolomite that occur within the pyroclastic rocks of the upper part of the Irene Volcanic Formation mark the resumption of deposition of conglomerate and a transition to the base of the Monk Formation.

The Monk Formation attains a maximum thickness of 1.5 km and consists of a conglomeratic unit at the base with poorly sorted angular clasts of dolomite in a mudstone matrix, except in the north part of the area where an abrupt facies change to well sorted quartz cobble conglomerate occurs south of the Mine Stock.

¹Department of Geological Sciences; Queen's University, Kingston, Ontario.

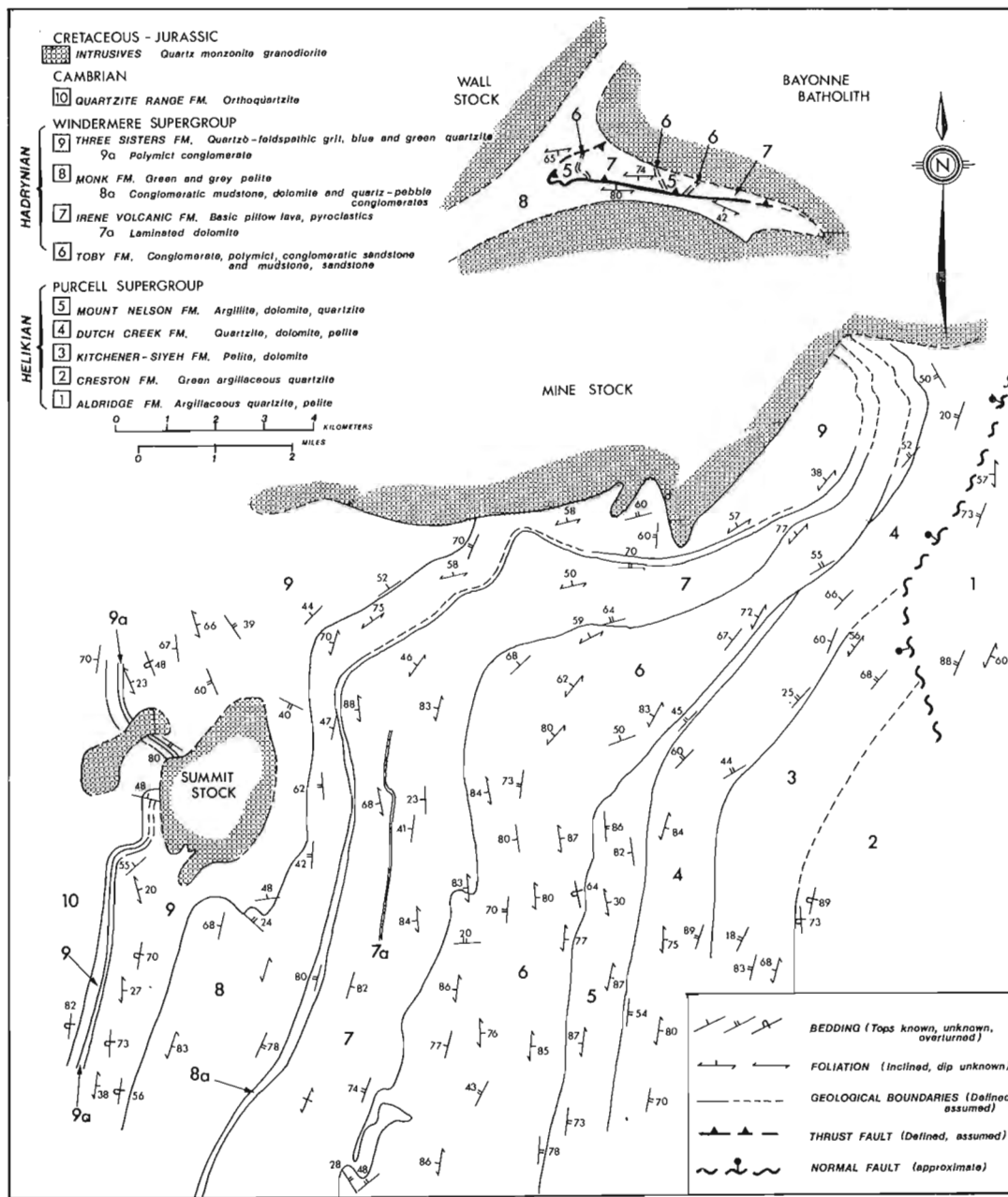


Figure 6.2. Geological map.

Locally the conglomerates of the Monk Formation are overlain by a thin stromatolitic dolomite unit which is succeeded by laminated green and grey pelite.

The Three Sisters Formation is at least 1.5 km thick and consists of quartzo-feldspathic grits interbedded with green and blue-grey medium-scale cross-bedded quartzite, quartz-pebble conglomerates, pink quartzite and interbedded grit, and rare argillite. A distinctive conglomerate unit at the top contains clasts of grit, quartzite, shale, vein quartz and greenstone, and contains channel-fill structures and evidence of thin sedimentary faulting. Above this there is a gradation from green and blue-grey quartzite to light grey quartzite over an interval in which the

relative proportion of interbedded grit decreases. The contact with the overlying Quartzite Range Formation is placed above the highest bed of grit. This coincides with the appearance of white orthoquartzites with abundant ripple marks and shallow planar cross-bedding. There is no evidence of an erosional hiatus between the Windermere Supergroup and the overlying Quartzite Range Formation. However, nearby in the western Purcell Mountains, Lower Cambrian white quartzites (which are lateral equivalents of the Quartzite Range Formation) lie with angular unconformity on rocks comprising the middle part of the Purcell Supergroup (Rice, 1941).

The character and thickness of the Windermere Supergroup in this area and its stratigraphic relationships with the underlying Eo-Cambrian or Cambrian beds of the Quartzite Range Formation support the conclusion (Lis *et al.*, 1975; Price and Lis, 1975) that the Windermere Supergroup is a syntectonic deposit which accumulated, probably during the East Kootenay Orogeny (White, 1959; Leech, 1962), along the northwesterly and westerly flanks of an uplifted fault block of Purcell strata from which much of the coarse clastic detritus was eroded. The basic volcanic rocks which are intercalated with the sediments of the Windermere Supergroup are probably related to deep crustal fracturing associated with this faulting.

Geologic Structure

All the rocks in the study area are metamorphic tectonites in the lower greenschist facies of regional metamorphism. They contain a well developed, pervasively penetrative foliation, and locally a less well developed, crenulation cleavage. Deformed clasts in the conglomerate and pillows in the Irene Volcanic Formation show that the penetrative strain, although quite variable from place to place, involved apparent flattening in the plane of the foliation, and a maximum elongation parallel with the axes of the earliest, small scale, northerly plunging z-shaped folds (Fig. 6.2).

The overall structure of the area, as outlined by the main stratigraphic units, is a steep westerly facing homocline upon which is superimposed a shallow to moderate, northerly plunging large z-shaped fold (Fig. 6.3). This structure is most obvious in the southern part of the area where the stratigraphic succession and primary sedimentary structures show that the Three Sisters Formation and the lower part of the Toby Formation are overturned toward the west, but the intervening section is upright and westerly dipping. Penetrative foliation changes congruently with the dip of the bedding and it is obvious that the structure developed after the foliation had become defined. In the middle part of the area the structure is modified by a steep northwesterly plunging anticline (Fig. 6.3) which is outlined by an easterly swing in the strike of both bedding and foliation.

The structural evolution of the area can be accounted for by a model in which small northerly plunging z folds and associated penetrative foliation developed in conjunction with the Purcell Anticlinorium in its steeply dipping west flank. This stage is responsible for the bulk of the finite strain and the apparent flattening field recorded by deformed conglomerates and volcanics within the succession. As deformation proceeded larger coaxial folds formed, and were accompanied by external rotation of the entire rock mass, which led to the development of a superimposed crenulation cleavage.

The Mine and Summit stocks occur within short limbs of large-scale z folds, which suggests a structural control of their emplacement. However, both plutons have narrow structural aureoles within which small, commonly isoclinal flow folds are present. In the northeast part of the area westerly directed thrusting

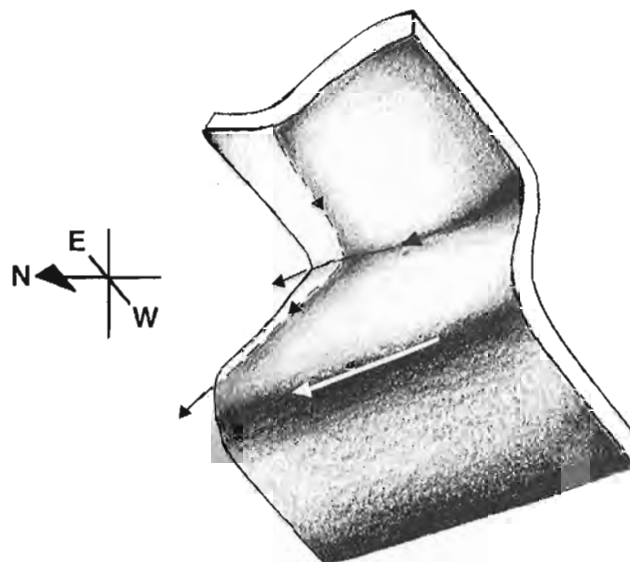


Figure 6.3. Schematic diagram of the generalized fold morphology.

of Lower Windermere and Upper Purcell over the Monk Formation is thought to be due to the emplacement of the Bayonne Batholith.

References

- Aalto, K.R.
1971: Glacial marine sedimentation and stratigraphy of the Toby Conglomerate (Upper Proterozoic) southeastern British Columbia, northwestern Idaho and northeastern Washington; *Can. J. Earth Sci.*, v. 8, no. 7, p. 753-787.
- Leech, G.B.
1962: Metamorphism and granitic intrusions of Precambrian age in southeastern British Columbia; *Geol. Surv. Can.*, Paper 62-13.
- Lis, M.G., Price, R.A., and Glover, J.K.
1975: Late Precambrian (Hadrynian) block faulting across the western margin of the North American Craton in southeastern British Columbia; *Geol. Soc. Am., Abstr.*, v. 7, no. 6, p. 809-810.
- Little, H.A.
1960: Nelson map-area, west-half, British Columbia; *Geol. Surv. Can.*, Mem. 308.
- Price, R.A. and Lis, M.G.
1975: Recurrent Displacements on Basement-Controlled Faults Across the Cordilleran Miogeocline in Southern Canada; *Geol. Soc. Am., Abstr.*, v. 7, no. 7, p. 1234.
- Rice, H.M.A.
1941: Nelson map-area, east-half, British Columbia; *Geol. Surv. Can.*, Mem. 228.
- White, W.H.
1959: Cordilleran tectonics in British Columbia; *Am. Assoc. Pet. Geol. Bull.*, v. 43, no. 1, p. 60-100.

Project 740012

George Patton

Atlantic Geoscience Centre, Dartmouth

Two estuaries entering the Minas Basin of the Bay of Fundy have been under investigation for two summers. The rivers, and Avon and the Kennetcook, enter the Minas Basin near Windsor, Nova Scotia (Fig. 7.1). Prior to 1970 the estuary of the Avon was tidal, but since then it has become a brackish-water lake owing to the construction of a causeway from Windsor to Falmouth. The Kennetcook River, on the other hand, is a relatively undisturbed estuary and appears to be in a more-or-less natural state in its lower reaches.

When the causeway was constructed at Windsor in 1970 it prevented the waters of the rising tide from flowing up the estuary: the volume of this flow is estimated at $1.5 \times 10^6 \text{ m}^3$ for each half of the tidal cycle. The most outstanding feature developed as a result of the changed hydraulic regime is the extensive tidal mudflat to the north of the causeway. This was unexpected, but by the summer of 1974 approximately $3.5 \times 10^6 \text{ m}^3$ of mud has been deposited. This spectacular buildup of sediment prompted this study

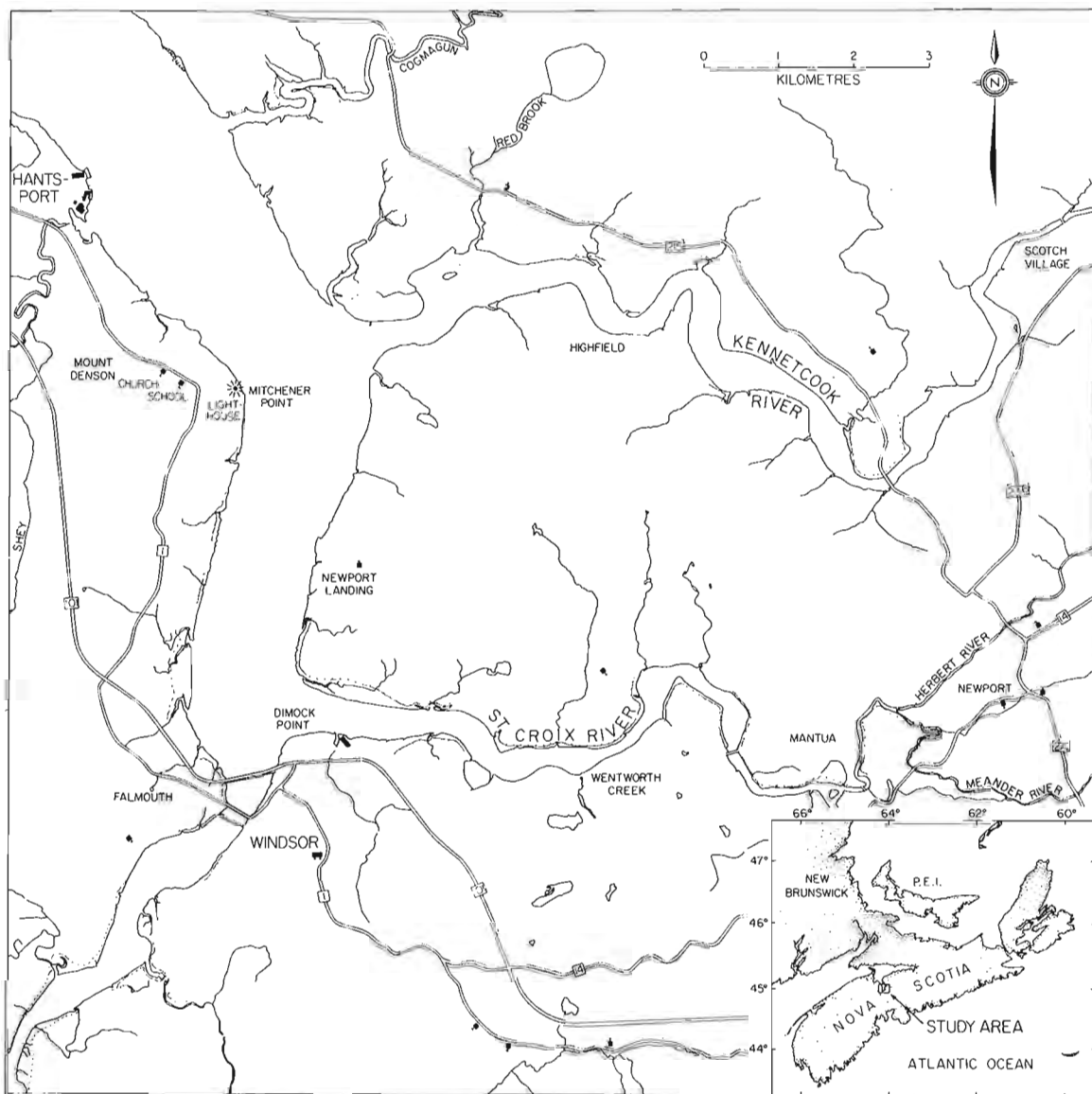


Figure 7.1. Location of study map.

which was undertaken to determine what relationships exist in estuaries of the Minas Basin between tidal currents and sediment type, and between tidal currents and primary bedforms, or, more specifically:

- (i) To determine which sedimentary structures and features are particularly associated with unmodified estuaries in the Minas Basin.
- (ii) To relate these features to tides and currents and associated parameters such as suspended loads, salinity, etc.
- (iii) To determine which combinations of bedforms and tidal currents constitute a dynamic equilibrium condition for unmodified estuaries in an environment where a large tidal range exists.
- (iv) To evaluate the effects of man-made barrages of coastal and estuarine hydrodynamics and geodynamics.
- (v) To interpret modifications in sedimentary structures as a result of an altered tidal flow.
- (vi) To determine, if possible, the factors which govern the amount of time required for the estuarine system to reach equilibrium after the construction of a barrage.

As Figure 7.1 shows, the causeway across the Avon River lies near the point where the St. Croix River discharges into the Minas Basin. Figure 7.2a shows the position of the intertidal sediment bodies in 1966 prior to the construction of the causeway. There is a small area which appears, from the aerial photographs, to be an incipient mudflat. The probable cause was the fish weir which at that time stood a few hundred metres upstream and effectively diverted the strongest currents away from the centre of the river. Figure 7.2b shows the situation in 1973, three years after the construction of the causeway. It can clearly be seen that the area to the north of the causeway, predominantly sand in

1966, had become covered by a thick tidal mudflat which, by 1974, had become populated by a fairly prolific bivalve fauna. By 1975 (Fig. 7.2c), the mud had extended farther to the north and the sand bar upon which the mud was encroaching was itself achieving a higher elevation. By 1975 the low tide discharge from the St. Croix River was entirely confined to the permanent channel which lies between the causeway and the tidal flat. The immediate conclusion is that there is a continuing deposition of both sand and mud in the area to the north of the Windsor causeway, but it should be borne in mind that the summer of 1975 was uncharacteristically dry and, during wet year, the discharge from the St. Croix River may be powerful enough to once more cut through the sand and mud so that the low-tide channel resumes the course which existed in 1973 and 1974. Alternatively, the channel between the causeway and the mudflat itself may fill in. In this case, the low tide discharge would either cut across the sand bars, as in 1973, or it would hug the shore near Newport Landing.

It is, perhaps, surprising that a deep channel should exist between the causeway and the tidal flat, but owing to poor techniques applied to the construction of the causeway, a large quantity of water leaks from the lake behind it. This flow, combined with the discharge from the St. Croix River helps to keep the channel open. The small tidal bore which passes through this channel on the flooding tide probably also helps to keep the channel open.

In 1974 the edges of the tidal mudflat at Windsor were observed to have slopes which were quite steep on nearly every side. Although the slopes were less pronounced to the north, the interpretation was that considerable erosion was taking place around the edges of the mudflat. By 1975, however, the edges of the tidal flat had extremely variable slopes. To the south,

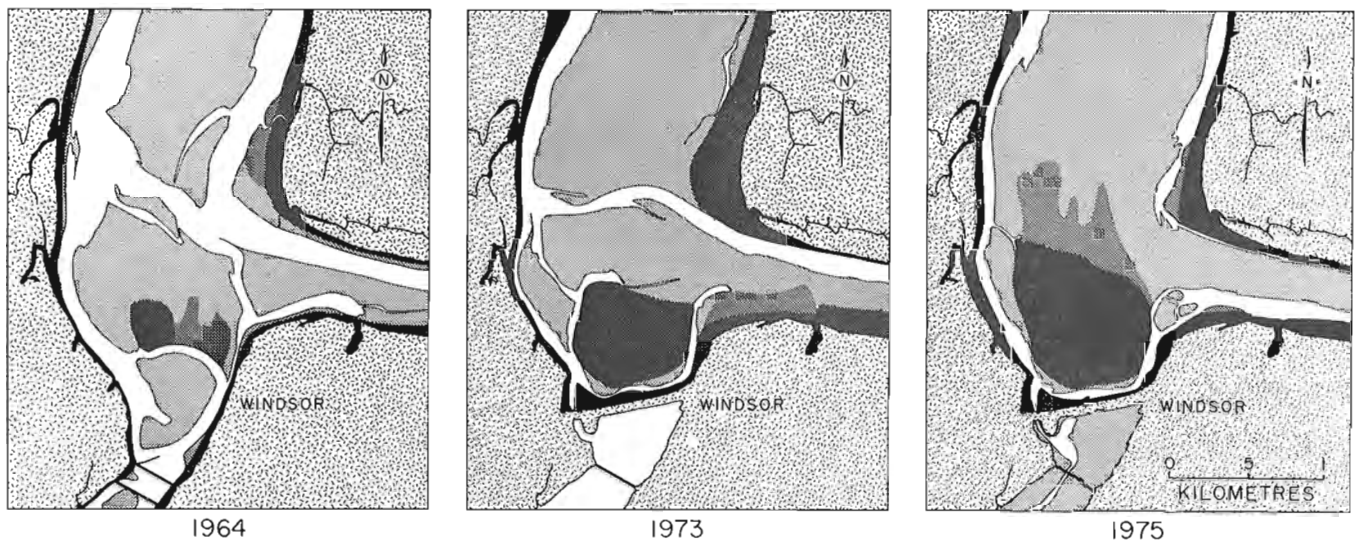


Figure 7.2a

Figure 7.2b

Figure 7.2c

Figure 7.2. Schematic representation of sediment accretion adjacent to the Windsor causeway. Data compiled from aerial photographs taken in 1964, 1973 and 1975.

near the causeway, the edges were still steeply sloping and, on one occasion, the southeast corner of the mud-flat was observed to retreat about three metres in the space of two weeks. In the north, however, the mud had extended nearly one kilometer and the edge of the tidal flat sloped very gently down to the level of the adjacent sand bar.

Like the Avon River prior to 1970, the Kennetcook is characterized by sand and gravel bars in its bed. The banks border salt marshes or cut through exposures of Pleistocene till and Tertiary bedrock outcrops. In some places the latter form cliffs, sometimes as high as 12 m or more. The Kennetcook is tidal for some 16 km, but only the lower reaches of the estuary were studied and work took place only downstream of the first significant man-made structure on the river; the bridge at Upper Burlington.

Downstream from the bridge there are three major sand bars which are exposed at low tide. Between them, in the semipermanent low tide channel, the river flows over a bed of gravel, cobbles, or boulders. Although they are not delineated on the map (Fig. 7.1), these bars are extensive. They show, at low tide, a number of large scale bedding features, some of which appear to be characteristic of an area of great tidal range, such as this is. The most prominent large scale features are the current ripples which vary in size and type according to the local tidal-current environment. In some places these megaripples are nearly symmetrical in outline and have low wave amplitudes (20 cm) and moderate wavelengths (6 - 10 m). These occur in particular on highly elevated parts of the bar which lies to the south and east of the island at the mouth of the Kennetcook estuary. They are located on a part of the bar which is protected from the full force of the incoming tide by the island itself. Large-scale eddies are features of the area during the tidal flood and, during the subsequent ebb, the area is quickly exposed so that the megaripples formed by the ebb-tide currents do not appear to undergo the same degree of development as those commonly found elsewhere.

In many places the bedforms generated by the ebbing tide show to traces of the "reactivation surfaces" described by Klein in 1970. Apparently the currents are strong enough to obliterate all traces of bedforms generated by the previous flood tide, at least to the depth that it is possible to dig during the low tide period. In other locations it is possible to see the reactivation surfaces where the bedforms generated by the flood tide have been modified by the subsequent ebb-tide currents to form downstream-facing megaripples which contain cross-beds set in an upstream direction. In a few places, however, where the ebb currents are less strong, the large scale bedforms retain the orientation which they derive from the flood tide, but often they show some modification by the ebb-tide currents.

Another type of large-scale feature are the 'terraces' which predominate in certain areas of strong ebb-tide currents. These are large, nearly flat sand "waves" arranged in a sort of step-wise fashion on bars where there is a considerable drop in elevation from the top to the downstream end. Of particular interest is the

fact that these terraces appear to be plane-bedded rather than cross-bedded as is true of all of the other large-scale bedforms investigated.

What happens to these bedforms as the tide rises has been investigated by means of echo-sounding and by side-scan sonar. It has been shown that in many cases the bedforms generated by the ebb-tide currents are completely destroyed and are subsequently replaced by upstream-facing waves. Other areas are merely planed flat, whilst a few maintain the orientation generated by the ebb tide, although it must be assumed that the latter megaripples are modified superficially at least.

Other large-scale features are often found associated with the leeside of large-scale ripples. They take the form of oval-shaped scours and are generally associated with their own ripplefans and are separated by spurs attached to the large scale ripples. The scours vary in size and may be over 2 m in diameter and up to 60 cm in depth. They appear to be associated with currents which trend across existing sand bars.

Apart from the large scale ripple bedforms, which are generally themselves covered with smaller scale features associated in particular with the last stages of runoff, there exist in several places plateaux which at low tide are almost featureless. The two basic types appear to be of an erosional or depositional character. The depositional plateaux consist of fine to medium sand and appear to be formed in areas where eddying current interrupt the full force of the ebbing tide. Trenches dug in these flat areas show that they are not conspicuously cross-bedded.

The erosional plateaux appear to be areas of semi-consolidated sand and silt which are gradually being worn down. Often they contain considerable organic matter. They are covered in the centre by a layer of sand, but at the edges this becomes thinner and, since often have abrupt edges averaging about 20 cm in height, it is possible to see that the layers of sand and silt are being worn away laterally by the tidal currents. Of particular interest are secondary phenomena which are developed as a result. In some places the flattish chunks of broken-off plateau material (up to approximately 5 cm in diameter and rarely more than 2 cm thick) accumulate in the troughs of adjacent ripples and megaripples. They can subsequently be incorporated in the megaripple structure where they follow closely the general bedding pattern, or they can be rolled and tumbled over the river bed until they are formed into balls of mud, sand and gravel which may be up to 12 cm in diameter. The shapes of the mudballs vary from nearly spherical, to shapes which resemble two cones attached by their bases.

Measurement of Currents

During the summer of 1975 the velocities of tidal currents in the Avon and Kennetcook rivers were measured at 20 locations. Table 7.1 shows the maximum velocities obtained by tidal currents in mm/s. during the flood and ebb for 9 of the 20 stations. At five of the stations listed, a comparison is made of the currents

Table 7.1
Maximum current velocity (mm/s.)

Station	Spring Flood	Tides Ebb	Diff.	Neap Flood	Tides Ebb	Diff.	Differences (Spring - Neap)
C	887	461	426	351	342	9	576 119
E	1763	1137	626	799	567	232	964 570
K	1240	1567	327	737	770	33	503 797
L	2441	1467	972	1137	954	183	1304 515
J	704	970	266	603	687	84	101 283
	Spring Flood	Tides Ebb	Diff.	Other Flood	Tides Ebb	Diff.	Differences (Spring - Neap)
B	419	176	243	194	41	153	225 135
F					1286		
H				1440			
I				1594	1697	103	
M(i)				1800	1748	52	
M(ii)				1877			
N				1646	1620	26	

Current meter locations

Station	Location
B*	On tidal flat at Windsor, about 300 m north of causeway.
C*	On tidal flat at Windsor, about 600 m north of station B.
E*	On sand bar in Avon River estuary, about 800 m north of station C.
F	At mouth of Kennetcook River.
H	On sand bar near island in Kennetcook River.
I	In channel to north of island in Kennetcook River.
J*	On sand bar to southeast of island in Kennetcook River.
K*	On sand bar north-northeast of Highfield in Kennetcook River.
L*	On sand bar east of Highfield in Kennetcook River.
M	In channel east of Highfield in Kennetcook River.
N	On sand bar east of Highfield in Kennetcook River.

* indicates that recording current meters were used.

which occur during spring tides and those which occurred during the ensuing neap tide period. Such a comparison is only possible where recording current meters were used, and where the recording took place over a complete neap-spring tidal cycle. In other areas a less satisfactory record has been obtained by using partial data furnished by recording current meters and by the use of direct-reading current meters. Table 7.1 explains the locations of the current meters listed.

The direct reading current meters were suspended from a boat for up to one day. The recording current meters were mounted on aluminum davits which were embedded in the sand and mud. Generally, this means that the direct reading current meters were used in channels in which the rivers continued to flow even at low tide.

It is interesting to note that in many cases the relationship between flood and ebb tide maximum velocities is less striking than the fact that the velocity of the flood or ebb tidal currents may change drastically in response to the spring and neap tidal cycles. As a result, there is often a corresponding change in both the size and type of bedform in a certain location. Because of this, it appears that certain areas may alternate as areas of deposition and erosion, but other areas appear to have a relatively stable sedimentary budget which remains unaffected by changes in the tidal regime.

Some of the data, however, indicate a continuing trend in sediment movement. An excellent example of the latter is exhibited by the current data for station B and, to a lesser extent, by stations C and E. Station B was located on top of the tidal mudflat at Windsor, and station C was similarly placed about 600 m to the north, where the influence of currents generated as a result of the confluence of the St. Croix and Avon rivers would be felt. Station E was 800 m farther north and was located on the sand bar contiguous with the tidal flat. The data for station B show that the difference between flood and ebb tidal current velocities is greater than the ebb velocity itself. This indicates that a relatively strong surge is made by the rising tide which can be compared with a gentle period of runoff which occurs when the tide falls. Such a regime obviously promotes the buildup of the tidal flat since fine grained sediment brought in as a suspension by the flood will settle during the high tide slack and will be left behind by the gentle ebb currents. Measurements of deposition of sediment upon the mudflat using plugs made of silica cement indicate that such is the case. Stations C and E also show a strongly unbalanced tidal cycle in which the flood tide dominates the ebb, and reference to Figure 7.2 shows that the tidal flat appears to be growing in a northerly direction as a result of this imbalance.

The rest of the stations listed all lie within the Kennetcook River. Most of the discrepancies in flood and ebb tidal current velocities can be attributed to the fact that the meters were located on the edges of the sand bars and, since most of these lie fully in the centre of the river, the currents tend to be greatest near the

river banks. The meandering of the river and the inertia of the flowing water means that on a flood tide one side of a sand bar will often experience higher velocities than the other, and vice versa during the ebb. This indicates a cyclic movement of sediment, and thus nearly a dynamic equilibrium on most of the sand bars studied.

At station L in the Kennetcook River the differences in flood tide velocities during spring and neap tides is remarkable, and the bottom bedforms can be expected to reflect the change from a maximum velocity of 2441 mm/s. during the spring tides to only 1137 mm/s. during the neap period. The ebb velocities differ by some 515 mm/s. and even at the relatively low velocities involved, the amplitudes of the megaripples in the area were observed to vary from less than 50 cm to nearly 2 m.

It is interesting to note that the current velocities so far obtained in the Kennetcook River are everywhere much greater than those which exist on the Windsor

tidal flat and the area immediately to the north. Of particular importance is the fact that in the Kennetcook River the ebb velocities are often greater than the flood velocities and that, even when this is not the case, the difference between the two flows is not enough to cause a sustained deposition in any area for which data are now available. It is unlikely then, that large deposits of sediment will suddenly appear in those parts of the Kennetcook River which have been under investigation. On the other hand, it is apparent that the tidal mudflat at Windsor will continue to extend to the northwards, unless some catastrophic event should change the dynamics of the estuary as they now stand.

Reference

- Klein, G. DeV.
1970: Depositional and dispersal dynamics of inter-tidal sand bars; *J. Sed. Petrol.*, v. 40, p. 1095-1127.

Project 730084

I. A. Hardy and D. C. Umpleby
Atlantic Geoscience Centre, Dartmouth

Introduction

The southern Labrador Shelf is underlain by a wedge of Meso-Cenozoic sediments up to 20 000 feet (6150 m) thick. A lithostratigraphic analysis of these deposits, based on the study of three non-confidential wells, is presented herein. The wells are:

- (a) Tenneco *et al.* Leif E-38 (54°17'29.57"N;
55°05'52.17"W)
- (b) Eastcan *et al.* Leif M-48 (54°17'45.92"N;
55°07'20.17"W)
- (c) Eastcan *et al.* Bjarni H-81 (55°30'29.35"N;
57°42'05.52"W)

As the Leif wells are only 1.09 miles (1750 m) apart and encountered similar sections, they are treated as a single well. Bjarni H-81 is approximately 134 miles (216 km) northwest of the Leif wells (Fig. 8.1).

The lithostratigraphy of the wells is based on microscopic examination of samples (cuttings) taken at ten-foot intervals. The encountered lithologies were correlated to mechanical logs and the sequence penetrated was subdivided into correlatable informal units.

Recognised lithostratigraphic units are named according to their dominant lithologies and do not necessarily coincide with the biostratigraphic boundaries determined by Gradstein and Williams (in press), McWhae and Michel (in press), Eastcan (1973a, b) and

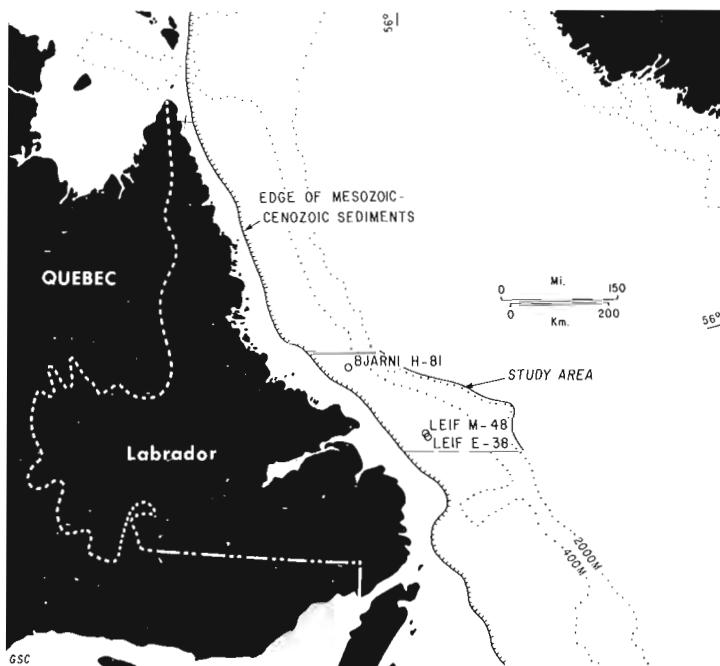


Figure 8.1. Location map for wells discussed in text.

Tenneco (1971). These units are summarised in Tables 8.1 and 8.2, and described below in descending order (see also Fig. 8.2).

A continuous Upper Cretaceous to Pleistocene sequence is present in both wells, except for Bjarni H-81 where the Pliocene appears to be absent and Pleistocene sands overlie Miocene mudrocks. In addition, the Upper Cretaceous-Pleistocene succession in Bjarni disconformably overlies a Lower Cretaceous sandstone. In each well the sediments are underlain unconformably by coeval basaltic volcanics.

Lithostratigraphic Units

10. COARSE SAND UNIT: occurs above 1420 feet (432 m) in Leif and above 1560 feet (477 m) in Bjarni. It comprises unconsolidated, arkosic sand with up to 25 per cent silt and clay fractions. The clasts consist mainly of quartz grains, mostly well-rounded, frosted and iron-stained. Minor pebbles of varied metamorphic rocks, vein quartz, feldspar and black chert also occur. In both wells, the unit has been dated as Quaternary. Abundant fossil fragments, particularly worm tubes, bryozoa and ooliths indicate rapid deposition in very shallow water.

9. FINE SAND AND SILT UNIT: approximately 50 to 75 per cent of this unit consists of sandstone; grey, very fine- to fine-grained, poorly sorted, with abundant silty and argillaceous matrix. This sand is often silicified and is interbedded with, and grades downwards into, silts and shales. Occasionally, the sand is cemented by pyrite, and has lignitic and pyritized wood fragments scattered throughout. Bryozoa, shell fragments, worm tubes and occasional fecal pellets are common and are indicative of shallow shelf deposition. This unit has been dated as Pleistocene.

8. SILT, SAND AND SHALE UNIT: occurs only in the Leif wells. This unit consists of approximately 85 per cent shale; greyish brown, silty, calcareous and carbonaceous. Pyrite and floating quartz grains of fine- to granule-size occur throughout. Minor interbeds of very fine grained, silty and poorly sorted sand are also present.

A Miocene-Pliocene age has been assigned to this unit which was probably deposited in a neritic environment. This unit is absent in Bjarni H-81, where Pleistocene sands (units 9 and 10) directly overlie beds of Miocene age (unit 7).

7. SHALE AND MUDSTONE UNIT: consists of interbedded shale and mudstone, both being variably silty, calcareous and carbonaceous. Minor interbeds of sand and limestone also occur throughout. The sand is grey, fine- to coarse-grained, poorly sorted and friable; the limestones are dark grey, silty micrites.

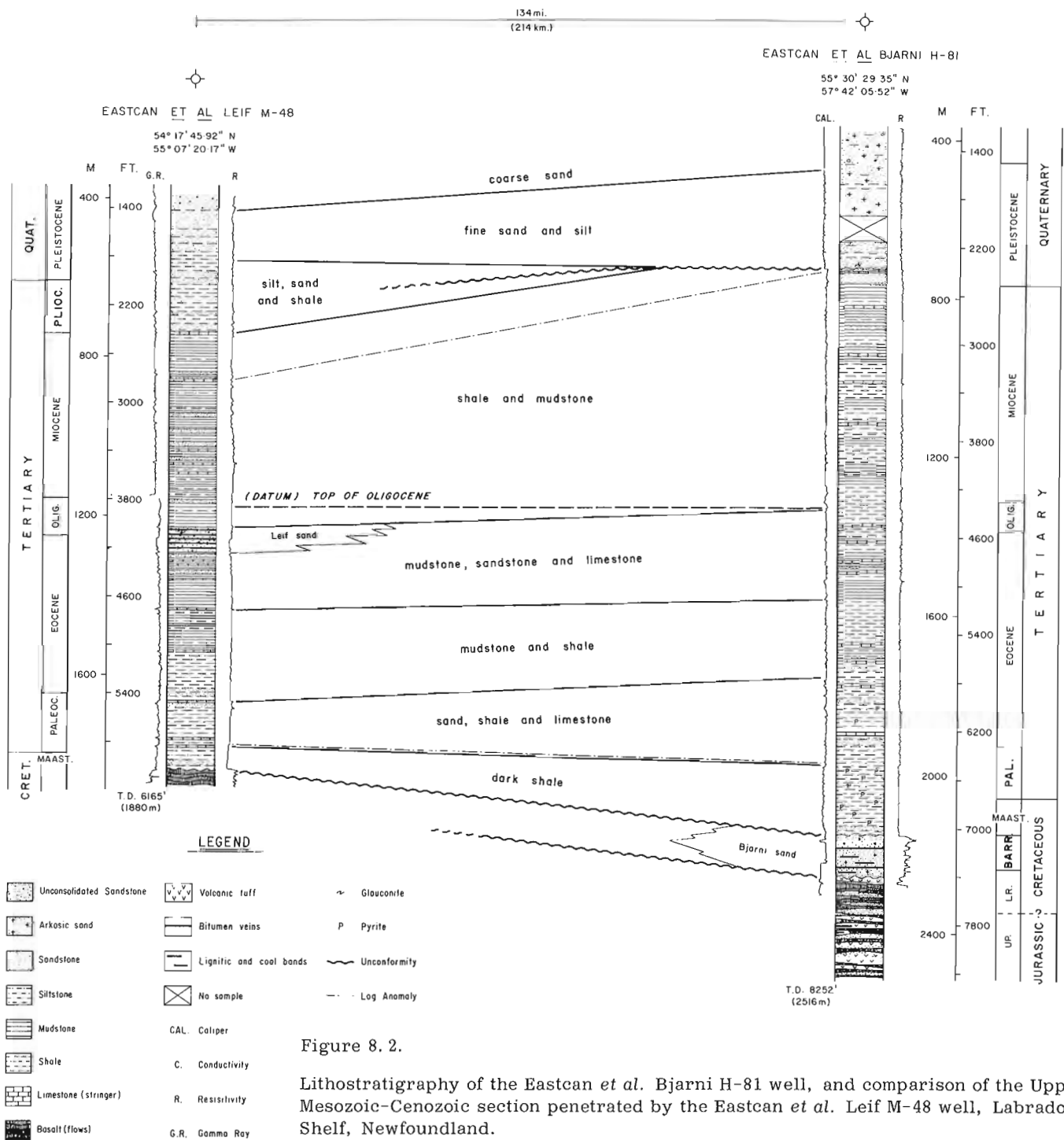


Figure 8.2. Lithostratigraphy of the Eastcan *et al.* Bjarni H-81 well, and comparison of the Upper Mesozoic-Cenozoic section penetrated by the Eastcan *et al.* Leif M-48 well, Labrador Shelf, Newfoundland.

Although these limestone beds are very thin, they may prove to be correlatable markers.

This unit is Oligocene-Miocene and was deposited in a neritic to bathyal environment (outer shelf conditions).

6. MUDSTONE, SANDSTONE AND LIMESTONE UNIT: approximately 75 per cent of this unit in Leif, and 60 per cent in Bjarni is mudstone and siltstone. Both

these rock types are greyish brown, silty, micaceous and calcareous. Minor interbeds of sand and limestone are present throughout. The sands are quartzose, greyish brown, very fine grained with abundant silt and clay matrix. The limestones are slightly dolomitic micrites, rarely over two feet thick.

Between 4120 and 4260 feet (1256.1 and 1298.8 m) in Leif M-48, a glauconitic, greyish brown, very fine

Table 8.1

The lithostratigraphy is briefly summarized for Leif M-48, with all depths measured from KB.

LITHOLOGIC SUBDIVISION	DEPTH (FOOTAGE)	THICKNESS	AGE	ENVIRONMENT
coarse sand*	?-1410'	>150' (>45.7 m)	Pleistocene	inner neritic
fine sand and silt*	1410-1825'	415' (126.5 m)	Pliocene/ Pleistocene	inner neritic
silt, sand and shale*	1825-2450'	625' (190.5 m)	Pliocene and Miocene	inner-outer neritic
shale and mudstone*	2450-4025'	1575' (480.2 m)	Miocene and Oligocene	inner-outer neritic to outer bathyal
mudstone, sandstone limestone	4025-4705'	680' (207.3 m)	Upper Eocene and Oligocene	upper bathyal
mudstone and shale	4705-5464'	759' (231.4 m)	Eocene	upper bathyal to neritic
sand, shale and limestone	5464-5838'	374' (114 m)	Paleocene	neritic
dark shale	5838-6035'	197' (60.1 m)	Upper Cretaceous	inner neritic
unconformity at 6035' (1839.9 m)				
basalt (flows)	6035-6160' (6165'T. D.)	125' (38.1 m)	Lower Cretaceous	-----

* Also present in the Leif E-38 well.

grained, friable, silty and argillaceous sandstone occurs (the Leif Sand). Logs indicate little porosity development in this sand.

An Oligocene-Eocene age has been assigned to this unit, which was deposited in a neritic to upper bathyal environment.

5. MUDSTONE AND SHALE UNIT: consists of shale, dark greyish brown to black, friable, variably silty and micaceous; and mudstone, dark grey, silty and slightly calcareous. Several thin interbeds of slightly dolomitic micrite are also found throughout this unit.

This unit has an Eocene age. Deposition occurred within a neritic environment.

4. SAND, SHALE AND LIMESTONE UNIT: is mostly shale; dark greyish brown, silty, micaceous and calcareous. In Leif, the shale grades to mudstone; dark grey, silty and slightly calcareous. In both wells, thin stringers of dolomitized micrite and fine- to medium-grained sandy beds are common.

This unit has been given a Paleocene to early Eocene age and was deposited in shallow water.

3. DARK SHALE UNIT: consists of dark brown to grey, silty and calcareous shale grading downwards to a dark grey, argillaceous and silty, fine grained sandy sequence. Minor grey-brown, silty limestone interbeds occur throughout.

Paleontology indicates a Maastrichtian to Paleocene age for this unit with deposition in a neritic environment.

In Leif, this unit unconformably overlies basaltic lavas, described in more detail below. In Bjarni, this unit disconformably overlies a thick continental sandstone (the Bjarni sand) of Barremian age.

2. BJARNI (SAND) UNIT: consists of an arkosic, fairly well sorted sand with fine- to granule-sized quartz grains and a variably silty and clay matrix. Thin lignitic and coaly bands are scattered throughout. This sand is cemented by clay minerals and appears to have up to 25 per cent residual porosity.

Palynology indicates a Barremian age for the sand. Marine fossils are absent, suggesting deposition in a paralic to continental environment.

Table 8.2

The lithostratigraphy is briefly summarized for Bjarni H-81, with all depths measured from KB.

LITHOLOGIC SUBDIVISION	DEPTH (FOOTAGE)	THICKNESS	AGE	ENVIRONMENT
Coarse sand	?-1560'	>310' (94.5 m)	Quaternary	?littoral
Fine sand and silt	1560-2380'	820' (250 m)	Quaternary- Pleistocene	?littoral
Unconformity at 2380' (725.6 m); Unit III - Silt, sand and shale absent.				
Shale and mudstone	2380-4380'	2000' (609.8 m)	Miocene- Oligocene	inner neritic to outer neritic-upper bathyal
Mudstone, sandstone and limestone	4380-5110'(?)	730' (222.6 m)	Oligocene-Late Eocene	outer neritic-upper bathyal
Mudstone and shale	5110(?)-5755'	645' (196.6 m)	Late Eocene- Early Eocene	outer neritic-upper bathyal to neritic
Sand, shale and limestone	5755-6480'	725' (221 m)	Early Eocene- Paleocene	neritic to inner neritic
Dark shale	6480-7050'	570' (173.8 m)	Paleocene- Maastrichtian	inner neritic
Unconformity at 7050' (2149.4 m)				
Bjarni sand*	7050-7400'	350' (106.7 m)	Barremian	?non-marine
Unconformity at 7400' (2256.1 m)				
Basalt flows*	7400'-T.D.	>852' (259.8 m)	undated	

*Units not present in the Eastcan *et al.* Leif M-48 well.

1. BASALTIC VOLCANIC UNIT: unconformably underlies the sedimentary sequence in both wells. This unit was penetrated to a depth sufficient to give adequate responses on mechanical logs (125 feet (38.1 m)) in Leif and 825 feet (259.8 m) in Bjarni. Comparable lithologies and similar ages, as deduced from Eastcan's (1973a, b) radiometric ages, indicate that the basaltic volcanics in both sections are sufficiently similar for them to be considered as the same unit.

The volcanic unit consists of a series of discrete subaerial flows, averaging ± 60 feet (± 19 m) in thickness, with a weathered upper section and zeolitic bases.

In the lower section of the volcanic pile in the Bjarni well (below 8210 or 2503 m), thin lignitic and silty sands occur between flows. Also in this part of the section subaerial weathering appears to have been more intense, with the extensive development of reddened beds possibly suggesting intermittent extrusion.

A cored section from Leif shows a thin sill of olivine basalt with chilled margins and local hydrothermal alteration. It therefore appears that the basaltic volcanic unit consists of a series of discrete flows which have been subsequently altered, not only by subaerial weathering but also by hydrothermal metasomatism. The central portions of each flow appears to be unaffected.

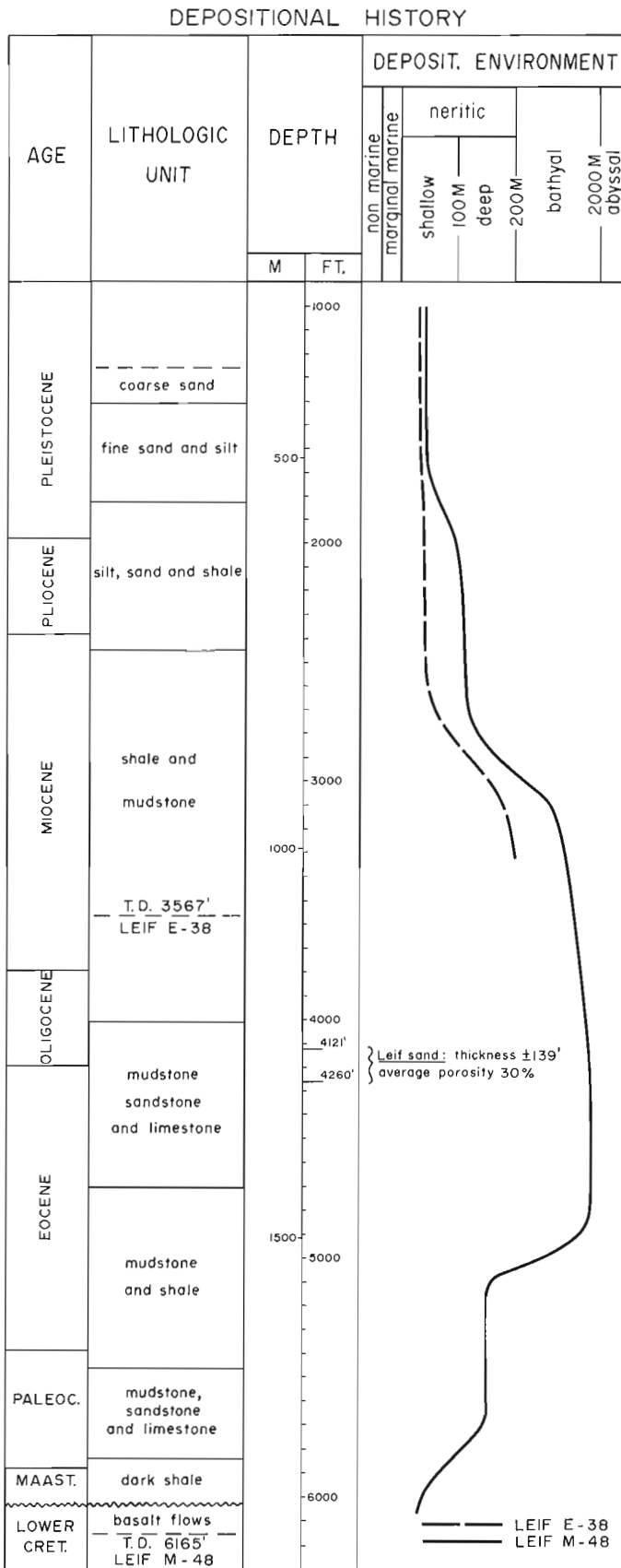


Figure 8.3. Summary of depositional environments for Tenneco *et al.*, Leif E-38 and Eastcan *et al.* Leif M-48, Labrador Shelf, Newfoundland.

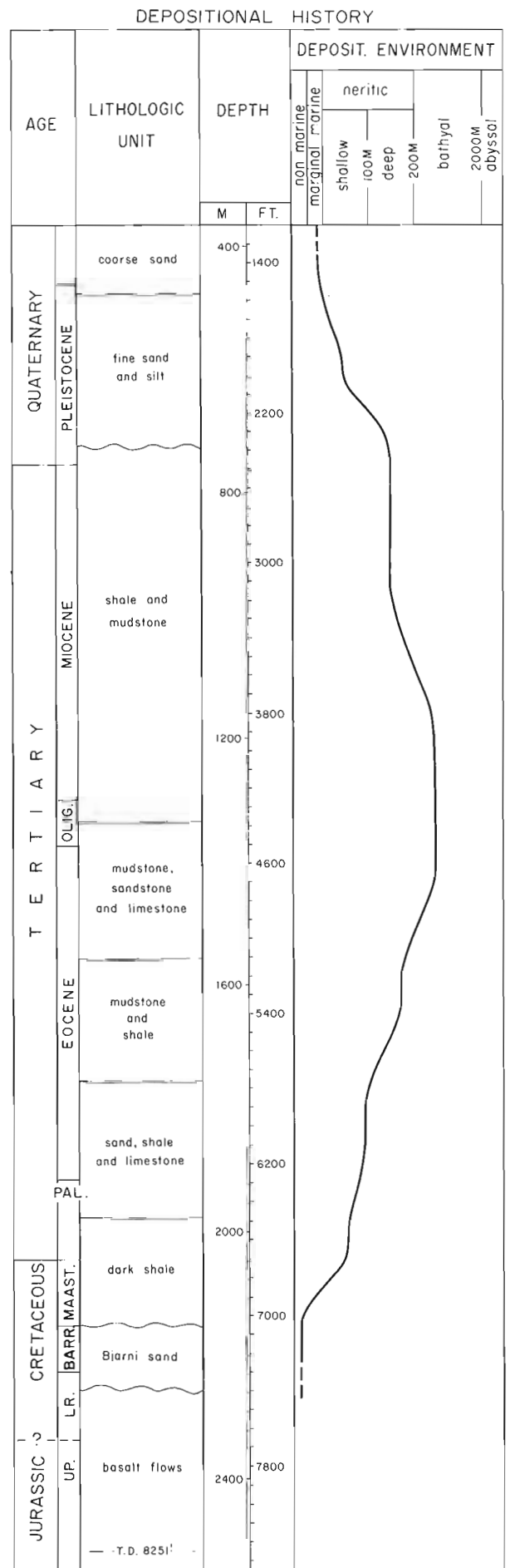


Figure 8.4. Summary of the depositional environment for Eastcan *et al.* Bjarni H-81, Labrador Shelf, Newfoundland.

Depositional History

Seismic profiles in the vicinity of the Leif and Bjarni wells show the basement to be faulted, although the faults rarely disturb the overlying sedimentary sequence (Grant, 1974). The major faults are normal and have westward-dipping fault planes, indicating downthrow towards the present coast. It seems probable that these faults are related to a Late Jurassic-Early Cretaceous taphrogenic episode that occurred prior to basin subsidence.

The present study that, after a phase of discontinuous continental sedimentation, sediments were deposited in a milieu of rapid deepening, followed by shallow water conditions (Figs. 8.3 and 8.4). Thus shallow neritic deposits of Paleocene to early Eocene age are overlain by outer neritic to upper bathyal deposits of middle Eocene to middle Miocene age. Succeeding sedimentation occurred under progressively shallowing environments, terminating with inner neritic Pleistocene sands.

Apparently this sequence of events is not one of simple transgression followed by regression. Instead, Cretaceous and lowermost Tertiary paralic and continental sedimentation was followed by basin subsidence about a hingeline. This subsidence appears to have been accelerated in the early Eocene, after which subsidence ceased and the basin became infilled.

References

- Eastcan Exploration Limited
1973a: Well history report, Eastcan *et al.* Bjarni H-81; released to Open File October 12, 1975 by Dep. Energy, Mines and Resources, Ottawa, Canada.
- 1973b: Well history report, Eastcan *et al.* Leif M-48; released to Open File August 29, 1975 by Dep. Energy, Mines and Resources, Ottawa, Canada.
- Gradstein, F. M. and Williams, G. L.
Biostratigraphy of the Labrador Shelf, Part I; Open File, Dep. Energy, Mines and Resources, Ottawa, Canada. (in press).
- Grant, A. C.
1974: Structural modes of the western margin of the Labrador Sea; Geol. Surv. Can., Paper 74-30, v. 2, p. 217-231.
- McWhae, J. R. H. and Michel, W. F. E.
Stratigraphy of Bjarni H-81 and Leif M-48, Labrador Shelf; Bull. Can. Pet. Geol. (in press).
- Tenneco Oil and Minerals Limited
1971: Well history report, Tenneco *et al.* Leif E-38; released to Open File September 25, 1975 by Dep. Energy, Mines and Resources, Ottawa, Canada.

Project 730160

E. J. Schwarz

Regional and Economic Geology Division

The Proterozoic Circum-Ungava fold belt extends from south of Schefferville northwards to Ungava Bay, then westwards via Cape Smith to Hudson Bay, subsequently turning southwards via Richmond Gulf and the Belcher Islands and finally turning westwards. Lithologically, the eastern and western parts of the belt are similar consisting of basaltic rocks of calc-alkaline composition and sediments some of which are red beds. The northern part consists essentially of mafic to ultramafic (komatiitic) flows and intrusions. The whole belt is strongly folded.

Paleomagnetic sampling programs (in 1973, Smith Island; in 1974, Richmond Gulf, Manitounuk and Hopewell Islands; in 1975, Schefferville area) were undertaken by the Paleomagnetic Section with the objectives of (1) settling the question whether the complex shape of the belt is primary or not, and (2) arriving at stratigraphic correlations between the various parts of the belt.

1. Smith Island results (Jujiwara and Schwarz, 1975). The komatiitic basalts (Schwarz and Fujiwara, in press) show weak and stable remanent magnetization which was tested using both alternating field and thermal techniques. The magnetization is carried by virtually pure magnetite with median unblocking temperatures around 450°C. The mean direction of magnetization is approximately given by declination = 220°, inclination = +70° (down) before correction for the tilt of the beds (Fig. 9.1). The corresponding pole position falls near the Hudsonian (~1750 m.y.) part of the polar wandering curve relative to the North American Precambrian Shield. This suggests that the magnetization is Hudsonian in age. Correcting for the tilt (90°) yields a mean direction of approximately declination = 300°, inclination = +25°. This direction would apply if the magnetization is pre-folding or, presumably, pre-Hudsonian. The corresponding pole position is southeast of Japan near the 900 m.y. part of the polar wandering curve (Fig. 9.2). This does not mean that the age of magnetization is 900 m.y. unless folding is younger than that, which is at variance with presently held views.

2. Richmond Gulf results.

Stable remanent magnetization was isolated for basaltic rocks and an andesite - red sediment series near Richmond Gulf. The magnetization is carried by magnetite and/or hematite with blocking temperatures generally well above 400°C. The rocks show little deformation.

The average directions for the basalts and andesite - sediments show good agreement. These directions are given approximately by: declination = 125°, inclination = -50° (up) as shown on Figure 9.1. Reversing these directions results in south-seeking directions near the pre-folding Cape Smith north-seeking direction as shown in Figure 9.1. The only internal check on

the age of the magnetization is provided by the strongly scattered directions of four samples taken from andesite - red bed layer. Attempts to isolate stable remanence in the collections from the basaltic rocks of one of the Manitounuk and one of the Hopewell Islands were not successful.

3. Schefferville area.

Samples collected from basalts, gabbros, red beds, and iron formation in an area between Schefferville and 90 miles to the north show complex remanent magnetization probably composed of superimposed components of different age. Very substantial within-core and within-site scatter is generally observed. These results are being further analyzed.

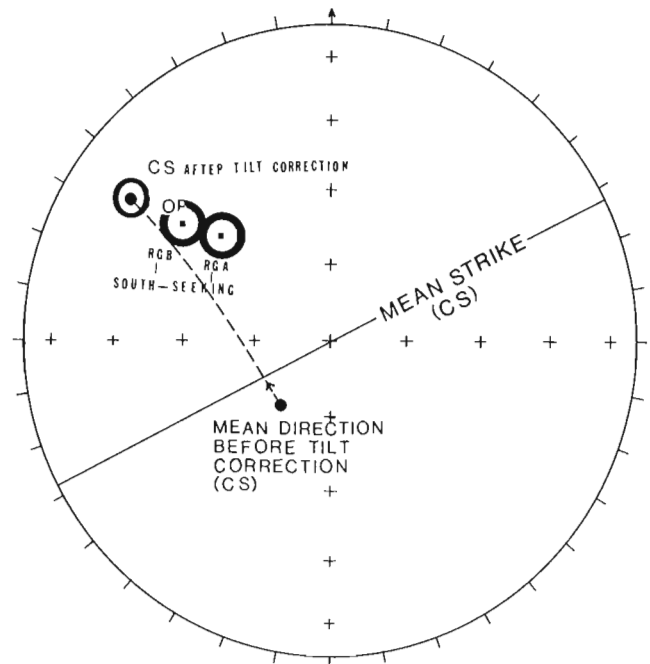


Figure 9.1. Stereographic projection showing mean direction of remanent magnetization after alternating field cleaning for Cape Smith (CS) and Richmond Gulf andesites and sediments (RGA) and basalts (RGB). The south-seeking directions of the Richmond Gulf rocks have been plotted for comparison with the north-seeking, tilt-corrected, Cape Smith direction. All directions are in lower hemisphere. Circles around the means indicate approximate limits of 95 per cent confidence.

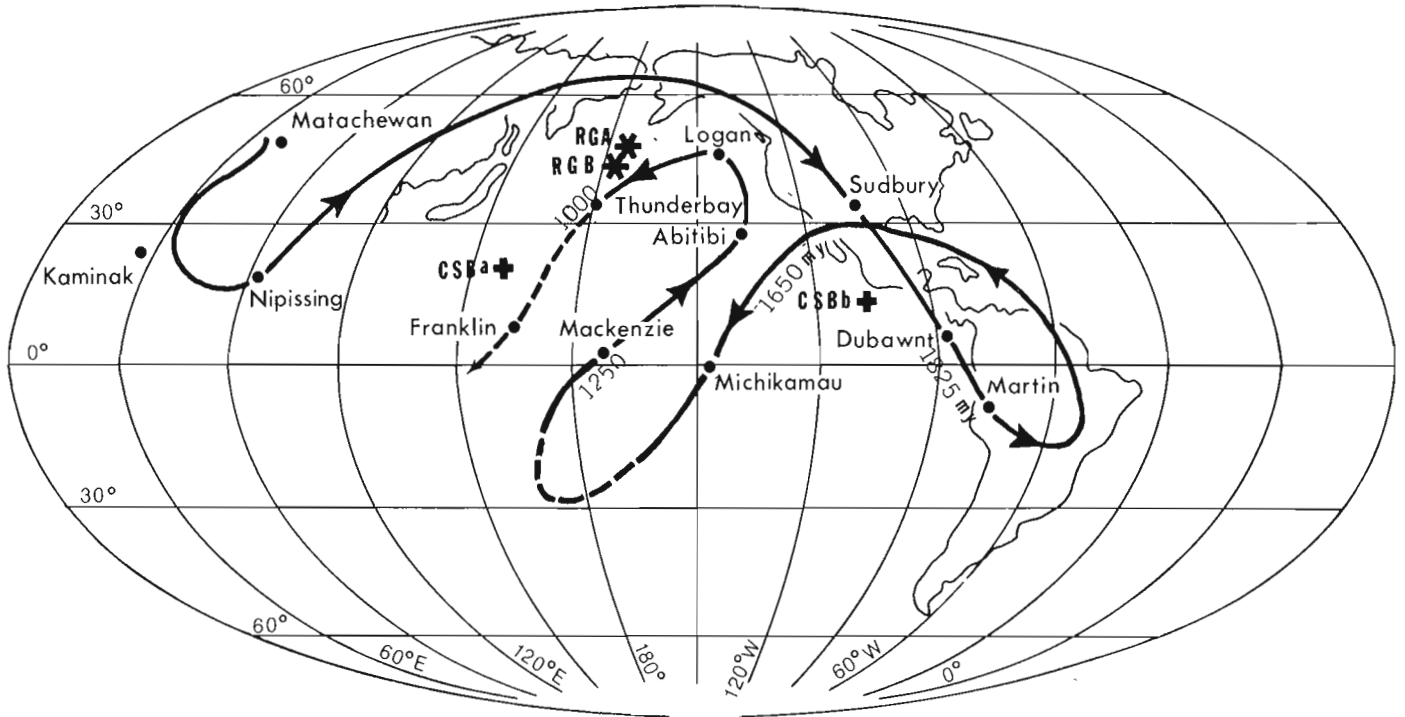


Figure 9. 2. Pole positions for Richmond Gulf andesites (RGA) and basalts (RGB) after tilt corrections and for Cape Smith Komatiitic basalts before (CSBb) and after (CSBa) tilt correction. Polar wandering path from Christie *et al.* (1975).

Significance of the results

The data for Cape Smith and Richmond Gulf raise the following possibilities:

1. The Richmond Gulf data and the Cape Smith data represent primary magnetization. The grouping of these poles suggests that at least the area between Richmond Gulf and Cape Smith can be regarded as one single block. If the rock ages are Aphebian, which is generally thought to be the case on geological grounds, a counter-clockwise rotation over 30° could have caused the discrepancy between the location of the poles and one of the most recent interpretations of the pre-Hudsonian part of the polar wandering curve (Fig. 9. 2).

2. The Richmond Gulf magnetization is primary (Aphebian) but the Cape Smith magnetization represents a Hudsonian direction. Then the tilt-incorrected Cape Smith pole applies. These magnetization ages are the most plausible from the present magnetic data. This would also suggest a counter-clockwise rotation of the Cape Smith - Richmond Gulf block, and the grouping of the Cape Smith (corrected) and Richmond Gulf poles is fortuitous.

3. The Richmond Gulf data represent secondary magnetization acquired at about 1100 m. y. ago and the Cape Smith results are Hudsonian or at least of the same age as the folding. This is at variance with the

results from the andesite breccia. Also, the Richmond Gulf magnetization shows a fairly narrow unblocking temperature spectrum up to 670°C. This magnetization should survive greenschist facies metamorphism. The Richmond Gulf rocks are generally fresh and show only evidence of very low greenschist metamorphism.

Discrimination between these and other possibilities cannot be made with reasonable certainty at this time so that more results are required from this unique Proterozoic structure.

References

- Christie, K.W., Davidson, A., and Fahrig, W.F.
1975: The paleomagnetism of Kaminak dikes; *Can. J. Earth Sci.*, v. 12, p. 2048-2064.
- Fujiwara, Y. and Schwarz, E.J.
1975: Paleomagnetism of the Circum-Ungava belt (I): Cape Smith komatiitic basalts; *Can. J. Earth Sci.*, v. 12, no. 10, p. 1785-1793.
- Schwarz, E.J. and Fujiwara, Y.
Komatiitic basalts from the Proterozoic Cape Smith range in Northern Quebec, Canada. In *Geol. Assoc. Canada, spec. paper 17*. Ed. W.R.A. Baragar, L.C. Colman, J.M. Ade Hall., in press.

E. M. R. Research Agreement 1135 - D13 - 4 - 217/75

L. D. Ayres¹ and D. J. Findlay¹
Regional and Economic Geology DivisionIntroduction

Large, low-grade copper and molybdenum deposits with porphyry affinities have been found at numerous localities in the Canadian Shield (Kirkham, 1972; Riley, *et al.*, 1971) and more are being found every year. At present, however, very little is known about most of them other than a few brief comments about the nature and grade of mineralization and the general host rock types. In order to facilitate further mineral exploration for such deposits, detailed examinations of individual deposits and their surrounding rocks must be made to determine relationship of mineralization to volcanism and plutonism, distribution patterns of alteration and mineralization, structural controls, and possible reorientation of the deposit. Studies are currently in progress on three deposits: (1) the Archean Setting Net Lake molybdenum deposit in northwestern Ontario; (2) the Archean Lang Lake copper deposit of Bochawna Copper Mines Limited in northwestern Ontario, and (3) the Aphebian Missi Island area in Amisk Lake, Saskatchewan, where numerous low-grade copper, molybdenum, and gold occurrences have been found.

Many of the known, Archean to Aphebian Precambrian porphyry deposits are associated with small plutons that were emplaced at high levels in volcanic sequences. Many of these plutons appear to be an integral part of the volcanism and may occupy the lower parts of volcanic vents. Precambrian porphyry deposits may thus be more akin to the poorly known deposits that occur in the volcanic island arcs of the southwest Pacific such as Paguna in Gougainville, than to the well-known, so-called typical deposits of the southwestern United States, many of which are associated with Mesozoic and Cenozoic plutons emplaced in Precambrian and Paleozoic sedimentary and meta-sedimentary country rocks. In the Canadian Shield, a few deposits have been found in the large mesozonal granitic batholiths that border the metavolcanic-metasedimentary belts, but these are not included in this study.

Unlike most younger deposits, Precambrian deposits have been subjected to the same regional metamorphism and deformation that affected the enclosing volcanic sequences. As a result, Precambrian porphyry deposits may differ from younger deposits in several ways. (1) The widespread zonal alteration that is associated with many porphyry deposits and is one means of identifying such deposits, may have been obliterated or transformed by metamorphism. (2) Regional metamorphism and deformation may have partly or completely destroyed

epizonal textures in the host pluton and may have modified the character of the mineralization. (3) The deposits may have been tilted during deformation. This last factor must be seriously considered when planning an exploration program for Precambrian porphyry deposits.

The Setting Net Lake porphyry molybdenum deposit

This deposit occurs in an oval, epizonal Archean porphyritic granodiorite-quartz monzonite pluton (Ayres, 1970; Ayres *et al.*, 1973; Wolfe, 1974) in the Favourable Lake area, 195 km north of Red Lake, north-western Ontario (52°49'N; 93°34'W). The stock has an area of 5.7 km², but mineralization is restricted to the northern 15 per cent where closely spaced, molybdenite-bearing quartz veins occur within a 2500-m long by 460-m wide zone. The veins have relatively consistent trend of N65°E and dip 75°S; most veins are 1 to 2 mm wide. Average grade in the east part of the zone is 0.06% MoS₂; minor copper is also present.

The stock was intruded into the central part of the Favourable Lake metavolcanic-metasedimentary sequence. Near the stock this sequence has a subvertical dip and faces southwestward. Textural and structural data within the stock such as width of chilled zone, distribution of phenocrysts, and attitude of primary flow lines suggest that it may have been intruded when the enclosing sequence was still relatively flat-lying. Both the stock and the enclosing formations were then tilted about 90° southwestward during regional deformation. Consequently the presently exposed section through the stock is actually a near-vertical cross-section with the western side representing the original top.

The mineralization formed prior to tilting, and thus the western side represents the original top of the deposit. Recognition of such tilting in this and other Precambrian porphyry deposits could have an important bearing on exploration. For example, its present attitude the Setting Net Lake stock exposes a 2.5-km vertical section through the mineralization. It is quite conceivable that, because of vertical changes in temperature, pressure, fugacities, and concentration gradients, both mineralization and associated alteration will vary more over a 2.5-km vertical distance, than over a similar, horizontal distance (in reference to original attitude). Thus if areas of higher grade mineralization or potentially favourable alteration are found within the mineralized zone, extensions of these zones must be looked for in the vertical rather than horizontal directions (in reference to present attitude).

Alteration in the mineralized zone consists of albitization and sericitization of plagioclase, chloritization of biotite, replacement of biotite by muscovite, decrease in overall biotite and chlorite content, increase

¹Department of Earth Sciences - University of Manitoba Winnipeg, Manitoba R3T 2N2

in pyrite content, decrease in abundance of primary iron-titanium oxide, replacement of sphene by secondary ilmenite, and increase in carbonate and epidote content. Intensity of alteration decreases away from the mineralized zone and alteration related to mineralization is slight to absent in the south part of the stock. The stock has been metamorphosed to greenschist facies, and the present alteration mineral assemblages are the result of both alteration and superimposed metamorphism.

The major objectives of the present study are twofold: (1) to obtain additional petrographic and structural data relative to the primary attitude of the stock, and (2) to examine, in detail, the alteration and mineralization in order to define more precisely alteration patterns and trends and to attempt to differentiate between alteration and metamorphism effects and consequently to determine the original alteration assemblages.

Lang Lake copper deposit

Field work was begun on the Lang Lake copper deposit of Bochawna Copper Mines Limited, 160 km east of Red Lake, northwestern Ontario (51°35'N; 91°32'W). The deposit is at the west end of the Lang-Cannon Lakes metavolcanic-metasedimentary belt (Fenwick, 1969; Riley, 1969). Outcrop is sparse on the property, and much of the study will be based on the extensive diamond-drill core.

On the property, a north-facing, steeply-dipping sequence of mafic to intermediate flows, pyroclastic rocks, and volcanoclastic greywacke and conglomerate is intruded by a suite of porphyritic to equigranular dykes, sills, and stocks ranging in composition from diorite to granodiorite. Chalcopyrite, pyrite, magnetite, and minor molybdenite, gold, and silver occur in disseminated form and as fracture-filling sulphide and sulphide-quartz veinlets in both the intrusive and metavolcanic-metasedimentary sequence, but sulphides are most abundant in the metavolcanics. Mineralization is concentrated in a 700-metre-long, east-trending zone immediately north of a small, equigranular to porphyritic trondhjemite stock that contains only minor mineralization. Within the mineralized zone, more leucocratic and finer grained porphyritic dykes are present and appear to be intimately associated with the mineralization; these dykes appear to be older than the trondhjemite stock.

Based on textural evidence and occurrence, the porphyritic suite is epizonal and subvolcanic. The mineralization is spatially and probably genetically related to the porphyritic suite but the precise relationship between mineralization and individual dyke types has not yet been established. Within the mineralized zone the rocks are weakly to moderately altered, and elucidation of the nature and distribution of this alteration and its relationship to mineralization is the major objective of this study. The host rocks for the mineralization have been metamorphosed to upper greenschist facies, and if the alteration is subvolcanic, then primary alteration assemblages will have been

transformed by metamorphism. We will try to read through the metamorphism and determine the original alteration assemblages.

The cause of the metamorphism is a large, mesozonal granitic batholith immediately west of the property. The batholith appears to be younger than the porphyritic suite and mineralization, but this relationship remains to be tested.

Missi Island volcanic centre

Reconnaissance mapping and logging of diamond-drill core were carried out at Missi Island in Amisk Lake, east-central Saskatchewan (54°40'N; 102°15'W). This preliminary work was in preparation for a detailed examination which will commence in 1976.

At Missi Island, the Aphebian Amisk Group comprising mafic to felsic flows, pyroclastic rocks, and volcanogenic greywacke is intruded by two felsic subvolcanic, plutonic suites: (1) an older porphyritic dyke suite, and (2) younger discrete stocks of altered trondhjemite. The plutonic rocks underlie slightly more than half of Missi Island (Byers and Dahlstrom, 1954), which has an area of about 75 km², but their abundance decreases rapidly away from the island.

The porphyritic dyke suite ranges in composition from gabbro to quartz monzonite and the dykes contain variable amounts of quartz, feldspar, biotite, and hornblende phenocrysts in a fine grained to aphanitic groundmass. Dykes range in width from a few centimetres to more than 50 metres and have diverse trends. Dyke abundance is variable and ranges from nothing to total with dykes being concentrated in the north and west parts of the island forming an arcuate outcrop pattern. In areas of abundant dykes, younger dykes are intimately injected into older dykes. Using variations in phenocryst population, groundmass texture, and composition, at least 10 dyke types have been recognized to date, but differences between many of the dykes are subtle.

The dykes and adjacent mafic metavolcanic country rocks are variably altered, although the later dykes appear to be relatively unaltered. Greenschist facies metamorphism appears to have been superimposed on the alteration which in turn appears to be related to dyke emplacement. There is a strong correlation between the presence of abundant porphyritic dykes, increasing alteration of mafic metavolcanics, and mineralization. Alteration is of two general types: (1) pervasive, and (2) concentrated adjacent to fractures containing narrow veins of one or more of quartz, carbonate, chlorite, hematite, and pyrite. Mineralization consists of pyrite and minor chalcopyrite disseminated in some of the dykes and country rocks, local pyrite veinlets, especially in country rocks, and sporadic molybdenite. As yet no pattern has been discerned between abundance and type of mineralization, intensity of alteration, and dyke type, but the possible relationships among these three factors is one of the major objectives of this study.

The porphyritic dyke suite may represent an eroded vent complex with the dykes being the intrusive equivalent of overlying felsic to intermediate metavolcanic formations (Kirkham, 1974). The general similarity of dyke types, apparent lack of a consistent intrusive sequence of different dyke types, complexity of outcrop pattern, subvolcanic textures, and associated alteration and mineralization all support this conclusion. In this type of environment, porphyry-type deposits might occur, and indeed, the sidespread mineralization may be indicative of such deposits, although assays are below ore grade.

The possible vent origin of the dyke suite and the potential porphyry environment are the major focuses of this study. Specifically, the study will examine: (1) areal distribution of dyke types, (2) general and local intrusive sequences of dykes as an indicator of magma chamber evolution, (3) areal variation in attitude and size of dykes, (4) relationship of dykes to the felsic to intermediate part of the Amisk Group which occurs immediately west of Missi Island, (5) relationship between mineralization, alteration, and dyke type, (6) areal distribution of alteration and mineralization, (7) effects of superimposed greenschist facies metamorphism on alteration assemblages, and (8) relationship between the dyke suite and the younger, altered trondhjemite plutons.

The younger altered trondhjemite (quartz-eye diorite of Byers and Dehstrom (1954)) forms small stocks with areas up to 10 km². The unit is medium-to coarse-grained, equigranular to porphyritic, massive to weakly foliated, and moderately to strongly altered; there are at least two distinct textural variants. Narrow quartz veins are abundant in many of the stocks, but no mineralization was observed.

Concluding Remarks

It is well known that microscopic petrography is a powerful tool in exploring for porphyry mineral deposits because it can document alteration patterns that have a direct relationship to mineralization (Lowell and Guilbert, 1970; Carson and Jambor, 1974). Microscopic study is especially important in Precambrian deposits because (1) primary alteration assemblages have been partly to completely transformed by metamorphism and their recognition is more difficult and (2) petrographic variations are one of the more reliable indicators of primary attitude of host plutons. Once porphyry mineralization has been discovered in the Precambrian, microscopic petrography should be one of the main exploration tools used to outline potential drill targets. For example, preliminary petrographic examination of the Setting Net Lake stock suggests that the highest priority drill targets are at the poorly exposed, western (upper) end of the mineralized zone, rather than at the better exposed, eastern (lower) end where previous drilling was concentrated.

References

- Ayres, L. D.
1970: Setting Net Lake area, District of Kenora: Ont. Dep. Mines, Prel. Map P. 538 (revised).
- Ayres, L. D., Averill, S. A., and Wolfe, W. J.
1973: The Early Precambrian, Setting Net Lake porphyry molybdenum deposit (abstract): Can. Min. Metall. Bull., v. 66, March, p. 48.
- Byers, A. R. and Dahlstrom, C. D. A.
1954: Geology and mineral deposits of the Amisk-Wildnest Lakes area: Sask. Dep. Min. Resour. Rep. 14, 177 p.
- Carson, D. J. T. and Jambor, J. L.
1974: Mineralogy, zonal relationships and economic significance of hydrothermal alteration at porphyry copper deposits, Babine Lake area, British Columbia: Can. Min. Metall. Bull., v. 67, p. 110-133.
- Fenwick, K. G.
1969: Lang-Cannon Lakes area (west half): Ont. Dep. Mines, Prel. Map P. 581.
- Kirkham, R. V.
1972: Geology of copper and molybdenum deposits: in Report of Activities, Pt. A, Geol. Surv. Can., Paper 72-1A, p. 82-87.
1974: Geology of copper and molybdenum deposits in Canada: in Report of Activities, Pt. A, Geol. Surv. Can., Paper 74-1A, p. 377-379.
- Lowell, J. D. and Guilbert, J. M.
1970: Lateral and vertical alteration-mineralization zoning in porphyry ore deposits: Econ. Geol., v. 65, p. 373-408.
- Riley, R. A.
1969: Bochawna Copper Mines Limited: Ont. Dep. Mines, Misc. Paper 23, p. 8-9.
- Riley, R. A., King, H. L., and Kustra, C. R.
1971: Mineral exploration targets in northwestern Ontario: Ont. Dep. Mines Northern Affairs, Misc. Paper 47, 72 p.
- Wolfe, W. J.
1974: Geochemical and biogeochemical exploration research near Early Precambrian porphyry-type molybdenum-copper mineralization, northwestern Ontario, Canada: J. Geochem. Explor. v. 3, p. 25-41.

NEARSHORE OBSERVATIONS ALONG THE EAST COAST OF
MELVILLE ISLAND, DISTRICT OF FRANKLIN

Project 730021

R. B. Taylor
Terrain Sciences Division

Introduction

Recent discoveries of oil and gas reserves in the Arctic Islands have led to much discussion on methods of transporting these fuels to southern markets. Current thinking favours a pipeline but whether a pipeline or sea-going fuel carriers are used, the dynamic coastal-nearshore zones will be involved and must be considered in any construction plans.

In 1973 P. McLaren, Terrain Sciences Division, began a study of the coastal characteristics and processes along the eastern coast of Melville Island and western coast of Byam Martin Island (McLaren, 1974).

The nearshore observations presented in this paper were collected in support of the above coastal project (Project 730020). Apart from collecting information on nearshore bottom topography, the research involved experimentation with and testing of commonly used oceanographic instruments in a shallow nearshore arctic environment.

The nearshore work took place during the month of August 1973 from a base camp established along 'Frustration Bay' a small bay north of King Point, Melville Island (Fig. 11.1). As the name implies considerable difficulties arose during the research for although Byam Channel was nearly completely ice free,

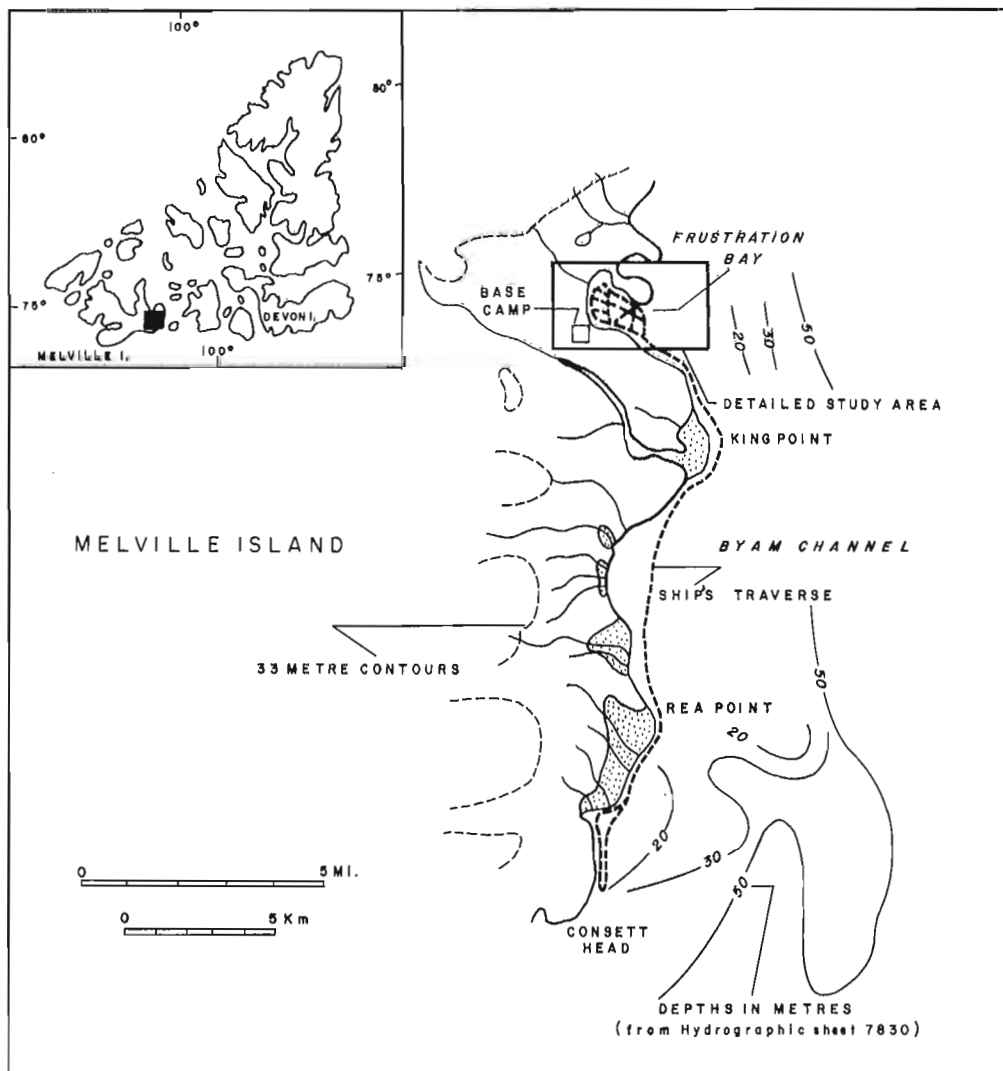


Figure 11.1. Location map of study area and boat transects.

the nearshore was congested with mobile multi-year ice which continually shifted north and south along the coast. Consequently, extensive boat work was prevented and detailed surveys were limited to 'Frustration Bay' and one additional traverse along the coast as far south as Consett Head (Fig. 11.1). Echo sounding, side-scan sonar, bottom sediment sampling, and some spot measurements of nearshore currents, salinity, and temperature within 'Frustration Bay', were carried out. Horizontal control for the marine research was provided by aerial photographs which were used to locate the physiographic features sighted on during the boat traverses.

Acknowledgments

The author wishes to thank Dr. A.J. Kerr of Canadian Hydrographic Service, Burlington for providing an echo sounder at very short notice and to Dr. E.L. Lewis of Frozen Sea Research Group, Victoria and H. Serson, Defense Research Group, Ottawa for the loan of oceanographic instruments and advice on the use of other marine instruments in the High Arctic. Thanks also are extended to Polar Continental Shelf, particularly F. Alt, for logistics support and to P. McLaren for additional field supplies and subsequent discussions. Field assistants J. Arcuri and D. Bernard provided valuable electronic and carpentry assistance during a frustrating field season. Dr. C.F.M. Lewis provided constructive criticism of the report.

Instrumentation

The working platform for the marine research was a 19-foot pneumatic boat (Fig. 11.2). Bathymetry within 'Frustration Bay' and farther along the coast was obtained using a Raytheon D.E. 719 fathometer with a high frequency (200 KHz) wide beam transducer. The fathometer together with a Klein model 400 side scan sonar provided a good picture of the nearshore bottom topography. The sonar system was also used to estimate the frequency of ice scouring in the nearshore. Bottom sediment samples were collected within the study area using a Petite Ponar grab sampler. Select *in situ* measurements of salinity and temperature were obtained using a Beckman RS₅ salinometer, and sea water samples were collected using a Van Dorn sampling bottle. Finally, nearshore current measurements were attempted with a Bendix Q-15 current sensor; however, it was not possible to determine current direction because of the proximity to the North Magnetic Pole. A list of advantages and disadvantages for each instrument is given in Appendix 1.

Physical Setting

Eastern Melville Island falls within the Innuitian physiographic region and more specifically is part of the Ridges and Plateaux physiographic division (Tozer and Thorsteinsson, 1964). The coastline of the study area is low lying and has relief of less than

30 m (100 feet) within 2 km of the shoreline. River deltas compose a large proportion of the coast; they range from micro-sized deltas formed by ephemeral spring-melt streams to large deltas such as at King Point (Fig. 11.1). The coastal sediments are composed primarily of light grey to white sandstone of the Hecla Bay Formation and small amounts of siltstone and shale from the Weatherall Formation (Tozer and Thorsteinsson, 1964).

Detailed beach observations were made along the coast between King Point and the northern headland of 'Frustration Bay'. Beach profile stations were not established by the author although a set of three profiles, zonal 7, at the west end of 'Frustration Bay' was surveyed by McLaren (1974). The beach stretching north from King Point delta is characterized by a partially vegetated sandy backshore fronted by a gradually sloping foreshore and a wide intertidal zone (Fig. 11.3). The beach sediment is medium to coarse sand with isolated occurrences of fine gravels. In contrast to these beaches, a more steeply sloping and narrower beach, backed by raised beach terraces, was observed at the southern headland and along the entire northern shoreline of 'Frustration Bay'. Bedrock here is exposed in the nearshore and partially exposed on the raised beach terraces; large cobbles are also common in the nearshore. Beach sediment visibly decreased in grain size from the headlands to the west end of 'Frustration Bay'.

Minor processes observed occurring in the backshore were gully erosion by spring meltwater and eolian action on the exposed, nonvegetated beach backshores (Fig. 11.4).

Nearshore Observations

'Frustration Bay'

Bathymetry: A hydrographic survey was completed initially on a reconnaissance scale throughout 'Frustration Bay' using headlands and physiographic features as reference points and later was done in detail with sounding lines running offshore of three established beach profiles, zonal 7 (McLaren, 1974). The track chart of the boat is shown in Figure 11.1 and the resultant isobath maps of 'Frustration Bay' and zonal 7 are shown in Figures 11.5 and 11.6.

'Frustration Bay' is outlined by a nearshore platform of varying width, which commonly only extends to depths of 1 or 2 m (at mean high tide) where a substantial break-in-slope occurs. This slope, based on the offshore surveys at zonal 7, has an inclination of 4.5 to 5.5 degrees and generally ends at depths of 12 to 15 m. Both the shoreline and nearshore break-in-slope have a cusp-like configuration which is clearly defined on the side-scan sonar records (Fig. 11.7 and 11.8). The foreshore also is characterized by small wave-formed cusps. The soundings within 'Frustration Bay' only exceeded 20 m in an elongated channel offshore of zonal 7 where depths of 22 m were recorded and at the mouth of the bay where depths reached 28 m. Shallow water areas within the bay include a small platform at



Figure 11.2

Boat and equipment used in the collection of field data. (GSC-202299).

Figure 11.3

Sandy beach foreshore north of King Point, Melville Island. (GSC-202728-A)



the entrance and a wide shallow zone at the northwestern end where 'Antler Creek' enters the bay.

A survey of 'Frustration Bay' with side-scan sonar and fathometer exhibited few bottom features. The sonar records however clearly did show the shoreline, the nearshore break-in-slope, grounded and floating sea ice, large marine life (i. e. seals), and some minor sea-ice scourings. Microrelief on the sea bed, as shown on the echograms, is limited to water depths of 3.5 to 14.5 m which basically include the edge of the nearshore break-in-slope and the shallow-water platform at the entrance to the bay. In the latter area linear sea-ice scours 20 to 50 m long, 2 to 11 m wide, and less than 0.8 m deep were detected criss-crossing the platform surface.

Elsewhere in the bay bottom microrelief was detected on the side-scan sonar records as small elongated or wedge-shaped depressions, probably created by the grounding of small ice cakes.

Zonal 7

Morphology: Three beach profiles established 100 m apart at the head of 'Frustration Bay' constitute zonal 7 (McLaren, 1974). Each profile was surveyed by fathometer from low tide mark to a distance of nearly 600 m offshore where the sea bed was considered below the reach of waves. Control for the survey was provided by nine positioned buoys, three per profile. At these buoys additional studies of water temperature and salinity and current measurements were conducted (Figs. 11.6 and 11.9).

At zonal 7 the nearshore platform varies in width from approximately 34 m at profile C to slightly wider than 100 m at profile A (Fig. 11.9); seaward of the platform, the nearshore break-in-slope is steepest (5.5 degrees) at profile C and most gradual (4.5 degrees) at profile A. Ripple marks cover most of the intertidal zone while a system of small bars has been created in



Figure 11.4

Beach backshore at same location as Figure 11.3; note the microdunes created during the storm of August 20, 1973. (GSC-202728).

the breaker zone at the upper edge of the nearshore break-in-slope. Farther offshore the sea bed becomes undulating.

Sediment Characteristics: Nine sediment cores were collected across the intertidal flats of zonal 7 using a plastic core tube. Although probing with a soil auger of 2 m length failed to reach the frost table, penetration with the core tube was limited to 0.3 to 0.4 m because of the compact nature of the sediment. The intertidal beach sediments are primarily a grey sand-silt mixture which commonly is oxidized at a level of 5 to 8 cm below the surface. Black bands of reduced sediment were most pronounced at a depth of 0.25 to 0.30 m beneath the rill channels and beach runnels.

Farther offshore, bottom samples were collected at each buoy with a sediment grab sampler. The sediments were unimodal and were composed of a very fine silt to coarse clay, i. e. +7.56 to +8.2 mean grain size. Furthermore, the bottom sediments were poorly sorted and negatively skewed throughout the nearshore except beneath buoy C_{B1} . At C_{B1} the positively skewed sediment was medium silt of +5.45 grain size. The only apparent reason for the sediment difference is that the sample from C_{B1} was close to a stream outlet and was from the nearshore slope; the rest of the samples were from farther offshore on a more gradual slope.

Salinity and Temperature: *In situ* water temperature and salinity measurements were collected at five stations within zonal 7 (Fig. 11.6) during high tide on August 16. The salinity values were relatively uniform throughout the water profile with the least saline water, 24‰, at the surface and the most saline, 31‰, at the sea bed. Water temperatures at the same sample sites were surprisingly cool for the post spring-melt season. The temperatures varied from -0.7°C at the water surface to -1.5°C at the sea bed. Warmer waters at the surface and sea bed offshore of profile C and the adjacent stream were found to be separated by a slightly cooler layer of water. The

cooler water was at a depth of 3 to 5 m within 200 m of shore and at a depth of 15 m farther offshore. The warmer waters are probably tongues of fresh water flowing from the stream. In contrast a gradual decrease in temperature with depth was recorded at the two sample sites offshore of profile A. The maximum depth at which these measurements were collected was 20 m.

Nearshore currents: Nearshore current measurements collected within zonal 7 were completed with only limited success. Current direction values were attempted by aligning the vane perpendicular to shore and then recording differences in angle deflection at each sample depth. Large variations in current direction however, were observed with repeated measurements at the same site. Consequently current direction is estimated solely on visual observations of the vane in near-surface depths. Current velocity was obtained by applying a predetermined calibration correction factor to the direct read-out from the Q-15 sensor.

Current direction was estimated to be into the bay, i. e. east to west, with a slight southwest deflection at profile A and a northwest deflection at profile C. The east to west current direction was expected since readings were collected near high tide stage. The average current velocities were small, ranging from 7 to 9 cm/s; peak velocities were 14 to 17 cm/s. The stronger currents were observed at depths of 5 and 10 m at stations one and two, respectively, of profile A. The stronger currents at profile C, on the other hand, occurred in the upper 2 to 3 m of the water profile. The latter currents may be fluvial and the primary cause of the difference in water temperature found in the near-surface waters off profile C.

'Frustration Bay' to King Point Delta

Nearshore Bathymetry and Morphology

On August 26, the sea ice moved far enough offshore to enable a transect by boat as far south as profile 7 (McLaren, 1974) situated on the south side of King Point delta. The objectives were to obtain nearshore bathymetry and to locate the areas of maximum sea-ice scouring. To achieve these goals a Klein side-scan sonar system and a Raytheon fathometer with a 200 Khz transducer were mounted in the Zodiac boat. The route was planned south along the immediate nearshore with a return northward via a transect much farther offshore. The latter, however, was prevented by a return of sea-ice and engine troubles. Horizontal control for the mapping of the nearshore bathymetry was obtained by using the side-scan sonar to measure the distance from shore and from the mouths of the larger streams as reference points along shore (Fig. 11.10).

A nearshore isobath map has been interpolated from the soundings (Fig. 11.10). At a distance of 50 to

80 m offshore of the nearshore break-in-slope, a consistent depth of 5 m was observed. Farther south at similar distances offshore of the King Point delta, however, water depths became considerably deeper, up to 24 m.

An examination of the nearshore topography between reference points A and B (Fig. 11.10) shows a zone of concentrated microtopography. Short sea-ice scours criss-cross the bottom while the presence of boulders near A and perhaps ice-melt features, produce a mottled and irregular picture on the sonar records. In water depths of 3 to 5 m the linear ice scourings were 33.5 to 55 m long, up to 11 m wide, but generally less than 1 m deep.

The most irregular bottom topography within the study area was viewed at the King Point delta front. Figure 11.10 shows a trace of the echogram produced across the delta front.

Superimposed on what appear to be extensions of the larger stream channels are numerous smaller depressions. From the side-scan sonar records these depressions have both a linear and circular form.

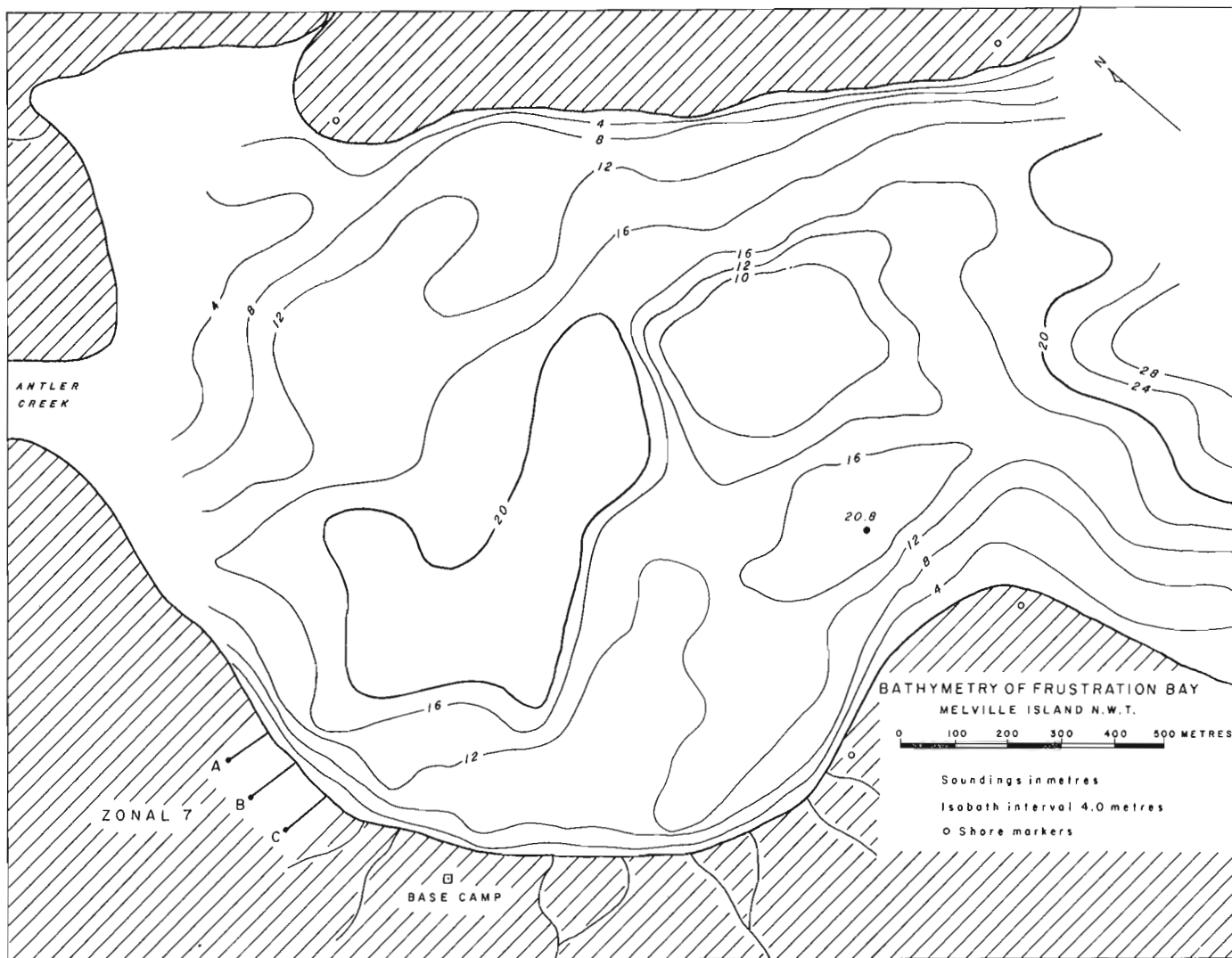


Figure 11.5. Bathymetric contour map of 'Frustration Bay', Melville Island.

Some may be pits created by concentrated flood waters flowing through "strudel marks" (Reimnitz *et al.*, 1974) in the nearshore ice or may be formed by the melting of bottom-fast ice by the input of warmer fresh waters. The occurrence of bottom-fast ice in the nearshore area is inferred from observations of this ice in the shallow waters off Little Point, Melville Island. The occurrence of bottom-fast ice there was common. Nevertheless, the majority of the nearshore bottom markings are created by sea-ice groundings. The King Point delta front and the entire eastern Melville Island coast were subjected to continually shifting sea-ice during August. On August 26, 1973 the delta front was lined with small mobile sea-ice and a few much larger multi-year ice blocks. At the delta front the linear ice scourings were short and narrow, having an average length and width of only 37 m and 7 m respectively. Sea-ice scourings between reference points E and F (Fig. 11.10) were slightly larger with dimensions up to 55 m long and 8 m wide. The depth of scour did not exceed 2 m; however, this depth is based only on a couple of scours which were recorded on both the side-scan and echo sounding records.

Observations were made of the sea bed adjacent to a piece of ice island grounded on the delta front. Surprisingly no large linear ice scour was found, but rather a wide area of lighter coloured tone was exhibited on the side-scan records which may be the result of removal of a thin layer of surficial sediments. The piece of ice island and a large block of multi-year ice nearby both produced wide and strong reflection markings on the sonar records. In contrast, the small pieces of younger ice grounded in the nearshore produced much lighter and thinner markings on the records.

From these observations one might conclude a relationship between ice age and width and intensity of the reflector on the side-scan sonar records. This hypothesis cannot be proven with the few examples observed in this study because it may well be that size and thickness of ice, rather than age (i. e. hardness), govern the properties of the resultant markings on the charts. Further research or observations therefore will have to be made in correlating sea-ice age and thickness with resultant characteristics viewed on side-scan sonar records.

In summary, the largest number of linear ice scours were recorded between reference points A and B, and E to G. The dimensions of these scours in comparison to ice-scour marks reported in the Beaufort Sea (Reimnitz *et al.*, 1973; Pelletier and Shearer, 1972) are very minute.

Rea Point

Nearshore Bathymetry and Morphology

The presence of sea ice at zonal 6 (McLaren, 1974) prohibited the planned offshore surveys, consequently two brief impromptu runs were completed at and to the south of Rea Point using sounding and sonar equipment.

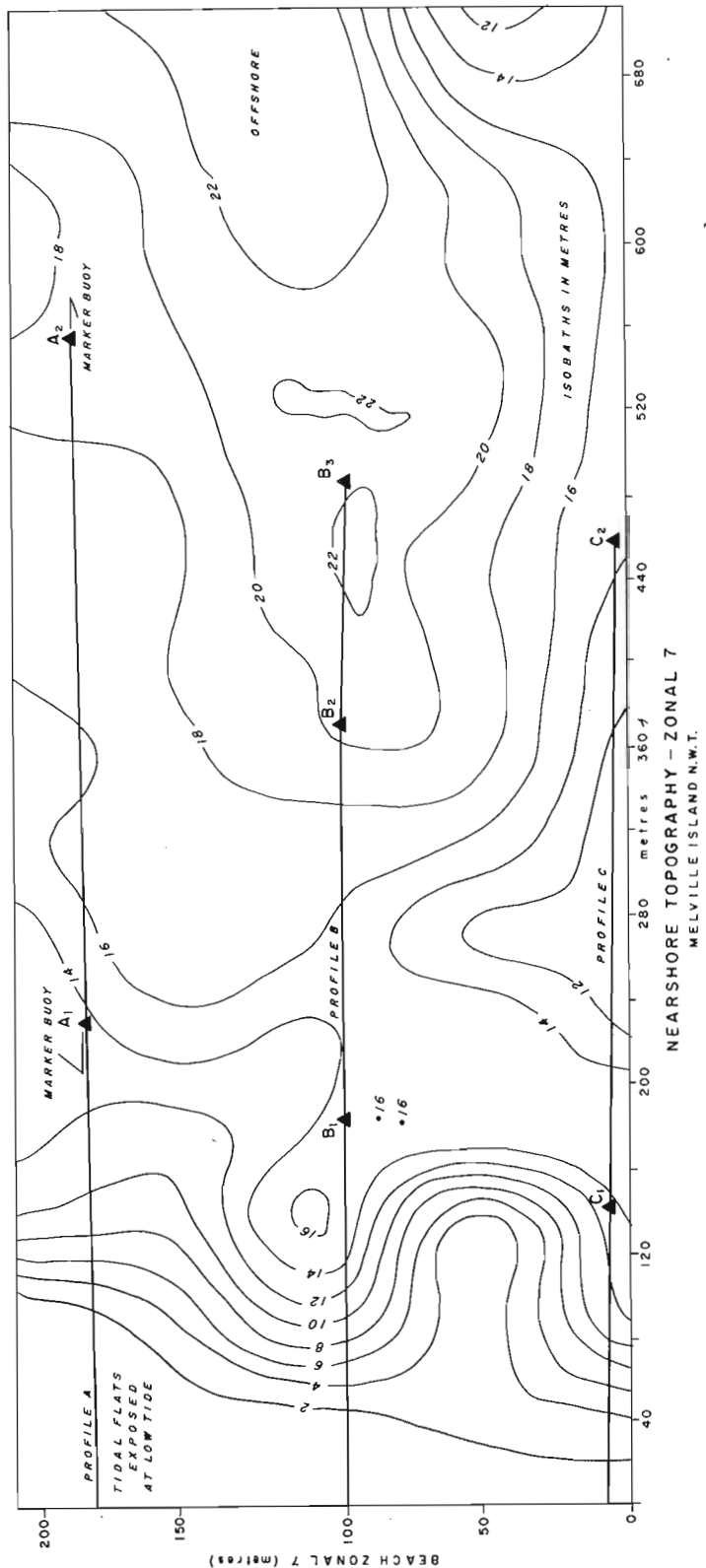


Figure 11.6. Plan shape of the north shore of 'Frustration Bay' as viewed on the side-scan sonar records.

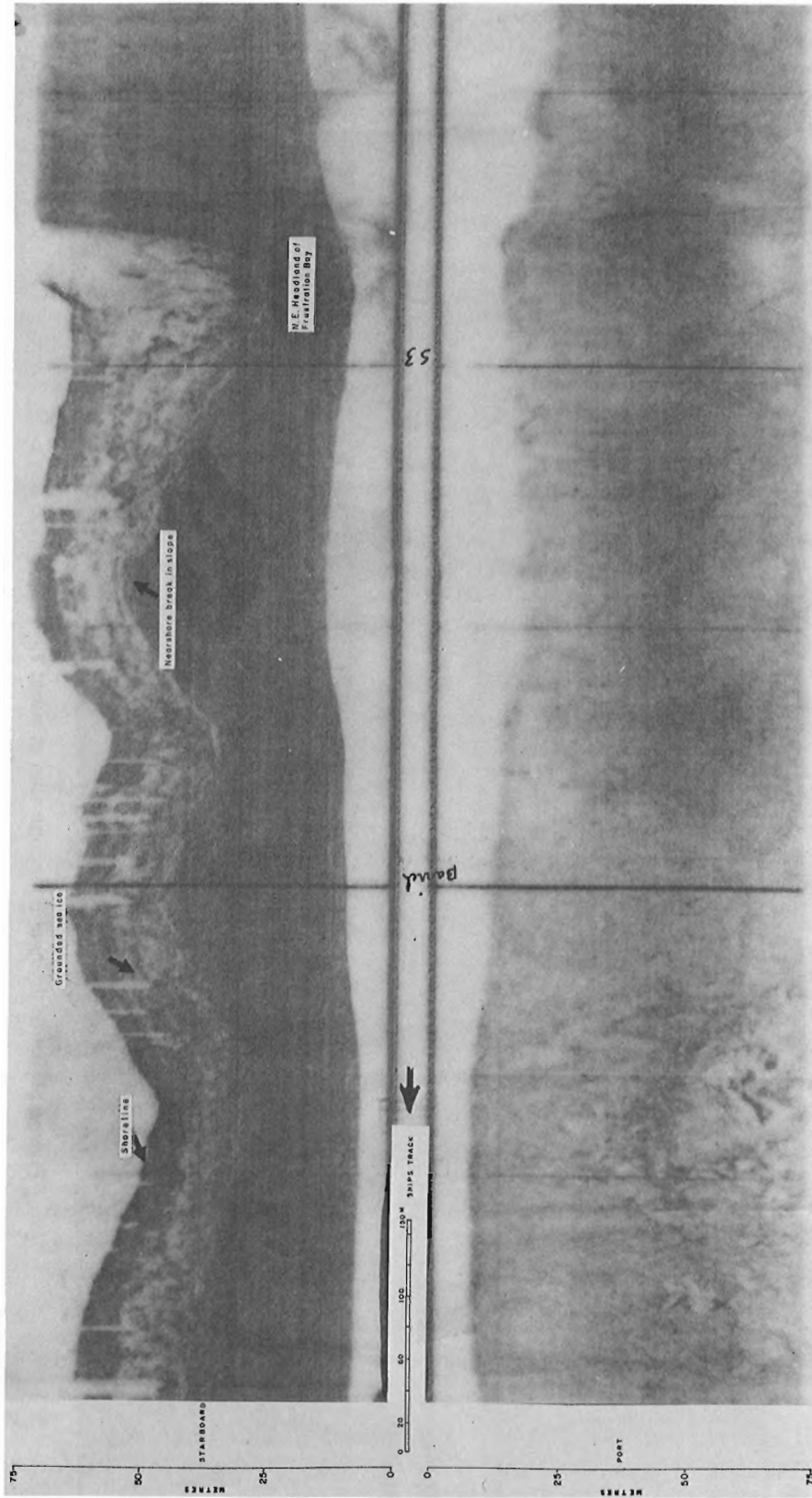


Figure 11.7. Side-scan sonar record of the southeast headland of 'Frustration Bay'. Note the increase in bottom microrelief at the headland and along the open coast of Melville Island.

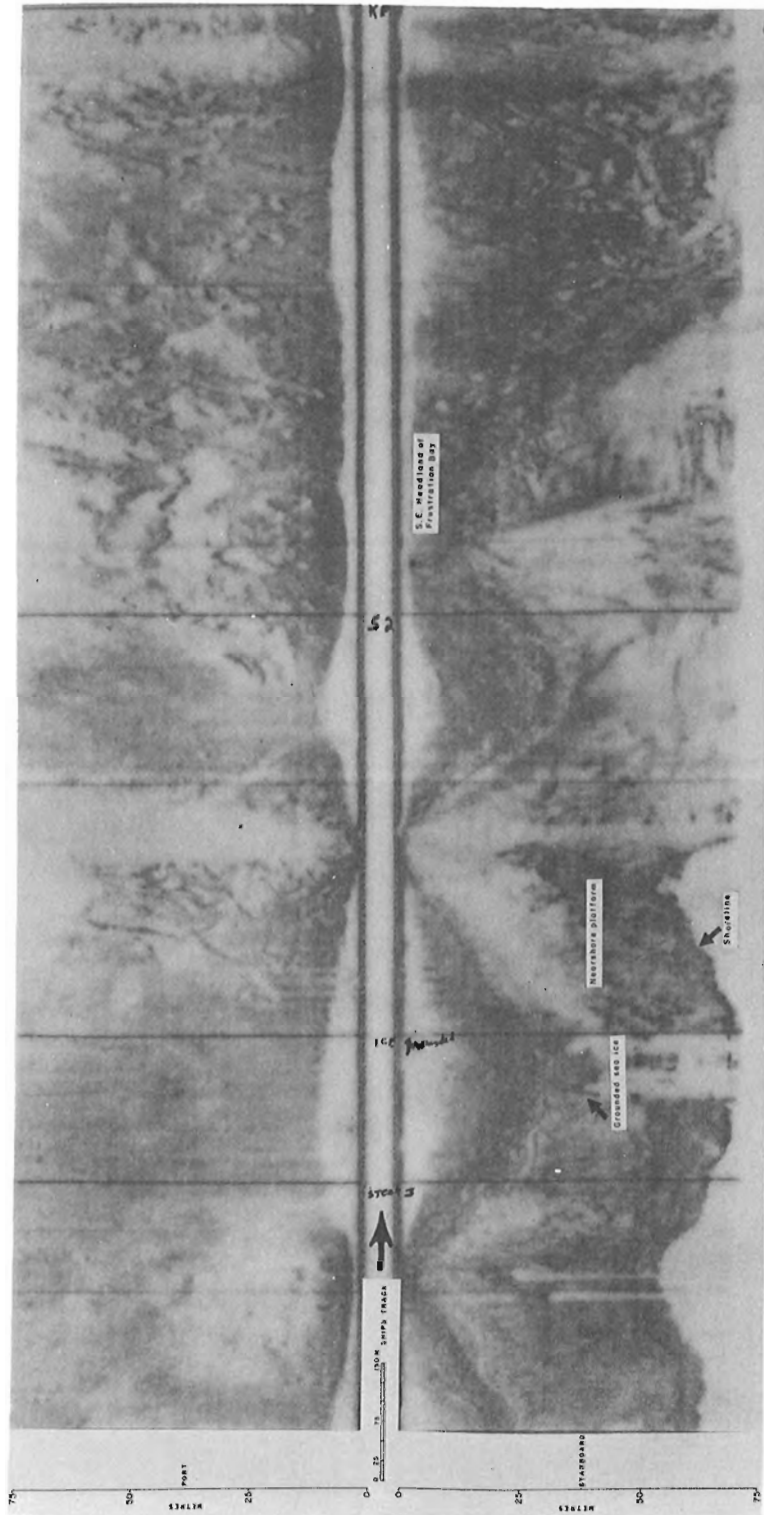


Figure 11. 8. Bathymetric contour map of zonal 7, 'Frustration Bay'.

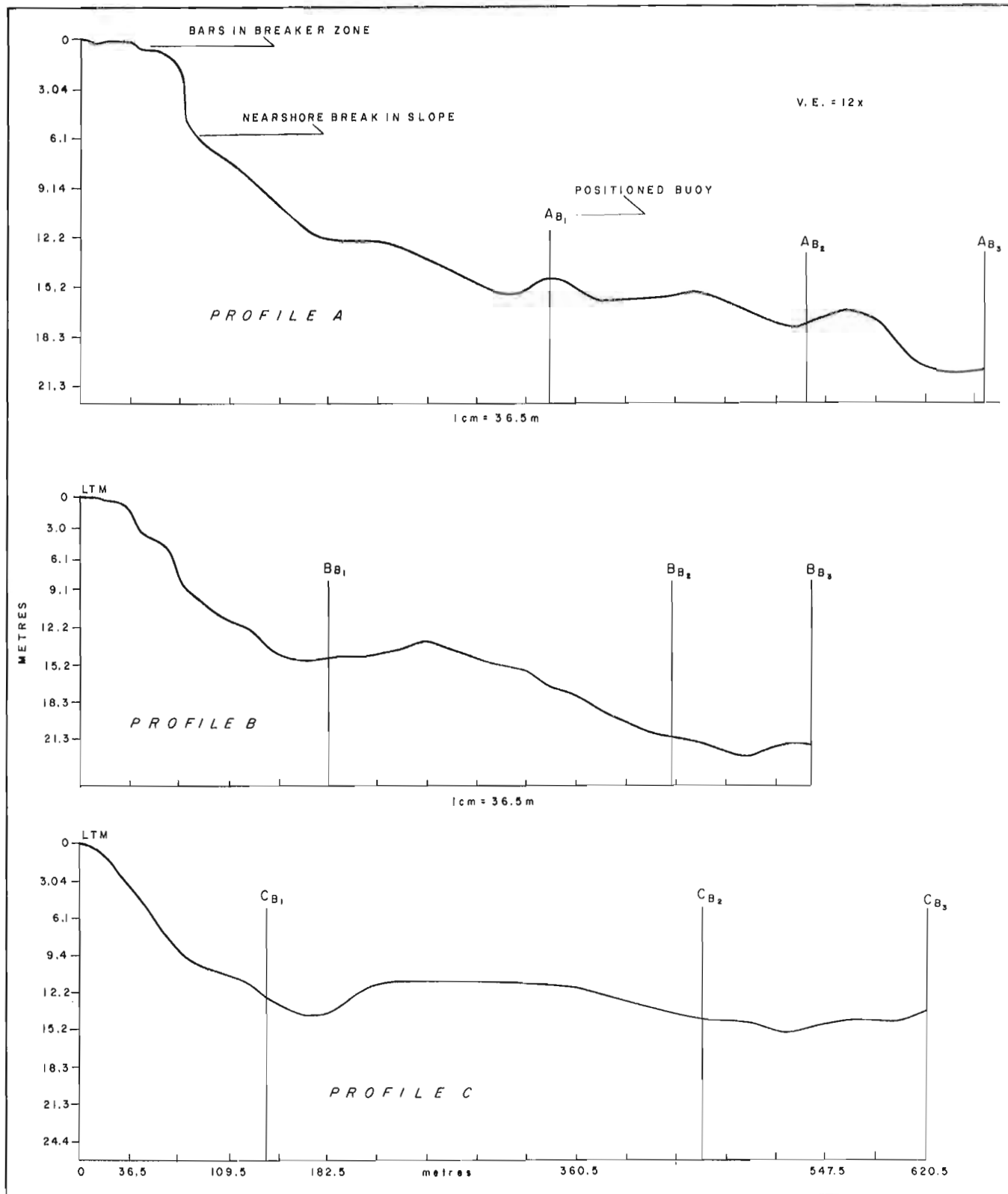


Figure 11. 9. Cross-sectional profiles of the three sounding lines completed at Zonal 7 and the location of the marker buoys.



Figure 11.10. Trace of echo sounding records across the front of King Point delta; reference map and nearshore bathymetric contours between 'Frustration Bay' and King Point delta, Melville Island (insert).

An earlier bathymetric survey in 1969 by the vessel Irving Birch showed that depths of 23 to 51 feet (7 to 15 m) occur just beyond low tide limit of the harbour area at Rea Point (Hydrographic sheet 4243). The present survey confirmed these depths and extended soundings farther into the small bay and across its entrance. A lack of horizontal control prevents the plotting of an isobath map, however, Figure 11.11 shows a few spot soundings together with the published data. The deeper waters were found to extend farther into the bay along its northern shore; however, this deep channel used by ships does not extend across the

entire entrance to the bay. Instead, depths as shallow as 10 feet (3 m) were recorded towards the southern portion of the entrance.

During the survey on August 30, the freighter Cabot was unloading along the northern shoreline of the bay and the oil tanker Palva had just set off from its beached position. A survey using the side-scan sonar failed to show any significant disruptions to the bottom topography where the Palva had been anchored. In Figure 11.12 which shows the side-scan records of the harbour area, the hull of the ship Cabot is distinguished along with a distinct bottom scouring

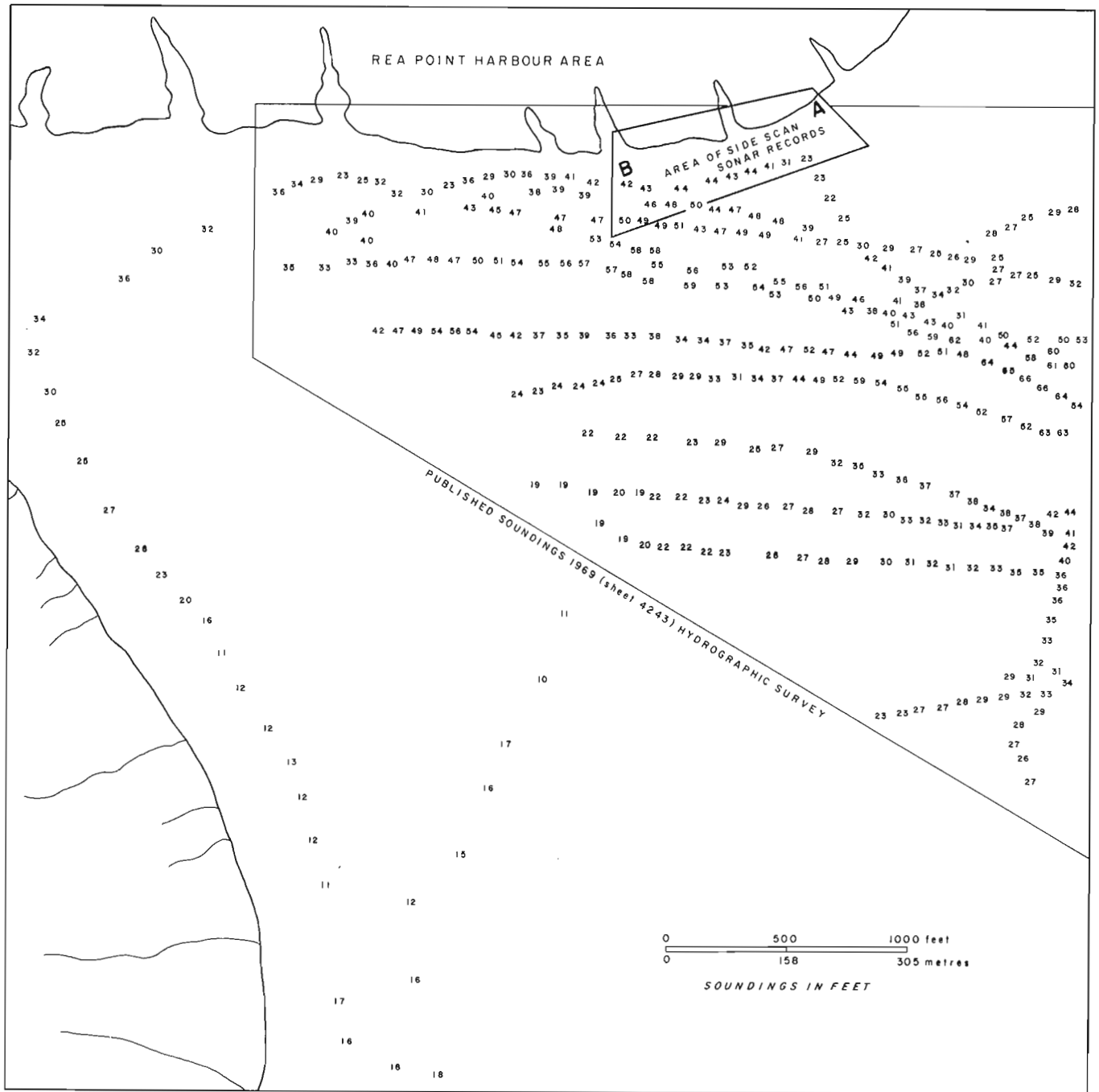


Figure 11.11. Published bathymetry and spot soundings at Rea Point harbour, Melville Island.

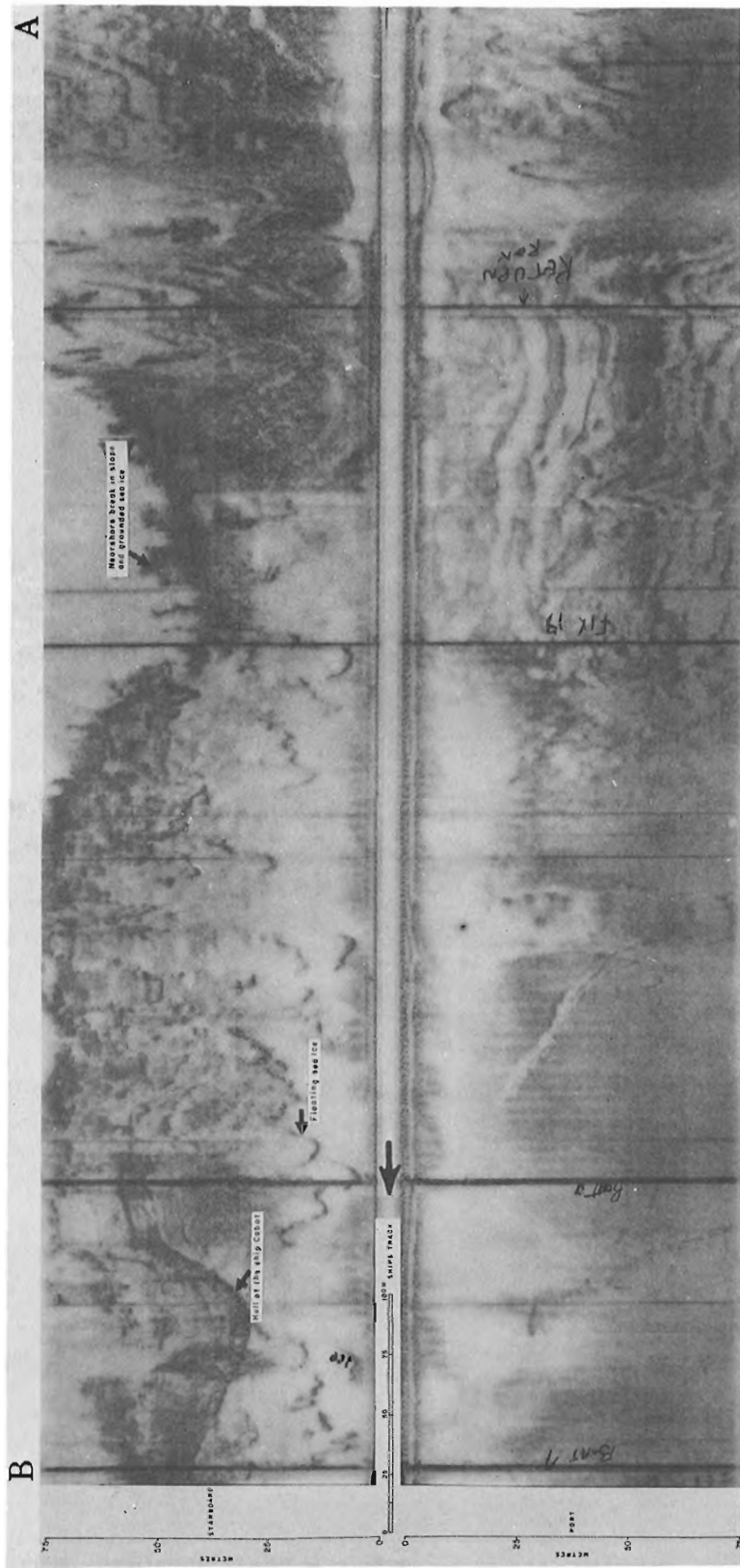


Figure 11. 12. Side-scan sonar record of the sea bed at Rea Point, Melville Island.



Figure 11.13

Two views of the kaimoo, composed of frozen swash, snow, and brash ice, formed during the storm of August 20, 1973, 'Frustration Bay', Melville Island. (GSC 165995, 165997)

offshore of the stern of the ship. The scour is 15 m (49 ft.) long at a water depth of 14 m (46 ft.) and probably was created by ice or the dragging of a ship's anchor. Much of the nearshore topography was masked on the sonar records by small cakes of floating sea ice. In general the nearshore was similar to the rest of the Melville Island coast which had been surveyed. Grounded sea ice, pitted bottom, and numerous criss-crossings of short ice scours were the most common nearshore features.

Some of the largest ice scours were observed farther south offshore of Consett Head. The largest linear scouring was estimated to be at least 60 m long and 4.5 m wide in water depth of 9 to 12 m. The approximate maximum relief of the scours was 1.8 m, based on microrelief recorded on the sounding records.

Considerably more scourings ran parallel to shore than were found in the nearshore area around King Point. Excluding the latter, the nearshore bottom was similar to the rest of the coastal areas examined in this study.

Storm Coastal Processes

Strong winds of up to 44 mph and air temperatures as low as -3.3°C were experienced on August 20 (Rea Point weather sheets, 1974). During the period August 19 to 20 the effect of winds on wave generation, sea-ice destruction, and backshore sediment transport were monitored.

Short choppy waves of two- to three-second period, formed by the north-northwest winds, pounded on the southern shore of 'Frustration Bay' throughout the

early morning of August 20, and by 0800 hours (C.D.T.) the swash and spray had frozen as a thin layer of new ice across the upper foreshore. During the same period, the sea-ice in the bay was broken down into brash ice and also was deposited along shore. The accumulation and freezing together of the brash ice, swash, and wave- and wind-entrained sediments at mean high tide limit created a kaimoo (Fig. 11.13a, b) A kaimoo is a form of icefoot found on the Alaskan coast which has been described previously by Rex (1964), Moore (1966), and Short and Wiseman (1974). The general absence of substantial quantities of brash ice and snow limited the development and size of the kaimoo; however, the dimensions did extend to 3 m wide and up to 0.3 m thick. A 500-ml sample of snow and ice from the kaimoo was collected to determine the amount of incorporated sediment. The results indicate that only 1.56 per cent of the sample was composed of organics and sediment. The incorporated sands were estimated, using a phi-size estimator (Hayes *et al.*, 1973), to be of +2.5 to +4.0 grain size.

Although the kaimoo was not permanent and had melted by August 22, its presence did illustrate the type of fast ice that probably occurs during final beach freezeup. Beach profile change during the storm was minor within 'Frustration Bay' because only locally generated waves struck the beach. Along the shoreline between 'Frustration Bay' and King Point delta, however, a small but distinct storm high-tide ridge was formed and some beach pitting occurred as a result of the melted kaimoo. In the backshore, sediments were entrained by the peak storm winds which transported and deposited them on the leeward side of clumps of vegetation, thus creating a microdune topography (Fig. 11.4). Eolian processes are not considered to be very important in terms of the overall coastal regime but nevertheless are one component of the storm processes.

Summary and Concluding Remarks

Low relief and sand beaches characterize the coastal area investigated along eastern Melville Island. The proximity of bedrock to the ground surface, e.g. north shore of 'Frustration Bay', suggests that the coastline in some locations is geologically controlled. Wave action was minimal, but in late August a storm was experienced which showed that significant wave action can scour despite the short wave fetches caused by the presence of sea ice.

The shoreline was outlined by a distinct break-in-slope which generally extended offshore at an angle of 4 to 5 degrees to depths of 12 to 15 m. Ripple marks and wave-formed beach cusps were common along the foreshore zone and bottom microrelief was most noticeable in water depths of 3.5 to 14.5 m, i.e. the near-shore break-in-slope. Sea-ice scourings were more common along the open coast of Melville Island than in 'Frustration Bay'. The latter area is protected from large pieces of multi-year ice by a shallow-water entrance. Along the open coast sea-ice scours commonly criss-crossed the nearshore platform as

short linear scars or as wedge-shaped depressions where the ice had grounded. The sea-ice scours were up to 60 m long, 12 m wide, and 2 m deep; however, observations were limited to the shallow nearshore area and a short section of the Melville Island coast.

The very fine silt to clay sediments sampled on the bottom of 'Frustration Bay' suggest some sedimentation from nearby rivers. The water temperature, of 'Frustration Bay' was below 0°C, much colder than expected, but the presence of sea ice and absence of warm fresh waters entering the bay in late August may account for the cooler temperatures.

It can be concluded from the experience of this field season that if a boat is to be used it must be portable, i.e. lightweight, yet durable so that movement through or over ice to open water areas can be achieved easily and quickly. The nature of the working platform dictates that the oceanographic instruments used be of minimum size and maximum portability. Below freezing water temperatures place a further restriction on many instruments.

Future research along the eastern Melville Island coast should include several transects running offshore in order to better document the nearshore break-in-slope and the presence of sea-ice scours farther offshore. In addition more observations of the relationship between the age and size of sea ice and its reflection on side-scan sonar records are needed. It also would be of interest to obtain a sediment core from the bottom of 'Frustration Bay' to gather information on rates of sedimentation and subbottom sediments.

References

- Hayes, M.O., Owen, E.H., Hubbard, D.K., and Abele, R.W.
1973: The investigation of form and processes in the coastal zone; in *Coastal Geomorphology*, ed. D.R. Coates, Binghamton State Univ., New York, p. 11-41.
- McLaren, P.
1974: Coastal erosion-sedimentation, southeast Melville and western Byam Martin Islands, District of Franklin; in *Report of Activities, Part A; Geol. Surv. Can., Paper 74-1A*, p. 267-268.
- Moore, G.W.
1966: Arctic beach sedimentation; in *Environment of Cape Thompson region, Alaska*, eds. N.J. Wilimousky and J.N. Wolfe, Oak Ridge (Tennessee), U.S. Atomic Energy Comm., Dep. PNE-481, p. 587-608.
- Pelletier, B.R. and Shearer, J.M.
1972: Sea bottom scouring in the Beaufort Sea of the Arctic Ocean; 24th Int. Geol. Congr., sec. 8, p. 251-261.

Reimnitz, E., Rodeick, C. A., and Wolf, S. C.
1974: Strudel scour: a unique arctic marine geologic phenomenon; *J. Sed. Petrol.*, v. 44, no. 2, p. 409-420.

Reimnitz, E., Barnes, P. W., and Alpha, T. R.
1973: Bottom features and processes related to drifting ice on the arctic shelf, Alaska; *U. S. Geol. Surv., Misc. Field Stud., Map MF-532*.

Rex, R. W.
1964: Arctic beaches, Barrow Alaska; in *Papers in Marine Geology, Shepard commemorative volume*, ed. R. L. Miller, The MacMillian Company, New York, p. 384-400.

Short, A. D. and Wiseman, W. J., Jr.
1974: Freezeup processes on Arctic beaches; *Arctic*, v. 27, p. 215-224.

Tozer, E. T. and Thorsteinsson, R.
1964: Western Queen Elizabeth Islands, Arctic Archipelago; *Geol. Surv. Can., Mem. 332*, 242 p.

APPENDIX

Instruments: Advantages and Disadvantages

1) Nineteen-foot pneumatic boat (manufacturer Zodiac):

Advantages: large floor space, relatively stable, portable, heavy-duty rubber withstands contact with mobile sea-ice; assembling of the boat becomes easier with repetition; has a shallow draft and is capable of working in shallow nearshore zones; easy to attach other instruments, etc. to the floor and sides of the boat.

Disadvantages: heavy - 440 lb when packed; when inflated it is awkward to move across land, is open, and subject to cold winds and sea spray; launching is hampered severely when sea ice grounds and accumulated along the shore; initial assembling of the boat is difficult.

Recommendations: use four or five inflatable boat rollers to launch the boat; use a smaller, e. g. 9-foot, pneumatic boat when only leads are available or when sea-ice concentrations prevent launching of the larger boat; set up a transparent wind screen at the bow of the boat to protect both researchers and instruments.

2) DE-719 fathometer (manufacturer Raytheon):

Advantages: portable, light; records are clear and continuous; resolution in both shallow and deep water is good; transducer can withstand contact with the numerous small pieces of ice common in Arctic waters; easy to mount system on a wooden platform which can be roped to the pneumatic boat.

Disadvantages: no subbottom capabilities; a large number of styluses sometimes are required.

Recommendations: place a small container with extra fuses and styluses within the recorder so that they are accessible during recording; mount the transducer such that it can be quickly pulled out of the water in case of an emergency and so nearshore profiles can be extended up the lower beach face at high tide.

3) Ponar bottom sediment grab sampler (distributor Wildco):

Both petite (20 lb.) and regular (45 lb.) ponar samplers were available for use but only the petite was needed.

Advantages: relatively light weight, portable, easy to use; works well in fine marine sediments; does not require a winch, but a small hand winch was used.

Disadvantages: in deep water the petite sampler tends to float, therefore may require some additional weights - for instance, a 3-lb. lead weight was added to sample a sand-silt sea bed; as with most grab samplers it requires many tries to obtain a sufficient sample from gravel sea beds.

Recommendations: carry extra weights for petite sampler; use a graduated rope and hand method rather than a winch when sampling in water depths less than 30 m (100 ft.); the petite sampler was found to be better than the larger sampler when sampling gravel-bedrock sea bottoms because of the weight difference since each sampler needed many attempts to obtain sufficient sediment.

4) In situ nearshore current sensor (manufacturer Marine Adivsers, Bendix Corporation):

Advantages: well protected and self-contained meter and recorder; works in water temperatures of less than 0°C; provides *in situ* nearshore current velocities of 0 to 5 knots; requires no external AC source, only batteries; works well in calm sea conditions.

Disadvantages: heavy; difficult to stabilize from a small pneumatic craft; current direction recorder not operative due to proximity to North Magnetic Pole, the extremely long vane was awkward to handle; not advisable to anchor current sensor offshore because of continual shifting of sea ice; if sea ice is present the sensor is difficult to lower over the boat because of the long vane.

Recommendations: use drogues with vanes set at various water depths to record current direction.

5) RS₅ *in situ* salinometer (manufacturer Beckman):

Advantages: portable, accurate, and easily readable; with factory alteration one can measure water temperatures as low as -2°C; easily used in the Arctic through seal holes, tidal cracks, or from small water craft to give water salinity and temperature; cable does not require a support line.

Disadvantages: very light probe can be deflected by strong water currents; difficult to determine when the probe has reached sea bottom; occasionally water freezes or ice particles collect in the probe; requires a more complicated initial calibration than some simpler salinometers; cable is heavy.

Recommendations: the cable could be placed on a take-up reel and the recorder mounted within the reel; a weight should be attached to the cable to give a better indication of when sea bottom is reached.

6) Side-scan sonar (manufacturer Klein Associates):

Advantages: once set up, the recorder provides a good picture of the nearshore bottom and is easy to

monitor; it is relatively portable and fits well on the floor or wooden platform across a 19-foot Zodiac boat; the fish is a bright yellow which is easily visible in the water; the fish is easily deployed over the side of the Zodiac; it is able to record floating and grounded sea ice, shoreline, nearshore break-in-slope, seals, sea-ice scour, and sea bed depressions and projections.

Disadvantages: the recorder is heavy and somewhat awkward to handle; the large size and weight limit its use to relatively large boats; the fish is subject to frequent groundings in the shallow near-shore; the cable is vulnerable if used in waters with sea-ice; the emulsion on the records continues to activate if the records are not dried soon after recording, which leads to severe fading of the records and loss of information; the recorder is vulnerable to damp, foggy weather and spray from waves in the small open-water craft.

Recommendations: carry extra plexiglass tail fins in case the original tail is lost; set up an area in camp where the records can be hung or laid out to dry each evening; secure a safety line from the fish tail and fish body to prevent loss of the tail if it hits the sea bottom.

Project 680047

J. Ross Mackay¹
Terrain Sciences Division

Ibyuk pingo, whose summit rises 48 m above sea level, is the best known pingo in Canada. When viewed from the settlement of Tuktoyaktuk, the pingo stands out prominently above the rolling tundra 6 km to the south-southwest. Unlike many other pingos, Ibyuk pingo does not appear to be old because it lacks a turf mat and a well developed tundra polygon system, and some slopes are unstable. As the rate of permafrost growth for a time span measured in hundreds or thousands of years is of scientific interest, field measurements were started in 1973 to determine if Ibyuk pingo is growing (Mackay, 1975). The purpose of this note is to discuss the measurement results and age interpretation for the 1973-75 period.

Description of Ibyuk Pingo

Ibyuk pingo rises nearly 47 m above the bottom flats of an old, drained lake. The lake flats, about 50 cm above sea level, are inundated during storm periods. The overburden above the ice core is 15 m thick, and if the overburden were returned to its original position, the present top would lie about 3 m below the lake flats (Müller, 1959, 1962). As pingos grow in residual ponds in the bottoms of drained lakes, the freezing plane at the bottom of permafrost at the initiation of pingo growth would then have been about 18 m below the lake flats. If the ice core is of pure ice, then the bottom of the ice core is about 65 m below the pingo summit. The maximum age of the pingo can be no more than 7000 to 10 000 years (Müller, 1962) as shown by the stratigraphy and radiocarbon dates of the overburden (Fyles *et al.*, 1972).

Survey Methods

In 1973, 8 antiheave bench marks (Mackay, 1973) were installed at least 2 m into permafrost (Fig. 12.1). Bench mark 1 (BM 1) was sited about 2.3 m above the lake flats and just above the driftwood level of storm surges. Bench marks 2 to 7 were in a straight line up the slope, with BM 7 on one of the four crater summits; BM 8 was on the highest summit. A theodolite (Wild T2 with ball centring and levelling device) was mounted on BM 3 and sights were taken to a target at BM 1, 2, 5, and 6. Bench marks 6, 7, and 8 were levelled (Wild NA2, optical micrometer, invar rod and struts). All surveys were repeated at least three times at each survey (in June, July, August 1973; early June 1974; early August 1975).

¹Department of Geography, University of British Columbia, Vancouver, B.C. V6T 1W5

Previous measurements of growing pingos (Mackay, 1973) have shown that the periphery remains stable, with growth increasing from the periphery to the summit. It was impractical to establish a reference datum on higher land, beyond the lake flats surrounding Ibyuk pingo, so BM 1 has been used as a zero datum. If Ibyuk pingo is growing at BM 1, which seems unlikely, the effect would be to underestimate any growth obtained. The 1973-75 surveys, using BM 1 as datum, show no growth for BM 2; 0.2 cm/yr for BM 3; 0.4 cm/yr for BM 4; 0.4 cm/yr for BM 5; 0.8 cm/yr for BM 6; 1.5 cm/yr for CM 7; and 2.8 cm/yr for BM 8. The increase in the rate of growth from the periphery to the summit is evident.

Interpretation

The downward growth of permafrost on a drained lake flat or the upward growth of the summit of a pingo can be estimated (Mackay, 1973) from Neumann's equation:

$$(1) \quad z = b \sqrt{t}$$

where z is the depth of permafrost on a lake flat or the height of the pingo summit above the freezing plane; b is a soil constant for the specific site, temperature, and ground conditions; and t is time. The annual freezing increment is then:

$$(2) \quad \Delta z = \frac{b}{2 \sqrt{t}} \quad (t \text{ in years})$$

From equations (1) and (2):

$$(3) \quad t = \frac{z}{2\Delta z}$$

$$(4) \quad b = \sqrt{2z \cdot \Delta z}$$

If the ice core of Ibyuk pingo is of pure ice, $z \sim 65$ m. For 1973-75 at BM 8, the fastest growing site, $\Delta z \sim 2.8$ cm/yr. The largest value for the soil constant b , under similar site, temperature, and ground conditions near Tuktoyaktuk, is $b \sim 170$ cm yr^{-1/2}. Substitutions of the above into equations (1), (2), (3), and (4) give:

- a. from equation (1), age (t) ~ 1460 years
- b. from equation (2), age (t) ~ 920 years
- c. from equation (3), age (t) ~ 1160 years
- d. from equation (4), $b \sim 190$ cm yr^{-1/2}

The above data suggest that Ibyuk pingo may be about 1000 years old or the growth may date back to the 10th century A.D.

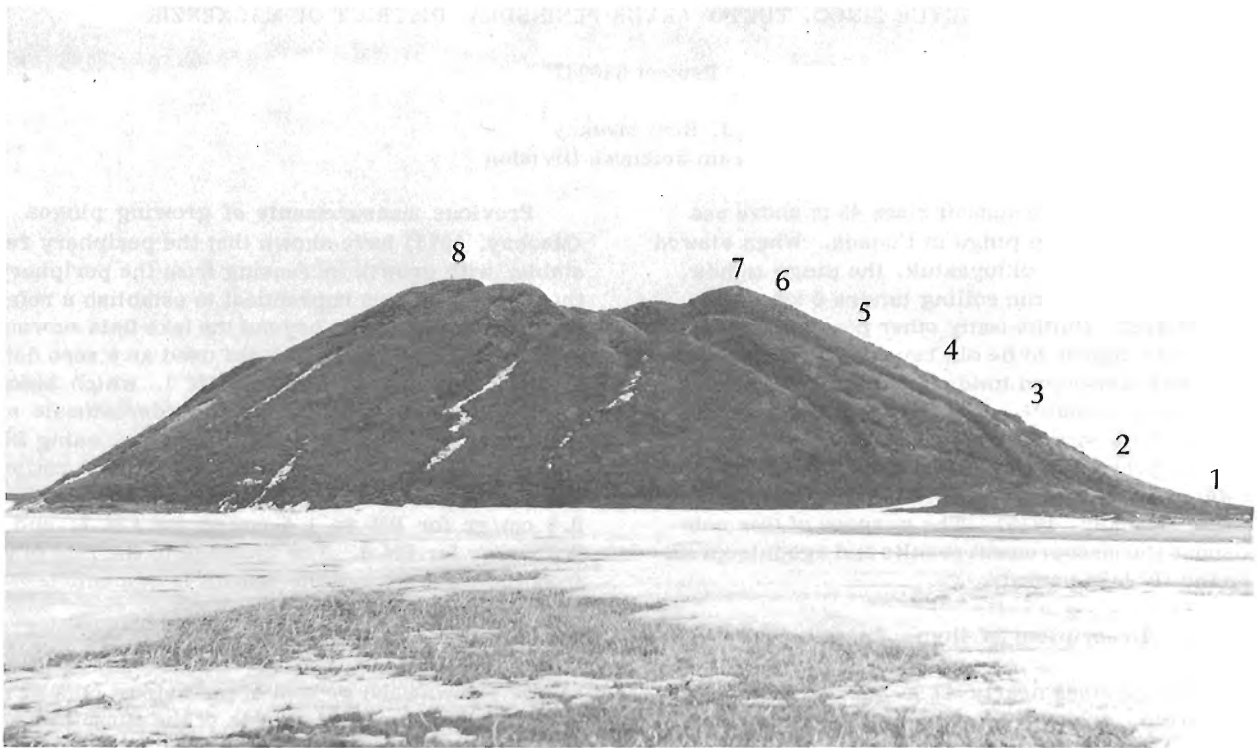


Figure 12. 1. Ibyuk pingo showing the lake flats of the old drained lake in the foreground and the locations of the bench marks.

Permafrost Creep

Ibyuk pingo is so large that permafrost creep must be considered in any attempt to estimate the age from growth rates. It is well known that permafrost will deform under a load and that viscoplastic flow is possible on a slope (Tsyrovich, 1975, p. 134). McRoberts (1975) has presented a model for deformations due to secondary creep on permafrost slopes. Since Ibyuk pingo can be viewed as an ice hill about 50 m high, loaded with a 15 m frozen overburden, the shear stresses would seem high enough to result in slow downslope creep of both overburden and ice. If such creep occurs, then the age estimates based upon growth rates may require modification.

Conclusion

Precise surveying of 8 bench marks on Ibyuk pingo for the period 1973-75 shows that the pingo is growing, with the growth rate increasing from the periphery to the summit. According to the 1973-75 growth rate, Ibyuk pingo is about 1000 years old, but the actual age could be several hundred years younger or older. As the drained lake bottom flats around Ibyuk pingo are only about 50 cm above sea level, lake drainage probably was caused by coastal retreat. Because the thickness of permafrost was at least 20 m on the adjacent lake flats a considerable time elapsed following lake drainage before pingo growth commenced. Permafrost on the surrounding lake flats is probably at least 150 m deep. There is a strong probability that the overburden and ice core of Ibyuk pingo deform and slowly creep, but no data are available to confirm or deny this opinion.

References

- Fyles, J. G., Heginbottom, J. A., and Rampton, V. N.
1972: Quaternary geology and geomorphology, Mackenzie Delta to Hudson Bay; XXIV Int. Geol. Congr., Excursion A-30, Montreal, 23 p.
- Mackay, J. R.
1973: The growth of pingos, western Arctic coast, Canada; *Can. J. Earth Sci.*, v. 10, p. 979-1004.
1975: Ice segregation at depth in permafrost; in *Report of Activities, Part A; Geol. Surv. Can., Paper 76-1A*, p. 287-288.
- McRoberts, E. C.
1975: Some aspects of a simple secondary creep model for deformations in permafrost slopes; *Can. Geotech. J.*, v. 12, p. 98-105.
- Müller, F.
1959: Observations on pingos (trans. from German); Ottawa, NRCC TT-1073, 1963, 117 p.
1962: Analysis of some stratigraphic observations and radiocarbon dates from two pingos in the Mackenzie Delta area, N. W. T.; *Arctic*, v. 15, p. 278-288.
- Tsyrovich, N. A.
1975: *The Mechanics of Frozen Ground* (trans. from Russian); McGraw Hill, New York, 426 p.

L. V. Hills¹ and R. M. Bustin¹
Terrain Sciences Division

Balkwill and Bustin (1975) reported the presence of *Picea banksii* from Axel Heiberg Island (79°53'N, 88°15'W). Examination of 64 complete or partial cones from this locality indicates that they exhibit a higher degree of morphologic variability than do those from Banks Island (Hills and Ogilvie, 1970). This variability is expressed in a smaller size range, 42 to 99 mm as compared to 63 to 110 mm for northwestern Banks Island, and a conspicuous basal taper to the cones. In general the cone scale morphology is similar to that of *P. banksii*.

Hills and Ogilvie (1970) stated that the only difference between *Picea banksii* and the extant species *Picea glauca* is the larger cone length of the fossil (63 to 110 mm as compared to 30 to 67 mm for *P. glauca*); the latter species could have evolved from the former by reduction in the length of the cone. Two of the specimens from Axel Heiberg Island are within the 40 to 50 mm length range typical of *Picea glauca*. They are assigned here to *P. banksii* because they appear to represent the shorter cones of a single species as indicated by a unimodal length distribution. Unfortunately too few complete specimens are available to demonstrate conclusively this unimodality. The specimens are significant in that if they are a single species population then they represent one in which the cone length overlaps both that of the fossil (*Picea banksii*) and that of the extant species (*Picea glauca*).

Regional palynologic and paleobotanic studies indicate that during upper Beaufort time, coniferous forests occupied the area at least as far north as Prince Patrick Island (evidence from northwestern Banks Island (Hills, 1969) and Prince Patrick Island). Unpublished palynologic data indicate a marked increase in ericaceous plants such as *Ledum*, as well as in *Betula* and *Alnus*, on northern Ellef Ringnes Island in comparison to Banks Island. Well preserved plant macrofossils including *Picea banksii*, *Pinus itelmenorum*, *Pinus* cf. *nagajevii*, *Ledum*, *Myrica*, *Betula*, and *Alnus* (Hills and Matthews, unpubl. data, 1973, 1975) have been recovered from Meighen Island (Hills and Matthews, 1974). These assemblages suggest that Ellef Ringnes Island and Meighen Island were at or near the treeline during Beaufort time.

The presence of *Picea banksii*, *Pinus itelmenorum*, and *P.* cf. *nagajevii* on Meighen Island indicates affinities with the Beaufort flora from Banks Island. Similarly, the presence of abundant cones of *Picea banksii* on Axel Heiberg Island indicates that the Beaufort Formation there is correlative with the upper member of the Beaufort Formation on northwestern Banks Island. If these correlations are correct, then the interpretation to be placed on the northward change

of the Beaufort Formation flora is that it represents differences in latitude as opposed to differences of age. The latitudinal position of the Axel Heiberg Island locality is similar to that of both Meighen and Ellef Ringnes islands; thus during Beaufort time it too was probably close to the treeline. The morphologic variation of the *Picea banksii* cones from Axel Heiberg, therefore, could be interpreted as the product of late Miocene environmental stress. Selection pressures associated with this condition could have resulted in the evolution of the shorter cones, characteristic of *Picea glauca*.

The basal taper (Fig. 13.1a — 13.1c) exhibited by the specimens from Axel Heiberg Island is significant in that this feature and the cone size cause them to resemble cones of *Picea breweriana* S. Wats (Fig. 13.1f — 13.1g). This similarity suggests that *P. breweriana*, a timberline species restricted to the Siskiyou Mountains and neighbouring coast ranges in southern Oregon and northern California (Harlow and Harrar, 1958), also may have developed as a treeline variant of *P. banksii*. If so, migration of the *P. breweriana* form from its northern origin would have occurred during latest Tertiary (Pliocene) and Quaternary times.

Single cones of *Metasequoia* and *Alnus*, as well as a *Carya* seed, also were recovered from these deposits. The flora suggests that the deposits are probably late Miocene in age (Hills and Ogilvie, 1970; Hills *et al.*, 1974; Wolfe and Leopold, 1967) and that they are probably equivalent to the upper part of the Beaufort Formation on northwestern Banks Island.

Two probable senior synonyms of *Picea banksii* Hills & Ogilvie recently have come to light. Heer (1868) described an undoubted spruce species (*Pinus (Abies) Mac Clurii*) from northwestern Banks Island. The specimens which he illustrates resemble more closely the Axel Heiberg material than the typical specimens from Banks Island. There can be little doubt, however, that Heer's species is conspecific with *P. banksii*. Prior to formally placing *P. banksii* in synonymy, attempts will be made to locate and examine the two specimens described by Heer, which according to him are in: "der geolog. Survey von London" and "der Dubliner Sammlung" (Heer, 1868, p. 186).

Examination of cones of the second species, *Picea anadyrensis* Krystoph. from the northern Pekul' neiveyemsk Suite, Anadyr River, Siberia, indicates that the species is conspecific with *P. banksii* and in all probability is also a junior synonym of Heer's species. In view of the fact that illustrated specimens assigned to *P. anadyrensis* apparently exhibit greater variability in size and morphology than do specimens from the Canadian Arctic, indiscriminate reassignment of this species of Heer's could result in further confusion. Reassignment, therefore, will await a thorough examination of the Russian literature.

¹Department of Geology, University of Calgary, Calgary, Alberta



a



b



c



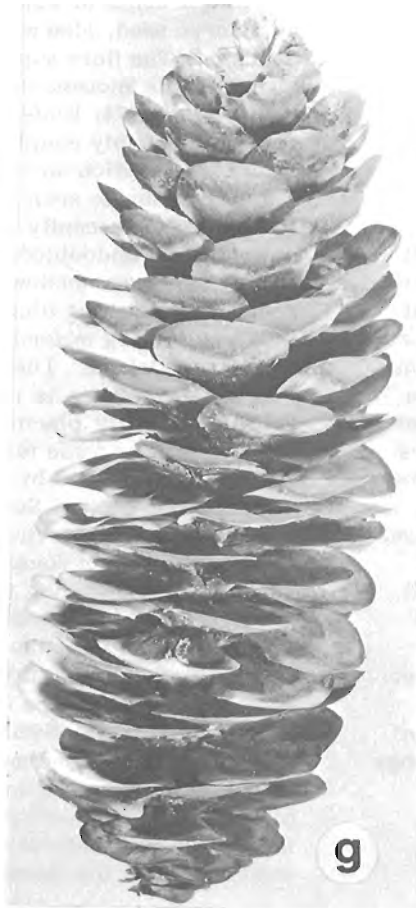
d



e



f



g



h

Plate 13. 1 (opposite)

Figs. a-f. *Picea banksii* cones illustrating the range in size and basal morphology x 1.

Fig. a GSC specimen no. 42545.

Fig. b GSC specimen no. 42546.

Fig. c GSC specimen no. 42547.

Fig. d GSC specimen no. 42548.

Fig. e GSC specimen no. 42549.

Fig. f GSC specimen no. 42550.

Fig. g *Picea breweriana* S. Wats. Typical cone illustrating scale morphology and basal taper.

Fig. h Same cone as in fig. g, basal view.

References

- Balkwill, H. and Bustin, R. M.
1975: Stratigraphic and structural studies; central Ellesmere Island and eastern Axel Heiberg Island, District of Franklin; in Report of Activities, Part A; Geol. Surv. Can., Paper 75-1A, p. 513-517.
- Harlow, W. M. and Harrar, E. S.
1958: Textbook of Dendrology; McGraw Hill, New York, Toronto, London, 561 p.
- Heer, O.
1868: Die fossile Flora Polarländer; in Flora Fossilis Arctica; F. Schulthess, Zürich, 192 p.
- Hills, L. V.
1969: Beaufort Formation, northwestern Banks Island, District of Franklin; in Report of Activities; Part A; Geol. Surv. Can., Paper 69-1A, p. 204-207.
- Hills, L. V., Klován, J. E., and Sweet, A. R.
1974: *Juglans eocinerea* n. sp., Beaufort Formation (Tertiary), southwestern Banks Island, Arctic Canada; Can. J. Bot., v. 52, no. 1, p. 65-90.
- Hills, L. V. and Matthews, J. V., Jr.
1974: A preliminary list of fossil plants from the Beaufort Formation, Meighen Island, District of Franklin; in Report of Activities, Part B; Geol. Surv. Can., Paper 74-1B, p. 224-226.
- Hills, L. V. and Ogilvie, R. T.
1970: *Picea banksii* n. sp., Beaufort Formation (Tertiary), Banks Island, Arctic Canada; Can. J. Bot., v. 48, no. 3, p. 457-464.
- Wolfe, J. A. and Leopold, E. B.
1967: Neogene and Early Quaternary vegetation of northwestern North America and northeastern Asia; in The Bering Land Bridge; ed. D. M. Hopkins, Stanford Univ. Press, Stanford, California, p. 193-206.

Project 750034

J. L. Jambor¹

Regional and Economic Geology Division

Tochilinite, $6\text{Fe}_{0.9}\text{S}_{0.5}(\text{Mg}, \text{Fe})(\text{OH})_2$, was first reported as an unnamed mineral from the Muskox Intrusion, N.W.T. (Jambor, 1969), and subsequently from the Lizard ultramafics in Cornwall, England (Clark, 1970). The mineral was named by Organova *et al.* (1971), who described its occurrence in serpentinites in the U. S. S. R. Tochilinite was also recognized as thin coatings on fractures in the nickel-bearing ultramafic intrusion of Dumont Nickel Corporation in the Amos area, Quebec (Jambor, 1975). A microprobe analysis of the Amos-area mineral is reported here, together with results obtained for a new occurrence in Pennsylvania.

Crystal-structure studies by Organova *et al.* (1972, 1973a, b, 1974) have shown that tochilinite consists of alternating "brucite" and "sulphide" layers. The latter are iron-deficient and have vacancies distributed in a regular pattern. In the variety "tochilinite-I", sulphide and brucite layers have the same unit cell, whereas in "tochilinite-II" the two layers have different cells. The distribution of the vacancies in the sulphide layer also differs in the I and II varieties, but the vacancies are always present (Organova *et al.*, 1974). This deficiency is taken into account in the sulphide molecule such that tochilinite has the general formula $6\text{Fe}_{0.9}\text{S}_{0.5}(\text{Mg}, \text{Fe})(\text{OH})_2$, or $2\text{Fe}_{0.9}\text{S}_{1.67}(\text{Mg}, \text{Fe})(\text{OH})_2$. Tochilinite I is $6\text{Fe}_{0.9}\text{S}_{0.5}(\text{Mg}_{0.7}\text{Fe}_{0.3})(\text{OH})_2$, and tochilinite-II is $6\text{Fe}_{0.8}\text{S}_{0.5}(\text{Mg}_{0.7}\text{Fe}_{0.3})(\text{OH})_2$.

Dumont Tochilinite

Microprobe analysis of the Dumont material is given in Table 14.1. The ideal composition $6\text{Fe}_{0.94}\text{S}$ for the sulphide layer (Organova *et al.*, 1973a) was assumed, and the remainder of the Fe was allocated to the brucite layer. This distribution yields a calculated (OH) of 20.99 weight per cent, and a total of 98.58 per cent. Additional cations were not detected, and thus the unadjusted total gives a formula of $2\text{Fe}_{0.94}\text{S}_{1.82}(\text{Mg}_{0.73}\text{Fe}_{0.27})(\text{OH})_2$. The value 1.82 for the brucite layer exceeds the theoretical 1.67, but similar results have been obtained by Organova *et al.*, who have attributed the excess to Fe and other hydroxide mixtures detected by means of electron diffraction patterns.

Pennsylvania Tochilinite

Samples containing tochilinite were collected by Mr. Byron Brookmeyer, an amateur mineral collector from Blue Ball, Pennsylvania. The material was examined initially by Robert C. Smith II, Economic Geochemist with the Pennsylvania Department of Environmental Resources. Dr. Smith recognized the similarity of the Muskox and Pennsylvania minerals, and he and Mr. Brookmeyer kindly offered material for further studies. Mr. Brookmeyer subsequently provided several specimens which have been donated to the Systematic Reference Series, National Mineral Collection.

Table 14.1. Microprobe analyses of tochilinite and related phases.

wt. %	1 Dumont, Amos, P.Q.	2 Penna. (Fig. 1)	3 Penna. (Fig. 2)	4 Penna.	5 Penna. Area 2	6 Penna. (Figs. 3, 4) Area 3	7 Area 1
Fe	44.92	34.64	35.27	35.44	33.61	9.77	8.86
Mg	10.94	13.23	13.24	14.37	14.13	21.56	22.26
Al	--	3.96	4.27	4.17	4.14	3.70	3.93
S	21.73	24.69	24.33	24.36	23.21	5.41	4.91
	77.59	76.52	77.11	78.34			
Si					0.97	13.38	13.75
					76.06	53.82	53.71

Analysis in column 1 by A. G. Plant, G.S.C.; remainder by D. R. Owens, CANMET. Analysis in column 4 is of material with a bronze colour; remainder are black. Energy-dispersive analysis indicates that Co, Mn, Ni and other cations are not present.

¹Present address: CANMET, 555 Booth Street, Ottawa.

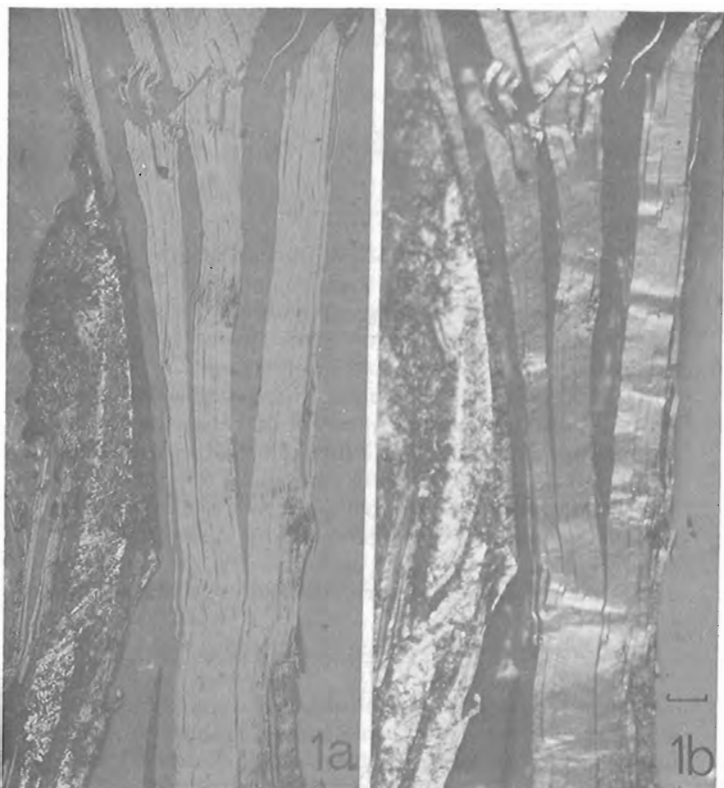


Figure 14.1. Toichilinite from Pennsylvania, polished section, reflected light; (a) analyzed grains (Table 14.1, column 2) in plain light; (b) same area showing the kinks evident with partly crossed nicols. Bar scale = 0.03 mm.

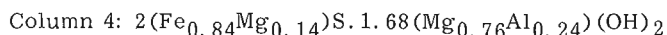
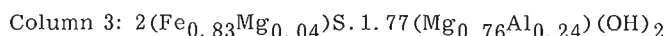
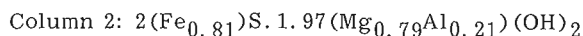
The Pennsylvania toichilinite occurs in calcite-healed breccia in limestone of the Cambrian Elbrook Formation at the Grace mine, Morgantown, Berks County. Although the occurrence is unusual in that it is not in ultramafic rocks, a Triassic diabase sheet lies about 50 feet below the collecting site. In the samples available, toichilinite is associated with clear and white calcites, some of which are coarse euhedral crystals. Black metallic masses of toichilinite up to 5 by 7 mm are in the calcite, and small amounts of the sulphide coat the carbonate crystals and can be scraped off in minute sheets resembling black foil paper. Some of the coatings have a distinctly bronze cast.

Although the bulk of the toichilinite is massive, several areas of the specimens have fibrous, partly radiating aggregates which, under a binocular microscope, can be seen to be groups of elongate, paper-thin tabular grains. These are up to 2 mm long and are striated parallel to the elongation. One large grain is almost cylindrical, about 3 mm long by 1 mm in diameter, and seems to consist of a bundle of curved plates; in cross-section the bundles are reminiscent of the appearance of a rolled newspaper viewed on end.

Both the massive and fibrous varieties are sectile and crinkle readily (Figs. 14.1, 14.3). The thin tablets of fibres can be bent repeatedly over a 180° arc before parting cleanly, normal to the elongation. Plucking during polishing is a severe problem except for grains mounted normal to the layering.

Microprobe analyses (Table 14.1) of the grains shown in Figures 14.1 and 14.2 gave similar results. The pronounced anisotropic banding of material in

Figure 14.2 is an optical rather than a compositional variation. Grains of material having a bronze cast were mounted in a separate polished section and gave similar results (Table 14.1). The average of the three analyses gave 4.1 weight per cent Al, or 11.86 weight per cent $\text{Al}(\text{OH})_3$. Gibbsite was not detected in any of the several X-ray powder diffraction patterns of the material. However, if it is assumed that $\text{Al}(\text{OH})_3$ is present, subtraction of this component and summation to 100% yields the formulas $6(\text{Fe}_{0.8})\text{S}.\text{Mg}_{4.6}(\text{OH})_{7.3}$, $6(\text{Fe}_{0.8})\text{S}.\text{Mg}_{4.3}(\text{OH})_{6.9}$ and $6(\text{Fe}_{0.8})\text{S}.\text{Mg}_{4.67}(\text{OH})_{6.4}$ for columns 2, 3, and 4 (Table 14.1), respectively. Although the low (OH) values suggest that some Mg could be shifted to the sulphide layer, the brucite layer is itself lower than the theoretical value. However, if it is assumed that Al is an integral part of the brucite layer, the resulting formulas are as follows:



The formula obtained from the results in column 4 is unsatisfactory because the sum of Fe + Mg is 0.98 in the sulphide layer. However, formulas obtained from the analyses in columns 2 and 3 are appropriate and are remarkably consistent even though the contents of the brucite layer are high. It may be that only part of the Al is present as admixtures, and part is incorporated in the structure. That the former occurs is clearly evident from the remainder of the analyses given in Table 14.1. The analysed area (Fig. 14.3) shows distinct compositional zoning: the optically darker bands are rich in silica (Fig. 14.4) and low in sulphur. A powder X-ray diffraction mount of the analyzed area gave a weak, serpentine-type pattern. The increase in analytical Mg and Si, the lack of significant increase in Al, and the absence of a 14 Å line in the powder diffraction pattern lend support to the identification of the silicate as a serpentine mineral rather than a chlorite. Thus, it is concluded that the zones material shown in Figure 14.3 consists of intimately interlayered toichilinite and serpentine.

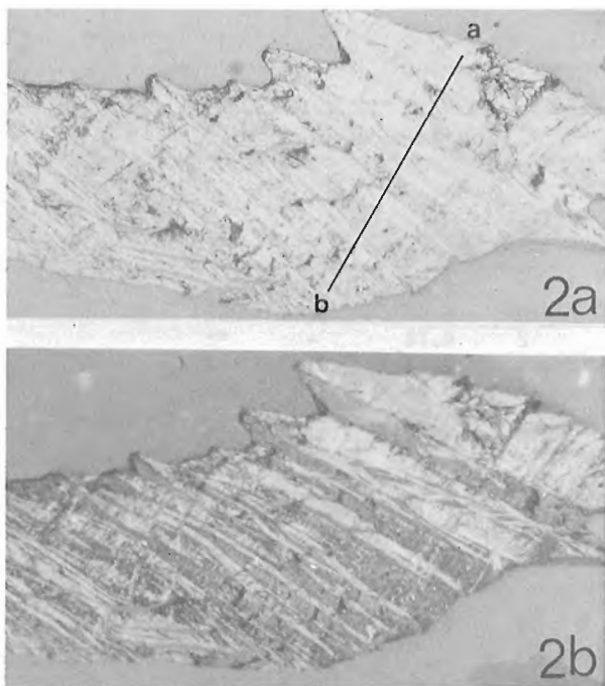


Figure 14.2. Tochilinite, Pennsylvania, in plain light (2a) and with partly crossed nicols (2b). A microprobe scan across a-b confirmed the compositional homogeneity of the grain, for which analytical results are listed in Table 14.1, column 3. Line a-b = 0.25 mm.

X-Ray Data

Numerous powder X-ray diffraction patterns were prepared from the Pennsylvania and Amos-area tochilinites. Data obtained from 114.6 mm Gandolfi and Debye-Scherrer films are listed in Table 14.2. Although preferred orientation effects hamper reproducibility, ground samples of tochilinite yield diffraction patterns which are more uniform but have fewer lines. It is possible that grinding disorders the structure of the mineral.

The powder data in Table 14.2 were indexed satisfactorily by using the cell dimensions of tochilinite-II as a starting point and subsequently using several lines for least-squares refinements. The final results are not much different from the cell dimensions reported by Organova *et al.* (1974) for tochilinite-I:

$$a = 5.37, b = 15.60, c = 10.72 \text{ \AA}, \alpha = \gamma = 90^\circ, \beta = 95^\circ.$$

Two of the best free-standing tablets of the Pennsylvania tochilinite were examined by the X-ray precession method. Both crystals gave diffuse, streaky, multiple diffraction spots which indicated that the grains were not single crystals. The O-level layer lines for both crystals were similar, and diffraction spots along the morphological elongation indicate that this axis is 10.8 \AA in one orientation, and 10.4 \AA in the plane normal to it. Diffraction rows normal to the elongation and

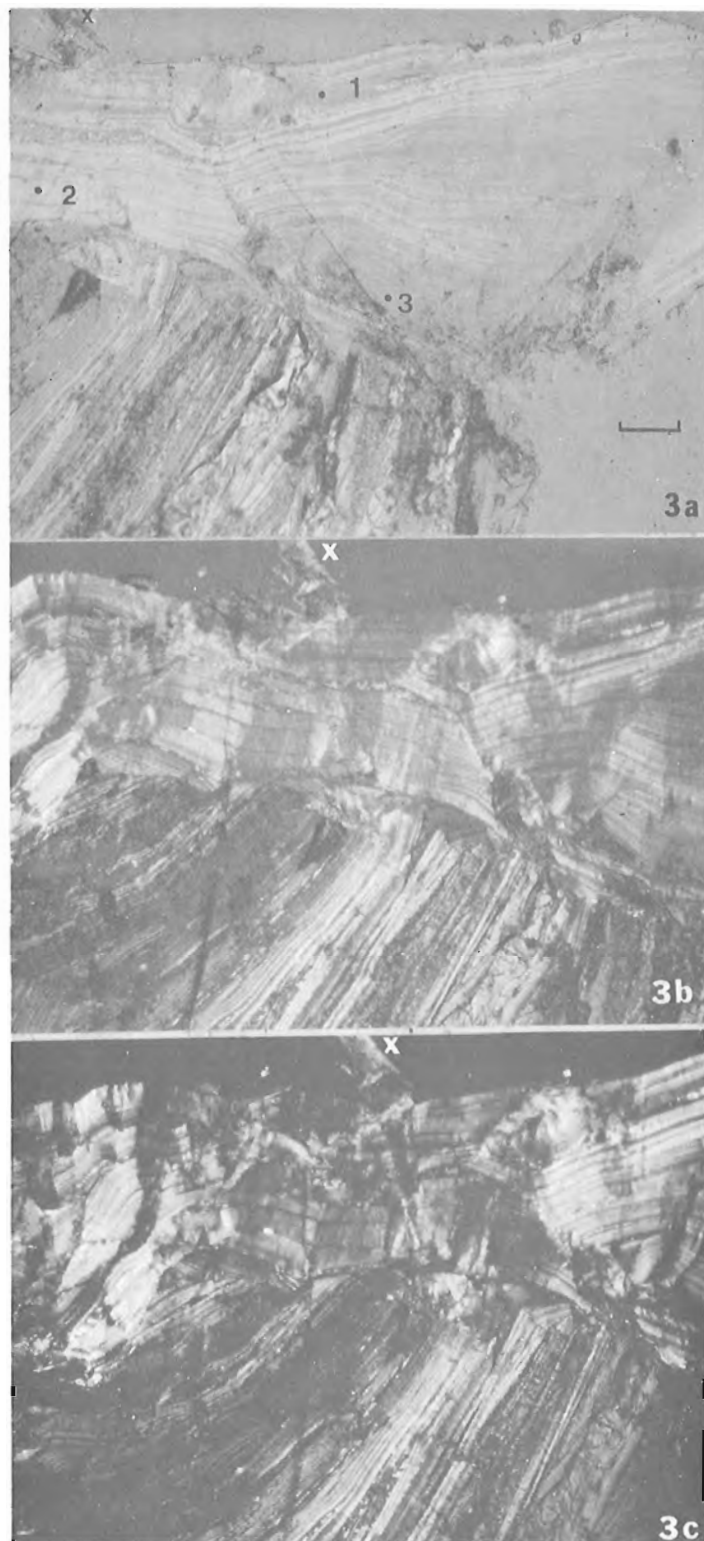


Figure 14.3. Tochilinite, Pennsylvania, in plain light (3a) and with partly crossed (3b) and crossed (3c) nicols, showing pronounced compositional zoning, kinks, and strong anisotropism. Common reference point is marked by an X. Areas 1, 2, and 3 in photo 3a mark areas analyzed (Table 14.1, columns 5, 6, 7). The darker zones at spots 1 and 3 are Si-rich. Bar scale = 0.05 mm.

Table 14.2.

Powder X-ray diffraction patterns of tochilinite.

Pennsylvania						Amos Area, Quebec			
1		2		d_{calc}	hkl	I_{est}	d_{meas}	d_{calc}	hkl
I_{est}	d_{meas}	I_{est}	d_{meas}						
4	10.84	6	10.87	10.85	001	7	10.83	10.88	001
10	5.41	10	5.41	5.43	002	10	5.43	5.44	002
1	4.13	1	4.12	-	**	2	4.14	-	**
-	-	-	-	-	-	<< $\frac{1}{2}$	3.83	3.85	$\bar{1}12$
1	3.61	-	-	3.62	003	2	3.64	3.63	003
$\frac{1}{2}B$	3.46	-	-	3.45	131	-	-	-	-
-	-	-	-	-	-	2	3.30	3.29	023
$\frac{1}{2}$	3.15	-	-	{3.16 3.15}	{042 $\bar{1}32$ }	-	-	-	-
< $\frac{1}{2}$	2.96	-	-	-	--	-	-	-	--
-	-	1	2.82	2.83	113	2	2.71	2.72	004
2	2.625	2	2.623	2.633	$\bar{1}51$	-	-	-	-
-	-	-	-	-	-	2	2.593	{2.597 2.587}	{060 151}
1	2.562	-	-	2.561	024	2	2.451	2.453	$\bar{1}52$
$\frac{1}{2}$	2.336	-	-	2.337	062	-	-	-	-
1	2.307	1	2.307	{2.317 2.314}	{202 114}	$\frac{1}{2}$	2.310	2.320	114,202
-	-	-	-	-	-	$\frac{1}{2}$	2.243	2.238	$\bar{2}03$
5	2.227	4	2.223	2.224	044	$\frac{1}{2}$	2.177	2.177	005
< $\frac{1}{2}$	2.103	-	-	2.106	063	-	-	-	-
$\frac{1}{2}$	2.072	-	-	2.065	203	-	-	-	-
2	2.051	1	2.059	2.054	$\bar{1}15$	-	-	-	-
-	-	$\frac{1}{2}$	1.988	{1.990 1.986}	{242 204}	< $\frac{1}{2}$	1.989	{1.993 1.988}	{242 204}
4	1.861	3	1.856	1.858	260	< $\frac{1}{2}$	1.921	1.926	224
$\frac{1}{2}$	1.814	$\frac{1}{2}$	1.808	1.809	006	4	1.838	1.833	135
3	1.751	2	1.748	{1.757 1.747}	{205 $\bar{1}16$ }	$\frac{1}{2}$	1.816	1.814	006(+)
1	1.616	$\frac{1}{2}$	1.618	1.618	205(+)	< $\frac{1}{2}$	1.714	1.715	$\bar{2}25$
2	1.533	2	1.535	1.538	0.10.1(+)	-	-	{1.561 1.558 1.555}	{ $\bar{2}06$ 0.10.0 007}
1	1.354	1	1.355	1.357	008(+)	3	1.560	-	-
-	-	-	-	-	-	1	1.358	1.360	008(+)
-	-	-	-	-	-	1	1.321	1.323	157(+)
-	-	-	-	-	-	2	1.300	1.298	0.12.0(+)

Column 1 data obtained from coarse, unground material, 114.6 mm Gandolfi camera; column 2 data from ground material, 114.6 mm Debye-Scherrer camera. X-ray mounts for column 3 made directly from powder obtained by scratching specimen surface with a needle; data from 114.6 mm Debye-Scherrer films. Columns 1-3: Co/Fe radiation, B=broad line

Pennsylvania tochilinite indexed with $a=5.35$, $b=15.54$, $c=10.89\text{\AA}$, $\beta=94.807^\circ$. Amos tochilinite indexed with $a=5.35$, $b=15.58$, $c=10.92$, $\beta=94.726^\circ$.

** Also recorded by Organova *et al.* (1971) who attribute the line to an epitaxial sulphide phase.

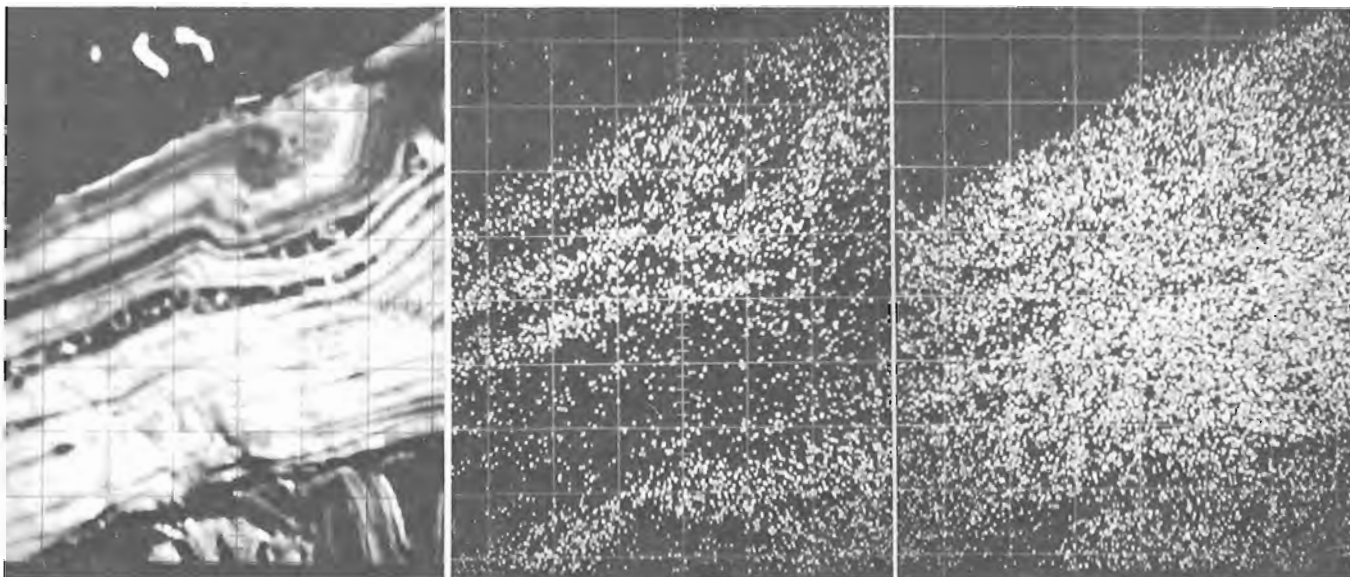


Figure 14. 4. Electron back-scatter image (left photo) of area slightly left of spot 1 in Figure 14. 3a. Middle photograph shows X-ray image for SiK α , and right side photo is for SK α .

along the broad, flat face of the crystals are at 5.38 Å, and the above values therefore correspond to the $hk0$ net of tochilinite. In the Pennsylvania material, the a^*b^* net is at 90°. According to Organova *et al.* (1974), microcrystals of tochilinite are elongate along b , with $a = 5.37$, $b = 15.60$ Å; the corresponding morphology and O -level dimensions for Pennsylvania material are $a^* = 5.38$, $b = \sim 10.6$ Å ($= 2/3 \times 15.6$). Additional spots, some of which are strong, also appear on the $hk0$ net of the Pennsylvania patterns. These spots form a hexagonal array with $d = 2.70$, corresponding to $a = 3.1$ Å as in brucite.

Precession photographs of the Ok_l net have multiple but relatively sharp, diffraction spots along OkO (10.8 Å); all others are streaky and multiple so that the lattice cannot be outlined with confidence. However, strong diffraction rows normal to b^* have $d = 2.66$ Å, and very weak supercell streaks suggest that this dimension is at least 2×2.66 Å. A 48-hour exposure using MoK α radiation confirmed the 5.32 Å for lkl , but again there were extremely weak, uncertain indications of supercell streaking, possible 4×5.32 Å. A final observation is that if the Ok_l diffraction spots are in an orthogonal array, then b^* appears to be 2×10.8 Å, with $k = 2n$. A possible alternative lattice is $b^* = 10.8$ Å and $b^* \wedge c^* = 96^\circ$.

Acknowledgments

The writer is grateful to Dr. R.C. Smith and Mr. B. Brookmyer for drawing attention to, and providing samples of, the Pennsylvania mineral. Powder diffraction and single crystal X-ray patterns of this material were kindly provided by E.J. Murray and J.M. Stewart of CANMET. Microporobe analyses of the Quebec and Pennsylvania tochilinites were done by A.G. Plant of the Geological Survey and D.R. Owens of CANMET.

References

- Clark, A.H.
1970: A probable second occurrence of Jambor's "fibrous iron sulphide"; *Am. Mineral.*, v. 55, p. 283-284.
- Jambor, J.L.
1969: Coalingite from the Muskox Intrusion, Northwest Territories; *Am. Mineral.*, v. 54, p. 437-447.
1975: Secondary minerals in an ultramafic intrusion, Amos area, Quebec; in *Report of Activities, Part A, Geol. Surv. Can., Paper 75-1A*, p. 261-263.
- Organova, N.I., Genkin, A.D., Drits, V.A., Dmitrik, A.L. and Kuzmina, O.V.
1971: Tochilinite-novyi sulfid-gidrookisel zheleza i magniya (Tochilinite: a new sulfide hydroxide of iron and magnesium); *Zap. Vses. Mineral. Obshch.*, v. 4, p. 477-487.
- Organova, N.I., Drits, V.A., and Dmitrik, A.L.
1973a: Structural study of tochilinite. Part 1. The isometric variety; *Soviet Phys. - Cryst.*, v. 17, p. 667-671.
1973b: Structural study of tochilinite. II. Acicular variety: Unusual diffraction patterns; *Soviet Phys. - Cryst.*, v. 18, p. 606-609.
1974: Selected area electron diffraction study of a type II "valeriite-like" mineral; *Am. Mineral.*, v. 59, p. 190-200.

15. TRACE METALS IN SNOW STRATA AS INDICATORS OF SILVER-ARSENIDE VEIN MINERALIZATION, CAMSELL RIVER AREA, DISTRICT OF MACKENZIE

Project 740081

I. R. Jonasson
Resource Geophysics and Geochemistry Division

Introduction

As part of a broad program designed to evaluate the usefulness or otherwise of snow strata sampling in geochemical prospecting (Jonasson and Allan, 1972), it was decided to apply the procedures already established in temperate regions, to a study in some permafrost areas of the Canadian sub-arctic in the winter of 1971-72.

With the close co-operation of Terra Mining and Exploration Limited and in particular, Mr. H. A. Sanche, some snow samples were collected from two locations, the Terra mine site near Camsell River, District of Mackenzie and from the nearby Norex property (see Mineral Claim Sheets, D.I.N.A., 86.E.9 and 86.F.12).

At the Terra, property mineralization consists primarily of vein deposits of native silver associated with copper, iron, cobalt and nickel arsenides (ramellsbergite, niccolite, etc.) and some bismuth and lead minerals (native bismuth, bismuthinite, matildite, galena). Minor pitchblende also occurs as spherules in the arsenides. Native silver is often highly mercuriferous. Rocks in the immediate area are mainly tuffaceous sediments and intermediate to acid volcanic rocks of the Proterozoic Echo Bay Group. The Terra property also has stratiform copper zinc (chalcocopyrite with minor sphalerite and galena) which is cut by the vein mineralization.

Norex Property yields similar minerals from similar rocks. However, the vein materials (arsenides) can be very bismuth rich. Disseminated galena occurs in wallrocks associated with the arsenide veins. In general, vein mineralization is somewhat less enriched in Zn and Cu than at Terra Mines, but perhaps more Pb-rich (R. I. Thorpe, pers. comm.).

Samples of clean snow were collected in early May, 1972 from immediately above soil surface at 20- to 50-foot intervals along 6 traverse lines at Terra Mine site. The lines were selected to traverse buried or suboutcropping mineralized veins as well as suspected barren zones.

Some of the vein occurrences are known to manifest significant radioactivity; in fact scintillometer surveys conducted by Sanche (pers. comm.) have proved useful in delineating small areas for more detailed prospecting. Consequently some of the snow sample lines also cross radiochemical anomalies which may be associated with silver mineralization.

The Norex samples are located at 25-foot intervals on a single line which strikes roughly N70°W and is perpendicular to a long fault valley that may contain mineralized vein material. An unknown depth of overburden covers bedrock in this area.

Results

Analyses for the trace metals, Zn, Cu, Pb, Ni, Ag, Bi were carried out by means of atomic absorption spectrometry on extracts of ammonium pyrrolidine dithiocarbamate complexes in methylisobutylketone. Analyses for As were made using a modified Gutzeit technique, U was determined fluorimetrically and F was determined with a fluoride specific ion electrode. Hg was not determined on these samples, although this was very desirable, because of problems related to sample transport and storage.

It is of interest to note the relative amounts of the metallic (and other) element of interest in ores from Terra and Norex. Table 15.1 provides some data for trace contents of ore beds, grab ore samples, tailings and concentrates. The metal values shown probably provide a fair estimate of the relative amounts of each species present. It was on the basis of these and other data that the metals to be determined in these snow samples were selected. Table 15.2 present analytical results (ppb) for the snow surveys at Terra. Table 15.2 also contains summary information of radiochemical activity of soil surfaces along the traverse lines at Terra. Generally, it can be seen that surface traces of known veins coincide with the highest activity (Fig. 15.1). The direction of drainage with respect to each traverse line is also shown, it is generally northeast towards the Camsell River (Fig. 15.1).

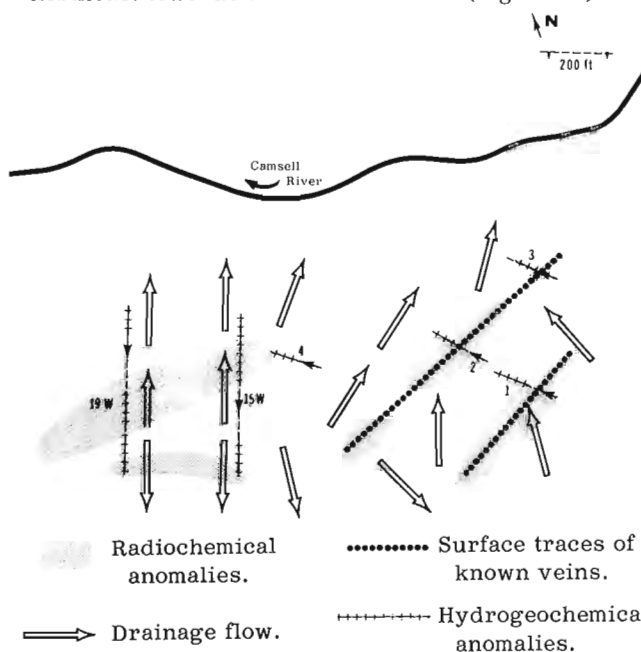


Figure 15.1. Snow traverse lines at Terra Minesite.

Table 15. 1. Ore geochemistry of some samples from Terra Mines and Norex property.

Nature of Sample	No	Zn	Cu	Pb	Ni	Co	Ag	Cd	Bi	Hg	As	Sb	Mo	Au	U	Mn	Fc
Native silver ore: Terra	01	773	564	149	4.3%	917	9.2%	6	82	2100	1557	8000	5	0.03	275	1.6%	3.61%
Ramellsbergite	02	79	344	1053	14.3%	2.59%	1613	0.5	3545	7.6	4.8%	3000	26	0.13	3700	-	-
Terra ore heads	03	870	5000	500	1400	1200	2000	4		50.0				0.03		3500	6.1%
mine tailings	04	325	255	135	620	450	150	3		10.4				0.01		3300	5.8%
jig concentrate	05	1300	1.30%	3200	2.10%	1.20%	13.0%	6		6100				0.31		3300	1.0%
flotation sulphide concentrate	06	6900	10.0%	8500	7500	9000	4.20%	22		1000				0.31		1500	20.0%
Norex ore heads	011	-	2100	7700	4500	1.50%	2.52%	-	4.61%	-	16.0%	-	-	-	-	-	-
Norex concentrate	021	-	6000	2.36%	1.50%	4.38%	5.54%	-	11.6%	-	26.8%	-	-	-	-	-	-

1. Samples 03, 04, 05, and 06 represent monthly composites for December, 1972.
2. All values in ppm unless otherwise indicated.
3. Norex values from R.I. Thorpe, (pers. comm.).

Discussion - Terra Mine site

For all three lines across known, but buried, veins (1, 2, 3) Zn, Pb and As consistently show as high levels as the same sample sites. Ag values are quite sporadic but tend to match up too. Surprisingly Ni, Bi and U which are reasonably abundant in ore specimens (Table 15.1) are virtually absent in all samples. F was sought but never found in quantities greater than 40 ppb. Cu is also somewhat low but its highs do match those for Zn, Pb and As. Consequently the anomalous zones of each traverse as shown in Figure 15.1 are composites of all elements which proved useful.

The anomalous zones match quite well the projected surface traces of the veins with one common feature - that they are all displaced about 60 to 80 feet down drainage.

The two lines, 15W and 19W, taken across radiochemical activity highs, also exhibit coherent anomalous zones, for Pb and Ag especially. In this they differ from lines 1, 2, 3 which produced solid multielement haloes in the snow, particularly strong for As and Zn. These also coincide with radiochemical activity highs of Figure 15.1 quite neatly. The traverse, line 4, across ground considered barren shows a few scattered anomalies in Zn, Pb and Ag which may or may not be meaningful. These do lie close to an anomalous zone of line 15W.

Discussion - Norex

Quick inspection of Table 15.3 reveals very strong and coherent snow haloes for Zn, Cu, Pb and As in two locations. One location is reinforced with some good values for Bi. Ag is significant by its absence. The contrast between highs and background values is quite exceptional, especially for Pb and Zn. The main anomalous zone, samples N.12 to N.15, cover that part of the traverse which crosses a fault valley in which mineralized veins are anticipated.

At present, little is known of the source of the measured snow haloes for Cu, Pb, Zn and Bi observed here.

Discussion - General

The best indicators of mineralization in the Norex and Terra areas are Pb, Zn, Ag and As. Occasionally Cu and Bi are useful. Some of the Pb values observed at Norex are considered to be very high when comparisons are made with previously reported data for this element at the New Calumet Mine area, Quebec (Jonasson and Allan, 1972).

Because it is now believed that dispersion haloes of metals in snow strata merely reflect what is present in the frozen soils beneath the snow, it is strongly recommended that soil geochemistry at the same detailed sampling scale be employed to map extensions of existing veins, or to search for new ones. Use of all of the metals considered in this study would be a reasonably initial approach. The usefulness of Ag,

Table 15.2

Trace element data: snow from Terra Mines

Element	Zn	Cu	Pb	Ni	Ag	Bi	As	U	F	Scintillometry counts/sec.
Detection Limit	5	1	5	1	0.3	5	0.5	0.1	40	
Sample No.	Known veins — covered by overburden.									
Line — Vein sample										
1-7-01	16	5	13	0	0	0	1.6	0	0	75
1-7-02	11	3	9	0	0	0	2.6	0	0	80
1-7-03	13	5	9	0	0	0	0	0	0	90
1-7-04	18	6	9	0	0	0	0	0	0	90
1-7-05	29	8	17	0	0	0	0	0	0	80
1-7-06	7	3	17	0	0.4	5	0	0	0	70
1-7-07	49	35	37	0	1.6	0	0	0	0	60
1-7-08	17	5	9	0	1.0	0	1.8	0	0	70
1-7-09	26	16	19	0	0	0	2.2	0	0	70
1-7-10	31	3	6	0	0.3	0	2.2	0	0	85
1-7-11	18	5	13	0	0	0	3.3	0	0	90
3-9-02	22	8	22	0	0.3	0	-	0	0	75
3-9-03	9	3	4	0	0	0	2.7	0	0	80
3-9-04	16	4	9	0	0.7	0	4.2	0	0	80
3-9-05	13	4	11	0	0.3	0	3.3	0	0	60
3-9-06	16	16	9	0	0	0	4.6	0	0	50
3-9-07	20	7	17	0	0	0	2.7	0	0	50
3-9-08	13	5	13	0	0	0	0	0	0	50
2-9-01	52	8	13	0	0.3	0	1.6	0	0	50
2-9-02	9	1	11	0	0	0	0	0	0	55
2-9-03	-	-	-	0	-	0	-	0	0	55
2-9-04	9	3	9	0	0	0	26.0	0	0	50
2-9-05	8	2	15	0	0.3	0	4.2	0	0	70
2-9-06	4	0	24	0	0	0	4.2	0	0	70
2-9-07	15	4	11	0	0	0	5.2	0	0	60
2-9-08	12	3	22	0	0	0	0	0	0	60
2-9-10	8	4	6	0	0	0	1.2	0	0	60
2-9-11	58	6	29	0	0	0	17.0	0	0	60
no known veins										
4-0-01	40	19	13	0	0.4	0	0	0	0	75
4-0-02	18	7	9	0	0	0	0	0	0	
4-0-03	8	4	6	0	0	0	0	0	0	50
4-0-04	12	2	17	0	0	0	0	0	0	50
4-0-05	97	30	41	0	0.8	0	-	0	0	50
4-0-06	8	4	9	0	0.3	0	3.5	0	0	50
4-0-07	17	4	15	0	0.3	0	0	0	0	50
4-0-08	7	2	6	0	0	0	0	0	0	40
4-0-09	18	8	33	0	0.3	0	0	0	0	40
4-0-10	13	5	6	0	0	0	0	0	0	40
Radiochemical anomalies										
15W. 0†00	18	5	29	0	0.6	0	0	0	0	50
0.06S	10	6	14	0	0.7	0	0	0	0	60
0.50S	40	13	50	0	1.3	0	0	0	0	70
0.100S	18	9	49	0	1.6	0	0	0	0	70
0.200S	10	4	38	0	1.1	0	0	0	0	75
1.50S	16	6	42	0	1.2	0	0	0	0	105
2.50S	10	5	45	0	1.4	0	0	0	0	200
3.00S	10	10	27	0	1.1	0	0.6	0	0	75
3.50S	10	4	18	0	0.4	0	0	0	0	75
4.00S	20	14	18	0	0.3	0	0	0	0	55
4.50S	14	4	23	0	0.3	0	0	0	0	55

Table 15.2 (cont.)

Element	Zn	Cu	Pb	Ni	Ag	Bi	As	U	F	Scintillometry
Detection Limit	5	1	5	1	0.3	5	0.5	0.1	40	counts/sec.
Sample No.	Known veins — covered by overburden.									
Line — Vein sample										
5.00S	10	3	11	0	1.3	0	0.5	0	0	55
5.50S	10	5	18	0	0.5	0	0	0	0	80
6.50S	12	8	23	0	1.1	0	0.5	0	0	75
7.00S	20	9	42	0	1.8	0	0.8	0	0	85
7.50S	14	8	27	0	0.9	0	0.5	0	0	90
19W.0.00	10	6	23	0	1.9	0	0	0	0	55
0.50	8	3	34	0	0.4	0	0	0	0	55
1.00	5	2	5	0	0.3	0	0	0	0	55
1.50	5	3	16	0	0.4	0	1.2	0	0	55
2.00	5	2	9	0	1.1	0	0	0	0	70
2.50	8	3	9	0	0.5	0	0.3	0	0	70
3.00	8	6	20	0	0.5	0	0	0	0	55
3.50	5	4	18	0	2.3	0	0.5	0	0	90
4.00	5	4	18	0	0.3	0	0	0	0	90
4.50	10	8	7	0	0.4	0	0	0	0	55
5.00	5	3	14	0	0.5	0	0	0	0	90
5.50	48	29	74	0	4.0	10	4.4	0	0	90
6.00	8	4	23	0	0.3	0	0	0	0	55
6.50	16	7	31	0	0.7	0	0.5	0	0	50

Notes: 1. All values in nanograms/ml (ppb) unless otherwise indicated.

Table 15.3

Trace element data: Norex property

Element	Zn	Cu	Pb	Ni	Ag	Bi	As	U	F
Detection Limit	5	1	5	1	0.3	5	0.5	0.1	40
Sample No.									
N-01	5	2	27	0	0	0	0.8	0	0
N-02	5	0	7	0	0	0	1.6	0	0
N-03	8	5	14	0	0	0	0.7	0	0
N-04	16	17	56	0	0	0	0	0	0
N-05	15	22	75	0	0	0	0.7	0	0
N-06	5	2	11	0	0	0	0	0	0
N-07	5	5	23	0	0	0	0	0	0
N-08	0	1	9	0	0	0	0	0	0
N-09	0	0	5	0	0	0	0	0	0
N-10	5	3	18	0	0	0	0.8	0	0
N-11	23	52	155	0	0	5	0.7	0	0
N-12	104	2	5	0	0	0	0.5	0	0
N-13	14	35	95	0	0	5	0	0	0
N-14	5	2	9	0	0	0	0	0	0
N-15	20	79	200	0	0	10	14	0	0
N-16	0	1	0	0	0	0	0	0	0
N-17	8	0	14	0	0	0	0.5	0	0
N-18	12	23	74	0	0	0	0	0	0
N-19	8	4	71	0	0	0	0	0	0
N-20	0	0	25	0	0	0	0.5	0	0
N-21	5	0	16	0	0	0	0.5	0	0
N-22	5	2	5	0	0	0	0	0	0
N-23	0	2	18	0	0	0	0	0	0

Notes: 1. All values in nanograms/ml (ppb) unless otherwise indicated.

Pb and As cannot be overemphasized in these regions of continuous and discontinuous permafrost because of their restricted abilities for migration (dispersion). Zn which is much more mobile, may be useful in outlining broader zones for more detailed studies using Ag, Pb and As.

The absence of Ni from the snow samples remain puzzling; perhaps it should also be sought, along with Co and U in the deeper soil horizons in the initial stages of any soil surveys. Perhaps nickel arsenides do not weather appreciably at depth in the bedrock, or else there may be a mutual restriction on the migrational abilities of Ni and As in these soils. Bi may be similarly restricted. Ni was found elsewhere to be quite high in snow overlying tetrahedrite veins wherein Ni reached only 0.7% in content (Jonasson and Allan, 1972).

The absence of U is also something of a problem. Its geochemistry is such that in the VI oxidation state, U is very mobile, usually as uranyl ion, UO_2^{++} , or as anionic complexes of this ion with carbonate or humate ligands. It is, therefore, quite likely that any UO_2^{++} moving into the surface soils is quickly dispersed or washed out of them. Usually a C horizon soil is the preferred sampling material for U. U in snow has been

sought elsewhere above known U showings and so far it has not been detected in excess of 0.1 ppb.

In general, metal elements suspected of acquiring anionic character in surface soils seem to be either absent or in very low concentrations in snow strata above mineralization (e.g., U, As, Sb) wherein they are often quite abundant.

Acknowledgments

The close co-operation of Terra Mining and Exploration Ltd. is acknowledged. The advice and discussion of data proffered by Mr. H.A. Sanche, who also collected the samples, proved invaluable to this study.

The technical assistance of Mr. G. Gauthier who was responsible for the analyses of these, at times, difficult samples is also gratefully acknowledged.

Reference

Jonasson, I.R. and Allan, R.J.

1972: Snow — a sampling medium in hydrochemical prospecting in permafrost and temperature regions; in "Geochemical Exploration -- 1972", Proc., 4th Internat. Geochem. Explor. Symp., (London, U.K.) Ed. Jones, M.J. (I.M.M. Lond. 1972), p. 161-176.

Project 720084

R. L. Grasty

Resource Geophysics and Geochemistry Division

Introduction

Previous workers, e.g. Kogan *et al.* (1969), and Duval *et al.* (1971) have carried out theoretical studies to determine the percentage of the total detected gamma radiation from an infinite homogeneous source that originates from within a circular area directly beneath the aircraft. This circular area is termed a 'circle of investigation' and they have found for instance, that approximately 50 per cent of the total radiation detected at an altitude of 400 feet originates from within a circular area with an approximate radius of 400 feet. However, these calculations have assumed the detector to be spherical which means that the detector sensitivity is independent of the angle the gamma-ray photons strike the detector. Grasty and Holman (1974) carried out experiments with a variety of different detectors commonly used in airborne detector survey operations and showed that for some detectors there was a large variation in sensitivity with angle of incidence. The results for three of these detectors are shown in Figure 16.1. This paper shows how the detector response can be incorporated into the theory to arrive at the percentage of the detected radiation from an infinite source that originates from within 'circles of investigation' of different radii.

Detector Response

From the experimental results of Grasty and Holman (1974) it was found that at an energy of 2.62

MeV, the sensitivity of all detectors studied could be satisfactorily represented by the equation:

$$S = \frac{1 + a \cos \theta}{1 + a} \dots \dots \dots (1)$$

where θ is the displacement angle of the source from the detector axis and S is the normalized sensitivity to give unit sensitivity along the detector axis, a is a constant which varies for each detector. This particular form of the detector response was chosen since terms involving $\cos \theta$ can readily be incorporated into the theory.

The responses of the seven different crystals were computer fitted to Equation (1) to determine the value of the parameter a. These results are shown in Table 16.1 and the computed curves are plotted in Figure 16.1 for the 5 x 5, 9 x 4, 11.5 x 4 inch detectors. The assumed detector response given by Equation (1) can be seen to adequately represent the experimental data.

Theory

As shown by Kogan *et al.* (1969) the number of unscattered photons, $N\theta_1$ of energy 2.62 MeV originating from within a cone of half-angle θ_1 (the aircraft at the apex of the cone) is given by:

$$N\theta_1 = \frac{n}{2\lambda} \int_{\sec \theta_1}^{\infty} \frac{\Lambda \epsilon e^{-\mu h \sec \theta}}{|\sec \theta|^2} d(\sec \theta) \dots \dots \dots (2)$$

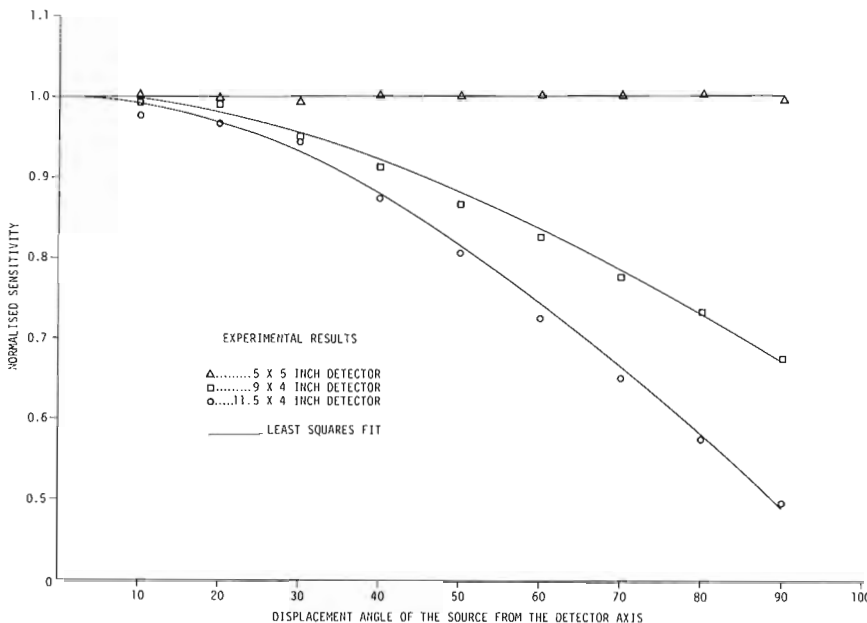


Figure 16.1
Variation of detector sensitivity with angle of incidence.

n is the number of primary photons emitted per unit volume.
 μ is the linear absorption coefficient of air at 2.62 MeV.
 λ is the linear absorption coefficient of the ground at 2.62 MeV.
A is the cross-section area of the detector.
 ϵ is the photo peak efficiency of the detector at 2.62 MeV, defined as the fraction of incident photons striking the detector that are totally absorbed.
h is the aircraft height.

The percentage of the total detected gamma-ray photons from an infinite source that originate from within an angle θ_1 is then given by:

$$P = 100 \times \frac{\int_0^{\theta_1} \frac{A \epsilon \epsilon^{-\mu h \sec \theta} d(\sec \theta)}{(\sec \theta)^2}}{\int_0^{\infty} \frac{A \epsilon \epsilon^{-\mu h \sec \theta} d(\sec \theta)}{(\sec \theta)^2}} \dots (3)$$

For a spherical detector the product $A\epsilon$ is independent of θ and P reduces to:

$$P = 100 \times \frac{[E_2(\mu h) - \cos \theta_1 E_2(\mu h \sec \theta_1)]}{E_2(\mu h)} \dots (4)$$

where E_2 is the exponential integral of the second kind.

From the work presented here the product $A\epsilon$ can be represented by the equation:

$$A\epsilon = k (1 + a \cos \theta) \dots (5)$$

where k is a constant. Incorporating this detector response into Equation (3) and integrating we obtain for any detector:

where E_3 is the exponential integral of the third kind.

This equation satisfactorily reduces to Equation (4) for a spherical detector in which $a=0$.

Results and Discussions

The percentage of the total gamma radiation from an infinite source, P, that originates from circular areas of different radii beneath the aircraft is shown in Figure 16.2 for the 11.5- by 4- and 5- by 5-inch detector. An altitude of 400 feet was assumed. In spite of the extreme variation of response between a 5- by 5- and 11.5- by 4-inch detector, there is surprising little variation between the two crystals. For the 5- by 5-inch detector 51.4 per cent of the radiation from an infinite source originates from a circle of radius 400 feet, whereas for the 11.5- by 4-inch detector the same area contributes 56.7 per cent of the total infinite source yield. This small difference can best be explained from a consideration of the two detector

responses in Figure 16.1. It is only at large angles from the detector axis that the 11.5- by 4-inch detector has a significantly reduced sensitivity. At right angles to the axis of the detector the sensitivity has reduced to approximately 50 per cent of the along-axis value. However, no radiation can reach the detector at this angle because an infinite air path must be traversed. Similarly, at other large angles air absorption is significantly more important than the reduced sensitivity of the detector.

Table 16.1

Variation of Angular Sensitivity Parameter for Different Detectors (Equation 1)

Crystal Size (inches)	Angular Sensitivity Parameter (a)
3 x 3	0.14 ± 0.03
5 x 4	0.01 ± 0.01
5 x 5	-0.03 ± 0.02
6 x 4	0.12 ± 0.02
8 x 4	0.46 ± 0.02
9 x 4	0.48 ± 0.02
11.5 x 5	1.04 ± 0.04

In order to reach the detector, the gamma-ray photons must also pass through the aircraft structure and detector housing. For the Geological Survey of Canada system the material below the crystals was estimated to be equivalent to 1.15 cm of aluminium. This thickness of material was incorporated into the theory. The percentage of the infinite source yield as a function of the radius of the 'circle of investigation' is shown in Table 16.2 for four detectors, both with and without this 1.15 cm of aluminium. It can be seen that the assumption of a spherical detector is a reasonable approximation even for the 11.5- by 4-inch detector which exhibits the largest angular sensitivity variation.

Table 16.2

The Percentage of the Infinite Source Originating from Within A Circle of Radius 400 Feet (Aircraft Altitude 400 Feet)

Detector	Percentage (without aircraft structure)	Percentage (with aircraft structure)
Spherical Detector	51.4	52.7
8 x 4, 9 x 4	54.5	55.7
11.5 x 4	56.7	57.9

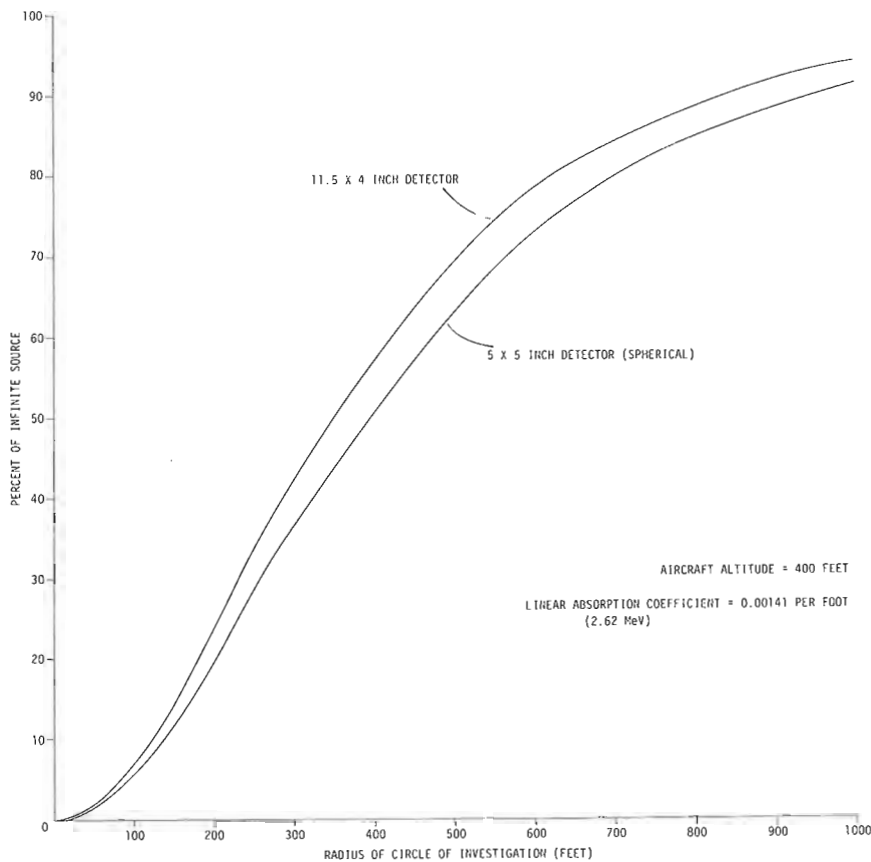


Figure 16.2

The percentage of the infinite source yield as a function of the radius of the circle of investigation.

These results are applicable to uniform circular sources centred directly beneath the aircraft. In this particular case there is little difference between detectors. However, this would not necessarily be the case for distributed sources, in particular for strong sources at large horizontal distances from the aircraft.

References

Duval, J. S. *et al.*

1971: Circle of investigation of an airborne gamma-ray spectrometer; *J. Geophys. Res.*, v. 76, p. 8466-8470.

Grasty, R. L. and Holman, P. B.

1974: Optimum detector sizes for airborne gamma-ray surveys; in *Report of Activities, Part B, Geol. Surv. Can., Paper 74-1B*, p. 72-74.

Kogan, R. M., Nazarov, I. M., and Fridman, Sh. D.

1969: Gamma spectrometry of natural environments and formation, *Israel Program for Scientific Translations*, no. 5778, Jerusalem, 1971.

Project 720084

R. L. Grasty

Resource Geophysics and Geochemistry Division

Unlike a camera, an airborne gamma-ray detection system does not have a fixed 'field of view', since it can receive radiation equally well from any angle. In airborne gamma spectrometry the 'field of view' of a detector is commonly thought of as the circular area directly beneath the aircraft contributing a fixed percentage of the total detected radiation. This fixed percentage of the total detected radiation has no accepted standard and different values will give different 'fields of view' for the same detector. Only in the very special case of a flat infinite homogeneous source can this concept of 'field of view' be applied.

Aeromagnetic and radioactivity surveys both provide an average physical measurement from an infinite number of sources distributed in the ground. If sources are strong, they can be detected at considerable distances from the aircraft. Yet one would never conceive of a 'field of view' in aeromagnetism. Why is it so commonly used in gamma-radiation surveys? Probably because it is generally believed that the measurement relates directly to a physical property of the ground immediately beneath the aircraft whereas it actually relates to the average contribution of a large number of sources.

The origin of the detected radiation depends solely on the distribution of sources in the ground. If the ground is inhomogeneous or has varied topography the concept of 'field of view' no longer applies. It can readily be appreciated that by flying over a lake, radiation could be detected from the shore, that did not originate from a circular area beneath the aircraft. A strongly radioactive source can also be detected even if it is outside a nominal 'field of view'.

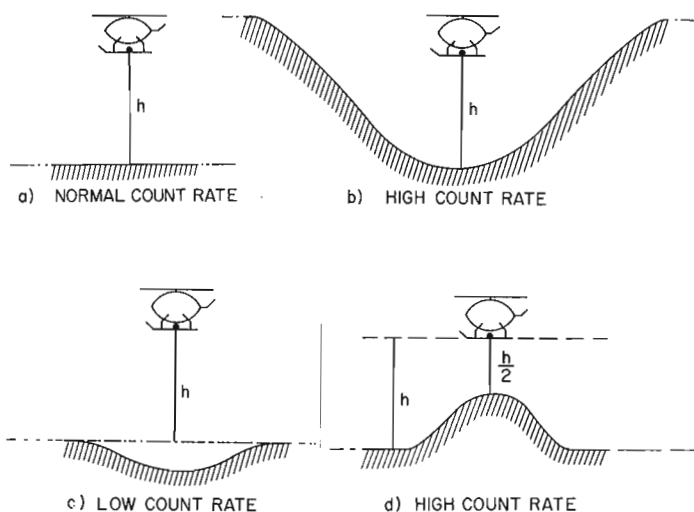


Figure 17.1. The effect of source geometry upon count rate.

An airborne detection system receives ground radiation from horizon to horizon, a total angle of 180 degrees. Under the special circumstance of flying within a valley, the radiation can originate from a total angle greater than 180 degrees, and will produce a higher count rate compared to a measurement at the same altitude over ground of the same composition (Figs. 17.1a and 17.1b). Figures 17.1c and 17.1d illustrate the effects of flying over a valley and over a ridge. The total detected radiation depends on the distribution of sources over all space and the 'field of view' concept can lead to some wrong conclusions in relation to the count rate obtained in the examples illustrated here.

The concept of 'field of view' is often used to establish the percentage of ground covered by an airborne system. As previously stated, a 'field of view' is quite arbitrary, and depending on one's particular choice of the 'field of view' any 'suitable' value could be selected. As an example, for an energy of 2.62 MeV, a circle of radius 400 feet beneath an aircraft at an altitude of 400 feet will produce approximately 50 per cent of the total detected radiation from a homogeneous radioactive infinite half-space. In terms of a moving aircraft, this circle can be envisaged as a swath, 400 feet either side of the aircraft path that is producing 50 per cent of the total detected radiation. For an airborne survey with a line spacing of 2000 feet, a percentage ground coverage of 40 per cent $\left(\frac{2 \times 400}{2000} \times 100\right)$ would be

calculated. For this particular survey it should be stated that approximately 50 per cent of the detected radiation originated from 40 per cent of the area. The word 'approximately' should be used since the calculations are all based on a homogeneous source. For exactly the same survey, using a 90 per cent instead of 50 per cent 'field of view', there would be almost complete coverage (Duval *et al.*, 1969). What coverage should be quoted? Obviously the choice is arbitrary and certainly should not be quoted to any high degree of accuracy. Furthermore, the area beneath the aircraft contributing to a fixed percentage of the detected radiation is strongly dependent on the particular gamma-ray energy under consideration. This is particularly true if high percentage 'fields of view' are considered. For instance the radius of the circle producing 90 per cent of the total detected radiation has a value of approximately 850 feet for potassium at 1.46 MeV and a value of approximately 950 feet for thorium at 2.62 MeV (Duval *et al.*, 1969), once again demonstrating that percentage coverage should not be quoted to a high degree of accuracy.

The ultimate aim of any airborne survey is to map a property of the ground as economically as possible. To achieve this it is necessary to know the physical

field at the aircraft altitude. The 'field of view' concept should not be the basis for establishing the optimum line spacing required for detailed airborne gamma-ray surveys designed for locating small targets. The concept is only valid for a uniform homogeneous ground and is thus not applicable to this type of survey. In order to select the appropriate flight line spacing for a detailed survey it is necessary to know the variation of the gamma-radiation field at the survey altitude, due to small radioactive sources on the ground. At an altitude of 400 feet, the radiation over a small source has dropped to half its intensity at a horizontal distance of approximately 300 feet from the source (Tammenmaa *et al.*, in press). This response due to a small source should be the physical basis for flight line selection. The 'field of view' concept provides no information on

the desired separation of the flight lines for detailed surveys and in this regard has no more relevance than it would in aeromagnetism.

References

- Duval, J. S. *et al.*
1971: "Circle of investigation of an airborne gamma-ray spectrometer"; J. Geophys. Res., v. 76, p. 8466-8470.
- Tammenmaa, J., Grasty, R. L., and Peltoniemi, M.
"The reduction of statistical noise in airborne radiometric data"; Can. J. Earth Sci. (in press).

Project 720072

M. J. Copeland

Regional and Economic Geology Division

Canadian paleontological literature is replete with references to leperditiid ostracodes as '*Leperditia* sp.', 'leperditiid ostracode indet.' and so forth. To varying degrees all micropaleontologists dealing with early Paleozoic ostracodes have been guilty of this 'large, smooth ostracode syndrome' approach to a perplexing but often soluble taxonomic problem. As a result, leperditiids have fallen into general disrepute as reliable stratigraphic indices, despite the fact that they may be the only visible organic constituents of the carbonate strata in which they occur. To continue to neglect the possible value of one of the most common and easily collectable types of Early Paleozoic ostracodes is to ignore what may prove to be a most valuable biostratigraphic tool.

Leperditicopid ostracodes are common in Canada in strata of Middle Ordovician to Early Devonian age. They 'exploded' as several distinct lineages during the Ordovician, flourished along generalized lines of development during the Silurian, and their sometimes bizarre, large-sized relicts survived until well into the Devonian. This evolutionary sequence may be related to the increasingly widespread, shallow, often restricted epicontinental marine environments in which leperditiids thrived. Both physical and faunal evidence points to the high subtidal to intertidal habitat of these often gregarious ostracodes (Berdan, 1968). Within a sedimentary unit, consistent lateral increase in number and type of pelagic or benthic marine fossils may prove useful as a relatively reliable indicator of decreasing water depth. Also, the association with *Hormotoma*-like gastropods, fish, eurypterids and *Ceratiocaris*-type phyllocarids would seem to indicate a leperditiid tolerance, by Silurian time, to extreme variations of salinity (Copeland, 1971b).

Ordovician and Devonian leperditiids have been studied more extensively than those of the Silurian. This is due to the initial diversity of Ordovician forms usually associated with 'normal' marine faunas, and the large size and often unique morphologies of the relatively less common Devonian species. Cosmopolitan Silurian species have been considered as monotonously similar in size and morphology and consequently their usefulness as biostratigraphic indicators has been doubted. The first worker to critically examine Canadian Silurian leperditiids was the English entomostracan specialist T. Rupert Jones (1856, 1858a, b, 1891). Collections submitted to him were from isolated occurrences, their descriptions were based on a few specimens collected by Arctic explorers of western mappers from general geographic localities with little stratigraphic information. It was not until 1949 that Swartz critically analyzed and classified some North American Silurian Leperditacea and, using his work as a basis, Abushik (1960) expanded our knowledge

of the Silurian leperditiids by study of specimens from the Siberian Platform. Utilizing their results, Copeland (1971a) reported on several occurrences of Canadian leperditiids and attempted to stratigraphically relate Middle Silurian leperditiid and beyrichiid faunas from the northern mid-continent region.

Whereas previously, lateral shape, marginal features and hinge length were general distinguishing criteria, many leperditiid genera are now established on the occurrence and number of right valve internal marginal denticles (Copeland, 1970b, pl. V, fig. 27; 1974, pl. V, fig. 7), presence of marginal flanges, surface ornamentation, 'eye' tubercles and dorsal protuberances, all well shown on Plate I, figure 17, and size of muscle tubercles forming the large adductorial and/or chevron muscle impressions (pl. I, figs. 10, 11; Copeland, 1970a, pl. III, figs. 6-15). It has also been considered that anastomosing ridges radiating from the adductorial muscle impression of some leperditiid specimens (Pl. I, fig. 22) may be of possible taxonomic and evolutionary significance. The assumption that these ridges represented 'blood canals' and, therefore, that a relationship existed between leperditicopid and heart-bearing myodocopid ostracodes was dismissed by Sohn (1974). He concluded (*ibid.*, p. 726) that "the markings on the leperditiids probably represent the organic framework because they are present also within the calcified part of the shell." In assemblages studied thus far, patterns traced by these markings appear to be subject to a degree of variation, but sufficiently large samples of well preserved specimens are very difficult to obtain. To be ultimately useful these morphological refinements in leperditicopid taxonomy must be applicable at the specific level where a combination of external and internal valve characteristics may be assessed. Determination of sufficient specific characteristics is more often based on observations from numerous dolomitic steinkerns in a monospecific assemblage than from the fortunate find of calcareous or silicified valves and carapaces on which such structures are readily discernible. Obviously, the fewer morphological criteria that apply the greater the possibility of determinations only at the generic level. Now, however, the terms '*Leperditia* sp.' or 'leperditiid ostracode indet.' may be replaced in many instances by other taxonomic nomenclature that has more exact stratigraphic significance.

Few attempts have been made to determine the stratigraphic sequence of Canadian Silurian leperditicopids. Within the Appalachian Basin, zonation of predominantly clastic Clinton strata has been based on zygodolbine beyrichiids (Ulrich and Bassler, 1923). This zonation was erected for the central Appalachian belt but zygodolbine assemblages also occur on Anticosti Island,

Plate 18.1

- Figures 1-4. *Herrmannina baltica* (Hisinger)
Left and right lateral, dorsal and ventral views of a carapace, X2,
Island of Gotland, Sweden, hypotype, GSC No. 45719.
- Figures 5-7. *Herrmannina fabulina* (Jones)
5. Left lateral view of a valve, X3, (*Leperditia Hisingeri* Schmidt of
Jones, 1891, pl. XIII, fig. 9), hypotype, GSC No. 8752b.
6. Left lateral view of a valve, X3, (*Leperditia Hisingeri* Schmidt var.
fabulina Jones, 1891, pl. X, fig. 5), cotype, GSC No. 6052.
7. Left and right lateral views of two valves, X3, (*Leperditia Hisingeri*
Schmidt var. *fabulina* Jones, Jones, 1891, pl. X, fig. 7), cotype,
GSC No. 6052b. (All specimens from Cedar Lake Formation, Long Point,
east side of Lake Winnipegosis, Manitoba.)
- Figures 8, 9. *Herrmannina caeca* (Jones)
Left lateral views of two silicified carapaces, X15 and X10, locs. 22184
and 22187, Cape Phillips Formation, Baillie-Hamilton Island, District of
Franklin, hypotypes, GSC Nos. 45720, 45721.
- Figures 10, 11. *Leperditia arctica?* Salter
Right lateral view of a valve, X3, and adductorial and chevron muscular
impressions, X18, River gorge ca. 2 miles south of Strzelecki Harbour,
east coast of Prince of Wales Island, District of Franklin, 7 feet above
base of Read Bay Formation, hypotype, GSC No. 45722.
- Figures 12, 13. *Leperditia guelphica* Jones
Left and right lateral views of two valves, X3, (*Leperditia balthica*
(Hisinger) var. *guelphica* Jones, 1891, pl. XIII, figs. 12 and 13),
Guelph Formation, Durham, Ontario, cotypes, GSC Nos. 3013c and 3013.
- Figure 14. *Leperditia longigibbera* Swartz
Left lateral view of a valve, X4, (*Leperditia Hisingeri* Schmidt var.
gibbera Jones, 1891), Cedar Lake Formation, Long Point, east side of
Lake Winnipegosis, Manitoba, paralectotype, GSC No. 8754a.
- Figures 15-17. *Leperditia gibbera* Jones
15. Right lateral view of a valve, X4, 136 feet above base of the Peel
Sound Formation, hypotype, GSC No. 45723.
16, 17. Left lateral views of two valves, X3, 253 and 84 feet above base
of the Peel Sound Formation, hypotypes, GSC Nos. 45724, 45725. (All
specimens from river gorge ca. 1 mile south of Strzelecki Harbour, east
coast of Prince of Wales Island, District of Franklin.)
- Figure 18. *Leperditia* sp. cf. *L. arctica* Salter
Left lateral view of a valve, X3, River gorge ca. 2 miles south of
Strzelecki Harbour, east coast of Prince of Wales Island, District of
Franklin, 310 feet above base of the Read Bay Formation, hypotype,
GSC No. 45726.
- Figures 19-22. *Leperditia arctica* Salter
Left lateral, ventral, right and left lateral views of four silicified
carapaces, X10, loc. 88184, Cape Phillips Formation, Baillie-Hamilton
Island, District of Franklin, hypotypes, GSC Nos. 45727-45730.

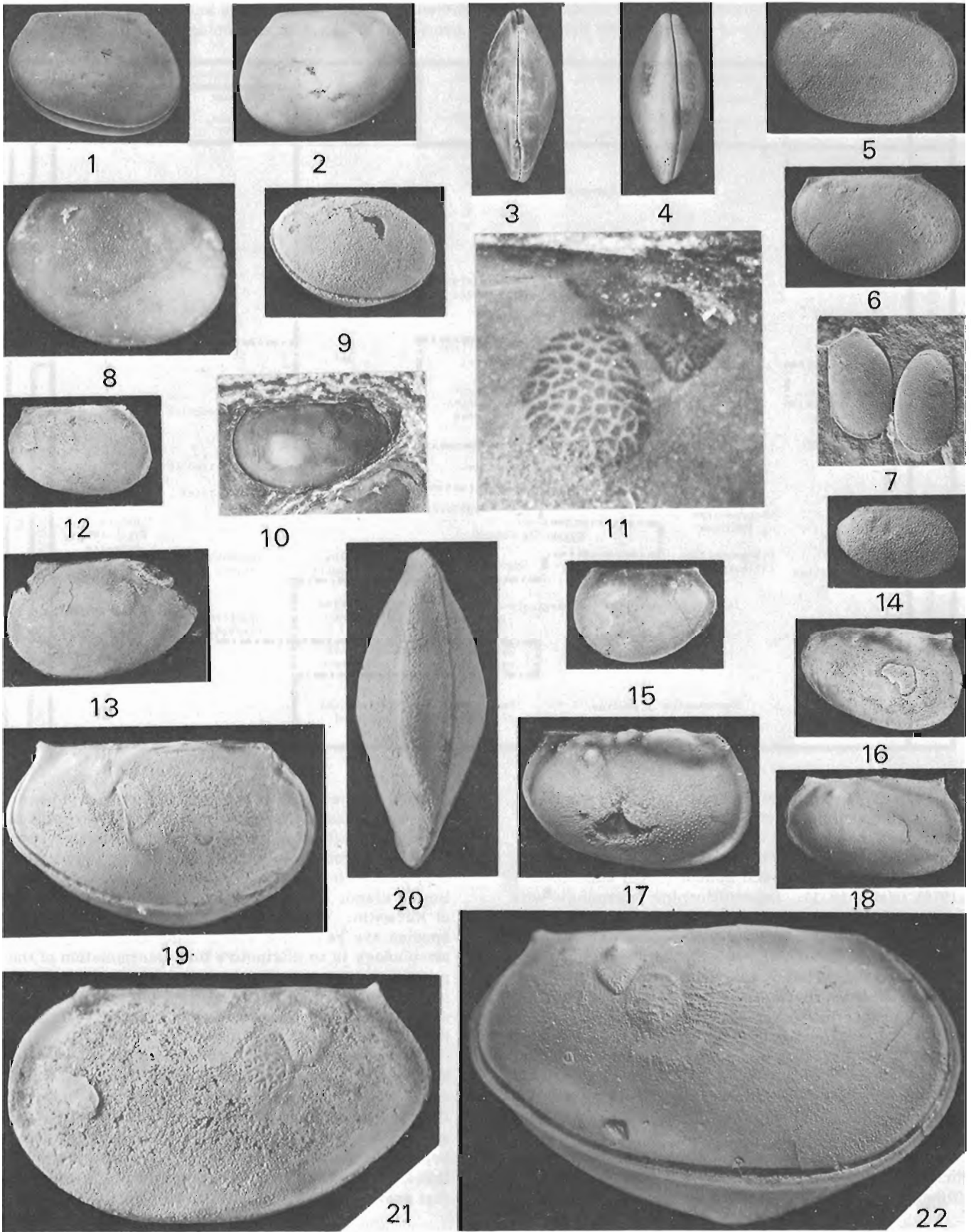


Table 18.1

Relationship between Silurian leperditicopid and palaeocopid ostracode faunas discussed in text. Solid lines surround prominent palaeocopid assemblages

	SOUTH-CENTRAL ARCTIC ISLANDS	SOUTHERN MANITOBA (Stearn, 1956)	MICHIGAN (Ehlers and Kesling, 1957)	ONTARIO (GENERAL) (Copeland, 1971a)	ANTICOSTI ISLAND, QUEBEC (Copeland, 1974)	STANDARD SEQUENCES		SALINA CAYUGAN	LOCKPORT	NIAGARAN	MEDINA
						NEW YORK (Rickard, 1975)	APPALACHIAN (Berry and Boucot, 1970)				
PRIDOLIAN	Beyrichia (Beyrichia) sp.										
			Leperditia scalaris								
LUDLOVIAN	Leperditia gibbera										
	Leperditia gibbera		Leperditia? sp.	Leperditia guelphica							
WENLOCKIAN	Leperditia arctica										
	Beyrichia (Beyrichia) sp.										
LLANDOVERIAN	Leperditia arctica										
	Herrmannina caeca	Leperditia longigibbera	Herrmannina marginata	Drepanellina clarki	Paraechmina spinosa						
		Herrmannina caeca	Herrmannina marginata	Zygobolba decora							
		Herrmannina fabulina	Zygobolba twenhofeli								
		Dihogmochilina latimarginata	Zygobolba logani								
	Dihogmochilina boothia	Herrmannina fabulina	Zygobolba sp.	Zygobolba anticostiensis							
		Dihogmochilina latimarginata	Herrmannina selwyni								
		Herrmannina fabulina	Zygobolba excavata								
			Zygocosta williamsi	Zygobursa praecursor							
		Herrmannina fabulina	Herrmannina aff. selwyni	Herrmannina selwyni							

northern Gaspé and Maine, Hudson Bay Lowland, Lake Timiskaming outlier on the Canadian Shield, and Michigan Basin. Slight modification of this zonation, proposed by Gillette (1947) for northern New York, has been adopted by Berry and Boucot (1970) and Rickard (1975) (Table 18.1). Leperditicopids intermingle with zygobolbine ostracodes throughout part of the Niagaran Series of Ontario and Michigan and are the only ostracodes present in the Silurian rocks of southern Manitoba (Stearn, 1956). They are commonly contained within dense calcareous rocks of shallow, restricted marine deposition that are widely distributed across the mid-western and northern part of the North American craton. In the central Arctic Archipelago, Wenlockian and Pridolian species of *Beyrichia* (*Beyrichia*) occur with distinctive boreal leperditiid species (Copeland, 1971b). The exact extent of the intermingling of these Arctic ostracodes is not yet known.

Although three leperditicopid genera predominate throughout eastern and northern Canada, only one (*Dihogmochilina*) is restricted to the Silurian, as

species of the other two genera (*Herrmannina* and *Leperditia*) also occur in the Devonian. Two species of *Dihogmochilina* are present in these Silurian strata, *D. boothia* from the central Arctic and *D. latimarginata* from southern Manitoba, northern Michigan, Hudson Bay Lowland, and Southampton-Coats Island, District of Keewatin. As presently known, *Dihogmochilina* species are restricted to the Late Llandovery; their morphology is so distinctive that determination of the prominent 'fish-tailed' sulcus, posterior of the chevron muscle impression and dorsally enclosing the large scars of the adductor muscle impression is sufficient for generic identification (Copeland, 1970a).

Canadian species of *Herrmannina* and *Leperditia* also may have biostratigraphic significance within the Silurian, though not as time restricted as those of *Dihogmochilina*. In general, *Herrmannina* species appear as a southern, Llandoveryan assemblage and *Leperditia* species as a northern post-Llandoveryan fauna. Variation exists among species of *Herrmannina* that presents certain taxonomic difficulties. All are

what may be termed 'smooth' in that they have no distinctive surface ornamentation, and adductorial and chevron muscle patterns are indistinct of unknown on the valves of many species. One herrmanninid group that includes *H. baltica* (a north European species), *H. selwyni* and *H. caeca*, displays ventral overlap by the right valve, short hinge line and indistinct dorsal angles (Pl. 18.1, figs. 1-4, 8, 9). The other herrmanninids, of which *H. fabulina* and *H. marginata* are prominent species, have long hinge lines, prominent dorsal angles, marginal flanges and, apparently, are almost equivalved (Pl. 18.1, figs. 5-7). Possibly two generic (or subgeneric) assemblages are contained within our present concept of *Herrmannina* but this taxonomic uncertainty does not alter the biostratigraphic usefulness of the genus as presently constituted.

Species of *Leperditia* are distinctive in that each bears a posterodorsal swelling only on the left valve. This swelling is a long, relatively indistinct dorsal fold in such species as *L. guelphica* and *L. longigibbera* (P. 18.1, figs. 12-14), more pronounced and posteriorly situated in *L. scalaris* (Berdan, 1972) and *L. arctica* (Pl. 18.1, figs. 18, 19, 22) and prominent and often dissected in *L. gibbera* (Pl. 18.1, figs. 16, 17). The size and shape of the dorsal swellings displayed by species in this morphologic sequence of Silurian forms may be related to increased carapace volume. Also, the right valve of these larger *Leperditia* species strongly overlaps the left valve along the free margin. This feature may form a rounded keel such as is present along the posteroventral margin of *L. guelphica* (Pl. 18.1, fig. 13) and the entire ventral margin of *L. arctica* (Pl. 18.1, figs. 19-22). These shell-strengthening structures combined with effective closure, strong musculature and thick valve walls indicate that leperditiids were benthonic forms capable of living under extreme physical conditions.

As yet insufficient information is available on other Canadian Silurian leperditicopid taxa to warrant their inclusion in Table 18.1. Abushik (1960) has described several biostratigraphically important genera from the USSR, species of which should be present in northern Canada. Such may indeed have already been reported, but because the specimens lacked sufficient morphological detail or such details were misinterpreted, they languish in collection as '*Leperditia* sp.' or 'leperditiid ostracode indet.' Whatever the cause, and the present author is probably as much to blame as anyone, a change in our mental apathy toward Leperditicopida is necessary before they can assume their rightful role in North American Silurian biostratigraphy.

References

- Abushik, A. F.
1960: Silurian ostracodes of the Siberian Platform; VSEGEI, v. 39.
- Berdan, J. M.
1968: Possible paleoecologic significance of leperditiid ostracods; Geol. Soc. Am., Northeast Section, Program, p. 17.
- Berdan, J. M. (cont'd.)
1972: Brachiopoda and Ostracoda of the Cobleskill limestone (Upper Silurian) of central New York; U. S. Geol. Surv., Prof. Paper 730.
- Berry, W. B. N. and Boucot, A. J.
1970: Correlation of the North American Silurian rocks; Geol. Soc. Am., Spec. Paper 102.
- Copeland, M. J.
1970a: Redescription of the Middle Silurian leperditicopid ostracod *Dihogmochilina latimarginata* (Jones); Geol. Surv. Can., Bull. 187, p. 9-14.
1970b: Ostracoda from the Vauréal Formation, Upper Ordovician of Anticosti Island, Québec; Geol. Surv. Can., Bull. 187, p. 15-29.
1971a: Biostratigraphy of some early Middle Silurian Ostracoda, eastern Canada; Geol. Surv. Can., Bull. 200, p. 1-13.
1971b: Additional Silurian Arthropoda from Arctic and eastern Canada; Geol. Surv. Can., Bull. 200, p. 19-26.
1974: Middle Ordovician Ostracoda from southwestern District of Mackenzie; Geol. Surv. Can., Bull. 244.
- Ehlers, G. M. and Kesling, R. V.
1957: Silurian rocks of the northern peninsula of Michigan: Mich. Geol. Soc. Ann. Field Excursion, June, 1957.
- Gillette, T.
1947: The Clinton of western and central New York; N. Y. State Mus. Bull. n. 341.
- Jones, T. R.
1856: Notes on the Palaeozoic bivalved Entomostraca. No. III. Some species of *Leperditia*; Ann. Mag. Nat. Hist., ser. 2, n. 98, p. 81-101.
1858a: Notes on the Palaeozoic bivalved Entomostraca. No. IV. Some North American species; Ann. Mag. Nat. Hist., ser. 3, n. 4, p. 241-257.
1858b: On the Palaeozoic bivalve Entomostraca of Canada; Geol. Surv. Can., Can. Organic Remains, dec. III, p. 91-102.
1891: 5. On some Ostracoda from the Cambro-Silurian, Silurian, and Devonian rocks; Contrib. Can. Micro-Pal., pt. 3, p. 59-99.
- Rickard, L. V.
1975: Correlation of the Silurian and Devonian rocks in New York State; N. Y. State Mus. and Sci. Service, Map and Chart Series No. 24.

Sohn, I. G.

- 1974: Evidence of the presence of a heart in Paleozoic ostracodes inconclusive; *J. Res. U.S. Geol. Surv.*, v. 2, n. 6, p. 723-726.

Stearn, C. W.

- 1956: Stratigraphy and palaeontology of the Interlake Group and Stonewall Formation of southern Manitoba; *Geol. Surv. Can.*, Mem. 281.

Swartz, F. M.

- 1949: Muscle marks, hinge and overlap features, and classification of some Leperditiiidea; *J. Paleontol.*, v. 23, n. 3, p. 306-327.

Ulrich, E. O. and Bassler, R. S.

- 1923: Systematic paleontology of Silurian deposits; Ostracoda; *Maryland Geol. Surv.*, Silurian, p. 500-704.

Convention de recherche E. M. R. 1135/D13-4-172/75

Jean-Marie Dubois¹

Division de la science des terrains

Localisation et accessibilité

Le complexe morainique de Manitou-Matamek a progressivement été levé par photo-interprétation lors de travaux de cartographie pendant les étés 1974 et 1975 (Dubois, 1975, 1976). Il se localise principalement sur la carte de Manitou Lake (22 I) et déborde un peu sur les cartes adjacentes, soit Havre-Saint-Pierre (12 L) et Sept-Iles (22 J) (fig. 19. 1).

Ce complexe est parallèle à la côte et se situe généralement entre 15 et 20 milles (24 et 32 km) à l'intérieur des terres. Ses divers segments s'étirent ainsi sur 125 milles (200 km) entre les rivières Moisie et Romaine. La moraine du lac Daigle à l'ouest de la rivière Moisie a elle-même été levée sur 8 miles (13 km) par Dredge (1971). Tremblay (1975) postule son prolongement sur 6 à 7 milles (10 à 11 km) vers l'ouest en ceinturant la baie des Sept-Iles.

A l'exception de la moraine du lac Daigle, aucune route ne mène au complexe et les deux rivières les plus canotables qui le rejoignent sont les rivières Matamek et (petite) Manitou. Cette inaccessibilité est la raison pour laquelle seulement deux sites ont pu être sommairement visités (Dubois, 1976) et la raison pour laquelle beaucoup de composantes demeurent problématiques et sont affublées de points d'interrogation sur la carte.

Relations avec la topographie

Dans l'ensemble aucune relation évidente n'existe avec l'énergie du relief (dénivellation moyenne entre les talwegs et les interfluves) ou avec le degré de dissection du relief. Cependant le tracé général du complexe se subdivise en quatre arcs de moins en moins nets vers l'est; ces lobes se caractérisent par des constantes altimétriques et de position (fig. 19. 1).

1er arc: lobe de Moisie

Cet arc va de la rivière des Rapides à la rivière au Bouleau et il est centré sur la grande dépression de la rivière Moisie (fig. 19. 2a). Sa corde mesure 45 milles (72 km). L'altitude moyenne à la base de l'arc est de 350 à 450 pieds (105 à 140 m) alors que la zone nodale avec l'arc de Manitou se situe à des altitudes de 1000 à 1825 pieds (305 à 555 m). A l'ouest du lac Matamek les segments morainiques sont en position de bas de versant tandis qu'au nord-est de ce dernier les segments sont en position d'interfluve.

Le tracé de cet arc tend à démontrer la possibilité d'un raccord vers l'ouest avec la moraine du lac Daigle; en effet, il faudrait pour cela confirmer l'existence des deux segments litigieux entre la rivière Moisie et le lac Thom (fig. 19. 2a).

2^e arc: lobe de Manitou

Cet arc va de la rivière au Bouleau à la rivière Sheldrake et il est centré sur la dépression du lac Manitou et du lac des Eudistes (fig. 19. 1). Sa corde mesure environ 27 milles (43 km). L'altitude moyenne à la base de l'arc est de 500 à 750 pieds (150 à 230 m) alors que la zone nodale avec l'arc de Magpie se situe à des altitudes de 1100 à 2000 pieds (335 à 610 m). Ces divers segments sont en position d'interfluve sauf à la base de l'arc, soit entre le lac des Eudistes et la rivière à la Chaloupe, et aux abords immédiats de la rivière Tortue où ils sont en position de cuvette ou de mi-versant (fig. 19. 2a).

3^e arc: lobe de Magpie

Cet arc va de la rivière Sheldrake à la rivière au Saumon et il est centré sur la dépression du lac Magpie (fig. 19. 1). Sa corde mesure environ 30 milles (48 km). L'altitude moyenne à la base de l'arc est de 650 à 750 pieds (200 à 230 m) alors que la zone nodale avec l'arc de Mingan se situe à des altitudes de 1250 à 1500 pieds (400 à 460 m). Cet arc est un peu plus morcelé que les deux précédents et la plupart de ses segments sont en position de cuvette ou de mi-versant à l'exception des segments de la zone nodale avec l'arc de Mingan qui sont en position d'interfluve (fig. 19. 2b).

4^e arc: lobe de Mingan

Ce dernier arc se situe à l'est de la rivière au Saumon et semble être axé sur la vaste dépression de la rivière Mingan et probablement de la rivière Romaine (fig. 19. 1). La section levée présente une corde de plus de 45 milles (72 km). L'altitude moyenne à la base est de 350 à 450 pieds (105 à 140 m) tout comme l'arc de Moisie. Cet arc est très morcelé et n'exprime qu'une tendance en reliant diverses cuvettes qui sont le siège de formes morainiques.

Relations avec la lithologie

Aucune relation évidente n'existe entre les formes morainiques et la nature de la roche en place au nord du complexe si ce n'est que les segments morainiques semblent plus discontinus dans les anorthosites à l'est de la rivière à la Chaloupe que dans les gabbros, les gneiss ou les paragneiss (Greig, 1945; Sharma et Franconi, 1973) à l'ouest de cette dernière. De plus,

¹Université de Sherbrooke, Département de géographie,
Section de géographie physique, Sherbrooke, Québec.

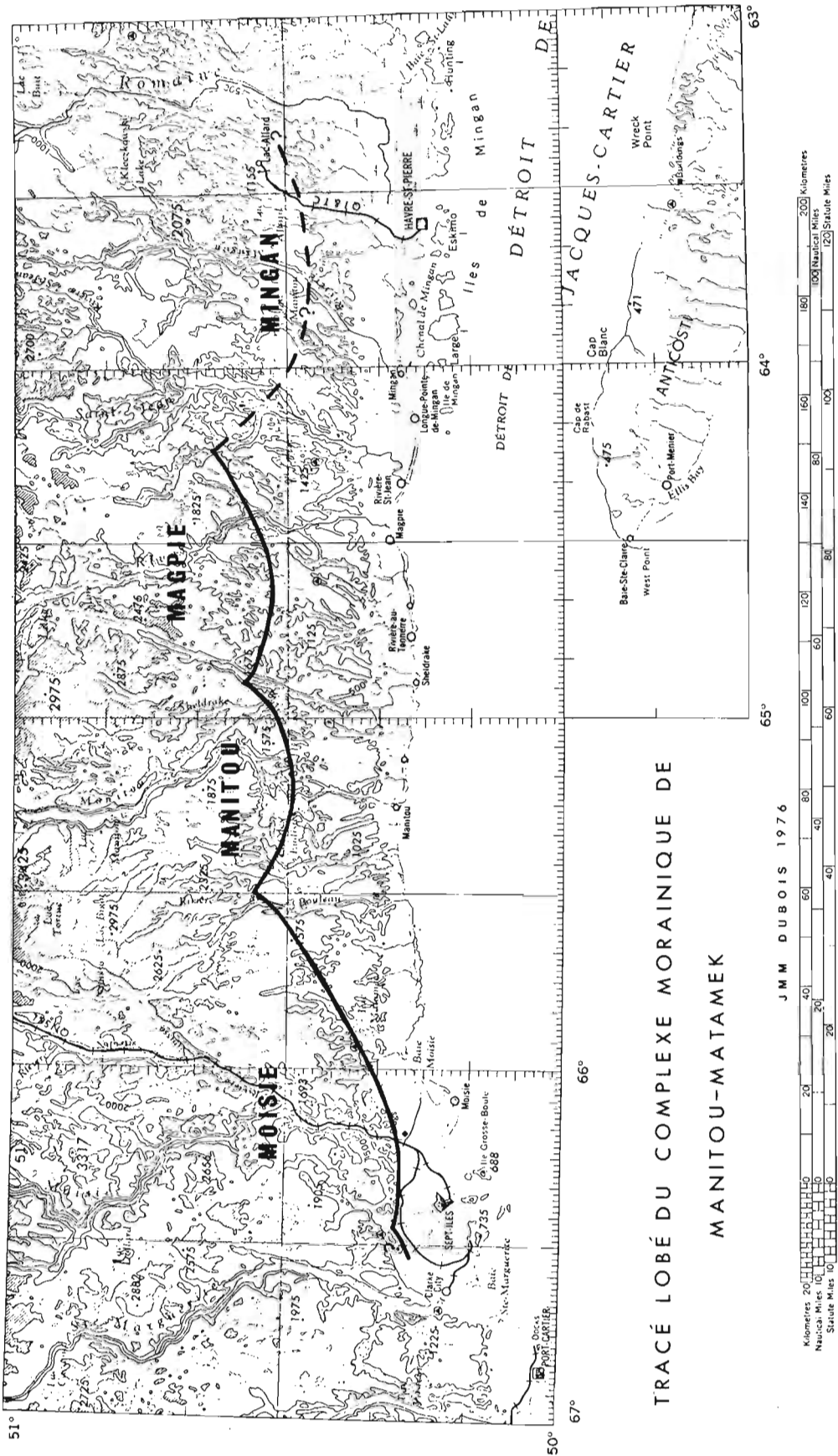


Figure 19.1.

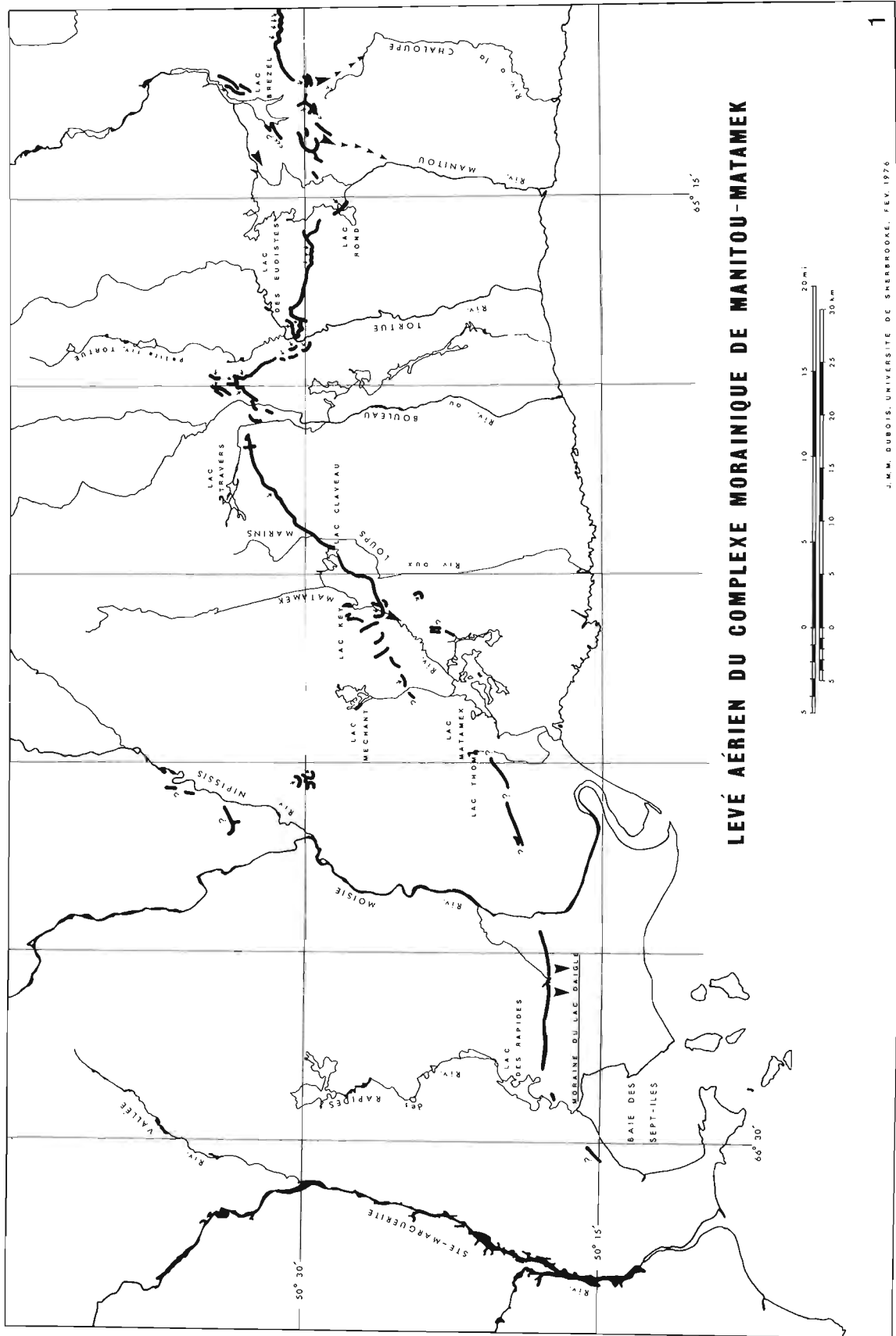


Figure 19. 2a.

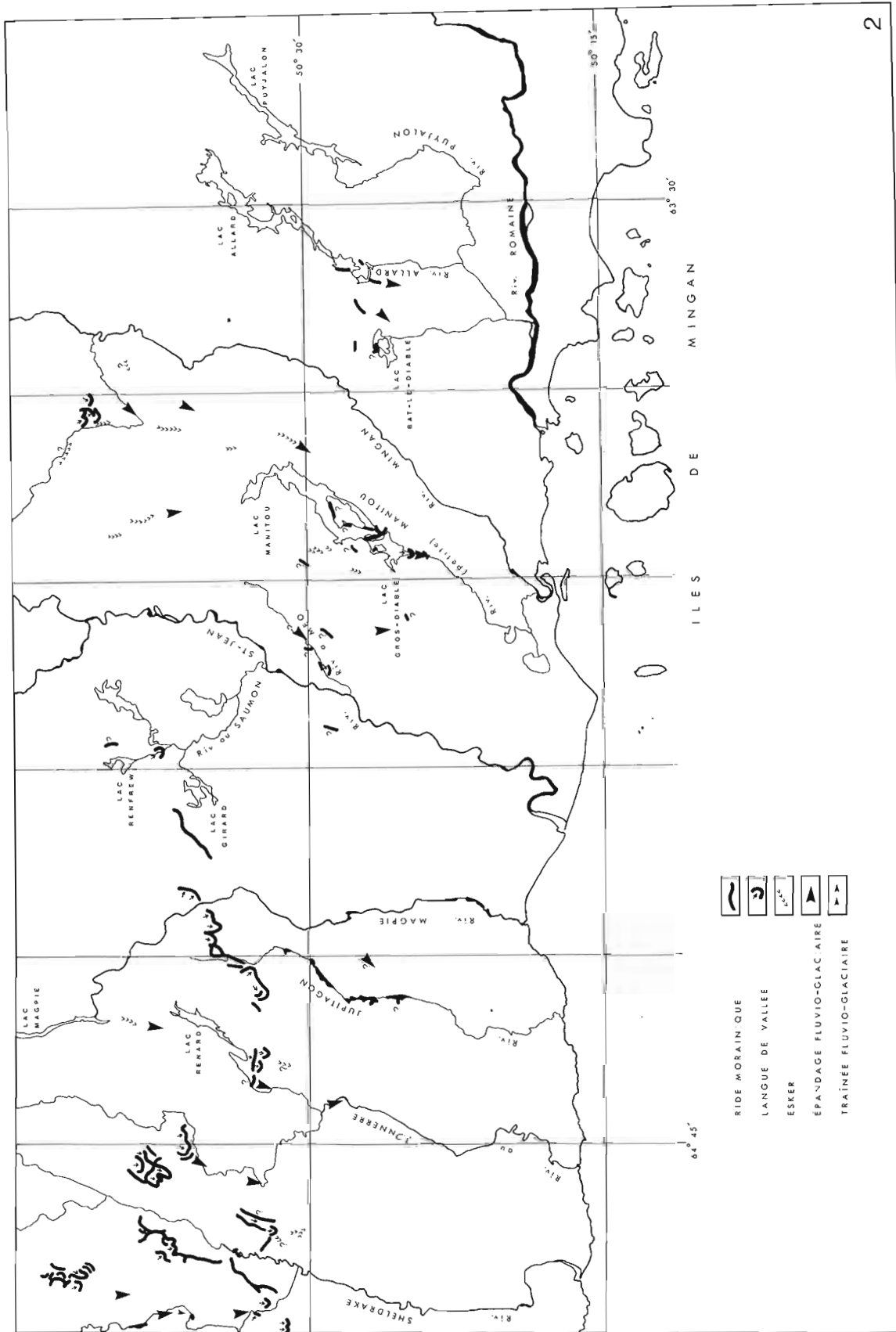


Figure 19. 2b.

il faut noter qu'il y a une lacune dans le complexe situé exactement sur le massif d'anorthosite du lac Matamek entre le lac Méchant et le lac Thom (fig. 19. 2a).

Composition et dynamique

En position de cuvette ou de bas de versant, les rides morainiques ont tendance à prendre du volume, à présenter une très grande variabilité granulométrique et à être associées directement avec des épandages fluvio-glaciaires ou avec des dépôts de fusion. Les trois segments suivants sont de ce type: 1- la ride entre les lacs Gros-Diable et Manitou (fig. 19. 2b); 2- la ride entre les lacs Rond et des Eudistes (fig. 19. 2a); 3- la moraine du lac Daigle. Pour cette dernière on peut se référer aux descriptions de Dredge (1971) et de Tremblay (1975).

En position d'interfluve ou de mi-versant, les rides morainiques sont très minces et semblent plutôt être composées de gros blocs si l'on se fie à la section survolée en hélicoptère entre la rivière Matamek et le lac Claveau¹ (fig. 19. 2a).

La plupart des rides morainiques semblent donc marquer un court temps de stagnation des lobes glaciaires en retraite et la petite dimension des moraines de poussée dans les vallées et vallons indiquent la faible ampleur des langues qui les ont édifiées.

Dredge (1971, p. 82) date la moraine du lac Daigle entre 9300 et 10 000 B.P. Tous les lobes du complexe morainique sont-ils synchrones? Y a-t-il un décalage chronologique de l'est vers l'ouest? Ces deux questions demeurent en suspens.

Conclusions de l'étude préliminaire

1. Le complexe morainique de Manitou-Matamek semble se subdiviser en au moins quatre arcs incluant la moraine du lac Daigle. De plus, il est permis de penser à la possibilité que le segment postulé par Tremblay (1975) à l'ouest de la baie des Sept-Iles soit l'aboutissement d'un cinquième arc.
2. Les arcs de Moisie et de Manitou sis dans les gabbros, les gneiss ou les paragneiss sont mieux définis que les arcs de Magpie et de Mingan sis sur les anorthosites.
3. L'ampleur des arcs semble directement proportionnelle à l'ampleur des dépressions tandis que leur altitude moyenne minimale à la base y est indirectement proportionnelle.

4. De façon générale les arcs présentent des segments morainiques en position de cuvette, de bas et de mi-versant aux basses altitudes de leur base et des segments en position d'interfluve aux hautes altitudes de leurs zones nodales.

5. En position de cuvette ou de bas de versant les segments sont plus volumineux, présentent une granulométrie plus variable et sont associés à des dépôts de fusion contrairement à ceux d'interfluve et de mi-versant qui sont minces et composés de gros blocs.

6. Ce complexe semble marquer un court arrêt des lobes glaciaires en retraite.

Références

- Dredge, L. A.
1971: Late-Quaternary sedimentary environments, Sept-Iles, Québec; unpubl. M.Sc. thesis, McGill University, Montreal, 102 p.
- Dubois, J. M. M.
1975: Le Quaternaire de la Côte Nord de l'estuaire maritime du Saint-Laurent; dans Report of Activities, Part A, Comm. Géol. Can., Paper 75-1A, p. 403-405.
1976: Le Quaternaire de la Côte Nord de l'estuaire maritime du Saint-Laurent: secteurs de Rivière-aux-Graines, Sheldrake et Mingan; dans Report of Activities, Part A, Comm. Géol. Can., Paper 76-1A, p. 33-36.
- Greig, E. W.
1945: Région du lac Matamek, comté de Saguenay; min. des Mines du Québec, rapp. géol. no. 22, 29 p., carte au 1: 63 360.
- Sharma, K. N. M. et Franconi, R. A.
1973: Grenville Project 1970; Geology of the rivière Magpie, rivière Saint-Jean and rivière Romaine area, Duplessis County, Quebec; min. des Rich. Nat. du Québec, rapp. GM-28405, 66 p., cartes au 1: 250 000.
- Tremblay, G.
1975: Géologie du Quaternaire; région de Sept-Iles/Port-Cartier; min. des Rich. Nat. du Québec, rapp. DP-304, 43 p., cartes au 1: 63 360.

¹Nous remercions Woods Hole Oceanographic Institution Mass. pour cette excursion.

Projects 740062, 710049

D. Swan
Terrain Sciences Division, VancouverI. Frydecky and R. G. Currie
Regional and Economic Geology Division, Vancouver

The need for increased precision in position fixing during marine geophysical and geological surveys has led to the use of electronic systems based upon the generation of pairs of stationary wave patterns by synchronized radio transmissions from two or more stations. The patterns generated may be either hyperbolic or circular and the ship's location is given in terms of the intersection of two pattern lines. A package of eight FORTRAN subroutines (with supporting documentation) has been compiled to facilitate conversions between pattern readings (range-range or hyperbolic) and UTM or geographic co-ordinates. The subroutines have been designed to be as flexible as possible so as not to place limitations on the survey procedure.

Two of the problems encountered during the formulation of these subroutines merit further discussion. All the algorithms used in this package are based upon plane geometry. However, pattern readings are observed over the spherical surface of the earth and

hence a correction or scale factor must be applied to the observed data before an accurate position can be obtained. Omitting this scale factor introduces a variable error of as much as several hundred metres in both the north-south and east-west directions. The second problem involves consideration of alternate mathematical solutions for regions on opposite sides of the baselines (lines joining transmitter sites), what is referred to as "back-cover". The problem of what "cover" to use arises from symmetry in the geometry of navigation station chains (Fig. 20.1).

The subroutines in this package deal with the problem of what "cover" to use by considering *a priori* knowledge of probable position to make calculations using "front" or "back" cover, whichever is appropriate. To facilitate the identification of "cover" type in position listings, patterns corresponding to areas of back cover are made negative.

Documented program listings are available from I. Frydecky in Vancouver.

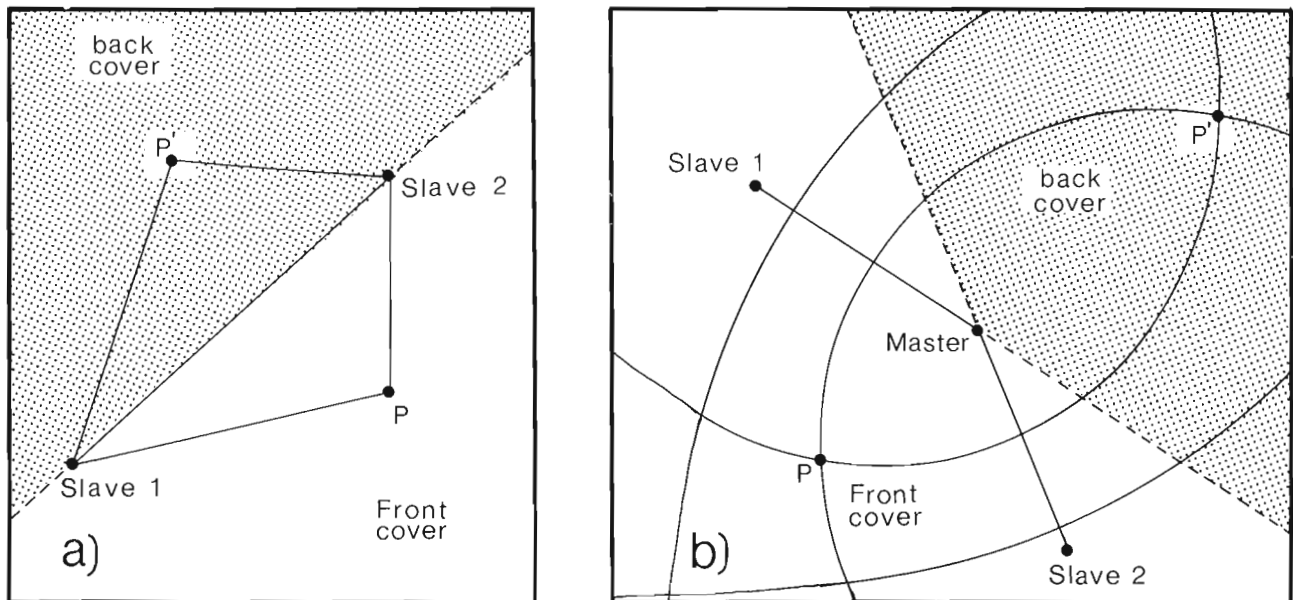


Figure 20.1. The configuration of navigation station chains in a) range-range and b) hyperbolic modes. P and P' are the positions calculated using front and back cover respectively.

MAGNETIC SUSCEPTIBILITY AS A DIAGNOSTIC PARAMETER OF
VANCOUVER ISLAND VOLCANIC ROCKS

Projects 710048 and 730036

R. G. Currie and J. E. Muller
Regional and Economic Geology Division, Vancouver

Field identification of the different volcanic units present on Vancouver Island is commonly difficult. The Karmutsen and Metchosin volcanics are tholeiitic basalts with similar pillow lavas, pillow breccias and flows that are lithologically almost identical. The Sicker and Bonanza volcanics are andesite to rhyodacite with flows, tuffs, and breccias. Although the Sicker volcanics are generally more metamorphosed, in many cases they look very much like the Bonanza volcanics.

An examination of available aeromagnetic data indicates that the volcanic units have associated magnetic anomalies of significantly different amplitude which may reflect differences in magnetic volume susceptibility. To investigate the relationship between rock unit and magnetic properties, a random selection of previously collected hand specimens from the major units present were examined. The major volcanic units are:

- (i) Metchosin volcanics – Eocene
– pillow basalts, flows, breccia, dykes and sills.
- (ii) Bonanza volcanics – Lower Jurassic
– ranging from basaltic andesite to rhyodacite.
- (iii) Karmutsen volcanics – Upper Triassic
– pillow basalt, flows, breccia, intruded by diabase dykes and weakly metamorphosed.
- (iv) Sicker volcanics – Paleozoic
– chiefly greenstones derived from volcanic breccias and tuffs.

Susceptibilities were determined from crushed samples with a Geophysical Specialties Company Magnetic Susceptibility Bridge Model MS-3. The reproducibility of the measurements was ± 2 scale divisions which is equivalent to from ± 50 per cent to ± 1 per cent with precision increasing with increasing susceptibility. The susceptibility of 8 cores of Metchosin volcanics were determined by Dr. E. J. Schwarz of the Geological Survey of Canada, Ottawa.

The histogram of the measured values (Fig. 21.1) is multimodal and the peaks in the histogram can be related to the mean susceptibility of each volcanic unit. The individual distributions approximate lognormal, a tendency that has been noted by Puranen *et al.* (1968). Although it has been suggested (Platou, 1974) that the median is a better way of describing the normal susceptibility than the mean value, the mean value, in units of 10^{-6} emu, is used in this report.

Differentiation between the units is suggested by the parameter means (Table 21.1) and distribution (Fig. 21.2). The Metchosin and the Karmutsen have comparable densities but the difference in mean susceptibility is statistically significant to a 95 per cent

confidence limit. The Karmutsen exhibit a bimodal distribution of susceptibilities which has been separated as A and B on Table 21.1. The bimodal distribution of Karmutsen susceptibilities appears to be inherent as it cannot be definitely related to sample location or lithology. There is an indication that holocrystalline medium grained rocks have higher susceptibilities than hypocrySTALLINE fine grained rocks with abundant palagonite. The difference between the mean susceptibility of the Metchosin and Karmutsen (B) is statistically significant to a 90 per cent confidence limit but Metchosin and Karmutsen (A) cannot be differentiated on the basis of susceptibility.

Table 21.1
Magnetic Susceptibility and Density of
Vancouver Island Volcanics

	1	2	3	4	5	6	7
Metchosin	3.01	0.56	1023	2.95	0.06	18	
Bonanza	2.35	0.90	224	2.76	0.07	8	
Karmutsen	2.42	0.88	263	2.93	0.08	10	
Mode A	3.24	0.12	1738	2.93	0.06	(5)	
Mode B	1.60	0.23	40	2.93	0.11	(5)	
Sicker	1.50	0.36	32	2.85	0.09	11	

1 = formation. 2, 3 = arithmetic mean and standard deviation of the logarithm of susceptibility. 4 = antilog (mean susceptibility). 5, 6 = arithmetic mean and standard deviation of density. 7 = number of samples.

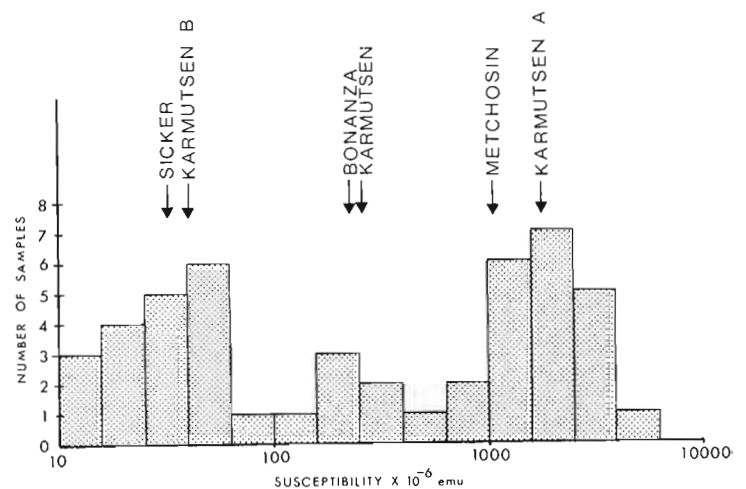


Figure 21.1. Histogram of magnetic susceptibility determinations with mean values, by rock unit, indicated.

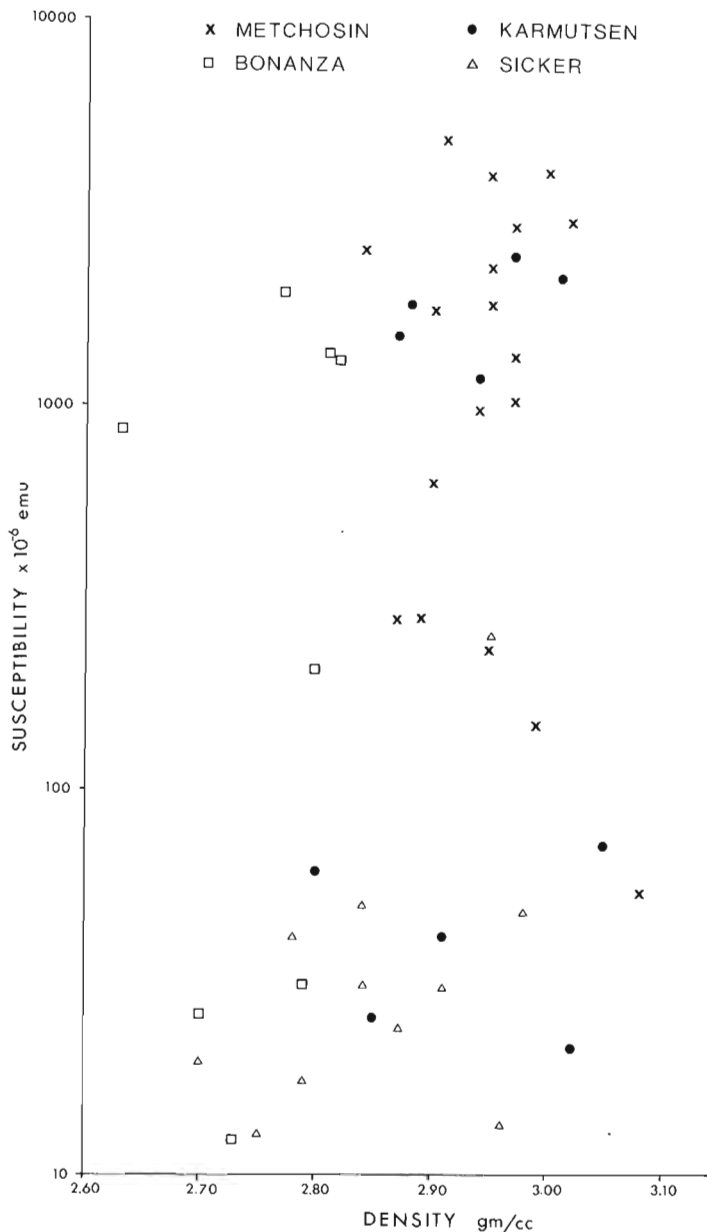


Figure 21.2. Magnetic susceptibility versus density.

The Bonanza volcanics have a wide range of susceptibilities and the lowest mean density, 2.76 gm/cc s. d. 0.07. The Sicker volcanics have the lowest mean susceptibility. The difference between the susceptibilities of the Bonanza and Sicker volcanics is statistically significant to a 95 per cent confidence limit. A correlation between susceptibility and age is observed with the older rocks tending to have lower susceptibility. This appears to be related to the degree of alteration or metamorphism.

In an attempt to improve the discrimination on the basis of an individual sample rather than on mean parameters, the chemical composition of the sample was also considered. The usefulness of rock chemistry, density, and susceptibility in discriminating between Karmutsen and Metchosin, or between Sicker and Bonanza volcanics was assessed by applying stepwise discriminant analysis (Cooley and Lohnes, 1962). This technique consists of looking for linear combinations of the variables to form canonical variables which give the optimal representation of the separation of the groups. This type of analysis is of special interest in that it selects the variables in order of their ability to differentiate between groups and it generates equations that can be evaluated to predict in which group a particular sample belongs. The analysis showed that of the variables considered, susceptibility was the most important parameter and that chemistry and density offer no additional aid in distinguishing between the Sicker and Bonanza volcanics. A knowledge of the rock chemistry improved the separation of the Karmutsen and Metchosin volcanics with H_2O and FeO being the most important parameters. The underlying assumption, that the sample means approximate the population means, cannot be assessed until a larger sample is examined. It has been suggested by Puranen *et al.* (1968) that approximately 100 samples are required to determine an average susceptibility within an accuracy of 5 to 10 per cent.

Despite the notorious variability of magnetic susceptibility, this preliminary investigation suggests that susceptibility can be used to distinguish between Bonanza and Sicker volcanics but its application in distinguishing between Metchosin and Karmutsen volcanics is uncertain unless the bimodality of the Karmutsen susceptibilities persists. The ease and speed with which magnetic susceptibility can be determined makes its application as a diagnostic aid in geologic mapping an area worth further study.

References

- Cooley, W. W. and Lohnes, P. R.
1962: *Multivariate Procedures for Behavioral Sciences*; Wiley.
- Platou, S. W.
1974: The relations between magnetic properties and magnetic anomalies; *Geol. Foeren. Stockh., Foerh.*, vol. 96, p. 253-260.
- Puranen, M., Marmo, V., and Hämäläinen, U.
1968: On the Geology, aeromagnetic anomalies and susceptibilities of Precambrian rocks in the Virrat region (Central Finland); *Geoexploration*, vol. 6, p. 163-184.

Project 710059

L. F. Jansa

Atlantic Geoscience Centre, Dartmouth

Introduction

A program of shallow drilling to obtain bedrock samples underlying parts of the southeastern Baffin Island shelf was undertaken by B. MacLean and S. P. Srivastava from CSS HUDSON during the period September 15-17, 1975 (Cruise 75-009, Phase V). The samples were collected using the Bedford Institute of Oceanography's underwater electric core drill.

The shelf southeast of Baffin Island (Hudson Strait to Cape Dyer) was previously investigated by Grant (1975) who inferred six distinct bedrock units on the basis of continuous seismic reflection and magnetic profiling. Grant's investigations also revealed that the structure of the southern Baffin shelf is considerably more complex than that of the Labrador Shelf to the south. Bedrock sample data are not available for control of the offshore geology north of the Eastcan *et al.* Bjarni H-81 well on the Labrador Shelf, 520 km south of Hudson Strait, except for a short sandstone core collected by Srivastava (1974) at a site about 130 km northeast of locality 9 (Fig. 22.1) and samples of rocks of possible Silurian age dredged by Grant (1975) from Hudson Strait.

Fifteen drilling attempts were made during CSS HUDSON Cruise 75-009 (MacLean and Srivastava, 1976) at nine different localities and six cores totalling 544 cm in length were recovered from four of these localities (Fig. 22.1). Cores from three localities consisted of limestone, whereas the fourth consisted of gneiss. Results of the petrographic study of the cores (Jansa, 1975, GSC Open File) and their regional geological implications are presented in this report.

As paleontological age data are not available at this time the stratigraphy of the suggested unit is tentative.

Results

Igneous and Metamorphic Rocks

The metamorphic and igneous rocks recovered by drilling off southern Baffin Island are considered to represent basement only at stations 9 and 9A, and erratics at all other stations (MacLean and Srivastava, 1976). The cores of igneous and metamorphic rocks can be grouped into six main petrographic categories (Table 22.1). With the exception of the biotite gneiss at station 9, all other rock types can be correlated with similar rocks outcropping on southern Baffin Island. According to Blackadar (1967) the rocks on southern Baffin Island are predominantly gneisses of Precambrian age, with the gneiss complex being metamorphosed during the Aphebian. The region is part of the

Churchill Structural Province. The regional distribution of the rock types cored on the shelf during the HUDSON 75-009 cruise is shown in Figure 22.1. For the abbreviation of rock types see Table 22.1.

Table 22.1

Comparison of the metamorphic and igneous rocks drilled on the Baffin shelf and outcropping on southern Baffin Island.

Southern Baffin shelf-station	Southern Baffin Island (Unit Number according to Blackadar, 1967)
biotite gneiss (basement) -9, 9A (Bi gn)	
acidic gneiss (erratics) -2, 3 (Ac gn)	3 (grey granite gneiss)
pyroxene gneiss (erratics) -1, 2, 3 (Py gn)	3 (grey granite gneiss)
garnet-biotite gneiss (erratics) -3, 5 (Gar gn)	7 (garnet-biotite-quartz-feldspar gneiss)
granite gneiss (erratics) -8A (Gr gn)	12 (granite gneiss)
granite (erratics) -8A, 8B (Gr)	13 (biotite granite)

Biotite gneiss: The light grey biotite gneiss cored at stations 9 and 9A, regarded as basement is characterized by the occurrence of olive coloured biotite. Composition, texture, and biotite colour is similar to the light grey biotite gneiss found by the author on Monumental Island, situated 60 km south-southwest from station 9. Erratics of biotite gneiss were recovered at stations 8 and 2. Both stations are located relatively close to the biotite gneiss outcrops.

Acidic gneiss: Considering the small diameter of the core, size of pebbles, and the wide variation in composition of the acidic rocks, plus the presence of migmatites on southern Baffin Island, the identification of this rock is uncertain. Pebbles of light grey acidic gneiss were recovered at stations 2 and 3. These may be derived from the migmatite or the leucocratic portion of the biotite gneiss.

Pyroxene gneiss: The occurrence of pebbles composed of pyroxenic gneiss is limited to the southern and central part of the study area (Fig. 22.1, stations 1, 2, and 3). The composition of the gneiss on the shelf is

similar to the rocks described by Blackadar (1967) as quartz-feldspar gneiss (unit 3), which contains hypersthene and therefore could be called charnockite. The pyroxene gneiss occurs widely on southern Baffin Island and outcrops along the northwest shore of Frobisher Bay, which may be the source of the erratics.

Garnet-biotite gneiss: Pebbles of light grey garnet-biotite gneiss were recovered in the central and northern part of the investigated area at stations 3 and 5. Similar rocks outcrop extensively on Hall Peninsula, southern Baffin Island (unit 7, Blackadar, 1967).

Granite gneiss: A pebble of granite gneiss was recovered at station 8A. This rock type may correspond to the granite gneiss (unit 12, Blackadar, 1967), which outcrops widely throughout southern Baffin Island.

Granite: Pebbles of granite were recovered at stations 1, 8A and 8B. Coarse crystalline biotite granite outcrops were noted by the author in 1974 on Monumental Island, and on the eastern Part of Hall Peninsula by Blackadar (1967). The pebbles could be derived from these sources.

Sedimentary Rocks

The sedimentary rocks recovered by coring are dominantly carbonates. The cores from stations 4, 5, 8A and 8B were considered by MacLean and Srivastava (1976) to represent subsea outcrops. The carbonate rocks at stations 3 and 8 are erratics.

From detailed studies of the limestones in thin sections and considering composition, colour, sedimentary structures and fossil assemblages, three distinctive

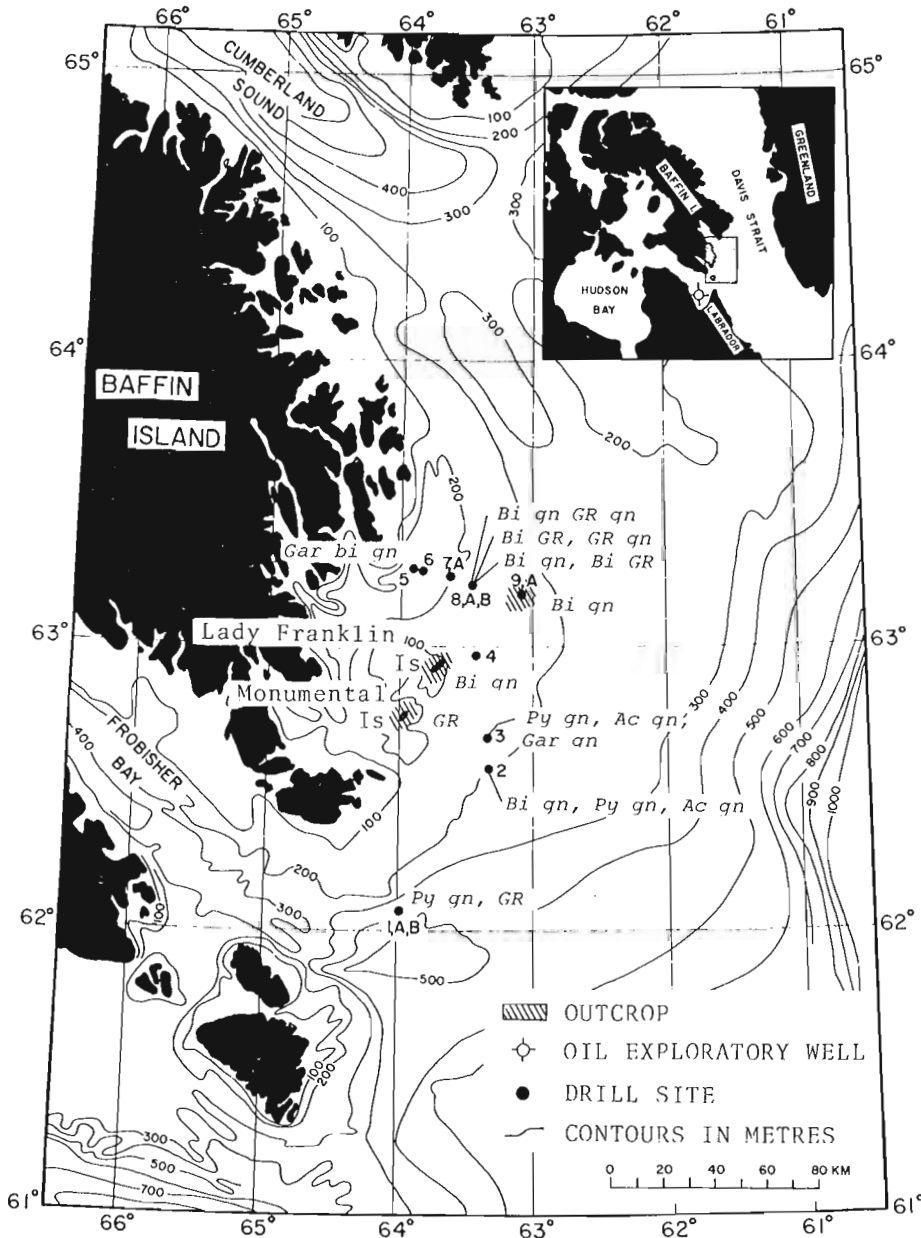


Figure 22.1.

Distribution of igneous and metamorphic rock types recovered at drill sites off southern Baffin Island.

lithostratigraphic units were recognized. The tentative stratigraphic superposition of the limestones is summarized in Table 22. 2.

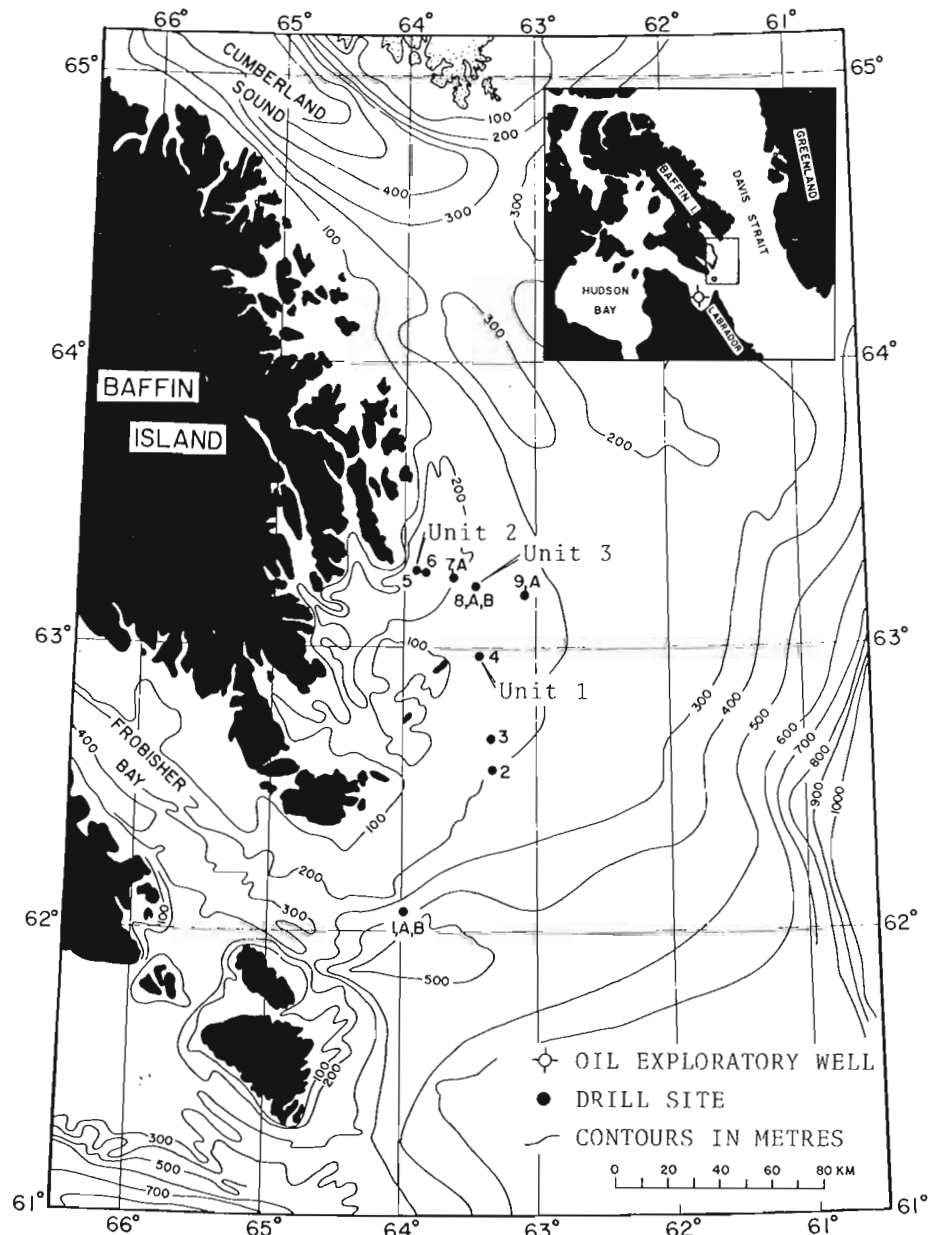
Unit 1 (Station 4, Fig. 22.2): This unit is composed of mottled, olive grey dolomitic limestone with laminae of flat pebble conglomerate and breccia (Fig. 22. 3a). The mottling is caused by preferential dolomitization of the micrite-filled burrows. Dolomitization increases toward the bottom of the core. The micrite intraclasts are angular in some of the laminae, and rounded in others. Intraclasts are jumbled with trilobite, mollusc, and crinoid fragments. Rare Chitinozoa and scolecodonts occur in the insoluble residue. In some of the micritic intraclasts, authigenic feldspars and minute quartz crystals are abundant. The bioclasts in the breccia laminae are unsorted without preferential orientation,

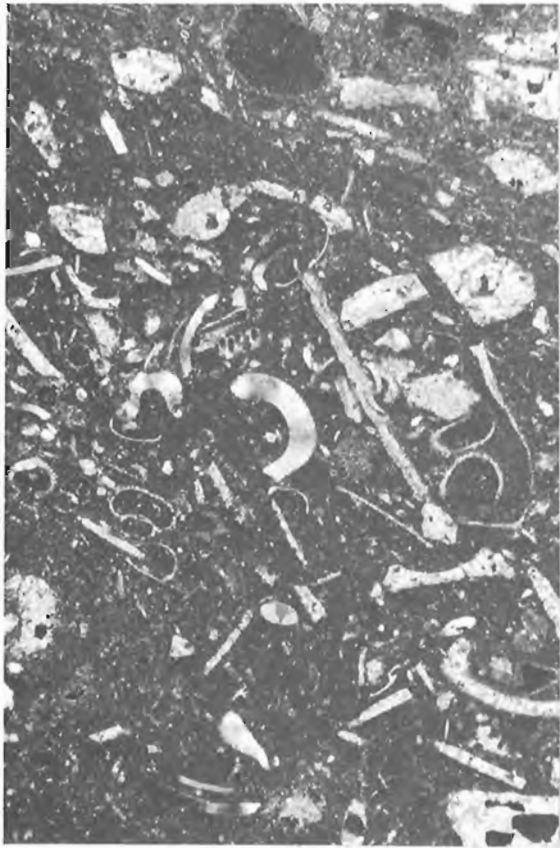
which indicates turbulent flow and rapid deposition of the sediment. The composition and texture of the sediment indicate deposition was in the intertidal to shallow subtidal zone, with the flat pebble breccia beds probably representing storm deposits.

Unit 1 can be compared to Member A of the Baillarge Formation and the Bad Cache Rapids Group of the Hudson Platform (B.V. Sanford, pers. comm., 1976; Trettin 1969, 1975; Thorsteinsson and Tozer 1970) which are Middle Ordovician in age. Another sequence lithostratigraphically similar to unit 1 is present in Foxe Basin; it was mapped by Trettin (1975) as map-unit DSc6 and is Lower Silurian in age. The seismic interpretation of the geology of the southern Baffin Shelf by Grant (1975) indicates that unit 1 is overlapped by unit 3. This supports the stratigraphic superposition of the units as indicated in Table 22. 1, but until

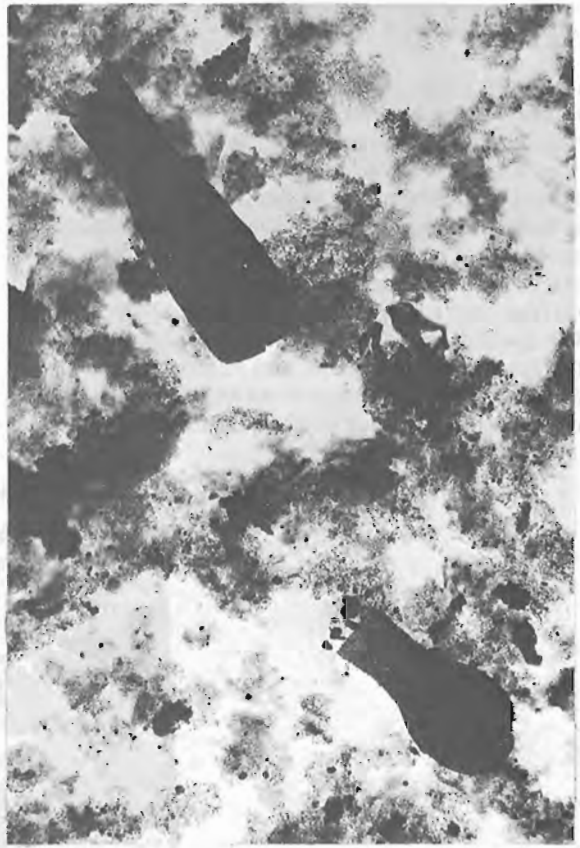
Figure 22. 2.

Occurrence of limestone units at drill sites off southern Baffin Island.





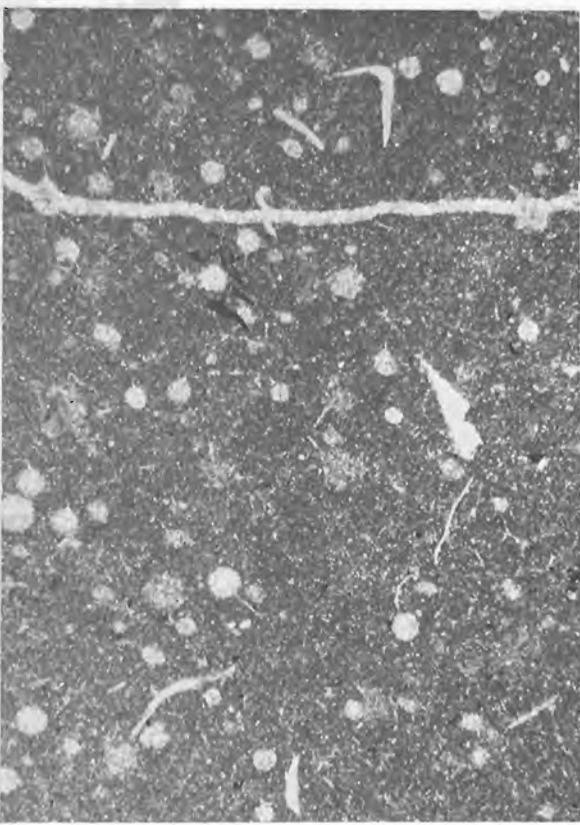
b



d



a



c

Figure 22. 3a. Intraclast breccia (unit 1). Subangular and subrounded clasts of dark grey micrite, fragments of mollusc with prismatic structure of shell and rare echinoderms are cemented by coarse sparry calcite. Euhedral dolomite replaces cement and to a lesser degree the intraclasts (?storm breccia deposited in a shallow subtidal environment). Thin section, ordinary light; station 4 - 45 cm. Bar scale equal to 1 mm.

22. 3b. Skeletal wackestone (unit 2), bioturbated, composed of fragments of trilobites, brachiopods, gastropods and echinoderms in a micritic matrix (infralittoral depositional environment, below wave base). Thin section, ordinary light; station 5 - 115.5 cm. Bar scale is equal to 1 mm.

22. 3c. Radiolaria-bearing micrite (unit 3). The radial skeleton of the Radiolaria with occasionally preserved spines is replaced by iron rich sparry calcite. Fragments of thin shell mollusc and Chitinozoa are rare. Matrix is composed of a mixture of micrite, microsparite, argillaceous and fine organic matter (epibathyal depositional environment). Thin section parallel with the bedding plane, ordinary light. Bar scale equal to 1 mm.

22. 3d. Insoluble residue from Radiolaria-bearing limestone (site 8) shows large concentration of very fine, fluffy, organic matter and well preserved Chitinozoa (unit 3). Bar scale equal to 0.1 mm.

biostratigraphic data are available, this remains speculative.

Unit 2 (Station 5, Fig. 22.2): This unit is massive, pale yellowish brown skeletal wackestone (Fig. 22.3b), slightly bioturbated and partially dolomitized. Dolomitization of the limestone is a secondary, post-diagenetic feature. Euhedral dolomite crystals locally replace the micritic matrix of the wackestone. Skeletal remains in the limestone were identified as fragments of echinoderms, trilobites, articulate brachiopods, rare cephalopods, favositid corals, and bryozoans. Scolecodonts, Chitinozoa, and acritarchs are rarely found in the insoluble residue. The fossil assemblage indicates an open marine, low energy, possibly deeper infralittoral depositional environment. The presence of the favositid coral and associated fossils suggests a late Ordovician-Silurian age for the unit. The lithology and fossil assemblage is similar to the limestone outcropping at the cliffs of Akpatok Island, dated as late Middle and early Upper Ordovician by Workum *et al.* (1976). A similar sequence is present within the Churchill River Group, Hudson Bay (B.V. Sanford, pers. comm., 1976; Workum *et al.*, 1976). The fossil assemblage from unit 2 is similar to those described from Silliman's Fossil Mount at Frobisher Bay by Miller *et al.* (1954). The lithological appearance of the limestones of unit 2 is also similar to the limestones dredged in Ungava Bay (Dredge DW 71-030, No. 1, Grant, 1975) and the limestones described by Trettin (1969) as unit B of the Baillarge Formation. The limestone sequences at all these localities are interpreted as Late Ordovician. Because the limestone of unit 2 represents a deeper water facies than unit 1, and considering the transgressive nature of the Upper Ordovician in this region, a Late Ordovician age of unit 2 seems likely.

Unit 3 (Stations 8A, 8B, Fig. 22.2): This unit is composed of dark yellowish brown, slightly dolomitized Radiolaria-bearing bituminous micritic limestone. Radiolaria in the limestone are poorly preserved as casts filled by sparry calcite (Fig. 22.3c). The Radiolaria are rounded in shape, 0.14 mm in diameter, occasionally with poorly preserved spines. The Radiolaria are tentatively identified as belonging to the Suborder *Spumellina* Ehrenberg, 1875 (Campbell and Moore, 1954). Other fossils present in the limestone are sparsely occurring trilobite fragments, sponge spicules, and traces of ?graptolite. Chitinozoa and acritarchs are common in the insoluble residue (Fig. 22.3d). Finely disseminated organic pigment between micrite particles constitute several per cent of the limestone. Silt grains and argillaceous matter are rare. Silt-sized dolomite crystals are scattered in the micrite matrix.

Unit 3 may be correlative to the Red Head Rapids of the Hudson Platform (Trettin, 1975; B.V. Sanford, pers. comm., 1976). Limestones, similar in colour and composition, were described within Member B of the

Table 22.2

Lithostratigraphic Units	Colour	Texture	Fossils
3	pale brown (5YR5/2)	massive, faint lamination and bedding, bioturbation minor	Radiolaria, trilobites, sponge spicules, ?graptolite
2	pale yellowish brown (10YR6/2)	massive, minor bioturbation	echinoderms, trilobites, brachiopods, favositid corals, gastropods
1	olive grey (5Y4/1; 5Y6/1)	mottled, flat pebble intraclasts, mud cracks (?), scouring, minor bioturbation	molluscs, trilobites, crinoids

Baillarge Formation on northwestern Baffin Island, considered by Trettin (1969) to span late Middle Ordovician to early Silurian.

None of the authors (Workum *et al.*, 1976; Trettin, 1969, 1975; Miller *et al.*, 1954; Blackadar, 1967) describing the Paleozoic rocks on Baffin Island mentioned the occurrence of radiolarians. The Radiolaria could easily be overlooked in the limestone as their presence can be recognized only by careful examination of thin sections. Alternatively, the Radiolaria may not occur in the rocks described by Workum *et al.*, and Trettin, if these limestones represent nearshore facies.

The fossils, the micritic matrix, and the presence of organic matter indicate pelagic deposition in a low energy environment, with poorly oxygenated bottom water, probably as a result of sluggish bottom water circulation. Such depositional conditions can develop in a semirestricted environment or in the deeper parts of the marine basin. The presence of a dominantly planktonic fossil assemblage and lack of other "shelf dominated" fossils in unit 3 are strong indications of an outer littoral to epibathyal depositional environment.

Other occurrences of Radiolaria in the Ordovician of eastern North America were described from the New York Late Ordovician cherts by Ruedemann and Wilson (1936) and were mentioned from the Lower and Middle Ordovician cherts of Newfoundland by Sampson (1923) and Kay (1973).

When commenting on the fossil assemblage from Silliman's Fossil Mount in Frobisher Bay, Miller *et al.* (1954) noted that the fossils are similar to those on northwestern Greenland. The occurrences of "deeper water" facies in the offshore of southern Baffin Island is an indication that the northern Labrador Sea was a deeper "oceanic" basin in the Lower Paleozoic, with the sea connected to the Appalachian geosyncline. The limestones at Frobisher Bay and northwest Greenland

are the "paleoshelf" deposits of a Late Ordovician sea, which probably extended from Baffin Bay southward along the Labrador and western Greenland margins into the Newfoundland area.

The existence of a Late Ordovician "deeper water" basin off southern Baffin Island has implications for the tectonic interpretation of the Labrador Sea Basin (LePichon *et al.*, 1971; Laughton, 1972; Grant, 1975; van der Linden, 1975; Beh, 1975; and others), and opens at least two alternative explanations for the tectonic development of the region: a) the Lower Paleozoic basin opened and closed in similar manner to the Ordovician basin in central Newfoundland (Kay, 1973) and opened again along almost the same suture zone in the Late Mesozoic-Tertiary; or b) the northern Labrador Sea area is a region of mainly vertical tectonic movement, with the late Mesozoic-Tertiary tectonic stage mainly one of axial collapse accompanied by volcanism and extension in the central Labrador Sea. The recent geophysical studies in the Labrador Sea (Grant, 1975; van der Linden, 1975), seem to favour the latter hypothesis.

References

- Beh, R. L.
1975: Evolution and geology of western Baffin Bay and Davis Strait, Canada; in Canada's Continental Margins and Offshore Petroleum Exploration; eds. C. J. Yorath, E. R. Parker, and D. J. Glass; Can. Soc. Pet. Geol., Mem. 4, p. 453-476.
- Blackadar, R. G.
1967: Geological reconnaissance, southern Baffin Bay Island, District of Franklin; Geol. Surv. Can., Paper 66-47, 32 p.

- Campbell A. S. and Moore, R. C.
1954: Protista 3; in *Treatise on Invertebrate Paleontology, Part D* (Ed. R. C. Moore).
- Grant, A. C.
1975: Geophysical results from the continental margin off southern Baffin Island; in *Canada's Continental Margins and Offshore Petroleum Exploration*; eds. C. J. Yorath, E. R. Parker, and D. J. Glass; *Can. Soc. Pet. Geol., Mem.* 4, p. 411-431.
- Kay, Marshall
1973: Tectonic evolution of Newfoundland; in *Gravity and Tectonics*; eds. K. A. DeJong and Robert Scholten; John Wiley and Sons, New York, p. 313-326.
- Laughton, A. S.
1972: The southern Labrador Sea - A key to the Mesozoic and Early Tertiary evolution of the North Atlantic; in *Initial Reports of the Deep Sea Drilling Project*, Laughton, A. S., Berggren, W. A. *et al.*; v. XII, Washington (U. S. Government Printing Office), p. 1155-1179.
- LePichon, X., Hydmann, R. D., and Pautot, G.
1971: Geophysical study of the opening of the Labrador Sea; *J. Geophys. Res.*, v. 76, p. 4724-4743.
- MacLean, B. and Srivastava, S. P.
1976: Shallow core hole drilling on the Baffin Island shelf; in *Report of Activities, Part A*, *Geol. Surv. Can., Paper 76-1A*, p. 141-143.
- Miller, A. K., Youngquist, W., and Collinson, C.
1954: Ordovician cephalopod fauna of Baffin Island; *Geol. Soc. Am., Mem.* 62, 234 p.
- Ruedemann, R. and Wilson, T. Y.
1936: Eastern New York Ordovician cherts; *Geol. Soc. Am., Bull.*, v. 47, p. 1535-1586.
- Sampson, E.
1923: The terrigenous chert formations in Notre Dame Bay, Newfoundland; *J. Geol.*, v. 31, no. 7.
- Thorsteinsson, R. and Tozer, E. T.
1970: Geology of the Arctic Archipelago; in *Geology and Economic Minerals of Canada*; ed. R. J. W. Douglas, p. 547-590.
- Trettin, H. P.
1969: Lower Paleozoic sediments of northwestern Baffin Island, District of Franklin; *Geol. Surv. Can., Bull.* 157, 70 p.

1975: Investigations of Lower Paleozoic geology, Foxe Basin, northeastern Melville Peninsula, and parts of northwestern and central Baffin Island; *Geol. Surv. Can., Bull.* 251, 177 p.
- van der Linden, W. J. M.
1975: Crustal attenuation and sea-floor spreading in the Labrador Sea; *Earth Planet. Sci. Lett.*, v. 27, p. 409-423.
- Workum, R. H., Bolton, T. E., and Barnes, C. R.
1976: Ordovician geology of Akpatok Island, Ungava Bay, District of Franklin; *Can. J. Earth Sci.*, v. 13, p. 157-178.

E. M. R. Research Agreement 1135-D13-4-71/75

Erich Dimroth¹

Regional and Economic Geology Division

Introduction

This project has as its purpose the detailed reconstruction of the historical evolution of a typical segment of the Archean Abitibi greenstone belt. The area investigated comprises the 12 townships surrounding Rouyn-Noranda, Québec (Fig. 23.1).

Work is done in the form of Ph.D. and M.Sc. theses at various universities, under the field supervision of the writer. Field work has been financed by the Quebec Department of Natural Resources. Funds for laboratory work have been obtained from the National Research Council of Canada (Operating Grant No. A 9145) and the Geological Survey of Canada. Detailed progress reports have been issued by the Quebec Department of Natural Resources (Dimroth *et al.*, 1973, 1974, 1975a).

Two large longitudinal faults, the Cadillac and Duparquet-Destor faults (not shown on Fig. 23.1) segment the area in east-west trending slices. Correlation across these faults is difficult. For this reason, there is some controversy concerning the regional stratigraphy (cf. Wilson, 1962; Graham, 1954). Figure 23.2 gives a tentative stratigraphic scheme that appears to agree best with the field relations observed so far. However, there is still considerable doubt about the mutual relations of the Malartic, Lake Caste and Kinojevis groups.

VolcanologyVolcanic stratigraphy

Mapping of marker units permits the subdivision of the volcanic sequences by means of an interdigitating system of key horizons. Porphyritic and variolitic flows or flow groups serve as markers in intermediate-mafic volcanic sequences. Subaqueous pyroclastic flows are excellent marker units unless they are hyalotuffs related directly to lava flows. Distinct phenocryst associations permit mapping of individual rhyolite flows. Very few marker units can be followed for more than 20 km. Marker units, being products of a single extrusion or of an extrusive period, are time-rock units.

Volcanic facies

Systematic study of the facies of volcanic rocks permits certain conclusions regarding the mechanism of their emplacement, and the bathymetry at the site of extrusion or of emplacement. Facies of mafic and intermediate rocks are defined by variation of the

following properties: (1) Vesicularity; (2) proportion of massive, pillowed or brecciated rocks in the flow units; (3) absence or presence of stratified hyalotuff at the top of flows and (4) the petrography of the aquagene tuffs. Hyalotuffs are tuffs in which fragmentation occurred largely by hyaloclastic processes, but which were dispersed by minor explosions and which were emplaced as local pyroclastic falls and flows. They contain the same type of phenocrysts as the underlying lava flow from which they are derived. Vesicularity, the proportion of pillow breccia in flow units, and the proportion of hyalotuffs increase with decreasing water depth at the site of emplacement, but are functions of magma composition as well.

Facies of pyroclastic rocks are defined by, (1) the morphology and vesicularity of essential fragments, both functions of the mechanism of eruption (Heiken, 1972), and (2) the sequence of sedimentary structures which are a function of the mechanism of emplacement and nearness to source. Ballistic fall-back breccias, and subaqueous pyroclastic falls and flows have been distinguished (Dimroth *et al.*, 1975b). Facies of acidic flows defined by characteristic flow ribbing, flow folding and by several types of breccias, appear to reflect proximity to the feeding vent (Provost, in Dimroth *et al.*, 1975a).

Volcanic associations

Integration of data on the stratigraphy and facies of the volcanic rocks permits us to define volcanic associations comparable to associations of Cenozoic volcanic rocks. These associations are interpreted to have formed in specific environments. Figure 23.3 illustrates the way in which volcanic associations are defined and the way in which their formative environment is interpreted.

The Blake River Group, in the area between Hébécourt Lake and Cléricy (area 1, Fig. 23.1), may be subdivided into several stratigraphic divisions, defined by marker units (Dimroth *et al.*, 1974, 1975), and distinguished by their chemistry (Gélinas *et al.*, 1975). A prominent variolitic basalt unit, about 500 feet above the base of the group, can be followed for more than 100 km along strike. This basal unit of the Blake River Group shows minimal changes of thickness and of facies. It is composed of massive and pillowed basalt, without substantial quantities of pillow breccia or aquagene tuff. Its vesicularity is low (generally below 2 per cent), and vesicle size is small. The rocks are tholeiitic basalts (Gélinas *et al.*, 1975). Thus, the association has the geometry of a thin, flat sheet of large lateral extent. The low vesicularity and the absence of products of explosion suggest eruption of this basalt sheet in deep water (2000 m +, Jones, 1969; Moore, 1965).

¹Sciences de la Terre, Université du Québec à Chicoutimi

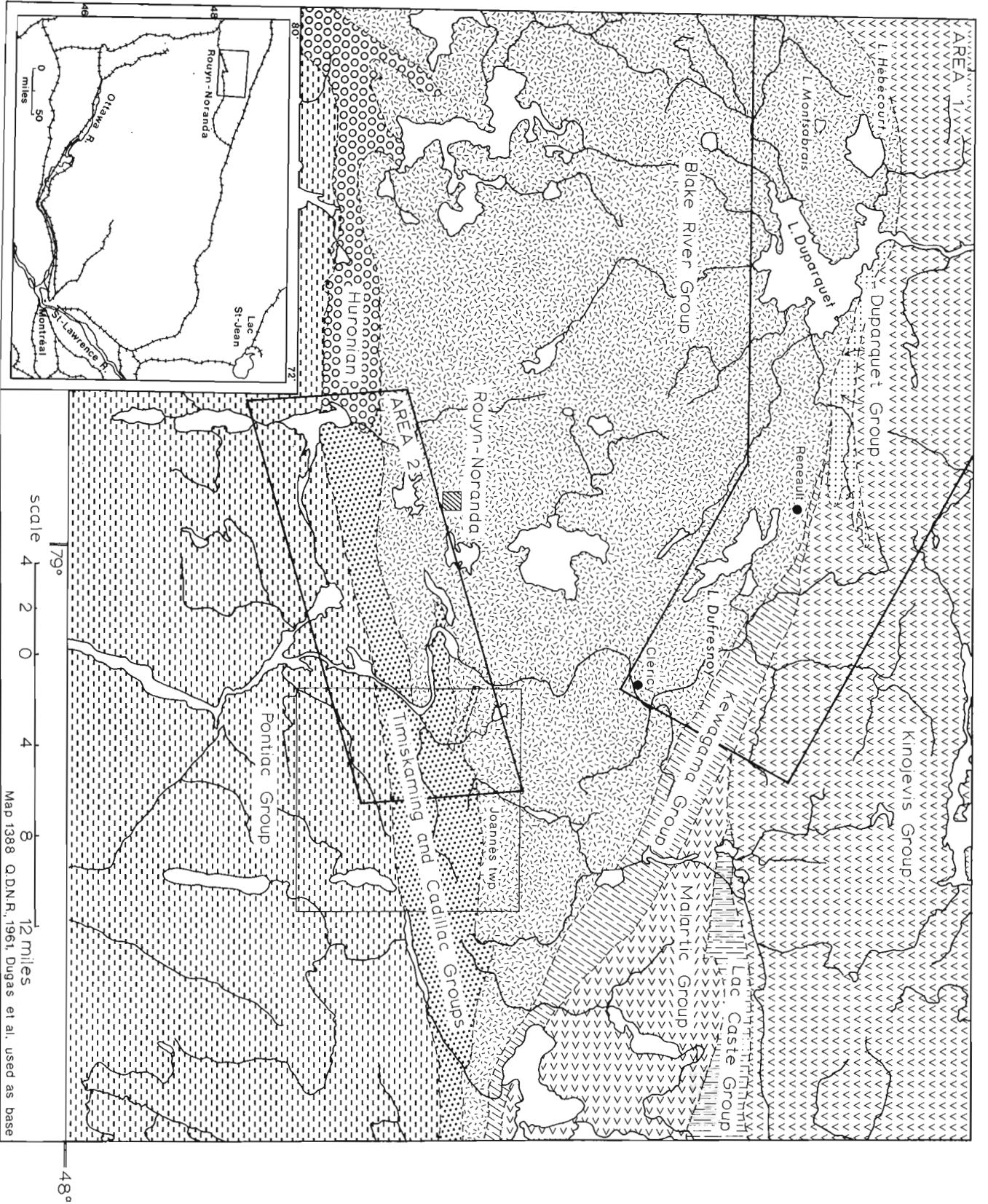


Figure 23.1. Index map of the area.

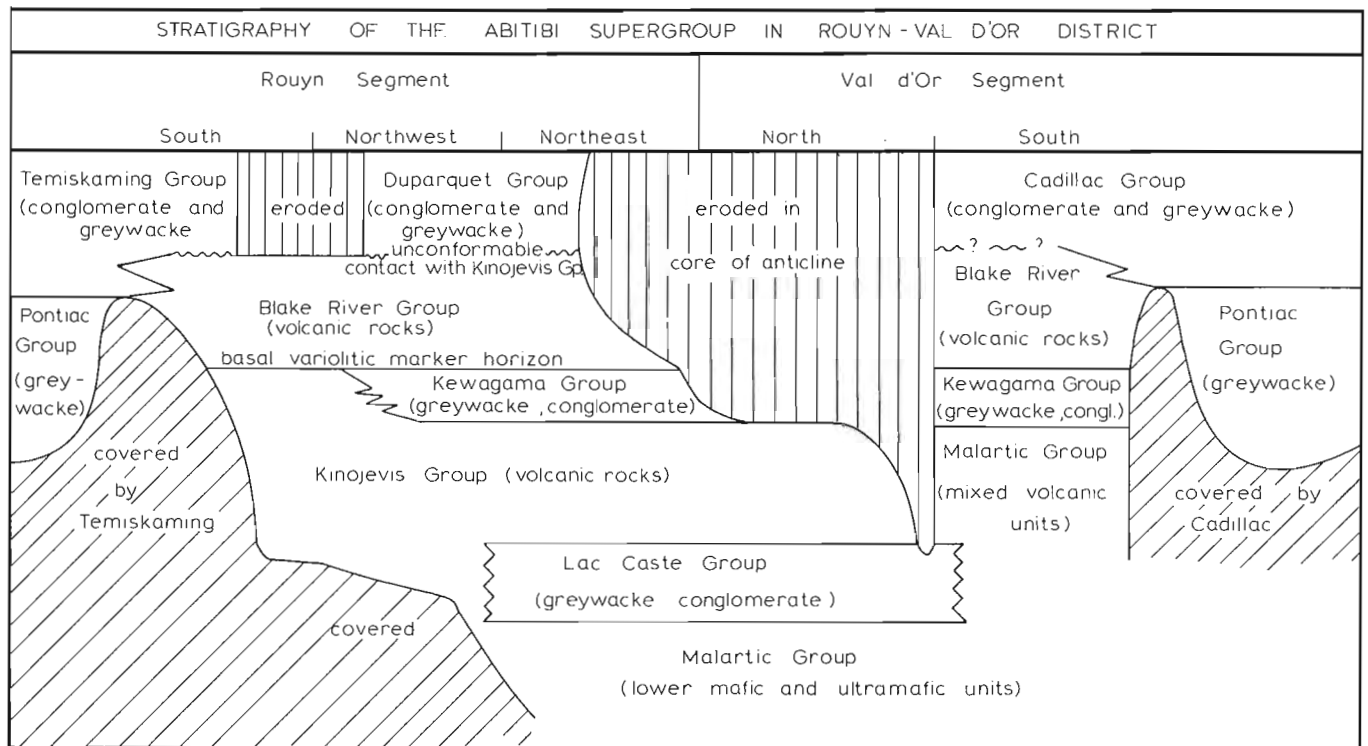


Figure 23. 2. Tentative stratigraphic table of Rouyn-Val d'Or area.

The basal phase of the Blake River Group is overlain by two associations of andesite and basalt. In the west, fine feldspar-porphyrific andesites and basalts predominate whereas east of Duparquet Lake the andesites and basalts are aphanitic, except for two well defined marker units (porphyritic marker and Dalembert tuff). The thickness of both associations increases from about 1500 m at Duparquet Lake to a maximum of about 5000 m at Montsabrias Lake and at Reneault. Vesicularity of flows, as well as the proportion of pillow breccia and of layered hyalotuff, increase in the western association toward the top of the sequence and, laterally, toward Montsabrias Lake. Facies relations of the andesitic sequence east of Duparquet Lake are more complicated; however, pyroclastic flows are in very proximal facies west of Reneault, whereas distal facies are exposed on Duparquet Lake and Lac Dufresnoy. These two associations are interpreted as shield volcanoes that were growing on a nearly horizontal platform and that became nearly emergent at the end of their activity.

Small flows of high magnesium basalt (komatiite), rhyolite domes, and dykes of comparable composition occur in a narrow zone north of the Duparquet-Destor-Manneville break. They may suggest the existence of a long-lived fault that began to form during the eruption of the volcanic sequence and that was rejuvenated repeatedly thereafter.

Sedimentology

The mechanisms and environments of deposition of the sediments of the Duparquet, Timiskaming and Cadillac groups are being investigated by M. Rocheleau (Université de Montréal). Sediments were deposited in four basic environments: (1) fluvial; (2) coastline (fluvial sediments and turbidites interfingering); (3) turbidite fans and (4) pelagic sediments deposited in areas protected from the influx of large quantities of terrigenous detritus. Sediments were derived from a volcanic terrane containing an appreciable volume of coarse grained, granitic plutonites. Transport was grossly from north to south. Details on the sedimentology of the area have been published by Rocheleau (in Dimroth *et al.*, 1975a, b).

Tentative Basin Model

At present, it appears that the paleogeography of the investigated area can be interpreted in terms of a volcanic chain in the north, adjoined to the south by a marine sedimentary basin. The volcanic chain apparently was built southward in successive steps. During the earlier stage of evolution (Kinojevis Group) most of the volcanic chain was deep marine and consisted of a vast, thick, basalt sheet interfingering to the east with a shield volcanic complex (Destor Complex). Later, a thin basalt sheet erupted to the south of the Destor Complex (basal unit of Blake River Group) and a complex system of overlapping shield volcanoes grew upon this base (main part of Blake River Group). Some

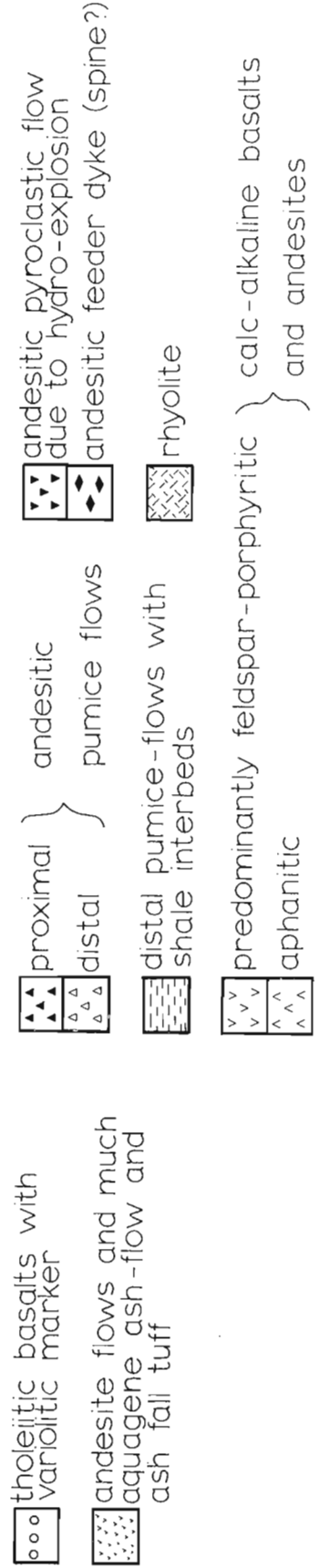
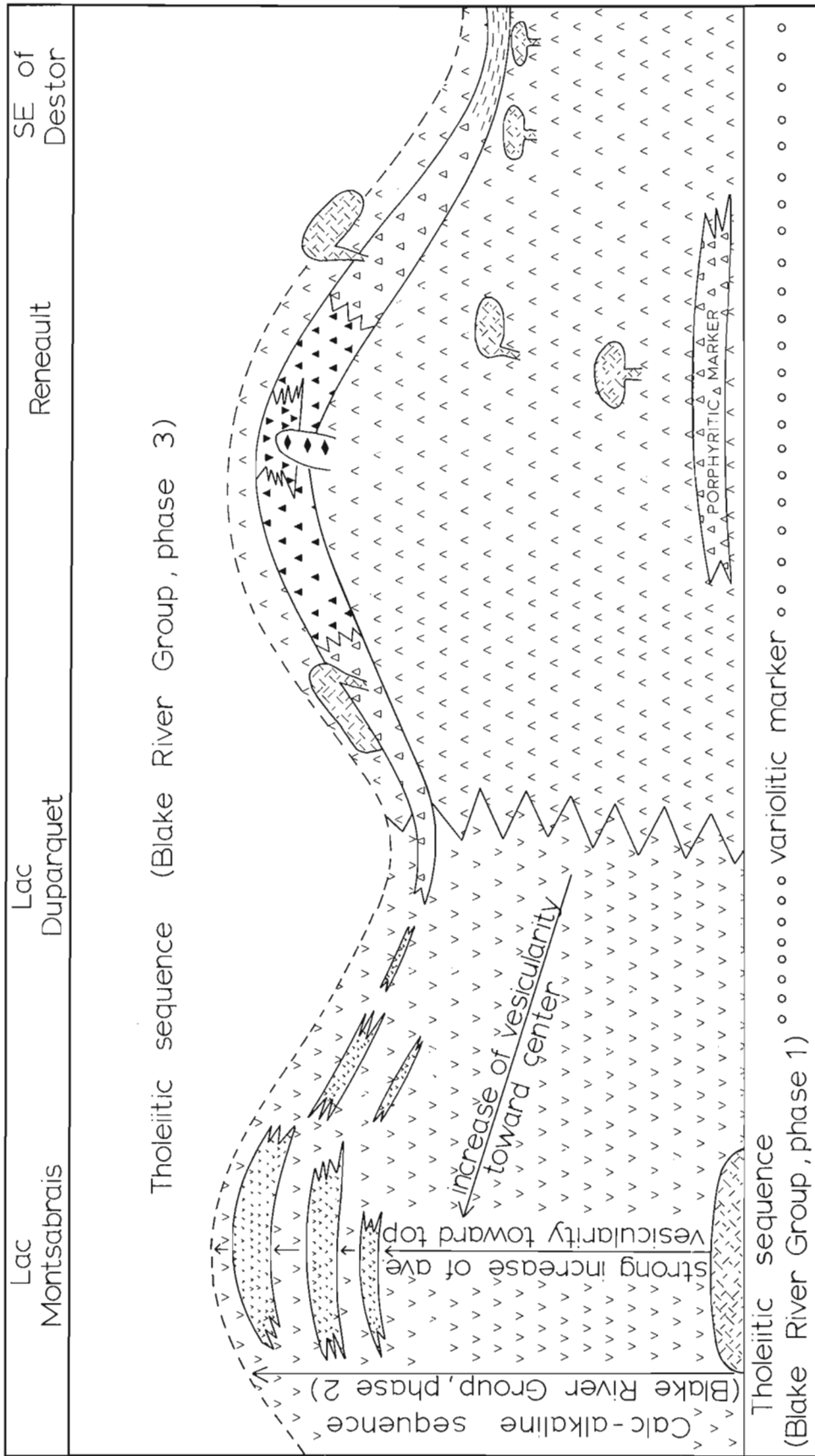


Figure 23.3. Generalized volcanic stratigraphy of the Blake River Group in area 1 outlined in Figure 23.1.

of these emerged at the end of the main phase of Blake River activity, and shed fans of conglomeratic turbidites composed exclusively of volcanic (mostly andesitic) fragments to the south (basal conglomeratic sandstone of the Cadillac Group in Joannès township). Minor volcanism (e.g. tuff turbidites in the Rouyn basin, andesite flows and flow breccias interfingering with the Joannès conglomerate) was contemporaneous. Somewhat later the volcanic chain with its large granitic plutons emerged, and shed southward the turbidites of the upper part of the Pontiac Group and of the Timiskaming and Cadillac groups. Marginal equivalents of the turbidite conglomerates at McWatters were deposited in fluvial environments. It is likely that a regional fault system, the ancestor of the Cadillac fault zone, separated the emergent volcanic chain in the north from the turbidite basin in the south. Interfingering and overlapping fans of turbidite conglomerate can be followed for over 100 km from Larder Lake to east of Val d'Or, suggesting that the emergent volcanic chain formed a relatively large island. Minor volcanic activity still took place on the volcanic island, as indicated by the presence of tuff turbidites in the Timiskaming Group.

Acknowledgments

This report is based on a synthesis of the work done by the writer and the following geologists: Pierre Boivin (Université de Clermont-Ferrand; stratigraphy of Hébécourt, Duparquet and parts of Destor townships), Marc Larouche (Université Laval; stratigraphy of the Destor-Montbrun area), Normand Goulet (Queen's University; stratigraphy and tectonics along the Cadillac fault zone), Richard Côté (Ecole Polytechnique; Stratigraphy of the Blake River Group south of Rouyn), Pierre Trudel (Ecole Polytechnique; stratigraphy of the Blake River Group between Reneault and Cléricy), Gilles Provost (Ecole Polytechnique; facies and emplacement mechanism of rhyolite flows), Michel Rocheleau (Université de Montréal; sedimentology), Normand Tassé (Université de Montréal; sedimentology of pyroclastic flows) and Claude Larouche (Carleton University; intrusive granitic rocks, Bellecombe-Rémigny area).

References

- Dimroth, E., Goulet, N., and Larouche, M.
1973: Preliminary report on tectonic and volcanological studies in Rouyn-Noranda area. Quebec Dep. Nat. Resour., Open file G.M. 28491.
- Dimroth, E., Rocheleau, M., Boivin, P., Larouche, M., and Côté, R.
1974: Preliminary report on stratigraphic and tectonic work in Rouyn-Noranda area. Quebec Dep. Nat. Resour., Open file Report DP-246.
- Dimroth, E., Côté, R., Provost, G., Rocheleau, M., Tassé, N., and Trudel, P.
1975a: Third progress report on the stratigraphy, volcanology, sedimentology and structure of Rouyn-Noranda area. Quebec Dep. Nat. Resour., Open file Report DP-300.
- Dimroth, E., Gélinas, L., Rocheleau, M., Provost, G., and Tassé, N.
1975b: Guidebook, Field trip and field Conference on the volcanology and sedimentology of Rouyn-Noranda area*.
- Gélinas, L., Brooks, C., Perrault, G., Carignan, G., Grasso, F., Trudel, P., and Côté, R.
1975: Chemical Stratigraphy in Archean Volcanic rocks of the Abitibi belt, Rouyn-Noranda Region, Quebec (abs.): Geol. Soc. Am./Geol. Assoc. Can. Annual Meeting, Programs with Abstracts, v. 7, p. 762.
- Graham, B.
1954: Parts of Hébécourt, Duparquet and Destor townships. Quebec Dep. Mines, G.R. 61.
- Heiken, G.
1972: Morphology and petrography of volcanic ashes. Geol. Soc. Am., Bull., v. 83, p. 1961-1988.
- Jones, J. G.
1969: Pillow lavas as depth indicators. Am. J. Sci., v. 267, p. 181-195.
- Moore, J. G.
1965: Petrology of deep-sea basalt near Hawaii, Am. J. Sci., v. 263, p. 40-52.
- Wilson, M. E.
1962: Royun-Beauchastel map area, Quebec; Geol. Surv. Can., Mem. 315.

* Available from Dr. L. Gélinas, Dep. Génie Minéral, Ecole Polytechnique.

W. H. Poole

Regional and Economic Geology Division

Abstract

The Canadian Appalachian belt comprises Hadrynian to Middle Devonian deformed sedimentary, volcanic and plutonic rocks overlain by an internal successor basin of Middle Devonian to Lower Permian deformed and undeformed post-orogenic sediments. Superimposed are Upper Triassic continental sediments and basalt in a half-graben and the Early Cretaceous alkaline Monteregean Intrusions. The Appalachian belt evolved upon and apparently between the disrupted edges of a probably once-continuous pre-Hadrynian crystalline basement now appearing as the Canadian and African shields, and as isolated blocks both identified and suspected within the Appalachian orogen. Plate movement was mainly one of extension during the Hadrynian, of extension and pull-apart during Cambrian and Early Ordovician time, of contraction from the Ordovician to Devonian and of collision during the Devonian. Polydeformation, regional metamorphism as high as amphibolite grade, and plutonism occurred several times from Hadrynian to Devonian in different localities.

Hadrynian-Cambrian extension of the crystalline basement resulted in a two-part proto-Atlantic ocean. Thick miogeoclinal sediments were deposited along the depressed inner northwest margin of the northwestern ocean, and Cambrian (with "Pacific" trilobite fauna) and Ordovician carbonates transgressed the stable platform to the northwest. In the Avalon belt, on the southeastern side of the northwestern ocean, Hadrynian volcanism and associated sedimentation changed in later time through mature quartz sand to Cambrian and Early Ordovician platformal pelite deposition (with "Atlantic" trilobite fauna).

In the southeastern ocean, southeast of the Avalon belt, thick turbidites derived from the southeast (African Shield?) were deposited in a deep trough in southern Nova Scotia.

During Early Ordovician time, ophiolitic assemblages developed along a mid-ocean ridge in northwestern ocean and were carried away from the ridge. They became partly buried by island arc volcanics and greywacke above a subduction zone which probably dipped northwest. Parts of the miogeoclinal and ophiolitic assemblages were thrust and slid north-westward (Taconian orogeny) into an Ordovician exogeosynclinal flysch trough formed upon the depressed carbonate platform.

During Late Ordovician to Early Devonian time, generally shallow-water sedimentation and volcanism filled basins and troughs between the Ordovician uplifted areas. In mid-Devonian time (Acadian orogeny), almost the entire belt was deformed, intruded, uplifted and eroded.

Post-Acadian continental clastics with one marine incursion (late Mississippian) filled a depressed area central to the Appalachian belt, especially along a fault-fold zone (Maritime Disturbance) that extended through the middle of the area.

Introduction

The Appalachian orogen consists of Paleozoic and Hadrynian sedimentary, volcanic, metamorphic and plutonic rocks and extends 3300 km along eastern North America from Newfoundland to Alabama. The system was probably once continuous with the Caledonian orogen of Ireland, Britain and Scandinavia. Although continuity seems assured in late Precambrian and Paleozoic times, the integral tectono-stratigraphic elements, the rocks, the tectonic styles, the geological processes and the intensity of development varied from place to place along the entire system.

The northeastern end of the Appalachian orogen, within Canada, is as long as 1500 km, as wide as 600 km and covers 360 000 km² onshore (Fig. 24.1). The central part is submerged beneath the Gulf of St. Lawrence and Bay of Fundy, and on the east and north-east, the orogen extends to the continental slope beneath unconformably overlying Mesozoic and Cenozoic sediments. These submerged parts add 650 000 km² nearly twice the onshore area.

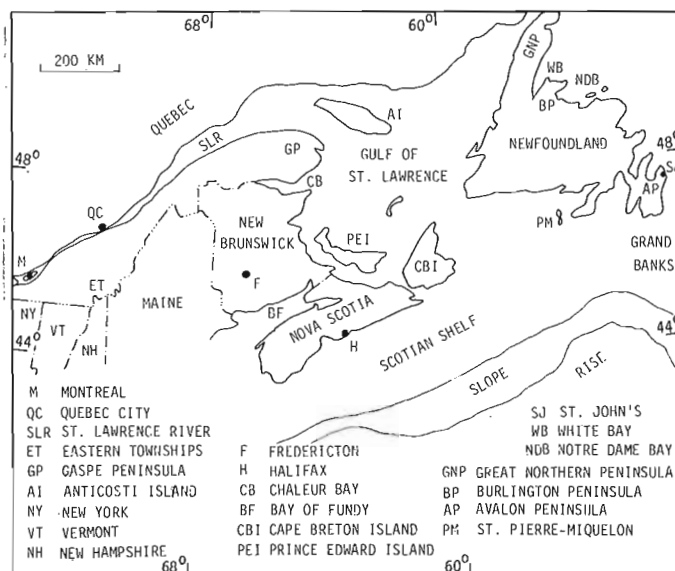


Figure 24.1. Geographical names, Appalachian region of Canada.

¹This paper was presented in Rennes, France in August 1974 to Colloque international sur la chaîne varisque d'Europe moyenne et occidentale. A version in French will be published by Centre National de la Recherche Scientifique (C. N. R. S.), Paris.

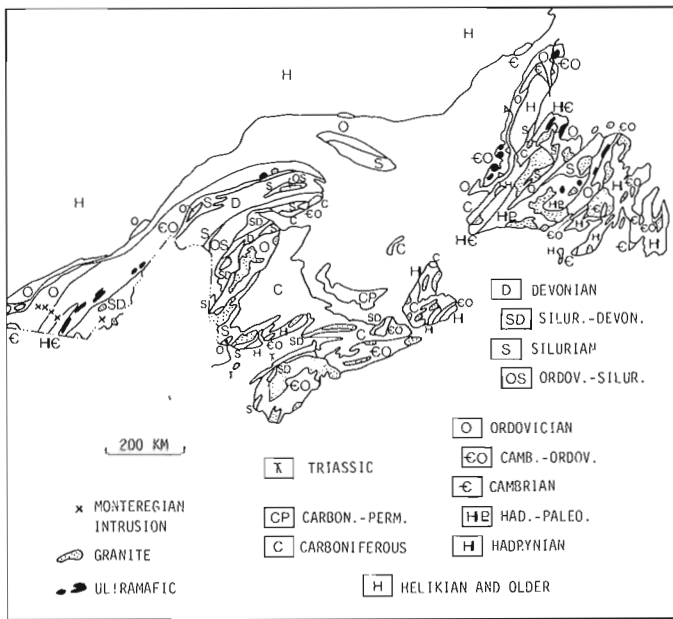


Figure 24.2. Generalized geology.

The Appalachian orogen is bordered on the north, west by flatlying Paleozoic carbonates of the St. Lawrence Platform that rest unconformably upon and now fringe the crystalline craton of the pre-Hadrynian Canadian Shield.

The orogen consists of five broad tectono-stratigraphic elements (Figs. 24.2 and 24.3):

1. On the northwest, a southeastward thickening miogeocline of Hadrynian, Cambrian and Ordovician flysch, the upper parts of which grade northwestward into carbonates of the St. Lawrence Platform bearing "Pacific" or "American" Cambrian trilobite fauna. Most of these rocks are now allochthonous, following northwestward thrusting and sliding in the Ordovician and some are autochthonous or allochthonous and regionally metamorphosed as high as amphibolite grade in the Western Crystalline belt.

2. In the axial zone Ordovician, Silurian and Devonian autochthonous, generally little metamorphosed sedimentary and volcanic rocks with some ultramafics cut by voluminous granite batholiths of Devonian and Ordovician ages. These rocks occupy the original site of the northwestern proto-Atlantic ocean. Ordovician shelly faunas are of the "Appalachian" realm.

3. In the southeast the Avalon belt of Hadrynian, Cambrian, Ordovician and some Silurian and Devonian autochthonous, sedimentary and volcanic rocks. The Hadrynian volcanic and sedimentary rocks are overlain unconformably and conformably by relict synclines of Cambrian and Lower Ordovician platformal pelites bearing trilobite fauna of the "Atlantic" or "European-Mediterranean" realm. In the Eastern Crystalline belt the northwest border has been regionally metamorphosed as high as amphibolite grade.

4. In the extreme southeast, Cambrian to Devonian autochthonous sedimentary and some volcanic rocks of the Meguma belt, deposited in the southeastern proto-Atlantic ocean. They are little metamorphosed except at the southern end, and are cut by Devonian batholiths. Devonian faunas are like those of central Europe.

5. Upon the Devonian Acadian orogen and extending east and north onto the continental shelves beneath Mesozoic-Cenozoic sediments, a successor basin of Middle Devonian to Lower Permian continental clastic rocks including one formation of marine carbonates and evaporites, unmetamorphosed and folded-and-faulted along a central zone flanked by thinner, flat-lying strata. Flora and fauna are European.

A late Triassic half-graben of continental red clastic sediments and basalt, essentially flat-lying, occurs in the southwest and is considered related to the initial development of the present Atlantic Ocean. Early Cretaceous alkaline intrusions of the Monteregian suite cut rocks of the St. Lawrence Platform and Appalachian orogen near Montreal.

Modern concepts of the tectonic evolution of the Appalachian region began with the classification by Kay (1951) of geosynclines and their characteristic sedimentary and volcanic infilling. His models, developed mainly in United States, were applied to the Canadian Appalachians to greater or lesser degree by Weeks (1957), Williams (1964), Poole (1967), Poole *et al.* (1970), Rodgers (1970) and Williams *et al.* (1972). Recent concepts of present-day ocean floor spreading and plate tectonics brought about attempts to reconstruct the Paleozoic evolution of the Appalachian belt in the same style (Dewey, 1969; Dewey and Bird, 1971; Bird and Dewey, 1970; Church and Stevens, 1971; Kennedy and McGonigal, 1972; Schenk, 1971, 1972; St. Julien and Hubert, 1975; and others). Consensus is far from complete on such questions as the location and dip of former subduction zones, the nature of the crust

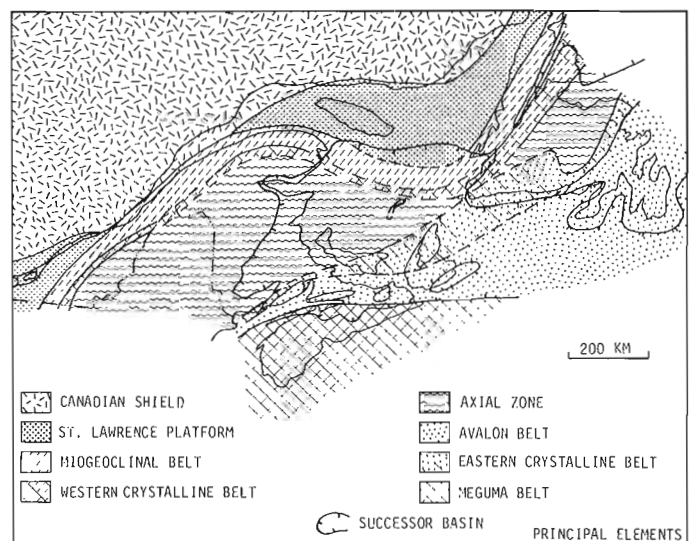


Figure 24.3. Principal geological elements.

underlying various parts during evolution of the Appalachian orogen, not to mention such basic questions as the age of deposition of some older strata and some metamorphosed strata, and the age of the older multiple deformation and metamorphism in the crystalline belts. Strong *et al.* (1974) and Strong (1974) have briefly summarized the postulated plate tectonic models and the place and variation of mineral deposits and of geochemistry of some granitic rocks in Newfoundland.

An attempt will be made in the following pages to place the tectono-stratigraphic units in a necessarily schematic representation of a plate tectonic development model of the Canadian Appalachians. The writer approaches the task with no little trepidation. That plate tectonics was operative during Appalachian evolution is assumed. Not all possible models of development can be treated; what is presented is the model which at this time finds most favour with the writer. Space limitations so not permit adequate documentation and arguments.

Pre-Hadrynian

Before the opening of the proto-Atlantic ocean, the North American and European-African continents, comprising Precambrian crystalline rocks, are assumed to have been continuous. The Canadian Shield northwest of the Canadian Appalachian belt consists of schist, gneiss, granulite, granite, anorthosite, marble, etc., of Archean to Helikian age, which were deformed, metamorphosed, intruded, and uplifted and eroded during the Grenvillian orogeny (ca. 1000 m.y.). Grenvillian rocks are exposed within the Appalachian orogen along its northwest margin in the Green Mountains of Vermont, the Eastern Townships of southern Quebec and in western Newfoundland (Fig. 24.4). Smaller inliers occur in western Newfoundland within the (Phanerozoic) Western Crystalline belt. Grenvillian (or older) basement is believed to underlie other parts of the orogen and to have originated as blocks and belts within the proto-Atlantic ocean during the opening.

Hadrynian

During the Hadrynian (Fig. 24.5), the Canadian-European-African Shield thinned by extension along the axis of the Appalachian belt and was depressed beneath the early proto-Atlantic ocean. A broad belt ("micro-continent" of Schenk, 1971) of continental crust on the southeast side of the axial zone became the site of Hadrynian island arc volcanism, the Avalon belt. A subduction zone is postulated to have dipped southeast beneath the island arc.

Hadrynian rocks occur in two belts (Rodgers, 1972):

1. Northwest marginal miogeocline

Upon the northwestern thinned and depressed margin, southeast-thickening immature clastic strata derived from the Canadian Shield to the northwest were deposited, perhaps mainly by turbidity currents, in a miogeocline along an Atlantic-type margin. The

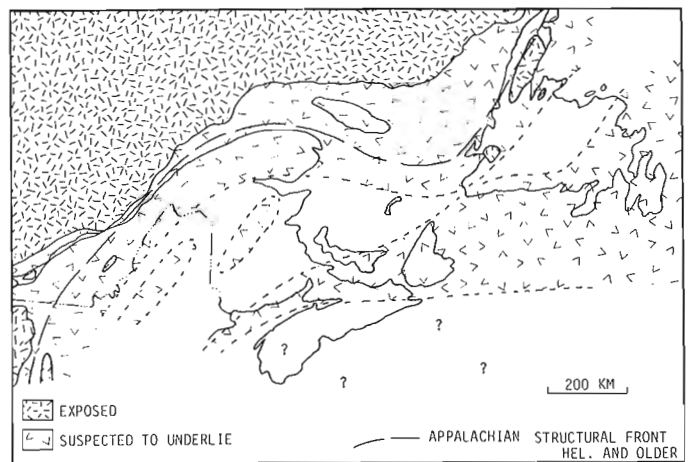


Figure 24.4. Helikian and older rocks.

rocks now appear in the Western Crystalline belt as psammitic and pelitic schist and gneiss with some marble, amphibolite and greenschist (Fleur de Lys, Shickshock(?), lower Oak Hill)¹. In Burlington Peninsula, the assemblage rests upon an inlier of Grenvillian basement (de Wit, 1974), and a sliver of Grenvillian basement has been upthrust south of Quebec City (St. Julien and Hubert, 1975). Hadrynian strata have not been recognized nor are they suspected to occur at surface in the axial zone of the orogen. Nevertheless, what must have been an enormous volume of detritus eroded from the Grenvillian orogen seemingly cannot be accounted for in the exposed and longitudinally projected miogeocline; some may have been lost through Paleozoic subduction.

2. Avalon volcanic belt

The Avalon belt widens northeastward from 50 km in southern New Brunswick to 200 km in onshore eastern Newfoundland to which can be added 500 km additional width if most of the Grand Banks of Newfoundland are included (the Virgin Rocks on the Grand Banks, 160 km southeast of Newfoundland, consist of probable Hadrynian rocks; Lilly, 1966). The Newfoundland part is the most varied: calc-alkaline or weakly alkaline, acidic to basic volcanics and volcanoclastic sedimentary rocks (Harbour Main Group) pass upward and laterally into marine volcanic grey-wacke and siltstone (Conception, Connecting Point; Rose, 1952; McCartney, 1967; Hughes and Brückner, 1971), and thence into nonmarine volcanic red sandstone, conglomerate and local acidic to basic volcanics (Cabot, Hodgewater, Musgravetown) deposited in taphrogenic troughs. Hadrynian plutons of granodiorite and adamellite are probably subvolcanic. Deformation is simple and moderate, and metamorphism is low greenschist to subgreenschist (except in the Eastern Crystalline belt). Similar but less variable volcanic and sedimentary rocks occur on Cape Breton Island

¹ Names of selected formations are placed in parentheses.

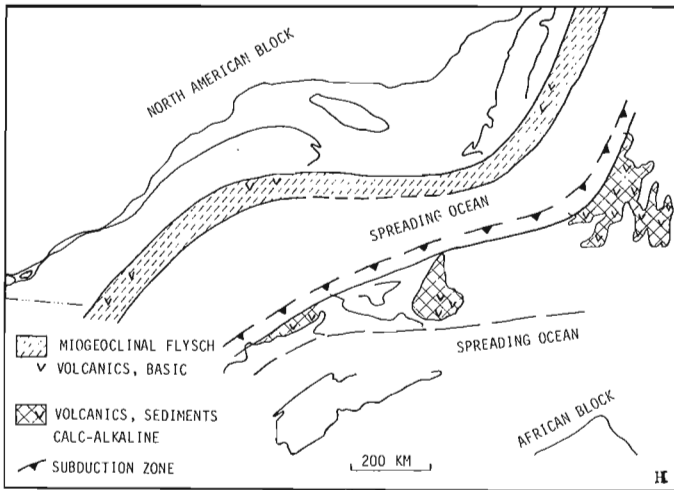


Figure 24.5. Hadrynian, schematic restoration.

(Fourchu; Weeks, 1954) and southern New Brunswick (Coldbrook; Ruitenbert *et al.*, 1973). The orogenic events have been referred to the Avalonian disturbance (orogeny). A subduction zone is presumed to have dipped southeast beneath a Cordilleran-type margin. Some metamorphism and deformation occurred on the northwestward side (the future site of the Eastern Crystalline belt) during Hadrynian (pre-Musgravetown time).

Carbonate, quartzite and pelite, now partly metamorphosed (Green Head, George River) are older than the Hadrynian volcanics and occur in fault blocks in southern New Brunswick and Cape Breton Island. Their age is unknown; Schenk (1971) suggested correlation with Helikian strata in Morocco and in the Canadian Shield.

Cambrian

During the Cambrian (Fig. 24.6), the continental crust in the axial zone continued to thin by extension and marginal normal faulting, and probably began to pull apart by the generation of oceanic crust at a mid-ocean ridge although Cambrian ophiolites have not been positively recognized. Some time late in the Cambrian, a northwest-dipping subduction zone produced island arc volcanics and (?) plutons in the northwestern margin in Newfoundland followed by deformation and metamorphism of the miogeoclinal strata of the upper plate. The subduction zone beneath the Avalon belt was inactive, and mainly shale was deposited on the eroded island arc. Southeast of the Avalon belt, another branch of the proto-Atlantic ocean had formed by at least late Cambrian at which time flysch was carried into the resulting miogeocline from the African Shield on an Atlantic-type margin.

Cambrian strata occur in three belts; the Northwest Marginal miogeocline, the Avalon Belt at the Meguma Belt.

1. Northwest marginal miogeocline

As in Hadrynian time, Cambrian detritus from the Canadian Shield was carried into the miogeoclinal flysch belt. In western Newfoundland (Church, 1969) the upper part of the unfossiliferous metamorphic terrane (Fleur de Lys) passes southeasterly into basic volcanics (Pacquet Harbour) and thence to dominantly acidic volcanics (Cape St. John) whose ages are questioned but are treated in this report as probably Cambrian. To the northwest on the St. Lawrence Platform thinner equivalents are carbonate, quartzite and minor basic volcanics (Labrador) which rest unconformably upon the Grenvillian basement. The onlapping carbonates bear a "Pacific" trilobite fauna. Diabase dyke feeders to the volcanics cut the Grenville basement and parallel the continental margin. Spectacular limestone breccias (lower Cow Head) formed along the southeast front of the carbonate platform (Kindle and Whittington, 1958). Strata intermediate between the carbonate of the platform and the deep-water facies of the metamorphic terrane appear in the Ordovician allochthons (Maiden Point, Humber Arm; Stevens, 1970).

In southern Quebec very thick Cambrian deep-water flysch sequences were deposited (Quebec, upper Oak Hill, Maquereau; St. Julien and Hubert, 1975). Greywacke and periodically limestone breccias (Lévis type), conglomerate, quartz sand and polymictic conglomerate were carried from the Shield in canyons through a carbonate platform into deep water of the proto-Atlantic ocean (Lajoie *et al.*, 1974). Trilobites in the limestone clasts of the breccias are of the "Pacific" realm. Cambrian carbonate is not exposed on the St. Lawrence Platform, and is presumed to underlie the Quebec allochthon; Cambrian carbonate is exposed in a small window (?) in eastern Gaspé Peninsula.

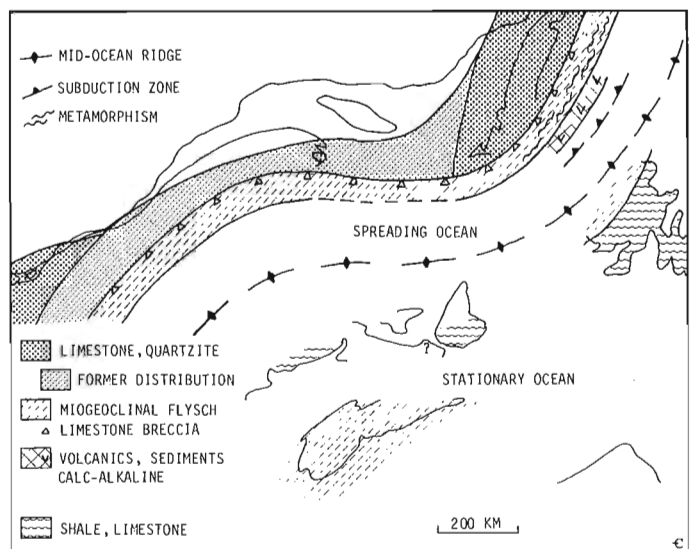


Figure 24.6. Cambrian, schematic restoration.

Ordovician

In latest Cambrian or earliest Ordovician time, the miogeoclinal strata on the northwest margin in western Newfoundland became multiply deformed and regionally metamorphosed to greenschist and amphibolite grades (Kennedy, 1971) to form the Newfoundland part of the Western Crystalline belt. Deformation and metamorphism decrease southeasterly into the island arc rocks. Small ultramafic bodies emplaced early in the deformation may be true intrusions rising above the subduction zone (cf. Stevens *et al.*, 1974).

2. Avalon belt

The Avalon belt behaved as a platform during the Cambrian. Trilobite faunas are of the "Atlantic-Mediterranean" realm. Hadrynian red beds grade upward into mature quartzite (Random, upper Morrison River, Glen Falls) and thence into Cambrian shale and siltstone, red and green with limestone in the Lower Cambrian, and dark grey in the Middle and Upper Cambrian (Hutchinson, 1952, 1962). Manganiferous shale occurs near the base of the Middle Cambrian. Some volcanics appear locally in the Middle Cambrian. The Hadrynian-Cambrian contact is conformable or disconformable in most places, nonconformable and angularly unconformable in others. Low-lying land was present locally. The tectonic state during the Cambrian is that of a platform by virtue of the stability during near-continuous deposition despite the lack of carbonates. Whether the water was generally deep or shallow is debatable and perhaps irrelevant depending upon the reader's definition of the term "platform".

Northwest of the Avalon and Eastern Crystalline belts, in central Newfoundland, are fine grained strata (Gander Lake; Kennedy and McGonigal, 1972) whose age is known only as pre-Middle Ordovician. They are probably of Cambrian and/or Early Ordovician age, and were possibly deposited on the ocean side of the Hadrynian volcanic belt contemporaneous with platformal strata within the belt.

3. Meguma belt

A deep trough formed southeast of the Avalon belt during Cambrian (and ? Hadrynian) time, perhaps on thinned and extended continental crust of the African Shield-Avalon belt. Oceanic volcanics and ultramafic rocks are lacking in the Meguma belt. In late Cambrian(?) time, turbidity currents from a meta-igneous, metasedimentary terrane to the southeast (African Shield?) carried thousands of metres of monotonous slope and rise quartzose greywacke (Goldenville of Meguma) into the trough (Schenk, 1970). The currents flowed northwestward into southern Nova Scotia and then arced eastward parallel to the present structural grain of the strata. No stratigraphically similar rocks have been recognized southeast of the Avalon belt in North America.

The Ordovician was a time of the most active plate motion in Canadian Appalachian evolution. Carbonate deposition continued on most of the St. Lawrence Platform. Ocean-floor ophiolitic assemblages and northwesterly bordering miogeoclinal clastic strata as young as Early Ordovician became uplifted and slid northwestward into an exogeosyncline developed upon the platform. Miogeoclinal strata in Quebec became multiply deformed and metamorphosed (Western Crystalline belt). Island arc volcanism developed in the axial zone. Pelitic deposition continued to the southeast of the volcanism. Avalon Platform pelitic deposition stopped following deposition of the Lower Ordovician (Arenig) iron-formation, and the northwest margin of Avalon Platform became multiply deformed and metamorphosed (Eastern Crystalline belt). All these orogenic and suborogenic events can be attributed to a multifaceted Taconian orogeny.

Early Ordovician

1. Northwest margin: Carbonate, mainly dolomite (Beekmantown, Romaine, St. George), was deposited gradationally above the Cambrian on the St. Lawrence Platform as the seas continued their transgression of the Canadian Shield, and carbonate breccias (upper Cow Head, Lévis type) continued to be formed on the southeastern, ocean side (Fig. 24.7).

In western Newfoundland, miogeoclinal flysch (now in the Humber Arm allochthon) was bordered to southeast by metamorphosed miogeoclinal flysch in the still depressed Western Crystalline belt, farther to the southeast by an ophiolite belt (Snooks Arm) and finally by an island arc (Catchers Pond, lower Wild Bight). As in the Cambrian, a subduction zone dipped northwest beneath the arc. Perhaps the former trench is marked by the Dunnage Mélange of Kay (1972). The

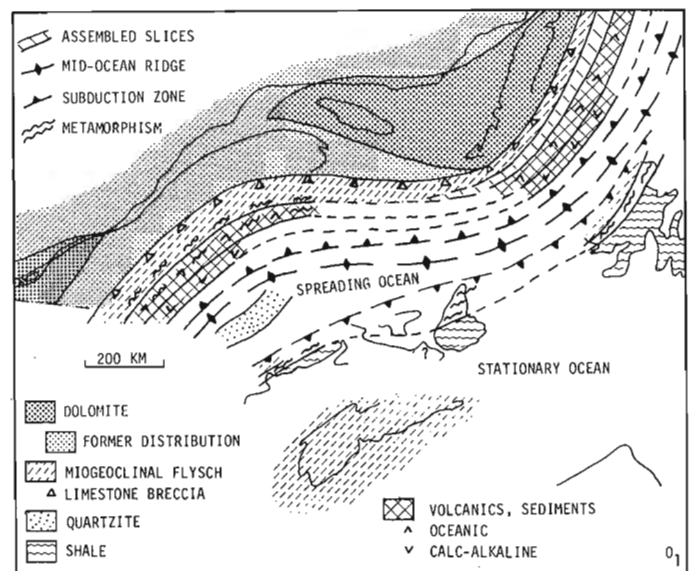


Figure 24.7. Early Ordovician, schematic restoration.

individual slices within what became the western Newfoundland allochthon became assembled above or just northwest of the crystalline belt (wildflysch between some slices has a Lower Ordovician black-and-green shale matrix); ophiolitic slices were slid on top of flysch slices from southeast to northwest, while the crystalline belt began to rise. Detritus from the assembling slices was carried southeastward to be deposited above the remaining ophiolites (Snooks Arm) and northwestward above flysch-bearing carbonate breccia about to be incorporated in the slice assemblage (Blow-me-Down). The stage was set for final emplacement of the allochthon during the Middle Ordovician.

In southern Quebec, miogeoclinal flysch deposition continued throughout Early Ordovician (upper Quebec) time and was apparently bordered to the southeast by ophiolites (Serpentine belt) and farther southeast by an island arc (Ascot, Weedon). The ages of the ophiolites and island arc rocks are quite uncertain; by analogy with western Newfoundland an Early Ordovician age is assumed in this report. Development of allochthons apparently did not begin until Middle Ordovician, but in perhaps early Middle Ordovician, time the southeast margin of the miogeoclinal flysch belt (Sutton, Bennett, Shickshock) and southeast-bordering ophiolite and island arc became multiply deformed and the flysch belt regionally metamorphosed to high greenschist facies (Western Crystalline belt). A subduction zone presumably dipped northwest beneath the island arc. The Mount Albert hot dunite and peridotite pluton was probably intruded at this time in northern Gaspé Peninsula.

2. Axial region: In central New Brunswick and adjacent parts of Maine, thick mature quartzite bearing an Early Ordovician (Arenig?) Appalachian shelly fauna like that of the volcanic terrane in northeastern Newfoundland (Neuman, 1972) forms the oldest strata beneath Middle Ordovician volcanics. This quartzite occurs nowhere else in the Canadian Appalachians. Its maturity leads to the inference that central New Brunswick and central Maine are underlain in subsurface by a crystalline basement, possibly Grenvillian (Poole, 1967).

3. Avalon Platform: Platformal conditions in the Avalon belt continued throughout the Early Ordovician with deposition of dark grey pelites. In eastern Avalon Peninsula a thicker sequence (over 1500 m) of Arenig sandstone, micaceous siltstone, shale and shallow-water iron-formation (hematite, chamosite, phosphatic shells of Wabana mine; Rose, 1952) was deposited. Deposition on the platform ceased at the end of Early Ordovician time; no Middle and Upper Ordovician strata have been recognized in the belt.

Multiple deformation and regional metamorphism to amphibolite grade in the Eastern Crystalline belt along the northwestern side of the Avalon Platform occurred between Hadrynian and Middle Ordovician time, probably in the early Middle Ordovician coincident with probable uplift of the platform. Perhaps folding of the platformal strata also occurred then, rather than

in the Devonian as is generally assumed. The cause could have been renewed activity on the Hadrynian southeast-dipping subduction zone.

4. Meguma belt: The southeast-derived greywackes of the Meguma belt became in the Early Ordovician (Tremadoc) time gradationally overlain by deep-water, dark grey shale (Halifax), as much as several thousand metres thick, a possible continental rise deposit (Schenk, 1970, 1971). The southeastern proto-Atlantic was apparently stationary.

Middle Ordovician

During Middle Ordovician time (Fig. 24.8), the St. Lawrence Platform bordering the Appalachian system became depressed, and allochthons were driven out of the northwestern proto-Atlantic ocean into an exogeosynclinal shale trough, while island arcs were active within the ocean. The location and dip of the operative subduction zone is debatable northwest-dipping from southeast of the island arc zone (Bird and Dewey, 1970) or southeast-dipping from northwest of the island arc zone (e.g. Stevens *et al.*, 1974). A northwest-dipping zone is depicted in Figure 24.8.

1. Northwest margin: On the bordering St. Lawrence Platform of western Newfoundland dark grey limestone of early Middle Ordovician (Llanvirn: Table Head) age was deposited upon the uplifted, karst topography of Lower Ordovician dolomites (with stratabound zinc bodies) and then was depressed deeply to be overlain by exogeosynclinal dark grey shale and greywacke carried from the southeast. The Western Crystalline belt and assembled slices were uplifted, and the slices slid as a unit (as a continuous allochthon over the entire western Newfoundland) northwestward into the exogeosyncline with attendant production of wildflysch and mélangé of Llandeillian age. Almost immediately,

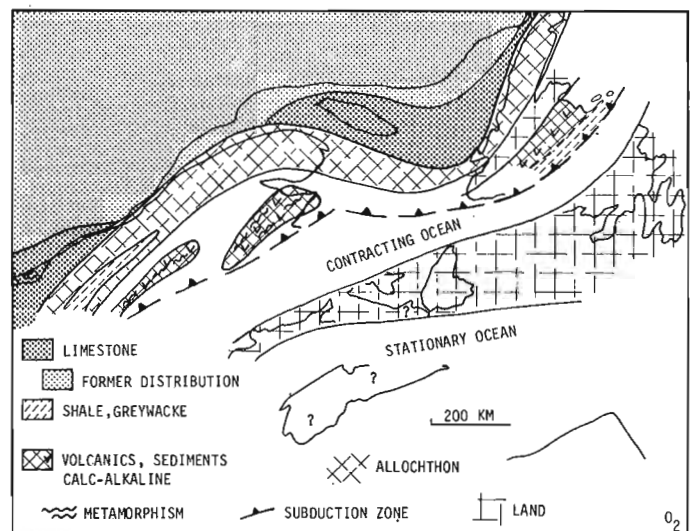


Figure 24.8. Middle Ordovician, schematic restoration.

the platformal conditions returned and the eroded surface of the southwestern part of the allochthon became overlain unconformably by reefal limestone and siltstone of Caradocian age (Long Point).

In southern Quebec, on the other hand, platformal carbonate continued to be deposited throughout the Middle Ordovician (Chazy, Black River, Trenton) to about middle Caradoc time when exogeosynclinal black shale (Canajoharie, Utica) began to be deposited on the subsided platform, and several slices of older miogeoclinal rocks (Sillery, Lévis, Quebec, Oak Hill and Shickshock) slid into the trough, again with accompanying production of wildflysch and mélange. In contrast to Newfoundland, the Western Crystalline belt in Quebec is believed by the writer to be also allochthonous along with the ophiolitic rocks in the Serpentine belt and island arc rocks.

2. Axial zone: Southeast of the zone of allochthon development, Middle Ordovician island arc volcanism prevailed in Newfoundland (Exploits), New Brunswick (Tetagouche) and Maine, in the latter two upon the Lower Ordovician (and older?) quartzite terrane. Again a northwest-dipping subduction zone is postulated.

3. Avalon and Meguma belts: Rocks of Middle and Late Ordovician age are unknown in the Avalon and Meguma belts. Presumably, the Avalon Platform had been uplifted following probably early Middle Ordovician deformation and metamorphism along its northwest margin, now the Eastern Crystalline belt. Middle and Upper Ordovician rocks may exist in the undated White Rock Group (see below).

Late Ordovician

During Late Ordovician time, much of the Canadian Appalachian belt was undergoing erosion; Upper Ordovician strata are rare (Fig. 24.9). Green and red detritus from the emplaced and uplifted allochthon in southern Quebec was carried northwestward and westward onto the St. Lawrence Platform, well into Ontario and New York State, in what is called the "Queenston Delta". Curiously, very little if any detritus reached the carbonate deposition area of Anticosti Island in the northern Gulf of St. Lawrence. Within the axial zone, island arc volcanism apparently continued in Newfoundland, but in New Brunswick and adjacent Maine, the Middle Ordovician island arc assemblage became deformed, in some places multiply deformed and regionally metamorphosed to greenschist and low amphibolite grade, and uplifted and eroded. In eastern Notre Dame Bay, on New World Island, Upper Ordovician greywacke with a northerly provenance was folded, uplifted and eroded, and then overlapped from the southeast by Lower Silurian polymictic conglomerate (Kay, 1969). A northwest-dipping subduction zone probably lay southeast of the deforming belt in New Brunswick and Maine and southeast of the island arc belt in Newfoundland. The northwestern proto-Atlantic ocean was probably almost closed in Late Ordovician time.

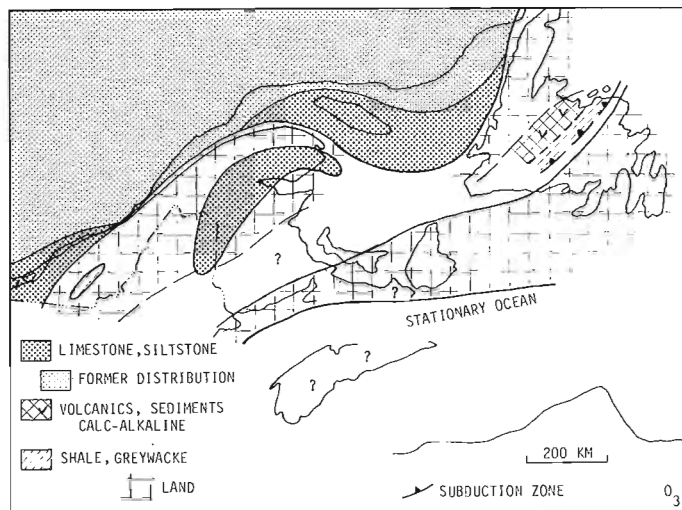


Figure 24.9. Late Ordovician, schematic restoration.

A marine trough existed in Gaspé Peninsula and along the New Brunswick-Maine boundary zone. Late Middle Ordovician clastics (Honorat) grade upward into Upper Ordovician-lowermost Silurian (Llandovery A) deep-water, poorly fossiliferous ribboned limestone (Matapedia, Whitehead, parts of Meduxnekeag). The strata record continuous deposition, unaffected by the uplift to the northwest and the deformation and uplift to the southeast. The trough developed upon the backside of the Quebec allochthon in Gaspé Peninsula and extended southward between two parts of the former island arc. Its character and apparent insensitivity to bordering uplifts are a puzzle.

The Avalon Belt continued as a low-lying area, presumably one of nondeposition undergoing weak erosion. In the Meguma belt, no Upper Ordovician strata have been recognized paleontologically; Schenk (1972) suggested that paraconglomerates in the White Rock Formation may indeed be of glacial origin and of Late Ordovician age like similar glacio-genetic strata in northwest Africa.

Silurian to Middle Devonian

During the Silurian to Middle Devonian (Figs. 24.10 and 24.11), the axial region subsided and marine shallow-water sediments and volcanics unconformably overlapped the land areas raised during the Ordovician. Nonmarine conditions were attained in Newfoundland by mid-Silurian time while marine conditions prevailed in the Quebec-Maritimes sector during the Silurian and Early Devonian at which time nonmarine conditions developed. A subduction zone probably dipped northwestward beneath the Avalon belt.

On the St. Lawrence Platform, Lower and Middle Silurian (Llandovery and Wenlock) limestone is exposed on Anticosti Island; probably limestone and some clastics of Late Silurian to Middle Devonian age were also present at one time. Red beds with some limestone (Pridoli) of Late Silurian-Early Devonian age

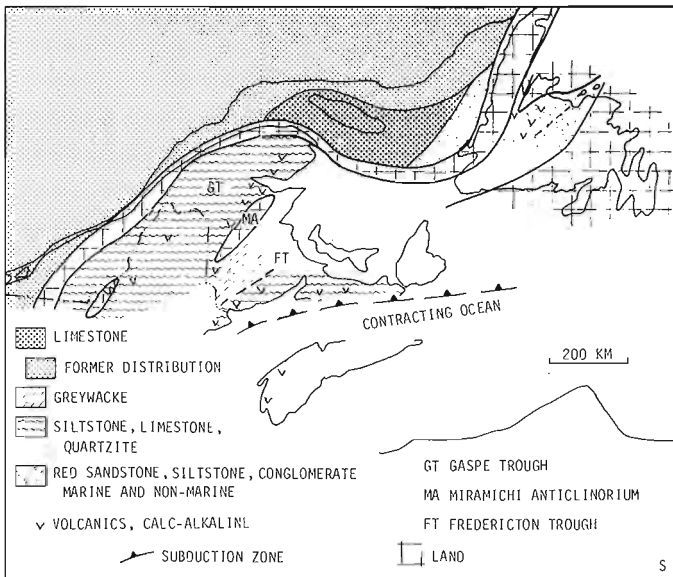


Figure 24.10. Silurian, schematic restoration.

(Clam Bank) were deposited upon the neo-autochthonous Ordovician strata (Long Point) in southwestern Newfoundland in response to uplift to the southeast.

Whereas there is a gross similarity of Cambrian and Ordovician Appalachian strata between the Newfoundland and Quebec-Maritimes sectors, the Siluro-Devonian strata are markedly different in lithology and age.

In Newfoundland there are three outcrop areas. In the northwest, between the uplifted St. Lawrence Platform that bears the Ordovician allochthon and the Western Crystalline belt shallow-water sandstone and basic and acidic volcanics (Sops Arm, Lock, 1969) were deposited; the conglomerates were derived from Grenvillian terrane to the north. To the southeast, gently deformed acidic and basic volcanics are interbedded with red sandstones and conglomerates in the Springdale belt, where they lie unconformably above Ordovician and older rocks. Farther southeast, in the Botwood belt, red and green fluviatile micaceous sandstones are more common, and volcanics are rare. Basal Botwood strata, the Goldson polymictic conglomerates, overlapped northward across a latest Ordovician unconformity. These Newfoundland Silurian rocks are several thousand metres thick, are deformed and are of Early to Middle Silurian age (Llandovery and Wenlock). They record the transition from marine in late Ordovician to continental conditions in mid-Silurian time. No Ludlovian strata are known to exist in Newfoundland.

Lower to Middle Devonian, plant-bearing polymictic conglomerate, sandstone and slate (Bay du Nord) occur in southwestern Newfoundland where they grade laterally into schist and gneiss, that were metamorphosed during the Acadian orogeny. Most of Newfoundland was probably land during Late Silurian and Devonian time.

In the Quebec-Maritimes sector, Siluro-Devonian strata are much more widespread, extend from earliest

Silurian through to Middle Devonian time, and are several thousand metres thick. In the Gaspé Trough to the northwest, Silurian and Devonian strata overlapped northward unconformably upon the Quebec allochthon on the northwest and upon the Miramichi anticlinorium to the southeast, but lie conformably upon intervening Upper Ordovician Matapedia strata. Siltstone is the dominant lithology; conglomerate is common at the base and throughout; and quartzite and limestone are about Wenlockian in age. Acidic and basic volcanics associated with limestone and local slope breccias are common in the Ludlovian and Early Devonian in a zone extending diagonally southward from northern Gaspé to southwestern Miramichi anticlinorium. In Early and Middle Devonian time, limestone (Gaspé Limestone) developed on the northwestern edge of the Gaspé Trough while a parallel marginal trough of thick Lower Devonian siltstone (Fortin, Témiscouata, Seboomook, Compton) developed to the southeast, to be succeeded in Gaspé Peninsula by even thicker feldspathic sandstone and finally conglomerate (Gaspé Sandstone) in the early Middle Devonian at the top of the sequence. This trough of clastics developed in response to early Acadian tectonism to the southeast.

In the Fredericton Trough, thick, sparsely graptolitic greywacke turbidites of known Wenlockian and Ludlovian age were deposited southeast of the Miramichi anticlinorium in what may be the relict of the northwestern proto-Atlantic ocean. On the southeast side of the trough, and presumably intergradational with the turbidites, are shallow-water sediments and acidic and basic volcanics ("Mascarene") that lie upon and along the northwest side of the older Avalon rocks. In northern Nova Scotia, on the other hand, is the classic Arisaig sequence of relatively thin para-platformal fossiliferous shale ranging through the entire Silurian. The Fredericton Trough strata reach just into the Devonian in New Brunswick, but in northern Nova Scotia, Lower Devonian red and green sandstone and siltstone (Knoydart) top the sequence.

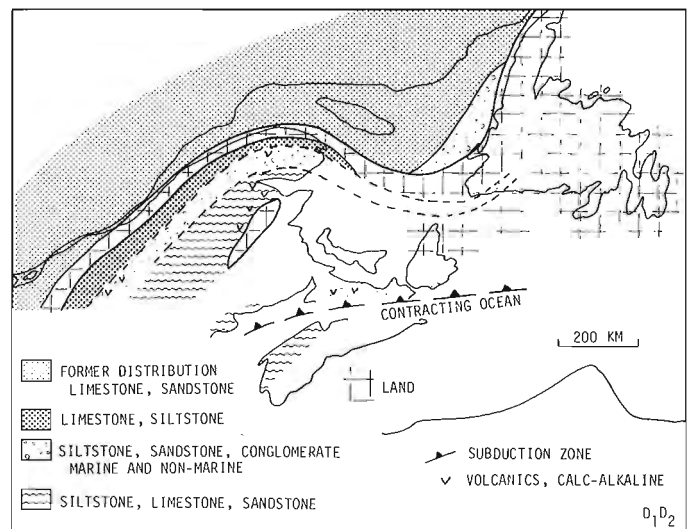


Figure 24.11. Early and Middle Devonian, schematic restoration.

In the Meguma belt, the Lower Ordovician Halifax slates are overlain in the northwest by undated slate and mature quartzite 100 m thick which thicken to over 5000 m about 200 km to the southwest by the addition of acidic to basic volcanics, greywacke and polymictic conglomerate (White Rock). These rocks are overlain gradationally by Upper Silurian (Ludlovian) slate (Kentville) and thence Lower Devonian slate, quartzite, limestone and iron-formation (Torbrook) bearing a European fauna.

Middle Devonian

The climatic orogeny in the Canadian Appalachians, the Acadian orogeny, occurred in mid-Devonian time (Fig. 24.12). It resulted in tight, upright folds across the entire Appalachian region but for a narrow strip of the allochthonous zone along the northwest margin, and was accompanied by axial-plane cleavage, granitic plutons, and faults. Regional metamorphism reached greenschist and low amphibolite grades in small areas in southern Newfoundland and in southern Nova Scotia, the latter co-extensive with widespread high-grade metamorphism in southern Maine, New Hampshire and Vermont.

Faults are steep, some are normal and others transcurrent. Many (transcurrent?) faults follow a broad open "Z" trace, mimicking the trace of the St. Lawrence Platform–Appalachian orogen boundary. A few faults along the northwest Appalachian margin are steep northwest-directed thrusts but no zone of imbricate flat to gently dipping thrusts was developed. In order to explain the scarcity of Middle Ordovician syn-allochthonous exogeosynclinal flysch and the lack of Upper Ordovician erosion products within the carbonate sequence of the Anticosti Island. Crustal shortening by thrusting is suggested to have occurred in the St. Lawrence River between Appalachian rocks of Gaspé Peninsula and St. Lawrence Platform carbonate of Anticosti Island.

Acadian intrusions of mainly granodiorite and adamellite are widespread in the Acadian orogen. Some seem to favour Siluro-Devonian volcanic belts (as in

New Brunswick and Gaspé Peninsula) but others do not. A few hot ultramafic plutons were emplaced northwest of the Avalon belt: the St. Stephen body in southern New Brunswick and some in east-central Newfoundland (Stevens *et al.*, 1974).

The Acadian orogeny is said to have been caused by continental collision in which the European–African continent collided with the Appalachian geosynclinal belt (Bird and Dewey, 1970). The Meguma belt probably became attached to the Avalon zone at this time along a suture now covered by younger strata. But evidence of closed mid-Devonian subduction zones, marked by wide crush zones, intense folding, metamorphism and/or serpentinites, have not been recognized. Rather it appears that the crust beneath the Appalachian belt thickened by shortening and as a result the supracrustal Paleozoic rocks were thrown into upright folds and were intruded in Devonian time by Late Silurian–Early Devonian magmas some of which had produced the volcanism of that age.

The entire Appalachian belt, the Acadian orogen, become uplifted and eroded in Middle and Late Devonian and Carboniferous time. A system of faults disrupted the orogen from the Bay of Fundy to White Bay, and possibly on the Grand Banks of Newfoundland, in a zone which developed into the Maritime fold belt in Carboniferous time.

Late Devonian to Early Permian

A successor basin of mainly continental clastics, a molasse, was deposited upon the Acadian orogen (Fig. 24.13). No trough of clastics marginal to the Appalachian system on the northwest and no flat thrusts of Carboniferous–Permian age were developed as in the central Appalachians of the United States.

Post-Acadian molasse deposition began in the taphrogenic zone (Maritime fold belt) of the Bay of Fundy–White Bay belt in Middle and Late Devonian. This happened in Late Devonian time in southern Newfoundland (Fig. 24.14) and in the Late Devonian in an isolated sag in Chaleur Bay between Gaspé Peninsula and New Brunswick. In Chaleur Bay, thin conglomerate (Fleurant) and siltstone (Escuminac with its famous fossil fishes) were deposited in rivers and lakes.

The taphrogenic zone contains the most complete formational sequence, the thickest strata (totalling over 8 km), and most of the few, locally occurring volcanics. The zone was bordered by platforms of similar strata, thinner, less complete and flat-lying. Deposition in the zone occurred in sub-basins much like fault-troughs, bordered by local highlands of pre-Acadian rocks periodically uplifted and tilted on boundary faults. Deposition was thus a response to a complex interplay of down-sinking troughs adjacent to episodically renewed source areas; folding was related to fault movement; basin-edge coarse clastics and unconformities grade basinward to finer clastics and conformities; and younger strata overlapped older onto the basement. Tectonic activity (referred to the Maritime Disturbance) and volcanism decreased during

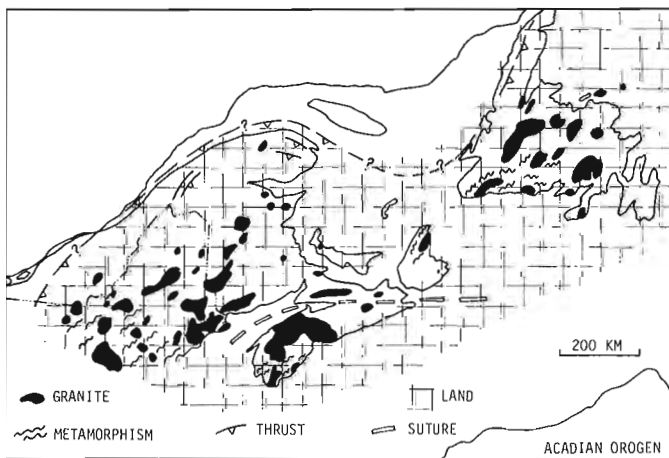


Figure 24.12. Mid-Devonian, Acadian orogen.

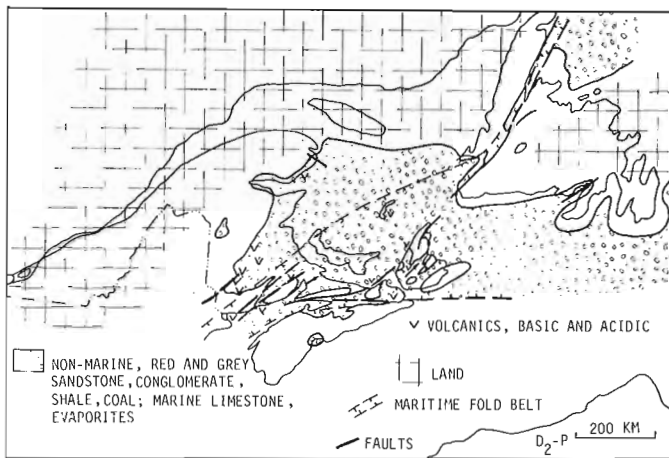


Figure 24.13. Middle Devonian to Early Permian, distribution of strata. Distribution on Atlantic continental shelf from B.V. Sanford, pers. comm. 1974.

the late Paleozoic: Devonian and Mississippian strata are generally more deformed than Pennsylvanian-Permian strata. Uppermost Pennsylvanian-Permian strata are slightly warped if at all and cover much of the older strata.

Kelley (in Poole *et al.*, 1970) and Hacquebard (1972) have summarized the geology recently.

Middle and Upper Devonian and Lower Mississippian (Tournaisian and Viséan) red and grey polymictic conglomerate, sandstone and shale with some oil shale and a trace of salt were deposited mainly in the taphrogenic zone (Perry, Horton s.l., Anguille, Great Bay de l'Eau). Local volcanics are basic in older parts (Perry) and acidic and basic in the upper parts (Fisset Brook, Piskahegan). During the Viséan and early Namurian, seas occupied the taphrogenic zone and platforms to deposit limestone, gypsum, anhydrite and salt, and red beds and local basin-edge conglomerate (Windsor, Codroy), with a few local thin basic and acidic volcanics. Continental deposition returned in late Viséan and Namurian, and continued through to Early Permian, the youngest strata exposed. Shale, sandstone, and conglomerate were deposited in rivers, fans, lakes and swamps over the entire successor basin (Canso, Riversdale, Cumberland, Pictou). Coal deposits are mainly Westphalian. Lower Permian strata occur only on Prince Edward Island, and represent the last stage in the evolution of the Appalachian system as related to the proto-Atlantic ocean. While the provenance of the older successor basin deposits was mainly internal to the Appalachian belt, it is possible that the St. Lawrence Platform and Canadian Shield yielded detritus to the younger strata, perhaps by an ancient St. Lawrence River system.

Upper Permian and lower Triassic strata are not present, and perhaps the Appalachian region and bordering Canadian Shield were undergoing erosion at this time (although strata of this age are nowhere to be found in Eastern Canada). In the Late Triassic (Fig. 24.14), a taphrogenic fault-trough was formed in the Bay of Fundy-northern Nova Scotia zone, in which a half-graben with a boundary fault on the north became filled with continental red clastics (Klein, 1962) and some 300 m of zeolitic tholeiitic basalt; this was beginning of the formation of the present-day Atlantic Ocean. On the Atlantic continental shelf, Lower (?) Jurassic salt was deposited unconformably upon the Appalachian orogen, to be succeeded by Jurassic to Recent marine and nonmarine limestone and fine clastics in a prograding wedge over 7 km thick on the continental slope and rise (McIver, 1972; Sherwin, 1973). The alkaline Montereian plugs and dykes were emplaced near Montreal during the Early Cretaceous.

Conclusions

The tectonic evolution of the Canadian Appalachians can, with some uncertainties, be interpreted using plate tectonic models. Unanimity is far from complete, the "rules of the game" are still being established, and major problems remain.

From a plate-tectonic viewpoint, the Canadian Appalachian system evolved in the following stages:

1. Extension, tensional faulting and eventually pull-apart on a mid-ocean ridge of a pre-Hadrynian crystalline craton which began in middle to late

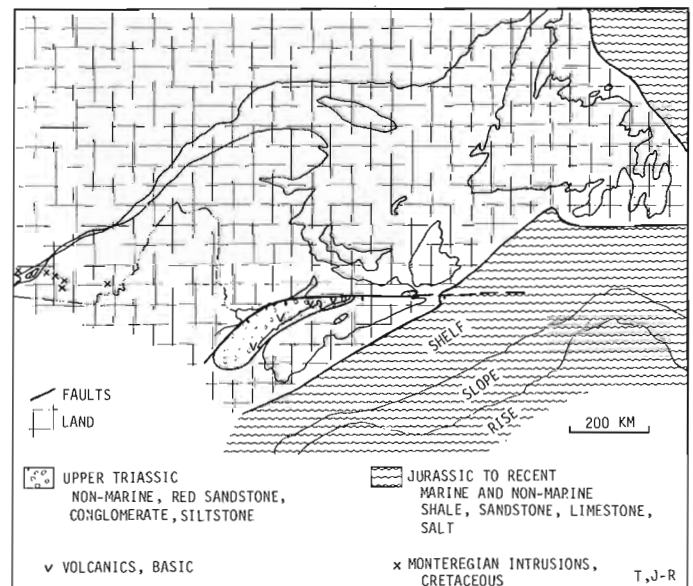


Figure 24.14. Late Triassic and Jurassic to Recent, distribution of strata; and Early Cretaceous Montereian Intrusions. Distribution of strata on Atlantic continental shelf from B.V. Sanford, pers. comm. 1974.

Hadrynian time, with the foundering of the northwestern Appalachian margin and the deposition of miogeoclinal Hadrynian and Cambrian clastics in Newfoundland and Hadrynian to Early Ordovician clastics in Quebec in the newly formed northwestern proto-Atlantic ocean. Platformal Cambrian and Ordovician carbonates were deposited on the bordering Canadian Shield, the St. Lawrence Platform. Cambrian(?) island arc volcanism on the oceanward edge of the miogeoclinal belt in Newfoundland resulted from a presumed subduction zone dipping northwest beneath the arc.

In the Avalon belt, Hadrynian island arc volcanism and sedimentation occurred on a continental basement (perhaps a remnant of the European-African Shield) and was caused by a southeast-dipping subduction zone located in the northwestern proto-Atlantic. Some regional metamorphism during the Hadrynian along the northwestern margin of the Avalon belt was followed by mainly molassal upper Hadrynian clastics in fault-troughs bordering the former volcanic belts. Platformal Cambrian and Early Ordovician pelites (including iron-formation) were deposited on the quiescent Hadrynian belt, at the same time as possibly Cambrian and/or Lower Ordovician turbiditic strata were deposited on the northwest side of the belt.

Cambrian and Lower Ordovician miogeoclinal turbidites in the apparently restricted southeastern proto-Atlantic ocean were deposited on a continental slope and rise on thinned continental crust of the bordering European-African Shield.

2. In the northwest margin, in western Newfoundland, latest Cambrian or earliest Ordovician polydeformation and regional metamorphism (Western Crystalline belt) of miogeoclinal strata and assembly of flysch and ophiolitic slices. Detritus from the assembled slices was carried northwestward toward a developing exogeosynclinal trough and southeastward upon autochthonous ophiolites. Island arc volcanism prevailed farther southeast above a northwest-dipping subduction zone.

In the northwest margin, in southern Quebec, by contrast, early Middle Ordovician polydeformation and regional metamorphism (Western Crystalline belt) of miogeoclinal strata took place in the same manner as in western Newfoundland. Lower(?) Ordovician ophiolites, and to the southeast island arc volcanics, were deformed on the southeast of the crystalline belt. The northwest-dipping subduction zone lay farther to the southeast.

Carbonate deposition on the bordering craton in western Newfoundland and Quebec was interrupted by a short-lived epeirogenic uplift at the end of the Early Ordovician, and again in Quebec in early Middle Ordovician time, reflecting tectonism in the bordering Appalachian belt.

On the northwest margin of the Avalon belt (southeast side of the northwestern proto-Atlantic ocean), possible early Middle Ordovician polydeformation and regional metamorphism (Eastern Crystalline belt) of Hadrynian and bordering miogeoclinal Cambro-

Ordovician strata developed above the reactivated southeast-dipping subduction zone, synchronous with folding of Cambrian and Lower Ordovician platformal strata of the Avalon belt itself.

Events in the Meguma belt in the Middle and Late Ordovician are uncertain; possibly glacio-genic deposition and accompanying volcanism prevailed.

3. In the northwest margin in western Newfoundland, in early to middle Middle Ordovician time, further uplift of the deformed and metamorphosed miogeoclinal strata, subsidence of the bordering platform to form a deep-water exogeosynclinal flysch trough, and gravity sliding of the assembled slices northwestward into the trough sediments occurred. Platformal deposition returned immediately on the front of the allochthon during middle and late Middle Ordovician. Island arc volcanism and greywacke deposition occurred farther southeast in the ocean above a northwest-dipping subduction zone.

In the northwest margin, in southern Quebec, in middle and late Middle Ordovician time, uplift of the deformed and metamorphosed miogeoclinal strata, subsidence of the bordering platform to form a deep-water exogeosynclinal flysch trough, and gravity sliding of slices during middle and late Middle Ordovician northwestward into the trough sediments, accompanied and followed immediately by thrusting of the frontal flysch zones occurred. Deep-water flysch deposition occurred southeast of the crystalline belt. Island arc volcanism in New Brunswick and northwestern Maine took place upon a Lower Ordovician and(?) older quartzite substrate that is presumed to overlie Grenvillian crust. A northwest-dipping subduction zone formed beneath the arc. There were no known late Middle and Late Ordovician events on Avalon Belt: possibly it was an uplifted, low-lying region undergoing gentle erosion.

4. In late Middle and Late Ordovician, in western Newfoundland, uplift of Great Northern Peninsula and erosion occurred thus dividing the allochthon into two klippe; uplift of Western Crystalline belt and contiguous northern Notre Dame Bay region occurred at end of Ordovician time. Island arc volcanism and flysch continued to the southeast above a northwest-dipping subduction zone.

In Late Ordovician time, in southern Quebec and New Brunswick, fine molasse from eroding allochthons was carried westward onto St. Lawrence Platform ("Queenston Delta") while deposition of flysch continued southeast of the crystalline belt. Deformation (in places multiple) and regional metamorphism of the Middle Ordovician island arc in New Brunswick and northwestern Maine took place. There was deposition of syn-deformational clastics and then deep-water ribboned limestone (Matapedia) upon the back of the Quebec allochthon in Gaspé Peninsula extending southward across deformed island arc along New Brunswick-Maine boundary zone. A northwest-dipping subduction zone lay beneath the island arc.

5. During Early and Middle Silurian, in Newfoundland, conversion from marine to continental environment by deposition of volcanics and coarse red bed clastics of molasse character derived from uplifted pre-Silurian rocks occurred. Upper Silurian-Lower Devonian red clastics derived from the uplifted orogen to southeast were deposited on the St. Lawrence Platform. Lower or Middle Devonian continental clastics were deposited in southwestern Newfoundland.

During Silurian and Early Devonian time, in the Quebec-New Brunswick sector, deposition of shallow-water sediments with local volcanics took place upon and against the uplifted Quebec allochthon and stabilized Ordovician island arc rocks and within the intervening Matapedia belt. Formation of a "marginal" trough of Lower and Middle Devonian clastics occurred upon the Ordovician allochthon. In southern New Brunswick, deep-water Middle and Upper Silurian turbidites were deposited in a trough representing a relict of the northwestern proto-Atlantic ocean; the turbidites grade southeastward to shallow-water sediments and volcanics along and upon the Avalon belt. A new subduction zone dipping northwest beneath the Avalon belt was formed.

In the Meguma belt, there were thick shallow- and deep-water sediments and volcanics of post-Early Ordovician to Late Silurian age, succeeded by Upper Silurian shale and Lower Devonian sedimentary rocks (including iron-formation).

6. In the mid-Devonian Acadian orogeny, crustal shortening resulting in upright folding with axial-plane cleavage of Paleozoic and (?) Hadrynian supracrustals occurred; there was regional metamorphism in southern Newfoundland and in southern Nova Scotia, Maine and adjacent states; transcurrent faulting (left-lateral?) was followed by minor steep thrusting on the northwest margin and extensive plutonism; this was succeeded by uplift of the entire Appalachian system (particularly anticlinorial zones of older rocks) and extensive erosion. The cause of these events is said to be continental collision; the suture is along the southeast side of the Avalon belt.

7. In Middle Devonian to Early Permian time, successor basin molasse deposits were formed with one evaporitic marine incursion (Viséan and early Namurian). Local volcanism in the early stage change from basic to mixed acidic and basic by Viséan time; coal is common in late stages. Thickest deposition is in a taphrogenic zone extending across the Acadian orogen where deposition was accompanied by interrelated faulting, folding, subsidence of sub-basins and uplift of source areas, all referred to the Maritime Disturbance. Tectonism decreased throughout the Late Paleozoic. This marked the end of the evolution of the Appalachian system as related to the proto-Atlantic ocean.

8. In Late Triassic, time half-graben faulting and continental clastic and basalt infilling took place along a zone extending across the Maritime fold belt; this signaled the beginning of the opening of the present-day Atlantic Ocean. Jurassic to Recent salt, limestone

and finally marine and nonmarine clastics, were deposited on the continental shelf, slope and rise. The intrusion of Cretaceous Montereian plugs occurred at this time.

Noteworthy are other aspects of evolution of the Canadian Appalachian belt:

1. The northwest-dipping subduction zones stepped progressively to the southeast from Cambrian to Devonian.

2. Although tectonic events in the Newfoundland sector and Quebec-Maritimes sector were similar, those in Newfoundland occurred before those in the Quebec-Maritimes sector, as for example, tectonism in the western crystalline belt, development of allochthons on the northwest margin, and transition from marine to nonmarine conditions during the Siluro-Devonian.

3. The "Z"-shaped curve of the St. Lawrence Platform — Appalachian orogen boundary probably originated when the proto-Atlantic ocean began to form in the Hadrynian. The close approach and apparent merging of the Western and Eastern Crystalline belts between Newfoundland and Cape Breton Island at the outermost point of the platform-orogen curve corresponds to the widest part of the metamorphic belt and to an area of uncertain size of Acadian regional metamorphism. This "bow tie knot" zone may have been present by the end of Ordovician, and may have served to separate the Newfoundland and Quebec-Maritimes sectors and allowed each to have its own Silurian and early Devonian development.

References

- Bird, J.M. and Dewey, J.F.
1970: Lithosphere plate: continental margin tectonics and the evolution of the Appalachian orogen. *Geol. Soc. Am., Bull.*, v. 81 p. 1031-1060.
- Church, W.R.
1969: Metamorphic rocks of Burlington Peninsula and adjoining areas of Newfoundland, and their bearing on continental drift in North Atlantic. *in: "North Atlantic — Geology and Continental Drift"*, ed. M. Kay. *Am. Assoc. Pet. Geol., Mem.* 12, p. 212-233.
- Church, W.R. and Stevens, R.K.
1971: Early Paleozoic ophiolite complexes of Newfoundland Appalachians as mantle-ocean crust sequences. *J. Geophys. Res.*, v. 76, p. 1460-1466.
- Dewey, J.F.
1969: Evolution of the Appalachian — Caledonian orogen. *Nature*, v. 222, p. 124-129.
- Dewey, J.F. and Bird, J.M.
1971: Origin and emplacement of the ophiolite suite: Appalachian ophiolites in Newfoundland. *J. Geophys. Res.*, v. 76, p. 3179-3206.

- Hacquebard, P. A.
1972: The Carboniferous of Eastern Canada. Septième Congrès International de Stratigraphie et de Géologie du Carbonifère, Krefeld, 1971, *Compte Rendu*, Bd. 1, p. 69-90.
- Hughes, C. J. and Brückner, W. D.
1971: Late Precambrian rocks of eastern Avalon Peninsula, Newfoundland — a volcanic island complex. *Can. J. Earth Sci.*, v. 8, p. 899-915.
- Hutchinson, R. D.
1952: The stratigraphy and trilobite faunas of the Cambrian sedimentary rocks of Cape Breton Island, Nova Scotia. *Geol. Surv. Can.*, Mem. 263, 124 p.
1962: Cambrian stratigraphy and trilobite faunas of southeastern Newfoundland. *Geol. Surv. Can.*, Bull. 88, 156 p.
- Kay, M.
1951: North American Geosynclines. *Geol. Soc. Am.*, Mem. 48, 143 p.
1969: Silurian of northeast Newfoundland. *in*: "North Atlantic — Geology and Continental Drift," ed. M. Kay. *Am. Assoc. Pet. Geol.*, Mem. 12, p. 414-424.
1972: Dunnage Mélange and Lower Paleozoic deformation in northeastern Newfoundland. *Int. Geol. Congre.*, 24th, Canada, Sec. 3, p. 122-133.
- Kennedy, M. J.
1971: Structure and stratigraphy of the Fleur de Lys Supergroup in the Fleur de Lys area, Burlington Peninsula, Newfoundland. *Geol. Assoc. Can.*, Proc., 24 (1), p. 59-71.
- Kennedy, M. J. and McGonigal, M. H.
1972: The Gander Lake and Davidsville Groups of northeastern Newfoundland: new data and geotectonic implications. *Can. J. Earth Sci.*, v. 9, p. 452-459.
- Kindle, C. H. and Whittington, H. B.
1958: Stratigraphy of the Cow Head region, western Newfoundland. *Geol. Soc. Am.*, Bull., v. 69, p. 315-342.
- Klein, G. deV.
1962: Triassic sedimentation, Maritime Provinces, Canada. *Geol. Soc. Am.*, Bull., v. 73, p. 1127-1146.
- Lajoie, J., Heroux, Y., and Mathey, B.
1974: The Precambrian Shield and the Lower Paleozoic shelf: the unstable provenance of the Lower Paleozoic flysch sandstones and conglomerates of the Appalachians between Beaumont and Bic, Quebec. *Can. J. Earth Sci.*, v. 11, p. 951-963.
- Lilly, H. D.
1966: Late Precambrian and Appalachian tectonics in the light of submarine exploration on the Great Bank of Newfoundland and in the Gulf of St. Lawrence, preliminary views. *Am. J. Sci.*, v. 264, p. 569-574.
- Lock, B. E.
1969: Silurian rocks of west White Bay area, Newfoundland. *in*: *North Atlantic — Geology and Continental Drift*, ed. M. Kay. *Am. Assoc. Pet. Geol.*, Mem. 12, p. 433-442.
- McCartney, W. D.
1967: Whitbourne map-area, Newfoundland, *Geol. Surv. Can.*, Mem. 341, 135 p.
- McIver, N. L.
1972: Cenozoic and Mesozoic stratigraphy of the Nova Scotia Shelf. *Can. J. Earth Sci.*, v. 9, p. 54-70.
- Neuman, R. B.
1972: Brachiopods of Early Ordovician volcanic islands. *Int. Geol. Congr.*, 24th, Canada, Sec. 7, p. 297-302.
- Poole, W. H.
1967: Tectonic evolution of Appalachian region of Canada. *in*: "Geology of the Atlantic Region, Hugh Lilly Memorial Volume", ed. E. R. W. Neale and H. Williams. *Geol. Assoc. Can.*, Spec. Paper 4, p. 9-51.
- Poole, W. H., Sanford, B. V., Williams, H., and Kelley, D. G.
1970: Geology of southeastern Canada. *in*: "Geology and Economic Minerals of Canada", ed. R. J. W. Douglas. *Geol. Surv. Can.*, Econ. Geol. Rep. 1, 5th edition, p. 227-304.
- Rodgers, J.
1970: The tectonics of the Appalachians. *Wiley-Interscience*, 271 p.
1972: Latest Precambrian (post-Grenville) rocks of the Appalachian region. *Am. J. Sci.*, v. 272, p. 507-520.
- Rose, E. R.
1952: Torbay map-area, Newfoundland. *Geol. Surv. Can.*, Mem. 265, 64 p.
- Ruitenberg, A. A., Venugopal, D. V., and Giles, P. S.
1973: "Fundy Cataclastic Zone", New Brunswick: evidence for post-Acadian penetrative deformation. *Geol. Soc. Am. Bull.*, v. 84, p. 3029-3044.

- Schenk, P. E.
 1970: Regional variation of the flysch-like Meguma Group (Lower Paleozoic) of Nova Scotia, compared to recent sedimentation off the Scotian Shelf. *in*: "Flysch Sedimentology in North America", ed. J. Lajoie. Geol. Assoc. Can., Spec. Paper 7, p. 127-152.
- 1971: Southeastern Atlantic Canada, northwestern Africa, and continental drift. *Can. J. Earth Sci.*, v. 8, p. 1218-1251.
- 1972: Possible Late Ordovician glaciation of Nova Scotia. *Can. J. Earth Sci.*, v. 9, p. 95-107.
- Sherwin, D. F.
 1973: Scotian Shelf and Grand Banks. *in*: "The Future Petroleum Provinces of Canada — their Geology and Potential", ed. R. G. McCrossan. *Can. Soc. Pet. Geol.*, Mem. 1, p. 519-559.
- Stevens, R. K.
 1970: Cambro-Ordovician flysch sedimentation and tectonics in west Newfoundland and their possible bearing on a proto-Atlantic ocean. *Geol. Assoc. Can.*, Spec. Paper 7, p. 165-177.
- Stevens, R. K., Strong, D. F., and Kean, B. F.
 1974: Do some eastern Appalachian ultramafic rocks represent mantle diapirs produced above a subduction zone; *Geology*, v. 2, p. 175-178.
- St. Julien, P. and Hubert, C.
 1975: Evolution of the Taconian orogen in the Quebec Appalachians. *Am. J. Sci.*, 275-A, p. 337-362.
- Strong, D. F.
 1974: Plate tectonic setting of Appalachian — Caledonian mineral deposits as indicated by Newfoundland examples. *Soc. Min. Eng. AIME, Trans.*, v. 250, p. 121-128.
- Strong, D. F., Dickson, W. L., O'Driscoll, C. F., Kean, B. F., and Stevens, R. K.
 1974: Geochemical evidence for a east-dipping Appalachian subduction zone in Newfoundland. *Nature*, v. 248, p. 37-39.
- Weeks, L. J.
 1954: Southeast Cape Breton Island. *Geol. Surv. Can.*, Mem. 277, 112 p.
- 1957: The Appalachian region. *in*: "Geology and Economic Minerals of Canada", ed. C. H. Stockwell. *Geol. Surv. Can.*, Econ. Geol., Rep. 1, 4th edition, p. 123-205.
- Williams, H.
 1964: The Appalachians in northeastern Newfoundland — a two-sided symmetrical system. *Am. J. Sci.*, v. 262, p. 1137-1158.
- Williams, H., Kennedy, M. J., and Neale, E. R. W. co-ordinators
 1972: The Appalachian Structural Province. *in*: "Variations in Tectonic styles in Canada", ed. R. A. Price and R. J. W. Douglas. *Geol. Assoc. Can.*, Spec. Paper 11, p. 181-261.
- Wit, M. J. de
 1974: On the origin and deformation of the Fleur de Lys metaconglomerate, Appalachian fold belt, northwest Newfoundland. *Can. J. Earth Sci.*, v. 11, p. 1168-1180.

Project 750010

V. Ruzicka

Regional and Economic Geology Division

The pyritiferous quartz-pebble conglomerate uranium ores of the Elliot Lake - Blind River area of Ontario are the most productive and comprise the greatest uranium resources of any area of similar size in Canada. For this reason, the highest priority was given to the area when evaluating the uranium resources of Canada. Furthermore, the Elliot Lake - Blind River area served as a model in evaluating the Huronian and other Lower Proterozoic basins that might contain similar conglomeratic ores (i. e. inferred and prognosticated uranium resources).

The methodology used in the uranium resources evaluation process was based on a conceptual genetic model. This model, which simulates processes leading to the formation of pyritiferous quartz-pebble conglomerate uranium deposits, was established on the basis of criteria derived from studies of the Elliot Lake deposits and from literature describing studies done on the South African Witwatersrand uranium deposits.

The model postulates a sedimentary syngenetic ("paleoplacer") mineralization process with some authigenic modifications during the diagenetic phase of the ore-forming process (Ruzicka, in press). It is postulated that: (a) the uranium mineralization was derived from source rocks containing anomalous amounts of radioelements and uranium minerals; (b) the liberation of uranium minerals took place by physical, chemical and, possibly, biological mechanisms under oxygen deficient conditions; (c) transportation of uranium minerals in the detritus occurred in water streams under an oxygen deficient atmosphere, combined with volcanic exhalations, and possibly in a periglacial environment. Some uranium minerals were probably transported as suspensions in colloidal organic matter (Ruzicka and Steacy, 1976); (d) concentration and deposition of uranium and accompanying minerals was governed by hydraulic action of streams within an area of extensively developed water drainage; (e) abundant sulphur, a product of volcanic activity, caused sulphurization of some minerals (e. g. magnetite) and hydrocarbon, which was apparently derived from organic material; (f) preservation of the uranium minerals was possible (with some local redistribution of uranium) due to presence of reducing agents, such as pyrite, in the beds and by burial, but some local redistribution of uranium may have occurred.

Using the above mentioned conceptual genetic model the data required for resource evaluation were gathered mainly from available drillhole logs (e. g. Leahy, 1973) and further processed according to another model - the "Uranium Resources Evaluation Model" (Ruzicka, in prep., and Fig. 25.1). The evaluation procedure consisted of several operations (see Fig. 25.2), such as: (a) adjustment of absolute elevations of

selected fiducial points on a topographical base map; (b) compilation of a contour map of the structurally restored paleosurface; (c) construction of an isopach map of the uranium-bearing Matinenda Formation or equivalents; (d) plotting of mineralization grades (G), thicknesses (T), and accumulations (GxT = DEL) on geological maps; (e) delineation of areas with identified and surmised uranium mineralization using interpretation of the above mentioned information (i. e. interpretation of the paleodrainage pattern, morphology of the uranium-bearing formations, grade - thickness - accumulation trends); (f) computation of uranium resources using a volumetric and a probabilistic formula.

The data were coded and processed using a computer MARS system. The coding of the selected data was done manually by support geologists on specially designed coding sheets. The coded data were then transferred into eighty-column two-card sets, recorded in the computer memory, retrieved, statistically analyzed and quantified.

Special attention was paid to the areal distribution of the uranium mineralization. It was postulated that the paleodrainage systems persisted and served as loci for deposition of the uranium-bearing sediments throughout the Matinenda period.

The interpreted distribution of uranium mineralization is shown on Figure 25.3, which was compiled from an original more detailed map and simplified for the purpose of illustration. Thirteen mineralized zones were delineated in the Elliot Lake - Blind River area: (numbers in brackets correspond with numbers on Fig. 25.3) (1) Quirke, (2) Nordic, (3) Corner Lake, (4) Whiskey Lake, (5) Elliot Lake I, (6) Elliot Lake II, (7) Moon Lake, (8) Matinenda Lake, (9) Pronto, (10) Peak Lake, (11) Demorest Lake, (12) Parkinson Township, and (13) Thessalon Township.

The mineralized zones were further classified according to economic parameters that were used in the 1975 assessment of Canada's uranium resources. This classification was based on price per lb. U_3O_8 categories: (A) up to \$20; (B) more than \$20 up to \$40; (C) more than \$40. (This classification is not shown in Fig. 25.3.)

Because of the computer based evaluation system, all subsequent modifications of the evaluation process, either due to input of new data from exploration, or to changes in economic conditions, can be made rapidly and efficiently. It is therefore anticipated that the annual assessments of the Canadian uranium resources can be updated in this way not only for the conglomeratic deposits, but also, by suitable modification, for the remaining genetic types of deposits and thus serve for periodic analyses of the uranium mineral endowment of Canada.

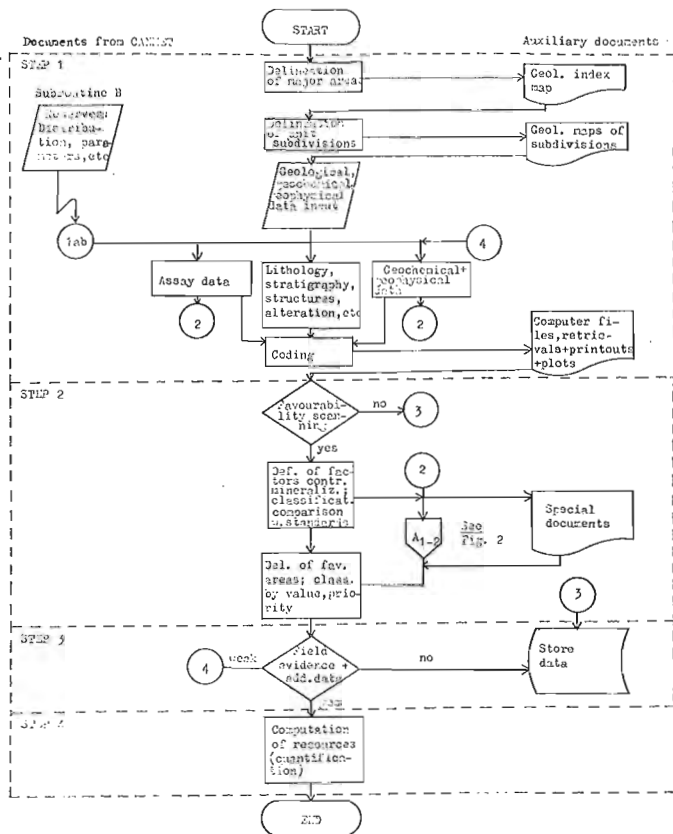


Figure 25.1. Uranium Resources Evaluation Model (Standard Routine).

Remarks: (1) CANMET is an abbreviation for "Canada Centre for Mineral and Energy Technology", a branch of Department of Energy, Mines and Resources.

(2) Abbreviations used in the scheme: Def. = Definition; Del. = Delineation; fav. = favourable; class. = classification; contr. = controlling; w. = with; Geol. = Geological.

(3) The symbols used in this flowchart conform to the International Organization for Standardization (ISO) International Standard 1028 "Information Processing - Flowchart Symbols".

(4) Operations shown by a special "off page connector" A₁₋₂ are detailed in Fig. 25.2.

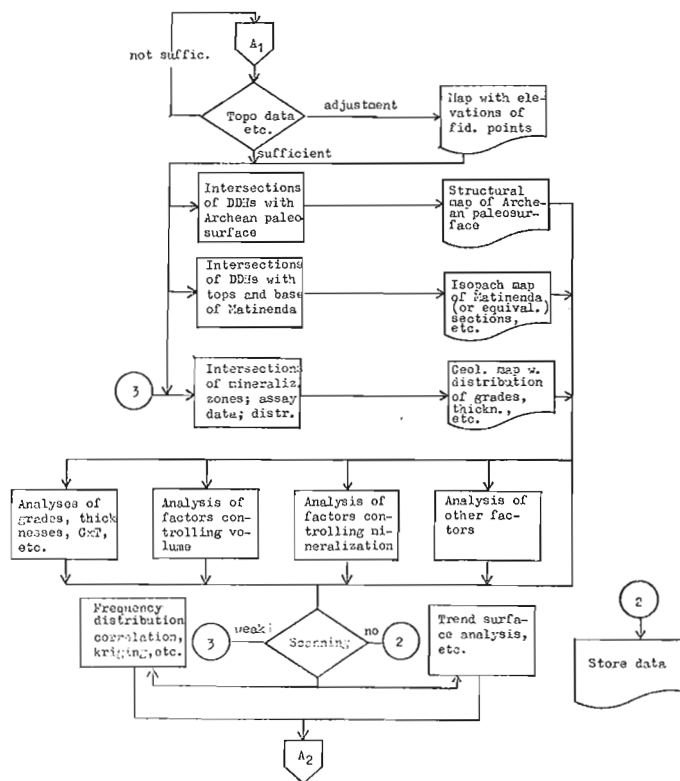


Figure 25.2. Uranium Resources Evaluation Model sub-model A₁₋₂.

Remarks: (1) Abbreviations used in the scheme: distr. = distribution; w. = with; thickn. = thickness;

(2) This scheme simulates a sub-routine, which is substituted in Fig. 25.1 by an "off page connector" A₁₋₂.

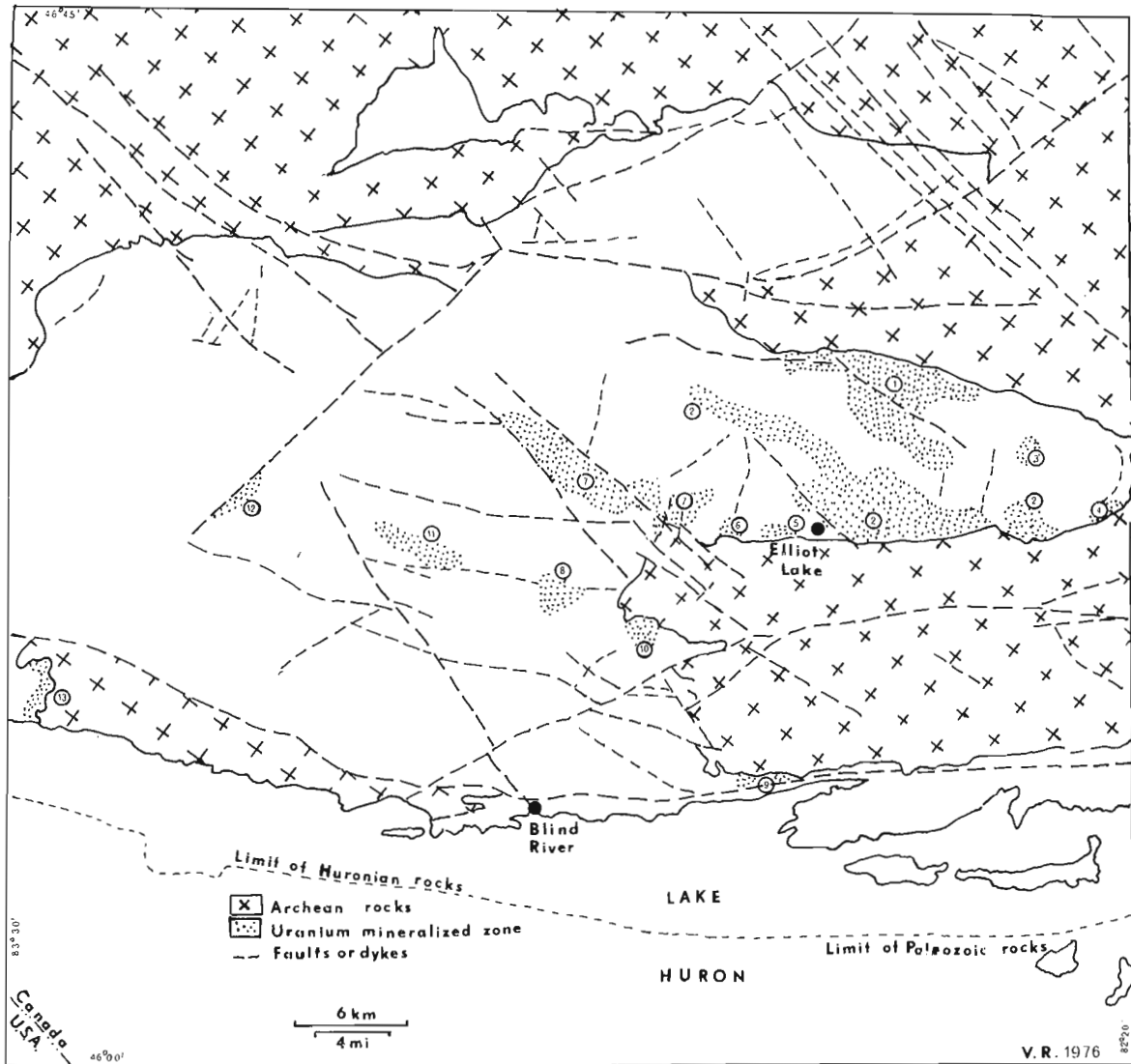


Figure 25.3. Elliot Lake - Blind River uranium-bearing area; mineralized zones:

- | | |
|--------------------------|--|
| (1) Quirke, | (2) Nordic, |
| (3) Corner Lake, | (4) Whiskey Lake, |
| (5) Elliot Lake I, | (6) Elliot Lake II, |
| (7) Moon Lake, | (8) Matinenda Lake |
| (9) Pronto, | (10) Peak Lake, |
| (11) Demorest Lake, | (12) Parkinson Township, |
| (13) Thessalon Township. | (Geological base after Robertson, 1971.) |

References

Leahy, E. J., compiler

1973: Diamond Drilling in the Huronian Supergroup, Sault Ste. Marie - Elliot Lake Area; v. 1, Ont. Div. Mines, Geol. Br., Open File Report 5093.

Robertson, J.A., compiler

1971: Blind River - Elliot Lake Sheet, District of Algoma and Sudbury; Preliminary Map P. 304 (1971 revision), Geological Compilation Series, Ont. Dep. Mines Northern Affairs.

Ruzicka, V.

Some metallogenic features of the Huronian and post-Huronian uraniferous conglomerates; U. S. Geol. Surv. Prof. Paper. (in press).

Uranium resources evaluation model as an exploration tool; Geol. Surv. Can. (in prep).

Ruzicka V. and Steacy H. R.

1976: Some sedimentary features of conglomeratic uranium ore from Elliot Lake, Ontario in Report of Activities, Pt. A, Geol. Surv. Can., Paper 76-1A, p. 343-346.

Project 680109

M. S. Barss and B. Crilley
Atlantic Geoscience Centre, Dartmouth

Barss and Williams, 1973, described the use of Clearcol and Cellosize as dispersant-mounting media for palynology residues on coverslips, prior to their mounting on microscope slides.

Clearcol is the trade name for a mounting medium manufactured by H. W. Clark, Melrose, Massachusetts, which is presently not available.

Cellosize (hydroxyethyl cellulose) is manufactured by Union Carbide Chemicals Company, and is in abundant supply.

Both mounting media have certain disadvantages. Clearcol, because of its acidity, removes the stain from specimens over a period of time; it cannot be used to mount nannofossil residues, and it can crack quite severely if left for an extended period without mounting on a slide. Cellosize tends to retain more air bubbles than Clearcol and can become cloudy. The latter may be a result of improper preparation rather than the age of the medium.

Because of the non-availability of Clearcol and the abundant supply of Cellosize, experiments were undertaken to develop a mounting medium utilizing several additives in a Cellosize base in an attempt to develop a medium without the disadvantages listed above.

The formula and preparation technique given below appears to meet most of the requirements. The authors emphasize that there should be no deviation from the preparation technique.

Formula and Preparation Technique

- Step 1. Place 5.0 ± 0.1 g of Cellosize (hydroxyethyl cellulose WP-09 low viscosity) in a 250 ml pyrex beaker, with a calibrated 85 ml mark. No more than this amount should be prepared at a time because of the difficulties in filtering.
- Step 2. Add 20 ml of methanol to beaker.
- Step 3. Add 100 ml of distilled water to beaker.
- Step 4. Heat mixture on hotplate at 71°C (160°F) for 20 minutes (by this time most of the methanol should be driven off). If a stirring magnet is used be sure to account for its volume. Also counter stir the mixture with a glass rod to prevent mixture from sticking to the sides of the beaker and burning. After 20 minutes of heating, turn hotplate down and allow mixture to cool to $57^{\circ}\text{--}60^{\circ}\text{C}$ ($135^{\circ}\text{--}140^{\circ}\text{F}$). Heat at this temperature (with stirring every 2-3 minutes if magnet is not used) for 40 to 60 minutes until mixture is within 5 ml of premeasured 85 ml mark. Reheat mixture to 71°C (this takes approximately 10 to 15 minutes). The mixture should now be at premeasured mark.

- Step 5. Pour half of mixture (while hot) into a Reeve Angel 934-AH glass-fiber filter paper (12.5 cm diameter) in a plastic funnel (65 mm top inner diameter, 25 mm stem) placed in a suitable size reagent bottle (a plastic funnel is used because a glass funnel cools the mixture faster). Because the mixture becomes quite viscous when cool, it is suggested, therefore, that two filtering apparatuses should be used. Filtering may take an hour or more. Approximately 70 per cent is recovered in the reagent bottles. Transfer mixture to one reagent bottle.
- Step 6. Add three drops of ethylene glycol monomethylether (Cellosolve) to the mixture in the reagent bottle and shake well. Dispensing instrument is a disposable Pasteur pipette, heavy wall, 7.0-7.5 mm diameter, $5\frac{3}{4}$ inches long, Fisher Cat. No. 13-678-5A, 1975, p. 633; a bulb is attached to dispense the drops.
- Step 7. Let mixture stand (in closed bottle) for a few days before using.
- Step 8. Transfer a two-week supply to a small dropping bottle, having a glass pipette with rubber bulb stopper. Pipette should have a $3/32$ inch diameter dispensing opening. Discard mixture when viscosity increases by exposure to air during slide making or if dispersal quality is lost.

Two drops of the above medium are sufficient for spreading residues and forming a satisfactory film on the coverslip. Better spreading of residue has been noted during slide making if residue to be spread is placed on coverslip and medium dropped on the residue. Mixture is spread over the coverslip using a toothpick which is discarded after use. When the mixture is dry the coverslip is mounted permanently on a slide with Elvacite (Barss and Williams, 1973, p. 15).

This mounting medium has been used in the Eastern Petroleum Geology Subdivision palynology laboratory, Atlantic Geoscience Centre since September 1, 1975, on all types of residues, including coarse fractions, fine fractions from screened residues, mixed, oxidized, unoxidized and with nannofossils. After several months of testing and general use since September, 1975 it is concluded that this medium has qualities that equal and/or surpass Clearcol and the Cellosize medium described by Barss and Williams (1973, p. 20).

The dispersal quality appears to be satisfactory, the medium does not appear to cloud when stored, it does not crack when left for extended periods of time (even when placed in oven at 25°C for two weeks), and

since it is not acidic can be used for stained specimens and nannofossils.

This medium is presented as a substitute for any of several other media presently in use in palynology laboratories. Any criticism of or suggestion for improving this procedure as well as any reports of

adverse effects from the use of this mounting medium are welcome.

Reference

- Barss, M. S. and Williams, G. L.
1973: Palynology and nannofossil processing techniques; Geol. Surv. Can., Paper 73-26, 25 p.

Project 720078

S. Lichti-Federovich
Terrain Sciences DivisionIntroduction

The site selection and collection of the core from which the diatoms were extracted (Station 95; 74°45.7'N, 83°13.2'W) were carried out under the direction of W. Blake, Jr. during cruise 74-026 of *C. S. S. Hudson*. The site is situated in the central inner part of Croker Bay, the easternmost bay along the south coast of Devon Island, approximately 20 km north-northeast of Cape Rosamond and 6.5 km south of the snout of an unnamed outlet glacier from the Devon Island Ice Cap. The core investigated, together with one nearby at Station 93, was from a basin where a thick sequence (at least 65 m) of sediments is present, in a water depth of 222 fathoms (406 m) (Blake and Lewis, 1975).

This preliminary investigation has shown that all samples from Station 95 in Croker Bay contain only Pleistocene assemblages (Pl. 27.1, 27.2), as shown by a comparison with the comprehensive floristic surveys of Grøntved and Seidenfaden (1938) and Seidenfaden (1947). The former gives a detailed account of the phytoplankton material collected in the waters west of Greenland on the Godthaab Expedition 1928, whereas the latter represents an extensive compilation of the phytoplankton species of the Canadian Eastern Arctic.

Future analysis of additional samples by critical identification of the many species and forms, as well as determination of their climatic/geographical affinities, should permit detailed paleoecological inferences to be drawn.

List of Diatoms

SAMPLE NO. 1 (0 cm depth – top of core section 1)

1. Marine planktonic forms of Silicoflagellates are present: *Distephanus speculum* Ehr.
2. Both marine plankton forms and marine littoral, epiphytic forms which have been reported from the coastal areas of cold seas: *Biddulphia aurita* (Lyngb.) Bréb. & God., *Rhabdonema minutum* Kütz., *Triceratium arcticum* f. *balaena* (E.) Meunier.
3. Marine form found in coastal plankton of polar seas: *Chaetoceros capreolus* (Bail.) Cleve.
4. Coastal planktonic forms of the northern Arctic Ocean: *Bacterosira fragilis* Gran., *Chaetoceros capreolus* Ehr., *Chaetoceros subsecundus* (Grun.) Hust.
5. Oceanic forms of the Arctic Ocean: *Stenoneis inconspicua* v. *baculus* Cleve, *Nitzschia seriata* Cleve.

6. Littoral forms occurring on coastal areas of many oceans: *Rhabdonema arcuatum* (Lyngb. ? Ag.) Kütz., *Cocconeis costata* Greg., *Podosira* spp., *Cocconeis pseudo-marginata* Greg., *Cocconeis soutellum* Ehr.

7. Oceanic forms present in plankton of all oceans: *Trachyneis aspera* (Ehr.) Cleve, *Coscinodiscus asteromphalus* Ehr., *Coscinodiscus marginatus* Ehr., *Coscinodiscus* spp.

8. Neritic form found in coastal plankton of all oceans: *Coscinodiscus curvatulus* Grun.

9. Marine forms occurring in many oceans: *Diploneis Smithii* (Bréb.) Cleve, *Plagiogramma staurophorum* (Greg.) Heib.

10. Marine forms of the Arctic Ocean: *Diploneis entomon* (A. S.) Cleve, *Nitzschia socialis* Greg.

11. Marine plankton forms of northern waters: *Rhizosolenia hebetata* f. *hiemalis* (Bail.) Gran., *Rhizosolenia hebetata* f. *semispina* (Hensen) Gran.

SAMPLE NO. 2 (100 cm depth – top of core section 2)

1. Silicoflagellates present: *Distephanus speculum* Ehr.
2. Several oceanic, planktonic diatoms of northern and arctic types: *Chaetoceros atlanticus* Cleve, *Rhizosolenia hebetata* f. *hiemalis* (Bail.) Gran., *Navicula directa* W. Smith, *Navicula Henedyi* v. *luxuosa* A. Cleve, *Thalassiosira kryophylus* Grun.
3. Coastal plankton forms of polar seas: *Porosira glacialis* (Grun.) Jörg., *Bacterosira fragilis* Gran., *Chaetoceros capreolus* Ehr., *Chaetoceros furcellatus* Bail.
4. Littoral, epiphytic form common on the coastal areas of cold seas: *Triceratium arcticum* f. *balaena* (E.) Meunier.
5. Littoral, marine forms found in most coastal areas: *Achnanthes brevipes* Agardh, *Podosira* spp., *Cocconeis costata* Greg., *Cocconeis pseudo-marginata* Greg.
6. Oceanic forms occurring in the plankton of most oceans: *Coscinodiscus centralis* Ehr., *Coscinodiscus oculus-iridis* Ehr., *Coscinodiscus asteromphalus* Ehr., *Coscinodiscus marginatus* Ehr., *Trachyneis aspera* (Ehr.) Cleve, *Coscinodiscus* spp.

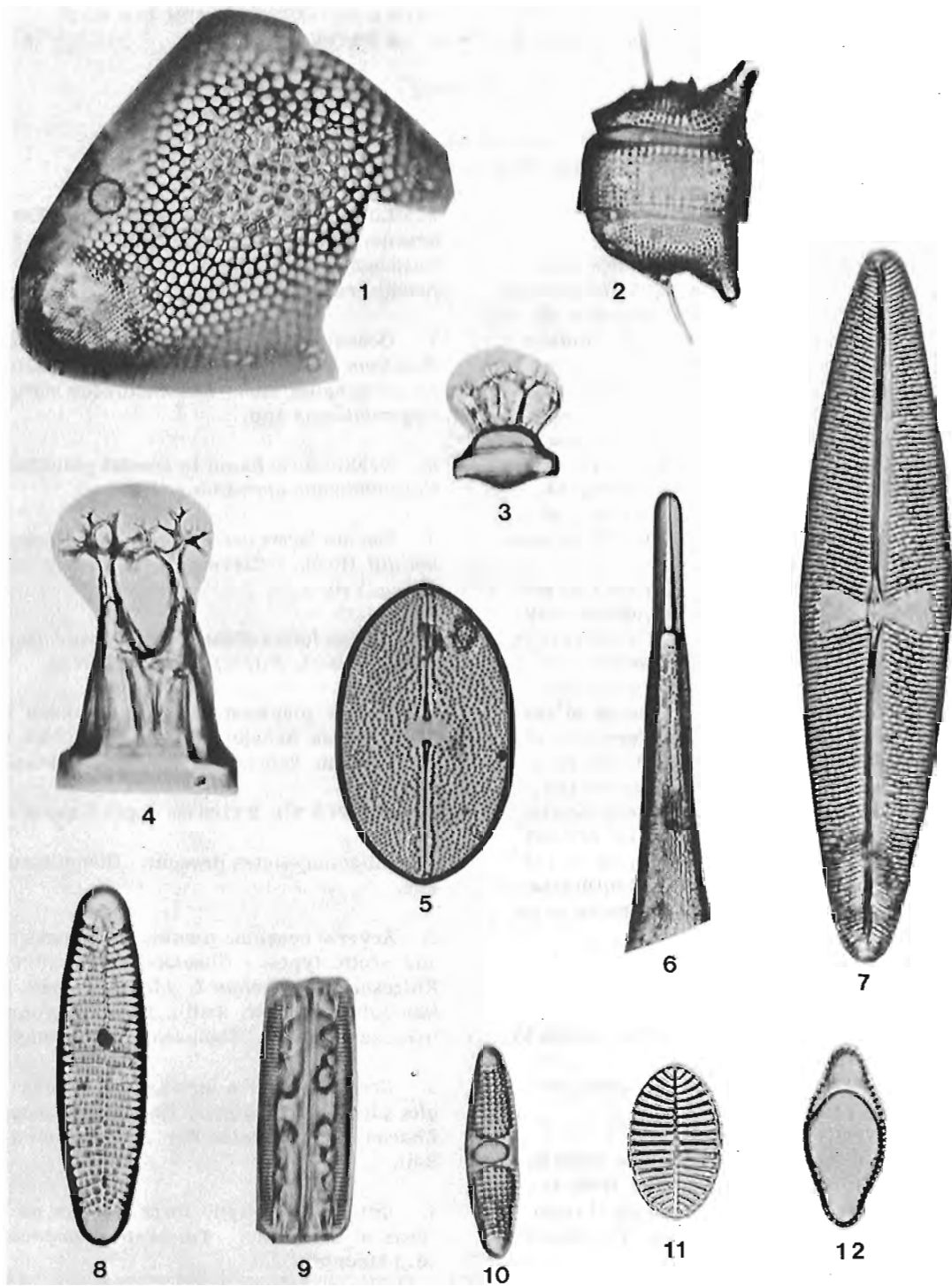


Plate 27. 1

(Magnification x 800)

- | | |
|--|---|
| Figure 1. <i>Triceratium arcticum</i> fo. <i>balaena</i> (E.) Meunier. | Figure 7. <i>Trachyneis aspera</i> (Ehr.) Cleve |
| Figure 2. <i>Biddulphia aurita</i> (Lyngb.) Bréb. & God. | Figure 8. <i>Rhabdonema arcuatum</i> (Lyngb. ? Ag.) Kütz. |
| Figure 3. <i>Chaetoceros subsecundus</i> (Grun.) Hust. | Figure 9. <i>Grammatophora angulosa</i> Ehr. |
| Figure 4. <i>Chaetoceros capreolus</i> Ehr. | Figure 10. <i>Plagiogramma staurophorum</i> (Greg.) Heib. |
| Figure 5. <i>Navicula glacialis</i> (Cleve) Grun. | Figure 11. <i>Cocconeis costata</i> Greg. |
| Figure 6. <i>Rhizosolenia hebetata</i> fo. <i>hiemalis</i> (Bail.) Gran. | Figure 12. <i>Rhabdonema minutum</i> Kütz. |

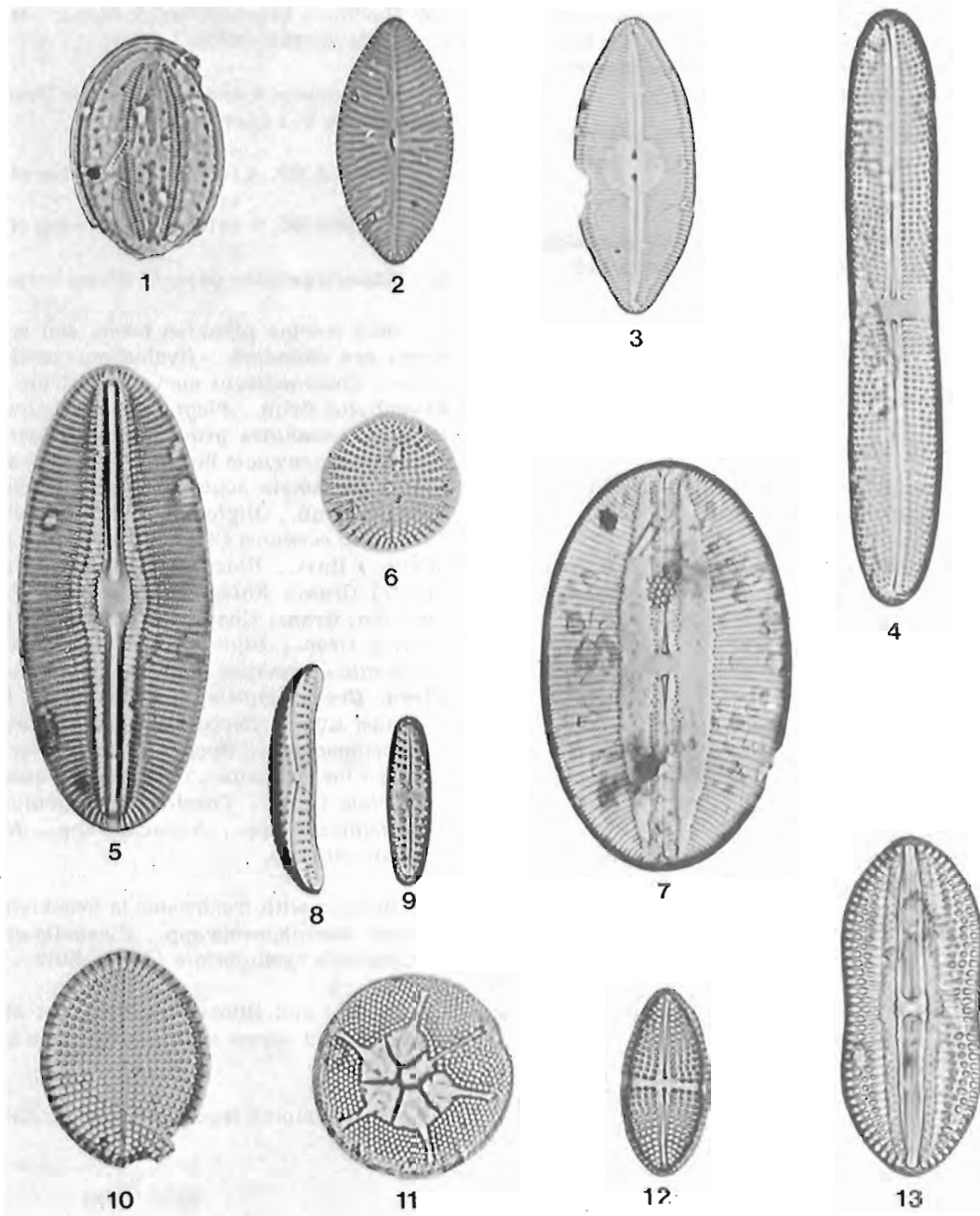


Plate 27. 2

(Magnification x 800)

- Figure 1. *Cocconeis pseudo-marginata* Greg.
- Figure 2. *Navicula valida* Cleve & Grun.
- Figure 3. *Caloneis brevis* (Greg.) Cleve
- Figure 4. *Achnanthes arctica* Cleve
- Figure 5. *Diploneis Smithii* (Bréb.) Cleve
- Figure 6. *Cocconeis pediculus* Ehr.

- Figure 7. *Navicula Hennedyi* var *luxuosa* A. Cleve
- Figure 8. *Amphora costata* W. Sm.
- Figure 9. *Achnanthes groenlandica* (Cleve) Grun.
- Figure 10. *Cocconeis scutellum* Ehr.
- Figure 11. *Asteromphalus robustus* Castrac.
- Figure 12. *Achnanthes brevipes* Agardh
- Figure 13. *Diploneis entomon* (A. S.) Cleve

7. Several littoral, marine-arctic forms are present: *Navicula glacialis* (Cleve) Grun., *Hyalodiscus subtilis* Bail., *Grammatophora arcuata* Ehr., *Grammatophora arctica* Cleve, *Rhabdonema Torellii* Cleve.

8. Neritic and littoral form most abundant in arctic and boreal seas: *Biddulphia aurita* (Lyngb.) Bréb. & God.

9. Neritic, boreal-arctic form found in the plankton of northern waters: *Thalassiosira Nordenskiöldi* Cleve.

SAMPLE NO. 3 (216 cm depth – top of core section 3)

1. Silicoflagellates present: *Distephanus speculum* Ehr., *Distephanus minutus* Bachm., *Distephanus octangulatus* Wailes, *Distephanus octonarius* Defl.

2. Cold-water marine form of coastal plankton: *Chaetoceros subsecundus* (Grun.) Hust.

3. Oceanic plankton form ranging from the Mediterranean to the Arctic Ocean: *Asteromphalus robustus* Castracane.

4. Nordic-alpine freshwater form: *Eunotia papilio* (Grun.) Hust.

5. Several marine-arctic forms are present: *Navicula valida* Cleve & Grun., *Navicula directa* W. Smith, *Thalassiosira hyalina* (Grun.) Gran., *Porosira glacialis* (Grun.) Jörg.

6. Littoral, marine forms: *Opephora Martyi* Hérribaud, *Podosira* spp., *Achnanthes brevipes* Agardh., *Biddulphia aurita* v. *robustus* (Kütz.) Hust., *Grammatophora arcuata* Ehr., *Amphora proteus* Greg., *Amphora costata* W. Smith.

7. Marine, pelagic form of the North Atlantic Ocean: *Nitzschia delicatissima* Cleve.

8. Marine form occurring on arctic coasts: *Achnanthes arctica* Cleve.

9. Pelagic, marine, arctic form common on the coastal areas of cold seas: *Chaetoceros capreolus* Ehr.

10. Freshwater to brackish-water forms: *Cocconeis pediculus* Ehr., *Cocconeis scutellum* v. *stauroneiformis* W. Smith, *Amphora ovalis* Kütz., *Amphora libyca* Ehr.

11. Marine, pelagic, or neritic forms found in most oceans: *Coscinodiscus curvatulus* Grun., *Coscinodiscus marginatus* Ehr., *Coscinodiscus oculus-iridis* v. *borealis* (Bail.) Cleve, *Coscinodiscus asteromphalus* Ehr.

12. Littoral form of coastal areas of cold oceans, especially arctic coasts: *Rhabdonema minutum* Kütz.

13. Littoral form common to coastal areas of many oceans: *Rhabdonema arcuatum* (Lyngb. ? Ag.) Kütz.

14. Marine to brackish-water forms: *Amphiprora* spp., *Diploneis Smithii* (Bréb.) Cleve.

15. Marine form found in the Arctic Ocean: *Diploneis entomon* (A. S.) Cleve.

SAMPLE NO. 4 (333 cm depth – top of core section 4)
and

SAMPLE NO. 5 (418 cm depth – top of core section 5)

1. Silicoflagellates present *Distephanus speculum* Ehr.

2. Both marine plankton forms and marine littoral forms are abundant: *Hyalodiscus scoticus* (Kütz.) Grun., *Coscinodiscus curvatulus* Grun., *Thalassiosira kryophylus* Grun., *Plagiogramma staurophorum* (Greg.) Heib., *Achnanthes groenlandica* (Cleve) Grun., *Rhabdonema arcuata* Ehr., *Trachyneis aspera* (Ehr.) Cleve, *Cocconeis scutellum* Ehr., *Navicula glacialis* (Cleve) Grun., *Diploneis Smithii* (Bréb.) Cleve, *Fragilaria oceanica* Cleve, *Chaetoceros subsecundus* (Grun.) Hust., *Rhizosolenia hebetata* f. *hiemalis* (Bail.) Gran., *Rhizosolenia hebetata* f. *semispina* (Hensen) Gran., *Chaetoceros capreolus* Ehr., *Bacterosira fragilis* Gran., *Diploneis Smithii* v. *borealis* Grun., *Achnanthes brevipes* Agardh, *Achnanthes septata* A. Cleve, *Grammatophora arctica* Cleve, *Rhabdonema minutum* Kütz., *Cocconeis pseudo-marginata* Greg., *Pleurosigma* spp., *Opephora Martyi* Hérribaud, *Navicula valida* Cleve & Grun., ? *Pinnularia quadratarea* v. *constricta* Oestr., *Coscinodiscus oculus-iridis* Ehr., *Coscinodiscus* spp., *Nitzschia* spp., *Navicula* spp., *Chaetoceros* spp.

3. Diatoms with freshwater to brackish-water distribution: *Gomphonema* spp., *Cymbella cistula* Hempr. or *Cymbella cymbiformis* (Ag. ?) Kütz.

4. Neritic and littoral species most abundant in northern and boreal seas: $\alpha\delta\delta\theta\pi\eta\alpha\ \alpha\theta\rho\iota\alpha$ (Lyngb.) Bréb. & God.

5. Nordic-alpine freshwater form: *Eunotia praerupta* Ehr.

References

- Blake, W., Jr. and Lewis, C. F. M.
1975: Marine surficial geology: observation in the High Arctic, 1974; in Report of Activities, Part A; Geol. Surv. Can., Paper 75-1A, p. 383-387.
- Grøntved, J. and Seidenfaden, G.
1938: The Godthaab Expedition 1928: The phytoplankton of the waters west of Greenland: Medd. Grønland, v. 82, no. 5, p. 1-380.
- Seidenfaden, G.
1947: Marine phytoplankton; in Botany of the Canadian Eastern Arctic; ed. N. Polunin; Nat. Mus. Can., Bull. 97, p. 138-177.

Project 740067

C. Tarnocai¹
Terrain Sciences Division

Introduction

Soils on Bathurst, Cornwallis, and adjacent small islands (Fig. 28.1), an area of approximately 11 000 square miles, were studied during the 1975 field season. This soil study was one component of the terrain inventory initiated by the Terrestrial-Environmental Program (TEP-1) for the Environmental-Social Program, Northern Pipelines (Barnett *et al.*, 1976).

During the field work, 248 stops were made (Fig. 28.1) along helicopter traverses. Information obtained from these sites includes a general description of the terrain, a description of the soil based on soil pits dug to the frost table and a description of vegetation around the soil pit. In most cases, either a soil parent material sample was collected or all horizons of the soil profile were sampled. In addition, detailed studies also were carried out at 6 sites (approximately 1 day was spent at each site). At these sites detailed soil studies were conducted using an electric hammer to dig into the perennially frozen portion of the soil to a depth of 1 to 1.5 m. Ground traverses also were carried out using a Honda ATC motor tricycle. The field activities resulted in the collection of 275 soil samples, 50 soil moisture and ice content core samples, and 10 samples for carbon dating.

This interim report is intended to provide a general description of soil parent materials and dominant soil types and a discussion of the soil development.

Soil Parent Materials

Soil parent materials were grouped according to their physical and chemical characteristics. Seventeen groups were identified, and their physical and chemical characteristics are summarized in Table 28.1.

In general, calcareous deposits dominate Bathurst Island eastwards from a line drawn between May Inlet in the north and Allison Inlet in the south (Kerr, 1974). West of this line and on the adjacent islands to the west, noncalcareous (medium-acid to neutral) deposits dominate. Cornwallis and Little Cornwallis islands are dominated by strongly to extremely calcareous, stony deposits with generally high silt content.

The conductivity of all materials is generally low with higher values occurring indiscriminately above and below the marine limit. Some of the higher values (above 1.0 mmhos/cm) are associated with areas above the 400-foot elevation. Low values below the marine limit are probably due to the leaching of salts from the active layer materials in the marine zone.

¹Canada Soil Survey, University of Manitoba, Winnipeg, Manitoba.

Some of the materials designated as noncalcareous showed a trace amount of calcium carbonate (less than 1 per cent and a pH higher than 7.0). The slight amount of calcium carbonate was probably due to the movement of carbonate materials by wind or groundwater.

Description of Soils

Soils of the study area have a shallow active layer and various amounts of ice in the perennially frozen layer. Cryogenic processes, especially cryoturbation, play a major role in the formation of these soils. Soils with these characteristics are classified as Cryosols, according to the Canadian System of Soil Classification*.

Regosolic Turbic Cryosol

This is one of the major soil types on Bathurst Island and the adjacent islands to the west; on Cornwallis and Little Cornwallis islands it is the dominant soil type. This soil is completely lacking in horizon development. Some organic-rich surface horizons and subsurface intrusions occur, especially on Bathurst Island. This soil, however, lacks organic-rich intrusions on both Cornwallis and Little Cornwallis islands. Cryogenic processes have strongly affected this soil. Sorted and nonsorted patterned ground types are characteristic except on sandy and strongly eroded materials. The soil is generally well to imperfectly drained. The active layer, however, was moist all summer on Bathurst Island and moderately dry on Cornwallis Island in August when these soils were examined. A Regosolic Turbic Cryosol examined on Bathurst Island (site DB6/4) had 32 per cent** moisture content in the active layer and 53 to 57 per cent ice content in the near-surface frozen layer.

Brunisolic Turbic Cryosol

This soil occurs commonly on Bathurst and adjacent islands to the west but was not found on Cornwallis and Little Cornwallis islands. Brunisolic Turbic Cryosols have a brownish Bmy horizon, which is strongly affected by cryoturbation as shown by organic-rich intrusions and extremely irregular and broken boundaries. An organic-rich surface horizon (Ah) may or may not be present but organic-rich intrusions, organic smears, or subsurface organic-rich (Ahy)

*Tentative Classification for Cryosolic Soils; Proc. of the Ninth Meeting of the Canada Soil Survey Committee, Univ. of Saskatchewan, Saskatoon, 1973, p. 350-358.

**All moisture and ice contents are on a volume basis.

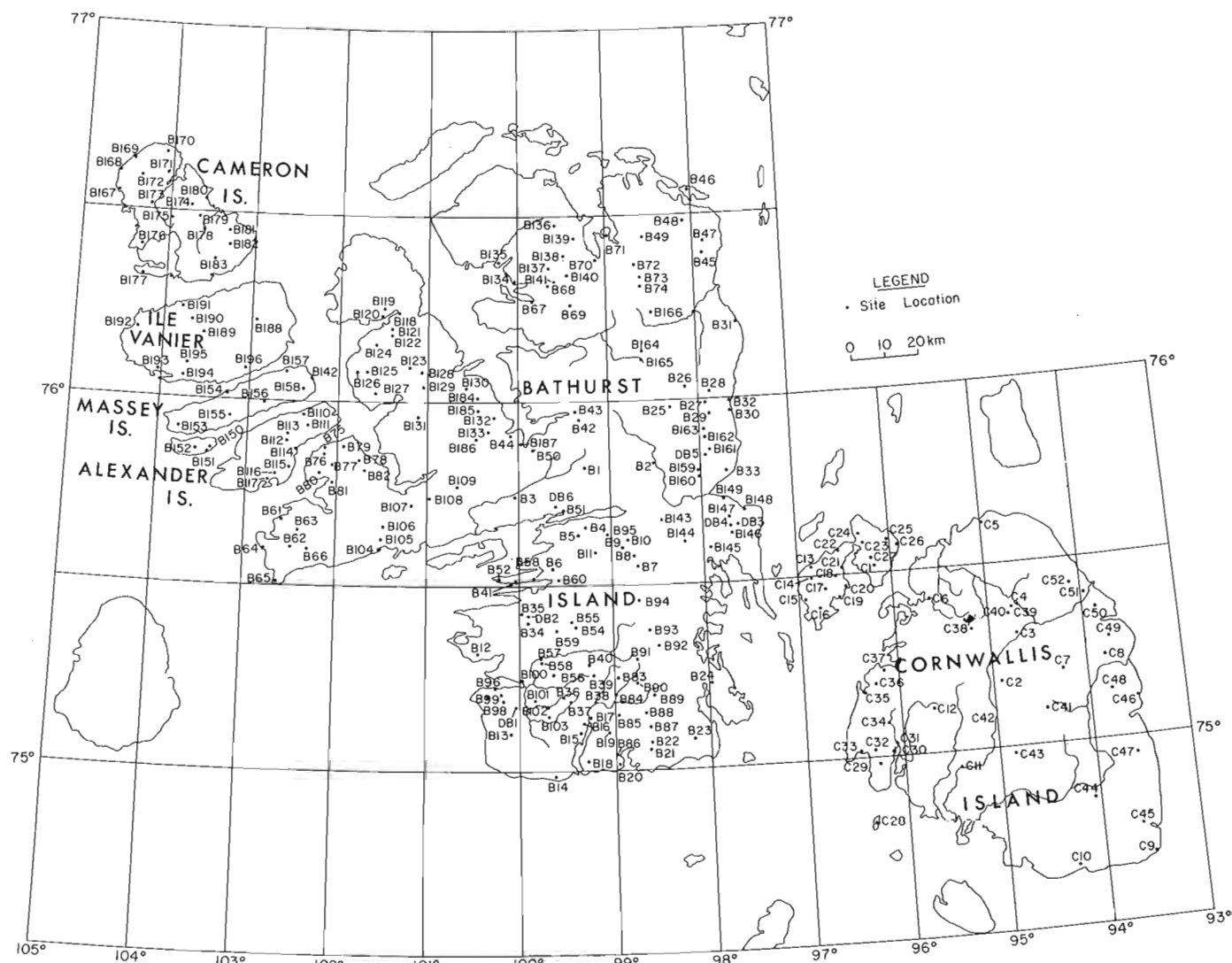


Figure 28.1. Location of sample sites in the study area. The B and C sites represent helicopter stops and DB sites are detailed study sites.

cryoturbated mineral horizons commonly occur. This soil is generally well to imperfectly drained. A Brunisolic Turbic Cryosol examined on Bathurst Island (site DB4) had a moisture content of between 18 and 22 per cent in the active layer and an ice content of 42 to 74 per cent in the near-surface frozen layer. Sorted and nonsorted patterned ground types are characteristic of these soils.

Gleysolic Turbic Cryosol

This soil is associated with poorly and very poorly drained areas and sometimes has a thin surface peaty layer or an organic-rich mineral horizon. The mineral horizons are gleyed and in places are weakly mottled. This soil, in most cases, has a continuous vegetation cover. Due to the continuous vegetation cover and the thin peat or organic-rich mineral surface horizon, this soil has a very shallow active layer. The permafrost

layer of Gleysolic Turbic Cryosols has a very high ice content. A clear ice layer was noted at the top of the permafrost table at many of the sites studied. A Gleysolic Turbic Cryosol associated with earth hummocks examined on Bathurst Island (site DB2) had a relatively dry active layer (12 to 16 per cent moisture content) at the apex of the hummock and a very high ice content in the near-surface frozen layer (56 to 91 per cent ice content).

Regosolic Static Cryosol

This soil is the dominant type occurring on sandy materials and also occurs, to a lesser extent, on loamy sand and sandy loam textured materials. Generally, it is lacking a surface, organic-rich (Ah) horizon. This soil is unaffected or slightly affected by cryoturbation and thus can be considered as a stable soil. In most cases, it is strongly eroded by wind, and the surface

Table 28.1

Physical and chemical composition of soil parent materials (for location of sample sites, see Fig. 1)

Description of Material	Sample No.	Statistic	Sand % (2.0-0.05 mm)	Silt % (0.05-0.002 mm)	Clay % (less than 0.002 mm)	pH	Conductivity mmhos/cm	CaCO ₃ Eq. %	Calcite %	Dolomite %	Stones %
Moderately to very strongly calcareous loamy sand	B47, D84, B26	Range Mean	81.4-82.5 82.0	11.7-12.0 11.8	5.8-6.9 6.2	7.5-7.9 7.7	0.3-1.4 0.7	6.9-28.6 16.4	1.1-8.7 5.3	5.3-18.6 10.0	0-49.8 24.1
Weakly to moderately calcareous sandy loam	B89, B127, B146, B165, B166, DB6/3	Range Mean	53.3-74.4 64.5	15.6-28.8 21.3	10.0-17.9 14.2	7.5-7.8 7.6	0.2-1.0 0.4	2.5-12.6 7.4	1.8-7.0 3.3	0.7-6.1 3.8	2.8-35.4 17.7
Strongly to extremely calcareous sandy loam	B2, B22, B43, B10, B46, B48, B49, B70, B73, B84, B85, B87, B135, B161, B163, B164, D85	Range Mean	52.2-77.4 60.6	14.2-40.2 28.7	3.6-14.5 10.6	7.6-7.9 7.7	0.2-1.3 0.5	15.9-79.1 30.7	0.2-37.4 12.5	0.2-72.8 16.7	8.3-51.9 25.9
Weakly to moderately calcareous loam	B34, B44, B45, B130, B141, B145, B185	Range Mean	27.3-49.3 43.2	28.7-47.2 35.2	14.8-25.5 21.6	7.6-7.8 7.7	0.2-0.8 0.4	3.8-15.4 9.5	0.8-9.8 6.2	0.2-8.7 3.1	0.2-17.0 10.1
Strongly to very strongly calcareous loam	B1, B4, B5, B6, B7, B25, B27, B60, B71, B74, B88, B139	Range Mean	26.8-51.8 41.4	34.3-48.4 42.1	7.8-27.4 16.4	7.6-7.8 7.7	0.3-0.8 0.3	15.6-36.6 23.1	0.2-28.1 12.9	0.2-14.1 9.4	0.2-28.7 12.0
Very strongly to extremely calcareous silt loam	B24, B40, B83, B86, B93, B94, B159	Range Mean	15.4-40.7 34.1	50.1-73.0 56.0	2.7-19.2 9.9	7.7-7.8 7.7	0.2-1.2 0.5	34.5-79.6 57.8	0.2-19.5 7.9	13.9-73.3 44.9	0.2-39.5 14.3
Weakly to moderately calcareous sandy clay loam, clay loam, silty clay loam and silty clay	B11, B50, B54, B68, B118, B121	Range Mean	18.2-54.7 33.0	20.4-40.6 35.3	24.9-41.2 31.7	7.2-7.7 7.6	0.2-0.3 0.3	4.0-9.9 7.0	3.1-7.0 5.8	0.2-2.9 1.1	0.2-12.1 8.5
Non-calcareous sand	B14, B36, B75, B76, B96, B97, B172, B173, B190, B192, B193, DB1	Range Mean	90.0-98.2 93.9	1.6-8.5 3.8	0.1-7.3 2.3	4.4-7.4 6.0	0.1-1.0 0.2	- -	- -	- -	0.2-12.3 2.7
Non-calcareous loamy sand	B110, B155, B175, B188, B98	Range Mean	83.0-95.5 85.5	2.4-21.5 7.9	2.1-12.2 6.5	4.5-7.5 5.8	0.1-0.4 0.2	- -	- -	- -	0.2-3.2 1.8
Non-calcareous sandy loam	B15, B39, B65, B66, B69, B91, B101, B106, B124, B128, B132, B140, B144, B153, B157, B178, B191, B194, B195, DB6/4	Range Mean	52.1-77.5 66.4	13.5-37.8 21.1	2.3-17.4 12.6	4.6-7.7 6.4	0.1-0.9 0.2	- -	- -	- -	0-46.9 28.5
Non-calcareous loam	B12, B62, B77, B78, B81, B82, B109, B115, B124A, B133, B138, B158, B189	Range Mean	37.5-52.0 46.5	29.9-38.0 32.9	11.9-27.1 20.5	5.4-7.6 6.9	0.1-0.4 0.2	- -	- -	- -	0-32.0 9.5
Non-calcareous silt loam, sandy clay loam and silty clay loam	B3, B35, B51, B57, B100, B108, B123, B151, B154, B176, B196, DB2	Range Mean	16.0-62.4 38.7	16.9-55.5 32.9	20.4-36.3 28.5	5.0-7.6 6.6	0.1-0.6 0.3	- -	- -	- -	0-9.7 2.7
Moderately to strongly calcareous sandy loam	C12, C26, C27	Range Mean	56.8-66.8 61.3	17.9-26.5 21.5	51.3-19.7 17.2	7.5-7.8 7.7	0.3-0.8 0.5	15.1-19.4 17.7	7.8-11.9 9.2	6.8-9.8 7.8	0-47.1 22.9
Very strongly to extremely calcareous sandy loam	C2, C3, C4, C5, C18, C38, C42, C44, C48	Range Mean	44.9-64.8 58.7	22.5-48.2 29.8	6.9-15.3 11.55	7.6-8.0 7.7	0.2-0.6 0.3	29.0-80.0 54.0	0-69.0 15.8	0-74.4 35.3	11.9-46.5 27.3
Strongly to extremely calcareous loam	C1, C8, C11, C15, C16, C36, C41, C49, C50, C51, C52	Range Mean	33.1-51.2 41.6	34.7-49.5 42.6	10.7-20.8 15.8	7.6-8.0 7.7	0.3-0.6 0.4	21.6-82.9 46.2	10.9-59.2 29.8	2.9-48.9 14.7	2.5-43.4 21.5
Very strongly to extremely calcareous silt loam	C6, C7, C10, C19, C43, C45, C47	Range Mean	30.6-41.9 36.2	50.3-58.8 53.8	6.6-13.8 10.0	7.6-7.8 7.7	0.2-0.9 0.4	36.9-87.9 63.8	0-48.2 25.3	0-81.0 36.2	2.6-58.3 24.3
Moderately calcareous clay loam	C30		21.1	35.0	37.9	7.7	0.5	11.4	1.6	9.0	4.9

is covered with a gravelly pavement. This soil has a moist (15 to 25 per cent) active layer and a low ice content, frozen layer.

Brunisolic Static Cryosol

This soil occurs mainly on sandy, sandy loam, and loamy sand textured materials. It may have a surface organic-rich mineral horizon and a brownish Bm horizon,

which forms the surface horizon or, in some cases, may be overlain by an organic-rich, mineral surface horizon (Ah). This soil is unaffected or very slightly affected by cryoturbation and thus can be considered as a stable soil. It has a moist (well to imperfectly drained) active layer and a low ice content, frozen layer.

Gleysolic Static Cryosol

This poorly drained soil occurs mainly on sandy materials. The surface horizon may contain various amounts of organic matter but no surface peat layer was found on this soil. The mineral horizons are gleyed and in places are weakly mottled. The frozen layer of this soil contains a medium amount of ice. The soil is unaffected or very slightly affected by cryoturbation and thus can be considered as a stable soil.

Organo Cryosol

Organo Cryosols have developed from organic (peat) materials. They are associated with eroded low-land ice-wedge polygons. They occur in small areas but are found on all islands in the study area. The depth of these soils is dominantly 120 to 150 cm, but in some locations they reach a depth of 370 to 400 cm. These soils are characterized by a very high ice content. In addition to this, pure ice bodies, mainly in the form of ice wedges, are common. An Organo Cryosol examined on Bathurst Island (site DB3) had a relatively dry active layer (11 per cent moisture content) and a very ice-rich frozen layer (79 to 94 per cent ice content).

Soil Development

Cryogenic processes play a major role in the formation of soils in the study area. The most striking of these processes, as evidenced by its effect on the soils, is cryoturbation. There is evidence that cryoturbation affects even the sands, notably those with a high moisture content. This is contrary to what was found in the southern regions of the Arctic, where sandy materials were unaffected by cryoturbation. Cryoturbation tends to mix the soil materials; thus, instead of classical soil horizon development, the result is a strongly disrupted (frost-churned) soil profile. In the extreme case of no horizon development, a moderately homogeneous active layer is the result. Cryoturbation also enriches the shallow soils with fresh frost-heaved bedrock materials. This process tends to rejuvenate the soil by the continuous addition of fresh materials.

The effect of parent materials on soil development can be demonstrated by comparing the soils on the Cornwallis Island group (Cornwallis and Little Cornwallis islands) with the soils on the Bathurst Island group (Bathurst Island and the adjacent islands to the west). On the Cornwallis Island group, very little or no soil development was found. All soils have developed on extremely calcareous materials which impede soil development because of their extremely high carbonate content. On the Bathurst Island group, however, much greater soil development was found. The occurrence of a brownish, oxidized Bm horizon was not a rare phenomenon. One of the best developed soil profiles was found in the northwestern part of the study area, on Cameron Island. Not only was a well developed Bmy horizon present, but in some places a very thin, discontinuous, poorly developed, leached Ae horizon

also was found. This corresponds with the findings of McMillan (1960) on Cameron Island.

The other important factor affecting soil development in the study area is downslope movement of materials. Evidence of downslope movement was found on slopes as low as 1 degree. This process not only mixes the materials but also deposits new soil materials on the lower slopes and removes materials from the upper slopes.

In the literature (Tedrow, 1966) high arctic soils commonly are referred to as polar desert soils; the latter term (desert) gives the impression that these soils are very dry, but just the opposite was found. All soils on the Bathurst Island group were found to be very moist, and on several occasions during the month of July all soils (even on well drained positions) were saturated, sometimes to the point where sheet runoff took place. This happened after heavy rain or wet snow fell. On the other hand, in some cases, soils on the Cornwallis Island group were found to be fairly dry during August. It is easy to understand this phenomenon as even a small amount of precipitation can have a great effect on the moisture status of these soils where the active layer is very shallow (30 to 45 cm). The moisture content of the active layer is generally high during the summer months and requires very little additional moisture to reach the point of saturation.

Even though the soils have a high moisture content and often are saturated, gleying is not very common. Gleying is associated mainly with fine textured materials (silts and clays) in the area. Some poorly drained sands exist that are gleyed, but these are associated with drained lakes. The lack of gleying is likely due to the fact that most of these waters are oxygen rich, and the soil is well aerated. Aeration is facilitated by a well developed vesicular pore structure and small polygonal cracks where air exchange can take place. Thus, water flowing through the soil system results in oxidation rather than in reduction.

Most Turbic Cryosols have a vesicular pore structure. These pores, having a diameter of 3 mm or less, are especially common in the upper 20 cm of the soil. The development of pores is associated with micro-scale ice lens formation in the soil. The melting of these ice lenses in the spring creates an oversaturated condition (Washburn, 1969). In this condition the slightest disturbance, e.g. vibration, will cause liquification of the soil material. This phenomenon is known as rheotropy (Yong and Warkentin, 1966).

In summary, the development of mineral soils is affected by cryoturbation, which tends to rearrange the soil materials or to slow down the development of soil horizons. Downslope movement results in the redistribution of soil materials. Extremely calcareous parent materials impede soil development. The flow of oxygen-rich waters in the shallow active layer causes oxidation. All of these processes tend to produce a soil which has weak soil horizon development or, more specifically, a soil with an oxidized, slightly brownish, active layer and an unaltered perennially frozen parent material.

Probably the most striking phenomenon observed was the occurrence of organic soils (Organo Cryosols) in the study area. These Organo Cryosols cover only small areas but are found on even the most northerly islands. These soils are strongly eroded and probably developed when climatic conditions were more favourable for peat development than they are at present. This theory is supported by the observations that very little active peat development currently is taking place in the area and that most of these deposits are very shallow (5 cm) and have no actively forming, deeper deposits.

References

Barnett, D.M. , Dredge, L.A. , and Edlund, S.A.

1976: Terrain inventory: Bathurst, Cornwallis, and adjacent islands, Northwest Territories; in Report of Activities, Part A; Geol. Surv. Can. , Paper 76-1A, p. 201-204.

Kerr, J. Wm.

1974: Geology of Bathurst Island Group and Byam Martin Island, Arctic Canada (Operation Bathurst Island); Geol. Surv. Can., Mem. 378, 152 p.

McMillan, N. J.

1960: Soils of the Queen Elizabeth Islands (Canadian Archipelago); J. Soil Sci. , v. 11, p. 131-139.

Tedrow, J. C. F.

1966: Polar desert soils; Proc. Soil Sci. Soc. Am. , v. 30, no. 3, p. 381-387.

Washburn, A. L.

1969: Weathering, frost action, and patterned ground in the Mesters Vig District, Northern Greenland; Medd. Groenland, bd. 176, nr. 4, 303 p.

Yong, R. N. and Warkentin, B. P.

1966: Introduction to Soil Behavior; The Macmillan Company, New York, 451 p.

Project 750071

S. C. Zoltai¹ and V. Woo²
Terrain Sciences Division

The soils and vegetation of Somerset Island and the northern part of Prince of Wales and surrounding islands, an area of about 43 500 km², were surveyed in conjunction with terrain studies of surficial geology, geomorphology, and geophysical conditions (Netterville *et al.* 1976). The objectives of this survey were: 1) to determine and map the vegetation of the area, 2) to determine and map the soils of the area, and 3) to determine conditions and areas that are sensitive to disturbances. In this paper a summary of the findings is presented.

During the survey all major terrain types, which were identified in the terrain studies, were visited and information was gathered on the soils and vegetation. The soil and vegetation were described at 200 sites, but many more informal observations were made. Detailed studies were carried out at 24 sites; at each site a soil pit was excavated at least 50 cm below the permafrost table and detailed sampling was made. A number of traverses were made on foot and on all-terrain vehicles. A total of 204 soil samples were collected for mechanical and chemical analyses and 129 core samples for moisture determination. Voucher specimens of 300 vascular plants and 100 moss and lichen samples were collected. Buried organic material was collected from 5 sites for radiocarbon dating.

Ecological Regions

While examining the biophysical characteristics of a large area, certain differences in plant distribution, frequency, or successional patterns become evident in similar physiographic areas. Such differences may be recognized as ecological regions (or zones) which may be defined as land areas within which vegetation growth and pedogenic processes will be similar in similar physiographic sites and influenced by uniform regional climate. The term "ecological region" or zone is equivalent to the "site region" of Hills (1960) and the "land region" of Lacate (1969).

The High Arctic ecological region (Fig. 29.1) is characterized by very sparse vegetation and by the absence of soil profile development. In the Mid-Arctic region (Fig. 29.1) the vegetation covers a larger proportion of the surface but is seldom continuous, except in wet depressions. The soils generally show a weak B horizon development. Differences in plant species occurrence were noted in the two regions. Such differences may be the absence or presence of some species or differences in habitats occupied by the same species.

Soils

The permafrost table is encountered within 1 mile of the surface on all soils within the study area, therefore all soils are classified as Cryosols. Soils developed on fine to medium grained materials show effects of mixing by frost heave (cryoturbation). Frost-induced microrelief, such as sorted and nonsorted circles, nets, and stripes, is common and widespread. Stripes develop on slopes and commonly curve around obstructions, showing that mass movement is associated with them. On sparsely stony soils, stripes and evidence of mass movement can be found even on very gentle slopes (less than 3%). Ice-wedge polygons commonly develop on coarse textured materials (boulders, gravel, sand).

Many soils are rheotropic in character. Rheotropy is a condition in plastic soils that occurs when the water content is below the liquid limit but is within the plastic range. Shaking causes the structure of the absorbed water on clay particles to break up, and the particles are rearranged, with a resulting plastic flow of the material.

The moisture content of the near-surface permafrost is high, commonly twice as high in the permafrost than in the active layer above, even on well drained sites. The highest moisture content was found under earth hummocks (a form of nonsorted circles) where the moisture by volume was 95 per cent in the near-surface permafrost but only 40 per cent 20 cm below the surface.

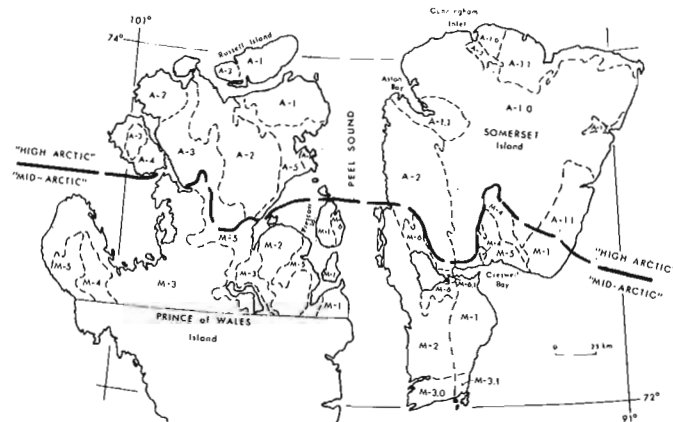


Figure 29.1. Ecological regions and districts of Somerset and Prince of Wales Islands.

¹ Northern Forest Research Centre, Environment Canada, Edmonton, Alberta.

² Soil Science Department, University of Manitoba, Winnipeg, Manitoba.

Permafrost conditions make the determination of the origin of soil materials very difficult. Frost shattering breaks up solid bedrock, and frost heave moves the rock to the surface. Cryoturbation in the active layer mixes the surface soil, and downslope mass movement further disturbs the surface materials. Chemical and physical weathering is pronounced on some upland areas of the High Arctic region. Thus the term 'till', used to denote the unconsolidated surface materials containing erratics, in fact may contain much material derived from the site and modified by frost and colluvial action.

Vegetation

The vegetation in the study area may be grouped into three basic types: polar desert, arctic dwarf shrub, and arctic sedge meadows. On highly calcareous materials the polar desert has scattered vegetation which seldom exceeds 5 per cent in cover, the *Papaver lapponicum*, ssp. *occidentale*, *Dryas integrifolia*, and species of *Draba* being the most frequent components. Except for sites enriched by wastes of owls and lemmings, the surface is barren. On Precambrian bedrock the polar desert appears as felsenmeer, where crustose lichens such as *Umbellicaria* spp., *Rhizocarpon* spp., and bryophytes like *Andraeae* are the main species. The cover of crustose lichen on bedrock may be as high as 30 per cent, otherwise the surface is barren except for occasional mosses, fruticose lichens, and *Cassiope tetragona* growing in crevices.

Arctic dwarf shrubs cover most of the area on Somerset Island and a large part of Prince of Wales Island. The basic pattern is the association of various herbaceous and nonvascular species with one or several of dwarf shrub components, namely *Salix* spp., *Saxifraga oppositifolia*, *Dryas integrifolia*, and *Cassiope tetragona*, the last of which can only be found on soil that is not strongly calcareous. Vegetation cover of this group ranges from 10 to 80 per cent; but the cover is never continuous in the Mid-Arctic and High Arctic ecological regions.

Sedge meadows are common throughout the Arctic. In the study area the graminoid components of sedge meadows are *Carex* spp., *Luzula* spp., *Eriophorum* spp., and grasses such as *Arctagrostis latifolia*. Moss species of *Dicranum*, *Dreplanocladus revolvens*, *Distichium capillaceum*, and *Calliergan giganteum* are found. The vegetation cover is between 80 and 100 per cent.

Moist seepage sites are characterized by mosses such as *Bryum cryophilum* and *Philonotis fontana* and grasses such as *Alopecurus alpinus*. On northern Prince of Wales and western Somerset islands the lichen *Polyblastia* forms a black or grey crust and is associated with black coloured mosses, such as *Blindia acuta* and *Cephaloziella* sp.. This association is very conspicuous, both on the ground and from the air, but represents very little plant material.

Ecological Districts

The ecological regions can be subdivided on the basis of major physiographic or geologic patterns that influence the development of soils and plant communities. The resulting ecological districts are broad subdivisions of ecological regions based on significant changes in the nature (texture, chemistry) and relief of surficial materials. The characteristic soils and vegetation of the different ecological districts are shown in Tables 29.1 and 29.2 and their extent is shown in Figure 29.1.

The dominant material on both islands is a highly calcareous, dolomite-rich till (districts: Somerset A-1.0, A-1.1, A-1.2, M-1; Prince of Wales A-3, M-3) over sedimentary bedrock, with various extents, of marine sediments in some ecological districts (Somerset A-1.1, A-1.2; Prince of Wales A-4, M-4). On Prince of Wales Island moderately calcareous, calcite-rich till covers large areas (A-1, M-1), with local marine silt and sand deposits (A-2, M-2). On Somerset Island similar materials are present in the Creswell River basin (M-4). Crystalline Precambrian bedrock areas are found mainly on Somerset Island and are covered by boulder fields and moderately calcareous till in the north (Somerset A-2) but by highly calcareous till in the south (Somerset M-2, M-3.0, M-3.1; Prince of Wales M-6). The Eureka Sound Formation, consisting of highly siliceous sands, underlies small areas on Somerset Island (A-3, M-6, M-6.1) together with various amounts of marine silts and sands. Large deposits of marine silts and sands occur on both islands (Somerset M-5; Prince of Wales A-5, M-5).

Sensitive Environments

The peculiar terrain, soil, and vegetation characteristics of the study area will present problems which should be considered when planning the routing and construction methodology of pipeline and associated activities. Some of these considerations are:

- 1) Tabular ground ice was found in certain areas of both islands in association with retrogressive-thaw flow slides. These features most commonly are associated with marine sediments and silty till of moderate surface relief. Such areas, marked by active or relict flow slides, should be avoided.
- 2) The vegetation and the active layer should be avoided where possible. There is evidence that the destruction of the vegetative layer, however thin, will lead to degradation of the permafrost. This in turn will initiate thermal subsidence, ponding, and channelling of runoff, causing further terrain damage.
- 3) Heaving of rocks was observed in consolidated bedrock areas. Large blocks of bedrock were noted to be uplifted about 1 m by frost heave. Blasting of bedrock for a pipeline trench would shatter the adjacent rock. If water were to seep into the cracks, uplift could result, leading to possible pipeline rupture.

4) The active layer is subject to flow even on gentle slopes. Active layer flow was noted on 3% slopes on silty loam materials. Structures, such as the berm of a pipeline, road, or gravel pads, may block the active layer flow and create pressures sufficient to erode the structure.

5) The sensitivity of the soil in the active layer to mechanical vibration may pose problems by greatly increasing the active layer flow. Vibration caused by compressor stations or by the pipeline itself may initiate the liquefaction of the soil. Soils susceptible to liquefaction upon disturbance are generally sparsely stony and have a high silt content.

6) Habitats for muskoxen and caribou are limited, especially on Somerset Island. Such well vegetated areas should be avoided by pipeline routing.

References

Hills, G. A.

1960: Regional site research; *For. Chron.*, v. 36, p. 401-423.

Netterville, J. A., Dyke, A. S., Thomas, R. D., and Drabinsky, K. A.

1976: Terrain inventory and Quaternary geology, Somerset, Prince of Wales and adjacent islands; in *Report of Activities, Part A*; *Geol. Surv. Can.*, Paper 76-1A, p. 145-154.

Lacate, D. S.

1969: Guidelines for biophysical land classification; *Can. For. Serv.*, Publ. No. 1264., 61 p.

Project 740057

J.E. Gale, K. Raven, J. Dugal, and P. Brown
Terrain Sciences Division

Atomic Energy of Canada Limited (AECL) and the Geological Survey of Canada (GSC) have undertaken a joint hard rock project to determine if igneous (intrusive) or metamorphic rocks are a suitable host rock for the storage of solidified radioactive wastes in a mined repository (Tammemagi, 1975). The immediate objective of this project is to select a number of sites within the Ontario portion of the Canadian Shield (Fig. 30.1) that appear to meet the requirements of a radioactive waste repository. This will be accomplished in early 1976 and immediately will be followed by reconnaissance mapping of six of the more favourable sites during the 1976 field season. From these six sites the most favourable site(s) will be evaluated by detailed geological, geotechnical, and geophysical investigations which should be completed by late 1978. At that time sufficient information should be available, from these investigations and parallel studies of other rock types, to permit a decision on which rock type, and presumably which site, will be used for the construction of a pilot storage facility (Fig. 30.2).

Factors for Consideration

The hard rock project was initiated by compiling a list of factors that were considered to be important in the selection of both the host rock type and the geographic location for the repository. These factors fall into three principal categories -- (1) site and environmental, (2) legal and political, and (3) geological and geotechnical (Table 30.1). Ongoing efforts are being directed towards ranking and quantifying the various factors in each category taking into account their relative significance with respect to the study of crystalline rocks in the hard rock project and to parallel studies of other rock types.

Many factors can only be quantified by reference to a specific study area, other factors can only be given a relative ranking, but as many factors as possible will be quantified by literature surveys and field and laboratory studies.

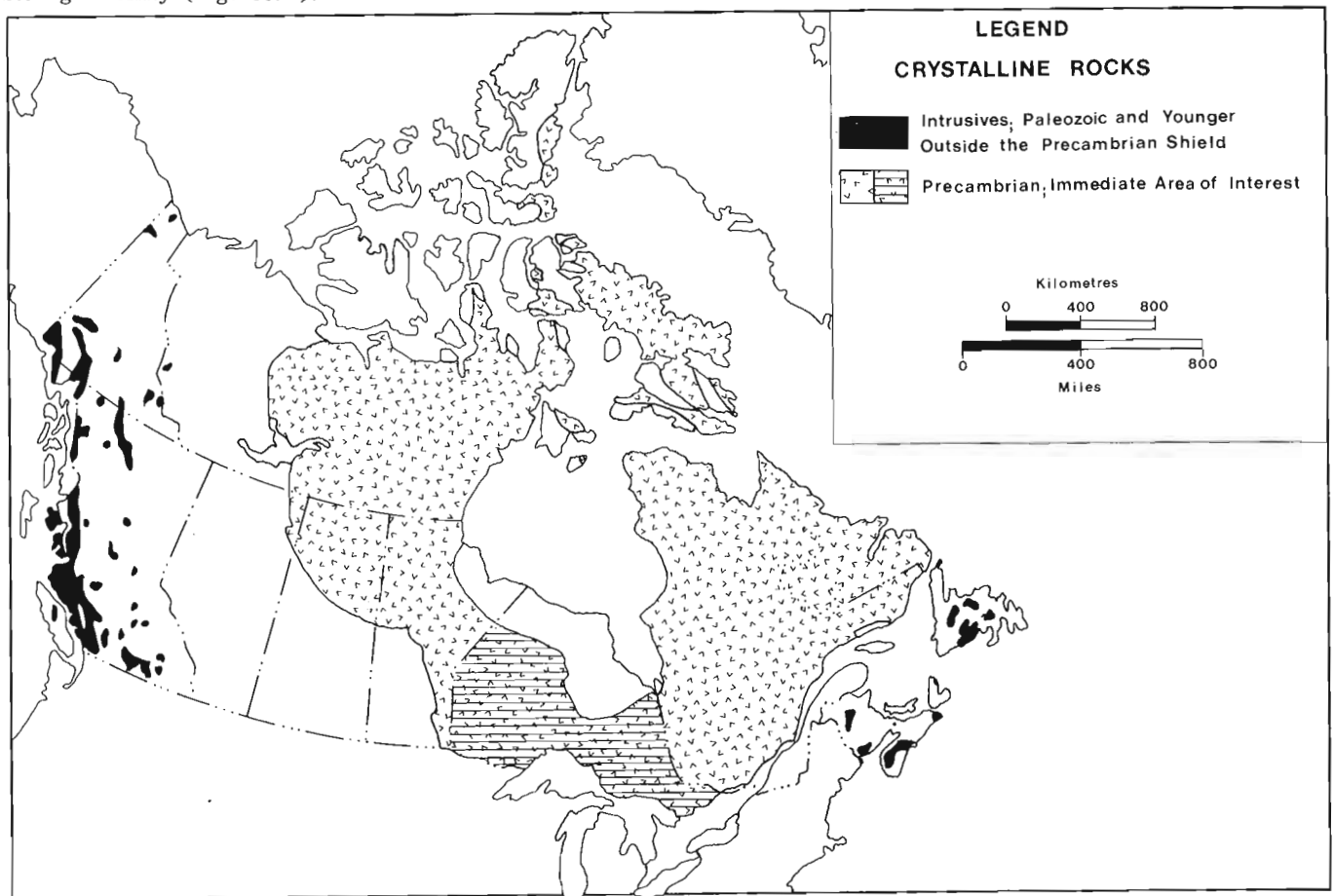


Figure 30.1. Distribution of potential host rocks for nuclear waste storage.

HARD ROCK PROJECT

Geological	Geotechnical	Laboratory
<hr/>		
Program started in May 1975.		
Selection of six potential sites in northern Ontario (May 1976).	Development of field and laboratory program: drilling, fracture analysis, injection testing, borehole and surface geophysics, computer programs for data analysis, etc. Evaluation of structural and groundwater conditions at mines in northern Ontario and Quebec and at major underground excavations in Canada (to be completed in September 1976). Establishment of a test site in granitic rocks near Ottawa in order to test and evaluate geotechnical tools and exploration methods. Other studies to be developed as required.	Initiation of laboratory studies (early 1976) to determine those rock types that are most favourable with respect to the safe storage of nuclear waste material. Specific thermal-mechanical tests on individual rock types, etc.
Reconnaissance field mapping of sites. Selection of from 1 to 3 promising sites (October 1976).		
Detailed mapping of most promising sites will start in early 1977 and continue through 1978.	Geotechnical field tests and laboratory studies will start in early 1977 and continue through 1978.	
 Analysis of the geological, geotechnical, and laboratory data from specific rock types and areas will be completed by late 1978. The analysis of these data and the results from additional studies on crystalline and metamorphic rocks and data from parallel studies, on other rock types, within EMR will make it possible to select the best host rock and the most suitable area in which to construct the radioactive waste storage facility.		

Figure 30.2. Components of hard rock program.

Hard Rock Project

The AECL-GSC hard rock project, which is one component of the AECL-EMR radioactive waste program (Tammemagi and Scott, 1975), consists of three inter-related areas (Fig. 30.2): geological, geotechnical, and experimental. The geological aspects of the project are concerned primarily with the selection of potential sites within designated parts of the Canadian Shield (Fig. 30.2) and their evaluation by reconnaissance and detailed mapping. Initial efforts have been directed towards areas of "intrusive granitic" rocks including both basic and acidic rock types. Approximately ten potential sites have been selected by analysis of aerial photographs, review of the geological literature, and discussions with field geologists who have been active in different areas of the Canadian Shield. It is hoped that at least twenty potential sites representing a variety of rock types, structural settings, and geographic locations will have been identified before the start of the 1976 season. The six most promising sites will then be selected for reconnaissance mapping during the 1976 season.

In order to select the sites for reconnaissance mapping, fundamental criteria dealing with structural geology, hydrogeology, and other geotechnical aspects of the different rock types must be established to permit a realistic ranking of the various sites. This requires being able to predict, with some degree of confidence, subsurface structural and groundwater conditions from surface observations. Attempts to develop these criteria have involved (1) an ongoing review of the surface and subsurface structural and groundwater conditions encountered at major underground excavations in Canada - four underground excavations, including Churchill Falls powerhouse, have been reviewed to date; (2) review of the literature on fracture systems and the fracture permeabilities of different rock types; and (3) the initiation of a study that involves an evaluation of the relationships, if any, between structural and groundwater conditions in underground mines located in the Canadian Shield. A field reconnaissance of the surface and subsurface conditions at nine mines in northern Ontario and Quebec already has been completed. An extensive questionnaire was sent to thirty-five mines and the information on the

Table 1

Factors for Consideration

A. <u>Site and Environmental</u>	- major lineaments - frequency, orientation, and character
1. Accessibility - rail or road	- fracture frequency and orientation
2. Distance from major population centres and waste load centres	- rock fabric
3. Distance from areas of restricted land use	3. Short and long term stability of underground openings
4. Availability of buffer zone	- structural integrity of rockmass
5. Topography	- depth, thickness, and extent of both host rock and adjacent rocks
6. Hydrology and hydrogeology	- mineable depths
7. Overburden characteristics	- existing stress field
8. Association with known mineral deposits or metallogenic provinces	- rock strength properties as a function of time and temperature
9. Mining and drilling activity	4. Rock characteristics
10. Mine waste disposal	- petrology and mineralogy
11. Seismicity - natural and induced	- rock homogeneity or purity
12. Geothermal environment	- ion exchange properties
13. Future geological events, i. e. glaciation	- content of gases and liquids and temperature stability field
14. Possibility of site operation being affected by other, nonwaste related, industrial accidents	- permeability and porosity of both fractures and rock blocks
B. <u>Legal and Political</u>	5. Erosional stability over geological time
1. Existing land use rights	6. Thermal properties of rock over specified temperature range: expansion, conductivity, fracture potential, etc.
2. Alternate use conflicts	7. Effect of thermal stress gradients on fractures and rock properties
3. Population density	8. Effect of fractures on the heat transfer properties of the rockmass
4. Site security	9. Groundwater flow in the vicinity of high thermal gradients
5. Public acceptance	10. Effect of hydration and dehydration
C. <u>Geological and Geotechnical</u>	11. Effect of radiation on structural properties
1. Economic value	
2. Structural Geology - tectonic framework - dip and nature of rockmass	

structural and groundwater conditions at these mines is now being compiled. After the data from the reconnaissance study and the questionnaire have been analyzed, four mines will be selected and their surface and subsurface structural and groundwater conditions will be studied in detail during the 1976 field season.

Preliminary results of the mine study show that, in the absence of major structural discontinuities, these mines do not have visible groundwater seepage from the mine roof and walls at depths below 2500 to 3000 feet. The physics of groundwater flow in fractured rocks suggests several reasons why this may be a valid observation. These reasons of concepts will be investigated using a finite element groundwater flow computer program.

In order to ensure the maximum return from geotechnical investigations of individual site areas, a test site, consisting of one inclined (45 degrees from the horizontal) NX size (\approx 3 inches in diameter) borehole, 258 feet in length and five vertical NX boreholes

approximately 100 feet deep, has been established in a small granitic pluton approximately 50 miles northwest of Ottawa. This site will be used to test both the equipment and theoretical concepts being developed for the evaluation of the permeability of each potential repository site as well as various surface and borehole geophysical tools. Also, the drilling and hydraulic testing will permit an evaluation of a new aeromagnetic technique (Hood *et al.*, 1975), developed at the Geological Survey of Canada that will be used to examine each potential site.

The experimental part of the hard rock project will be initiated in the early part of 1976 and will involve literature reviews and experimental studies to determine those rock types that have the most favourable response to thermal-mechanical loads. In addition, studies will be undertaken to determine the thermal and mechanical properties of specific rock types as a function of the temperature and pressure ranges that will exist during the operational life of the repository.

References

Hood, P., Sawatzky, P., Kornik, L. J., McGrath, P. H., and Holryod, M. T.

1975: An inboard digital-recording aeromagnetic gradiometer system, A progress report; Soc. Explor. Geophys., Denver, Colorado, U. S. A., October 13-16, 1975.

Tammemagi, H. Y.

1975: A development program for geological storage of radioactive wastes; internal rep., Atomic Energy Can. Ltd., Whiteshell Nuclear Res. Establ., Pinawa, Manitoba, 19 p.

Tammemagi, H. Y. and Scott, J. S.

1975: The Canadian program for geological disposal of radioactive wastes; Proc. Seminar on the Disposal of Radioactive Wastes into Geologic Formations, Clausthal-Zellerfeld, Dec. 1-3, 1975, sponsored by Nuclear Energy Agency, OECD, Paris.

E. M. R. Research Agreement 1135-D13-4-190/73

D. C. Ford¹ and H. P. Schwarcz²
Terrain Sciences Division

The $^{230}\text{Th}/^{234}\text{U}$ dating technique has been used to measure ages of speleothems (calcite stalactites, stalagmites, and flowstones) from natural caverns in Banff National Park and Crowsnest Pass (Rocky Mountains) and the South Nahanni region (Mackenzie Mountains). A new batch of samples has been collected on Vancouver Island and is being evaluated. Collections on Anticosti Island and in Newfoundland are planned for 1976. Results so far show that most specimens are in the age range of 100 000 to more than 350 000 years B. P.

Analysis of $^{18}\text{O}/^{16}\text{O}$ ratios in dated specimens has yielded paleotemperature information for the period 90 000 to 155 000 years B. P. from a cave in Banff National Park. Principal periods of stalagmite deposition have been related to sequences of glaciations in the Mackenzie Mountains. Current developments include measurement of D/H (deuterium/hydrogen) and $^{18}\text{O}/^{16}\text{O}$ ratios in fluid inclusions in calcite to derive absolute temperature changes and to infer change of continental storm tracks during Quaternary time (Schwarcz *et al.*, in press). Relationships of trace element abundance to $^{18}\text{O}/^{16}\text{O}$ variation are being evaluated. A new technique to prepare 'dirty' specimens (contaminated with detrital ^{230}Th) is being investigated; if successful, the dating method may be extended to cave entrance facies, caliche, and molluscs. The possibility of extending the range by paleomagnetic studies of dated speleothems is being studied also.

A detailed evaluation of all results up to May 1975, including a comparison of Canadian results with others obtained from American, Mexican, and Bermudan sites and with marine foraminiferal and terrace records, has been completed as a Ph. D. dissertation by Harmon (1975). Other recent reports arising from this project are those by Harmon *et al.* (1976, in press) and Thompson *et al.* (1975, in press).

Results

Castleguard Cave, Banff National Park, Alberta

This cave is the longest in Canada and terminates beneath the Columbia Icefield. A collection of specimens taken in 1973 has been dated and evaluated for oxygen paleotemperature information. Although most specimens display kinetic fractionation of oxygen isotopes, which nullifies the temperature record, sample 73010 (which grew between 155 000 and ca. 50 000 years B. P. but has suffered erosion of the record after 93 000 years B. P.)

¹Department of Geography, McMaster University, Hamilton, Ontario.

²Department of Geology, McMaster University, Hamilton, Ontario.

yielded good paleotemperature information. Warm climate peaks are indicated at ca. 145 000, 125 000, and (most strongly) 105 000 years B. P. The latter peak is also very strongly attested to in American specimens from extraglacial regions and is taken to indicate the maximum of the Sangamonian Interglacial. A modern specimen from Castleguard Cave indicates climatic amelioration during the last 6000 years.

Maximum fluctuation of ca. 0.5°C about the present-day mean annual temperature of +3.5°C in the interior of the cave is indicated. Together with hydrologic and geothermal observations, this has been used to infer that the Columbia Icefield probably has persisted throughout the past 155 000 years and has been temperate at its base during that period (Ford *et al.*, in press). Precise calibration of Castleguard paleotemperatures by the fluid inclusion method is anticipated shortly.

Crowsnest Pass, Alberta-British Columbia

Speleothems from relict cave systems scattered between the floor of the Pass (4400 feet a. s. l.) and surrounding summits (9000 feet a. s. l.) have been dated. Ages are greater than 100 000 years B. P. with 50 per cent of specimens being older than 350 000 years. It is inferred that the mean rate of entrenchment of the Pass has not exceeded 2 feet per 1000 years during the past 200 000 years. Collection of additional specimens is planned for 1976.

South Nahanni region, Mackenzie Mountains, N. W. T.

The karst belt, extending 35 miles north of First Canyon, South Nahanni River, is one of the most accentuated karst terrains in North America. It contains many relict caverns with speleothems. Two collections have been analyzed and a third (collected in 1975) awaits study. More than half of the specimens yield U/Th ages greater than 350 000 years; all are uranium-rich and contain other trace elements in abundance.

The U/Th chronology has been used to assign recognized Cordilleran and Laurentide ice advances within South Nahanni National Park to the 'classical' Wisconsinan, the Illinoian, and a glaciation older than 350 000 years (Ford, in press). Two successive proglacial lakes have been assigned to the Wisconsinan and Illinoian, respectively, by means of speleothems embedded in lacustrine fill in the caves. Similarly, an estimate of the rate of tectonic uplift of Nahanni Plateau, a domal high, has been derived from the U/Th chronology.

A South Nahanni speleothem has been adopted as a standard in an international program of interlaboratory calibration.

The South Nahanni and Crowsnest speleothems appear particularly well suited to a program of paleomagnetic investigations that is proposed.

Vancouver Island, British Columbia

Because of its oceanic location, isotopic fractionation effects in ancient precipitation on Vancouver Island can be inferred with greater confidence than in more continental locations. This makes it a particularly suitable location for the investigation of oxygen isotope fractionation in calcite and fluid inclusions. Accordingly, a first collection of speleothems from four caves was made in May 1975.

The samples are now being dated. Initial results indicate that they are amongst the youngest Canadian specimens, being less than 100 000 years in age. This supports geomorphological evidence in the caves which suggests a Sangamonian or later origin. Certain samples are porous textured and recrystallized and display uranium-migration, making them unsuitable for the $^{230}\text{Th}/^{234}\text{U}$ dating method. An additional counting chamber has been purchased to apply the $^{231}\text{Pa}/^{230}\text{Th}$ method to them.

Eastern Canada

Stalagmite specimens from Ontario that have been submitted to the McMaster University laboratory have proved too 'dirty' for conventional U/Th dating.

A particular effort is now being made to obtain specimens of significant age from eastern Canada. In 1976 Ford will investigate caves on Anticosti Island and in Newfoundland. A specimen has been obtained from upstate New York that should give some indication of conditions in nearby Quebec.

New methods

Most speleothems from cave entrance locations and some from cave interiors are 'dirty' in that they contain detrital ^{230}Th , vitiating the U/Th and Pa/Th methods applied so far. R.L. Ku (University of Southern California) has suggested a new extraction method to overcome this same problem in caliches, and a post-doctoral fellow at McMaster, A. Fallick, is testing it upon speleothems and interstitial calcites from breccias. If successful, this method should permit a substantial increase in the choice of samples from eastern and northern Canadian locations.

Analysis of trace element concentrations in speleothems and their associated drip waters has been extended to Vancouver Island. The aim is to determine partition coefficients, which are potential indicators of the temperature of deposition. A new method of concentrating solute uranium from groundwaters is being tested.

Preliminary arrangements have been made with D.W. Strangway (University of Toronto) to begin an appraisal of speleothems as paleomagnetic indicators.

The work will be undertaken by A.E. Latham, a Ph.D. candidate who has an M.Sc. in paleomagnetic work. He will attempt to establish whether sample speleothems contain sufficient iron to enable the determination of magnetic field characteristics at time of deposition. If this is so then (a) paleomagnetic records less than 350 000 years B.P. may be calibrated by the U/Th dating method; (b) speleothems older than 350 000 years might be dated by means of paleomagnetic reversals (e.g. Brunhes/Matuyama at ca. 700 000 years B.P.) and lesser excursions. In this program, top priority will be given to the ancient, metal-rich stalagmites of Nahanni and Crowsnest Pass regions.

References

- Ford, D. C.
Evidences of multiple glaciation in South Nahanni National Park, Mackenzie Mountains, N.W.T.; *Can. J. Earth Sci.* in press.
- Ford, D. C., Harmon, R. S., Schwarcz, H. P., Thompson, P., and Wigley, T. M. L.
Geohydrologic and thermometric observations in the vicinity of the Columbia Icefield, Alberta-B.C., Canada; *J. Glaciol.* in press.
- Harmon, R. S.
1975: Late Pleistocene climates in North America as inferred from isotopic variations in speleothems; unpubl. Ph.D. thesis, McMaster University, Hamilton, Ont., 279 p.
- Harmon, R. S., Thompson, P., Ford, D. C., and Schwarcz, H. P.
1976: Uranium-series dating of speleothems; *Natl. Speleo. Soc. Am., Bull.*, v. 37, no. 2, p. 21-33.
- Harmon, R. S., Thompson, P., Schwarcz, H. P., and Ford, D. C.
Late Pleistocene palaeoclimates of North America as inferred from stable isotope studies of speleothems; in press.
- Schwarcz, H. P., Harmon, R. S., Thompson, P., and Ford, D. C.
Stable isotope studies of fluid inclusions in speleothems and their palaeoclimatic significance; *Geochim. Cosmochim. Acta.* in press.
- Thompson, P., Ford, D. C., and Schwarcz, H. P.
1975: U/234-U/238 ratios in limestone cave seepage waters and speleothem from West Virginia; *Geochim. Cosmochim. Acta.*, v. 39, p. 661-669.
- Thompson, P., Schwarcz, H. P., and Ford, D. C.
Stable isotope geochemistry, geothermometry and geochronology of speleothems from West Virginia; *Geol. Soc. Am., Bull.* in press.

Project 740104

W. F. Fahrig
Regional and Economic Geology DivisionIntroduction

North-trending, unaltered olivine diabase dykes intersect Aphebian strata of the Kaniapiskau Supergroup near Schefferville, Quebec. The dyke intrusions occur along two subparallel lines, and within the lines the dykes have an en echelon arrangement (Frarey, 1961). This suggests that only two dykes are present at greater depth.

Two whole-rock K/Ar ages have been obtained on material from the dykes. The ages are concordant within the limits of accuracy and are 1255 ± 52 m. y. (Leech, *et al.*, 1963) and 1146 ± 104 m. y. (Wanless, *et al.*, 1968). The second determination was carried out during a later stage of the Geological Survey dating program, so, from a strictly analytical standpoint it more accurately reflects the age of intrusion of the dykes.

Two specimens from site 66 (666 and 667) and one specimen from site 67 (673) were chemically analyzed by the Geological Survey Rapid Method. Specimen 667 was also analyzed by the Classical Method. The results of these analyses are given in Table 32. 1.

Table 32. 1
Chemical Analyses

Sample	666	667	673	667
Method	Rapid	Rapid	Rapid	Classical
SiO ₂	46.9	46.9	46.6	47.88
Al ₂ O ₃	16.6	16.0	15.6	16.19
Fe ₂ O ₃	3.1	2.4	2.9	-
FeO	10.5	10.1	9.8	9.67
MgO	5.8	5.5	6.7	6.27
CaO	9.4	8.7	8.6	8.78
Na ₂ O	3.1	3.2	3.1	-
K ₂ O	1.37	1.05	1.26	-
TiO ₂	2.15	2.00	1.92	-
P ₂ O ₅	0.38	0.38	0.37	0.26
MnO	0.16	0.18	0.18	0.19
CO ₂	0.2	0.2	0.1	-
H ₂ O (T)	1.2	1.5	2.4	1.52

Chemical analyses by staff of the analytical section of the Geological Survey of Canada.

Fifteen samples oriented with sun compass were collected for paleomagnetic study from four sites on one of the dykes (Fig. 32.1). Two specimens were obtained from each sample and the mean magnetization direction of the specimen pairs was used to represent the sample.

Measurement and Results

Two specimens from each site were demagnetized in steps from 50 to 800 oe to determine the optimum cleaning field. All of these test specimens exhibited a stable end-point direction well away from the present earth's field direction in cleaning fields ranging from 150 to 250 and sometimes 300 oe, so all specimens were demagnetized in fields of 200 and 250 oe. Data were used for final site statistics (Table 32.2, Fig. 32.2) which resulted in the best grouping after cleaning in either of these two fields.

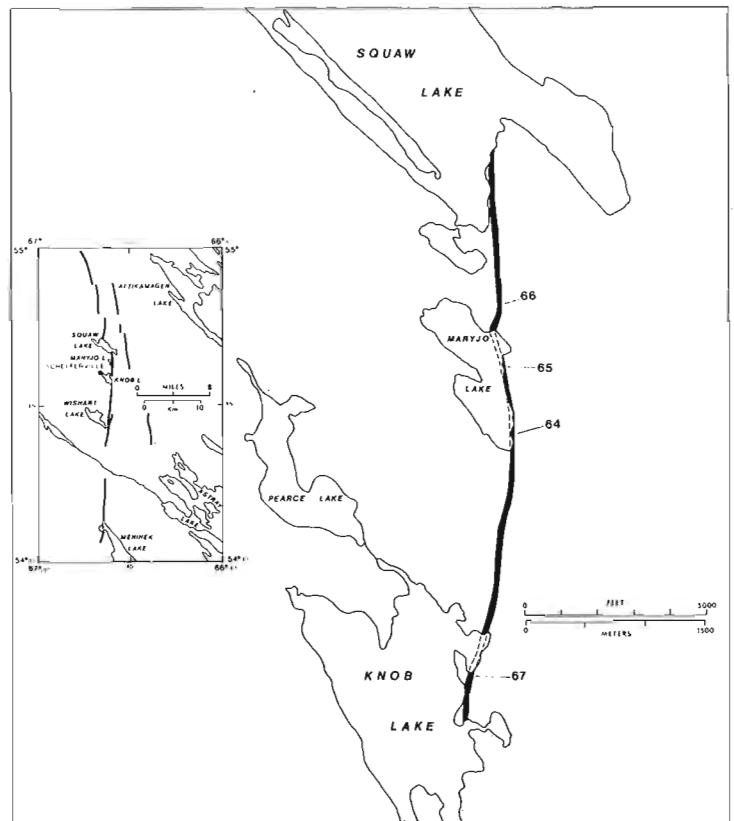


Figure 32.1. Schefferville diabase dykes from Geological Survey Map 1087A, detailed sketch (showing paleomagnetic sample locations) from a map of the Iron Ore Company of Canada.

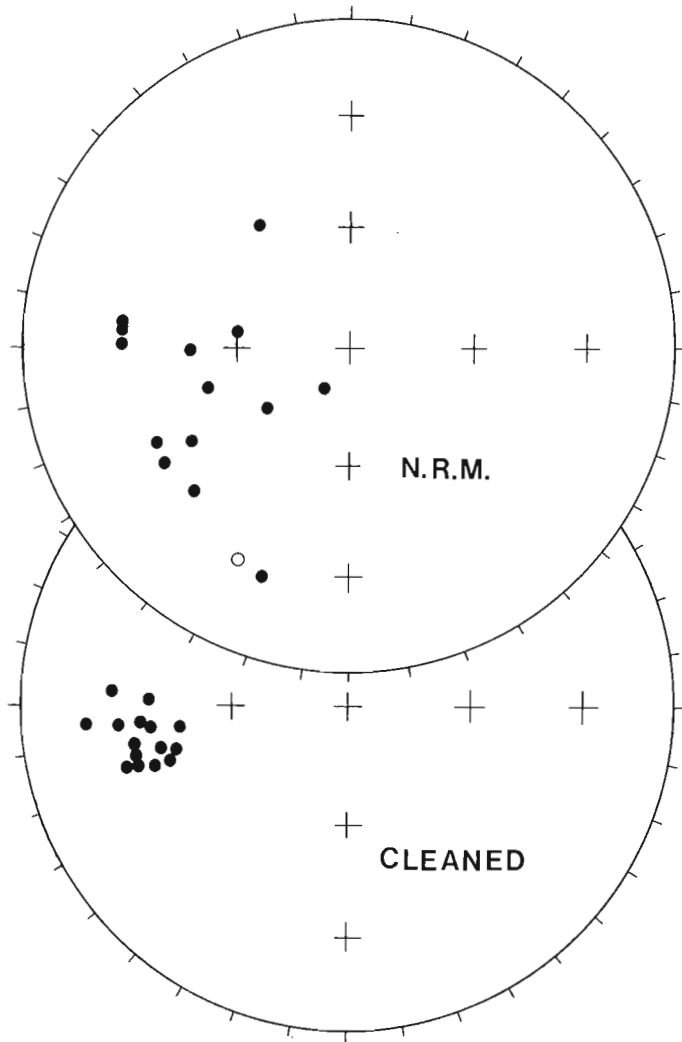


Figure 32.2. Magnetization directions of 15 independently oriented samples before (N.R.M.) and after optimum partial A.F. demagnetization. Solid circles indicate downward inclination, open circles upward inclination.

Discussion

The paleomagnetic pole (136.5°W, 11.0°N, $\alpha = 2.2^\circ$, Table 32.2) is close to that obtained for the Michikamau anorthositic intrusion, 144.7°W, 0.5°S (Murthy, *et al.*, 1968) which has an age of 1400-1500 m.y. The Michikamau intrusion also lies within the eastern Churchill Orogen so that it is unlikely that there has been relative tectonic movement between it and the Schefferville dykes. It is possible, however, that the paleomagnetic data from the Schefferville dykes do not adequately average out paleosecular variation if such variation was comparable to that of recent geologic time. Presumably the blocking temperature time span in passing from the chilled margins to the coarse central zone would be a few hundred years. This would depend on the ambient temperature of the

present erosion surface at the time of intrusion. Furthermore, the North American polar wandering path for the periods 1450-1600 m.y. and 1250-1200 m.y. are subparallel and separated by only 10 to 30 degrees of arc (Fig. 32.3). Comparison with this curve suggests the dykes may be as young as 1200 m.y. but the best fit suggests an age closer to 1500 m.y.

The only other paleomagnetic data for what are presumed to be the same dykes are those reported by Seguin (1975) on Montagnais* diabase dykes. He presented data from 11 sites, with a mean magnetization direction of $D = 247^\circ$, $I = 06$ and also stated that many sites yielded mixed polarities. It is extremely unusual in completely unaltered diabase dykes to isolate normal and reversed components from the same site, especially with a narrow A.F. cleaning range (in this case 100 to 200 oe). Seguin also reported considerable within-sample and within-site inhomogeneity, such that the data from an additional seven sites could not be used in the analysis. He did not give the exact localities of his sampling sites so they may not include material from sites or dykes represented in the present study.

The results from the present four sites (15 separately oriented samples) reflect the isolation and measurement of an excellent, stable, Thermoremanent magnetization which undoubtedly dates from the consolidation of the intrusion. The results are therefore more reliable than those previously reported (Seguin, 1975).

Table 32.2

Paleomagnetic data for the Schefferville diabase dykes

Site	N. R. M.				Cleaned					
	N	D	I	k	A. F.	D	I	k	δ°	
64	4	243	44	2.9	250	257	41	71	9.6	
65	4	255	52	11.6	250	260	36	66	10	
66	5	243	34	9.2	200	260	35	97	8.2	
67	2	277	50		250	262	36			
Sites	4	254	46	36		260	37	731	3.0	
Samples	15	250	44	6.3		259	37	85	8.8	
Mean pole*	after cleaning 136.5°W, 11.0°N, $k=1033$, $\alpha=2.2^\circ$									

N = number of independently oriented specimens per site

D = declination.

I = inclination.

k = Fisher's (1953) best estimate of precision.

A. F. = cleaning field in oersteds.

δ° = angular standard deviation.

α = half angle (degrees) of the cone of confidence at $P=0.95$.

*Note - Mean pole position calculated from site pole positions.

*The term Montagnais intrusives has already been used for another suite of basic and ultrabasic intrusive rocks (Frarey and Duffell, 1964) so should not be used for these different olivine diabase dykes.

References

- Fahrig, W.F.
Paleomagnetic correlation of the Riphean of North America; in proceedings of the international symposium, "Correlation of the Precambrian", held in Moscow, 1975 (in press).
- Fisher, R.A.
1953: Dispersion on a sphere; R. Soc. London, Proc., Ser. A, v. 217, p. 295-305.
- Frarey, M.J.
1961: Menihek Lakes, Geol. Surv. Can., Map 1087A.
- Frarey, M.J. and Duffell, S.
1964: Revised stratigraphic nomenclature for the central part of the Labrador Trough; Geol. Surv. Can., Paper 64-25.
- Leech, G.B., Lowdon, J.A., Stockwell, C.H., and Wanless, R.K.
1963: Age determinations by the Geological Survey of Canada; Geol. Surv. Can., Paper 63-17.
- Murthy, G.S., Fahrig, W.F., and Jones, D.J.
1968: The paleomagnetism of the Michikamau anorthositic intrusion, Labrador. Can. J. Earth Sci., v. 5, p. 1139-1144.
- Seguin, M.K.
1975: Paleomagnetism of the Montagnais diabase dikes of the west central sector of the Labrador Trough; Pageoph., v. 113, p. 435-445.
- Wanless, R.K., Stevens, R.D., Lachance, G.R., and Edwards, C.M.
1968: Age determinations and geological studies; Geol. Surv. Can., Paper 67-2, pt. A.

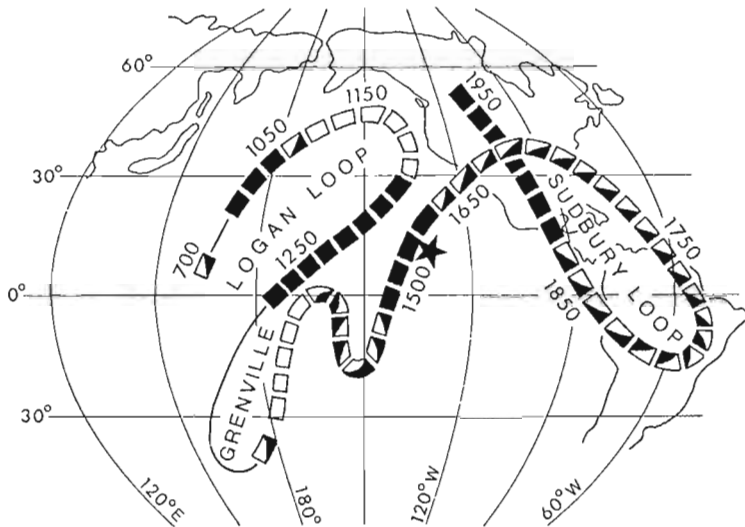


Figure 32.3. Pole position (indicated by star symbol) of Schefferville dykes relative to apparent polar wandering path (Fahrig, in press) for the Precambrian of North America. Intervals represented by solid rectangles indicate periods of normal polarity only, by open rectangles reversed polarity only and by partly shaded rectangles, mixed polarity. A single line indicates uncertainty regarding polar wandering during these periods.

Project 740063

J. J. Clague

Terrain Sciences Division, Vancouver

Introduction

The Georgia Depression, located between the Vancouver Island Ranges and the Coast Mountains of southwest British Columbia, is a major physiographic subdivision of the Canadian Cordillera (Holland, 1964). The morphology of the Georgia Depression, include of repeated subsidence and deposition since Late Cretaceous time and of subaerial and glacial erosion (Mathews, 1972).

Bathymetric elements in the Strait of Georgia, the submerged part of the Georgia Depression, include basins and troughs up to 430 m in depth and banks elongate in a northwest-southeast direction. These features are ascribed to glacial scour of Pleistocene sediments and perhaps Tertiary and Cretaceous strata (Mathews, 1968; Clague, 1975a).

Late Pleistocene sediments underlie much of the lowland bordering the Strait of Georgia and many of the islands within the strait (e. g. , see Armstrong, 1956, 1957; Fyles, 1963; Halstead, 1966; Clague, 1975a). These sediments in many places are continuous with Pleistocene strata underlying the sea floor. Tiffin (1969), for example, concluded from seismic reflection data that Pleistocene sediments up to 550 m thick occur over a large area on the northeast side of the central Strait of Georgia adjacent to major subaerial Pleistocene deposits. Also, many islands in the northern sector of the strait consist of Pleistocene sediments which rest on platforms of older unconsolidated materials extending below present sea level (Clague, 1975a).

Methods

The areal distribution and thickness of unconsolidated sediments in the northern Strait of Georgia have been determined from continuous seismic reflection profiles. Fifty profiles, representing about 900 line kilometres, were obtained during 1973 and 1974 with air gun sources of 16 cm³ (1 cu. in.) and 82 cm³ (5 cu. in.) (Fig. 33.1).

Pleistocene sediments were identified in the profiles using the following criteria (Fig. 33.2): (1) Seismic units considered to represent Pleistocene sediments unconformably overlie a basement complex which is continuous onshore with bedrock. These units are unconformably overlain in basins and troughs by Holocene sediments. (2) Some strata identified in the profiles are continuous with Pleistocene deposits onshore. (3) Units thought to be Pleistocene in age are characterized by horizontal and near-horizontal reflectors, which in many places are truncated by the present topography. Subordinate to these, but common near unconformities within the sediment pile, are possible deposits of glacial drift characterized by discontinuous, chaotic acoustic reflectors.

The above criteria do not preclude the possibility that some of the submarine sediments here considered to be Pleistocene may be of Tertiary age. Subaerial and submarine Tertiary rocks have been identified in the central and southern parts of the Georgia Depression (Hopkings, 1966, 1968; Muller and Carson, 1969; Rouse *et al.*, 1970). Deformation of unconsolidated sediments in the Strait of Georgia, however, is minor; these sediments, in general, are flat lying and are not extensively faulted. In contrast, seismic reflectors in the underlying basement complex are inclined and offset by faults. Muller and Carson (1969) stated that much of the faulted in the Georgia Depression occurred during Tertiary time, thus it is reasonable to assume that the little-deformed sediment piles overlying basement are largely Pleistocene in age. A similar conclusion was reached by Tiffin (1969) who analyzed seismic profiles from the southern and central Strait of Georgia.

Distribution and Character of Pleistocene Sediments

Pleistocene sediments underlie much of the sea floor of the northern Strait of Georgia (Fig. 33.1). Locally in excess of 550 m thick¹, these sediments occur to depths up to several hundred metres below sea level. Some of the thickest Pleistocene deposits underlie shallow banks and islands such as those northwest of Powell River (Figs. 33.2 and 33.3). Some banks and islands, however, are underlain directly by bedrock, and others consist of a bedrock core and overlying unconsolidated sediments. Locally in the troughs Pleistocene sediments underlie Holocene deposits; elsewhere, however, the latter are in direct contact with bedrock.

The distribution of Pleistocene sediments beneath the sea floor adjacent to Vancouver Island is not known, in large part because the available seismic records in this area are of poor quality. Thus, little information is shown on Figure 33.1 adjacent to Vancouver Island. At a few sites on the Vancouver Island slope, however, dipping reflectors occur immediately beneath the sea bottom, indicating that at least parts of this slope are underlain by bedrock with only a thin sediment cover.

Pleistocene sediments in the northern Strait of Georgia comprise a variety of lithologies. Samples of till or glaciomarine diamicton have been collected from large areas of the sea floor (Clague, 1975b). Much of the Pleistocene fill, however, consists of fine grained

¹Thicknesses are based upon an assumed seismic velocity of about 2000 m/s (Tiffin, 1969). Included in the maximum thickness cited above is about 100 m of sediment exposed in sea cliffs above the submarine sediment piles.

sediment. For example, outcrops of horizontally bedded silty clay were observed by the author between depths of 80 and 225 m during a traverse by submersible of the bank shown in Figure 33.3. The seismic profile of Figure 33.3 indicates that this bank consists largely of sediments of the same character as those outcropping at the bank edge. It is likely that other sediment bodies of similar seismic character also consist of stratified clay. This clay is thought to be marine in origin, in large part because of its position relative to present and past sea levels.

Discussion

The Pleistocene sediments are remnants of a formerly more extensive fill in the Georgia Depression. Horizontal strata are truncated by the present sea floor (Figs. 33.2 and 33.3), indicating that there has been significant erosion of the fill. The remnants in places extend above sea level to form islands consisting of late Wisconsin stratified, terrestrial sediments unconformably overlain by till deposited during the last continental glaciation (Fraser Glaciation). It is thought

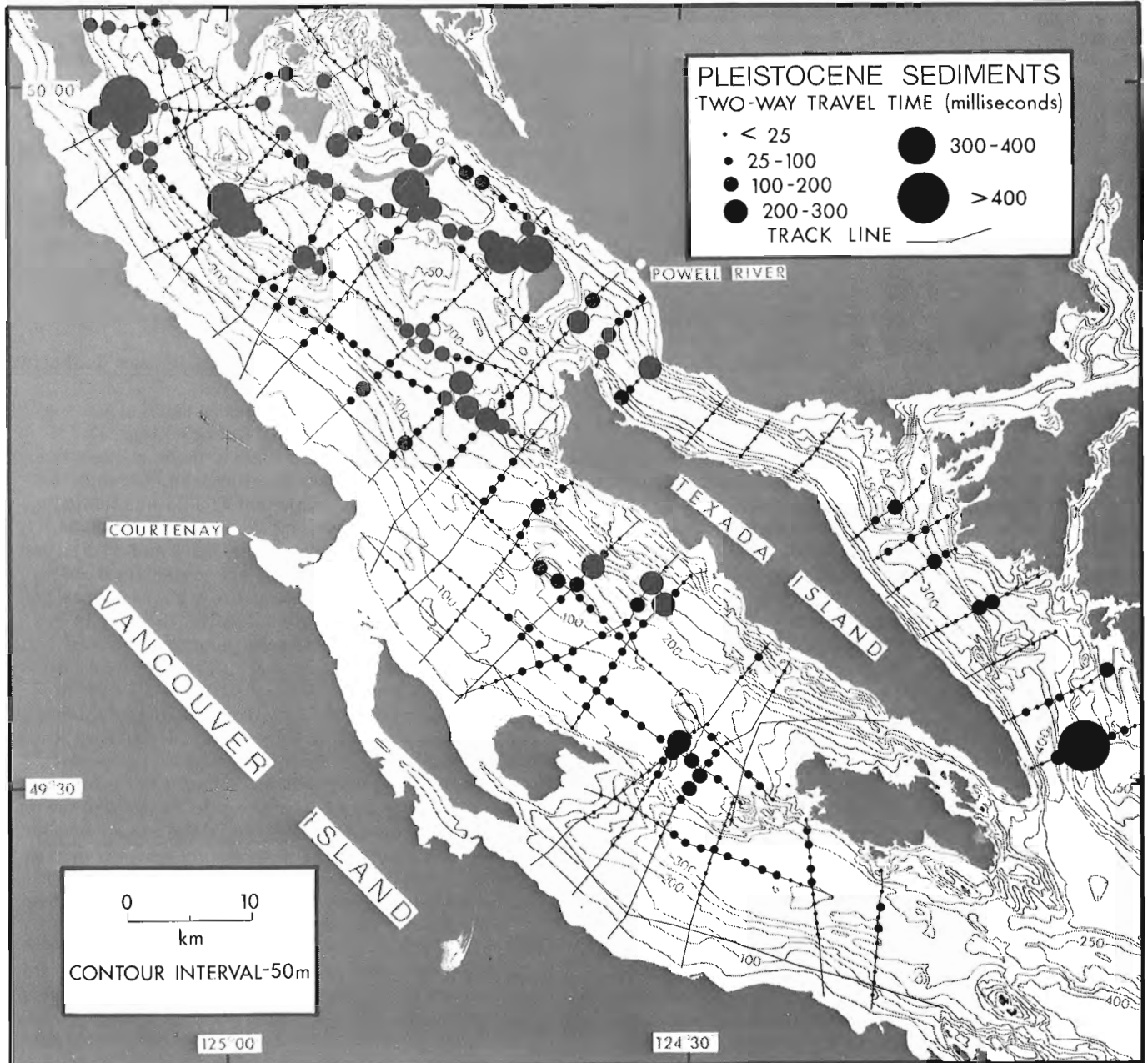


Figure 33.1. Distribution and inferred thickness of Pleistocene sediments in the northern Strait of Georgia. If the seismic velocity through the Pleistocene sediments is assumed to be 2000 m/s (Tiffin, 1969), two-way travel times are equal to thicknesses in metres. The thickness of sediments over those parts of track-lines for which no data are shown is unknown.

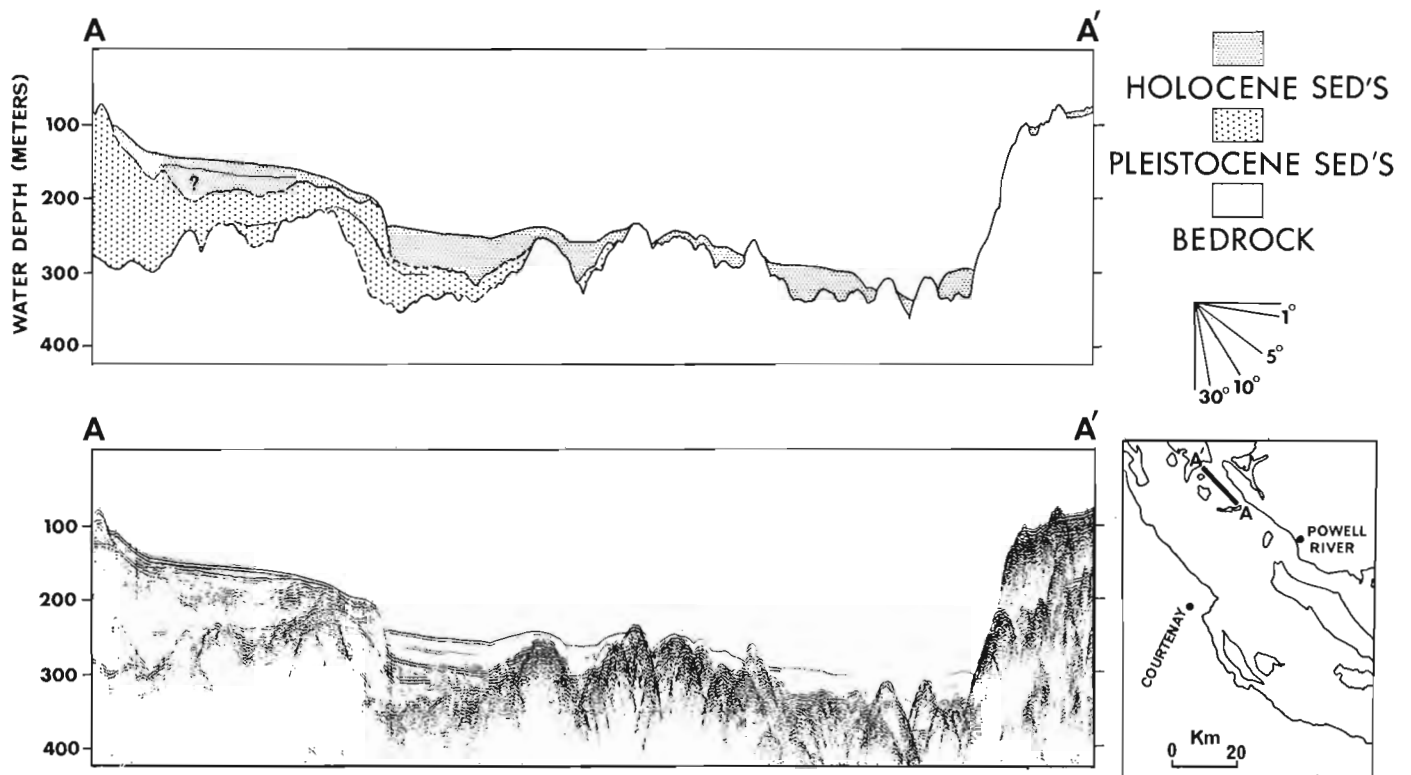


Figure 33.2. Seismic profile showing criteria by which Pleistocene sediments are identified. Horizontal reflectors at the south end of the profile (A) and hyperbolic reflectors at the north end (A') are continuous onshore with Pleistocene sediments and bedrock, respectively. Holocene strata, in general, are parallel to the sea floor and, in places, unconformably overlie the truncated Pleistocene beds.

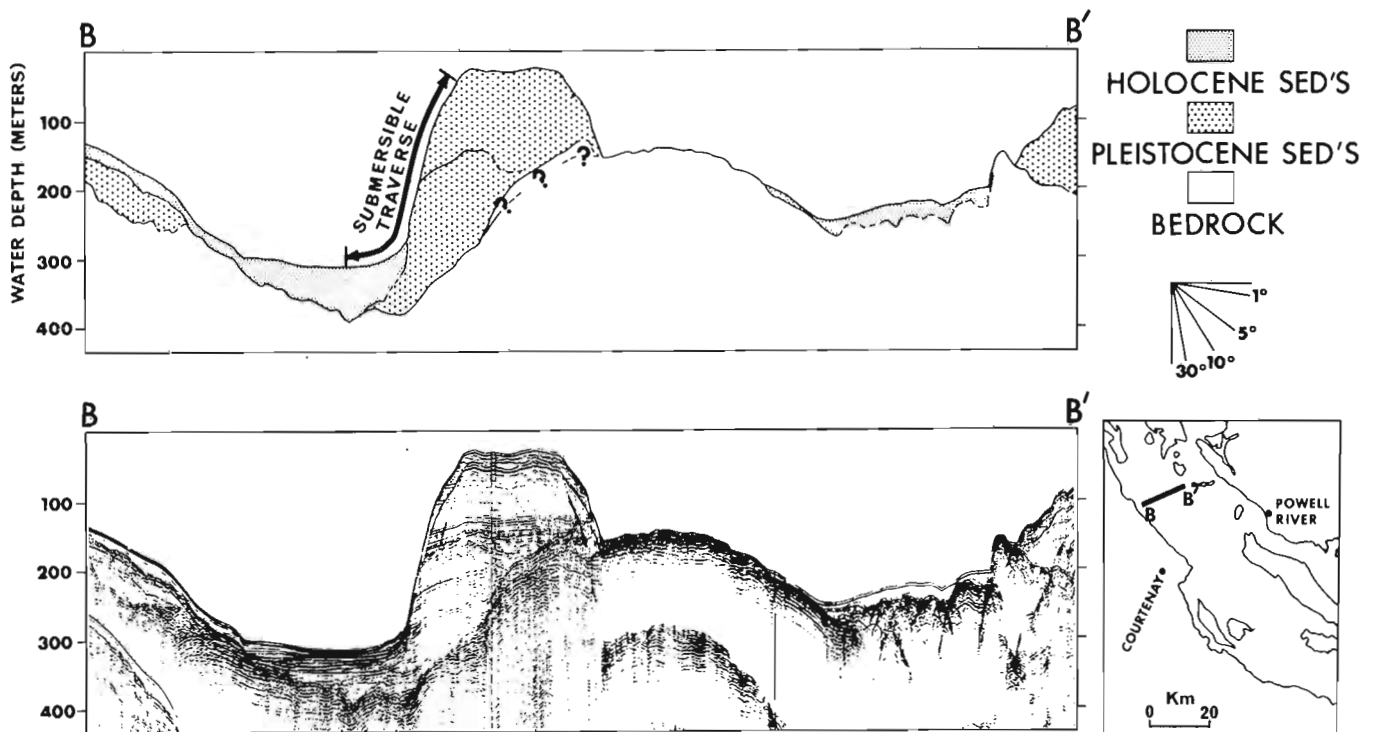


Figure 33.3. Seismic profile across a shallow bank underlain by stratified Pleistocene sediments. These sediments predate stratified terrestrial deposits of late Wisconsin age, which are exposed on nearby islands, and represent remnants of a more extensive marine fill that has been extensively eroded during the Fraser Glaciation. A major unconformity occurs within the sediment pile.

that stratified sediments were deposited above present sea level over the full width of the northern Georgia Depression during late Wisconsin time (Clague, in press). If so, much of the fill upon which these terrestrial sediments were deposited was eroded during the Fraser Glaciation.

If parts of the strait were filled with sediment before the late Wisconsin glacial advance, one or a combination of the following must be concluded: (1) The fill formed during the Olympia nonglacial interval before the Fraser Glaciation but after the penultimate, or Salmon Springs (Crandell, 1963) glaciation. (2) The fill predates the penultimate glaciation, and Salmon Springs glacial activity in the Strait of Georgia region was such that the area was not as extensively scoured by glaciers as it was during the Fraser Glaciation. In actual fact, the fill is probably of composite age. Unconformities within the sequence indicate that intervals of deposition alternated with intervals of glacial scour.

Whatever the detailed history of the fill, it is apparent that the volume of unconsolidated sediments in the Strait of Georgia was greater during at least part of the Pleistocene Epoch than during Holocene time.

Acknowledgments

D.L. Tiffin of the Geological Survey of Canada supplied the technical expertise and equipment with which the seismic reflection data were collected. Also gratefully acknowledged is the ship-board assistance provided by I. Frydecky, J.L. Luternauer, K.E. Ricker, J.W. Scott, D.L. Tiffin and crew members of the C. S. S. *Parizeau* and C. S. S. *Vector*.

References

Armstrong, J. E.

1956: Surficial geology of Vancouver area, British Columbia; Geol. Surv. Can., Paper 55-40, 16 p.

1957: Surficial geology of New Westminster map-area, British Columbia; Geol. Surv. Can., Paper 57-5, 25 p.

Clague, J. J.

1975a: Quaternary geology, northern Strait of Georgia, British Columbia; in Report of Activities, Part A; Geol. Surv. Can., Paper 75-1A, p. 397-400.

1975b: Surficial sediments of the northern Strait of Georgia, British Columbia; in Report of Activities, Part B; Geol. Surv. Can., Paper 75-1B, p. 151-156.

Quadra Sand and its relation to the late Wisconsin glaciation of southwest British Columbia; Can. J. Earth Sci. in press

Crandell, D. R.

1963: Surficial geology and geomorphology of the Lake Tapps quadrangle, Washington; U. S. Geol. Surv., Prof. Paper 388-A, 84 p.

Fyles, J. G.

1963: Surficial geology of Horne Lake and Parksville map-areas, Vancouver Island, British Columbia; Geol. Surv. Can., Mem. 318, 142 p.

Halstead, E. C.

1966: Surficial geology of Duncan and Shawnigan map-areas, British Columbia; Geol. Surv. Can., Paper 65-24, 3 p.

Holland, S. S.

1964: Landforms of British Columbia, a physiographic outline; B.C. Dep. Mines Pet. Resour., Bull. 48, 138 p.

Hopkins, W. S. Jr.

1966: Palynology of Tertiary rocks of the Whatcom basin, southwestern British Columbia and northwestern Washington; unpubl. Ph.D. thesis, Univ. British Columbia, Vancouver, B. C., 184 p.

1968: Subsurface Miocene rocks, British Columbia-Washington, a palynological investigation; Geol. Soc. Am., Bull., v. 79, p. 763-768.

Mathews, W. H.

1968: Geomorphology, southwestern British Columbia; in Guidebook for Geological Field Trips in Southwestern British Columbia, ed. W. H. Mathews, Univ. British Columbia, Dep. Geol. Sci., Rept. 6, p. 18-24.

1972: Geology of Vancouver area of British Columbia; 24th Int. Geol. Congr., Guideb., Field Excursion A05-C05, 47 p.

Muller, J. E. and Carson, D. J. T.

1969: Geology and mineral deposits of Alberni map-area, British Columbia (92 F); Geol. Surv. Can., Paper 68-50, 52 p.

Rouse, G. E., Hopkins, W. S. Jr., and Piel, K. M.

1970: Palynology of some Late Cretaceous and Early Tertiary deposits in British Columbia and adjacent Alberta; in Symposium on Palynology of the Late Cretaceous and Early Tertiary, eds. R. M. Kosanke and A. T. Cross; Geol. Soc. Am., Spec., Paper 127, p. 213-246.

Tiffin, D. L.

1969: Continuous seismic reflection profiling in the Strait of Georgia, British Columbia; unpubl. Ph.D. thesis, Univ. British Columbia, Vancouver, B. C., 177 p.

Project 730026





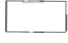
J. S. O. Lau and D. E. Lawrence¹
Terrain Sciences Division

Introduction

Information from the Mackenzie Valley Geotechnical Data Bank (Lawrence, 1974a, b, c) was used to study the distribution of ground ice in three selected map-areas in Mackenzie Valley (Camsell Bend 95 J, Norman Wells 96 E, and Travallant Lake 106 O). Soils containing ground ice may present serious problems of settlement and stability if allowed to thaw, especially in the case of fine grained soils. The amount, form, and distribution of ground ice were found to vary considerably with soil type and location in Mackenzie Valley.

Data Analysis

A retrieval system using COBOL programming was used to extract data from the data bank for analysis (Lau and Lawrence, 1976). Computer programs "GET-MAP", "RETRIEVE", and "SCATTER" were used to produce one-page cross-tabulation frequency plots of permafrost type vs. depth for various soil groups of the Unified Soil Classification System (USCS) for specified National Topographic System (NTS) map-areas. Cumulative frequency plots of the occurrence of various types of ice in frozen soils vs. depth were constructed. Unfrozen soils also were plotted. ICE, V, N, and F are modified alphabetic codes after the permafrost classification of Pihlainen and Johnston (1963). As this classification is used widely in geotechnical and geological investigations carried out in Mackenzie Valley, it also has been adopted for this study. In symbolic form, visible ice greater than one inch thick is designated as ICE, visible ice less than one inch thick as V, nonvisible ice as N, and unknown type of ice as F (Table 34.1, below).

	ICE	Ice is discernible by eye and is greater than one inch thick.
	V - VISIBLE ICE	Ice is discernible by eye and is less than one inch thick.
	N - ICE NOT VISIBLE	Ice is not discernible by eye. The impression received by the unaided eye is that none of the frozen water occupies space in excess of the original voids in the soil.
	F - FROZEN, TYPE UNKNOWN	
	SOILS NOT FROZEN	

It should be noted that this classification is intended for the description of undisturbed samples. Samples obtained in these three map-areas were recovered by air drilling, power auger, or rotary hydraulic methods which gave disturbed samples. Consequently, erroneous classification of permafrost is possible. The occurrence and amount of ground ice reported, when using disturbed sampling methods, are likely to be considerably less than those using continuous undisturbed sampling methods or estimated by geological observation (Lawrence, 1974a). Hence, the description of permafrost in this study should be treated as tentative.

Results and Discussion

In the discussion of results, all percentages are expressed as the percentage of the total number of samples in the specified soil groups:

Camsell Bend (95 J)
(62°00' to 63°00'N)

The samples from Camsell Bend were obtained from lacustrine sediments, alluvial deposits, and morainal till (Rutter *et al.*, 1973). From the cumulative frequency plots (Figs. 34.1, 34.2, and 34.3), the following observations can be made:

- 1) Most coarse grained soils recorded are frozen (92%) in winter with 3% containing visible ice (V).
- 2) Most ML and CL soils are frozen (88%). Six per cent of the samples contain visible ice (V).
- 3) Less than one quarter of CI and CH soils recorded (17%) are frozen; ice in these soils is commonly of the visible type (V), and visible ice is found in 7% of the samples.
- 4) Virtually all the peat recorded (95%) in this area freezes in winter. Visible ice is the major ice type and is found in 78% of the peat samples.

Norman Wells (96 E)
(65°00' to 66°00'N)

In Norman Wells, the samples were obtained from alluvial deposits, morainal till, glaciolacustrine sediments, and glaciofluvial deposits (Hughes, 1970). From the cumulative frequency plots (Figs. 34.4, 34.5, 34.6, and 34.7), the following observations can be made:

¹Department of Indian Affairs and Northern Development.

CUMULATIVE FREQUENCIES OF OCCURRENCE OF ICE, V, N, AND F TYPES OF ICE, AND SOILS NOT FROZEN

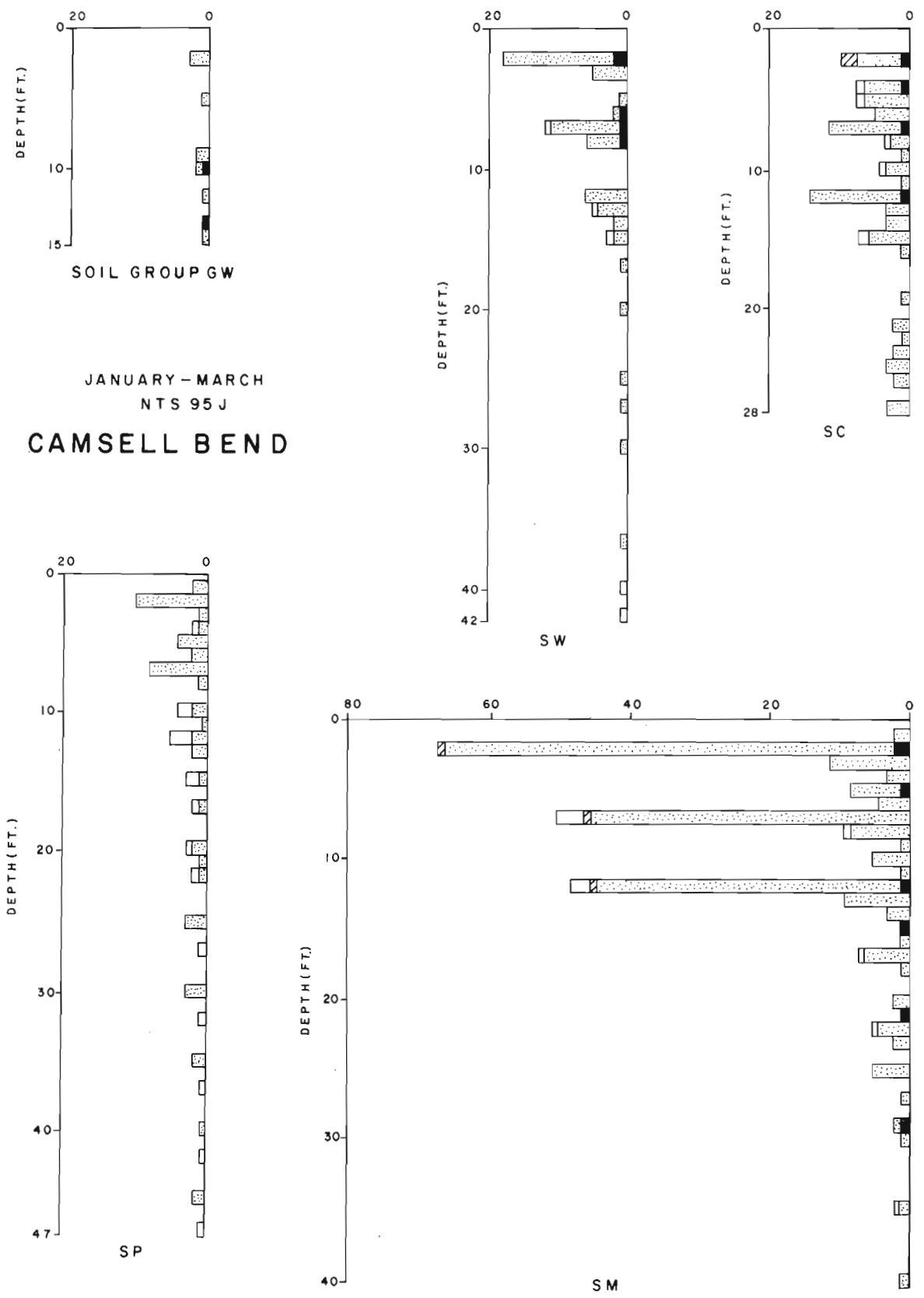


Figure 34. 1. Cumulative frequency plots of the occurrence of various types of ice for coarse grained soil groups (Camsell Bend NTS 95J).

CUMULATIVE FREQUENCIES OF OCCURRENCE OF ICE, V, N, AND F TYPES OF ICE, AND SOILS NOT FROZEN

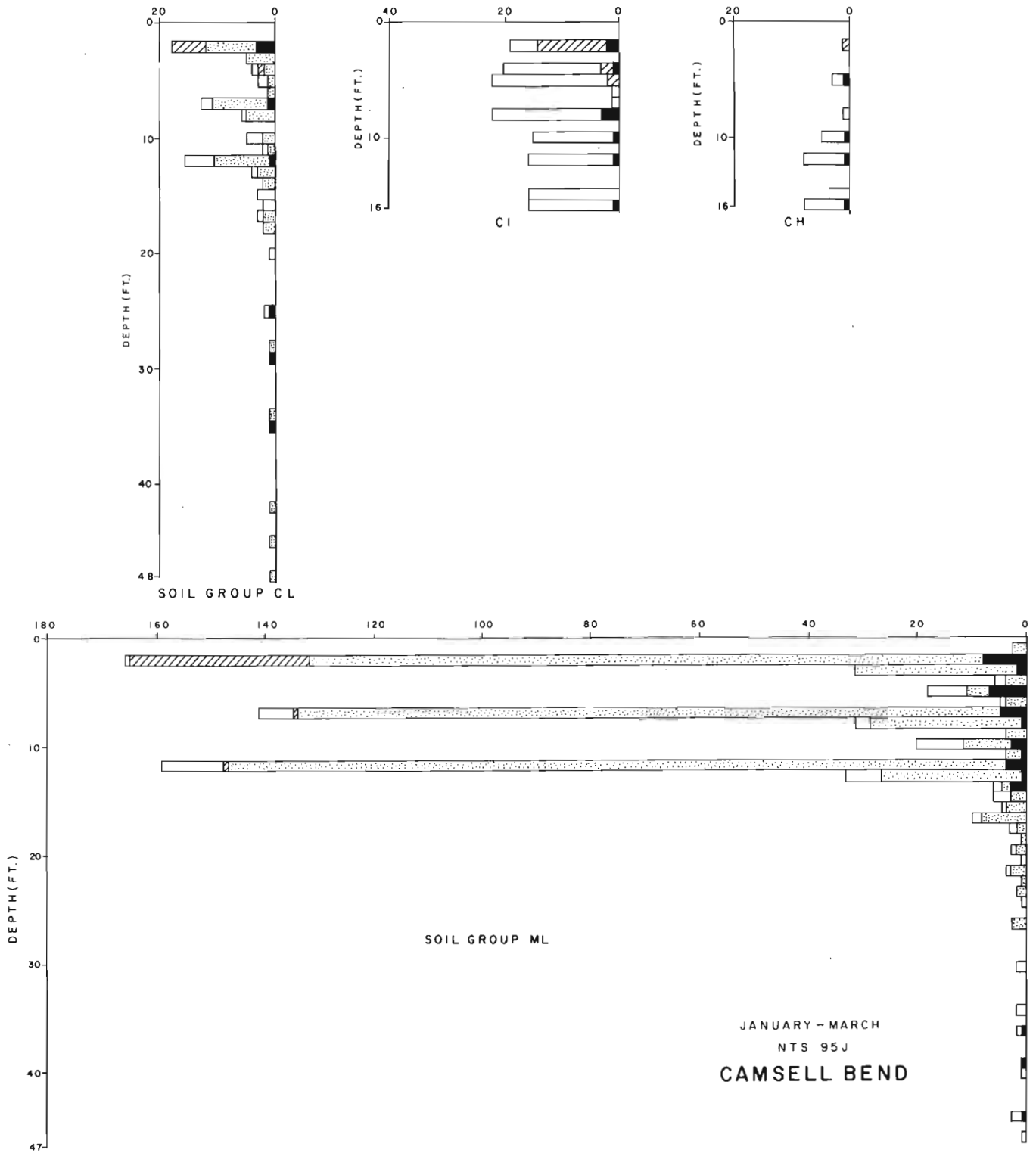


Figure 34. 2. Cumulative frequency plots of the occurrence of various types of ice for fine grained soil groups (Camsell Bend NTS 95J).

JANUARY - MARCH
NTS 95 J
CAMSELL BEND

CUMULATIVE FREQUENCIES OF OCCURRENCE OF ICE,
V, N, AND F TYPES OF ICE, AND SOILS NOT FROZEN

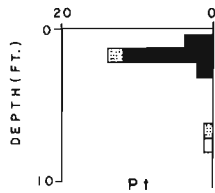
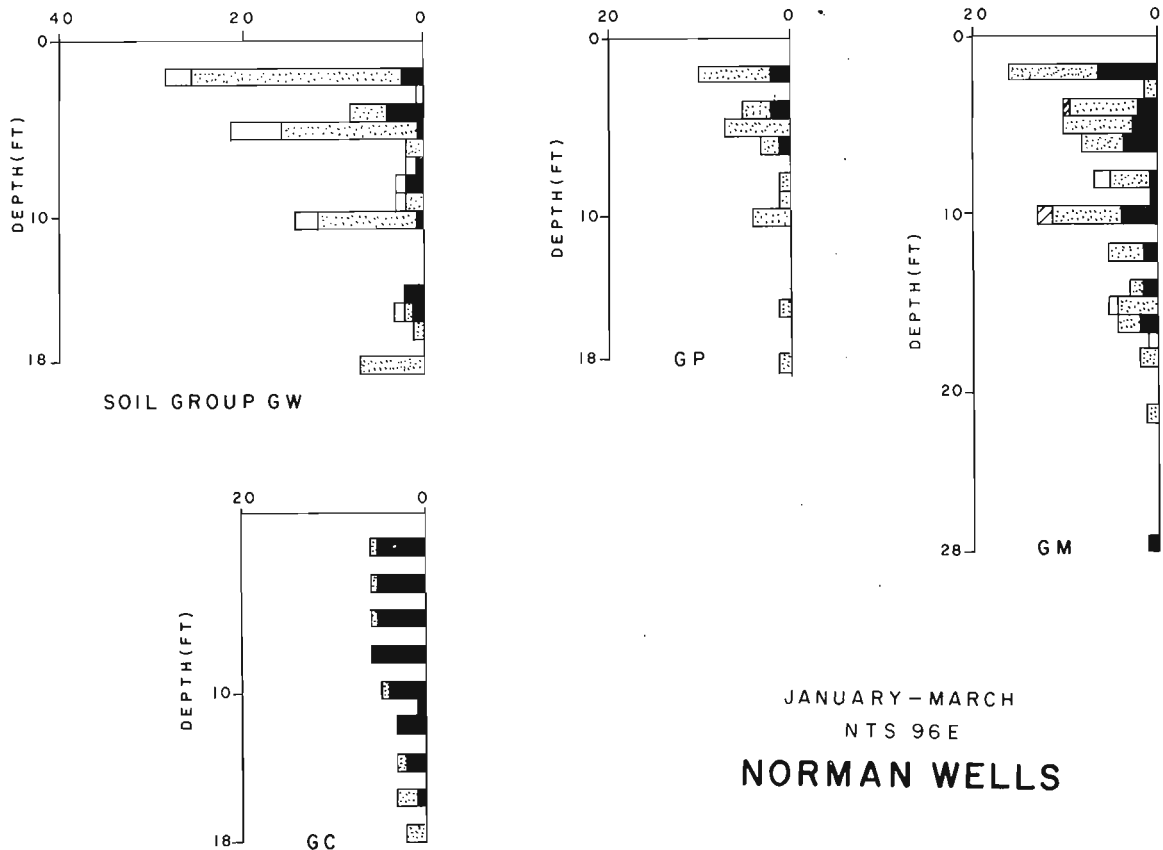


Figure 34.3. Cumulative frequency plot of the occurrence of various types of ice for the peat soil group (Camsell Bend NTS 95J).

- 1) Large proportions of coarse grained soils are frozen (82%) in winter; 22% of these soils contain visible ice (V).
- 2) The quantity of visible ice in gravels and sands appears to increase as the amount of fines increases (14%, 15%, 32%, 78% V in GW, GP, GM, GC soils and 26%, 12%, 20%, 35% V in SW, SP, SM, SC soils respectively).
- 3) Most (92%) fine grained soils are recorded as frozen and all ice types are present; however, visible ice (V) appears in 52% of all samples and ICE in 0.3%.
- 4) There is considerably more V type ice in fine grained soils than in coarse grained soils.
- 5) Visible ice apparently is encountered more frequently in CL and CI soils than in ML and CH soils (56% of CL soils and 61% of CI soils, while 40% of ML soils and 38% of CH soils contain visible ice).
- 6) Virtually all organic soils and peat recorded (97%) are frozen with visible ice (V) appearing in 89% of samples.

CUMULATIVE FREQUENCIES OF OCCURRENCE OF ICE, V, N, AND F TYPES OF ICE, AND SOILS NOT FROZEN



JANUARY - MARCH
NTS 96 E
NORMAN WELLS

Figure 34.4. Cumulative frequency plots of the occurrence of various types of ice for gravels (Norman Wells NTS 96E).

CUMULATIVE FREQUENCIES OF OCCURRENCE OF ICE, V, N, AND F TYPES OF ICE, AND SOILS NOT FROZEN

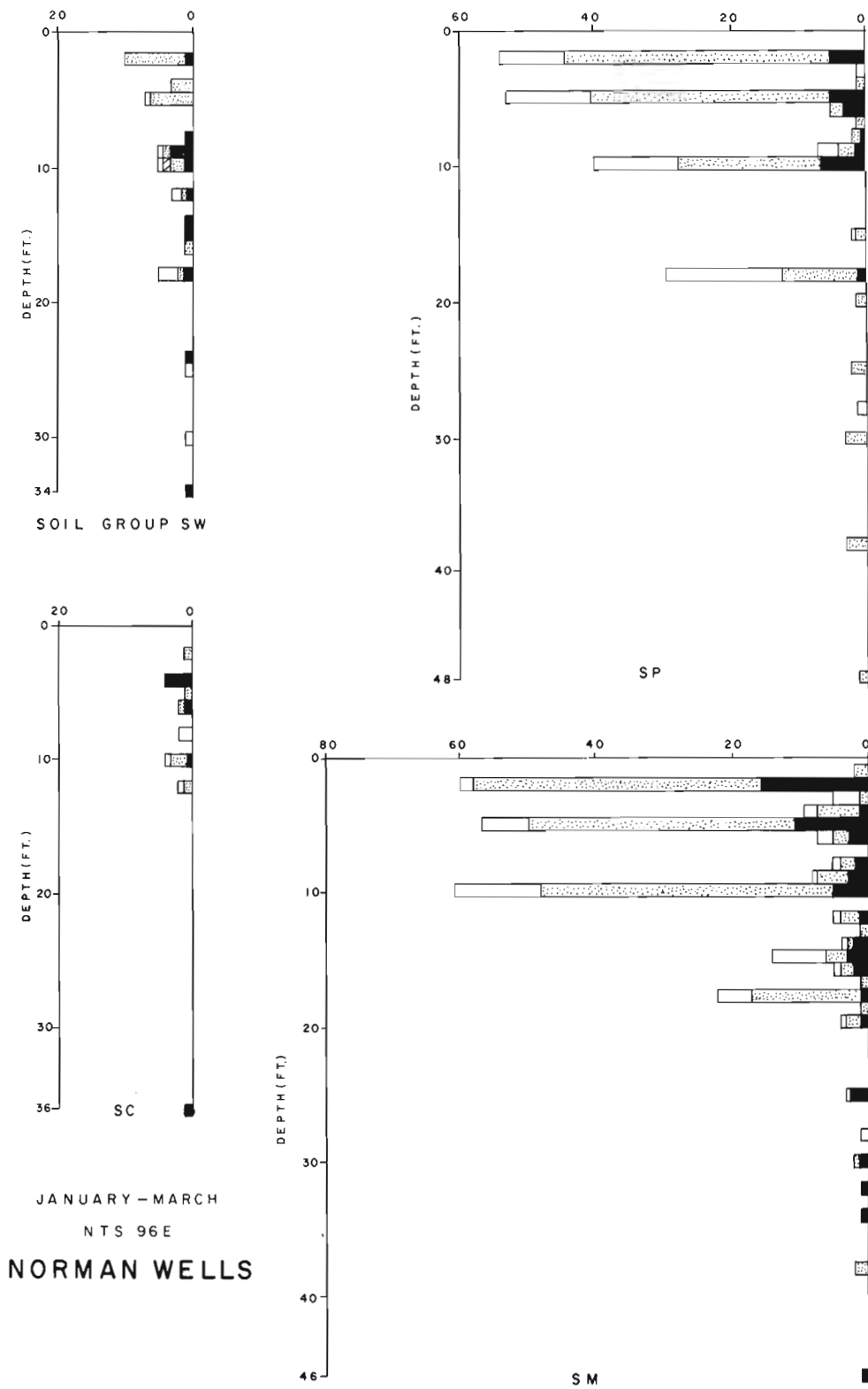


Figure 34.5. Cumulative frequency plots of the occurrence of various types of ice for sands (Norman Wells NTS 96E).

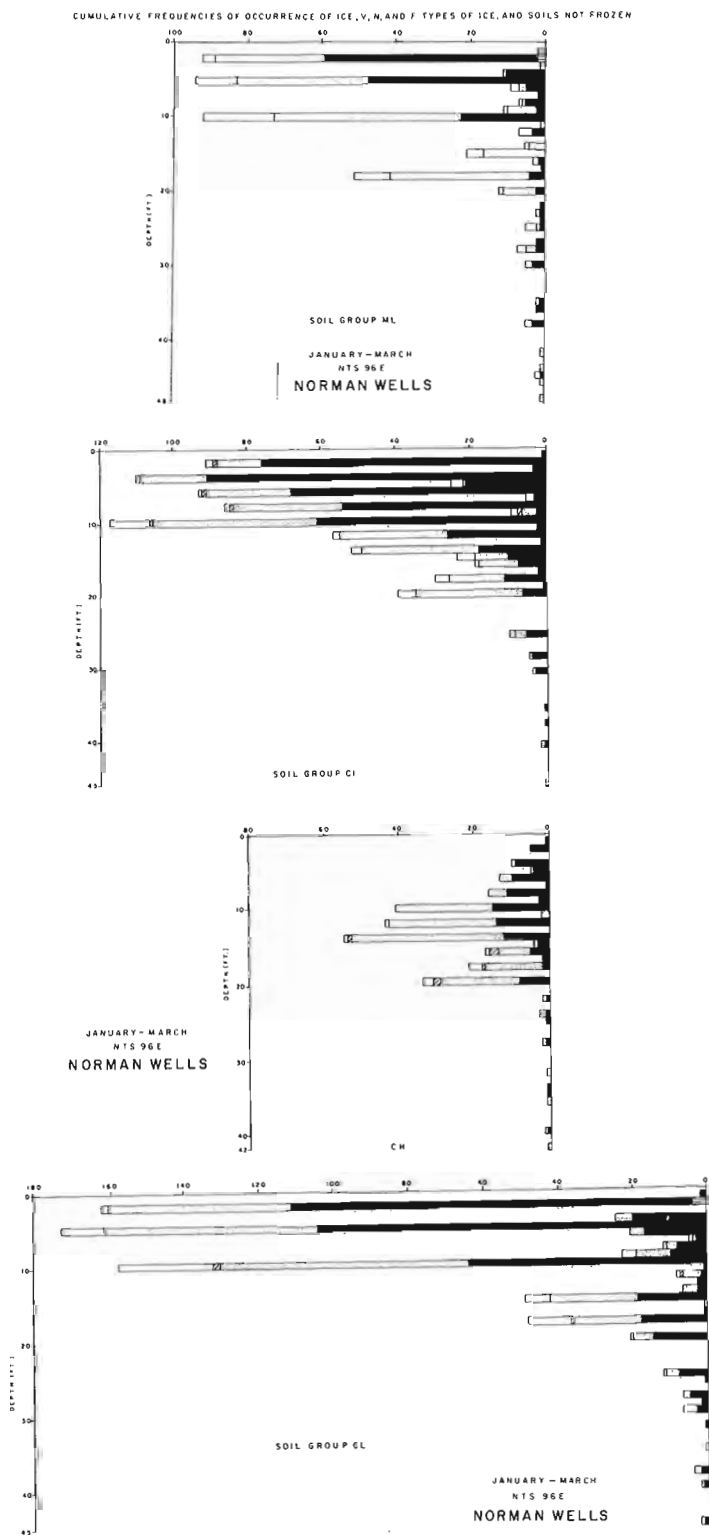


Figure 34.6. Cumulative frequency plots of the occurrence of various types of ice for fine grained soil groups (Norman Wells NTS 96E).

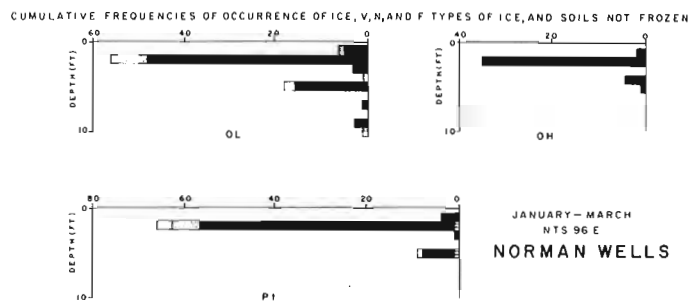


Figure 34.7. Cumulative frequency plots of the occurrence of various types of ice for organic soil groups (Norman Wells NTS 96E).

Travaillant Lake (106 O) (67°00' to 68°00'N)

The samples from Travaillant Lake were obtained from glaciofluvial deposits, organic terrain, and thin morainal till (Hughes, 1972). From the cumulative frequency plots (Figs. 34.8, 34.9, and 34.10), the following observations can be made:

- 1) Coarse grained soils apparently are all frozen in winter, and visible ice is the predominant type of ice (V, 93% of the samples and ICE, 0.2% of samples).
- 2) The quantity of ice in gravels and sands appears to increase as the amount of fines increases (78%, 87%, 97% V in GW, GP, GC soils and 100%, 94%, 97% V in SW, SP, SM, SC soils respectively).
- 3) Apparently all fine grained soils are frozen, and extremely large proportions of the ice are classified as being of the visible type. Visible ice (V) is found in 95.8% of samples, and ICE appears in 0.9% of samples.
- 4) Virtually all CI soils contain the V type of ice; 99.1% of samples contain visible ice (V) while 0.5% contain visible ice (ICE).
- 5) Organic soils and peat apparently are all frozen, and visible ice predominates in organic and peat soils (94.5% of samples contain visible ice (V) and 0.9% contain ICE).

Conclusions

From the study of winter ground-ice distribution in the three map-areas, the following conclusions can be drawn:

- 1) Most coarse grained soils in Mackenzie Valley are frozen in winter. The ice type is variable; however, there is a marked increase northwards of the quantity of visible ice.
- 2) The quantity of visible ice in gravels and sands appears to increase as the amount of fines increases.
- 3) Except in Camsell Bend, most fine grained soils are frozen in winter. Visible ice is the main type of ice, the quantity of which increases noticeably from south to north.
- 4) Visible ice apparently is encountered more often in CL and C1 soils than in ML and CH soils.

CUMULATIVE FREQUENCIES OF OCCURRENCE OF ICE, V, N, AND F TYPES OF ICE, AND SOILS NOT FROZEN

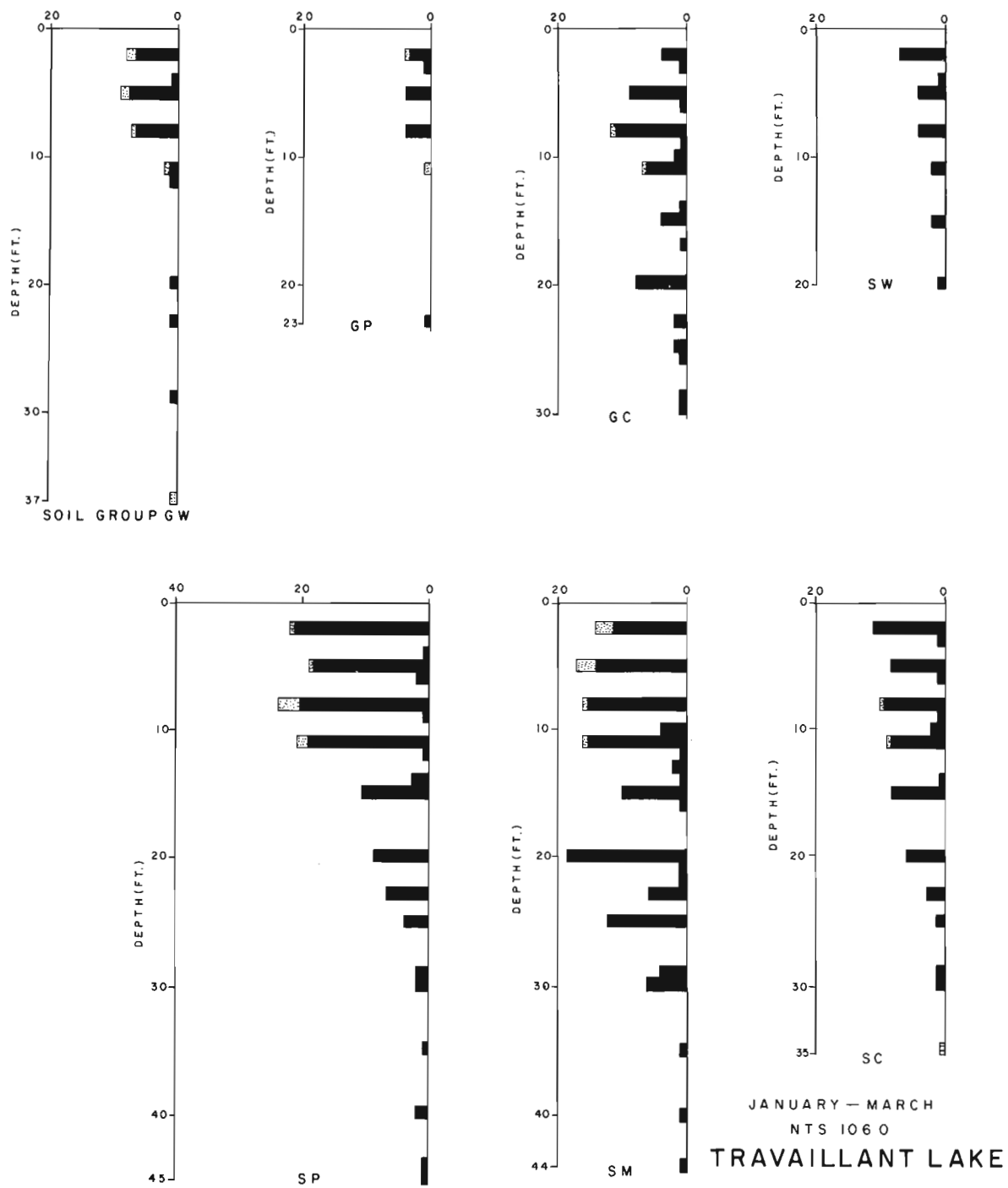
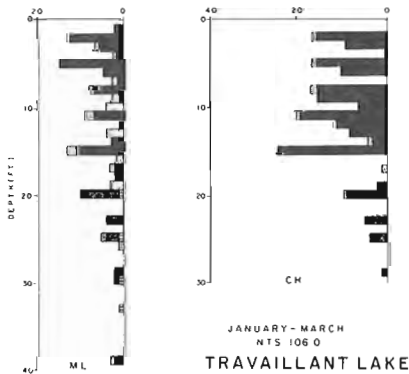
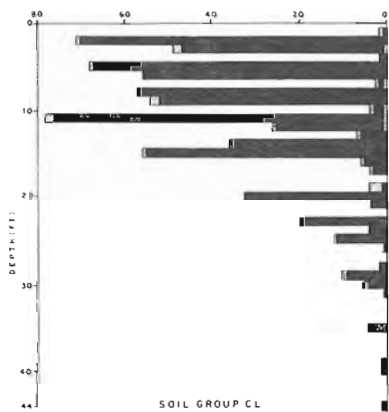
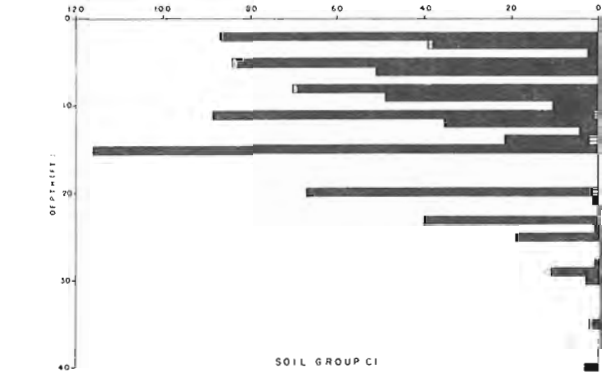


Figure 34. 8. Cumulative frequency plots of the occurrence of various types of ice for coarse grained soil groups (Travaillant Lake NTS 1060).

JANUARY-MARCH
NTS 1060
TRAVAILLANT LAKE

CUMULATIVE FREQUENCIES OF OCCURRENCE OF ICE, V, N, AND F TYPES OF ICE, AND SOILS NOT FROZEN



JANUARY-MARCH
NTS 1060
TRAVAILLANT LAKE

Figure 34.9. Cumulative frequency plots of the occurrence of various types of ice for fine grained soil groups (Travallant Lake NTS 1060).

CUMULATIVE FREQUENCIES OF OCCURRENCE OF ICE, V, N, AND F TYPES OF ICE, AND SOILS NOT FROZEN

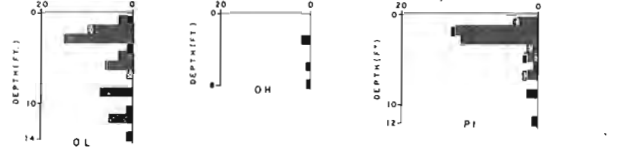


Figure 34.10. Cumulative frequency plots of the occurrence of various types of ice for organic soil groups (Travallant Lake NTS 1060).

5) Nearly all organic soils and peat freeze in winter and contain large amounts of visible ice.

6) The usefulness of the cumulative frequency plot in the study of ground-ice distribution is demonstrated, especially in the comparison of ground-ice distribution in two or more areas.

References

Hughes, O. L.

1970: Surficial geology maps; Geol. Surv. Can., Open File 26, scale 1: 125 000.

1972: Surficial geology map, Travallant Lake; Geol. Surv. Can., Open File 108.

Lau, J. S. O. and Lawrence, D. E.

1976: Review of Mackenzie Valley geotechnical data; in Report of Activities, Part A; Geol. Surv. Can., Paper 76-1A, p. 265-268.

Lawrence, D. E.

1974a: Geological review of geotechnical data Mackenzie Valley; in Report of Activities, Part A; Geol. Surv. Can., Paper 74-1A, p. 281.

1974b: Geological review of geotechnical data Mackenzie Valley; prepared for Mackenzie Highway Environmental Working Group, DIAND, 63 p.

1974c: Mackenzie Valley Geotechnical Data Bank; in Computer use in projects of the Geological Survey of Canada, eds. T. Gordon and W. W. Hutchison; Geol. Surv. Can., Paper 74-60, 100 p.

Pihlainen, J. A. and Johnston, G. H.

1963: Guide to a field description of permafrost for engineering purposes; Natl. Res. Coun. Can., Tech. Memo 79, 23 p.

Rutter, N. W., Boydell, A. N., Minning, G. V., and Netterville, J. A.

1973: Preliminary drafts of surficial geology and geomorphology maps, District of Mackenzie; Geol. Surv. Can., Open File 158, scale 1: 125 000.

Project 740062

John L. Luternauer
Terrain Sciences Division, Vancouver

Examination of the lithologic character of cores collected along the tidal flats of the Fraser River delta front (Luternauer, 1976) is still in progress. Reports on the following topics have been completed: (a) historical variations in the metallic ion content of Fraser Delta tidal flat sediments (contract to Department of Geological Sciences at the University of British Columbia), (b) preliminary assessment of the possible responses of the Fraser Delta slope to loading, wave pressures, and seismic disturbances (research agreement with Department of Civil Engineering, University of British Columbia) and, (c) preliminary assessment of historical morphologic changes on the Fraser Delta tidal flats (research agreement with the Survey Department at the British Columbia Institute of Technology).

A detailed inventory of the relief on the Fraser Delta slope was carried out as an aid to the interpretation of local patterns of sedimentation (Luternauer, 1976) and to make available additional information on the responses of the slope surface to local erosional/depositional regimes.

The echo sounding records examined for this purpose (Fig. 35.1) were produced during a revisory

survey of the slope performed by the Canadian Hydrographic Service in 1974. Over much of the slope, tracklines are 75 m apart and nowhere are more than 150 m apart.

The presence of relatively few submarine canyons on the slope has been noted earlier (Luternauer, 1976). The present report is concerned with all other relief not represented by these continuous channels.

On the whole, this relief is subdued (Fig. 35.2). In fact, over much of the slope no relief is apparent. Most striking relief is evident off Roberts Bank and here occurs only within three isolated patches. Slope relief off Sturgeon Bank is notable only on that part just northwest of the Main Channel mouth.

In general, relief off Sturgeon Bank reflects the fact that much of the sea floor here is mantled with fine mud. In fact, the progressive decrease in relief to the north of Main Channel is matched by a decrease in mean size of sediments in the same direction (Luternauer, 1976). There is no apparent increase in relief off the mouth of North Arm, however, where sediment character is comparable to that off Main Channel.

Sediment discharged from the Main Channel mouth and swept north appears to be gradually burying relict

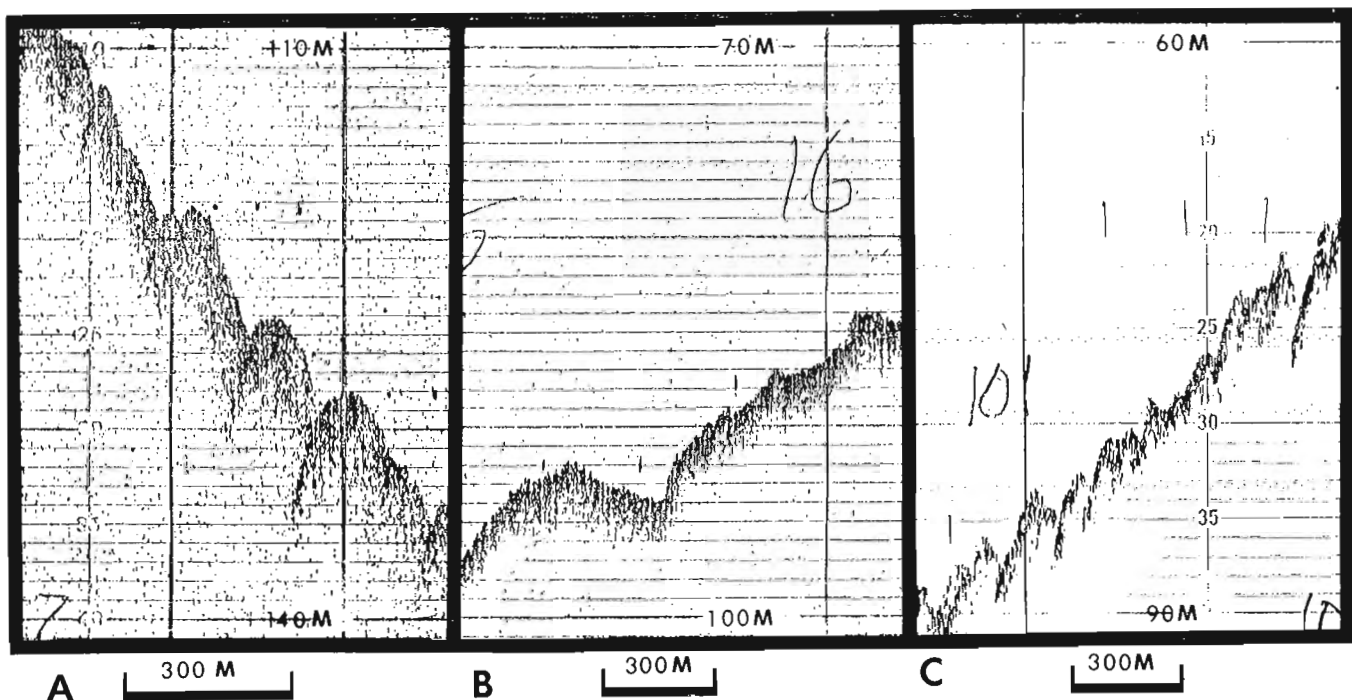


Figure 35.1. Echo sounding records (provided by the Canadian Hydrographic Service) illustrating the character of the Fraser River delta slope morphology at sites having highest relief. In all cases tracklines are oblique to the dip of the slope. Section A lies off the mouth of Main Channel, section B off central Roberts Bank, and section C off southernmost Roberts Bank (see Fig. 35.2).

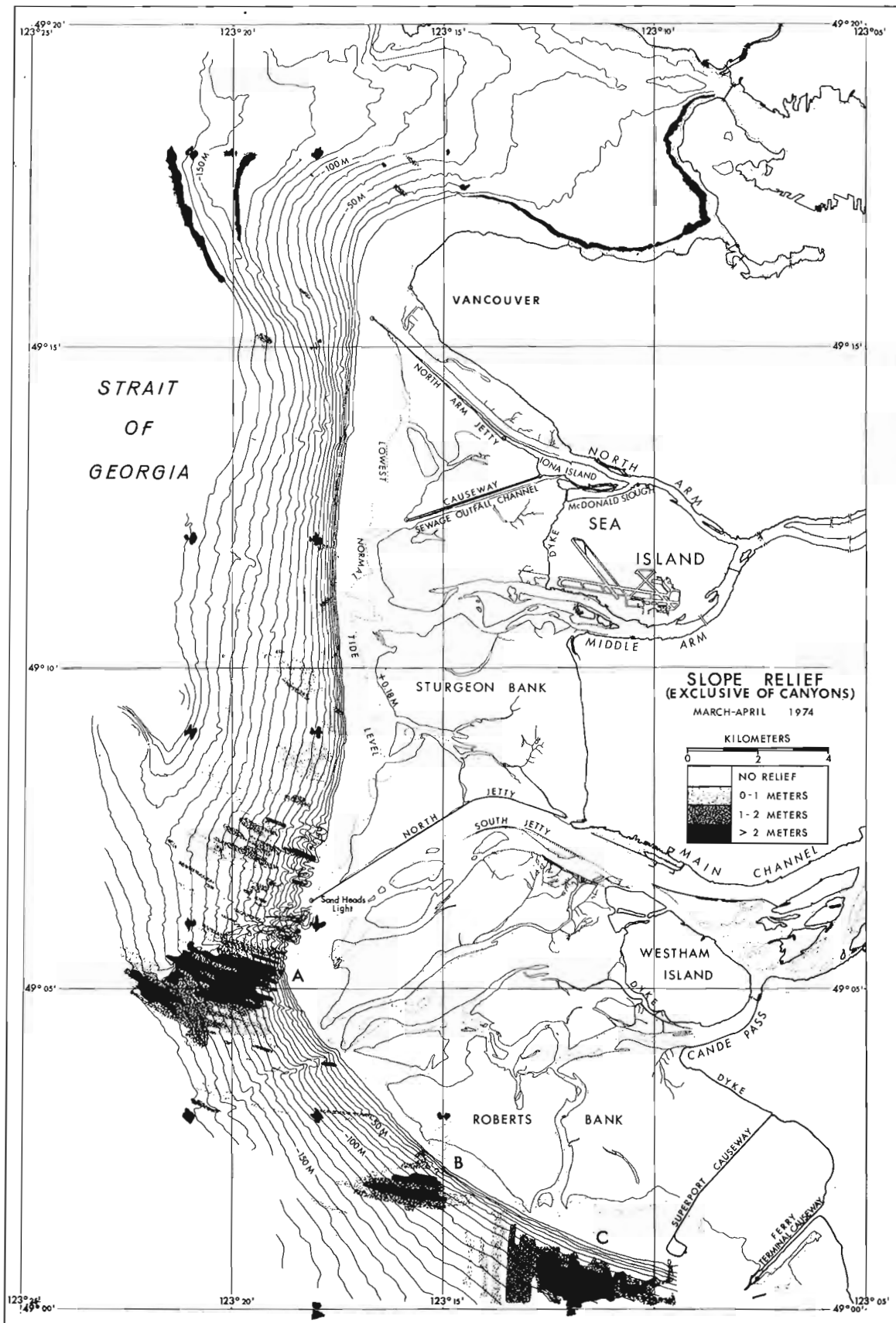


Figure 35.2. Maximum relief on the Fraser River delta slope (exclusive of canyons).

submarine canyons just northwest of the Main Channel mouth. These were formed when the flow of Main Channel was unobstructed by North Jetty and the Fraser disgorged its sediments to the north of Sand Heads Light. There is also evidence that fine muds, swept north in suspension from Main Channel and west from Middle Arm, almost entirely have concealed a canyon formed on the slope possibly when discharge from distributaries crossing Sturgeon Bank was higher and/or carried coarser sediment.

The patch of high relief off Main Channel (Figs. 35. 1A and 35. 2) may well represent a network of finer scale submarine tributary canyons that serve as conduits of coarser sediment which is discharged during the freshet. This zone terminates abruptly to the north along the Main Channel submarine canyon but to the south is not bounded by a distinct physiographic feature.

Although freshet-related sedimentation likely affects the slope between patches A and B in Figure 35. 2, sediment supplied in this fashion may not be coarse enough to permit the generation of features evident in patch A.

Patches of high relief B and C (Figs. 35. 1A, B, and 35. 2) lie outside the zone into which significant amounts of fine sediment are deposited during the freshet (Luternauer, 1976) and thus are mantled with sand throughout the year. Area B is represented by a few widely spaced shallow valleys and ridges. Their origin is not readily apparent although they may represent incipient canyons and/or outcrops of more resistant, older units. The character of area C is somewhat comparable to that of A although the relief in the former area appears to be more irregular. In area C tracklines have an orientation closer to that of the dip of the slope than do the tracklines off Main Channel. Thus, the features evident in area C are more readily attributable to mass wasting than canyon erosion (Luternauer, 1976) although the possible role of bottom currents also should be investigated. Areas B and C suggest that, although muddy sediments may not reach or may not remain on the southern Roberts Bank slope, sand may be washed out from Canoe Pass

distributaries that cross the tidal flats (patch B lies just off one of the distributaries which is not evident from the topographic contouring on the flats but is clearly apparent on recent airphotos taken at very low tides) and may be dumped at the head of the slope. This sand in turn may be transported downslope by a network of canyons as is likely the case in area A and, possibly, in area B or by means of mass wasting as may be the case in area C.

Summary

A preliminary appraisal of the relief (exclusive of continuous canyons) on the Fraser Delta slope was carried out employing echo sounding records obtained by the Canadian Hydrographic Service. A constraint on the precision of this sort of inventory is that tracklines are not always normal to the strike of the slope and/or the features thereon.

Over much of the slope there is little or no relief. Significant relief (2 to 5 m) is apparent only on isolated segments of the northern, central, and southernmost slope off Roberts Bank. The gently rolling morphology (on a 1 to 3 degree slope) in these areas may be maintained by the freshet-related dumping of coarser sediment which subsequently is transported downslope along finer scale tributary canyons or incipient larger scale canyons and/or by mass wasting. Bottom currents in part may be responsible for the features or may alter features created by other mechanisms.

A planned side-scan sonar survey should clarify what the true sea floor surface texture is in the areas of relatively high relief and should contribute to our understanding of their origin.

Reference

- Luternauer, J. L.
1976: Fraser Delta sedimentation, Vancouver, B. C. ;
in Report of Activities, Part A, Geol. Surv.
Can., Paper 76-1A, p. 213-219.

GEOMORPHOLOGY OF SOME ARCTIC GULLIES,
BANKS ISLAND, DISTRICT OF FRANKLIN

Project 750079

Terry J. Day and Robert J. Gale¹
Terrain Sciences Division

Introduction

During a reconnaissance study of surface processes on Banks Island, District of Franklin (71° to 75°N, 116° to 126°W) cursory observations were made of a number of gully forms. According to the classification of

Leopold *et al.* (1963) these gullies are continuous features in that their runoff network begins in small rills which coalesce to form the main channel. Gully forms discussed here range from small features with V-shaped cross-sections to larger features over 1 km in length with U-shaped sections.



Figure 36.1

Aerial view of Gausse E gully located just west of four surveyed gullies. Note wide gravel bed. View is to north (GSC 166333).



Figure 36.2

Aerial view of Gausse B gully. View is towards north. (GSC 166360).

¹Department of Geography, University of Calgary, Calgary, Alberta.

Morphology



Figure 36.3. Aerial view of Gausse D gully. View is towards north. Note (1) the vegetated upper channel; (2) rapid development of active bed for no apparent hydraulic reason; (3) terrace-like remnant along west bank indicating renewed downcutting. (GSC 166359).

As integral parts of river networks, tributary gullies are ubiquitous features. The two sites chosen for this study covered both a variety of form and scale. The first site, called Soo, consists of three small, predominantly V-shaped gullies located on the east bank of a lake (73°17'N, 121°25'W). These gullies are aligned along an east-west axis and are degrading through sands and gravels of an old meltwater channel (J. S. Vincent, pers. comm.). The second site is situated along the southern banks of "Gausse River" (73°22'N, 122°20'W) where four gullies were studied. Their alignment is north-south and they debouch directly into "Gausse River". These gullies are forming in a broad alluvial plain where the relative relief is determined by the depth of degradation of "Gausse River". In addition to data for these seven gullies, supporting information, principally in the form of photographs, is offered for a wide range of forms and locations.

Plan form geometries are variable, ranging from long, sinuous, wide-bottomed gullies (Fig. 36.1, Gausse E; Fig. 36.2, Gausse B; Fig. 36.3, Gausse D) to more typical gully forms, such as shown in Figures 36.4 (Soo Site), 36.5, 36.6, 36.7, and 36.8. Gullies in Figure 36.8 have formed along frost cracks. Some gullies at this site have headwalls common to discontinuous gullies but have slopes greater than the original surface. Headwall retreat results from thermal erosion of the exposed ice wedge. The effect of frost-crack distribution on the topology of gully networks is also shown in Figure 36.5. Other networks appear to be predominantly fluvial features (cf. Figs. 36.4 and 36.6).

The longitudinal slopes of the seven surveyed gullies range from 0.0063 to 0.1385 (Table 36.1). The relationship between gully length and slope is an exponential one, with the best fitting equation.

$$S = 11 L^{-1.05} \quad (1)$$

where S is slope and L the channel length. This equation explains 96 per cent of the variance. The strength of this relationship implies a continuity of form. Data from gullies in the Rocky Mountains (Heede, 1970) are also shown with the Banks Island data in Figure 36.9. The former data show no such continuity.

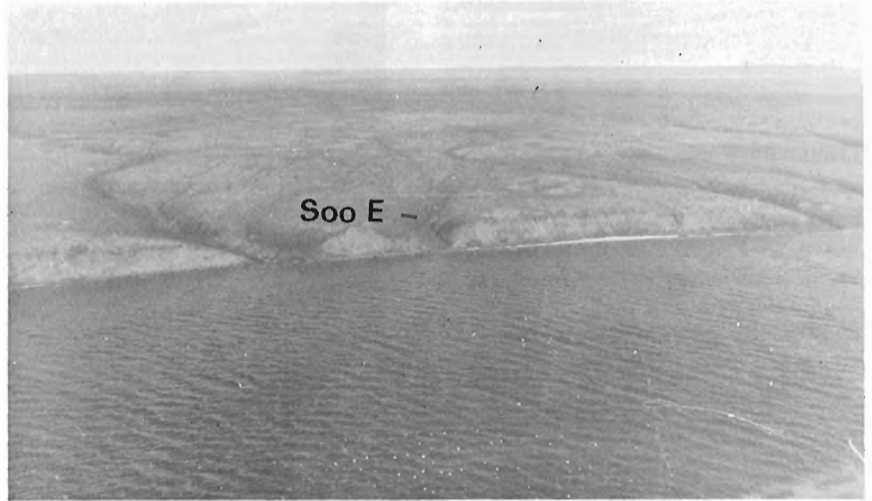
The long profiles are shown in Figure 36.10. For comparative purposes the upper origins of all profiles are made coincident by the following procedure: (height - lower end of the profile)/total height differential in the profile. This procedure results in a dimensionless height with all profiles having a common origin (0.0, 1.0). A variety of profile shapes is shown in Figure 36.10. Four profiles, Soo E, F, G, and Gausse B are linear, with regression equations explaining 99 per cent of the variance in each case. Generally, stream profiles are concave upward, but the concavity of gully long profiles has been found to be too weak to be expressed by curvilinear equations (Brice, 1964; Heede, 1970). Heede found that the lower end of gully profiles showed a slight concavity.

Table 36.1
Length and Slope Data of Gullies

Site	Length m	Drop m	Slope
Gausse A	274	7.1	0.0259
B	952	6.0	0.0063
C	455	6.4	0.0141
D	1210	10.9	0.0090
Soo E	65	9.0	0.1385
F	284	11.1	0.0391
G	104	9.2	0.0885

Figure 36.4

Aerial view of Soo Site; view is towards east. Note gullies are well vegetated with only active area confined to gully channels.



In the Banks Island features, however, the lower portions are convex as the gully exits into either a lake shore or river bed, forming small alluvial fans (cf. Fig. 36.7).

Two other profile shapes are evident. Gausse C profile exhibits a strongly parabolic shape ($h = 0.96 + 0.00019L - 0.0000464L^2$, where h is the dimensionless height). A possible explanation could be the renewed downcutting evident in the lower 20 to 30 m (Fig. 36.11). The remaining two profiles, Gausse A and D, have stepped profiles. Leopold *et al.* (1963, p. 450-451) have shown similar profiles for discontinuous gullies and explained them as slope adjustments where width is restricted. Although the Gausse gullies are not discontinuous, their steps may be due to local readjustments caused by renewed downcutting. The terrace-like remnant along the west side of Gausse D (Fig. 36.3) is evidence for this renewed downcutting.

The primary difference between V- and U-shaped cross-sections is the presence of wide, nonvegetated, nonchannelled alluvial beds as seen in Figures 36.1 to 36.3. In general terms, the difference between these two shapes must be in the predominant erosion direction; vertical erosion must dominate in the V-shaped sections whereas lateral erosion must dominate in the other. Although small gullies tend to be V-shaped and large ones U-shaped, the transition from one shape to another is not simply continuous with scale. Gullies of the same dimensions as Soo F and G have been observed to have U-shaped geometries. Some geometric properties of the surveyed gullies are listed in Table 36.2.

All Gausse sections are U-shaped (Figs. 36.12 and 36.13), although the uppermost sections are more difficult to describe. The strongest downslope patterns are in the increasing incision (ultimately determined by the river or lake bed) and increasing cross-sectional area, which, of course, is related to incision. Weaker trends indicate increasing top and bottom width downslope. The bottom width refers only to the alluvial



Figure 36.5. Aerial view of gullies along north bank of the westerly flowing Bernard River on western Banks Island. Note that the gullies tend to follow frost-crack patterns. There does not seem to be any preferential distribution of snow within the gullies.

Figure 36.6

Aerial view of gullies along north bank of Bernard River several kilometres upstream of Figure 36.5. Photo taken after spring flood; snow accumulations are still present. East-facing slopes appear to be steepest. (GSC 166920).

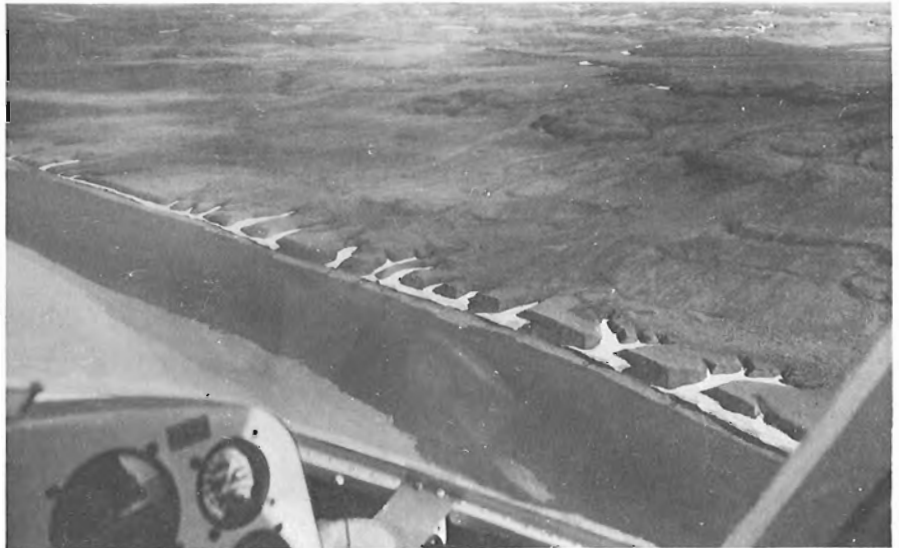


Figure 36.7

View of east bank gully of northerly flowing Thomsen River in eastern Banks Island. The north-facing slope is not only the steepest but is very active. Note the stable upper portions of the gully as well as the small fan on the Thomsen River bed.

Figure 36.8

Aerial view of east bank gully on Thomsen River. Topology of gully network is strongly related to frost-crack pattern. (GSC 166816).



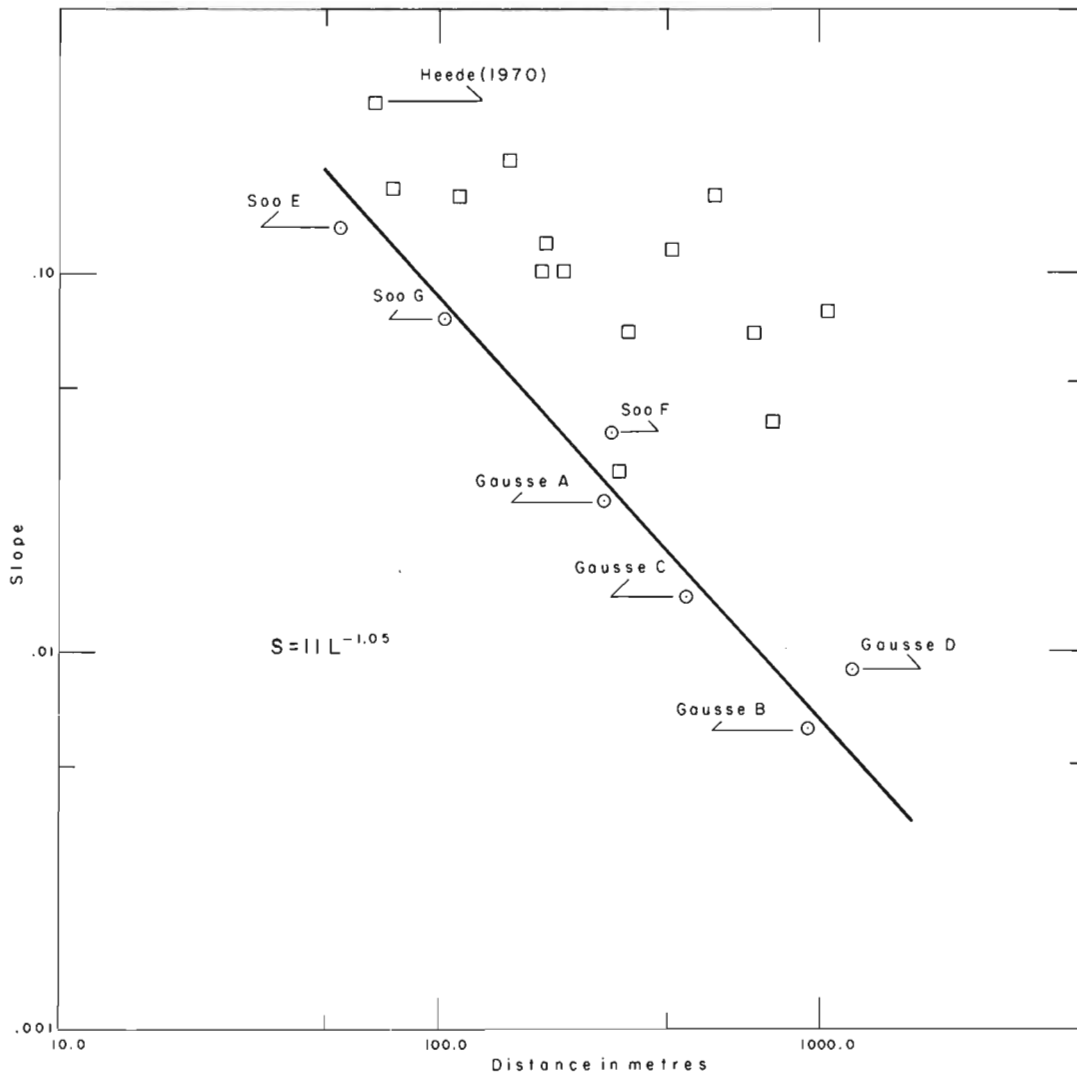


Figure 36.9. Logarithmic plot of gully slope versus gully length for the Gausse and Soo sites. Data from Heede (1970) also are shown.

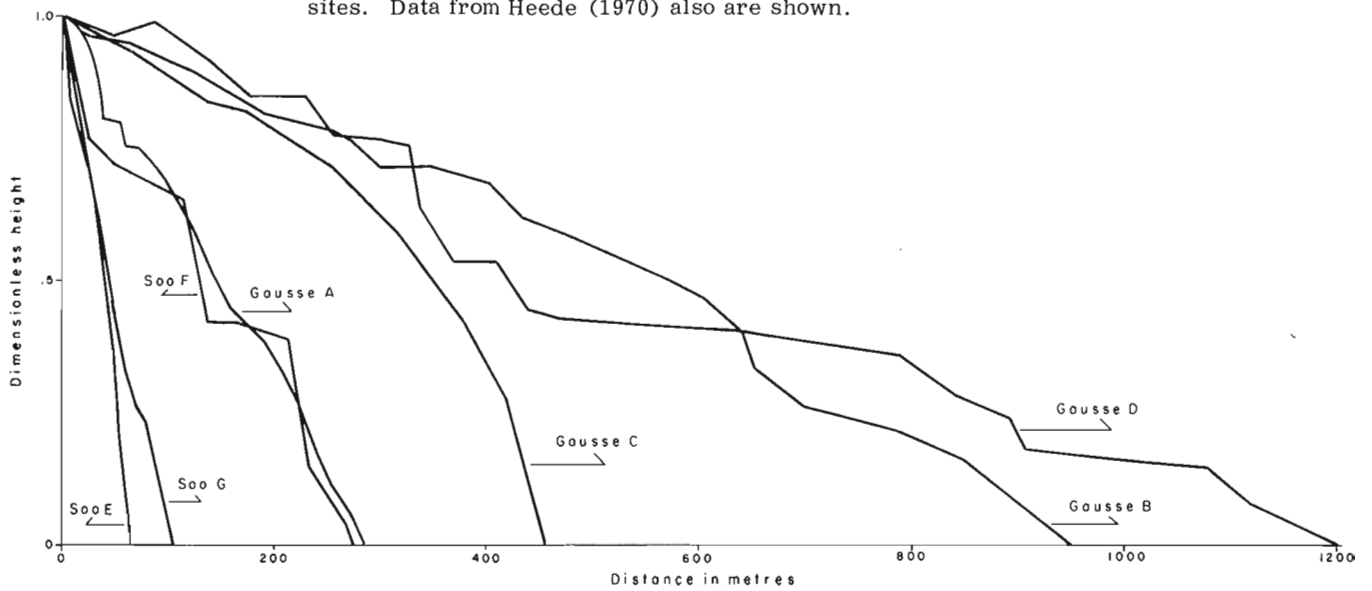


Figure 36.10. Comparison plot of gully long profiles.

Table 36.2. Geometric Properties.

Site and Cross-section	Location on Long Profile m	Top Width m	Bottom Width m	Incision Depth m	Width/Depth Ratio	Area m ²	Mean Bank Angles Slope Facing		Maximum Bank Angles Slope Facing	
							West	East	West	East
Gausse A 1	25	4.0	1.9	0.4	10.0	0.8	6.7	4.4	16.6	10.8
2	*	13.2	6.2	2.0	6.6	16.9	12.6	12.2	28.1	14.0
3	164	18.8	7.0	3.8	4.9	44.2	22.0	19.1	34.6	40.3
4	*	23.8	10.0	5.0	4.8	84.3	21.1	15.0	37.8	37.8
Gausse B 1	*	5.8	1.5	0.5	11.6	1.7	6.1	7.5	25.4	11.5
2	*	44.2	34.2	2.3	19.2	85.5	5.2	18.3	22.5	44.2
3	274	24.5	6.8	2.7	9.0	43.1	11.1	15.5	18.4	43.2
4	605	23.8	6.8	2.7	8.8	43.3	18.3	13.4	33.2	16.1
5	860	31.2	14.6	2.6	12.0	170.1	23.2	10.3	21.5	15.0
Gausse C 1	*	*	*	*	*	*	2.4	3.3	5.7	6.5
2	251	16.0	8.8	0.9	17.7	22.0	5.4	9.2	11.0	14.2
3	377	21.5	8.2	2.4	9.0	46.8	7.7	6.2	14.7	18.8
Gausse D 1	4	34.2	4.8	1.2	28.5	25.2	3.0	5.5	6.8	7.5
2	330	34.4	8.5	2.7	12.7	66.1	7.9	13.7	14.1	21.4
3	444	43.8	20.2	4.9	8.9	148.2	16.9	11.7	32.2	24.5
4	846	50.6	24.0	5.4	9.3	198.3	14.7	18.6	39.5	30.0
5	1122	63.0	19.0	6.7	9.4	292.7	13.1	17.5	20.4	62.7
Soo	E 1	15.0	-	0.7	21.4	8.4	North 7.7	South 4.4	North 27.0	South 17.5
2	*	18.7	-	4.6	4.1	57.3	25.2	13.3	54.6	21.3
Soo	F 1	8.0	-	1.3	6.2	4.4	10.5	8.6	43.2	17.9
2	*	7.0	1.5	1.6	4.4	6.9	18.2	17.3	34.8	47.2
3	*	23.0	2.5	3.0	7.7	25.7	13.3	9.4	40.3	28.2
Soo	G 1	8.0	-	0.5	16.0	2.1	7.2	4.1	10.7	5.5
2	*	18.0	-	3.5	5.1	29.5	19.2	14.1	34.2	25.4

* unmeasured

- V-shaped gullies, no distinct bottom width



Figure 36.11

Aerial view of Gausse C; view is towards south. Note the active channel in the lower portions. (GSC 166330).

bed and can develop very quickly for no apparent hydraulic reason as in the upper portion of Gausse D (Fig. 36.3). With the exception of cross-sections 2 and 3 of Soo F, the Soo sections are V-shaped (Fig. 36.14).

Most cross-sections possess an asymmetry and two methods were adopted to test for consistent forms. Both mean slope angles, i.e. the ratio of profile height to the ground length of slope, and maximum slope angles, i.e. the slope of the steepest section of the profile of more than 1.5 m in length (Kennedy and Melton, 1972) are listed in Table 36.2). These data indicate that there is no preferred asymmetry in the north-south oriented Gausse gullies, but the Soo gullies predominantly have their steepest slopes facing north (gully axis east-west). Bronhofer (1957) observed similar features on Southampton Island, Northwest Territories but found that the south-facing slopes generally were the steepest. He explained this asymmetry by longer acting gelifluction processes on the north-facing slope. French (1971) showed that valleys in the Beaufort Plain of northwest Banks Island have their steepest slopes facing the southwest and advanced the same argument as Bronhofer for their development. Even though the Soo data are limited, the predominance of steeper north-facing slopes is real and clearly shown in Figure 36.4 for Soo E and the gully immediately to the north. The most probable cause of this asymmetry is preferential snow storage caused by prevailing winter winds.

Channel development within the gullies is minor. In the Gausse gullies well defined channels are found only where flow is confined against a bank or at the gully mouth where channel slope increases over the fans. Minor levee-type sedimentary deposits probably result from channelization of the snow-filled bottoms. Poorly developed bars, such as seen in Figure 36.15 are present in the lower portions of Gausse B. The sporadic distribution of stagnant water shown in Figure 36.15 illustrates the poor channel development.

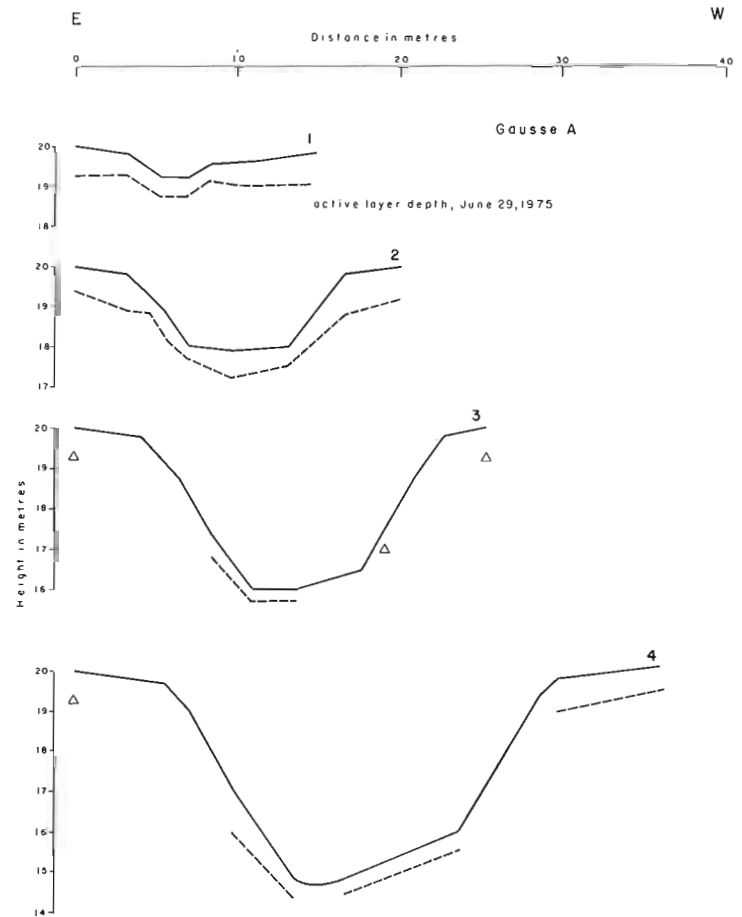


Figure 36.12. Surveyed cross-sections of Gausse A (solid line) including mean active layer depths (dashed line). These depths are joined where readings are continuous and marked with a triangle where only separate measurements exist.

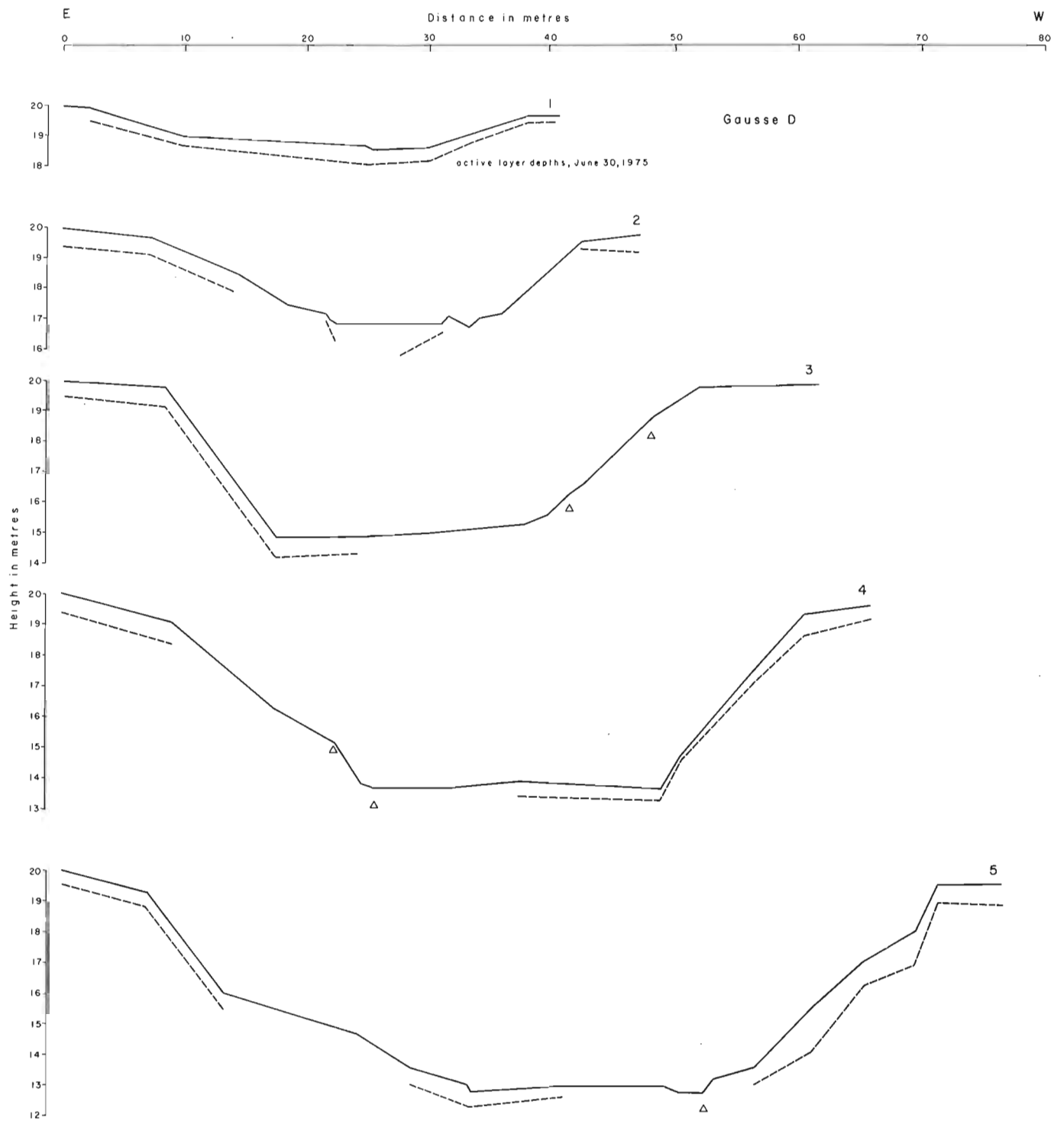


Figure 36.13. Surveyed cross-sections of Gausse D (solid line) including active layer depths (dashed line). These depths are joined where readings are continuous and marked with a triangle where only separate measurements exist.

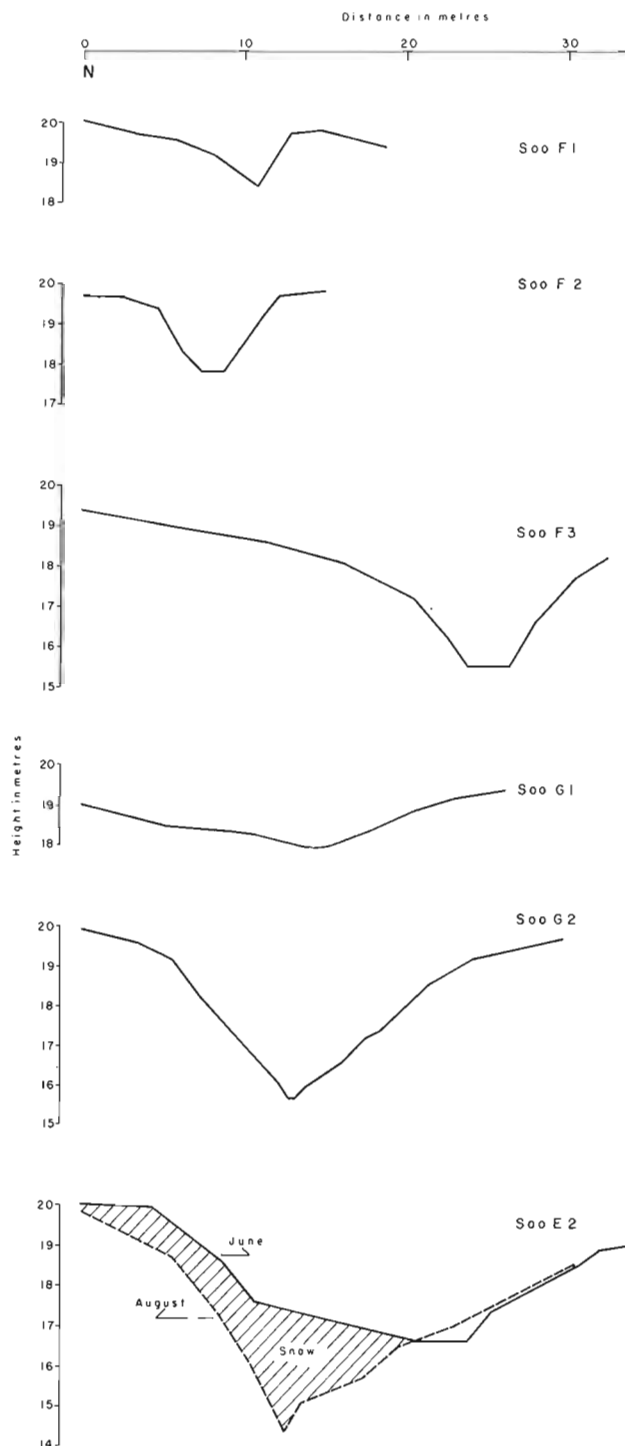


Figure 36.14. Surveyed cross-sections of Soo gullies.

Minor amounts of chaotic sediments were noted on some beds. These deposits appear to be the result of sediment deposition on top of snowbanks with subsequent redeposition upon melting. Sediment transport seems to occur in sheet form. Lines painted across the bed of a gully in the Gausse site in July 1974 indicated, when rechecked in 1975, that almost the entire bed had moved downstream, with individual particle movements up to several metres.

Grain-size data are available only for Gausse B and D, where surface samples were collected along a transverse line grid across the bed at each cross-section. The resulting grain-size distributions for Gausse B are shown in Figure 36.16. These distributions have characteristics common to surface fluvial gravels in that coarser size fractions dominate. When exposed to mild shear stresses, gravel mixtures lose their fines through selective transport until a stable armour coat eventually develops. The beds of the Gausse gullies were certainly armoured, although with loose packing. Downstream grain-size characteristics for Gausse B and D are shown in Figure 36.17, where the



Figure 36.15. Aerial view of lower portion of Gausse B showing poorly developed gravel bars. View is towards north (GSC 166335).

median grain size is shown to decrease downchannel. This decline in particle size is most probably a result of selective transport.

Processes

In a periglacial environment many factors influencing erosion and transportation by fluvial processes are similar to those in more temperate regions; however, some significant differences do exist. On Banks Island winter winds cause preferential accumulations of snow in topographic lows, such as the gullies studied here. As melt begins, small channels are formed on the snow fill in a similar manner to that shown in Figure 36.18. Slushflows caused by the decaying snow pack are common. As melt progresses the snow fill decays in place or is eroded around the channel (Fig. 36.19). Eventually the channel degrades through the snow fill until the gully bed is reached. By this time the snow fill is in advanced decay. Although no measurements are available, the gravel bed must still be frozen and as the flow reaches it, flow energy is expended against the less resistant snowbanks leading to an undermining of the snow fill. Sheet sediment flow probably is initiated during this period and vertical scour limited by frozen sediment. As runoff ceases, the gravel bed is exposed as are the bank sections from which the snow fill has been removed (cf. Fig. 36.20). The four main stages of this process are shown schematically in Figure 36.21.

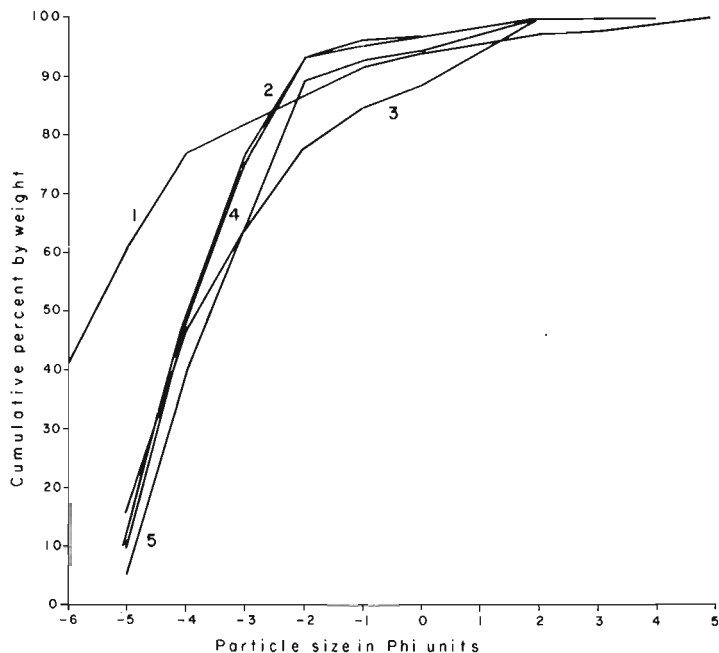


Figure 36.16. Grain-size distribution of surface samples from Gausse B. Samples identified by cross-section number.

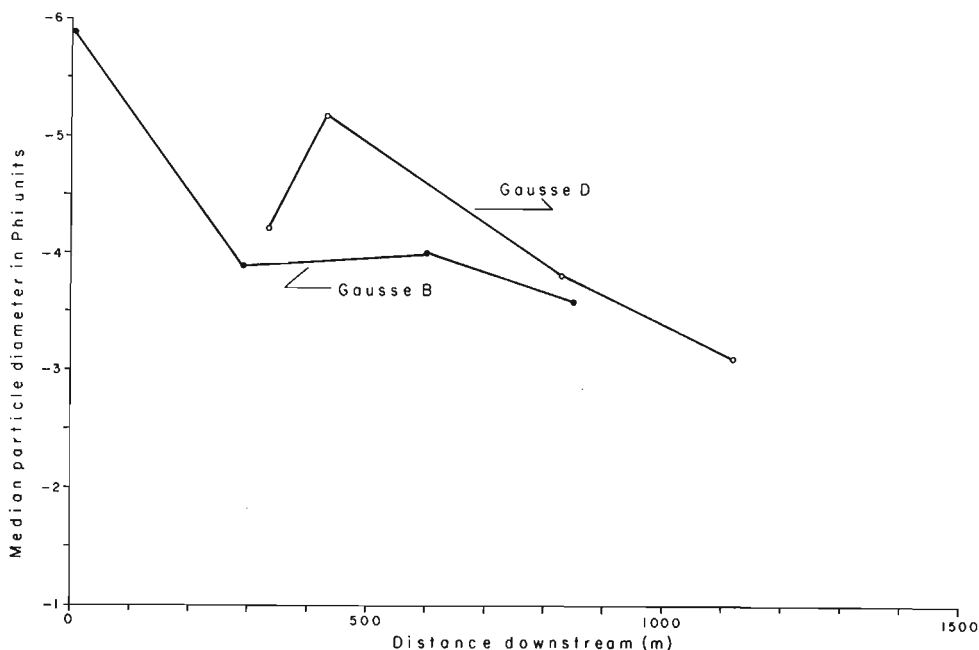


Figure 36.17
Downstream grain size characteristics for Gausse B and D.

With the recession of fluvial activity, gully geometry continues to be modified by periglacial processes. Solifluction processes are favoured either through microclimates existing upon differently exposed slopes or through the remnant snowbanks with their resultant sapping and soil saturation. A solifluction lobe on the west-facing bank of Gausse B is shown in Figure 36. 22. Block slumping also was noted along the east bank of Gausse A. The dimensions of these slumps seemed directly related to the spacing of frost cracks (up to 6 m in length).

Observations at Soo E showed that active layer depths developed from 30 cm on June 15 to 109 cm by July 15, 1975 and then increased only slightly to 111 cm by August 11. These measurements were taken in the upper portion of the south side of the lower cross-section. Active layer development followed a

similar pattern in the north bank. Depths on the extremities of the upper cross-section followed the same pattern but the maximum depths were 10 to 20 cm shallower. The shallowest depths were measured within the gully bottom, reaching only 39 cm by August 11 for the channel portion of the lower section. These shallow active layer depths were probably the result of the late season recession of the snow fill. Active layer depths for the Gausse gullies were measured only once during the study period of June 29 to August 1, 1975. Those depths measured for Gausse A and D are shown in Figures 36. 12 and 36. 13 respectively. The large variability among the profiles (11 to 106 cm) is a product of material, surface cover, and aspect but also is probably due to the variability in the location of remnant snowbanks. Insulation by snow is the most logical explanation for the variability of thaw depth across the various gravel beds of the Gausse gullies.



Figure 36. 18

Early runoff over a snow-filled gully. (GSC 166656).

Figure 36. 19

Advanced snow-fill decay during runoff in gully. (GSC 166494).





Figure 36. 20. Aerial view of Gausse D (July, 1974) at end of runoff period showing residual snowbanks mainly on west bank. (GSC 203025-J).

Summary

Geomorphologic studies of gully forms on Banks Island indicate that they may represent a continuum in that their slopes appear to follow an exponential relationship with gully length, and that smaller V-shaped gullies develop towards larger forms with a dominant U-shaped geometry. Their dimensions seem to be determined by both fluvial and periglacial processes, with the former operative only during the short runoff period and the latter probably dominating development in the larger gullies. Although the data presented here are limited, they are sufficiently consistent to permit a discussion of gully forms and processes in the Arctic.

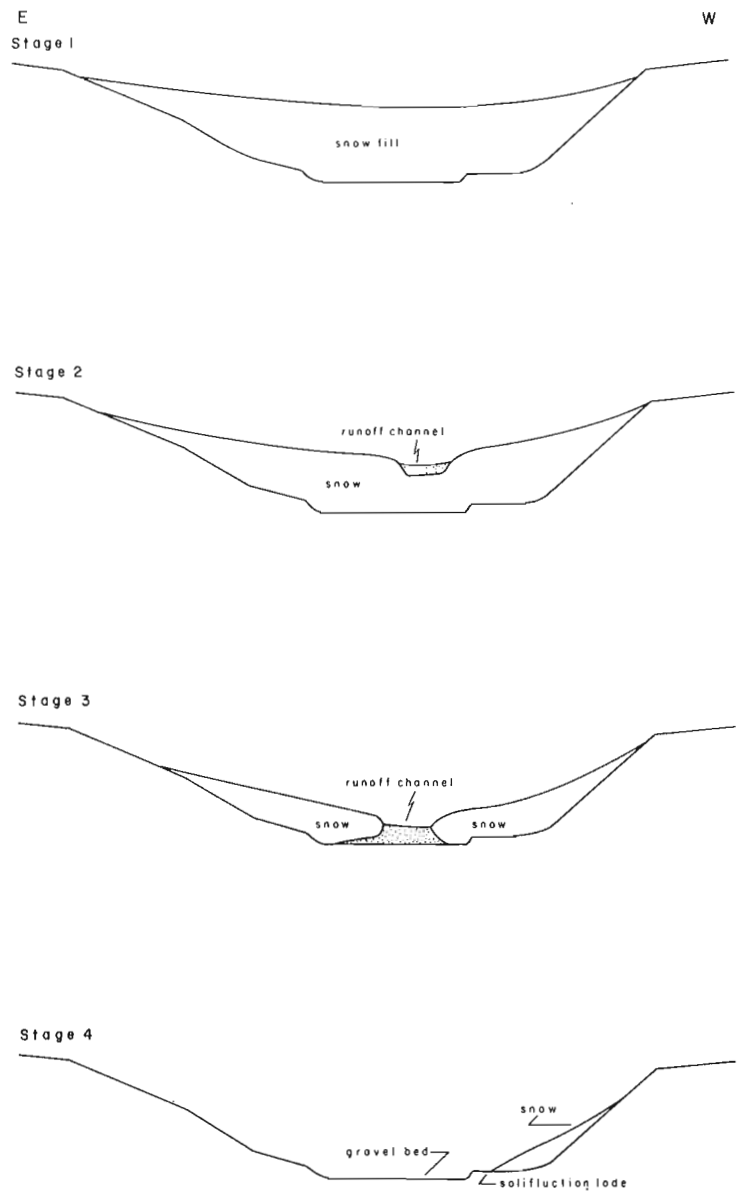


Figure 36. 21. Schematic diagram of processes acting in a snow-filled gully.

Figure 36.22

Solifluction lobe on east bank of Gausse B (Courtesy R. J. Gale)



References

- Brice, J. C.
1964: Channel patterns and terraces of the Loup Rivers in Nebraska; U. S. Geol. Surv., Prof. Paper 422-D, 41 p.
- Bronhofer, M.
1957: Field investigations on Southampton Island and around Wager Bay, Northwest Territories, Canada, 1956; The RAND Corp., Mem. 1936, Santa Monica, 294 p.
- French, H. M.
1971: Slope asymmetry of the Beaufort Plain, northwest Banks Island, N.W.T., Canada; Can. J. Earth Sci., v. 8, no. 7, p. 717-731.
- Heede, B. H.
1970: Morphology of gullies in the Colorado Rocky Mountains; Int. Assoc. Sci. Hydrol., Bull., v. XV, no. 2, p. 79-89.
- Kennedy, B. A. and Melton, M. A.
1972: Valley asymmetry and slope forms of a permafrost area in the Northwest Territories, Canada; in Polar Geomorphology eds. R. J. Price, and D. E. Sugden; Inst. Br. Geogr., Spec. Publ. no. 4, p. 107-122.
- Leopold, L. B., Wolman, M. G., and Miller, J. P.
1963: Fluvial Processes in Geomorphology; W. H. Freeman and Company, San Francisco, 522 p.

Project 750079

Terry J. Day and John C. Anderson¹
Terrain Sciences DivisionIntroduction

As part of a general reconnaissance of surface processes undertaken on Banks Island during May to August 1975, observations on the occurrence and characteristics of river ice were obtained with a view to assessing, in so far as possible, consequences of

jamming, scour, and channel stability. The majority of observations are concerned with Thomsen River (Fig. 37.1); however, limited supporting information from other rivers is discussed. Observations presented here are, of course, only for one breakup period, but relict ice features offer some substantiation.

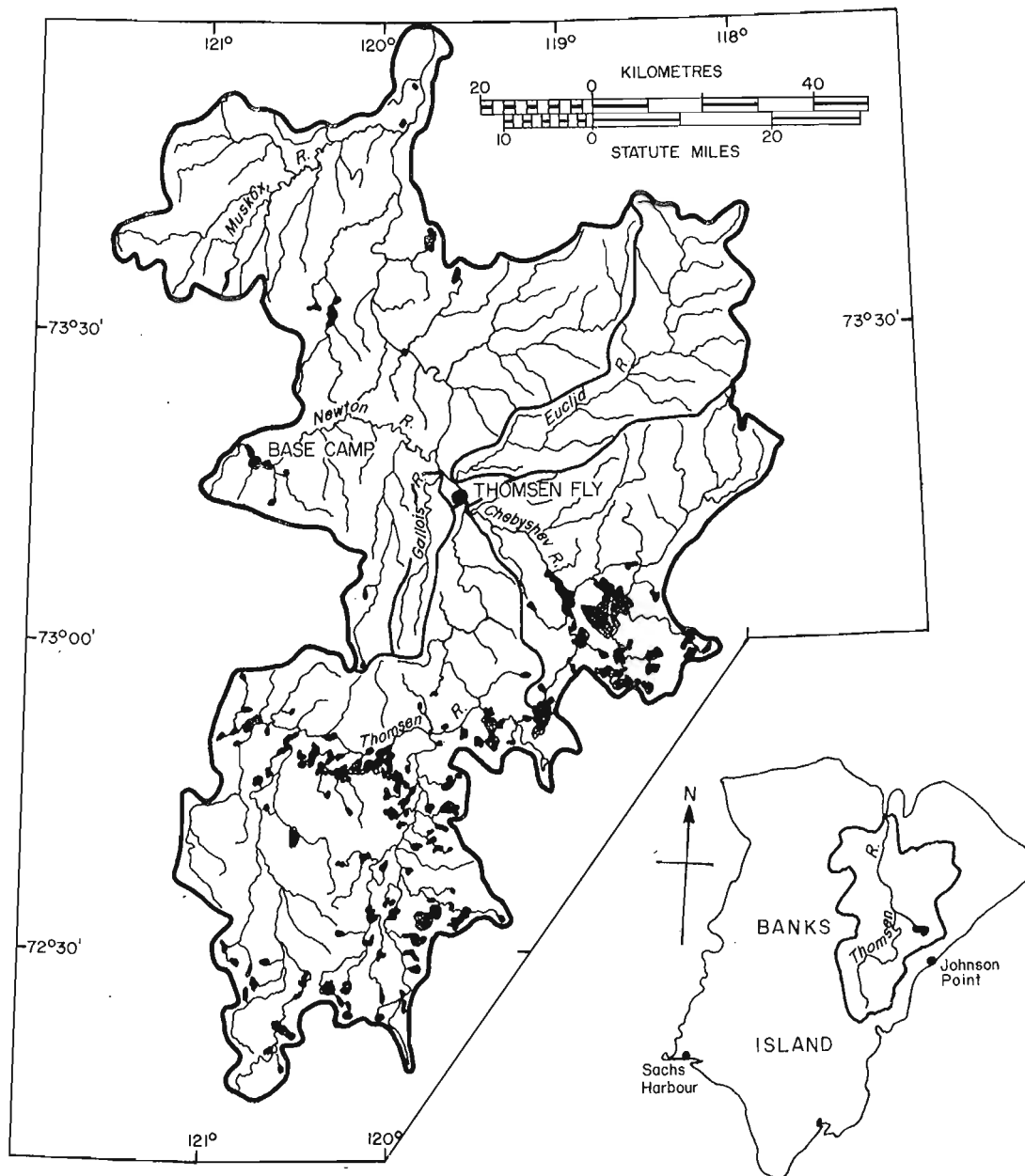


Figure 37.1. Location map of Banks Island and Thomsen River basin.

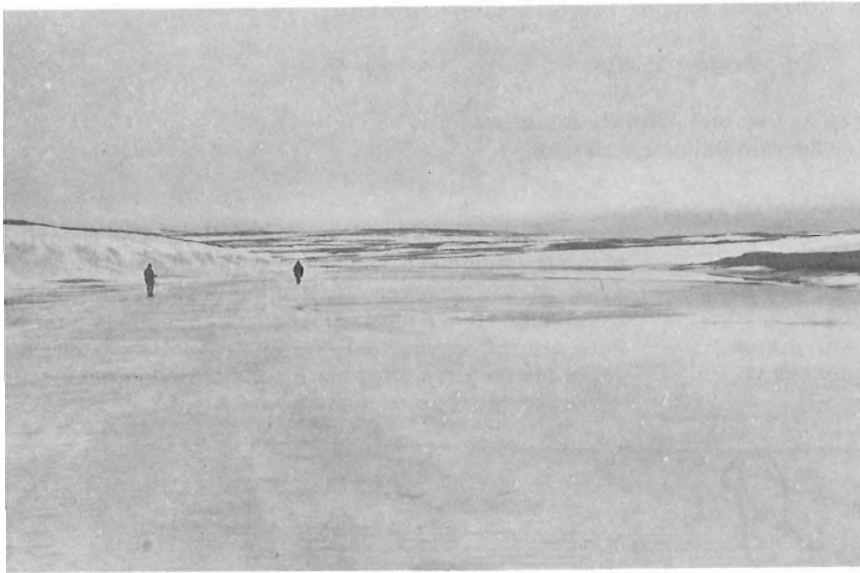


Figure 37.2

Thomsen River bed at "Thomsen Fly" looking downstream to the north. Note ponding of meltwaters. (GSC-166556).

Figure 37.3

Thomsen River at "Thomsen Fly" in early June. View is towards north. Note snow banks and width of ice-filled channel. (GSC-203025-B).



Banks Island, fourth largest in the Arctic Archipelago, lies between 71° and 75° N, and 116° and 126° W. Interpretation of meteorological records indicate that the thaw season at Sachs Harbour (Fig. 37.1) can begin as early as May 27 and as late as June 23 (based on 24 years of records). The length of thaw season for Sachs Harbour can range from 68 to 121 days, with a mean duration of 90 days. Thaw season is defined here as beginning on the first date when a sequence of days with mean temperature above 0°C was not followed by a sequence of the same or greater length with mean temperatures less than 0°C (Dingman, 1971, p. 22). Thompson (1963) showed that the thaw season on northern Banks Island can be expected to end about a week or two earlier than at Sachs Harbour. Thompson also indicated that duration of the thaw season decreases with increasing latitude, with a mean duration of approximately 80 days for northern Banks Island.

Thomsen River Observations

Thomsen River, largest on Banks Island, flows northward for 170 km to Castel Bay which opens into M'Clure Strait. The principle observation site was located at "Thomsen Fly" camp ($73^{\circ}14'N$, $119^{\circ}32'W$, Fig. 37.1) where hydrologic studies on several basins were undertaken (Anderson and Durrant, 1976). Hydrologic observations began at the beginning of June 1975 and continued until mid-August.

Pre-breakup conditions on Thomsen River at "Thomsen Fly" are shown in Figures 37.2 and 37.3. Figure 37.2 is a view downstream (north) and shows ponding of meltwater; Figure 37.3 is an aerial view of this site. Both photos were taken on or about June 2, 1975. Width of the ice at "Thomsen Fly" ranged from 44 to 77 m, about 1/3 to 1/2 the channel bed width. Ice thickness can be related to channel water depth at

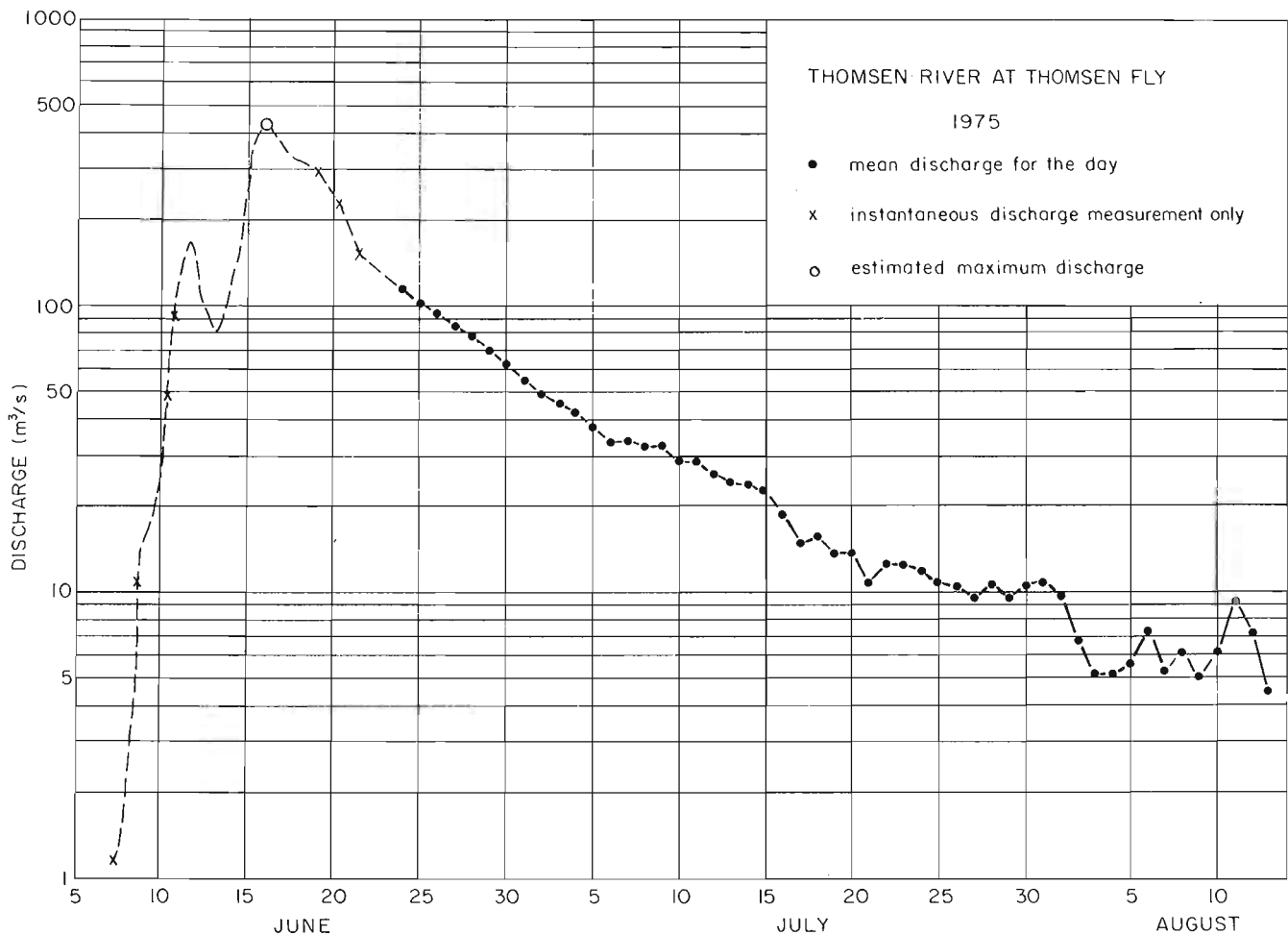


Figure 37.4. Hydrograph for Thomsen River at "Thomsen Fly", 1975.

freezeup and the air temperature regime over the winter. At "Thomsen Fly" pools were observed to be up to 2.7 m deep. Although ice thicknesses were not measured prior to breakup, a thickness of 2 m was observed for a lake 60 km to the west. Even though conditions for ice development differ between rivers and lakes, this 2 m depth is probably of the correct order of magnitude. These data suggest that some pools in the "Thomsen Fly" area may not freeze to the river bed. French (pers. comm. 1975) has evidence that some pools in the lower Thomsen do not freeze to the bottom. The largest occurrences are restricted to the main rivers, such as the Thomsen, that possess major channel storage associated with well developed pool and riffle sequences.

Thomsen River exhibits a typical arctic nival regime (Fig. 37.4) with the peak flood produced by snowmelt runoff. At "Thomsen Fly" runoff began in early June with some ponding over ice occurring from June 3 to 5. Water temperatures are shown in Figure 37.5 with cumulative, degree-day, air temperature values for the breakup period. As the pools increased in volume, flow was initiated with

broad channels forming in the ice. By June 7 thin ice began lifting from the riffles. As these ice pans moved downstream they grounded in the shallows or on the next riffle. Flow during this period increased from 1.2 m³/s on June 7 to about 11 m³/s on June 9 (instantaneous discharges). As flow increased, ice lifted from the pools in irregular pans of various size. The major pan shown in Figure 37.6 is about 20 m wide, 60 m long, and about 1 m thick. The largest pans originate in the pools, and their dimensions are limited by pool geometry. Some pans carried various amounts of sediment, indicating ice plucking of bed sediments.

In moving downstream these pans grounded on riffles. The resulting backwater effects were minor as water elevations were limited by the height of the grounded jam, usually only the single thickness of the ice (rafting was very minor). Upstream effects also were limited as the pool and riffle sequence still dominated flow geometry. Any increase in water depth probably would not be transmitted more than about two pool lengths upstream. Backwater effects also were limited because the observed jams did not extend across the entire flow section and only partial

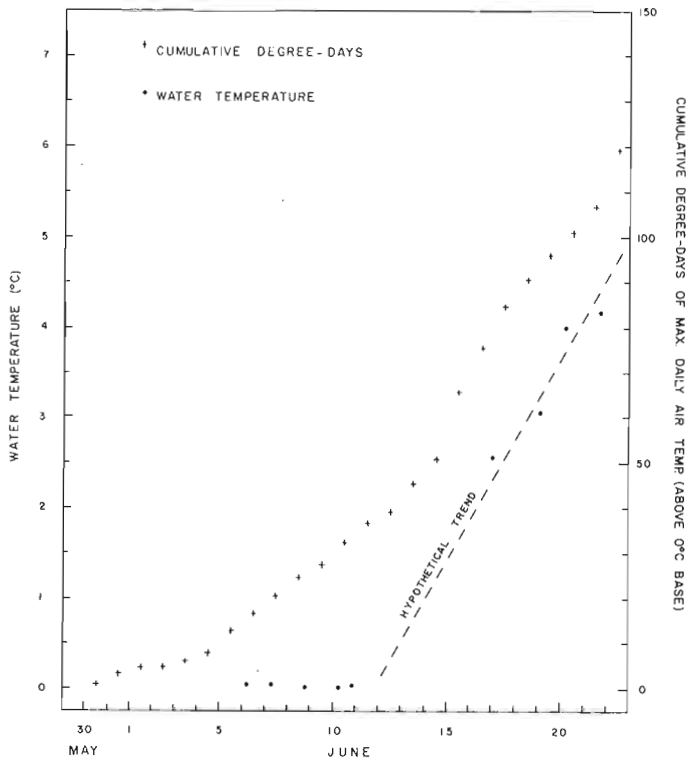


Figure 37.5. Thomsen River water temperatures and cumulative daily maximum air temperatures at "Thomsen Fly" during and immediately following river breakup.

blockage of flow resulted. Information on jam duration is limited; however, as an example, ice surfacing from a pool near "Thomsen Fly" jammed on a downstream riffle and remained there for 12 hours. Grounding and subsequent floating of ice-pans also was induced by stage fluctuations during the rise to peak flood.

As runoff progressed, large pans disintegrated into smaller pans (Fig. 37.7). Disintegration by candling was common; a slush load developed in the river from candling debris and calving of snowbanks. By about June 13, flow had increased to over 100 m³/s. The number frequency, and size of ice pans had decreased considerably, as had the slush load. By the occurrence of peak flow (June 16, estimated 425 m³/s) the ice had subsided considerably.

Ice run conditions in the lower Thomsen are shown in Figure 37.8 (June 11). Floating ice forms a long (several km) "stringer", shown in the upper right corner. The width of this ice is approximately that of the low-flow channel. Ice pan accumulations of a more chaotic nature are shown as well.

Supporting observations of ice runs on other rivers are limited. The other hydrologic sites near "Thomsen Fly" on "Gallois", "Euclid", and "Chebyshev" rivers (Fig. 37.1) also had ice-covered beds prior to runoff, although on a reduced scale. Ice breakup apparently occurs more swiftly on these smaller rivers, which is possibly due to lesser amounts of ice and an earlier rise in discharge. Sporadic observations on another major river, the Bernard, which drains the western half of the island, indicate a similar pattern of ice breakup and localized grounding. Ice dimensions seem to be largest in the Thomsen River channels, presumably due to higher flows at freezeup as flow is augmented by lake storage.



Figure 37.6

Large ice pan in Thomsen River at "Thomsen Fly". View is looking upstream to south. (GSC-203025-H).



Figure 37.7

Small ice pans grounded at "Thomsen Fly".
View is towards east; flow is from right
to left. (GSC-203025-P).

Figure 37.8

Ice run in lower Thomsen River.
View is to south (upstream).
(GSC-203025-M).



Figure 37.9

Ice-groove mark on the west bank of
Bernard River. (GSC-166318).

Figure 37.10

Scour holes on east bank of Thomsen River bed at "Thomsen Fly". View is towards south (upstream). (GSC-166557).



Figure 37.11

Scour holes on west bank of Bernard River. View is towards the east; flow is from right to left. (GSC-166320).

Figure 37.12

Ice-push crescent on west bank of Thomsen River. Flow is from right to left. (GSC-166446).





Figure 37. 13

Ice-push crescent on east bank of Thomsen River. View is towards north. (GSC-166864).



Figure 37. 14

Ice-push ridge on east bank of Thomsen, at same location as Figure 37. 13. (GSC-166865).



Figure 37. 15

Ice-push boulders on west bank of "Chebyshev River" just downstream of lake outlet. (GSC-166217).



Figure 37.16

Ice scalloping of east bank of mid-channel bar in lower Thomsen River. View is towards north. (GSC-166421).

Figure 37.17

Close-up view of ice scalloping shown in Figure 37.16. Depth of scalloping is about 0.3 m. View is towards north. (GSC-166461).



Forms and Occurrence of Ice Features in River Channels

The most common ice features on channel beds are groove marks associated with ice pans grounding in shallows, a typical example of which is shown in Figure 37.9 for Bernard River. Although these features can be extensive, they are of little consequence to bed scour. The maximum depths of grooves are only of the order of 0.10 to 0.15 m, with widths of up to 0.3 m and lengths of up to 30 m.

Crescent-shaped scour marks, caused by flow acceleration around grounded pans, are not as common although they exhibit greater scour depths. Figure 37.10 shows an array of scour holes located on the east side of Thomsen River at "Thomsen Fly". This is a zone of flow divergence where the channel expands at a bend. Typical dimensions (for the three scour

holes in the foreground of Fig. 37.10) are 8.8 x 4.5 x 0.6 m, 17 x 11.5 x 0.5 m, and 11.7 x 9.4 x 0.5 m, with the depth measurement being the most tenuous. Similar features are evident on the bar in Figure 37.11 for a section of Bernard River. Typical dimensions for the Bernard scour holes are 11.2 x 4.3 x 0.6 m, 8.5 x 5.8 x 0.5 m, and 19.5 x 12 x 0.8 m. These scour marks are also in a zone of flow divergence.

Other types of ice features include: (1) An ice-push crescent along the Thomsen (Fig. 37.12), typical of the area, is 2 to 3 m wide, 10 to 15 m long, and at the most 0.3 m deep. This site is in a zone of low expansion and shallowing. The area covered by these features was approximately 45 m x 100 m. (2) Crescent-shaped, ice-push features in coarse, angular bank material are shown in Figure 37.13. This site is in the lower Thomsen River where an alluvial fan impinges on the river. This, therefore, is a zone of flow convergence



Figure 37.18

Close-up view of ice scalloping shown in Figures 37.16 and 37.17. View is towards north. Closed arrow indicates scalloping resulting from 1975 ice run, open arrow indicates older scalloping marks. (GSC-166422).

Figure 37.19

Old ice-scour marks on midchannel bar in lower Thomsen River. View is towards west, flow direction from left to right. (GSC-166463).



where ice-push features result from jamming of ice pans in the channel and subsequent bankward movement. These marks are 3 to 5 m in length and extend for about 100 m along the east (inside) bank. Minor ice features also are found along the opposite bank. Evidence exists of an ice-push ridge (Fig. 37.14) on the east bank of this site above the crescent marks; ice push probably recurs here. (3) Ice-pushed boulders line the west bank of "Chebyshev River" where it exits a lake (Fig. 37.15). (4) Stable bars in the lower reaches of Thomsen River exhibit a scalloping feature (Figs. 37.16, 37.17, and 37.18) which is extensive several hundred metres long, but is a minor geomorphic feature. Evidence of previous ice push is shown in Figure 37.18. Long grooves also are found on the islands and are evidence of ice overriding during flood stage. These marks (Fig. 37.19), up to 4 to 5 m across and several hundred metres long, are higher

than 1975 flood levels, suggesting that much higher floods have occurred.

Conclusions

Observations on the pattern and geomorphic consequences of river breakup on Thomsen River on Banks Island indicate that, for the most part, rivers freeze to their bed. In the spring, ice disintegrates rapidly, forming a short run that is exhausted about the time of peak runoff with the bulk of it passing prior to peak flow.

Jamming is both a minor and localized phenomenon caused by the grounding of ice pans. Backwater effects are minor. Scouring associated with flow around grounded pans only produces features with depths less than one metre. Other ice features, such as grooves and push marks, also are minor individual

features, although large areas of the river bed can be disturbed.

Grounding of pans usually occurs where flow diverges or where a variable river stage alternately floats and grounds pans, as occurs during the rising limb of the spring flood. Ice-push features on banks, on the other hand, are found where flow converges, presumably resulting in an accumulation of ice pans with subsequent push against the banks. Observations also suggest that ice activity is repetitive at these sites.

In summary, these observations indicate that, even though ice can disrupt the river bed through plucking or push, the effects are minor and localized.

References

- Anderson, J. C. and Durrant, R. L.
1976: Hydrologic reconnaissance, Thomsen River basin, Banks Island, District of Franklin; in Report of Activities, Part A; Geol. Surv. Can., Paper 75-1A, p. 221-227.
- Dingman, S. L.
1971: Hydrology of the Glen Creek Watershed, Tanana River basin, central Alaska; U.S. Army, Cold Reg. Eng. Lab., Rep. 297, 112 p.
- Thompson, H. A.
1963: Freezing and thawing indices in Northern Canada; Proc. First Can. Permafrost Conf., NRC Tech. Memo. 76, p. 18-36.

Project 730155

John E. Armstrong and Stephen R. Hicock
Terrain Sciences Division, VancouverIntroduction

Coquitlam Valley is a glacier-carved bedrock valley (fiord), located 20 km east of Vancouver, which opens onto the Fraser Lowland at the southern limit of the Coast Mountains of British Columbia. Quaternary sediments more than 250 m thick are exposed on the west side of Coquitlam River in a number of gravel pits in which near-vertical sections up to 100 m thick are present. These sediments were deposited during several major glacial advances and retreats and during several nonglacial intervals. Each major ice advance and retreat was accompanied by eustatic and isostatic relative sea-level changes of up to 230 m.

Armstrong (1975) established five major Pleistocene geologic-climatic units in the Fraser Lowland. Armstrong and Hicock (1975) described buried Quaternary landscapes in Mary Hill, 3 to 8 km south of the area discussed in this paper. Buried landscapes are also common in the Coquitlam Valley Quaternary sediments, which exhibit periods of deposition followed by periods of erosion and reveal within them parts of one or more older valleys. Consequently, the unravelling of the stratigraphic succession becomes complex, especially as lithologic units of different chronologic ages may closely resemble one another and may be impossible to separate without absolute chronologic ages. Similar multiple valley development also must exist in other sediment-filled glaciated bedrock valleys bordering the Fraser Lowland.

Gravel pits have been operated in the west slope of Coquitlam Valley since the early 1940's, and since then millions of cubic metres of material have been removed. Armstrong examined the valley gravel pits several times between 1951 and 1965, Leaming (1968) described them, and the present writers studied them in detail between 1974 and 1976. The block diagram (Fig. 38.1) and much of the field work was done by S.R. Hicock.

Coquitlam Valley Stratigraphy

Figure 38.1 is a block diagram of the Pleistocene sediments underlying the west slope of lower Coquitlam Valley. It demonstrates that the sediment fill contains deposits related to at least two major glaciations and separated by at least one nonglacial interval. These geologic-climatic units are separated by unconformities which were modified by later stream and/or ice erosion.

The following stratigraphic succession has been established:

Fraser Glaciation (late Wisconsin; 11 000 to 22 000 years B.P.)

Capilano Sediments – fossiliferous raised marine and glaciomarine sediments; radiocarbon date 12 000 ± 100 years B.P.; GSC 2177.

Vashon Drift – at least three tills, glaciofluvial and ice-contact deposits.

Quadra Sand – proglacial outwash gravelly sand containing wood fragments; radiocarbon date 21 600 ± 200 years B.P.; GSC 2203.

Major Glaciation (mid-Wisconsin; probably > 62 000 years B.P.; QL-194)

Semiahmoo? Drift – at least two tills and one glaciomarine layer separated by outwash sandy gravel.

Nonglacial Interval (early Wisconsin?; > 49 000 and probably > 62 000 years B.P.)

Highbury? Sediments – rusty cross-bedded gravelly sand and wood-bearing silt; radiocarbon date > 49 000 years B.P.; GSC 2094-2).

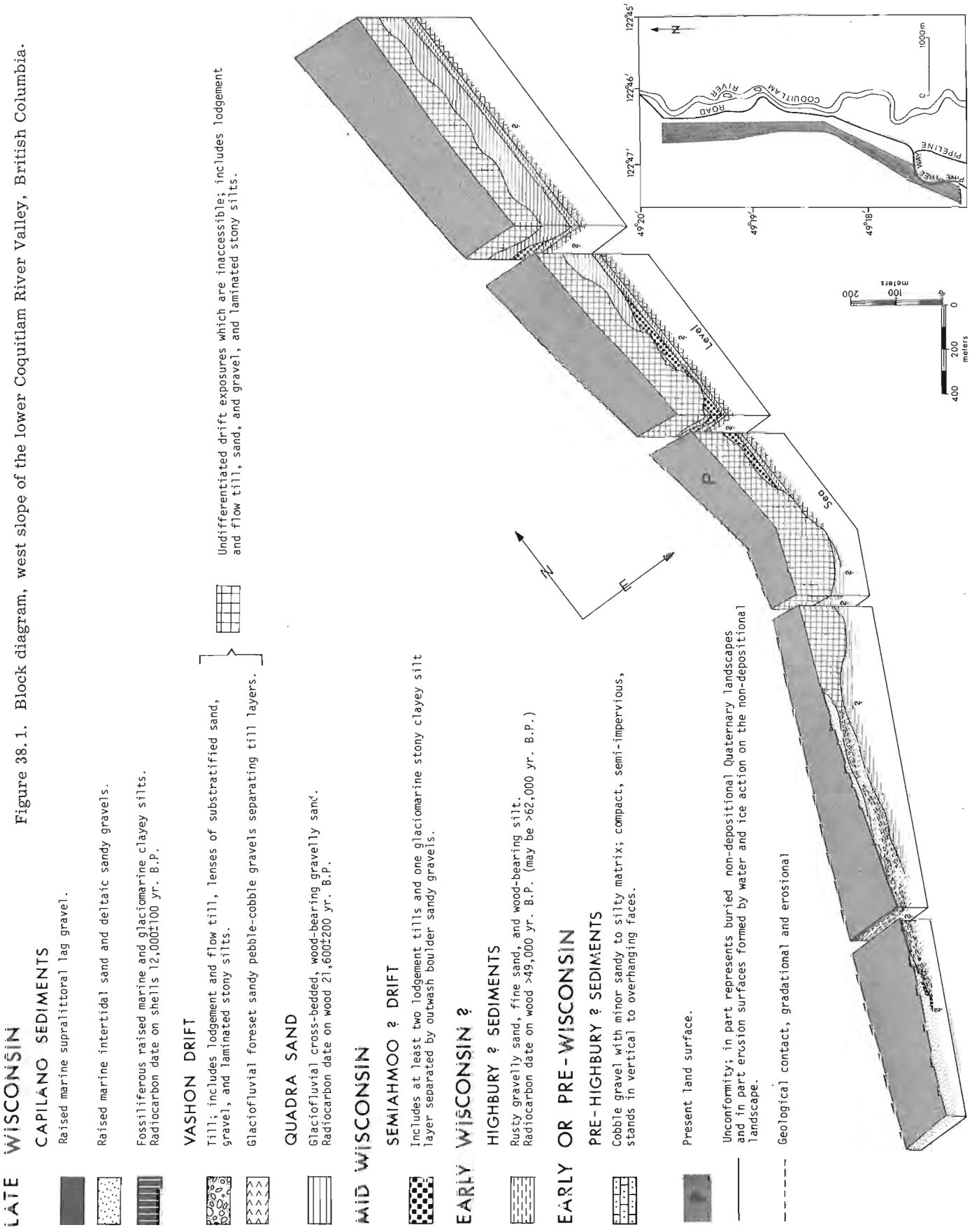
Glaciation? (early Wisconsin or pre-Wisconsin; > 62 000 years B.P.)

Pre-Highbury? Gravel – glaciofluvial? compact cobble gravel.

Most of the Capilano sediments occur as terraced raised marine deltas and are found up to 140 m a. s. l. abutting against a landscape formed on Vashon Drift. These deltas contain topset and southward-dipping foreset sandy gravels and gravelly sands which overlie thinly bedded bottomset sand containing shell casts. Fossiliferous marine and glaciomarine clayey silts are found in the basal part of the lowest delta, and a thin mantle of supralittoral lag gravel containing shell casts is found at the surface of all deltas.

Till fabric analyses and pebble provenance studies (to be presented in an ensuing paper) indicate that the major ice sheets which deposited the Vashon and Semiahmoo? drifts advanced southwards down the valley from the Coast Mountains. Both drift units

Figure 38.1. Block diagram, west slope of the lower Coquitlam River Valley, British Columbia.



LATE WISCONSIN

CAPILANO SEDIMENTS

Raised marine supralittoral lag gravel.

Raised marine intertidal sand and deltaic sandy gravels.

Fossiliferous raised marine and glaciomarine clayey silts. Radiocarbon date on shells 12,000±100 yr. B.P.

VASHON DRIFT

Till; includes lodgement and flow till, lenses of substratified sand, gravel, and laminated stony silts.

Glaciofluvial foreset sandy pebble-cobble gravels separating till layers.

QUADRA SAND

Glaciofluvial cross-bedded, wood-bearing gravelly silt. Radiocarbon date on wood 21,600±200 yr. B.P.

MID WISCONSIN

SEMAHMOO ? DRIFT

Includes at least two lodgement tills and one glaciomarine stony clayey silt layer separated by outwash boulder sandy gravels.

EARLY WISCONSIN ?

HIGHBURY ? SEDIMENTS

Rusty gravelly sand, fine sand, and wood-bearing silt. Radiocarbon date on wood >49,000 yr. B.P. (may be >62,000 yr. B.P.)

EARLY OR PRE-WISCONSIN

PRE-HIGHBURY ? SEDIMENTS

Cobble gravel with minor sandy to silty matrix; compact, semi-impervious, stands in vertical to overhanging faces.

Present land surface.

Unconformity; in part represents buried non-depositional Quaternary landscapes and in part erosion surfaces formed by water and ice action on the non-depositional landscape.

Geological contact, gradational and erosional

Undifferentiated drift exposures which are inaccessible; includes lodgement and flow till, sand, and gravel, and laminated stony silts.

thicken towards the valley axis and were deposited in troughs carved out of older sediments and parallel to Coquitlam Valley. Where exposed, Vashon Drift attains the greater thickness of the two drift units and truncates the older Semiahmoo? Drift. Similarly, each till within the drift units is truncated by the next youngest till. This successive truncation of sediment layers and units is a three-dimensional phenomenon.

Vashon Drift dips generally southward, most steeply where Coquitlam Valley opens onto the Fraser Lowland, and overlies a buried landscape that probably roughly parallels the bedrock surface. Beyond where Coquitlam Valley joins the Fraser Lowland pre-Vashon sediments are not exposed, and these materials apparently have been removed or buried by ice and water action during Vashon time.

Quadra Sand also thickens towards the axis of the valley, filling a north-south trending trough carved into older sediments and truncating Semiahmoo? Drift, and is truncated by Vashon Drift. Paleocurrent measurements indicate that the sands were deposited by southward-flowing streams, probably originated as proglacial outwash, in front of advancing Vashon ice to the north in the Coast Mountains. Both Vashon Drift and Quadra Sand have undulatory contacts with and truncate older sediments. These contacts were observed in north-south sections as well as in east-west sections, further emphasizing the three-dimensional character of these landscapes.

Highbury? sands and silts are thinly bedded, cross-bedded, and rippled and apparently were deposited by streams flowing northeastwards up and into Coquitlam Valley, probably during an interglacial period. These deposits are exposed only in a limited part of the valley, and in most of the exposures they underlie a buried landscape and are truncated by Vashon Drift.

Pre-Highbury? gravels are subhorizontally bedded and crudely cross-bedded and probably were deposited by glaciofluvial streams. Pebble imbrication and provenance studies indicate the streams were flowing southwards down the valley from the Coast Mountains. The gravels are moderately to well sorted, containing rounded, almost entirely granitic, cobbles and boulders surrounded by an angular sandy to silty matrix. Perhaps the angularity of the matrix grains permits these semi-impervious gravels to stand in vertical to slightly overhanging faces up to 20 m high.

At the base of each major sediment unit an unconformity (buried landscape) has been found that represents slopes of older river valleys which are roughly parallel to the present Coquitlam River valley. During the formation of each valley older sediments were eroded and removed by ice and/or water action, and then the valleys were infilled by more sediments.

Quaternary History

Commencing with the oldest sediments exposed, the geological history of Coquitlam Valley may be summarized as follows:

1) Pre-Highbury? coarse gravel is the oldest sediment found in the valley and is probably glaciofluvial in origin. It likely was deposited by streams flowing southwards down the valley from the Coast Mountains more than 62 000 years ago when the climate was cooler than that of today. This was followed by a period of erosion.

2. The climate warmed and Highbury sands and silts were deposited. This represents a radical change in sediment regime compared to that of Pre-Highbury gravel. Paleocurrent data from these deposits suggest northeastward transport of materials. Wood from the silts has been dated greater than 49 000 years but may be more than 62 000 years old. A landscape was developed on these deposits.

3) As the result of a cooling climate and the onset of another glaciation, southward-flowing glacial streams modified the landscape and covered it with Semiahmoo? outwash sandy gravels. The first Semiahmoo? till was deposited on the outwash when ice filled the valley. Upon a brief retreat of the ice more outwash was laid down, then the ice advanced again and deposited another till. Due to renewed climatic warming the ice retreated again, outwash again was laid down, and the sea invaded the valley and formed a fiord. The fiord later disappeared with further land uplift. During this Semiahmoo? deglaciation diamicton of probable glacio-marine origin were formed to at least 135 m a. s. l. Lack of radiocarbon dates prevents control on the absolute timing of these events. Landscapes were developed on each of these deposits.

4) After further isostatic uplift southward-flowing streams modified these landscapes, cutting into the older sediments; Quadra Sand was deposited by about 22 000 years ago on a new landscape, filling in the valley formed. Climatic cooling had begun again by this time, and the streams that carried the sands debouched from southward-advancing Vashon ice which was still far to the north in the Coast Mountains.

5) With continued climatic cooling Vashon ice entered the upper valley and southward-flowing meltwater streams cut into Quadra Sand and older sediments and formed a new valley, filling it with Vashon outwash gravels. As the ice filled Coquitlam Valley it remodeled previous landscapes and deposited till. At least three tills, separated by outwash gravels, were deposited in the valley by local Vashon ice advances in a similar way described for the Semiahmoo? tills. During the deposition of each till and outwash layer, ice and water action remodeled the older landscape and formed a new one. At the maximum advance of Vashon glaciers the land was depressed at least 210 m, and if eustatic lowering of sea level is considered, this figure would be at least 310 m.

6) By 13 000 years ago Vashon deglaciation was in progress. The climate had warmed, and as the ice retreated the sea entered the area, covering the landscape and depositing fossiliferous glaciomarine sediments up to 70 m a. s. l. in the Coquitlam fiord.

7) Following this, sand and gravel marine deltas were formed. As the land isostatically rose above the sea, surf pounded against the valley walls. Waves and spray reworked Vashon drift, forming a supralittoral lag gravel up to 175 m a. s. l. , and carved terraces up to 140 m a. s. l. into the deltaic sand and gravel. This marine action modified older landscapes and formed yet a new one, similar to the present day landscape.

Throughout the history of sediment deposition in Coquitlam Valley, tectonic adjustments probably occurred, as well as the isostatic and eustatic events mentioned, however, their importance and magnitude are completely unknown.

Conclusion

The main purpose of this short paper is to illustrate the complex geological makeup of the Quaternary sediment fills in glaciated bedrock valleys bordering the Fraser Lowland. Coquitlam Valley is the best illustrated example. Figure 38.1 demonstrates the sporadic occurrence of sediment units and the unreliability of attempting to correlate Quaternary deposits seen only in two dimensions or only from drill-holes. Correlations made on other than a three-dimensional study are at best tentative and should be supported whenever possible by radiocarbon dates.

Because of the multiple valley fills making up the Quaternary sediments in Coquitlam Valley, drillhole information could only result in completely misleading conclusions. For lower Coquitlam Valley nine sediment units have been mapped in Figure 38.1 and these can be subdivided further on a smaller scale. In some places a drillhole could penetrate as many as 12 different sediment layers, and in another drillhole, only a few metres away, as few as two.

References

Armstrong, J. E.

1975: Quaternary geology, stratigraphic studies, and revaluation of terrain inventory maps, Fraser Lowland, British Columbia; in Report of Activities, Part A; Geol. Surv. Can., Paper 75-1A, p. 377-380.

Armstrong, J. E. and Hicock, S. R.

1975: Quaternary landscapes: present and past - at Mary Hill, Coquitlam, British Columbia; in Report of Activities, Part B; Geol. Surv. Can., Paper 75-1B, p. 99-103.

Leaming, S. F.

1968: Sand and gravel in the Strait of Georgia area; Geol. Surv. Can., Paper 66-60, p. 40-45.

Project 750063

W. Blake, Jr.
Terrain Sciences DivisionIntroduction

This report is the second in a series of reviews being prepared to cover the coasts of Canada as part of the contribution of Terrain Sciences Division to the International Geological Correlation Program (IGCP) Project No. 61, entitled "Sea-level movements during the last deglacial hemicycle (about 15 000 years)". The first report dealt with the Pacific Coast (Clague, 1975); future reports will treat the southern islands of the Arctic Archipelago, the northern coast of the mainland (including Hudson Bay and James Bay), and the Atlantic Coast.

These reports are not intended to present new data as much as to cite pertinent references as sources of more detailed information. Among the important sources of data are the lists of radiocarbon age determinations, produced annually by the Geological Survey of Canada (GSC) since 1962 (two in 1970). From 1962 through 1971 these lists (numbers I to XI) were published in the journal *Radiocarbon* and then were reprinted as Geological Survey papers. In the lists reprinted as GSC papers from 1968 through 1971 (lists VII to XI) the original pagination from *Radiocarbon* was retained, but from 1962 to 1967 (lists I to VI) the reports unfortunately were given new pagination, so that the reader should consult *Radiocarbon* to obtain the proper bibliographical data. Commencing in 1972 annual lists of radiocarbon age determinations have been published only as GSC papers (publication no. 7 is reserved each year). Specific data relating to the last 15 000 years in the Queen Elizabeth Islands (Fig. 39.1) can be found in the eleven GSC dating lists cited at the beginning of the references to this paper. Prior to the establishment of the Geological Survey's own laboratory in 1959, numerous ^{14}C age determinations on samples of postglacial age from the Queen Elizabeth Islands were carried out by other laboratories, chiefly Lamont and Isotopes, Inc. (cf. Broecker *et al.*, 1956; Walton *et al.*, 1961; Trautman and Walton, 1962). In addition, a considerable number of dates relating to northeastern Devon Island have been produced by the University of Saskatchewan radiocarbon laboratory (Rutherford *et al.*, 1973), and numerous determinations on materials from northernmost Ellesmere Island have been made by the radiocarbon laboratory at the Smithsonian Institution (Long and Mielke, 1967; Mielke and Long, 1969; Stuckenrath and Mielke, 1973). These dating lists also are cited at the beginning of the references.

Chronology

In a general way the oldest marine molluscs appear to derive from the western Queen Elizabeth Islands

(Blake, 1972), although no determinations on *in situ* shells from anywhere in this island group are as old as those on a sample of *Portlandia arctica* (identified by F. J. E. Wagner) collected in 1959 by J. G. Fyles near the northwestern tip of Victoria Island in the vicinity of Peel Point. The original determination on these shells gave a value of $12\,400 \pm 320$ years B.P. (IGSC-18; Craig and Fyles, 1960; Walton *et al.*, 1961; Fyles, 1963), and a check determination gave $12\,600 \pm 140$ years B.P. (GSC-1707). On both Prince Patrick Island and southern Melville Island the most ancient marine samples postdating the last glaciation, all collected by Fyles, range in age from 11 000 to 12 000 years (Lowdon *et al.*, 1967; Lowdon and Blake, 1968). The oldest shell sample within this group, from an elevation of 3 to 6 m near the southern end of Prince Patrick Island (location 1, Fig. 1), is $11\,660 \pm 370$ years old (GSC-354; Blake, 1972).

An age of $14\,180 \pm 180$ years (GSC-432; 65 to 70 m elevation; Lowdon and Blake, 1968) has been obtained for *Hiatella arctica* shells from near the northern end of Axel Heiberg Island (location 2), but since much older shells of the same species are known to occur nearby (e.g., see Dyck and Fyles, 1964), the possibility that the dated sample comprised a mixture of 'old' shells with shells of Holocene age cannot be excluded. Another similar age has been reported on material from Ward Hunt Island, off the northern coast of Ellesmere Island. A date of $13\,200 \pm 440$ years (SI-719A) has been obtained there from calcilutite encrusting siliceous sponges in ice (Lyons and Mielke, 1973). Because carbonate bedrock occurs in the area, however, it seems unlikely that this age determination can be used as a valid indicator of ice-free conditions some 13 000 to 14 000 years ago, particularly in view of the fact that the organic fraction of the same sponges is only 3400 ± 140 years old (SI-719B; Lyons and Mielke, 1973; Stuckenrath and Mielke, 1973).

The oldest reliable age determination from the northernmost part of the Arctic Archipelago is on a sample of *Portlandia arctica* shells collected in 1972 by J. H. England from an elevation of 113 to 116 m, a few kilometres southwest of Alert, northern Ellesmere Island. The age of these shells, collected from silt and sand of a terrace, is $10\,100 \pm 210$ years (GSC-1815). England (1974a, 1976) has expressed reservations as to the validity of this age determination, as it is considerably older than others on raised marine deposits in northeastern Ellesmere Island, and it is not included in his critique of Lyons and Mielke's paper (England, 1974b). However, there is no reason to doubt the accuracy of the determination on these well preserved shells from a laboratory point of view; the sample was collected at a higher elevation than any of the other postglacial

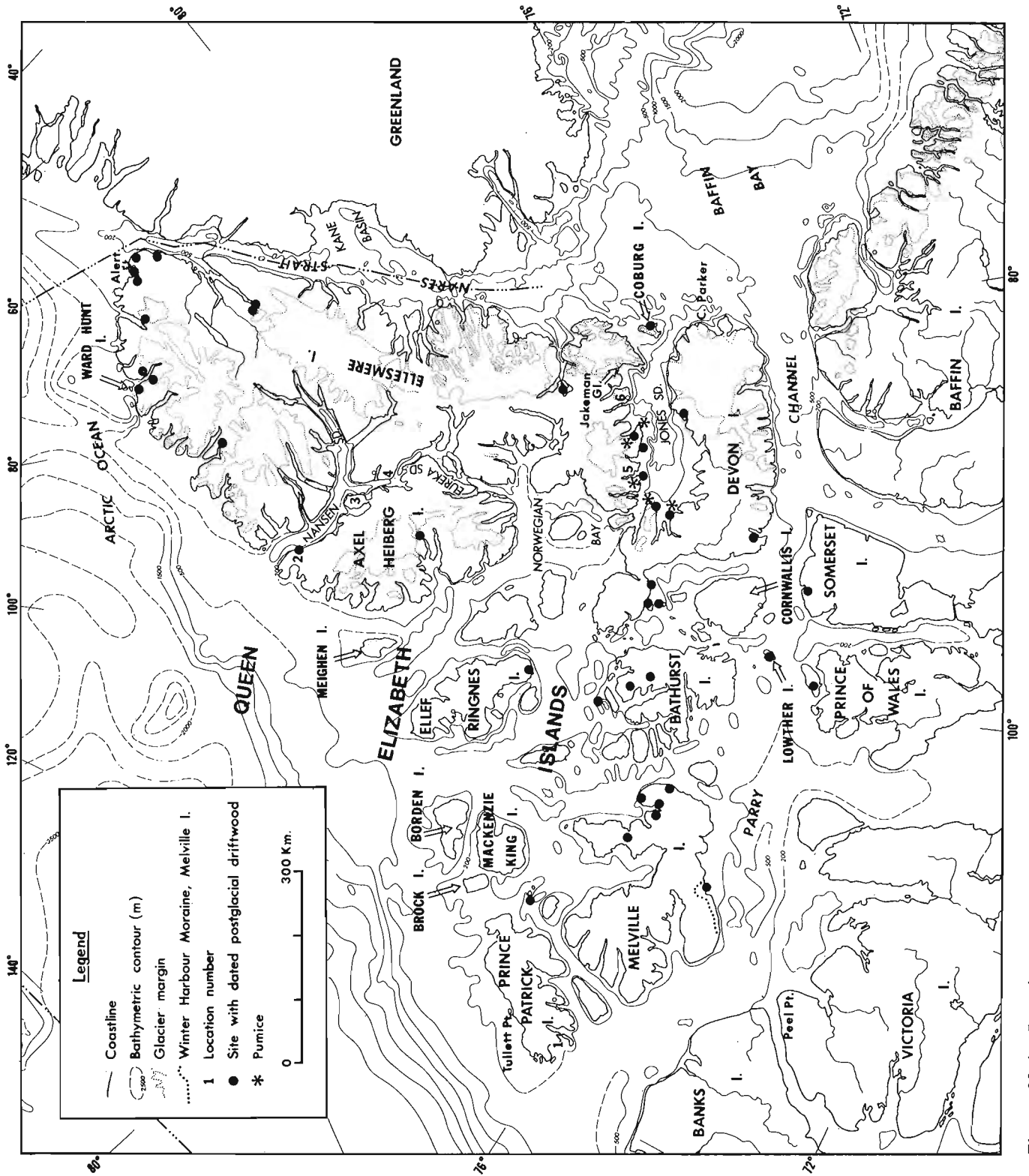


Figure 39.1. Location map.

shells in the region, hence its greater age seems reasonable to the present writer.

At the opposite end of Ellesmere Island, three ^{14}C age determinations of approximately 10 000 years have been obtained, but at least one of these collections, from Muskox Fiord (location 5), is known to be a mixture of postglacial shells with shells predating the last glaciation (Blake, 1975a). There is some evidence that the same problem may exist for a sample of shell fragments near Grise Fiord (location 6) and for one adjacent to Jakeman Glacier, farther east along the south coast of Ellesmere Island. At present it can be stated with certainty that the north coast of Jones Sound was open to the sea between 9500 and 9000 years ago, but additional study will be required to check the validity of the determinations which have given ages closer to 10 000 years.

The dates from the northern and southern extremities of Ellesmere Island are the oldest on Holocene marine deposits in this sector of the Queen Elizabeth Islands. They demonstrate that the penetration of sea into the eastern, more mountainous part of the archipelago, which is heavily glacierized at the present time, occurred well after (as much as 2000 years) the marine incursion into the channels separating the western islands.

General Pattern of Emergence

All islands investigated in the Queen Elizabeth Islands show some evidence of emergence during the last deglacial hemicycle. Age determinations from raised shorelines are available for every major island and for many minor islands. In places, however, the northwestern coasts of the westernmost islands – especially Prince Patrick Island, but also perhaps parts of Brock, Borden, and Ellef Ringnes islands – appear to be lacking in raised marine features; elsewhere these northwestern coasts are characterized by limits of postglacial marine submergence which do not exceed 10 m (Craig and Fyles, 1965; Fyles, 1965; Fyles and Blake, 1965). At Tullett Point, Prince Patrick Island, a 15-cm-thick band of peat was sampled in 1964 by J.G. Fyles. The peat was contained in an ice-push ridge composed of pebbly sand, and because the site was at an elevation of only 1.5 m, the peat was interpreted as having been pushed up from below present sea level (Fyles, pers. comm., 1976). The peat is 8910 ± 160 years old (GSC-473); thus this seems to be one site where the eustatic rise of sea level has equalled or exceeded the rebound due to glacial unloading.

An analogous situation may exist in the southeastern corner of the Archipelago; Barr *et al.* (1968) reported that conspicuous marine features were present up to only 4.5 to 6 m (and undisturbed felsenmeer occurred at 20 m) at Cape Parker, easternmost Devon Island.

By contrast, the areas exhibiting the greatest emergence seem to lie in a zone extending from Bathurst Island to the north-central part of Ellesmere Island (Craig and Fyles, 1965; Andrews, 1969, 1970a, 1970b; Blake, 1970, 1975a). Recognition of this pattern has necessitated modification of the original scheme proposed by Farrand and Gajda (1962), in which they

indicated that the highest marine limit (150 m or more) occurred in two areas – western Devon Island plus eastern Cornwallis Island and north-central Ellesmere Island plus adjacent Axel Heiberg Island – and that the elevation of the marine limit decreased westward across Bathurst Island towards the north-western margin of the Archipelago. The highest Holocene sample known to the writer was collected in 1960 by B.R. Robitaille at an elevation of ca. 155 m on Schei Peninsula, Axel Heiberg Island (location 3); the shells were 8080 ± 160 years old (I(GSC)-264; Sim, 1961; Trautman and Walton, 1962; Andrews and Drapier, 1967). In 1973 D.A. Hodgson (pers. comm., 1976) re-examined this part of Schei Peninsula. At the locality described by Robitaille the summit of the highest hill is only 135 m a.s.l., so there is a distinct possibility that the shells were from a lower elevation than indicated by altimetry at the time of collection. In addition, 60 km to the southeast near Blue Man Cape on Ellesmere Island (location 4), Fyles collected whole, paired valves of *Hiatella arctica* in silt at an elevation of 140 m (within 5 m of the limit of postglacial marine submergence). Two age determinations were made, resulting in ages of 8450 ± 140 years (GSC-243) and 8710 ± 140 years (GSC-254; Dyck *et al.*, 1965). Thus, unless postglacial uplift was considerably more rapid on Schei Peninsula than southward along Eureka Sound, the 8000-year-old shells at the former locality could be expected to derive from a lower, not a higher, elevation than the shells near Blue Man Cape.

Curves showing the relation between time and elevation have been constructed for a number of localities in the Queen Elizabeth Islands. The first was that produced by Farrand (1962) for northern Ellesmere Island, but it was based on sparse field data. The original radiocarbon age determinations from that area were on marine shells and driftwood collected by field parties under the direction of G. Hattersley-Smith (Broecker *et al.*, 1956; Crary, 1960; Christie, 1967). Time-elevation diagrams also have been constructed for Melville Island (Hench, 1964), northeastern Devon Island (Müller and Barr, 1966; King, 1970; Barr, 1971), and northern Ellesmere Island (Hattersley-Smith and Long, 1967; Lyons and Mielke, 1973; England, 1974a, 1976). Sea-level curves for Cornwallis, Bathurst, and Axel Heiberg islands have been published by Walcott (1972); he also included diagrams for two localities in southern Ellesmere Island which have since been treated in more detail by Blake (1975a, c). With the exception of the last-named area, where driftwood is abundant, all these time-elevation diagrams rely to a large extent on dated marine pelecypods. Recent work in southwestern Devon Island by S.B. McCann, B.T. Bunting, and others from McMaster University and in eastern Melville Island by D.M. Barnett (Barnett, 1973) and P. McLaren has resulted in a number of additional age determinations on driftwood, peat, and terrestrial organic detritus; time-elevation diagrams are expected to be constructed for those areas. A considerable body of data also exists for northern Eureka Sound, in addition to the sample from Blue Man Cape mentioned earlier; although the age determinations are mainly on marine pelecypods

(collected by J. G. Fyles in 1961 and D. A. Hodgson in 1972 and 1973), it should be possible to construct a reasonably accurate time-elevation diagram for this region also.

Driftwood

Perhaps the most reliable way in which data on former shoreline positions in the Arctic can be gathered is by dating accurately-levelled driftwood (preferably logs) embedded in emerged shingle beaches. During the last decade a particularly rich harvest of age determinations on wood has been obtained from the Queen Elizabeth Islands (Fig. 39.1). All available information up to the end of 1971 was summarized by the author (Blake, 1972), and ^{14}C ages determined since that time have not invalidated the earlier conclusions. A few points can be re-emphasized here:

1) As yet no Holocene driftwood has been found which is more than 8500 years old. This suggests that some channels may have been filled by glacier ice, and in other localities where the presence of dated marine pelecypods indicates that the incursion of the sea already had taken place, the cover of sea ice may have been sufficiently thick as to prevent the entry of driftwood.

2) Although there are a number of possible source areas for the wood, some of the larch (*Larix* sp.) logs at the modern shore as well as on raised beaches in southern Ellesmere Island are now known, on the basis of the characteristic resins they contain (Blake, 1975a), to be Eurasian species rather than of North American origin.

3) Along the northern coast of Ellesmere Island, on the landward side of the ice shelf adjacent to Ward Hunt Island (Fig. 39.1), most of the driftwood collected by G. Hattersley-Smith in 1972 either is 5000 to 6000 years old or is beyond the limit of radiocarbon dating (Blake, 1975b). Although no driftwood has been found so far that is as young as the two samples in the 3000 to 3500 year-range reported by Crary (1960), it is clear that the ice shelf, which now seals off the mouth of Disraeli Fiord (and hence blocks the entry of driftwood), was not in existence during at least part of the Hypsithermal Interval.

At the present time the main group of islands from which Holocene driftwood samples have not been recovered are those along the northwestern fringe of the Archipelago – Prince Patrick, Brock, Mackenzie King, Borden, northern Ellef Ringnes, and Meighen islands. It is hoped that accurately levelled collections can be made in this area in the future and that suites of samples can be collected from elsewhere in the Archipelago where data are sparse at present. In this way past positions of the shoreline eventually will be precisely documented throughout the Queen Elizabeth Islands.

Pumice

Driftwood can be used to great advantage in determining the age of individual emerged shorelines, but correlation between localities is made easier in some regions by the presence of pebbles and cobbles of pumice on beaches. Localities with pumice have been found along the northern and western shores of Jones Sound but, unfortunately, to date pumice has not been discovered elsewhere in the Queen Elizabeth Islands (Fig. 39.1). Details of the composition of the pumice, its mode of occurrence, and the time at which it arrived on the beaches around Jones Sound have been discussed in a series of papers by the writer (Blake, 1970, 1973, 1975a). It is worth re-emphasizing here, however, the usefulness of this tool in the hope that other workers in the Arctic will search carefully for pumice in their respective field areas. Because the pumice can be assumed to have arrived in widely separated beaches simultaneously (in this case approximately 5000 years ago, as shown by numerous age determinations on associated driftwood) and because it is usually concentrated within a narrow vertical interval (1 m), it serves as an excellent time line. Determination of the tilt of beach sequences, on the basis of the pumice, permits the delineation of areas where more rebound has occurred and hence where the cover of glacier ice was once thicker (Blake, 1975c). Without a guide horizon such as is provided by the pumice, in many cases it is difficult, or impossible, to correlate between islands or even along a stretch of coast where the shorelines cannot be traced physically.

Acknowledgments

Appreciation is expressed to W. Dyck, J. A. Lowdon, and their co-workers, who have operated the Radiocarbon Dating Laboratory at the Geological Survey of Canada with great care and attention to detail for the past 17 years. J. G. Fyles provided an unpublished age determination from Prince Patrick Island, and B. G. Craig and D. A. Hodgson were kind enough to provide helpful comments on a draft of this paper.

References

- GSC I Dyck and Fyles, 1962, p. 22-23.
GSC III Dyck and Fyles, 1964, p. 176-177.
GSC IV Dyck, Fyles, and Blake, 1965, p. 39-43.
GSC V Dyck, Lowdon, Fyles, and Blake, 1966, p. 123-124.
GSC VI Lowdon, Fyles, and Blake, 1967, p. 188-194.
GSC VII Lowdon and Blake, 1968, p. 239-242.
GSC IX Lowdon and Blake, 1970, p. 82-83.

- GSC XI Lowdon, Robertson, and Blake, 1971, p. 311-318.
- GSC XIII Lowdon and Blake, 1973, p. 38-45.
- GSC XIV Lowdon, Wilmeth, and Blake, 1974, p. 9.
- GSC XV Lowdon and Blake, 1975, p. 21-26.
- Isotopes I Walton, Trautman, and Friend, 1961, p. 53.
- Isotopes II Trautman and Walton, 1962, p. 37.
- Lamont III Broecker, Kulp, and Tucek, 1956, p. 9.
- Saskatchewan VI Rutherford, Wittenberg, and McCallum, 1973, p. 193-196.
- Smithsonian IV Long and Mielke, 1967, p. 380.
- Smithsonian V Mielke and Long, 1969, p. 176-177.
- Smithsonian VIII Stuckenrath and Mielke, 1973, p. 390-392.
- Andrews, J. T.
 1969: The pattern and interpretation of restrained, post-glacial and residual rebound in the area of Hudson Bay; *in* Earth Science Symposium on Hudson Bay, ed. P. J. Hood; Ottawa, Feb. 1968; Geol. Surv. Can., Paper 68-53, p. 49-62.
- 1970a: Present and postglacial rates of uplift for glaciated northern and eastern North America derived from postglacial uplift curves; *Can. J. Earth Sci.*, v. 7, p. 703-715.
- 1970b: A geomorphological study of postglacial uplift, with particular reference to Arctic Canada; *Inst. Br. Geogr.*, Spec. Publ. no. 2, 156 p.
- Andrews, J. T. and Drapier, L.
 1967: Radiocarbon dates obtained through Geographical Branch field observations; *Geogr. Bull.*, v. 9, p. 115-162.
- Barnett, D. M.
 1973: Radiocarbon dates from eastern Melville Island; *in* Report of Activities, Part B, Geol. Surv. Can., Paper 73-1B, p. 137-140.
- Barr, W.
 1971: Postglacial isostatic movement in northeastern Devon Island: a reappraisal; *Arctic*, v. 24, p. 249-268.
- Barr, W., Barrett, P. E., Hussell, D. J. T., King, R. H., and Koerner, R. M.
 1968: Devon Island programs, 1967; *Arctic*, v. 21, p. 44-50.
- Blake, W., Jr.
 1970: Studies of glacial history of Arctic Canada. I. Pumice, radiocarbon dates, and differential postglacial uplift in the eastern Queen Elizabeth Islands; *Can. J. Earth Sci.*, v. 7, p. 634-664.
- 1972: Climatic implications of radiocarbon-dated driftwood in the Queen Elizabeth Islands, Arctic Canada; *in* Climatic changes in Arctic areas during the last ten-thousand years, eds. Y. Vasari, H. Hyvärinen, and S. Hicks; Proc. symp., Oulanka-Kevo, Finland, 1971; *Acta Univ. Ouluensis, Ser. A, Sci. Rerum. Nat. no. 3, Geol. no. 1*, p. 77-104.
- 1973: Age of pumice on raised beaches, eastern Arctic Canada; *in* Report of Activities, Part B, Geol. Surv. Can., Paper 73-1B, p. 141-142.
- 1975a: Radiocarbon age determinations and postglacial emergence at Cape Storm, southern Ellesmere Island, Arctic Canada; *Geogr. Ann.*, Ser. A, v. 57, p. 1-71.
- 1975b: Studies of glacial history in the Queen Elizabeth Islands, Canadian Arctic Archipelago; *Naturgeogr. Inst., Stockholms Universitet; Forskningsrapport 21*, 14 p.
- 1975c: Pattern of postglacial emergence, Cape Storm and South Cape Fiord, southern Ellesmere Island, N. W. T.; *in* Report of Activities, Part C, Geol. Surv. Can., Paper 75-1C, p. 69-77.
- Broecker, W. S., Kulp, J. L., and Tucek, C. S.
 1956: Lamont natural radiocarbon measurements III; *Science*, v. 124, p. 154-165.
- Christie, R. L.
 1967: Reconnaissance of the surficial geology of northeastern Ellesmere Island, Arctic Archipelago; *Geol. Surv. Can., Bull.* 138, 50 p.
- Clague, J. J.
 1975: Late Quaternary sea level fluctuations, Pacific Coast of Canada and adjacent areas; *in* Report of Activities, Part C, Geol. Surv. Can., Paper 75-1C, p. 17-21.
- Craig, B. G. and Fyles, J. G.
 1960: Pleistocene geology of Arctic Canada; *Geol. Surv. Can., Paper* 60-10, 21 p.
- 1965: Quaternary of Arctic Canada; *in* Antropogenovye period v Arktike i Subarktika; *Trudy Nauchno-Issled. Inst. Geol. Arktiki*, Tom 143, p. 5-33 (in Russian with English summary).
- Crary, A. P.
 1960: Arctic ice island and ice shelf studies, Part II; *Arctic*, v. 13, p. 32-50.

- Dyck, W. and Fyles, J.G.
 1962: Geological Survey of Canada radiocarbon dates I; Radiocarbon, v. 4 p. 13-26; reprinted, together with list II, as GSC Paper 63-21.
 1964: Geological Survey of Canada radiocarbon dates III; Radiocarbon, v. 6, p. 167-181; reprinted as GSC Paper 64-40.
- Dyck, W., Fyles, J.G., and Blake, W., Jr.
 1965: Geological Survey of Canada radiocarbon dates IV; Radiocarbon, v. 7, p. 24-46; reprinted as GSC Paper 65-4.
- Dyck, W., Lowdon, J.A., Fyles, J.G., and Blake, W., Jr.
 1966: Geological Survey of Canada radiocarbon dates V; Radiocarbon, v. 8, p. 96-127; reprinted as GSC Paper 66-48.
- England, J.H.
 1974a: The glacial geology of the Archer Fiord/Lady Franklin Bay area, northeastern Ellesmere Island, N.W.T., Canada; unpubl. Ph.D. dissert., Univ. of Colorado, Boulder, Colo., 234 p.
 1974b: A note on the Holocene history of northernmost Ellesmere Island; Arctic, v. 27, p. 154-157.
 1976: Postglacial isobases and uplift curves from the Canadian and Greenland High Arctic; Arct. Alp. Res., v. 8, p. 61-78.
- Farrand, W.R.
 1962: Postglacial uplift in North America; Am. J. Sci., v. 260, p. 181-199.
- Farrand, W.R. and Gajda, R.T.
 1962: Isobases on the Wisconsin marine limit in Canada; Geogr. Bull., no. 17, p. 5-22.
- Fyles, J.G.
 1963: Surficial geology of Victoria and Stefansson Islands, District of Franklin; Geol. Surv. Can., Bull. 101, 38 p.
 1965: Surficial geology, western Queen Elizabeth Islands; in Report of Activities: field 1964; Geol. Surv. Can., Paper 65-1, p. 3-5.
- Fyles, J.G. and Blake, W., Jr.
 1965: Glaciation of the northwestern Canadian Arctic Islands; in Abstracts, VII Int. Cong., INQUA, Denver and Boulder, Colo., 1965, p. 156.
- Hattersley-Smith, G. and Long, A.
 1967: Postglacial uplift at Tanquary Fiord, northern Ellesmere Island, Northwest Territories; Arctic, v. 20, p. 255-260.
- Henoch, W.E.S.
 1964: Postglacial marine submergence and emergence of Melville Island, N.W.T.; Geogr. Bull., no. 22, p. 105-126.
- King, R.H.
 1970: An evaluation of postglacial isostatic rebound on Devon Island, Canadian Arctic Archipelago; Swansea Geographer, no. 8, p. 61-67.
- Long, A. and Mielke, J.E.
 1967: Smithsonian Institution radiocarbon measurements IV; Radiocarbon, v. 9, p. 368-381.
- Lowdon, J.A. and Blake, W., Jr.
 1968: Geological Survey of Canada radiocarbon dates VII; Radiocarbon, v. 10, p. 207-245; reprinted as GSC Paper 68-2, Part B.
 1970: Geological Survey of Canada radiocarbon dates IX; Radiocarbon, v. 12, p. 46-86; reprinted as GSC Paper 70-2, Part B.
 1973: Geological Survey of Canada radiocarbon dates XIII; Geol. Surv. Can., Paper 73-7, 61 p.
 1975: Geological Survey of Canada radiocarbon dates XV; Geol. Surv. Can., Paper 75-7, 32 p.
- Lowdon, J.A., Fyles, J.G., and Blake, W., Jr.
 1967: Geological Survey of Canada radiocarbon dates VI; Radiocarbon, v. 9, p. 156-197; reprinted as GSC Paper 67-2, Part B.
- Lowdon, J.A., Robertson, I.M., and Blake, W., Jr.
 1971: Geological Survey of Canada radiocarbon dates XI; Radiocarbon, v. 13, p. 255-324; reprinted as GSC Paper 71-7.
- Lowdon, J.A., Wilmeth, R., and Blake, W., Jr.
 1974: Geological Survey of Canada Radiocarbon dates XIV; Geol. Surv. Can., Paper 74-7, 11 p.
- Lyons, J.B. and Mielke, J.E.
 1973: Holocene history of a portion of northernmost Ellesmere Island; Arctic, v. 26, p. 314-323.
- Mielke, J.E. and Long, A.
 1969: Smithsonian Institution radiocarbon measurements V; Radiocarbon, v. 11, p. 163-182.
- Müller, F. and Barr, W.
 1966: Postglacial isostatic movement in northeastern Devon Island, Canadian Arctic Archipelago; Arctic, v. 19, p. 263-269.
- Rutherford, A.A., Wittenberg, J., and McCallum, K.J.
 1973: University of Saskatchewan radiocarbon dates VI; Radiocarbon, v. 15, p. 193-211.
- Sim, V.K.
 1961: A note on high-level marine shells on Fosheim Peninsula, Ellesmere Island, N.W.T.; Geogr. Bull., no. 16, p. 120-123.

Stuckenrath, R. and Mielke, J.E.

1973: Smithsonian Institution radiocarbon measurements VIII; Radiocarbon, v. 15, p. 388-424.

Trautman, M.A. and Walton, A.

1962: Isotopes, Inc. radiocarbon measurements II; Radiocarbon, v. 4, p. 35-42.

Walcott, R.I.

1972: Late Quaternary vertical movements in eastern North America: quantitative evidence of glacio-isostatic rebound; Rev. Geophys. Space Phys., v. 10, p. 849-884.

Walton, A., Trautman, M.A., and Friend, J.P.

1961: Isotopes, Inc. radiocarbon measurements I; Radiocarbon, v. 3, p. 47-59.

Project 750071

Arthur S. Dyke
Terrain Sciences Division

Introduction

During the summer of 1975 the writer was a member of a party mapping the surficial deposits of Somerset Island (Netterville *et al.*, 1976). This mapping led to the realization that the surficial materials over much of the island essentially consists of *in situ* weathered bedrock. Numerous tors were encountered on various types of bedrock, and a brief period was spent examining these landforms and their associated weathered materials.

Tors occur on all continents and in climatic zones ranging from tropical Africa to Antarctica. This implies that the same landform can evolve under widely different sets of processes. While some attention has been paid to the significance of tors with regard to ages of surfaces (i. e. time since deglaciation) in Arctic Canada, little information has been presented detailing the processes by which tors form under arctic conditions. Indeed, even the general distribution of tors within the Canadian Arctic is unknown. The purpose of this paper is to provide some initial information on the distribution and characteristics of tors in an area of the central Arctic and to outline the processes involved in their formation. It is hoped that this will encourage other earth scientists to present information regarding the distribution and characteristics of tors that they may have observed in their field areas. The following discussion of tors is ordered according to lithology and is preceded by a brief summary of the regional climate and geology.

The Study Area

Somerset Island lies between latitudes 72° and 74°10' and longitudes 90° and 96°. Although it is one of the more southerly islands of the Arctic Archipelago, its climate may be described as High Arctic. There are no official records of the local climate, but it appears to be similar to that of Cornwallis Island which has a fully equipped meteorological station at Resolute Bay, situated 80 km to the north. Resolute Bay has a mean annual temperature of -17°C, mean annual precipitation of 13 cm, and an average summer temperature (June, July, August) of 1.5°C. Despite the low recorded values for annual precipitation, summers in this area are often foggy and the soil layer, except in accumulations of coarse gravel and felsenmeer, is moist. Moisture is supplied by rainfall, ablation of late-lasting and perennial snow/firn packs, and melting of ground ice in the active layer.

The bedrock geology of the island is described by Blackadar (1967) and Blackadar *et al.* (1967). Figure 40.1 provides a generalized picture of the geology. The western portion of the island consists of Precambrian gneisses with small granite and gabbro intrusions. Over a small area near their northern

border, the gneisses are overlain by Precambrian metasediments consisting mainly of quartzites, dolomite, and chert. The northern and eastern portions of the island consist of Lower Paleozoic limestone and dolomite, interbedded with shaly and silty carbonates. Overlying the Lower Paleozoic carbonates in two areas are conglomerates, sandstones, and siltstones of Silurian and possibly Devonian age.

Aspects of the surficial geology of the island were first discussed by Craig and Fyles (1960) and later by Craig (1964) and Bird (1967). Netterville *et al.* (1976) provide the most recent interpretation of the surficial geology and Quaternary history. Generally, in the area north of Stanwell-Fletcher Lake and Creswell Bay (Fig. 40.1) the gneisses are overlain by felsenmeer with patches of till near the west coast; the Lower Paleozoic carbonates are overlain by a silty rubby veneer formed by weathering of the bedrock; the conglomerates, sandstones, and siltstones are overlain by similar materials. Only a few small areas of till are identifiable on the northern plateau, whereas south of Stanwell-Fletcher Lake and Creswell Bay the bedrock is mainly till covered. Two major phases of glaciation are proposed: the earlier involves one or more periods of complete coverage of the island by a Laurentide Ice Sheet, whereas during a later phase, Laurentide ice covered only the southern part of the island and retreated prior to or about 30 000 years B.P. The inferences as to extent of ice coverage and the tentative chronology are based mainly on the distribution of tills and erratics and on morphostratigraphic relationships between high-level (200 to 230 m) fossiliferous marine deposits and ice-marginal deposits.

Tors - a General Statement

An early attempt to derive a model describing the process of tor formation was made by Linton (1955). He proposed a two-stage model starting with deep differential chemical weathering of bedrock by groundwater and ending with mechanical stripping of the weathered overburden to expose the tors, which represent the more resistant, less weathered bedrock knobs. Linton's hypothesis stimulated a great deal of discussion of possible tor-forming processes, centering mainly around the validity of the earlier stage when applied to features in temperate latitudes. Pullan (1959) suggested that Linton's rather rigorous definition of "tor" be broadened, stating that "... a definition of tors must concentrate on their common origin as residuals of differential weathering and mass movement" but should not have a strictly defined morphogenesis. This general definition is used here. For a review of literature on tors the reader is referred to Brown and Waters (1974) - a collection of papers in

honour of D.L. Linton – and to Cunningham (1969) for a succinct summary of the various models of tor formation to that date.

Somerset Island Tors – Distribution

Tors have been observed on all the major bedrock lithologies of Somerset Island. Figure 40.1 contains a plot of those tors which are large enough to be recognized on airphotos of 1:60 000 scale. The distribution shown is incomplete because certain tors observed in the field are not recognizable on the photographs.

Figure 40.1 shows that the tors have a strikingly nonrandom distribution. The largest concentration occurs between Aston Bay and Stanwell-Fletcher Lake, within "Terrain Region 3" of Netterville *et al.* (1976); indeed, they constitute the most diagnostic geomorphic features within this large region. Here, the tors have developed on both mafic and felsic gneisses but predominantly on the latter. The more northerly tors in this region have developed on quartzite. The second

largest concentration is found north of Aston Bay, within "Terrain Region 7" of Netterville *et al.* (1976), which is underlain by Lower Paleozoic conglomerate, sandstone, and siltstone. Only a small number of distinct tors are detectable on the airphotos of the carbonate plateau. Fringing the northern and eastern coasts of the island, however, is a terrain of hummocky carbonate bedrock (Fig. 40.1, map-unit 5) containing numerous bedrock basin lakes interspersed with weathered bedrock knobs. This region is described by Netterville *et al.* (1976) under the heading "Terrain Region 1a". Although these rock knobs may represent a variety of tors, their interpretation is uncertain. A sharp margin exists around the area of hummocky bedrock. The bedrock lithology is the same on either side of this margin. It is necessary, therefore, to invoke a different geomorphic history to explain the morphologic contrast. The hummocky terrain may have been produced by severe glacial erosion, which the central portions of the carbonate plateau, have escaped but the writer is not aware of an analogous topography that is known to have been formed by glacial erosion.

Along the sides of several deep canyons, which criss-cross the carbonate plateau, there are numerous fragile stacks that may be classed as valley-side tors. Some of these are large enough to be visible on airphotos, but none of this variety have been plotted. Because they occur on cliff faces, where rates of mass movement are much accelerated and involve rockfall, it can be assumed that their rates of formation exceed those of the tors discussed below.

Gneissic Tors

Two days were spent examining part of a tor field lying south of Aston Bay. Figure 40.2 is a map of this area, illustrating the distribution of tors within the field, along with other relevant features. Circles show locations of either individual tors or tight clusters of tors. Thus, the number of circles, about 530, is a minimum for the number of tors present.

The tors are not distributed in any simple geometric pattern, but many linear associations occur. The north-south alignments are parallel to foliation of the gneisses, which in turn is parallel to a vertical joint system. Escarpments also show a strong tendency towards north-south and northwest-southeast alignments, and in several places lines of tors and tor clusters are oriented parallel to them. Both escarpments and the flanks of tors are sites of late-lasting snowbanks. These are clearly visible on airphotos and provide an aid to mapping.

Where foliation lines and joints have been mapped, the surficial material is a block field in which the bedrock structure is discernible. Over most of the tor field, however, surficial material consists of sand-size debris or a mixture of blocks and sandy colluvium. This material apparently moves downslope by both solifluction and fluvial transport along the main sediment paths shown in Figure 40.2. Such drainage lines within the tor field appear to act as conduits for surface runoff for only a brief interval of the summer, but the

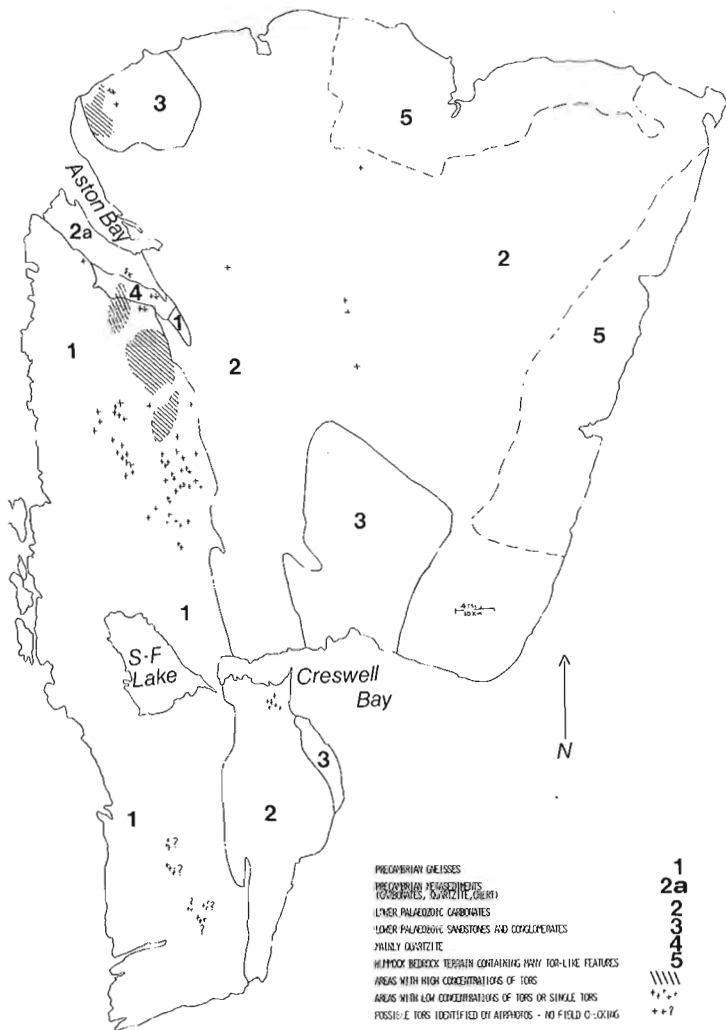


Figure 40.1. Distribution of tors on the various bedrock types of Somerset Island.

sandy material remains saturated throughout that season. For this reason the dominant mode of transport is thought to be soliflual rather than fluvial.

The tors and associated features shown in Figure 40.2 could have been formed by the following series of processes: (1) the landscape is initially weathered producing felsenmeer, presumably by frost shattering, as well as by weathering of felsenmeer blocks to grus. (2) Ensuing differential mass movement of the felsenmeer and grus exposes on the slopes low bedrock escarpments, the heights of which are determined by the spacing of horizontal joints or pseudobedding planes. (3) Continued mass movement leads to backwasting of these escarpments, a process similar to altiplanation described in Alaskan tor areas by Eakin (1916), and to isolation of remnant masses as tors. Because tors occur in linear associations that parallel directions of jointing, it is reasonable to assume that a tor marks a relatively less intensely jointed and, therefore, less easily dislodged rock mass. (4) Further continued weathering and mass movement leads to destruction of certain tors and "randomizing" of their distribution pattern.

A small area of the tor field, including four tor clusters, was selected for more detailed study. Attention was focused on the structure of the tor clusters and the nature and distribution of materials between them. Individual tors average three to four metres in height and have vertical or stepped faces (Fig. 40.3). The features consist of rhombohedrons with approximately one-metre-long edges defined by three joint planes – two nearly vertical, oriented roughly north-south and

northwest-southeast, and one nearly horizontal. The bedrock is felsic gneiss with well developed foliation, striking generally north-south.

Weathering of the tor rock is expressed most obviously by two microrelief types: (1) "Etching" has led to recession of those folia containing mafic minerals in a quartz matrix (most of which appear to be biotite) and relative protrusion of feldspar folia by about 3 cm. (2) Edge rounding and widening of joints have led to microrelief of up to at least 50 cm. This is more obvious on the tor tops than on their sides. On the tops, depressions along joints commonly are filled with gravelly, sandy grus consisting of mineral crystals, and easily crushed angular crystal aggregates, the whole being stained dark brown by iron oxides. Such accumulations of grus exceed 30 cm in depth and commonly fill joint spacings entirely. It is highly likely that the grus represents the material removed from the recessive folia and that the iron oxide staining was produced by weathering of the biotite. The original breakdown of the solid rock likely was accomplished by weathering of the biotite constituent. This reasoning is supported by Blackadar's (1967, p. 18) statement concerning the felsic gneisses: "Rusty bands are locally abundant in the succession. In contrast to the rusty gneisses of map-unit 1 (mafic gneisses), these rocks contain little graphite or pyrite. The rusty colour is due rather to the alteration of biotite-rich bands in the predominantly felsic complex". Mineralogical and chemical properties of the felsic gneisses of the region are contained in Tables 7 and 8

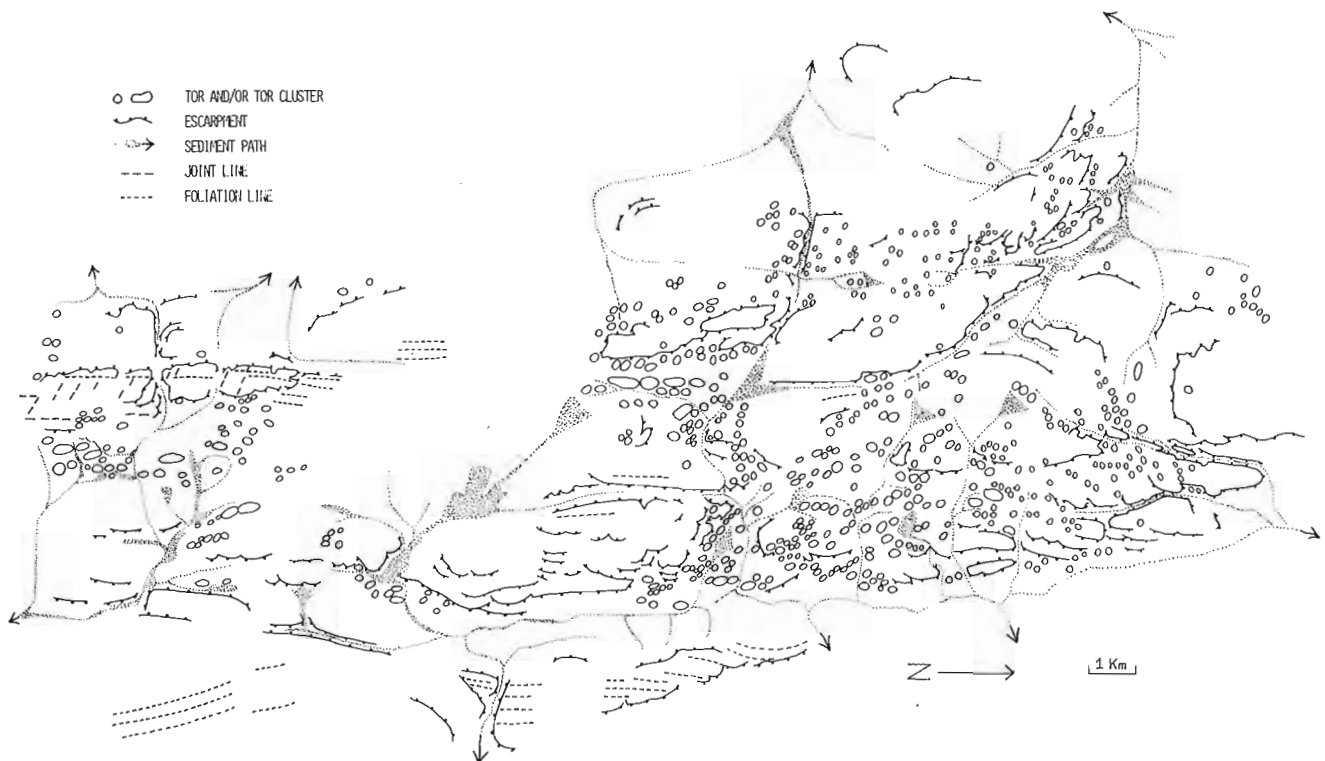


Figure 40.2. Distribution of tors and associated geomorphic features within part of the largest gneissic tor field south of Aston Bay.



Figure 40.3

One of the gneissic tors in the area of Figure 40.2. Note the joint pattern and the surrounding felsenmeer. (GSC-203014-E).

of Blackadar (1967). The considerable volume of grus found on the tors demonstrates the fine grained material is actively being produced in this environment by sub-aerial weathering of gneiss.

Figure 40.4 schematically summarizes the distribution of material around the tors, and Figure 40.5 provides an actual example. Each tor is surrounded by materials consisting of a mixture of joint blocks and frost-cracked joint blocks (60 to 80 per cent), and coarse sand and pea gravel (20 to 40 per cent) (Fig. 40.3). Where sufficient fines are present the assemblage is sorted into nets or circles with sandy centres. This material fills the space between tors of a cluster, surrounds the cluster, and in places bridges two closely spaced clusters.

Away from the tor clusters the block field grades into a unit containing roughly 50 per cent sand and pea gravel and 50 per cent blocks. This assemblage is arranged into sorted stripes oriented radially outward from the tor clusters. The striped unit is surrounded by a third unit in which block cover has decreased to 20 to 30 per cent, the whole being arranged into sorted circles. Beyond this, and occupying the spaces midway between widely spaced tor clusters, is a plain consisting almost entirely of sand and fine pea gravel. Boulders, commonly isolated, cover less than 5 per cent of the surface. One of the "clusters" consists of a single, small (ca. 1 m high and 2 m across) bedrock outcrop surrounded by a mixture of blocks and grus with the former dominating. This is interpreted as the remains of a former tor or cluster.

From the distribution of materials described above, the following is inferred concerning the weathering and tor evolution process:

- (1) The shape of the tors is dictated by the bedrock joint pattern.
- (2) Modifications to both shape and size are produced by dislodgment of joint blocks and subsequent mass

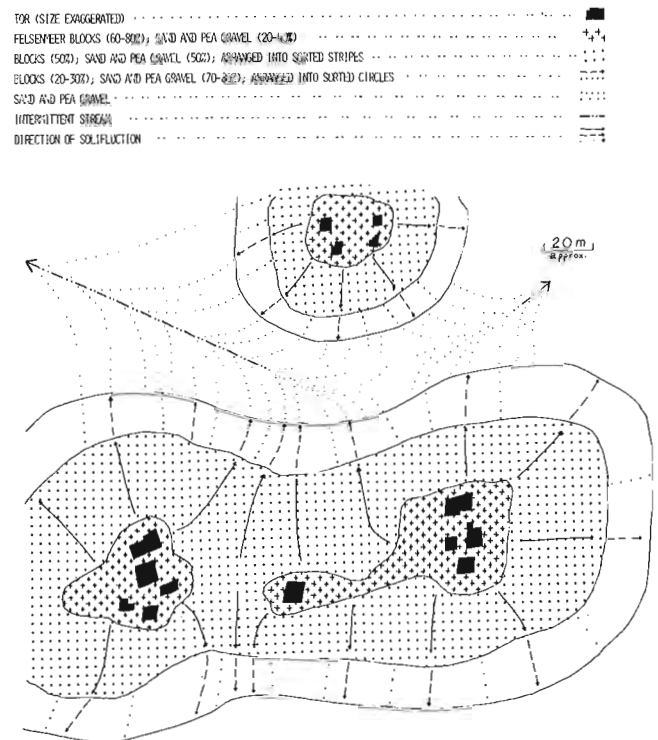


Figure 40.4. Schematic map of the surficial geology of a small portion of a tor field. This pattern appeared to be consistent throughout the field.

movement radially outward from their points of origin and by decomposition of the rock to grus. Both these processes presently are active in the study area.

- (3) The systematic decrease in the concentration of blocks on the surface, to the point where they are almost entirely absent from the areas midway between



Figure 40. 5

Photograph from approximately 50 m above the ground surface of a small portion of a gneissic tor field. (GSC-203014-D).

Figure 40. 6.

Portion of a large tor formed of interbedded carbonate, chert, and quartzite located immediately south of Aston Bay. The vertical face is approximately 2.5 m high. Strata are nearly horizontal and joints vertical. (GSC-203014-A).



the clusters (Fig. 40. 4), demonstrates that almost all solid blocks weather to sand-sized material in the length of time required for their transportation a distance of only a few hundred metres. In the area studied, the surface slope upon which the material moves is only 1 to 2 degrees. The rate of movement, therefore, is considered to be very slow.

(4) When the rate of denudation accomplished by lateral movement of weathered materials surrounding the tors remains for a period of time less than the rate at which material is removed from the sides and tops of the tors themselves, the features degenerate into small block fields which in turn are reduced to grus. Thus, the period of tor formation and relative increase in height is succeeded by a period of tor destruction. The critical factor controlling the conversion from growth to destruction may be the depth of materials overlying bedrock between the tors or tor clusters. During the period of tor formation this depth is less than the depth

of the active layer and the depth that frost shattering of bedrock can occur. Lateral movement of this shattered bedrock, and the grus which it produces, causes lowering of the bedrock surface and relative enhancement of tor heights. During this stage the tor rock continues to be more resistant to weathering than the surrounding bedrock for reasons discussed above. When the depth of weathered material surrounding the tors exceeds the depth of seasonal thaw, the only bedrock protruding above the permafrost table is that of the tors themselves. The tors then become more susceptible to weathering than the surrounding bedrock.

Within the area of Figure 40. 4 three or four carbonate erratic boulders are found near the tors. These are severely pitted and may represent relicts of a glaciation that predates the tors or may indicate that the tors have been overridden by ice with very little power to erode. The latter situation is similar to that invoked by Sugden and John (1976) to explain the presence of erratics near tors in the Cairngorms of Scotland.

Carbonate Tors

Tors developed on Proterozoic carbonates with interbedded chert and quartzite south of Aston Bay and those on Lower Paleozoic carbonates south of Creswell Bay were examined briefly. While the latter area contains the greater number, both groups are similar in size and structure (Fig. 40.6). Heights vary between an estimated two and five metres. Micro-relief imparted by weathering is controlled by the sedimentary and joint structures. Thus, chert, quartzite, and more resistant carbonate beds provide positive relief, while less resistant carbonate beds have recessed by weathering to a nearly homogeneous silt, which is easily removed by rainwash and wind. It is unknown whether this silt was produced by microglaciation or represents the less soluble portions of the parent strata. The more resistant carbonate strata

commonly display severely pitted surfaces which, likewise, may result from either solution or mechanical comminution. The resistant strata break into small blocks, presumably by frost shattering. When these blocks are mixed at the bases of the tors with the above mentioned silts, a diamicton easily mistaken for till, is produced.

Gneissic erratics in places are found near the tors to the south of Creswell Bay. This invokes either of two hypotheses: (1) the tors predate glaciation by noneroding ice or (2) the erratics represent the remnants of a till which predates the tors but which has not yet been completely swept away by the denuding processes. The highly fragile nature of the tors and their occurrence in exposed topographic situations makes it unlikely that they would have survived the passage of an ice sheet with the erosive capacity to produce a till. Although the till overlying the carbonate bedrock

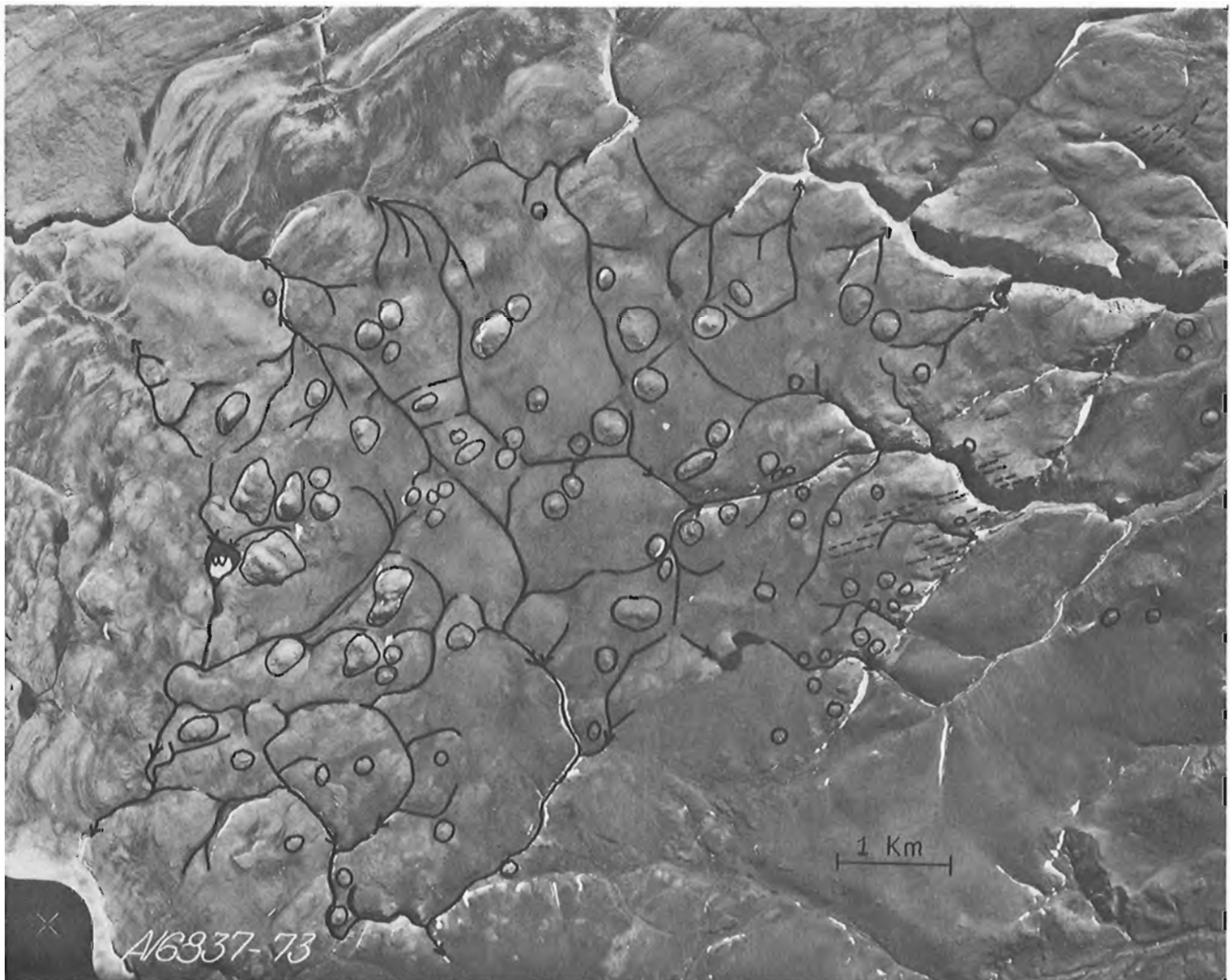


Figure 40.7. Portion of a vertical airphoto showing the distribution of tors on sandstones on northwestern Somerset Island. Circles locate tors and clusters of tors, broken lines follow bedrock strata, and solid lines with arrows show main sediment paths. (GSC-203012).

contains many gneissic erratics, it is dominantly composed of clasts of local derivation. This leads to the conclusion that the ice which overrode the area was not protective, but erosive. For this reason, the writer prefers the latter hypothesis.

Sandstone Tors

The main concentration of tors developed on rocks of the Peel Sound Formation of northwestern Somerset Island is illustrated in Figure 40.7. The surface drainage pattern and the main directions of movement of surficial materials by solifluction are shown. Smaller solifluction stripes are visible on the photograph and show convergence of materials towards the main sediment paths. The tors occupy local topographic highs which are being denuded by solifluction of weathered bedrock. The distribution of tors shows no obvious symmetrical geometry and no obvious relation to the bedrock structure. Field observations, however, indicate that the characteristics of the individual tors, to a large extent, are dictated by the sedimentary structure.

Conclusions and Implications

Subaerial weathering, both chemical and physical, combined with periglacial mass movement, has led to the evolution of tor landscapes on gneisses (both mafic and felsic), quartzites, metasediments (interbedded carbonates, chert, and quartzite), carbonates, conglomerates, and sandstones. While the tors are most abundant on gneisses and sandstones, they have similar average sizes on all rock types. The heights of tors provide minimum measures of the amount of denudation that has occurred since the initiation of tor formation, which may coincide with deglaciation.

The only data on current denudation rates on Somerset Island are supplied by Smith (1972), who concluded that denudation by removal of dissolved solids from limestone areas of the northern part of the island is about 2 mm per 1000 years. Assuming that this is representative of Holocene rates, only about 2 cm of denudation could have been accomplished by that process operating on areas of carbonate bedrock during Holocene time. This is obviously insignificant when compared to the heights of carbonate tors and is even less significant in explaining the sizes of gneissic, quartzite, or sandstone tors. No data are available on the rates of other denuding processes.

Most authorities have supported the concept of nearly complete coverage of the Canadian Arctic by ice sheets during late Wisconsin time (Bryson *et al.*, 1969; Prest, 1969; Blake, 1970; Blake, 1975; Barnett *et al.*, 1976), with Somerset Island lying near the central portion of the glaciated area. If this concept is correct, either the late Wisconsin ice must have been cold based and protective or bedrock denudation rates on Somerset Island have been suprisingly high throughout the Holocene. On the other hand, Netterville *et al.* (1967) have presented several lines of argument which suggest that at least a large portion of Somerset Island lay beyond the margins of the late Wisconsin ice sheets

(either Laurentide or Innuitian). Tors have not been reported from any area of Canada that is known to have been glaciated during late Wisconsin time. They are commonly encountered on surfaces which predate the late Wisconsin (and, indeed, the early Wisconsin) on Baffin Island (cf. Pheasant and Andrews, 1972) and have been reported from pre-late Wisconsin areas of the Yukon (Bostock, 1966). Furthermore, England (1974) noted tors on surfaces beyond the late Wisconsin moraines of northeastern Ellesmere Island. The data presented in this paper question the concept of an all-pervasive late Wisconsin ice cover in Arctic Canada.

Acknowledgments

Earlier typescripts of this paper were reviewed by D.R. Grant, J.A. Netterville, V.K. Prest, R.D. Thomas, and C.M. Tucker of Terrain Sciences Division, GSC, and by J.H. England of the University of Alberta. Each of the above provided useful comments which led to improvements in content or readability. I also gratefully acknowledge pertinent discussions during the course of the field season with K.A. Drabinsky, Terrain Sciences Division, B. Grey, Environment Canada, V. Woo, Manitoba Soil Survey, and S.C. Zoltai, Canadian Forestry Service. In addition, D.E. Sugden, University of Aberdeen, provided useful discussion of general problems involved in tor studies and the problem of deciphering the relationship between tor distribution and age of surface.

References

- Barnett, D.M., Dredge, L.A., and Edlund, S.A.
1976: Terrain inventory: Bathurst, Cornwallis, and adjacent islands, Northwest Territories, in Report of Activities, Part A; Geol. Surv. Can., Paper 76-1A, p. 201-204.
- Bird, J.B.
1967: The Physiography of Arctic Canada (with special reference to the area south of Parry Channel); Johns Hopkins Press, Baltimore, Maryland, 336 p.
- Blackadar, R.G.
1967: Precambrian geology of Boothia Peninsula, Somerset Island, and Prince of Wales Island, District of Franklin; Geol. Surv. Can., Bull. 151, 62 p.
- Blackadar, R.G., Christie, R.L., and Taylor, F.C.
1967: Somerset Island and Prince of Wales Island, District of Franklin; Geol. Surv. Can., Map 3-1967.
- Blake, W., Jr.
1970: Studies of glacial histories in Arctic Canada I: Pumice, radiocarbon dates, and differential postglacial uplift in the eastern Queen Elizabeth Islands; Can. J. Earth Sci., v. 7, p. 634-664.

- Blake, W., Jr. (cont.)
 1975: Radiocarbon age determinations and post-glacial emergence at Cape Storm, southern Ellesmere Island, Arctic Canada; *Geogr. Ann.*, Ser. A, v. 57, p. 1-71.
- Bostock, H. S.
 1966: Notes on glaciation in the central Yukon Territory; *Geol. Surv. Can.*, Paper 65-36, 18 p.
- Brown, E. H. and Waters R. S., eds.
 1974: Progress in geomorphology (papers in honour of David L. Linton); *Inst. Br. Geogr.*, Spec. Publ. no. 7, 255 p.
- Bryson, R. A., Wendland, W. M., Ives, J. D., and Andrews, J. T.
 1969: Radiocarbon isochrones on the disintegration of the Laurentide Ice Sheet; *Arct. Alp. Res.*, v. 1, p. 1-14.
- Craig, B. G.
 1964: Surficial geology of Boothia Peninsula and Somerset, King William, and Prince of Wales Islands, District of Franklin; *Geol. Surv. Can.*, Paper 63-44, 10 p.
- Craig, B. G. and Fyles, J. G.
 1960: Pleistocene geology of Arctic Canada; *Geol. Surv. Can.*, Paper 60-12, 21 p.
- Cunningham, F. F.
 1969: The Crow Tors, Laramie Mountains, Wyoming, U. S. A.; *Z. Geomorphol.*, Neue Folge, Band 13, p. 56-74.
- Eakin, H. M.
 1916: The Yukon-Koyukuk region, Alaska; *U. S. Geol. Surv.*, Bull. 631, p. 67-82.
- England, J. H.
 1974: The glacial geology of Archer Fiord/Lady Franklin Bay area, northeastern Ellesmere Island, NWT, Canada; in *A-The Humanities and Social Sciences; Dissertation Abstracts Int.*, Ann Arbor, Mich., v. 35, p. 2149A.
- Linton, D. L.
 1955: The problem of tors; *Geogr. J.*, v. CXXI, p. 470-487.
- Netterville, J. A., Dyke, A. S., Thomas, R. D., and Drabinsky, K. A.
 1976: Terrain inventory and Quaternary geology, Somerset, Prince of Wales, and adjacent islands; in *Report of Activities, Part A*; *Geol. Surv. Can.*, Paper 76-1A, p. 145-154.
- Pheasant, D. R. and Andrews, J. T.
 1972: The Quaternary history of northern Cumberland Peninsula, Baffin Island N. W. T.: Part VIII, Chronology of Narpaing and Quajon Fiords during the past 120,000 years; 24th Int. Geol. Congr., Sect. 12, Montreal, p. 81-88.
- Prest, V. K.
 1969: Speculative isochrones on the retreat of Wisconsin and Recent ice in North America; *Geol. Surv. Can.*, Map 1257A.
- Pullan, R. A.
 1959: Tors; *Scot. Geogr. Mag.*, v. 75, p. 51-55.
- Smith, D. I.
 1972: The solution of limestone in an arctic environment; in *Polar Geomorphology*, eds. R. J. Price and D. E. Sugden; *Inst. Br. Geogr.*, Spec. Publ. no. 4, p. 187-200.
- Sugden, D. and John, B.
 1976: *Glaciers and Landscape - a geomorphological approach*; Edward Arnold, London, 320 p.

Project 730027

John V. Matthews, Jr.
Terrain Sciences Division

Introduction

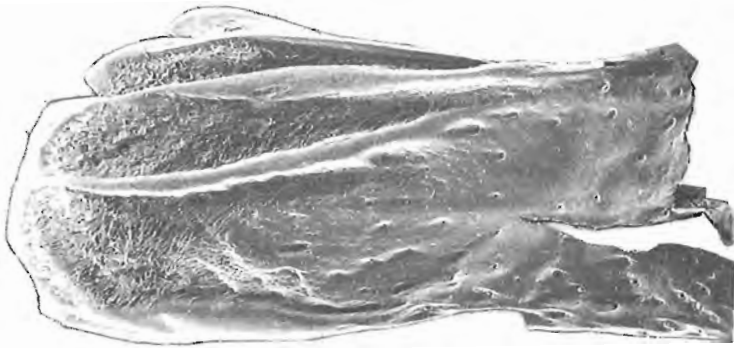
The late Tertiary Beaufort Formation, comprised chiefly of unconsolidated sands and gravels, outcrops extensively along the western and northwestern margin of the Canadian Arctic Archipelago (Fig. 41.1), and it occurs as outliers on some of the eastern islands of the Arctic Archipelago (Tozer and Thorsteinsson, 1964;

Balkwill and Bustin, 1975; Wilson, 1976). Beaufort sediments are primarily alluvial in origin. They possess sedimentary features indicating deposition by north to northwesterly flowing rivers prior to formation of the marine passages that now separate the islands.

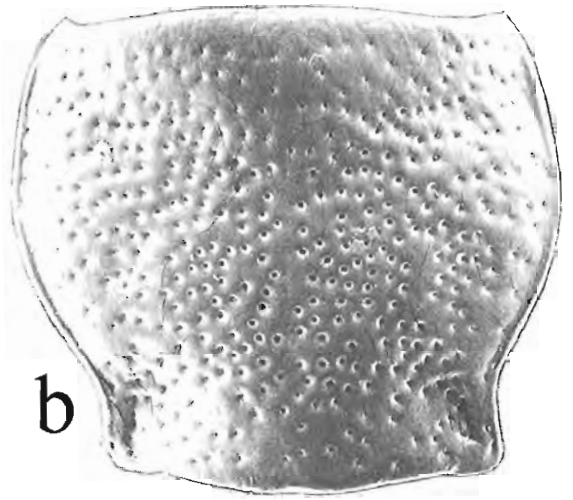
At some of the Beaufort exposures organics are interspersed with sands and gravels. These organics commonly consist entirely of large fragments of



Figure 41.1. Distribution of the Beaufort Formation and location of sites mentioned in text.



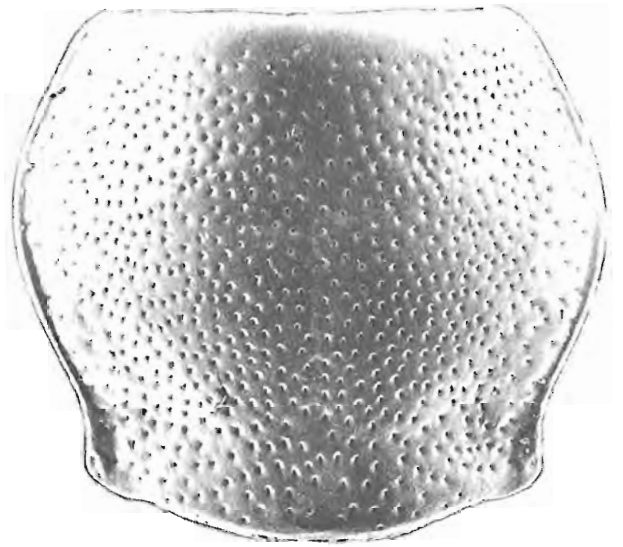
a



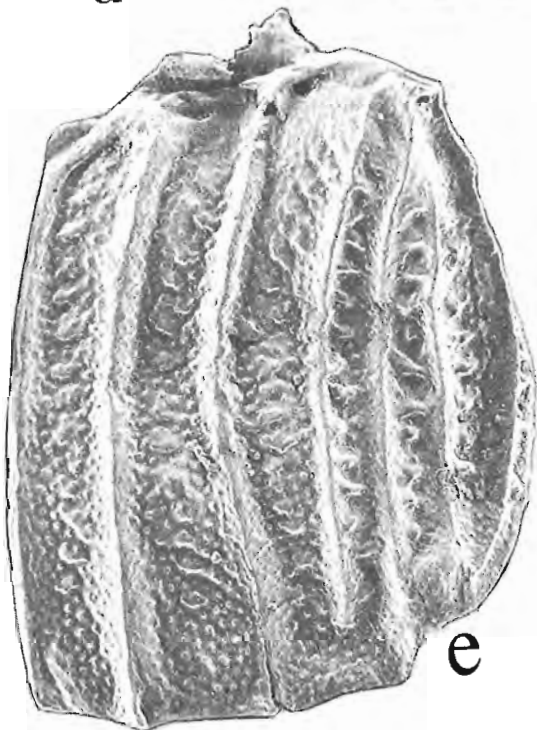
b



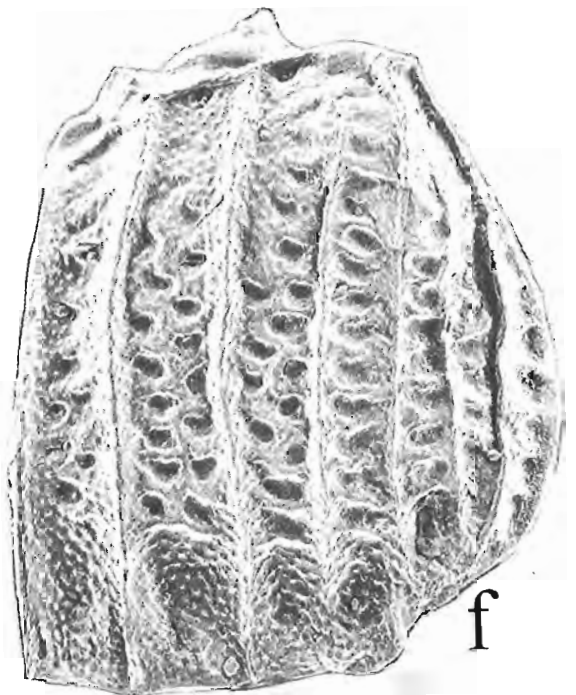
d



c



e



f

Figure 41. 2. Insect fragments (Beaufort Formation fossils and a modern counterpart) (opposite)
Scale bar = 0.5 mm. All photos are SEM micrographs, taken with the help of Louis Ling, Carleton University, uncoated at <1.4 kv.

- a) *Bombus* sp.; GSC-46917; left mandible; Meighen Island, Northwest Territories, Loc. 2-73, Sample JVM 5b-73
- b) *Diacheila* cf. *D. polita* Fald.; GSC-46918; pronotum; Meighen Island, Northwest Territories, Loc. 2-73, Sample JVM 5-73.
- c) *Diacheila polita* Fald.; modern; pronotum; College, Alaska, V-10-66, collected by J. Matthews. Note punctures smaller and more densely spaced than in Fig. 41. 2b. Arcuate base of specimen illustrated in Fig. 41. 2c is due to orientation.
- d) *Micropeplus sculptus* Lec.; GSC-46919; left elytron; Banks Island, Ballast Brook, Sample JVM 3-73.
- e) *Micropeplus hoogendorni* Matth.; GSC-46920; right elytron; Ballast Brook area, Banks Island, Northwest Territories, Sample JVM 3-73.
- f) *Micropeplus hopkinsi* Matth.; GSC-46921; right elytron; Ballast Brook area, Banks Island, Northwest Territories, Sample JVM 3-73.

redeposited wood. Zones of finer detritus and autochthonous peats are much rarer, having been found thus far only on northern Banks Island and on Meighen Island (Fig. 41. 1). Only Beaufort Formation sediments and a thin mantle of Pleistocene or Holocene (Koerner and Paterson, 1974) drift (till and marine sediments) occur on Meighen Island (Thorsteinsson, 1961), and they probably constitute just the upper part of a thick clastic wedge of Beaufort and earlier Tertiary sediments (Wilson, 1976). In addition to well preserved organic horizons, some of the sandy Beaufort exposures on Meighen Island also contain interdigitating black marine clays.

These clays contain fossils of Foraminifera and molluscs which, when they are studied, should provide valuable criteria for correlation of the northern Beaufort exposures with other late Tertiary sequences around the Arctic Basin. At present, the Beaufort Formation is dated by comparison of its fossil floras with those that define the Tertiary sequence in southern Alaska (Wolfe *et al.*, 1966). There the Clamgulchian Stage represents the upper Miocene and part of the Pliocene with the Homerian and Seldovian stages being of middle and middle to early Miocene age, respectively. Beaufort floras studied to date have a Homerian-Seldovian character (Hills and Ogilvie, 1970; Hills *et al.*, 1974; Hills and Bustin, 1976) which means that they are Miocene in age and, according to recent K-Ar dates from the Kenai Peninsula in Alaska (Turner *et al.*, 1975), are older than 8 million years.

Beaufort floras at northern localities like Meighen Island differ from those on Banks Island in the southern part of the Archipelago (Hills and Matthews, 1974; Hills *et al.*, 1974; Hills and Bustin, 1976). These differences are explained at present as a reflection of the eight degree latitudinal spread between Beaufort fossil localities, but it must be stressed that the differences are of the type that would be expected if northern Beaufort sediments were younger than those in the south.

In the past few years Beaufort Formation fossils have come under detailed study. L. V. Hills (University of Calgary) is dealing with plant fossils while the writer's efforts centre on insect fossils, particularly beetles (Coleoptera). Figure 41. 2 illustrates the excellent preservation of Beaufort insect fossils. The best preserved specimens come from organic zones exposed on Meighen Island. M. Kuc first noted beetle fossils within these organic horizons while collecting fossil mosses (Kuc, 1973), but it was not until Hills and Matthews visited the island in 1973 that the full paleontological potential of the Meighen Island exposures became obvious. The organic lenses occurring within the dominantly sandy exposures there contain some of the best preserved Miocene plant macrofossils yet discovered, and many of the beetle fossils are as well or better preserved than those from Pleistocene deposits. The 1973 work clearly revealed the need for another trip to the region, but this was not possible in 1974 due to the lack of summer thawing. In 1975, however, additional field work on the island was undertaken; the stratigraphy was studied in more detail; marine molluscs were collected; and large volumes of sediments were sieved for fossil insects and plants. Hills will report on the results of the stratigraphic studies and on new botanical finds in a paper now in preparation. This report contains an updated list of insect fossils, both from Meighen Island and from the Ballast Brook area of northern Banks Island. Such a list has been presented before (Matthews, 1974), but the one included here is considerably longer (based on 1973 and 1975 data) and is a better reflection of the former taxonomic diversity of the Meighen Island Beaufort fauna. This being so, the list forms a better basis for assessing the biological and geological implications of the Beaufort Formation insect fossils.

Evolutionary Implications

Although as a general rule insects are noted for their poor fossil record, in the last fifteen years there has been an explosion of information on fossil Coleoptera (Coope, 1970). Unfortunately, however, the majority of such fossils are of Quaternary age and refer to extant (living) species; so they are of little value for elucidating evolutionary history. Many of the Beaufort fossils can be assigned with confidence to extant genera (often the earliest record of these), but contrary to Matthews (1974) it is now known that the majority of those listed in Table 41. 1 do not fall within the range of variation of the extant species to which they are tentatively referred (note "cf" designation in the table).

Table 41.1

Arthropod Fossils -- Beaufort Formation¹

Taxon	Meighen ² Island	Banks ³ Island
INSECTA		
Homoptera "bugs"		
Cicadellidae "leafhoppers" ⁴		
<i>Athysanella</i> ap.	+	
Genus A	+	
Genus ?	+	
Coleoptera "beetles"		
Cicindelidae "tiger beetles" ⁵		
Genus ?	+	
Carabidae "ground beetles"		
<i>Trachypachus</i> cf. <i>T. holmbergi</i> Mann.	+	
<i>Trachypachus</i> sp. A.	+	
<i>Trachypachus</i> sp.		+
<i>Carabus</i> cf. <i>C. taedatus</i> Fab.	+	
<i>Carabus</i> sp.	+	
<i>Pelophila</i> cf. <i>P. borealis</i> Payk.	+	
<i>Nebria</i> cf. <i>gyllenhali</i> sp. grp.	+	
<i>Opisthius</i> cf. <i>O. richardsoni</i> Kirby	+	

¹Fossils identified as of March 1, 1976.

²District of Franklin, Northwest Territories; samples are from several fossil localities at different stratigraphic levels within the exposed portion of the Beaufort Formation.

³Upper Beaufort Formation, Ballast Brook area, northwestern Banks Island, District of Franklin; most fossils are from the same horizon that contained fossil mosses discussed by Kuc and Hills (1971).

⁴Identified by K. G. A. Hamilton, Biosystematics Inst., Dep. of Agriculture, Ottawa. Leafhopper fossil referred to as "Genus A" is the one cited in Matthews (1974) as representing a supraspecific taxon that is today unrepresented in the Nearctic region.

⁵All common names for beetle families are from Arnett (1963).

⁶Identified by H. Goulet, Department of Entomology, University of Alberta.

Table 41.1 (cont.)

Taxon	Meighen ² Island	Banks ³ Island
<i>Notiophilus</i> cf. <i>N. directus</i> Casey	+	
<i>Notiophilus</i> sp.		+
<i>Diacheila</i> cf. <i>D. polita</i> Fald (Fig. 41.2b)	+	
cf. <i>Diacheila</i>		+
<i>Blethisa</i> cf. <i>B. multipunctata</i> L.	+	
<i>B.</i> cf. <i>B. catenaria</i> Brown	+	
<i>Elaphrus</i> cf. <i>E. lapponicus</i> Gyll.	+	
<i>E.</i> cf. <i>E. clairvillei</i> Kirby ⁶	+	
<i>E. riparius</i> L. ⁶	+	
<i>E.</i> cf. <i>americanus</i> sp. grp. ⁶	+	
<i>Elaphrus</i> sp.		+
<i>Dischirius</i> spp.	+	+
<i>Patrobus</i> cf. <i>P. septentrionis</i> Dej.	+	
<i>Patrobus</i> sp.		+
<i>Asaphidion alaskanum</i> Wick.	+	+
<i>Bembidion</i> cf. <i>B. lapponicum</i> Zett.	+	
<i>B.</i> (<i>Chrysobracteum</i>) sp.		+?
<i>B.</i> cf. <i>B. nitidum</i> Kirby		+
<i>B.</i> cf. <i>B. dyschirinum</i> Lec.	+	
<i>B.</i> (<i>Plataphodes</i>) spp.	+	+
<i>B.</i> cf. <i>B. planatum</i> Lec.	+	
<i>B.</i> cf. <i>B. bimaculatum</i> Kirby	+	
<i>B.</i> cf. <i>B. nigripes</i> Kirby	+	
<i>B.</i> (<i>Trepanedoris</i>) spp.	+	
<i>Tachyta</i> cf. <i>T. angulata</i> Casey ⁷		+
<i>Pterostichus</i> cf. <i>P. circulosus</i> Lth.	+	
<i>P.</i> (<i>Derus</i>) sp.	+?	
<i>P.</i> (<i>Cryobius</i>) cf. <i>P. kotzebuei</i> Ball	+	
<i>P.</i> (<i>Cryobius</i>) cf. <i>P. tareumiut</i> Ball	+	
<i>P.</i> (<i>Cryobius</i>) <i>brevicornis</i> sp. grp.	+	
<i>P.</i> (<i>Cryobius</i>) <i>ventricosus</i> sp. grp.	+	
<i>P.</i> (<i>Cryobius</i>) spp.	+	+?
<i>P.</i> cf. <i>P. vermiculosus</i> Men.	+	
<i>P.</i> cf. <i>P. haematopus</i> Dej.	+	
<i>Pterostichus</i> spp.	+	+?

⁷Identified by T. L. Erwin, Dep. of Entomology, U. S. National Museum of Natural History, Washington, D. C.

Table 41.1 (cont.)

Taxon	Meighen ² Island	Banks ³ Island
<i>Agonum</i> cf. <i>A. consimile</i> Gyll.	+	
<i>A. (Stictanchus)</i> cf. <i>A. bicolor</i> Dej.	+	
<i>A.</i> cf. <i>A. cincticolle</i> Say	+	
<i>Agonum</i> sp.		+
<i>Amara</i> cf. <i>A. alpina</i> Payk.	+	
<i>A.</i> cf. <i>A. carinata</i> Lec.	+	
<i>Harpalus</i> cf. <i>H. amputatus</i> Say	+	
<i>Dromius</i> cf. <i>D. piceus</i> Dej.	+	
<i>Chlaenius</i> sp.	+	
Dytiscidae "predaceous diving beetles"		
<i>Hydroporus</i> sp.	+	
<i>Agabus</i> sp.	+?	
<i>Ilybius</i> sp.	+	
<i>Colymbetes</i> sp.	+	
Gyrinidae "whirligig beetles"		
<i>Gyrinus</i> sp.	+	+
Hydrophilidae "water scavenger beetles"		
<i>Helophorus (Cyphelophorus)</i> sp. B. ⁸	+	
<i>Helophorus</i> sp.	+	
<i>Hydrobius</i> sp.	+	
Georyssidae "minute mud-loving beetles"		
<i>Georyssus</i> sp. ⁹	+	
Staphylinidae "rove beetles"		
<i>Kalissus</i> sp. A.	+	
<i>Micropeplus hopkinsi</i> Matth. (Fig. 41.2f)		+
<i>M. hoogendorni</i> Matth. (Fig. 41.2e)		+
<i>M. sculptus</i> Lec. (Fig. 41.2d)	+	+
<i>Carpelimus</i> sp. ¹⁰	+	
<i>Bledius</i> sp.	+	
<i>Arpedium</i> sp.	+	
<i>Olophrum</i> sp.	+	

⁸New species described in Matthews (in press).

⁹Similar to the species found in Lava Camp sediments (Hopkins *et al.*, 1971).

¹⁰Identified by J. M. Campbell, Biosystematics Inst., Dep. of Agriculture, Ottawa.

Table 41.1 (cont.)

Taxon	Meighen ² Island	Banks ³ Island
<i>Acidota</i> sp.	+	
<i>Pycnoglypta</i> cf. <i>P. lurida</i> Gyll.	+	
<i>Omalium</i> sp.	+	+?
<i>Micralymma</i> cf. <i>M. brevilingue</i> Schiødt	+	
<i>Stenus</i> spp.	+	+
<i>Quedius</i> (<i>Raphirus</i>) <i>aenescens</i> sp. grp.	+	
<i>Tachinus</i> cf. <i>T. jacuticus</i> Popp.	+	
<i>Tachinus</i> sp.		+
<i>Tachyporus</i> sp.	+	
<i>Gymnusa</i> sp.	+	+
Pselaphidae "short-winged mold beetles"		
Genus?		+
Silphidae "carrion beetles"		
<i>Silpha</i> cf. <i>S. ramosa</i> Say	+	
<i>Phosphuga</i> cf. <i>P. atrata</i> L.	+	
Leptodiridae "small carrion beetles"		
<i>Colon</i> sp.		+?
Leiodidae "round fungus beetles"		
Genus?	+	
Scydmaenidae "ant-like stone beetles"		
Genus?	+	
Histeridae "hister beetles"		
<i>Platysoma</i> sp.	+?	
Scarabaeidae "scarab beetles"		
<i>Aegialia</i> sp.	+	
Byrrhidae "pill beetles"		
<i>Simplocaria</i> sp.	+	
<i>Byrrhus</i> sp.	+	
<i>Cytilus</i> sp.	+	
<i>Morychus</i> sp.	+	
<i>Curimopsis</i> sp.	+	
<i>Eusomalia</i> sp.		+?
Elateridae "click beetles"		
<i>Hypolithus</i> cf. <i>H. sandborni</i> (Horn) ¹¹	+	

¹¹Identified by E. C. Becker, Biosystematics Inst., Dep. of Agriculture, Ottawa.

Table 41.1 (concluded)

Taxon	Meighen ² Island	Banks ³ Island
Lathridiidae "minute brown scavenger beetles"		
<i>Stephostethus</i> sp.	+?	
Genus?		+
Colydiidae "cylindrical bark beetles"		
<i>Bitoma</i> sp.	+?	
Chrysomelidae "leaf beetles"		
<i>Donacia</i> sp.	+	
Curculionidae "weevils"		
<i>Apion</i> sp.	+	
<i>Vitavitus</i> cf. <i>V. thulius</i> Kissinger	+	
<i>Lepyrus</i> sp.	+	
<i>Grypidius</i> cf. <i>G. equiseti</i> Fab.	+	
<i>Notaris</i> sp.	+	
<i>Lixellus</i> sp.		+?
<i>Cleonus</i> sp.		+
<i>Ceutorhynchus</i> sp.	+	
Diptera "two-winged flies"		
Tipulidae "crane flies"		
<i>Tipula</i> sp.	+	
Coenomyiidae		
<i>Xylophagus</i> sp.	+	
Chironomidae		
Genus?	+	
Hymenoptera "wasps and ants"		
Ichneumonoidea "parasitic wasps"	+	
Diapriidae	+	
Formicidae "ants"		
<i>Leptothorax</i>	+?	
Apoidea "bees"		
<i>Bombus</i> sp. (Fig. 41.2a)	+	
ARACHNIDA		
Acari		
Oribatidae "oribatid mites"		
<i>Cepheus</i> cf. <i>C. corae</i> Jacot	+	
Genus?	+	
CRUSTACEA		
Notostraca "tadpole shrimp"		
<i>Lepiduris</i> sp.	+	

Undoubtedly they represent extinct species closely related to the named species, and in some cases (e. g. , the *Diacheila* fossils, Fig. 41. 2b) they seem more closely related to the referred extant species than to any other extant species of the genus. This characteristic of the Beaufort fossils, plus their abundance and excellent preservation, makes them a treasure-trove of information on evolutionary history.

Fossils, however, are not necessary for the study of evolutionary history, as illustrated by the fact that most entomologists, working as they must without fossil evidence, seek to construct phylogenies principally by examination of the characters displayed by living species. This approach is necessarily cladistic (i. e. , emphasizing branching relationships) and contrasts with that of most paleontologists, who, because of their different perspective of evolution, see it basically as a process of change within lineages (phyletic gradualism). The merits and demerits of these two approaches are not within the scope of this paper and are clarified elsewhere (Darlington, 1970; Eldredge, 1971; Eldredge and Gould, 1972; Harper, 1976). What is pertinent to note here is that any attempt to use the Beaufort fossils to elucidate evolutionary history brings one face to face with the two conflicting viewpoints. For example, the insect groups to which the fossils belong have been classified, and will continue to be classified, using cladistic methodology, but at the same time the similarity of some of the fossils to extant species is a persuasive argument for phyletic gradualism. Both approaches are accommodated by Ross (1974). The writer has followed (Matthews, in press), and will in the future continue to follow, Ross' rationale in attempting to construct phylogenies using the Beaufort fossils. This means that the study of each Beaufort species must be accompanied by detailed analyses of the related extant species (e. g. , Matthews, in press). The procedure is most easily followed in those cases where the fossils themselves preserve critical morphological characters necessary for establishment of phenoclines (character sequences) and where the genus or other supraspecific group to which the fossils are referred has few extant species. Accordingly, of the taxa listed in Table 41. 1, only a few, e. g. , *Trachypachus*, *Diacheila*, *Blethisa*, *Elaphrus*, some groups of *Bembidion*, *Helophorus*, *Georyssus*, *Kalissus*, and *Micropeplus*, are well suited at the present time for phylogenetic study using the Beaufort fossils.

Stratigraphic Implications

Insect fossils seldom have been used for correlation and dating; hence one of the more intriguing implications of Beaufort Coleoptera fossils is that they may be applied to just that end. This is discussed elsewhere (Matthews, in prep.), but it should be clear from what has been stated above that once the phylogenies of some of the groups mentioned in the table are established, even at a provisional level, the fossils representing these groups will inevitably take on added chronologic and stratigraphic significance.

One of the unknowns associated with the Beaufort Formation concerns the age equivalence of northern and southern exposures. As indicated earlier, one interpretation of the north to south differences of Beaufort floras is that they reflect an isochronous latitudinal gradient (Hills and Bustin, 1976). Such differences, however, could be due to diachronous Beaufort deposition. There is hope that insect fossils common to both northern and southern localities eventually may play a part in resolving this dilemma, but the most powerful evidence is likely to come from a comparison of the northern and southern Beaufort Coleoptera assemblages with the beetle assemblage from the 5. 7-million-year-old (Clamgulchian) Lava Camp site in western Alaska (Hopkins *et al.* , 1971). It is already possible to conclude, on the basis of one study of *Helophorus* fossils from Lava Camp and Meighen Island (Matthews, in press), that the latter region contains Beaufort sediments that are younger than the Lava Camp deposits and hence are younger than the Beaufort Formation on Banks Island. This conclusion, however, is based on only one of several possible interpretations of *Helophorus* (*Cyphelophorus*) phylogeny and requires confirmation. At present it does not seem to be supported by plant fossils from Meighen Island or by other beetle fossils from both Lava Camp and Meighen Island.

What is important to note at this state of study of Beaufort fossil insects is that several genera occur at both the southern and northern Beaufort exposures as well as at Lava Camp in Alaska. Among the most important of these for correlation purposes likely will be members of the subfamily Micropeplinae (Staphylinidae), for its fossils are replete with distinctive characters, and the overall diversity within the subfamily is low. For example, one of the Meighen Island sites contains fossils of an extinct species of the micropepline genus *Kalissus*, and the upper Beaufort Formation at Ballast Brook on Banks Island is now known (this paper) to contain two *Micropeplus* species, *M. hopkinsi* and *M. hoogendorni* (Figs. 41. 2e, f), which were formerly reported only at Lava Camp (Matthews, 1970). Moreover fossils of the distinctive species, *M. sculptus*, occur at both northern and southern Beaufort exposures (Table 41. 1).

Paleoecological Implications

The writer previously concluded that the Meighen Island assemblage represented the earliest record of lowland tundra because of the presence of fossils of beetle species, such as *Diacheila polita*, that have present-day tundra affinities (Matthews, 1974). Now that it is known that most of the fossils in the list do not represent extant species, such exact paleoenvironmental analogies are suspect. But the initial conclusion still stands – in fact is reinforced – because the much larger assemblage (Table 41. 1) contains numerous fossils whose closest extant relatives are forest-tundra species. Even though some of these fossils may represent species with slightly different ecological requirements than

their modern counterparts, it is unlikely that the entire assemblage would so closely resemble, taxonomically, a forest-tundra fauna without actually representing such an environment. This conclusion also is confirmed by the abundance of shrub birch fossils, by the small size of tree fragments (much smaller than at Beaufort exposures on Banks Island), and by negative evidence such as the absence of bark beetle (Scolytidae) fossils.

Some plant fossils imply that the forest-tundra environment of Meighen Island was not exactly like that of the present (Hills and Matthews, 1974). This is true as well of the beetle fossils since individuals of *Dromius*, *Chlaenius*, *Georyssus*, and Histerid beetles do not live in contemporary forest-tundra regions. Their northern limits are well south of that boundary today. Perhaps the explanation for this enigma lies with the rapid climatic fluctuations and glaciations of the Pleistocene.

A beetle which is interesting because of the absence of its fossils at Meighen Island is the weevil genus *Lepidophorus*. Individuals representing a number of the taxa listed in Table 41.1 occur today at or near northern riparian sites. *Lepidophorus lineaticollis* Kirby is abundant at those places, and its fossils are numerous in Pleistocene sediments which represent environmental conditions similar to those that must have prevailed on Meighen Island (Matthews, 1975). Yet despite a burgeoning number of fossils from Meighen Island Beaufort sediments, none of *Lepidophorus* have been found. The genus may not have evolved by Beaufort time. In this regard it is interesting that fossils of a weevil that appear similar to *Lepidophorus* do occur in the Alaskan Lava Camp assemblage (Matthews, unpublished data).

The Meighen Island assemblage contains a fossil of a bumblebee (*Bombus*). Bumblebees are critical for pollination of some of the northern leguminous plants, thus it is noteworthy that a seed of *Hedysarum* (Leguminosae) has been found in Meighen Island sediments (Hills and Matthews, 1974). *Bombus* fossils occur in the Oligocene Baltic Amber (Bachofen-Echt, 1949). The fossil from Meighen Island (Fig. 41.2a) shows that the genus was a member of forest-tundra communities in North America as early as the Miocene.

Discussion

The study of fossil insects, particularly beetles, has proven to be a powerful tool for analysis of Quaternary environmental change. Now there is the opportunity to study late Tertiary fossils with the same objective. Already such fossils from the Beaufort Formation have provided evidence for the existence of lowland tundra in northernmost Canada during the late Tertiary. Beaufort Formation fossils promise as well to yield valuable information on evolutionary history, and they may play a future role in dating and correlation.

The combined Beaufort plant and insect fossils provide us with a partial glimpse of an early forest-tundra ecosystem. Significantly, the biotic component of this ecosystem was more diverse taxonomically than its modern day North American counterpart. In other words, the contemporary forest-tundra biota is

impoverished. This may partly explain the well known propensity of some members of this ecosystem to undergo wild numerical fluctuations. If so, then continued study of Beaufort fossils can be viewed as providing the necessary historical perspective for a better understanding of the complexities of existing northern ecosystems.

References

- Arnett, R. H., Jr.
1963: The Beetles of United States; Catholic Univ. of America Press, Washington, D. C., 1112 p.
- Bachofen-Echt, A.
1949: Der Bernstein und seine Einschlüsse; Springer Verlag, Wien, 204 p.
- Balkwill, H. R. and Bustin, R. M.
1975: Stratigraphic and structural studies, central Ellesmere Island and eastern Axel Heiberg Island, District of Franklin; in Report of Activities, Part A; Geol. Surv. Can., Paper 75-1A, p. 513-517.
- Coope, G. R.
1970: Interpretations of Quaternary insect fossils; Annu. Rev. Entomology, v. 15, p. 97-120.
- Darlington, P. J., Jr.
1970: A practical criticism of Hennig-Brundin "Phylogenetic Systematics" and Antarctic biogeography; Syst. Zool., v. 19, p. 1-18.
- Eldredge, N.
1971: The allopatric model and phylogeny in Paleozoic invertebrates; Evolution, v. 25, p. 156-167.
- Eldredge, N. and Gould, S. J.
1972: Punctuated equilibria: an alternative of phyletic gradualism; in Models in Paleobiology ed. T. J. M. Schopf; Freeman, Cooper and Co., San Francisco, Calif., p. 82-115.
- Harper, C. W., Jr.
1976: Phylogenetic inference in paleontology; J. Paleontol., v. 50, no. 1, p. 180-193.
- Hills, L. V. and Bustin, R. M.
1976: *Picea banksii* Hills & Ogilvie from Axel Heiberg Island, District of Franklin; in Report of Activities, Part B; Geol. Surv. Can., Paper 76-1B, report 13.
- Hills, L. V., Klovan, J. E., and Sweet, A. R.
1974: *Juglans eocinerea* n. sp., Beaufort Formation (Tertiary) southwestern Banks Island, Arctic Canada; Can. J. Bot., v. 52, p. 65-90.

- Hills, L. V. and Matthews, J. V., Jr.
 1974: A preliminary list of fossils plants from the Beaufort Formation, Meighen Island, District of Franklin; in Report of Activities, Part B., Geol. Surv. Can., Paper 74-1B, p. 224-226.
- Hills, L. V. and Ogilvie, R. T.
 1970: *Picea banksii* n. sp., Beaufort Formation (Tertiary), northwestern Banks Island, Arctic Canada; Can. J. Bot., v. 48, p. 457-464.
- Hopkins, D. M., Matthews, J. V., Jr., Wolfe, J. A., and Silberman, M. L.
 1971: A Pliocene flora and insect fauna from Bering Strait region; Palaeogeogr. Palaeoclimatol. Palaeoecol., v. 9, p. 211-231.
- Koerner, R. M. and Paterson, W. S. B.
 1974: Analysis of a core through the Meighen Ice Cap, Arctic Canada, and its paleoclimatic implications; Quat. Res., v. 4, p. 253-263.
- Kuc, M.
 1973: Fossil flora of the Beaufort Formation, Meighen Island, NWT-Canada; ERA, Can. Polish Res. Inst., Ser. A, p. 1-44.
- Kuc, M. and Hills, L. V.
 1971: Fossil mosses, Beaufort Formation (Tertiary), northwestern Banks Island, Western Canada Arctic; Can. J. Bot., v. 49, p. 1089-1094.
- Matthews, J. V., Jr.
 1970: Two new species of *Micropeplus* from the Pliocene of western Alaska with remarks on the evolution of *Micropeplinae* (Coleoptera: Staphylinidae); Can. J. Zool., v. 48, p. 779-788.
 1974: A preliminary list of insect fossils from the Beaufort Formation, Meighen Island, District of Franklin; in Report of Activities, Part A; Geol. Surv. Can., Paper 74-1A, p. 203-206.
- Matthews, J. V., Jr. (cont.)
 1975: Insects and plant macrofossils from two Quaternary exposures in the Old Crow-Porcupine region, Yukon Territory, Canada; Arct. Alp. Res., v. 7, p. 249-259.
 Evolution of the subgenus *Cyphelophorus* (Genus *Helophorus*; Hydrophilidae, Coleoptera): description of two new fossil species and discussion of *Helophorus tuberculatus* Gyll.; Can. J. Zool. (in press).
- Ross, H. H.
 1974: Biological Systematics; Addison-Wesley Publishing Co., Don Mills, Ont., 345 p.
- Thorsteinsson, R.
 1961: The history and geology of Meighen Island, Arctic Archipelago; Geol. Surv. Can., Bull. 15, 19 p.
- Tozer, E. T. and Thorsteinsson, R.
 1964: Western Queen Elizabeth Islands, Arctic Archipelago; Geol. Surv. Can., Mem. 332, 242 p.
- Turner, D. L., Triplehorn, D. M., and Naeser, C. W.
 1975: Geochronology program, coal beds, Kenai Peninsula; Geophysical Inst., Univ. Alaska., Ann. Rep. 1974-75, p. 124-125.
- Wilson, D. G.
 1976: Eureka Sound and Beaufort formations, Yelverton Bay, Ellesmere Island, District of Franklin; in Report of Activities, Part A; Geol. Surv. Can., Paper 76-1A, p. 453-456.
- Wolfe, J. A., Hopkins, D. M., and Leopold, E. B.
 1966: Tertiary stratigraphy and paleontology of the Cook Inlet region, Alaska; U. S. Geol. Surv., Prof. Paper 398-A, 29 p.

Project 630049

T. J. Katsube

Resource Geophysics and Geochemistry Division

Introduction

A large portion of the problems in exploration for oil, coal, uranium, metallic and non-metallic minerals, and geotechnical engineering have a certain nature that make it possible for electrical and EM exploration methods to solve them. Ground, airborne and borehole electrical and EM exploration methods have shown a certain extent of success in various fields in the past, in locating indications of mineral deposits and certain geological structures and features. However, today a change can be seen in the requirements towards exploration geophysics. These new requirements are more on the quality of the target objects and necessitate the geophysical data to reflect more unique geological features. For example, methods must be developed to differentiate IP and low resistivity anomalies due to chalcopyrite and galena rich mineral deposits of economical value from those due to pyrites, clays and graphite rich zones of no economic value. Similarly, the amount of clay in coal beds must be detected for quality evaluation. One of the basic problems that arises in most of the past and current electrical and EM methods when faced with these requirements is that the electrical parameters measured by these systems are usually compound effects of many geological features and do not reflect unique geological information. The Three Electrical Polarization Model (TEPM) suggested by Katsube (1975a) is significant in this respect. Not only does it introduce 9 new electrical parameters of which some appear to be more dependent on unique geological features (Singh *et al.*, in prep.) but it also indicates a possibility of introducing a large number of parameters which may reflect individual geological features to a much greater extent. For example, there are indications that some of these new parameters reflect the effects of clays, fine grain sulphides, coarse grain sulphides, quantity of conductive minerals, and porosity of fractures and pores, independently.

In this paper, problem areas mainly in the fields of mineral, coal, uranium (including waste disposal) exploration and geotechnical engineering are discussed, and new directions to be taken in laboratory investigations for research and development of new electrical exploration techniques are presented.

The Three Electrical Polarization Model (TEPM)

The TEPM analytical technique suggested by Katsube (1975a) makes use of inphase and out of phase measurements expressed by real and imaginary resistivity (ρ_R and ρ_I), measured over a wide frequency range (usually 10^{-1} to 10^6 Hz) and plotting the results on a Cole-Cole diagram (Fig. 42.1). Usually the Cole-Cole plots for earth materials show a three arc pattern

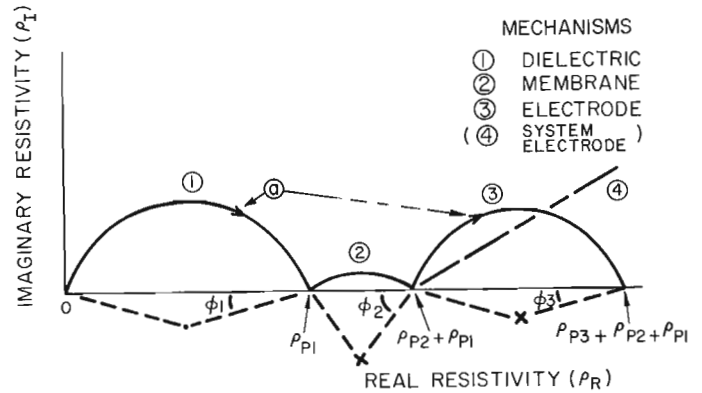


Figure 42.1. Cole-Cole or complex resistivity plot of the Three Electrical Polarization Mechanism Model for moist rocks (After Katsube, 1975a). a: Direction of the increase in frequency.

or part of the three arcs. These three arcs represent three different electrical mechanisms. From these three arcs 9 parameters: three resistivities (ρ_{p1} , ρ_{p2} , ρ_{p3}), three distribution angles (ϕ_1 , ϕ_2 , ϕ_3) and three dielectric constants (K_1 , K_2 , K_3) are determined. The methods for determining the dielectric constant from the Cole-Cole diagrams were discussed by Katsube (1975b) and will be described in a later paper. These 9 parameters are used to study the geological features of various earth materials.

In the past, the electrical characteristics of earth materials have usually been described by the frequency spectrum of resistivity, as shown in Figure 42.2. This is a modification of the resistivity curves shown by Katsube (1975c) and Keller and Licastro (1959). The relationship between the three arcs of the TEPM and the frequency spectrum of resistivity is shown in Figure 42.2. With decrease in frequency the resistivity rises to the levels of ρ_{p1} , $[\rho_{p1} + \rho_{p2}]$ and $[\rho_{p1} + \rho_{p2} + \rho_{p3}]$, sequentially. These three levels in resistivity reflect different electrical mechanisms in the earth material. In actual measurements, the gradient of the resistivity variation between the three levels is much smaller than shown in Figure 42.2. Thus, these levels can seldom be recognized in actual frequency spectrums of resistivity for earth materials, unless the data is plotted on the Cole-Cole diagrams. Resistivity (ρ), frequency effect (FE) and phase shift (θ) are the parameters usually used by state-of-the-art electrical and EM field systems. These parameters are usually measured at discrete frequencies or at two different frequencies along the frequency spectrum of resistivity as some examples are shown in Figure 42.2. It is evident from this diagram that these parameters represent compound effects of more than one electrical mechanism.

The author has discussed with scientists and engineers in the fields of oil, coal, uranium and mineral exploration, and geotechnical engineering, many of their problems. Conclusions from these discussions are presented, with references to the scientists involved.

Mineral Exploration

Electrical and EM methods for exploration of metallic mineral deposits have been designed and developed based on the assumption that these deposits can be characterized by low resistivity and large charge-abilities (large IP anomalies). However, today, it is well known that low resistivity and high IP anomalies are not a unique characteristic of metallic mineral deposits of economic value, but that pyrite, clay, and graphite also produce such anomalies. The mineral concentration, and in some cases the grain size of the minerals determine the economic value of a mineral deposit. Pyrite usually accompanies sulphide minerals of economic interest, but it also appears in veins of no economic interest, and in certain rock horizons due to organic origin. It is, thus, essential that techniques be developed to distinguish pyrite, clay, and graphite from minerals of economic interest, and to obtain information on the concentration and grain size of the minerals. These conclusions were reached in discussions with J. Hamilton and J. J. Lajoie, COMINCO Ltd.; Z. Nikic, and other members of the Geology Department, Pine Point Mines Ltd.; and F. M. Vokes, GSC.

Coal Exploration

It is essential that *in situ* techniques be developed to determine the quality of the coal beds. Though various logging techniques, such as density and resistivity are currently being used, none of the techniques can sufficiently measure the water, ash, carbon and sulphur contents. The result of discussions with B. A. Latour and J. A. Irvine of the Geological Survey was that a technique must be developed to determine all or any of these four factors.

Uranium Exploration and Waste Disposal

Geophysical methods other than radioactive techniques are also necessary for detection of uranium deposits. In some cases, certain clay minerals accompany the uranium deposits, and methods to detect the existence of clay could aid in locating uranium deposits. In certain cases uranium deposits are also related to subsurface water channels. Low resistivity anomalies are related to fractured zones or water bearing rocks, but in this case it is the regions related to the flow of water that are important. Clay minerals may indicate zones that are related to the

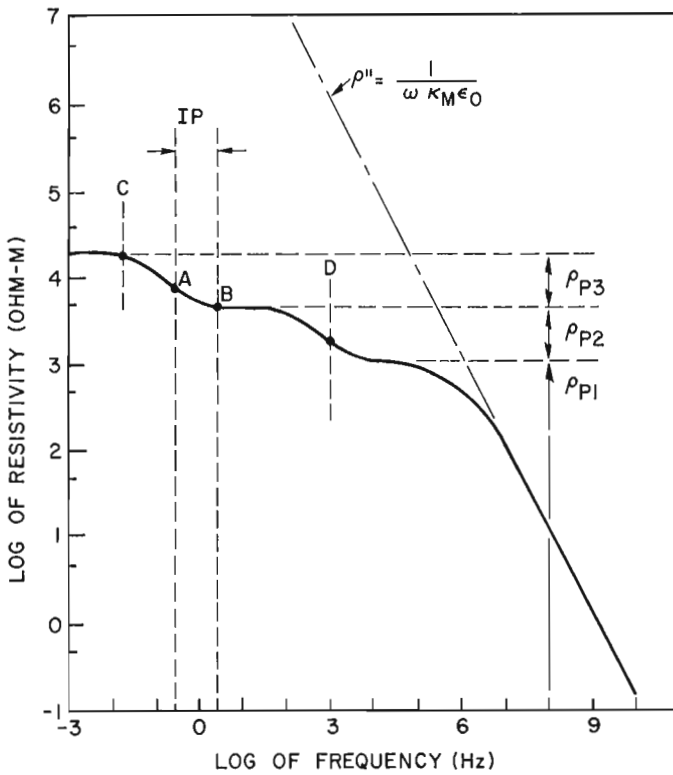


Figure 42.2. Idealized curve for the frequency spectrum of resistivity for moist earth materials. Points A and B indicate the frequencies at which the FE and θ are often measured for the IP method. Resistivity or low resistivity anomalies are detected at various frequencies (e. g. points C, D) depending upon the type of equipment that is used.

- ρ'' : Out of phase or imaginary resistivity
- K_M : Dielectric constant
- ϵ_0 : Dielectric constant of vacuum or air

Recent studies by Singh *et al.* (in prep.) show interesting relationships between some of the new parameters determined by the TEPM technique and geological features. For example, a good relationship between ρ_{p2} and the specific gravity has been observed for a suite of serpentinite samples. Rock containing clays have shown extremely large values for ρ_{p2} and ϕ_1 . A relationship between ϕ_1 and the amount of fractures and cracks has been observed. Large grains of conductive minerals in the rock seem to have an effect on ρ_3 and ϕ_3 , whereas fine grains of the same materials seem to have an affect on ρ_{p2} and ϕ_2 . These indications suggest that by the use of the new TEPM analytical technique, electrical exploration methods may gain a large potential for obtaining quantitative and unique geological information. It is now necessary to investigate various problems by use of this technique.

movement of water. Thus, techniques to detect clay are also important in this case. For disposal of radioactive waste material, water channels in the rock bodies are undesirable. Here again the detection of clays is important. It is thus necessary to develop borehole logging techniques or other surface geophysical techniques for the detection of clays. M. Best of Shell Canada Ltd., L.P. Tremblay, V. Ruzicka, and J.E. Gale of Geological Survey of Canada, and S.K. Singh, University of Quebec took part in these discussions with the author.

Geotechnical Engineering

In relation to construction of oil and gas pipelines, roads, and towns in arctic regions where continuous and non-continuous permafrost is dominant, the study of terrain sensitivity is important. One of the key factors in this study is the content and distribution patterns of ice in the overlying soils. It is thus necessary to develop techniques that can make a rapid *in situ* determination of these factors. These conclusions were reached in discussions with P.J. Kurfurst and L.S. Collett of the Geological Survey of Canada and with P. Hockstra of Northern Engineering Services Ltd.

Others

Camfield *et al.* (1976) reported their work on the North American Central Plains conductive body, which in part can be related to the Wollaston Lake Fold Belt. If the TEM techniques could be developed and used in some way to aid in understanding the medium of this conductive body, electrical methods may increase their value in geological mapping.

Direction of Research and Development

Many of the problems discussed in the former section are common to many fields. It is now necessary to consider how these problems can be tackled by electrical methods.

Grain-size Effect

Fine grained minerals can cause problems in the ore dressing process. Thus, even if the concentration of a useful mineral is high in a mineral deposit, it can be uneconomical because of the grain size. Wait (1959) has carried out theoretical work on the grain-size effect, and it is generally considered that the grain-size of conductive minerals have an effect on the IP phenomena. Recent studies on serpentinites by Singh *et al.* (in prep.) indicate that the effect of very fine grained magnetite is reflected on ρ_{p2} and ϕ_2 , and that the effect of larger grains is reflected on ρ_{p3} and ϕ_3 . The cause for this difference between the electrical characteristics of fine grains and larger grains of magnetite is yet to be clarified, but it is possible that similar trends will be found for other types of conductive materials.

Mineral Concentration

It is well known that the electrode polarization effect appears at frequencies below 10^{-10^2} Hz. Katsube (1974) and Katsube and Collett (1974) have observed that when large crystals of metallic minerals (pyrites, magnetite, chalcopyrite) exist, the third arc (ρ_{p3} and ϕ_3) is visible, but when these minerals are absent it is not visible. The third arc is, perhaps, the result of the electrode polarization. Therefore it is clear that a relationship between these mineral grains and the third arc exists, but whether or not it is quantitative relationship, has still to be clarified. In the case of certain serpentinites (Singh *et al.*, in prep.), there are indications that a relationship exists between the quantity of fine grained magnetites and ρ_{p2} .

Mineral Discrimination

Differentiation of different types of minerals is extremely important in mineral exploration, and will be in coal and uranium exploration. Though Katsube (1967), Zonge (1972), Collett and Katsube (1973), Katsube and Collett (1973), Katsube (1974a) indicated the possibilities of differentiation of minerals by their electrical characteristics, problems thought to be due to grain size and concentration effects appeared in subsequent laboratory studies. However, recent developments which may lead to establishing techniques to differentiate between different grain sizes opens up new possibilities in this field. In addition, it has become clear that, at present, the differentiation of pyrite, clay, and graphite from other economic minerals such as chalcopyrite and galena is most important. Recent work (Singh *et al.*, 1976) has indicated that there is a large difference between the effect of clays and other conductive minerals. It is expected that the difference in the effect of different minerals will appear in the third arc (ρ_{p3} , ϕ_3).

Detection of Clays

Detection of massive and finely distributed clays in necessary for aiding in exploration of uranium and coal, and for determining sites for waste disposal of radioactive materials. In the case of uranium exploration and waste disposal, the presence of clay in the rock and fractured zones must be detected. In the case of coal exploration, the quantity of clay must be detected. Recent studies (Singh in prep.) indicate that the effect of clay is reflected in ρ_{p2} and ϕ_1 . And there are indications that a quantitative relationship exists between the clay content and ρ_{p2} when the clay is finely distributed through the rocks. It is not yet known, however, whether the type of clay affects these relationships.

Moisture Detection

Moisture detection in soils and rocks is important for agriculture, hydrology, and other areas, and a considerable amount of work is being done in relation to this subject (e.g. Cihlar and Ulaby, 1975; Katsube and Collett, 1973; Davis and Chudobiak, 1975). Moisture detection in coal is also important for estimating the quality of the coal beds. Since a large contrast between the dielectric constant (K') of coal ($K' = 3-5$, Cook, 1970) and water ($K' = 80$) exists, principles similar to those applied in soil moisture detection may be applied to moisture detection in coal.

Ice Content Detection

Detection of ice content in soils is essential to study terrain sensitivity for pipeline and highway construction in arctic regions. Recent and past studies indicate that there is a large difference between the electrical characteristics of ice and other soil materials at low temperatures. The distribution patterns of ice in soils, however, varies to a great extent and can be a source of complication. Therefore a wide range of laboratory and theoretical studies are necessary in this area.

Conclusions

A number of discussions on exploration problems were carried out with scientists and engineers in the field of coal, uranium and mineral exploration and geotechnical engineering. As a result, it has been concluded that the following problems are significant, and should be tackled by the newly proposed TEMM technique in the laboratory:

1. Grain-size effect of sulphides.
2. Mineral concentration estimate.
3. Mineral discrimination.
4. Detection of clays.
5. Moisture detection in coal.
6. Ice content detection.

Though conclusions of the laboratory studies are not yet available, it is evident that IP, resistivity and EM systems with wide frequency ranges (up to 10^6 Hz) will be necessary for field follow-up investigations. Thus, it is pertinent that an effort should be made to start tackling the problems related to such field systems.

Acknowledgments

I am grateful to Mr. L. S. Collett for his guidance in relation to this work.

References

- Camfield, P. A., Alabi, A. O., and Gough, D. I.
1976: Electrical conductivity and Precambrian crustal structure in Saskatchewan and the northern U. S. A. Presented at the Stockwell Symposium, Ottawa, March 5, 1976.
- Cihlar, J. and Ulaby, F. T.
1974: Dielectric properties of soils as a function of moisture content. RSL Technical Report 177-47, University of Kansas.
- Collett, L. S. and Katsube, T. J.
1973: Electrical parameters of rocks in developing geophysical techniques; *Geophysics*, v. 38, no. 1, p. 76-91.
- Cook, J. C.
1970: R. F. electrical properties of Bituminous coal samples. *Geophysics*, v. 35, 1970, p. 1079-1085.
- Davis, J. L. and Chudobiak, W. J.
1975: *In situ* meter for measuring relative permittivity of soils. *Geol. Surv. Can.*, Paper 75-1A, p. 75-79.
- Katsube, T. J.
1967: The electrochemical transient phenomena of ore and rock samples; Dr. Eng. Thesis. Waseda Univ. Tokyo (in Japanese with English abstract).
1974a: Electrical characteristic differentiation of sulphide minerals. *Geol. Surv. Can.*, Paper 74-1A, p. 83.
1974b: Electrical characteristics and electrical mechanism of some ultramafic rocks. Presented at the Second Workshop on Electromagnetic Induction in the Earth. Ottawa, Ont., Aug. 22-28.
1975a: The electrical polarization mechanism model for moist rocks. *Geol. Surv. Can.*, Paper 75-1C, p. 353-360.
1975b: Electrical Characteristics of Serpentinites. Presented at the 45th Annual International Meeting of the Society of Exploration Geophysicists. Oct. 12-16, 1975.
1975c: The critical frequency and its effect on EM propagation; in Report of Activities, Part A, *Geol. Surv. Can.*, Paper 75-1A, p. 101-105.
- Katsube, T. J. and Collett, L. S.
1973: Electrical characteristics of rocks and their application to planetary and terrestrial EM sounding; Proc. Fourth Lunar Sci. Conference, Supplement 4, *Geophysics et Cosmochemica Acta*, Pergamon Press, v. 3, p. 3111-3131.
1974: Electromagnetic propagation characteristics of rocks. Presented at NATO Advanced Study Institute of Petrophysics, Newcastle upon Tyne, England, Apr. 23 (submitted to be published in "The Physics and Chemistry of Rocks and Minerals", John Wiley and Sons Ltd.)

Keller, G. V. and Licastro, P. H.

1959: Dielectric constant and electrical resistivity of natural-state cores; U.S. Geol. Surv., Bull. 1053H, p. 257-285.

Singh, S. K., Katsube, T. J., and Morency, M.

Application of new electrical parameters to analyse the petrographical features of serpentized ultramafic and other rocks. in prep.

Wait, J. R.

1959: A phenomenological theory of overvoltage for metallic particles. In *Overvoltage Research and Geophysical Applications*. Edited by Wait, J. R., Pergamon Press, 22-28.

Zonge, K. L.

1972: *In situ* mineral discrimination using a complex resistivity method. Presented at the 42nd Annual International Meeting of the Society of Exploration Geophysicists, Anaheim, Calif., Nov. 26-30.

Projects 710019 and 710036

W. W. Brideaux and D. W. Myhr
Institute of Sedimentary and Petroleum Geology, CalgaryIntroduction

The stratigraphy and dinoflagellate cyst succession in the Gulf Mobil Parsons N-10 well are discussed in this paper. The well is located approximately 2.4 km (1.5 miles) east-northeast of Parsons Lake (Fig. 43.1) and about 80 km (50 miles) north of Inuvik, District of Mackenzie (Lat. 69°59'48.52"N, Long. 133°31'50.33"W). It was spudded in ?Quaternary sediments and bottomed in Paleozoic or ?Proterozoic rocks at a depth of 10 515 feet (3205 m) (Fig. 43.2).

The well was drilled to test a Neocomian clastic succession which was found to be hydrocarbon-bearing in the discovery well, Gulf Mobil Parsons F-09 (Lat. 68°58'35"N, Long. 133°31'33"W). The Parsons N-10 well was spudded on February 24, 1973, and was completed as a gas well on May 29, 1973. Casing was set at 750 feet (229 m) and at 3900 feet (1189 m). Three drillstem tests were made and 487 feet (148 m) of core were taken from the gas-bearing sandstone and the underlying mudstone unit of Neocomian age. The present status of the well is a suspended gas well (Can., Dep. Indian Affairs and Northern Dev., 1973).

The reservoir geology and stratigraphy of the Neocomian rocks in the Parsons wells and nearby boreholes have been summarized by Cote *et al.* (1975). The Parsons N-10 and F-09 wells were drilled on a northeast-southwest anticlinal structure, situated along the northwestern margin of the Eskimo Lakes fault zone. The Parsons structure is considered to have resulted from ?late Tertiary normal faulting in conjunction with older fault movements contemporaneous with deposition of the Mesozoic sequences (Cote *et al.*, 1975).

The biostratigraphic divisions recognized in the Parsons N-10 well are based on a reconnaissance study of the dinoflagellate cyst succession in 95 composite cuttings samples taken between the depths of 900 and 10 220 feet (275-3115 m) (Fig. 43.3), and from 5 samples from conventional cores taken between the depths of 9025 and 9512 feet (2751-2899 m). Cuttings samples above the depth of 900 feet (275 m) were not of sufficient quality for use in these studies. This summary of the dinoflagellate succession, in which Upper Jurassic, Cretaceous, and lower Tertiary assemblages are recognized, is the first to be published for a comprehensive subsurface section in the northern Canadian mainland. Previously, Chamney (1971) had published a detailed study of the lithostratigraphy and micro-paleontology of the B. A.-Shell-IOE Reindeer D-27 well (Lat. 69°10'05"N, Long. 134°36'54"W).

Acknowledgments

The authors thank D. Morrow for critically reviewing the manuscript, and S. Pickering, H. Johnson and E. O'Keefe for their excellent palynological preparations.

Lithostratigraphy and PaleoenvironmentsQuaternary (undivided)

0-?100 feet (0-?30 m)

No samples are available for this interval. The base of the unit has been chosen arbitrarily at a depth of 100 feet (30 m). Rampton (1971) has mapped Quaternary deposits near Parsons Lake, but does not report a thickness. It is assumed that the basal contact is unconformable. Rampton's (*ibid.*, Fig. 1) map indicates that the Parsons N-10 borehole may have been spudded in glaciofluvial sediments consisting of sand and gravel.

Reindeer Formation

?100-5050 feet (?30-1509 m)

The Reindeer Formation is ?4950 feet (?1479 m) thick, and consists of sand, sandstone, siltstone,

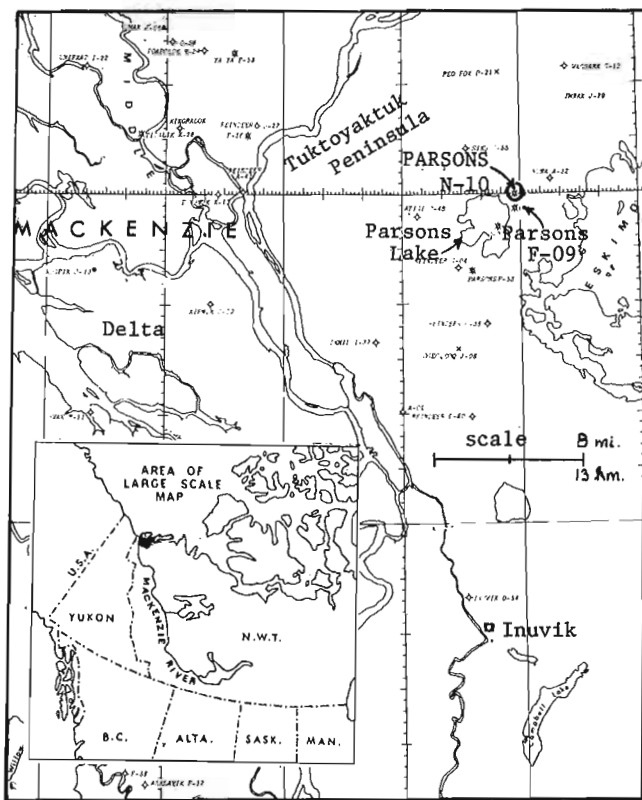


Figure 43.1. Index map.

mudstone and coal, with minor amounts of shale, wood (in part lignite), sideritic claystone, bentonite and bentonitic mudstone. Sand is common throughout the interval between 100 and 2900 feet (30-884 m); it is of coarse to granular and fine-pebble size (< 10 mm) and composed predominantly of dark grey (N3)¹ chert, very light grey (N8) quartz, light grey (N7) and dusky red (5R3/4) sandstone, K-feldspar granite, dusky red (5R3/4) to moderate red (5R4/6) jasper, dark grey (N8) dolomite and greyish-green (10G4/2)? volcanic fragments. Grey colour hues are more common between 850 and 2900 feet (259-884 m). Sandstone is present throughout, and is dominant in the interval from 1360 to 4750 feet (415-1448 m). A "salt and pepper" appearance is common, reflecting the dominance of quartz and medium dark grey (N4) chert or, less commonly, coal fragments and dark grey (N3) lithic fragments. Grain size commonly ranges from very fine to coarse. Calcite-cemented sandstone occurs throughout the interval between 1600 and 3620 feet (488-1103 m) and is indicated by a slow transit time log response (see gamma ray and sonic logs). Minor amounts of moderate brown (5YR3/4) siderite-cemented sandstone and medium grey (N5) argillaceous sandstone are present. The mudstone and siltstone are medium grey (N5) to dark grey (N4), with minor amounts of very light grey (N8) and moderate brown (5YR4/4). The lighter grey colours in the interval between 880 and 950 feet (268-290 m) are suggestive of a bentonitic component. Siderite and ferruginous cements impart brownish and reddish colour tones to these lithologies. Sideritic mudstone is commonly sandy and carbonaceous. Coal is very abundant below 900 feet (274 m). Reflectance values for coaly materials from the Reindeer Formation in the Parsons F-09 bore-hole indicate that the coals are of the subbituminous type

¹ Colour terms are those used in the Rock-Color Chart published by the Geological Society of America in 1963.

Legend for Figure 43.2

Lithology	code	Modifier	code
sand-sandst.		calcareous	⊥
siltstone		silty	..
mudstone		sulfates	*
shale		glauconite	~
bituminous shale		pyrite	Py
coal		bentonite	b
		chert	Δ
		concretionary	○
		wood	w

(P. Gunther, pers. comm., 1975). In the Parsons N-10 well, coal is typically greyish black (N2), has a low luster, is moderately brittle with expanded parting or fracture planes, and, in part, contains a fibrous, "woody" texture. Because coal is present in most sample vials, its stratigraphic position in Figure 43.2 has been inferred from interpretation of sonic and induction-lateralog logs. These logs display, respectively, a fast transit time and high resistivity

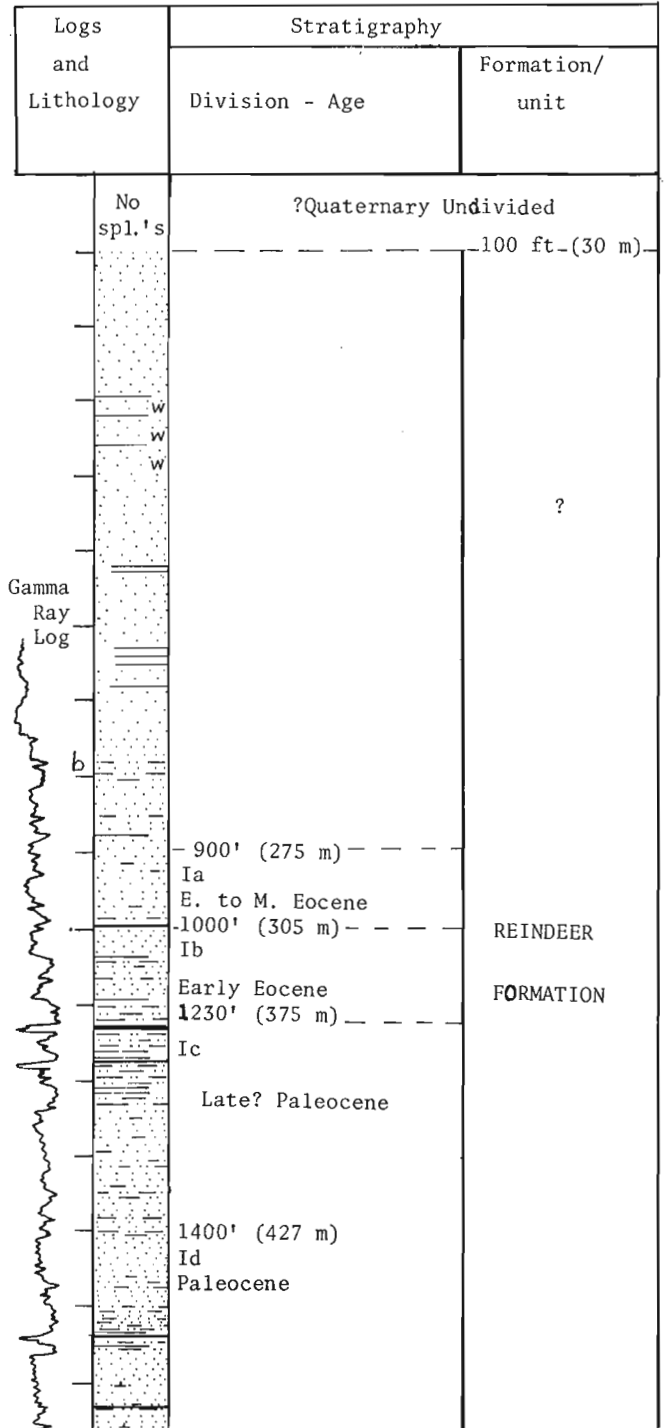


Figure 43.2. Stratigraphy, Gulf Mobil Parsons N-10.

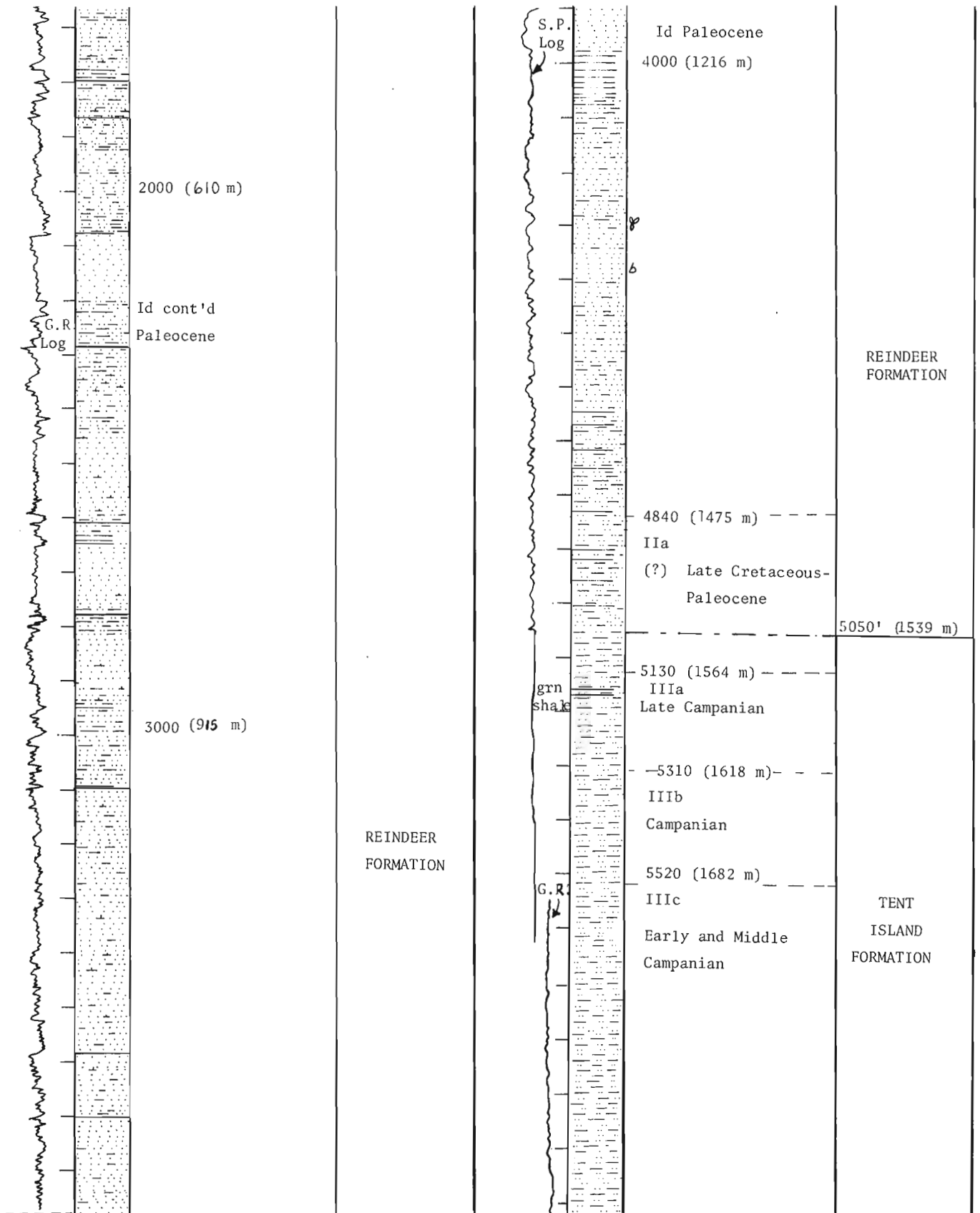


Figure 43.2 continued

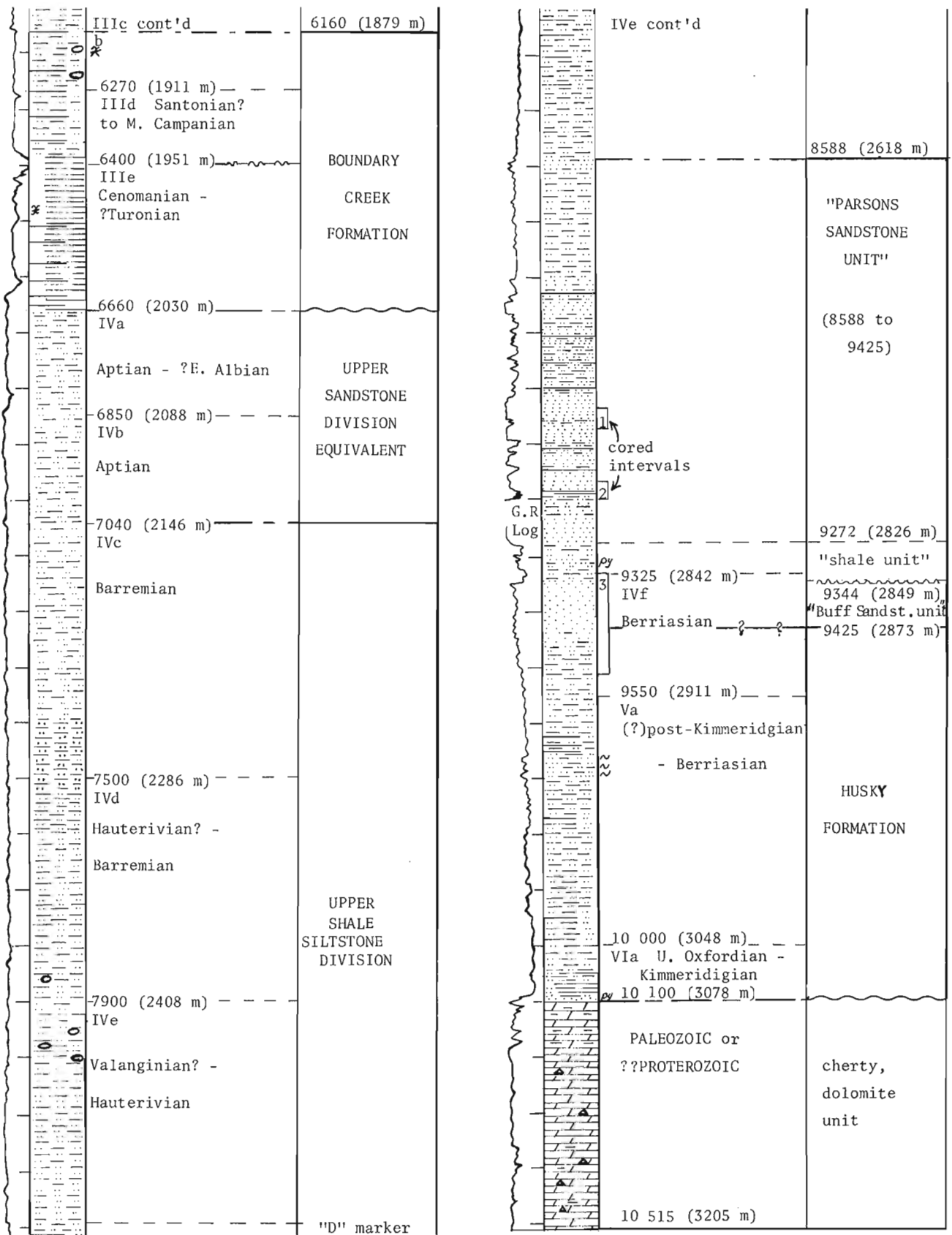


Figure 43.2 concluded

across a coal bed. Bituminous, brownish-black (5YR2/1) mudstone and shale may be associated with the coal-bearing intervals. Accessory lithologies of the Reindeer Formation include sideritic claystone and ironstone (dusky red, 5R3/4), ferruginous, scoracious lithologies (?bocanne deposits), and white (N9) to bluish-white (5B9/1) bentonite which first occurs at a depth of 4370 feet (1332 m). Foraminifers are common in samples below 4280 feet (1305 m). The contact with overlying Quaternary strata may be unconformable. The basal contact with the underlying Tent Island Formation is conformable(?). This interpretation is based on the following observations: a green shale marker found in other boreholes near the top of the Tent Island Formation is present also in the Parsons N-10 borehole; examination of the dipmeter log indicates that there is no abrupt change in azimuth or degree of dip across the contact; the borehole logs and sample material indicate a gradual change in lithology across the contact. The environment of deposition of the Reindeer Formation is primarily marine to transitional (paralic). The formation may be subdivided into two lithogenetic units. The upper unit, approximately 3600 feet (1098 m) thick, is considered to have been deposited in proximal delta-front and paralic (marsh and swamp) environments. The lithotope consists mainly of coarsening-upward (note gamma ray log, Fig. 43.2), stream-mouth bars, and ?nearshore sandstones with minor marsh and swamp deposits (coal-bearing and bituminous shale intervals). Shales and mudstones in the upper part of the formation are thought to have been deposited in an estuarine environment, as evidenced by the presence of dinoflagellate species in Divisions Ia and Ib. A basal unit, 1350 feet (412 m) thick, is interpreted to have been deposited in more distal delta-front, prodelta, and shallow-shelf environments. This lithotope consists of interstratified mudstone and minor argillaceous sandstone; coal is absent. Arenaceous foraminifers are common in the sample vials throughout the lower portion of the interval.

Tent Island Formation
5050-6160 feet (1509-1878 m)

The Tent Island Formation is 1110 feet (358 m) thick and consists of a homogeneous sequence of interstratified mudstone and argillaceous siltstone with minor amounts of shale. Mudstone is silty, dark grey (N3) to greyish red (10R4/2), and moderately indurated. Siltstone is less common, argillaceous, and grey in colour. Shale is a very minor constituent of the formation and occurs first at 5160 feet (1573 m). It is varicoloured [greyish green (5GS/2) and dusky yellow-green (5GY%/2)] and has a soft and waxy appearance. The colour tones enhance its usefulness as a lithostratigraphic marker [cf. 5080 ft. (1539 m) in the IOE Nuna borehole, Lat. 69°01'14"N, Long. 133°22'34"W]. Palynological studies and, to a lesser degree, the absence of an abrupt change in lithology, indicate a conformable basal contact.

The depositional setting is interpreted to be marine, based on lithology and dinoflagellate assemblages.

Boundary Creek Formation
6160-6660 feet (1878-2030 m)

This formation is 500 feet (152 m) thick and consists mainly of silty shale and shale with minor amounts of bentonite and ironstone. Gypsum crystals and sulphate compounds are common throughout.

The uppermost 216 feet (65 m) comprise shale, with minor amounts of bentonitic shale and ironstone. This interval contains abundant caved sand and mudstone from the overlying unit(s). The shale is silty and dark grey in colour. Minor amounts of very light grey (N8) to bluish-white (5B9/1) bentonitic clay and dark reddish-brown (10R3/4) ironstone are present also. White (N9), sulphate-bearing (?gypsiferous) compounds are common below 6170 feet (1881 m).

There is a gradual change in lithology from silty shale to fissile shale below 6380 feet (1944 m) that corresponds with a gradual increase in radioactivity (gamma ray log, Fig. 43.2); the high gamma counts (> 150 API) persist to a depth of 6420 feet (1958 m). These shales are bituminous, black to brownish black, of a low density, and highly radioactive over an interval of 44 feet (14 m). Euhedral and anhedral gypsum crystals are common below a depth of 6470 feet (1972 m).

The Boundary Creek Formation unconformably overlies Lower Cretaceous strata, as is indicated by age determinations and regional correlations made by other authors on nearby boreholes (i. e. Parsons F-09, Cote *et al.*, 1975; and Gulf Mobil East Reindeer G-04, Lat. 68°53'16"N, Long. 133°46'03"W, Chamney, 1973). The internal hiatus at 6400 feet (1951 m) is identified on the basis of palynological criteria and is not marked by a change in lithology or dip attitude.

These sediments were deposited in a euxinic (?restricted to semi-restricted) marine environment. This assertion is supported by the presence of bituminous, sulphate-bearing shale and a diverse dinoflagellate assemblage.

Aptian sandstone division equivalent and Upper shale-siltstone divisions, undivided
6660-8588 feet (2030-2618 m)

These strata are 1928 feet (588 m) thick. Both units are lithologically similar and consist of mudstone with minor amounts of siltstone. The mudstone is silty, and of a brownish-black (5YR2/1) to brownish-grey (5YR4/1) colour. Caved gypsum crystals occur throughout the interval to a depth of 7150 feet (2179 m), where a change in mechanical drilling procedures greatly improves the quality of sample material. The contact between Aptian strata and the older Barremian Upper shale-siltstone division is conformable and is placed at a depth of 7040 feet (2146 m) on palynological grounds. The Upper shale-siltstone division is slightly more arenaceous below 7400 feet (2256 m), where significant amounts of argillaceous siltstone first occur. This lithology is present throughout the remaining part of the sequence and, in part, may represent caved material. Brown dolostone (?sideritic concretions)

occurs throughout the interval between 7840 and 8050 feet (2390-2454 m), as indicated by sample and log response.

The basal 298 feet (91 m) of the Upper shale-siltstone division are more argillaceous than overlying strata, the upper contact being marked by a regionally correlative log marker at a depth of 8390 feet (2527 m). This change in lithology is recognizable on the gamma ray, sonic, and induction-laterolog logs and has been labelled as the "D" marker by Cote *et al.* (1975). Lithologies of this unit include mudstone and non-fissile shale, in part silty, and dark grey to brownish black in colour. The contact with the underlying unit is conformable.

Sediments of the Upper sandstone division equivalent and Upper shale-siltstone division were deposited in a marine environment, possibly in an offshore(?) or outer neritic(?) setting. The interpretation is based on the abundance of dinoflagellate species and the paucity of coarse arenaceous rocks (sandstone, conglomerate).

"Parsons sandstone unit"

8588-?9425 feet (2618-?2873 m)

The informally named "Parsons sandstone unit" (Cote *et al.*, 1975) is ?837 feet (?255 m) thick and is subdivided into four lithologic units, correlative with genetic subdivisions as proposed by Myhr and Young (1975). The youngest lithogenetic unit is 312 feet (95 m) thick and spans the interval between 8588 and ?8840 feet (2618-?2695 m). It consists mainly of dark grey to brownish-grey silty mudstone (\approx 89 per cent), interbedded with minor amounts of sandstone that is brownish grey and of a very fine texture. The basal contact of this unit is considered to be gradational and is chosen at the first occurrence of coal [8840 ft. (2695 m)]. This sequence was deposited in marine, prodelta-interdeltaic (mudstone lithofacies) and, in part, delta-front (sandstone lithofacies) environments. The interpretation is based on lithology, well log characteristics, and correlation of the lithofacies with the Parsons F-09 borehole (Myhr and Young, 1975; Cote *et al.*, 1975).

The underlying unit, between ?8840 and 9272 feet (?2695-2826 m), consists of sandstone, sand, and minor amounts of coal, siltstone, mudstone, and organic-rich shale. Core No. 2, from between 9172 and 9202 feet (2796-2805 m), contains these rock types and is considered to have been deposited in a deltaic setting by Young (1974) and Myhr and Young (1975). Reflectance values of the coal indicate its rank to be high volatile B bituminous (P. Gunther, pers. comm., 1974). The sandstone-mudstone lithology ratio is 7:1, compared with a ratio of 1:9 for the overlying unit. The arenaceous units are very fine to very coarse grained, with scattered 'floating' pebbles, and are generally poorly sorted, cross-stratified and in part ripple laminated. Measured porosities from core analysis range from 10.4 to 19.9 per cent, and the permeability maximum ranges from 0.16 to 1196 millidarcys. The sandstone units represent channel

and minor splay deposits in a delta-plain environment. The flood-basin deposits are represented by pelitic (shale-mudstone, siltstone) and coal lithologies, the former being carbonaceous, in part bioturbated, laminated and containing root borings. Although the unit is placed tentatively in a nonmarine setting, the upper part of the interval, between 8840 and 9010 feet (2695-2746 m), may have been deposited in a paralic (interdeltaic) setting. Evidence for this interpretation is the dominance of mudstone and siltstone over coal and sandstone.

The third unit, a "shale marker" (Cote *et al.*, 1975), is 72 feet (22 m) thick and occurs in the interval between 9272 and 9344 feet (2826-2848 m). It consists of sandy and silty, bioturbated mudstone, interstratified with organic-rich, pyritic shale and some arenaceous units of siltstone and very fine sandstone. Detailed descriptions and core photographs of this unit are presented in Cote *et al.* (1975) and in Myhr and Young (1975). The upper contact may be gradational with the overlying unit because there is a gradual decrease in gamma counts (gamma ray log, Fig. 2) across the contact. This infers a gradual change in lithology as the clay content of the shale unit ("shale marker") decreases upward. The basal contact is unconformable and is present in core 3 (Cote *et al.*, 1975; Myhr and Young, 1975). A thin (8 cm) polymictic lag conglomerate directly overlies the contact. The depositional environment is considered to be restricted, ?brackish to intermittently marine as indicated by the bituminous, pyritic nature of the shale and mudstone, the bioturbated texture, and the presence of dinoflagellate assemblages.

The basal unit, between 9344 and ?9425 feet (2848-?2873 m), is 81 feet (25 m) thick and has been designated informally as the "Buff sandstone member" by Cote *et al.* (1975). Cores from this unit consist mainly of sandstone (\approx 95 per cent) that is light brown, very fine grained, and interstratified with less abundant shale laminae in the interval between 9388 and 9408 feet (2863-2869 m). The upper 44 feet (13.4 m) of the unit consist of non-stratified and planar cross-stratified sandstone, in part coquinooid (thin-shelled ?pelecypods). A middle shaly interval consists of interstratified shale, mudstone and sandstone, in part cross-stratified, ripple-laminated and burrowed. The base of the unit consists of 17 feet (5.2 m) of non-stratified sandstone. Bioturbation may have destroyed completely primary sedimentary structures in this unit. The upper contact is abrupt and unconformable; the lower contact is gradational, and is chosen at the base of the non-stratified sandstone unit. The sedimentary features of this lithofacies are comparable to those found by Davies *et al.* (1971) in shoreface deposits of the Galveston Barrier Island complex. Core photographs and environmental interpretations are discussed in Myhr and Young (1975).

Husky Formation

?9425-10 100 feet (?2873-3078 m)

The Husky Formation is 675 feet (206 m) thick and comprises mudstone with minor siltstone, sandstone

and glauconitic mudstone. The upper 87 feet (27 m) of the unit were cored. The top 20 feet (6 m) consist of silty sandstone that contains parallel-to-burrowed sets typical of lower shoreface deposits (Davies *et al.*, 1971) and the remaining part of the cored interval comprises bioturbated mudstone which becomes increasingly more argillaceous with increasing depth. Samples indicate that a change in lithology occurs at 9652 feet (2942 m), where minor amounts of glauconitic mudstone, in part sandy, first occur and persist to about 9700 feet (2957 m). This unit is considered correlative with the Arenaceous member of the Husky Formation (Jeletzky, 1967) which outcrops in the Aklavik Range of the Richardson Mountains. Lithologies beneath this member also consist of mudstone with intercalated beds of argillaceous siltstone and organic-rich silty shale (base of the unit). The base of the formation contains approximately 10 feet (3 m) of pyritic sandstone that unconformably overlies a carbonate unit. Evidence from core and dinoflagellate assemblages suggests that the depositional environment of the Husky Formation is marine. The lithologies and sedimentary structures are representative of sediments deposited in a lower shoreface, offshore, and basinal marine setting.

Sub-Mesozoic (Paleozoic or ?Proterozoic)
10 100-10 515 feet (3078-3205 m)

This carbonate unit consists of dolomite with minor amounts of chert and dolomitic shale. The dolomite is mottled, dark grey to grey, micro-crystalline to very finely crystalline and, in part, argillaceous near the top. Dolomitic, dark grey shale and micritic dolomite are present in the upper 80 feet (24.3 m). Brownish-grey chert also is present in variable amounts. Porosity is low to negligible.

BIOSTRATIGRAPHY

The dinoflagellate succession in the Gulf Mobil Parsons N-10 well is based mainly on material from cuttings samples. Although the majority of cuttings samples have been prepared using methods outlined by Barss and Williams (1973), the oldest occurrence of a species in the section, or "species base", may be used only as a guide and cannot be considered reliable. The youngest occurrence of a species in the section, or "species top", remains the most reliable datum, despite the confusion engendered by reworking of species into younger rocks.

No comprehensive published palynological zonation exists for Mesozoic and Tertiary rocks of the northern Canadian mainland and Arctic Archipelago. Hence, biostratigraphic divisions recognized in this well cannot be compared with an existing zonation. Some information has been published for part of the Mesozoic-Tertiary section. McIntyre (1974, 1975) proposed three informal biostratigraphic divisions based on dinoflagellates and miospores recovered from Santonian-Maastrichtian rocks of the northern Canadian mainland. Other information basic to formulation of a dinoflagellate

cyst zonation for upper-most Jurassic and Lower Cretaceous rocks is in preparation, or will be published shortly (Brideaux and McIntyre, 1976; Brideaux and Fisher, in press; Pocock, in press; Brideaux, in prep.). A preliminary Tertiary zonation based on miospores, dinoflagellate cysts and fungal remains in subsurface sections from the Mackenzie Delta region is in preparation (Brideaux, 1975; F.L. Staplin, pers. comm.).

The ages assigned to the biostratigraphic divisions recognized in the well are based on known ranges of species in northern Canada given in the published and unpublished sources cited above, on data from the Canadian Atlantic Continental Margin (Williams and Brideaux, 1975; Williams, 1975) and, to a lesser extent, on compilations of published data from Europe, Asia and Australia (Jurassic — Riley and Sarjeant, 1972; Sarjeant, 1975; Cretaceous — Harker and Sarjeant, 1975; Milliod *et al.*, 1975; Tertiary — Drugg and Stover, 1975; Harker and Sarjeant, 1975).

A brief taxonomic sketch and illustrations of selected species designated referred to in the following discussion are presented in Brideaux (1976). Illustrations of certain previously published species also are included for reference. The occurrence of species in the well is given in Figure 43.3.

I. Lower Tertiary

Division Ia. 900-1000 feet (275-305 m)

Age/Formation: Early to Middle Eocene/Reindeer Formation

Discussion: The age is based on overlapping occurrences of *Wetzeliiella homomorpha* subsp. *homomorpha* Deflandre and Cookson, 1955, *W. homomorpha* subsp. *quinelata* Williams and Downie, 1966, *W. parva* Alberta, 1959 and *W. articulata* Eisenack, 1938. *Wetzeliiella homomorpha quinelata* has not been reported from rocks younger than Middle Eocene in age and *W. parva* has not been recorded in rocks older than Early Eocene in age.

Division Ib. 1000-1230 feet (305-375 m)

Age/Formation: Early Eocene/Reindeer Formation

Discussion: *Cyclonephelium ordinatum* Williams and Downie, 1966, *C. divaricatum* Williams and Downie, 1966 and *Wetzeliiella articulata* subsp. *coniopa* Williams and Downie, 1966 first appear at or near the top of this division. *Cordosphaeridium fibrospinum* Davey and Williams, 1966, *C. inodes* (Klumpp) Eisenack, 1963 and *Lanternosphaeridium* sp. BE first occur in the lower part of the division. The age is based on the overlapping of published ranges of these species. Two new species of *Wetzeliiella* also are associated with this assemblage, *Wetzeliiella* sp. AE and *Wetzeliiella* sp. BE.

Division Ic. 1230-1400 feet (375-427 m)

Age/Formation: Late? Paleocene/Reindeer Formation

Discussion: *Deflandrea oebisfeldensis* Alberti, 1959 and *Palaeoperidinium basilium* Drugg, 1967 first appear in this division. *Wetzeliella articulata articulata*, *W. articulata conioipa* and *W. parva* are no longer present in the assemblage. *Wetzeliella* sp. AE and *Wetzeliella* sp. BE are not recorded in the well below the depth of 1290 feet (393 m). *Palaeoperidinium basilium* has not been reported from rocks younger than Paleocene in age. Therefore, the known ranges of *Wetzeliella* sp. AE and *Wetzeliella* sp. BE are ?Upper Paleocene to Lower Eocene.

Division Id. 1400-4840 feet (427-1475 m)

Age/Formation: Paleocene/Reindeer Formation

Discussion: *Alterbia obscura* (Drugg) Lentin and Williams, 1976 and *Trithyrodinium evittii* Drugg, 1967 first appear at the top of this division associated with *Cyclonephelium ordinatum* and *C. divaricatum* in the topmost sample at 1400-1430 feet (427-436 m). *Cyclonephelium divaricatum* does not occur below 1430 feet (436 m) in the well. *Wetzeliella homomorpha homomorpha* is common in samples above the depth of 1760 feet (612 m) in the well.

Dinoflagellate cysts occur rarely in samples between 1760 and 3740 feet (612-1140 m). The occurrence of *Wetzeliella homomorpha quinquelata* at 2900-2960 feet (884-902 m) is interpreted as caving from Eocene rocks higher in the well. The sparse angiosperm pollen assemblages, however, indicate that this interval is Paleocene in age.

Dinoflagellates occur in samples between 3740 and 4840 feet (1140-1475 m). *Diphyes colligerum* (Deflandre and Cookson) Cookson, 1965 and *Cordosphaeridium exilimurum* Downie and Williams, 1966 appear for the first time in this well section. These species are associated with *Wetzeliella homomorpha homomorpha*, *Cordosphaeridium inodes*, *Lanternosphaeridium* sp. BE, *Palaeoperidinium basilium* and *Cyclonephelium ordinatum*. It is probable that indigenous specimens of this association are mixed with caved material, but this cannot be proved. With the exception of *Cordosphaeridium exilimurum*, the presence of these species in Paleocene rocks is consistent with their known range in North America and Europe. Except for obviously caved material, none of the species in this association occurs below the sample from 4710-4840 feet (1436-1475 m).

II. Cretaceous-Tertiary

Division IIa. 4840-5130 feet (1475-1564 m)

Age/Formation: (?)Late Cretaceous-Paleocene/Tent Island and Reindeer formations

Discussion: The quality and quantity of unwashed cuttings samples available for this study were very poor between 4710 and 5130 feet (1436-1564 m). The first productive sample below this interval was taken from 5130-5220 feet (1564-1591 m). Unfortunately,

this interval spans the contact between the Reindeer and Tent Island formations and also includes the Cretaceous-Tertiary contact. The formational boundary and, by implication, Cretaceous-Tertiary contact are placed at 5050-foot (1539 m) depth in the well (see discussion on lithostratigraphy).

III. Upper Cretaceous

Division IIIa. 5130-5310 feet (1564-1618 m)

Age/Formation: Late Campanian/Tent Island Formation

Discussion: Five species, including *Aeroligera* sp. of McIntyre, 1974, *Chatangiella vnigri* (Vozzhennikova) Lentin and Williams, 1976 and *Odontochitina operculata* (O. Wetzel) Deflandre and Cookson, 1955, first appear near the top of this division. The Late Campanian age assigned to this interval does not preclude the occurrence of Maastrichtian rocks higher in this well, possibly between 5050 and 5130 feet (1539-1564 m). However, because of limitations imposed by sample quality, it is not possible to cite evidence for or against this possibility.

Division IIIb. 5310-5520 feet (1618-1682 m)

Age/Formation: Campanian/Tent Island Formation

Discussion: Samples within this division are barren of diagnostic dinoflagellate cysts and miospores. Because the division is bounded above and below by rocks of Early to Late Campanian age, the age of the division is assumed to be Campanian.

Division IIIc. 5520-6270 feet (1682-1911 m)

Age/Formation: Early and Middle Campanian/Tent Island and Boundary Creek formations

Discussion: Thirteen species first occur in the interval between 5520 and 5790 feet (1682-1765 m) including: *Alterbia acuminata* (Cookson and Eisenack) Lentin and Williams, 1976, *Chatangiella biapertura* (McIntyre) Lentin and Williams, 1976, *C. ditissima* (McIntyre) Lentin and Williams, 1976, *Hystricho-sphaeridium* sp. cf. *H. difficile* Manum and Cookson, 1964 sensu McIntyre, 1974, *Palaeoperidinium basilium* Drugg, 1967 sensu McIntyre, 1974 and *Laciniadinium biconiculum* McIntyre, 1975. This part of the well section appears correlative in part with Divisions H1 (upper part), H2 and H3 (lower part) proposed by McIntyre (1974, 1975) for surface sections of the upper part of the Smoking Hills Formation and lower part of the Mason River Formation (Yorath *et al.*, 1975) of the Anderson Plain region on the northern Canadian mainland.

The sample from between 5790 and 6050 feet (1765-1844 m) is barren of dinoflagellate cysts and diagnostic pollen species. However, an assemblage of dinoflagellate cysts, which occurs for the first time between 6050 and 6270 feet (1844-1911 m), also permits correlation with McIntyre's following species:

Spinidinium clavum Harland, 1973, *Diconodinium firmum* Harland, 1973, *Chatangiella coronata* (McIntyre) Lentin and Williams, 1976 and *Adnatosphaeridium* sp. of McIntyre, 1974. On the basis of the presence of these associations of species, the division is assigned an Early to Middle Campanian age.

Division III d. 6270-6400 feet (1911-1951 m)

Age/Formation: Santonian? to Middle Campanian/
Boundary Creek Formation

Discussion: *Diconodinium arcticum* Manum and Cookson, 1964 and *Hystricho-sphaeridium* sp. 3 of McIntyre, 1974 first occur in the sample from 6270-6300 feet (1911-1920 m). At the 6370- to 6400-foot (1941-1950 m) depth, another fifteen species occur for the first time, of which only two persist below this depth. This assemblage includes: *Laciniadinium orbiculatum* McIntyre, 1975, *Nelsoniella* sp. AE (a species closely comparable to *N. aceras* Cookson and Eisenack, 1960), and *Spiniferites scabrosus* (Clarke and Verdier) Sarjeant, 1970, a species hitherto recorded from rocks no younger than Santonian. Based on the association of these and the other twelve species, the age of Division III d is considered to be Santonian?-Middle Campanian. Division III d appears correlative with Division H1 and H2 of McIntyre (1974, 1975). The sample from 6370-6400 feet (1941-1950 m) spans an easily recognizable lithologic change which first occurs at a depth of 6380 feet (1944 m); bituminous shale becomes abundant in sample cuttings.

Division III e. 6300-6660 feet (1951-2030 m)

Age/Formation: Cenomanian-?Turonian/
Boundary Creek Formation

Discussion: *Endoscrinium campanula* (Gocht) Vozzhennikova, 1967 and *Palaeoperidinium cretaceum* (Pocock ex Davey) Lentin and Williams, 1976 first appear in a sample from 6400-6430 feet (1951-1960 m) together with a few rare specimens of *Luxadinium propatulum* Brideaux and McIntyre, 1976. The former species have not been recorded in rocks younger than Turonian and the latter species in rocks younger than Cenomanian. *Dorocysta litotes* Davey, 1970 and *Chatangiella magna* (Davey) Lentin and Williams, 1976 occur first in a sample from 6630-6660 feet (2021-2030 m). These two species have not been reported from rocks older than Cenomanian in age and range into rocks of Santonian age. These data form the basis for assignment of a Cenomanian-?Turonian age for Division III e. Palynologic evidence indicates, therefore, that a hiatus, spanning some part of Turonian-Santonian time, occurs at 6400-foot (1951 m) depth in the well.

IV. Lower Cretaceous

Division IV a. 6660-6850 feet (2030-2088 m)

Age/Formation: Aptian-?Early Albian/?Upper sandstone division equivalent.

Discussion: Unfortunately, cuttings samples were not available for the interval in the well between 6660 and 6850 feet (2030-2088 m). The first productive sample below 6850 feet (2088 m) is from 6850-6880 feet (2088-2097 m). Lithostratigraphic studies indicate that the lower limits of the Upper Cretaceous Boundary Creek Formation and, by implication, the Lower-Upper Cretaceous contact, occur at the 6660-foot (2030 m) depth in the well. Because of this sample gap, it is not possible to determine the palynological contact between Early and Late Cretaceous assemblages. Neither is it possible to determine whether rocks of Albian age are present, or whether the Boundary Creek Formation rests directly on Aptian rocks correlative in age with those of the Upper sandstone division of Jeletzky (1958, 1960).

Division IV b. 6850-7040 feet (2088-2146 m)

Age/Formation: Aptian/Upper sandstone division equivalent.

Discussion: Eight species make their first appearance in the sample from 6850-6880 feet (2088-2097 m). "*Hemicystodinium*" sp. CA and *Muderongia* sp. A of Brideaux and McIntyre, 1976, are known to range into Lower Albian rocks (Brideaux and McIntyre, 1976; Brideaux, in prep.), but their association with a species of *Muderongia* similar to the *tetracantha*-type precludes an Albian age for this division. *Achomosphaera neptunii* (Eisenack) Davey and Williams, 1966 occurs in association with this assemblage from 6960 to 6990 feet (2121-2130 m). The reported range of this species is upper Valanginian to Aptian. Except for rare specimens interpreted as caved material, only five long-ranging species from Divisions III a to III e persist into or below Division IV b.

Division IV c. 7040-7500 feet (2146-2286 m)

Age/Formation: Barremian/Upper shale-siltstone division

Discussion: The Barremian age assignment is based on the first occurrence in the well of *Pseudoceratium* sp. cf. *P. gochtii* Neale and Sarjeant, 1962 (7040-7070 ft; 2146-2155 m), *Wallodinium krutzschii* Alberti ex Habib, 1972 (7120-7140 ft; 2170-2176 m), and *Heslertonia heslertonensis* (Neale and Sarjeant) Sarjeant, 1966 (7300-7320 ft; 2227-2233 m). None of these species is known to range above the Barremian in northern Canada; only *Wallodinium krutzschii* ranges higher elsewhere (Brideaux, manuscript report). *Lunatadinium dissolutum* Brideaux and McIntyre, 1973 and *Muderongia tetracantha* (Gocht) Alberta, 1961 also appear first in association with this assemblage, but are known to range into Middle Albian and Aptian rocks, respectively.

Division IVd. 7500-7900 feet (2286-2408 m)

Age/Formation: Hauterivian?-Barremian/Upper shale-siltstone division

Discussion: *Pseudoceratium nudum* Gocht, 1957, *Sirmiodinium grossii* Alberti, 1961, and *Hystrichosphaeridium* sp. AE of Brideaux (manuscript report) first appear in this interval in association with *Cyclonephelium* sp. GE and cf. *Ctenidodinium* sp. AE. The first three species do not range into rocks younger than Barremian in age; the other two species have been observed in this well section and rarely in surface samples of a general Hauterivian-Barremian age.

Division IVe. 7900-9325 feet (2408-2842 m)

Age/Formation: Valanginian?-Hauterivian/Upper shale-siltstone division; "Parsons sandstone unit"

Discussion: The age assignment is based on the recovery within this interval of three species thought to be restricted to Valanginian and Hauterivian rocks in northern Canada: *Oligosphaeridium* sp. cf. *O. complex* (White) Davey and Williams, 1966, *Canningia* sp. AE, and *Canningia* sp. BE. *Muderongia simplex* Alberti, 1961, whose reported range is Valanginian to Barremian, *Gonyaulacysta hyalodermopsis* (Cookson and Eisenack) Sarjeant, 1969, "*Psaliogonyaulax apatela*" auct. non (Cookson and Eisenack) Sarjeant, 1966 and *Meiourogonyaulax stoveri* milliod, 1969 also are associated with this assemblage.

Division IVf. 9325-9550 feet (2842-2911 m)

Age/Formation: Berriasian/"Parsons sandstone unit"; Husky Formation

Discussion: *Pareodinia* sp. BO occurs first in a conventional core sample at 9325-9346 feet (2842-2849 m). This species has not been observed in rocks younger than Berriasian in age in northern Canada (Brideaux and Fisher, in press; Brideaux, manuscript report). *Imbatodinium villosum* Vozzhennikova, 1967 occurs first in a core from 9480-9495 feet (2890-2894 m); in northern Canada, this species has been observed in Valanginian and lower Hauterivian rocks and in Russia (Vozzhennikova, 1967) has been reported from the Upper Jurassic (Upper Volgian - Upper Tithonian). These observations are the basis for the Berriasian age assignment.

A series of conventional cores were taken between 9022 and 9512 feet (2750-2899 m). Dinoflagellate species are rare in these cores and few in number. Cuttings samples within this interval, by contrast, yield a variety of species present in relatively large numbers. Many of these species do not range into Berriasian and Valanginian rocks in surface sections (Brideaux, unpubl. data). These observations indicate that most of the species occurring in the cuttings in the lower part of Division IVe and in Division IVf are caved material.

Lithostratigraphic studies suggest that the top of the Husky Formation in this well should be placed at 9425 feet (2873 m). In outcrop studies (Jeletzky, 1967, 1973), the Upper member of this unit has been assigned an Early and, in part, Late Berriasian age.

V. Upper Jurassic-Lower Cretaceous

Division Va. 9550-10 000 feet (2911-3048 m)

Age/Formation: (?)Post-Kimmeridgian-Berriasian/Husky Formation

Discussion: Excepting *Oligosphaeridium asterigium* (Gocht) Davey and Williams, 1966, *Oligosphaeridium* sp. cf. *O. complex* and *Pareodinia ceratophora* Deflandre, 1947, none of the other species recorded from the cuttings samples in this interval occurs in surface sections older than Hauterivian. Because of the strong indications of caved material in these samples, as discussed above, the age of this division based on dinoflagellates and miospores is problematical.

The interval between 9550 and 9652 feet (2911-2942 m), based on the lithostratigraphy, is assigned to subsurface equivalents of the Upper member and Red-weathering shale member of the Husky Formation. These units in surface outcrop are Early Cretaceous (Berriasian) in age (Jeletzky, 1967, 1973). The interval between 9652 and 9700 feet (2942-2957 m) is assigned, on lithostratigraphic evidence, to subsurface equivalents of the Arenaceous member of the Husky Formation. Jeletzky (1967, 1973) assigns a Late Jurassic (Late Tithonian) age to outcrop sections of the Arenaceous member. In the sections exposed along the eastern slopes of the Richardson Mountains, in the Aklavik Range, the contact between the Arenaceous member and the Red-weathering shale member is also the contact between rocks of latest Jurassic and earliest Cretaceous ages (Brideaux and Fisher, in press; Jeletzky, 1967). Therefore, it is probable that the upper part of this division, above 9652 feet (2942 m), is of early Cretaceous age; the lower part, extending to 10 000 feet (3048 m), is of latest Jurassic age (probably post-Kimmeridgian).

VI. Upper Jurassic

Division VIa. 10 000-10 100 feet (3048-3078 m)

Age/Formation: Upper Oxfordian-Kimmeridgian/Husky Formation, Lower member

Discussion: The age assignment is based on the association of *Lanterna* sp. SA, *Horologinella* sp. SP, *Endoscrinium luridum* (Deflandre) Gocht, 1969 and *Scriniodinium crystallinum* (Deflandre) Klement, 1960, recorded for the first time in the well from samples between 10 000 and 10 100 feet (3048-3078 m). *Pareodinia* sp. CA also occurs for the first time in the well in this interval but is known to range into Berriasian rocks (Brideaux and Fisher, in press). *Pareodinia* sp. BO also occurs in this interval. This association of species

has been termed the "borealis" assemblage and is indicative of a Late Oxfordian to Kimmeridgian age (Brideaux and Fisher, in press).

VII. Paleozoic or ?Proterozoic

Division VIIa. 10 000-10 515 feet (3078-3205 m)

Age/Formation: Paleozoic or ?Proterozoic/unnamed formation

Discussion: The samples from this interval contain only caved Jurassic dinoflagellates and miospores. Lithostratigraphic studies indicate that Jurassic rocks rest unconformably on cherty dolomites, in part argillaceous, of probable pre-Mesozoic, possibly Paleozoic or ?Proterozoic age.

BIOSTRATIGRAPHIC OBSERVATIONS ON SEVERAL CORED INTERVALS: GULF MOBIL PARSONS F-09 WELL

Information gained from the study of the dinoflagellate succession in the Gulf Mobil Parsons N-10 well has been applied to a restudy of some conventionally cored intervals in the Parsons F-09 well. Lithostratigraphic observations have been published on these cored intervals by Myhr and Gunther (1974) and Myhr and Young (1975). The following age determinations supersede those referred to in Myhr and Gunther (1974) and Brideaux (in Brideaux *et al.*, 1975, p. 4, 5).

Core 1: 9337-9346.8 feet (2846-2849 m) Paleo Services Slide
9337-9357 feet (2846-2852 m) GSC Slide C-22945

"*Palaeohystrichophora*" *brevispinosa* Pocock, 1962
Oligosphaeridium sp. cf. *O. complex* (White) Davey and Williams, 1966
Pareodinia ceratophora Deflandre, 1947

age: Hauterivian, correlative in part with Division IVE, Parsons N-10 well

Core 1: 9357-9377 feet (2852-2858 m) GSC Slide C-22946

Core 2: 9814-9824 feet (2991-2994 m) GSC Slide C-22380

Oligosphaeridium sp. cf. *O. complex* (White) Davey and Williams, 1966

age: ?Valanginian-Hauterivian, correlative in part with Division IVE, Parsons N-10 well

Core 2: 9824-9834 feet (2994-2997 m) GSC Slide C-22381 (*)
9833.2-9842.7 feet (2997-3000 m) Paleo Services Slide

"*Psaligonyaulax apatela*" *auct. non* (Cookson and Eisenack) Sarjeant, 1966 (*)

Imbatodinium villosum Vozzhennikova, 1967 (*)

Lunatadinium dissolutum Brideaux and McIntyre, 1973 (abundant)

Oligosphaeridium sp. cf. *O. complex* (White) Davey Williams, 1966 *Canningia* sp. BE

age: ?Valanginian-Hauterivian, correlative with Division IVE, Parsons N-10 well

The intervals mentioned above in the Gulf Mobil Parsons F-09 well are referred to the following informal unit: "Parsons sandstone unit".

References

- Barss, M. S. and Williams, G. L.
1973: Palynology and nannofossil processing techniques; Geol. Surv. Can., Paper 73-26.
- Brideaux, W. W.
1975: Status of Mesozoic and Tertiary dinoflagellate studies in the Canadian Arctic; Am. Assoc. Stratigr. Palynol., Contrib. Series, no. 4, p. 15-28
1976: Taxonomic notes and illustrations of selected dinoflagellates from the Gulf Mobil Parsons N-10 well; in Report of Activities, Part B; Geol. Surv. Can., Paper 76-1B, report 44.
- Brideaux, W. W., Chamney, T. P., Dunay, R. E., Fritz, W. H., Hopkins, William, S., Jr., Jeletzky, J. A., McGregor, D. C., Norford, B. S., Norris, A. W., Pedder, A. E. H., Sherrington, P. F., Sliter, W. V., Sweet, A. R., Uyeno, T. T., and Waterhouse, J. B.
1975: Biostratigraphic determinations of fossils from the subsurface of the Districts of Franklin and Mackenzie; Geol. Surv. Can., Paper 74-39.
- Brideaux, W. W. and Fisher, M. J.
Upper Jurassic-Lower Cretaceous dinoflagellate assemblages from Arctic Canada; Geol. Surv. Can., Bull. 259.
- Brideaux, W. W. and McIntyre, D. J.
1973: *Lunatadinium dissolutum* gen. et sp. nov., a dinoflagellate cyst from Lower Cretaceous rocks, Yukon Territory and northern District of Mackenzie; Bull. Can. Pet. Geol., v. 21, p. 395-402.
1976: Spores, pollen, dinoflagellates and acritarchs from Lower Cretaceous rocks on Horton River, District of Mackenzie, Canada; Geol. Surv. Can., Bull. 252.
- Canada, Department of Indian Affairs and Northern Development
1973: North of 60 Schedule of Wells; Northern Economics Development Branch, Oil and Mineral Division, Oil and Gas Section.

- Chamney, T. P.
 1971: Tertiary and Cretaceous biostratigraphic divisions in the Reindeer D-27 borehole, Mackenzie River delta; *Geol. Surv. Can.*, Paper 70-30.
- 1973: Tuktoyaktuk Peninsula Tertiary and Mesozoic biostratigraphic correlation; *in Report of Activities, Part B; Geol. Surv. Can.*, Paper 73-1B, p. 171-178.
- Cote, R. P., Lerand, M. M., and Rector, R. I.
 1975: Geology of the Lower Cretaceous Parsons Lake gas field, Mackenzie Delta, Northwest Territories in Canada's continental margins and offshore petroleum exploration, C. J. Yorath *et al.*, eds.; *Can. Soc. Pet. Geol.*, Mem. 4, p. 613-632.
- Davies, D. K., Ethridge, F. G., and Berg, R. R.
 1971: Recognition of barrier environments; *J. Sediment. Petrol.*, v. 43, p. 736-747.
- Drugg, W. S. and Stover, L. E.
 1975: Stratigraphic range charts. Selected Cenozoic dinoflagellates; *Am. Assoc. Stratigr. Palynol.*, Contrib. Series, no. 4, p. 73-77.
- Harker, S. D. and Sarjeant, W. A. S.
 1975: The stratigraphic distribution of organic-walled dinoflagellate cysts in the Cretaceous and Tertiary; *Rev. Palaeobot. Palynol.*, v. 20, p. 217-315.
- Jeletzky, J. A.
 1958: Uppermost Jurassic and Cretaceous rocks of Aklavik Range, northeastern Richardson Mountains, Northwest Territories; *Geol. Surv. Can.*, Paper 58-2.
- 1960: Uppermost Jurassic and Cretaceous rocks, east flank of Richardson Mountains between Stony Creek and Donna River, Northwest Territories; *Geol. Surv. Can.*, Paper 59-14.
- 1967: Jurassic and (?) Triassic rocks of the eastern slope of Richardson Mountains, northwestern District of Mackenzie, 106M and 107B (parts of); *Geol. Surv. Can.*, Paper 66-50.
- 1973: Biochronology of the marine boreal latest Jurassic, Berriasian and Valanginian in Canada; *in The Boreal Lower Cretaceous*, R. Casey and P. F. Rawson, eds.; *Geol. J.*, Spec. Issue 5, p. 41-80.
- McIntyre, D. J.
 1974: Palynology of an Upper Cretaceous section, Horton River, District of Mackenzie, N. W. T.; *Geol. Surv. Can.*, Paper 74-14.
- McIntyre, D. J. (cont'd.)
 1975: Morphologic changes in *Deflandrea* from a Campanian section, District of Mackenzie, N. W. T., Canada; *Geosci. Man*, v. 11, p. 61-76.
- Millioud, M. E., Williams, G. L., and Lentin, J. K.
 1975: Stratigraphic range charts. Selected Cretaceous dinoflagellates; *Am. Assoc. Stratigr. Palynol.*, Contrib. Series, no. 4, p. 65-72.
- Myhr, D. W. and Gunther, P. R.
 1974: Lithostratigraphy and coal reflectance of a Lower Cretaceous deltaic succession in the Gulf Mobil Parsons F-09 borehole, N. W. T.; *in Report of Activities, Part B; Geol. Surv. Can.*, Paper 74-1B, p. 24-48.
- Myhr, D. W. and Young, F. G.
 1975: Lower Cretaceous (Neocomian) sandstone sequence of Mackenzie Delta and Richardson Mountains area; *in Report of Activities, Part C; Geol. Surv. Can.*, Paper 75-1C, p. 247-266.
- Oilweek
 1974: Gulf Parsons data focuses attention on delta's Eskimo Lakes Fault Zone; *Oilweek*, v. 25, no. 5, March 18, 1974, p. 39-42.
- Pocock, S. A. J.
 A preliminary dinoflagellate zonation of the uppermost Jurassic and lower part of the Cretaceous in the Canadian Arctic and possible correlation southward in the Western Canada Basin; *Geosci. Man*, v. 12. (in press)
- Rampton, V. N.
 1971: Quaternary geology, Mackenzie Delta and Arctic Coastal Plain, District of Mackenzie; *in Report of Activities, Part A; Geol. Surv. Can.*, Paper 71-1A, p. 173-177.
- Riley, L. A. and Sarjeant, W. A. S.
 1972: Survey of the stratigraphical division of dinoflagellates, acritarchs and tasmanitids in the Jurassic; *Geophytology*, v. 2, p. 1-40.
- Sarjeant, W. A. S.
 1975: Stratigraphic range charts. Triassic and Jurassic dinoflagellates; *Am. Assoc. Stratigr. Palynol.*, Contrib. Series, no. 4, p. 51-64.
- Vozzhennikova, T. F.
 1967: Iskopaemye perodomeo yurskikh, melovykh i paleogenovykh otlozheniy SSSR; *Akad. Nauk SSSR, Sib. Otd., Inst. Geol. Geofiz.*, Tr. (Fossil peridinians of the Jurassic, Cretaceous and Paleogene deposits of the U. S. S. R.)

Williams, G. L.

- 1975: Dinoflagellate and spore stratigraphy of the Mesozoic-Cenozoic off-shore eastern Canada; in *Offshore Geology of Eastern Canada*, Volume 2, Regional Geology; Geol. Surv. Can., Paper 74-30, v. 2, p. 107-161.

Williams, G. L. and Brideaux, W. W.

- 1975: Palynologic analyses of upper Mesozoic and Cenozoic rocks of the Grand Banks, Atlantic Continental Margin; Geol. Surv. Can., Bull. 236.

Young, F. G.

- 1974: Deltas: a general review; in *Use of Sedimentary Structures for recognition of Clastic Environments*, M. S. Shawa, ed.; Can. Soc. Pet. Geol., p. 1, 8, Fig. 6.

Yorath, C. J., Balkwill, H. R., and Klassen, R. W.

- 1976: Franklin Bay (97C) and Malloch Hill (97F) map-areas, District of Mackenzie; Geol. Surv. Can., Paper 74-36.

Project 710019

Wayne W. Brideaux
Institute of Sedimentary and Petroleum Geology, CalgaryIntroduction

The lithostratigraphy, paleoenvironmental interpretations, and biostratigraphy based on dinoflagellate cysts for the Gulf Mobil Parsons N-10 well are discussed by Brideaux and Myhr (1976). This paper gives brief taxonomic descriptions of some of the species designated in that paper (*ibid.*, 1976) and illustrates these and other selected species in order to increase the practical value of the preliminary biostratigraphic divisions and facilitate their application to other subsurface sections in the Mackenzie Delta region. The morphologic terminology employed in the taxonomic notes follows the usage of Lentin and Williams (1976).

Slides containing figured specimens are stored in the collections of the Geological Survey of Canada, 601 Booth Street, Ottawa, Canada, K1A 0E8. Other slides and samples from this well are stored in the collection at the Institute of Sedimentary and Petroleum Geology, 3303 - 33rd Street N.W., Calgary, Canada, T2L 2A7.

Taxonomic notes on selected speciesTertiary

Genus *Wetzeliella* Eisenack, 1938 emend. Lentin and Williams, 1966. *Wetzeliella* sp. AE (Pl. 44.1, fig. 8)

Pericyst ambitus pentagonal; one apical horn, two pericingular horns and two antapical horns, the left one longer. Endocyst relatively small, ovoidal, elongate longitudinally. One apical, two pericingular and two antapical pericoels. Periphragm thin, with widely spaced nontabular, short, spiny processes. Peri- and endarcheopyle quadra intercalary. Peri- and endoperculum free, simple, slightly broader than long and nearly rectangular, formed by paraplate 2a.

Wetzeliella sp. BE (Pl. 44.1, fig. 4)

Pericyst ambitus pentagonal; one apical, two pericingular and two antapical horns, the left one longer. Endocyst large, ovoidal to subcircular. One apical, two pericingular and two antapical pericoels. Periphragm thin, with discrete nontabular spinose processes, distally acuminate to bifid. Peri- and endarcheopyle quadra intercalary; peri- and endoperculum simple, free, longer than broad, trapezoidal, formed by paraplate 2a.

Genus *Lanternosphaeridium* Morgenroth, 1966

Lanternosphaeridium sp. BE (Pl. 44.1, figs. 10, 12)

Pericyst and endocyst ambitus subcircular, slightly elongate longitudinally; apical and antapical horns absent; pericoel absent. Periphragm surface

granular to fibrous; periphragm forming groups of processes which are joined basally and variously terminated distally; processes intratabular and denoting a paratabulation of ?4', 6", ?6c, 1"', ?1p. Archeopyle precingular; operculum simple, free, formed by paraplate 3", subquadrate, slightly broader than long.

Upper Cretaceous

Genus *Nelsoniella* Cookson and Eisenack, 1960

Nelsoniella sp. AE (Pl. 44.1, fig. 7)

Pericyst ambitus ovoid, broader than long; apex and antapex rounded; endocyst relatively smaller, ambitus ovoid; hypopericoel. Periphragm thin, verrucate on the epiperiphragm, smooth on the hypoperiphragm; endoperiphragm smooth. Paratabulation indeterminate; archeopyle not developed on specimens encountered.

The apical verrucae are more pronounced than those of *Nelsoniella aceras* Cookson and Eisenack, 1960, p. 4, Pl. 1, figs. 12, 13.

Lower Cretaceous

Genus *Hemicystodinium* Wall, 1967

"*Hemicystodinium*" sp. CA (Pl. 44.2, fig. 10)

Autoblast spherical to subspherical; autophragm thin with scattered small grana and fine vermiculate ridges; shape of operculum and the projecting part of the hypocyst, which appears to represent the anterior sulcal paraplate, suggests presence of paratabulation; archeopyle formed by loss of apical and precingular paraplates; operculum simple, typically free but occasionally attached.

Genus *Ctenidodinium* Deflandre, 1938 emend. Sarjeant, 1966 Cf. *Ctenidodinium* sp. AE (Pl. 44.2, fig. 11)

Pericyst and endocyst outline subcircular; pericoel absent. Periphragm smooth and raised into low, parasutural ridges, from which arise variously formed flared bifurcate processes, their distal terminations either open or closed; greatest length of processes found on paracingular parasutures; processes often joined proximally by a thin membrane. Parasutural ridges and processes outline a paratabulation difficult to determine because of severe apical-antapical compression. Archeopyle formed by detachment of apical and precingular paraplates; operculum simple, attached.

Genus *Cyclonephelium* Deflandre and Cookson, 1955.

Cyclonephelium sp. GE (Pl. 44.2, fig. 13)

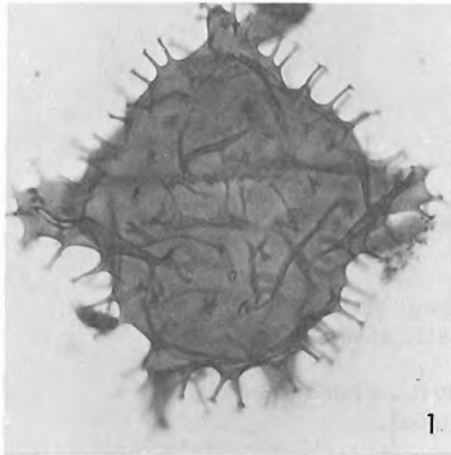
Pericyst and endocyst outline ovoid; pericoel absent. Periphragm thin, smooth on the central

PLATE LEGENDS

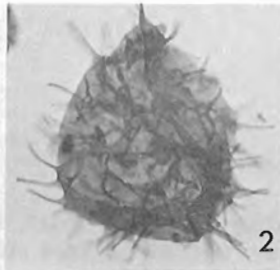
In the explanation of figures, the species name is followed by the GSC (ISPG) locality number, the depth in the well (ft.), the slide number, stage co-ordinates for Reichert Zetopan Microscope No. 56 395 at the Institute of Sedimentary and Petroleum Geology, Calgary, Canada, focus level and orientation if needed, the GSC Type Number, the magnifications and the size in microns. IC refers to Interference Contrast.

PLATE 44.1

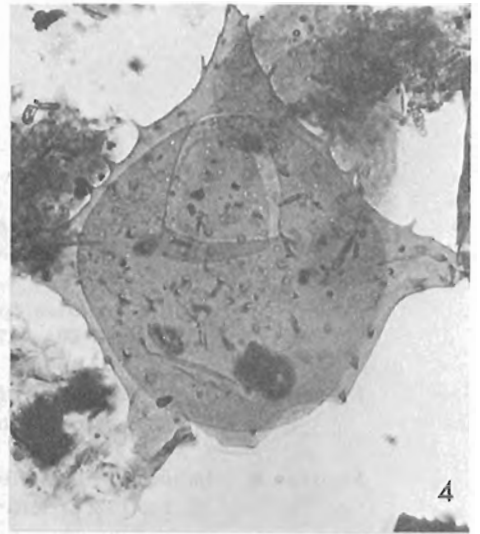
- Figure 1. *Wetziella articulata articulata* Eisenack, 1938; C-30335, 900-1000 ft., Slide P938-7B, 38.7 x 119.3, mid-focus, GSC 45797, x500 (102 μ).
- Figure 2. *Wetziella homomorpha homomorpha* Deflandre and Cookson, 1955; C-30335, 900-1000 ft., Slide P938-7B, 37.7 x 115.8, mid-focus, GSC 45798, x500 (54 μ).
- Figure 3. *Wetziella parva* Alberti, 1961; C-30335, 900-1000 ft., Slide P938-7B, 08.8 x 128.1, mid-focus, GSC 45799, x500 (75 μ).
- Figure 4. *Wetziella* sp. BE; C-30335, 1000-1030 ft., Slide P938-8A, 24.4 x 127.4, hi-focus on dorsal surface, GSC 45800, x500 (126 μ).
- Figure 5. *Diphyes colligerum* (Deflandre and Cookson) Cookson, 1965; C-30335, 4260-4290 ft., Slide P938-42A, 38.1 x 124.8, mid-focus, GSC 45801, x500 (60 μ).
- Figure 6. *Alterbia obscura* (Drugg) Lentin and Williams, 1976; C-30335, 1400-1430 ft., Slide P938-14A, 15.6 x 120.3, mid-focus, GSC 45802, x500 (60 μ).
- Figure 7. *Nelsoniella* sp. AE; C-30335, 6630-6660 ft., Slide P938-63A, 31.0 x 118.6, mid-focus, GSC 45803, x500 (62 μ).
- Figure 8. *Wetziella* sp. AE; C-30335, 1000-1030 ft., Slide P938-8A, 11.1 x 127.6, lo-focus on dorsal surface, GSC 45804, x500 (138 μ), IC.
- Figure 9. *Cyclonephelium ordinatum* Williams and Downie, 1966; C-30335, 1200-1230 ft., Slide P938-11A, 39.7 x 121.9, mid-focus, GSC 45805, x500 (width, 65 μ).
- Figures 10-12. *Lanternosphaeridium* sp. BE
10. C-30335, 1200-1230 ft., Slide P938-11A, 35.3 x 126.3, lo-focus on dorsal surface, GSC 45806, x500 (60 μ).
12. C-30335, 1200-1230 ft., Slide P938-11A, 07.1 x 132.2, lo-focus on right lateral surface, GSC 45807, x500 (70 μ).
- Figure 11. *Spiniferites* sp. CE; C-30335, 6380-6400 ft., Slide P938-60A, 22.6 x 125.5, mid-focus, GSC 45808, x500 (60 μ).
- Figure 13. *Wetziella articulata conioipa* Williams and Downie, 1966; C-30335, 1000-1030 ft., Slide P938-8A, 09.0 x 121.1, focus on processes, GSC 45809, x500 (115 μ).



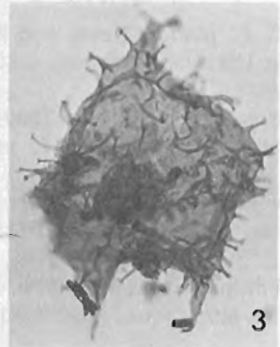
1



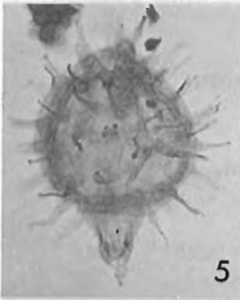
2



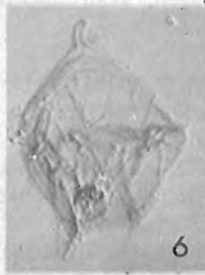
4



3



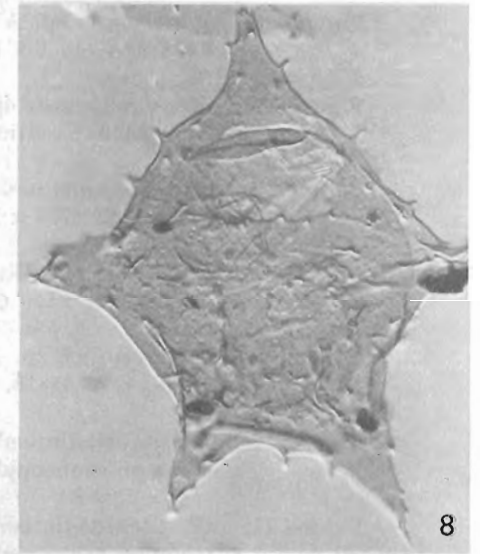
5



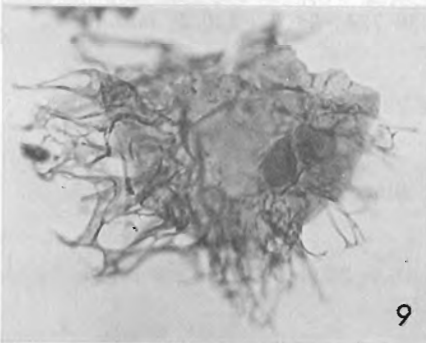
6



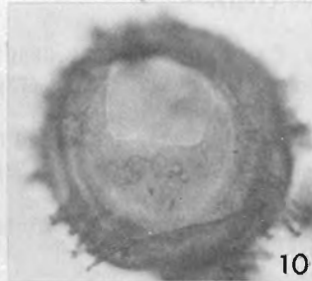
7



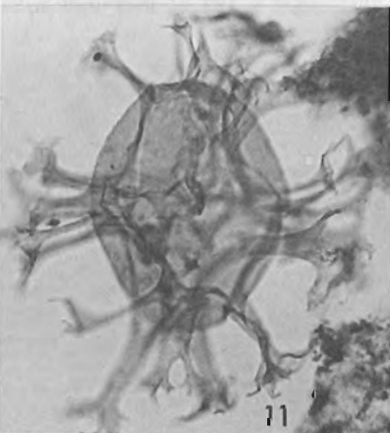
8



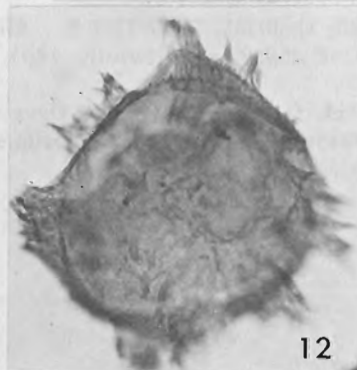
9



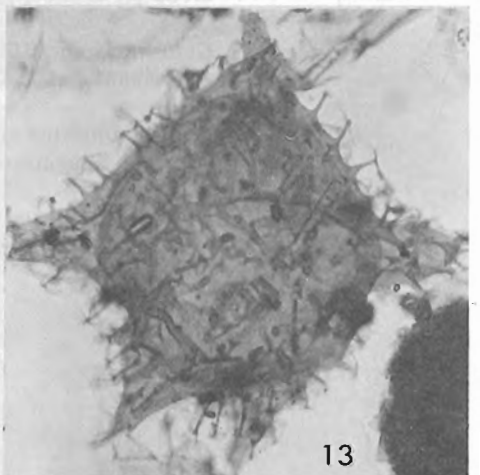
10



11



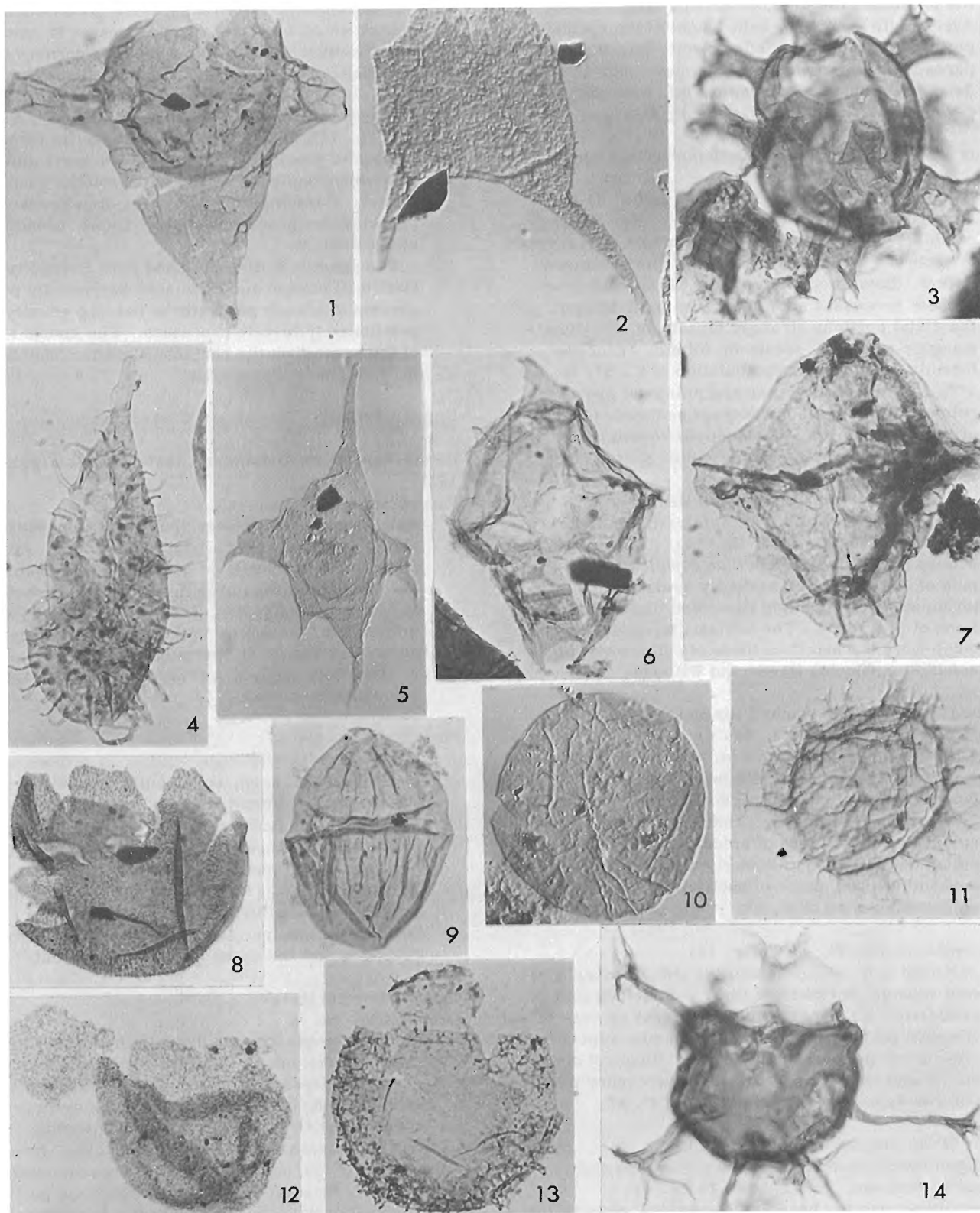
12



13

PLATE 44. 2

- Figure 1. *Muderongia simplex* Alberti, 1961; C-30335, 8100-8120 ft., Slide P938-76C, 31.8 x 116.7, mid-focus, GSC 45810, x500 (108 μ).
- Figure 2. *Pseudoceratium* sp. cf. *P. gochtii* Neale and Sarjeant, 1962; C-30335, 7300-7320 ft., Slide P938-69A, 27.2 x 120.5, mid-focus, GSC 45811, x500 (135 μ).
- Figure 3. *Hystrichosphaeridium* sp. AE; C-30335, 7500-7530 ft., Slide P938-71A, 07.4 x 118.2 ft., focus on archeopyle, GSC 45812, x500 (65 μ).
- Figure 4. *Imbatodinium villosum* Vozzhennikova, 1967; C-30335, 9480-9495 ft., Slide P938-5A, 35.3 x 133.3, mid-focus, GSC 45813, x500 (118 μ).
- Figure 5. *Muderongia* sp. A of Brideaux and McIntyre, 1976; C-30335, 7040-7070 ft., Slide P938-66A, 16.9 x 119.2, mid-focus, GSC 45814, x300 (160 μ).
- Figure 6. "*Psaligonyaulax apatela*" auct. non (Cookson and Eisenack) Sarjeant, 1966; C-30335, 8400-8420 ft., Slide P938-81C, 28.7 x 135.0, mid-focus, GSC 45815, x500 (100 μ).
- Figure 7. *Endoscrinium luridum* (Deflandre) Gocht, 1969; C-30335, 10 000-10 020 ft., Slide P938-97A, 37.9 x 121.2, mid-focus, GSC 45816, x500 (105 μ).
- Figure 8. *Canningia* sp. AE; C-30335, 8270-8290 ft., Slide P938-78A, 24.6 x 130.5, mid-focus, GSC 45817, x500 (width, 75 μ).
- Figure 9. *Dinogymnium* sp. AE; C-30335, 6380-6400 ft., Slide P938-60A, 31.2 x 116.7, mid-focus, GSC 45818, x500 (70 μ).
- Figure 10. "*Hemicystodinium*" sp. CA; C-30335, 6850-6880 ft., Slide P938-64A, 40.0 x 119.3, focus on archeopyle trace, GSC 45819, x500 (73 μ).
- Figure 11. Cf. *Ctenidodinium* sp. AE; C-30335, 7500-7530 ft., Slide P938-71A, 02.5 x 132.1, focus on archeopyle trace, GSC 45820, x500 (58 μ), IC.
- Figure 12. *Canningia* sp. BE; C-30335, 8300-8320 ft., Slide P938-79C, 43.1 x 123.5, mid-focus, GSC 45821, x500 (width, 63 μ).
- Figure 13. *Cyclonephelium* sp. GE; C-30335, 7500-7530 ft., Slide P938-71A, 22.8 x 115. a, focus on operculum, GSC 45822, x500 (width, 72 μ).
- Figure 14. *Oligosphaeridium* sp. cf. *O. complex* (White) Davey and Williams, 1966; C-30335, 8400-8420 ft., Slide P938-81C, 43.7 x 122.3, focus on processes, GSC 45823, x500 (width, 60 μ).



surface of the dorsal and ventral hypoperiblast, but otherwise densely ornamented with short apiculate processes and low, anastomosing ridges; the processes discrete, or arising from the ridges. Archeopyle formed by detachment of the apical paraplates; operculum simple, attached at the parasulcal region. Epipericyst paratabulation denoted by shape of operculum and accessory parasutures and determined as 4', 6".

Genus *Hystrichosphaeridium* Deflandre, 1937 emend. Davey and Williams, 1966

Hystrichosphaeridium sp. AE (Pl. 44.2, fig. 3)

Periblast and endoblast ambitus circular to subcircular; pericoel absent. Periphragm thin, smooth to scabrate, produced to form paraplate-centred, hollow, distally open, typically latispinous processes; processes often markedly infundibular, the distal portions strongly fenestrate, the distal margins aculeate, secate or foliate. Process formula denoting a paratabulation of 5', 6", 6c, 5"', 1"', 1p, ?s; postcingular and antapical processes robust, paracingular processes reduced, others of intermediate size. Archeopyle formed by loss of the apical paraplates; operculum simple, free.

Genus *Oligosphaeridium* Davey and Williams, 1966

Oligosphaeridium sp. cf. *O. complex* (White) Davey and Williams, 1966 (Pl. 44.2, fig. 14)

Differs from *Oligosphaeridium complex* in possession of clathrate, but markedly aculeate, distal terminations or strongly dissected distal terminations of processes. The aculeate terminations are much more marked than those of *Oligosphaeridium asterigium* (Gocht) Davey and Williams, 1966.

Genus *Canningia* Cookson and Eisenack, 1960

Canningia sp. AE (Pl. 44.2, fig. 8)

Complete specimens not seen; ambitus of remaining epipericyst and hypocyst semicircular to ovoid; pericoel absent. Periphragm thin, bearing densely spaced, short, apiculate ornament. Archeopyle apical, formed by loss of apical paraplates; operculum not observed. Strongly developed accessory parasutures and shape of archeopyle denote an epiparatabulation of 4', 6".

Canningia sp. BE (Pl. 44.2, fig. 12)

Periblast and endoblast ambitus subcircular; pericoel absent. Periphragm thin, the surface microreticulate. Archeopyle apical, formed by detachment of apical paraplates; operculum simple, typically attached in the parasulcal region. Shape of operculum and development of short accessory parasutures denote epiparatabulation of 4', 6".

Genus "*Psaligonyaulax*" Sarjeant, 1966

"*Psaligonyaulax apatela*" auct. non (Cookson and Eisenack) Sarjeant, 1966 (Pl. 44.2, fig. 6)

Periblast ambitus broadly rhomboidal; epiperiblast forming short apical horn; hypoperiblast distally

frustum-shaped, subquadrate in plan, open antapically. Epipericoel sensu stricto not developed; hypopericoel well developed. Periphragm thin, surface smooth, raised to form low parasutural ridges which bear trifurcate processes at junctions of parasutural ridges and at the four corners of the quadrate to subquadrate antapical opening.

Paratabulation, denoted by parasutural ridges and gonal processes, determined as ?4, 6", xc, 5"', ?p, 1'''. Peri- and endoarcheopyles formed by loss of precingular paraplate 3"; peri- and endoperculum simple, free, the latter smaller than the former. Paracingulum and parasulcus present; paracingular processes often reduced, broad-based and acuminate.

The species is distinguished from *Psaligonyaulax apatela* (Cookson and Eisenack) Sarjeant by possession of smooth parasutures bearing gonally positioned trifurcate processes. The known range of the species on the northern Canadian mainland is ?Berriasian-Barremian.

Upper Jurassic - lowermost Cretaceous

Genus *Pareodinia* Deflandre, 1947 emend. Wiggins, 1975

Pareodinia sp. BO

Autoblast length greater than maximum width; short, stout apical horn, rounded antapex. Autophragm surface smooth or scabrate and forming low, narrow parasutures denoting a paratabulation of ?4', 2a, 6", 5'''-?6"', 1''', ?1p. Archeopyle intercalary, formed by loss of two intercalary paraplates (1a, 2a); operculum free, simple; paracingular sutures outline paracingulum; parasulcus not observed.

Pareodinia sp. CA

Autoblast with tripartite outline, a prolonged, tapering apical horn, subcircular central part and moderately prominent antapical bulging. Autophragm bearing dense cover of solid, hairlike processes and lineations of processes denoting paratabulation; paratabulation determined as ?4', 2a, 6", 5'''-?6"', 1''', 1p. Archeopyle intercalary, formed by loss of two intercalary paraplates (1a, 2a); operculum free or attached, simple. Paracingulum and indistinct parasulcus present.

Genus *Lanterna* Dodekova, 1969

Lanterna sp. SA

Pericyst length greater than width; outline roughly truncated biconical; periblast and endoblast closely appressed; pericoel absent. Periphragm forming densely spaced intratabular sculpture, typically anastomosing basally and forming an irregular meshwork. Archeopyle apical, formed by loss of four apical paraplates; operculum simple, typically free but occasionally remaining partially attached at the parasulcal region. Paratabulation determined as 4', 6", Oc, ?6''', ?1''', ?1p. Paracingulum slightly offset, marked by paracingular

sutures bearing relatively long processes; parasulcus present but indistinct.

Genus *Horologinella* Cookson and Eisenack, 1962

Horologinella sp. SP

Autoblast longer than broad; ambitus hourglass-shaped; dorso-ventral compression. Autophragm bearing apiculate to vermiculate sculpture in more or less continuous bands, or in clusters denoting paratabulation; paratabulation determined as ?4', 5"-?6", Oc, 5"', ?O"". Archeopyle apical, formed by loss of apical paraplates; operculum simple, free. Medial, transverse and medially longitudinal areas lacking processes and interpreted in part

as denoting the positions of paracingulum and parasulcus.

References

Brideaux, W. W. and Myhr, D. W.

1976: Lithostratigraphy and dinoflagellate cyst succession in the Gulf Mobil Parsons N-10 well; in Report of Activities, Part B; Geol. Surv. Can., Paper 76-1B, report 43.

Lentin, J. K. and Williams, G. L.

1976: A monograph of fossil peridinioid dinoflagellate cysts; Bedford Inst. Oceanogr., Rept. Ser. BI-R-75.

Project 630003

R. L. Christie

Institute of Sedimentary and Petroleum Geology, Calgary

Introduction

The Tertiary rocks of the Lake Hazen region mainly underlie an area about 80 by 15 km (50 by 10 miles) extending northeasterly from the northeastern shore of Lake Hazen, but erosional remnants of similar rocks lie scattered in certain parts of the Hazen Plateau south and east of the lake. A Tertiary coal deposit near Discovery Harbour was mined by the British naval expedition of 1875-76 under Captain George S. Nares. Tertiary rocks also occur on Judge Daly Promontory, where they are down-faulted in a lower Paleozoic terrain (Fig. 45.1).

Clastic, coal-bearing beds were mapped by the author in 1957 and 1958 in the course of reconnaissance studies in the Lake Hazen region (Christie, 1964), and the same beds were studied in more detail in 1965 by A. A. Petryk (Petryk, 1969). Tertiary beds above the coal measures were examined subsequently in 1965, 1966 and 1973. The uppermost beds in the succession are coarse, weakly cemented boulder conglomerates that cap a series of isolated remnants, the 'Boulder Gravel Hills', north and northeast of Lake Hazen. The hills have been interpreted as remnants of a formerly widespread, upper Tertiary clastic deposit (Blackadar, 1954; Christie, 1964, 1967a, 1974; Petryk, 1969). The Tertiary coal measures along the north shore of Lake

Hazen (the lowest of the exposed Tertiary beds) were assigned to the Eureka Sound Formation on the basis of general lithological character, the presence of fossilized wood, and the subbituminous rank of the coal. A suggested age in the range of Paleocene to Oligocene was provided by D. C. McGregor, Geological Survey of Canada, based on pollen assemblages, and these ages seemed to confirm the correlation of the Lake Hazen rocks with those of the Eureka Sound region. However, G. E. Rouse, of the University of British Columbia, recently has identified floras from samples newly collected from measured sections and has suggested a younger age (Oligocene to Miocene*) for the beds. It now appears that the oldest Tertiary beds north of Lake Hazen were deposited contemporaneously with part of the Beaufort Formation of the Arctic Coastal Plain in the western islands of the Arctic Archipelago (Hills, 1969).

Structural setting

The nearly flat-lying Tertiary rocks at Lake Hazen lie adjacent to moderately folded Mesozoic and upper Paleozoic rocks, which occur as small, basin-like outlier of the Sverdrup Basin. The Tertiary beds appear to overlap the northeastern edge of the outlier. The structure of the Tertiary formation is one of open and irregular undulations except for a limited area or zone of extreme folding on lower Gilman River¹. These folds, presumably, are a consequence of movement on faults related to the Lake Hazen Fault Zone (Fig. 45.1).

Stratigraphy

The Tertiary rocks of the Lake Hazen region form a rolling lowland; the rocks are loosely consolidated and covered with solifluction debris so that few substantial exposures are available to measure stratigraphic sections in detail. Sections ranging in thickness from 90 to 270 m (300-900 ft.), however, are exposed in three areas: 1) along the north shore of Lake Hazen; 2) in deep channels cut by glacial meltwater a few miles north of the lake; and 3) on the flanks of the 'Boulder Gravel Hills' 16 km (10 miles) north of the lake (Fig. 45.1). Measured sections from these localities are presented in Figure 45.2. Section 1 is composite, after Petryk (1969).

The three sections occur at successively higher elevations and each appears to represent successively younger parts of the Tertiary sequence. A total thickness of about 600 m (2000 ft.) of beds is represented.

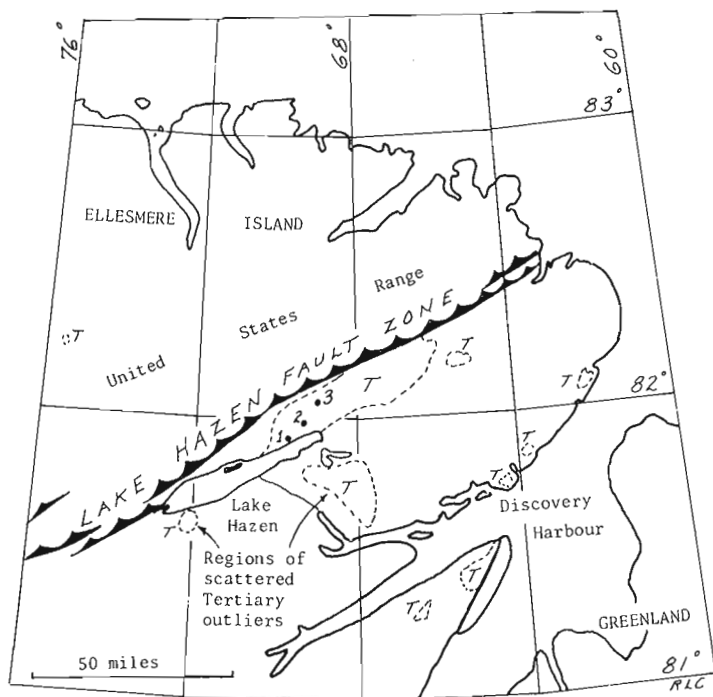


Figure 45.1. Index map showing distribution of Tertiary rocks and location of sections.

¹ Gilman River enters Lake Hazen from the northwest between localities 1 and 2 on Figure 45.1.

* see note, p. 262.

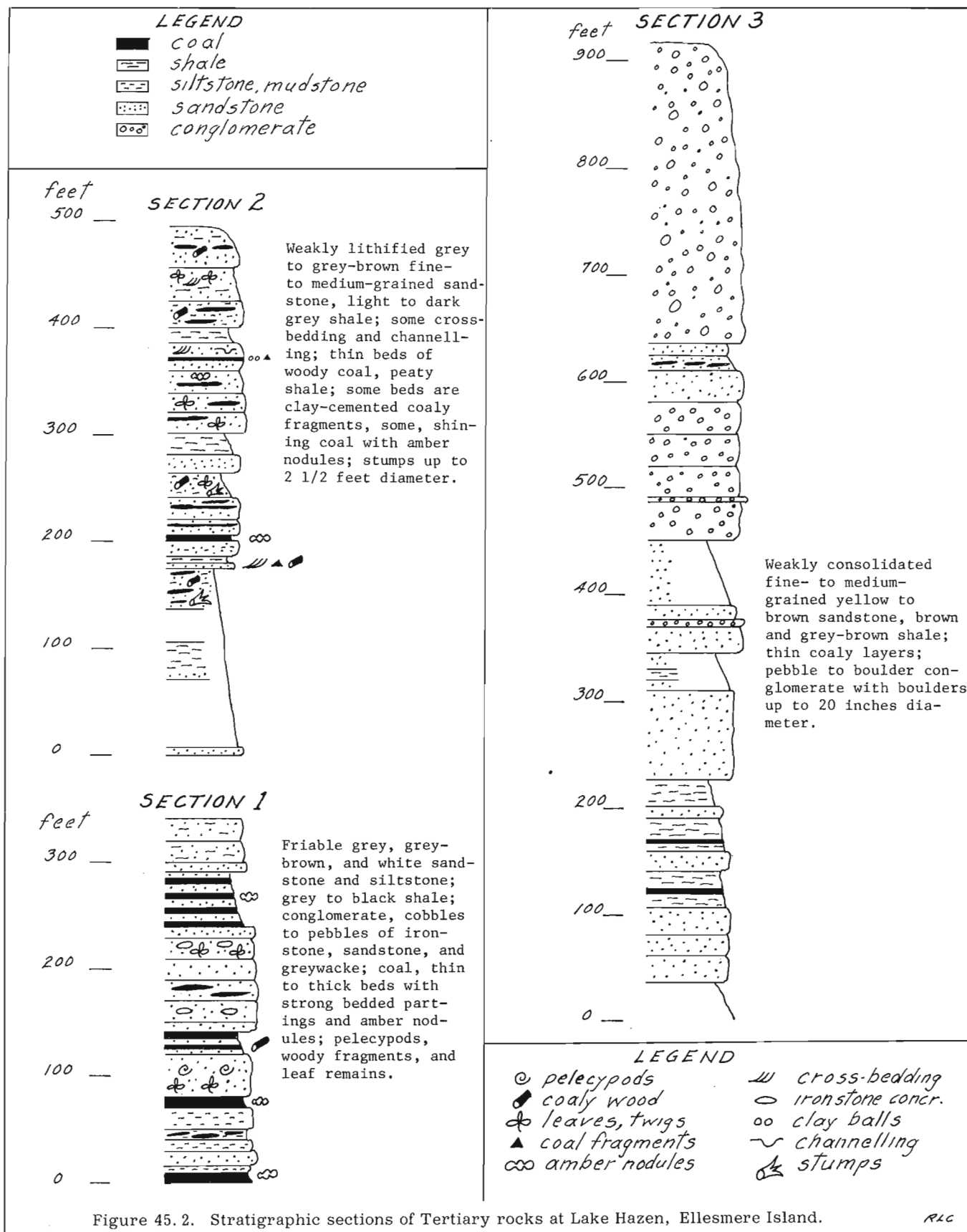


Figure 45. 2. Stratigraphic sections of Tertiary rocks at Lake Hazen, Ellesmere Island.

RLC

The Tertiary strata mainly comprise weakly lithified sandstone, siltstone, sandy shale, and shale with coal beds and coaly layers. Thick conglomerate beds, interbedded with sandstone and coaly shale, occur at the top of the section. The sandstones are fine to medium grained, white, brown, or grey, and weather to brown and yellow colours. The shales are variously grey to dark grey or brown. The coal, in beds up to 3 m (10 ft.) thick, is compact, shiny, and moderately friable. Although mainly black in colour, some coal is brownish; a subbituminous B rank (ASTM) has been determined. The conglomerates are brown weathering, weakly consolidated, and contain well-rounded cobbles and boulders, coarsening upward.

The lower part (Sec. 1, Fig. 45.2) of the Tertiary sequence is characterized by abundant crossbedding and channelling, coal layers, and ironstone concretionary bodies. Yellow amber is abundant in the coal. The azimuths of crossbeds, determined by Petryk (1969), are mainly east-northeast in southwestern exposures, and southwest in the northeastern exposures.

The proportion of coal appears to decrease upward in the sequence, so that in Section 2 both the thickness and abundance of coaly layers are much reduced. In addition, the grade of the coal in Section 2 appears distinctly lower than that of Section 1. Stumps, twigs, and fragments of carbonized and silicified wood are characteristic of the middle section.

The uppermost beds (Sec. 3) comprise mainly fine grained sandstone with few carbonaceous and shaly layers. A thin cobble conglomerate layer occurs within the sandstone sequence, and a unit of sandstone, several tens of feet thick, is interbedded with thick conglomerate units.

The conglomerate consists of well-rounded clasts in a brown sand matrix. The largest boulders in the lowest conglomerate bed are 25 cm (10 in.) in diameter; whereas in the upper beds they are up to 50 cm (20 in.). About half of the clasts resemble sandstone types that occur in the Permian Sabine Bay Formation, exposed in the mountainous region tens of miles to the northwest (Nassichuk, 1967); the remainder are composed of dark, bluish grey limestone typical of lower Paleozoic miogeosynclinal rocks that are developed extensively in the region. Diabase boulders form a conspicuous though minor part of the conglomerate.

Age and Correlation

The earliest estimate of the age of Cenozoic beds in the Lake Hazen region was by O. Heer (1878), who assigned a Miocene age to a rich flora from coal-bearing beds at Watercourse Valley (near Discovery Harbour). Heer's material was collected by the Nares expedition. A tree cone was recovered in 1953 from the eastern extremity of Tertiary exposures in the Lake Hazen area and was assigned by W. L. Fry (in Blackadar, 1954) to either *Picea* sp. or *Larix* sp. Fry suggested an age "not older than Miocene and possibly more recent". Palynological collections from Lake Hazen, assembled in 1957 and 1958, were assigned a Paleocene to Oligocene age by D. C. McGregor, who noted that plant remains

from Watercourse Valley (collected in 1958) indicated a Paleocene or possibly an Eocene age.

Samples collected by Petryk at Lake Hazen in 1965 (Sec. 1 of this paper) yielded a substantial suite of palynomorphs, which were examined by Rouse. According to Rouse (manuscript report), the following generalizations can be made concerning the palynomorph flora: (a) a considerable amount of reworking has taken place. Thus, a Miocene bed might be dominated by an Oligocene or earlier assemblage; and (b) the samples fall into an older, Oligocene and a younger, Miocene group. The Miocene palynomorphs include those that are found commonly in mid to lower upper Miocene deposits in the western Arctic.

Tectonic events

The Oligocene to Miocene ages now assigned to the Tertiary rocks in the Lake Hazen region invite a review of the correlation and tectonic setting of these deposits. The following relationships and assignments now appear to hold: (a) the Tertiary beds at Lake Hazen were deposited contemporaneously with part of the Beaufort Formation of the western Arctic Islands (Hills, 1969); (b) the Eureka Sound Formation (*sensu stricto*: lower Tertiary, pre-orogenic clastic beds) does not appear to be present in the Lake Hazen area; and (c) the ages or phases of Mesozoic-Tertiary orogenesis in the Lake Hazen region evidently were:

- i) Late Cretaceous or early Tertiary folding, perhaps accompanied by thrust faulting along the Lake Hazen Fault zone. Mesozoic and upper Paleozoic beds were folded during this episode.
- ii) Miocene or later thrust faulting – to juxtapose Oligocene-Miocene and upper Paleozoic-Mesozoic beds (with the older beds locally tectonically overlying the younger).

The sequence of events in late Mesozoic and Tertiary times at Lake Hazen apparently was as follows:

(a) Isolation of a part of the Sverdrup Basin due to faulting along the Lake Hazen Fault Zone in latest Cretaceous or early Tertiary time. During this event, presumably, an early Grant Land Mountains system formed; structures in the Mesozoic-upper Paleozoic rocks at Lake Hazen may be related entirely to faulting.

(b) More than one episode of compression may have occurred at Lake Hazen; an extensive hiatus – between Late Cretaceous and Oligocene time – is apparent, and during this interval, at Flat Sound on Axel Heiberg Island, the Paleocene and Eocene Eureka Sound Formation was folded by orogenesis (Balkwill *et al.*, 1975).

(c) Erosion of Paleozoic, Mesozoic, and possibly lower Tertiary beds resulted in detritus for Oligocene to Miocene beds of the Lake Hazen area; this detritus was deposited in a local, continental basin overlying the nearly peneplained Hazen Plateau.

(d) The Lake Hazen Miocene beds pass upward to coarse, molassic boulder beds; the detritus in these beds probably was derived from land to the north that was uplifted during a late (Miocene or later) phase of faulting, perhaps the phase during which the lower Miocene beds were displaced.

References

- Balkwill, H. R., Bustin, R. M., and Hopkins, W. S., Jr.
1975: Eureka Sound Formation at Flat Sound, Axel Heiberg Island, and chronology of the Eurekan Orogeny; *in Report of Activities, Part B*; Geol. Surv. Can., Paper 75-1B, p. 205-207.
- Blackadar, R. G.
1954: Geological reconnaissance, north coast of Ellesmere Island, Arctic Archipelago, Northwest Territories; Geol. Surv. Can., Paper 53-10.
- Christie, R. L.
1964: Geological reconnaissance of northeastern Ellesmere Island, District of Franklin; Geol. Surv. Can., Mem. 331.
1967a: Reconnaissance of the surficial geology of northeastern Ellesmere Island, Arctic Archipelago; Geol. Surv. Can., Bull. 138.
- Christie, R. L. (cont'd.)
1967b: Operation Grant Land, 1966; *in Report of Activities, Part A*; Geol. Surv. Can., Paper 67-1A, p. 2, 3.
1974: Northeastern Ellesmere Island: Lake Hazen region and Judge Daly Promontory; *in Report of Activities, Part A*; Geol. Surv. Can., Paper 74-1A, p. 297-299.
- Heer, O.
1878: Notes on fossil plants discovered in Grinnell Land by Captain H.W. Feilden; *Quart. J. Geol. Soc.*, v. 34, p. 66-72.
- Hills, L. V.
1969: Beaufort Formation, northwestern Banks Island, District of Franklin; *in Report of Activities, Part A*; Geol. Surv. Can., Paper 69-1A, p. 204-207.
- Nassichuk, W. W.
1967: Studies of Permo-Carboniferous and Mesozoic strata on northern Ellesmere Island; *in Report of Activities, Part A*; Geol. Surv. Can., Paper 67-1A, p. 10-12.
- Petryk, A. A.
1969: Mesozoic and Tertiary stratigraphy at Lake Hazen, northern Ellesmere Island, District of Franklin; Geol. Surv. Can., Paper 68-17.

N.B.: The palynological material has recently (May, 1976) been restudied by Rouse, and it now seems clear the Eocene and not Oligocene-Miocene ages are favoured; thus, many of the conclusions in this paper must be revised.

Projects 610007 and 690005

D. K. Norris

Institute of Sedimentary and Petroleum Geology, Calgary

In the preparation of final geological maps of the Interior Platform and Cordilleran Orogenic System north of Latitude 65°N and west of Longitude 132°W, the writer found that the inclusion of paleontological datings on the maps greatly facilitated the interpretation of the geology. A system of abbreviations of geological time terms, therefore, was devised to be included with GSC locality numbers. These datings were indispensable in the resolution of many structural and stratigraphic complexities. In some instances (for example, in deformed Jurassic and Lower Cretaceous clastics strata) it was not possible to arrive at a meaningful interpretation consistent and compatible with the regional geological framework without the aid of paleontology. Many parts of the Phanerozoic succession are fossiliferous and literally hundreds of collections have been made by industry, university, and government geologists throughout the project area. Some collections were more useful than others, but a large number of those studied by scientists of the Paleontology Subdivision were capable for precise dating. They have been used to advantage in the synthesis of the geology of the region (Norris, 1975a, b, 1976).

The writer is indebted to E. W. Bamber, W. W. Brideaux, W. H. Fritz, D. C. McGregor, B. S. Norford, T. P. Poulton and T. T. Uyeno for critically examining the manuscript, and for offering many constructive suggestions now incorporated in this paper.

Each abbreviation comprises a set of elements arranged hierarchically without punctuation, identifying the Period, Epoch and, wherever possible, the Age of the host rock determined by fossils. The symbols are qualified as to level of certainty of the paleontological determinations and as to whether the fossils may have been reworked. They are all tied to field stations and, normally, to specific GSC fossil localities plotted on the maps. A "C" preceding the locality number indicates curation at the Institute of Sedimentary and Petroleum Geology, Calgary, Alberta; otherwise the numbers represent curation at the Ottawa Headquarters of the Geological Survey of Canada.

A capitalized one- or two-letter element identifies a geological Period (e.g. C for Cambrian, Pe for Pennsylvanian). It is followed by a capitalized one- or two-letter element indicating an Age (e.g. Al for Albertan). The modifiers "e", "m", "l" (lower case, representing early, middle and late) before a Period identify the Epoch for those localities where no further refinement is possible (e.g. lK for Late Cretaceous), but when used before an Age (e.g. eBe for early Berriasian) they specify further refinement in the dating. The modifiers are in lower case letters when an integral part of an age symbol, but they must be capitalized when spelled out to modify a Period in accordance with the Code of the American Commission

on Stratigraphic Nomenclature. At localities where the fossils indicate more than one possible Age, that which is preferred is underlined. Thus KBe-V means a Cretaceous Berriasian age is preferred but a Valanginian age is possible.

A question mark (?) precedes that part of a paleontological age which may be in doubt. Should it precede the Period element, the whole of the age assignment is questioned. For example, ?DEm indicates a possible Devonian Emsian age for the host rock but the available fossils are either not well enough preserved or lack key specimens to determine precisely not only the Period but also the Age. An "i" specifies that the fossils collected at that locality were indeterminate. Where there is suspected or demonstrated reworking of fossils (so common in the Aptian and Albian Stages of northern Yukon Territory and northwestern District of Mackenzie), the whole symbol is embraced in brackets and the paleontological age(s) is (are) that (those) of the reworked assemblage(s), not necessarily that of the host rock. Period boundary uncertainties are acknowledged and symbols may have to be modified in due course. Thus the Tremadoc (OT) is implied to lie fully within the Ordovician Period, but it could conceivably span the boundary with the Cambrian.

Table 46.1 is not intended to be a correlation chart of European and North American time terms, nor is it intended to be complete. It is simply a tabulation of the most commonly used nomenclature for the northern Yukon and northwestern District of Mackenzie and will be included with all future open file maps and final reports of the region. It is necessarily subject to extension and refinement as further paleontological studies are carried out there, and it may well have application in principle far beyond the Operation Porcupine project area. The symbols need not be confused with those applied to formational names in legends and on geological maps. The element identifying an Age always begins with a capital letter whereas that identifying a formation is always in lower case. Thus JPo indicates a Jurassic Portlandian age assignment whereas Jpo identifies an unnamed Jurassic sandstone formation in the vicinity of Aklavik Arch.

References

- Norris, D. K.
 1975a: Geological maps of parts of Yukon and Northwest Territories; Geol. Surv. Can., Open File 279.
 1975b: Geological maps of part of Northwest Territories; Geol. Surv. Can., Open File 302.
 1976: Geological maps of parts of Northwest Territories and Yukon Territory; Geol. Surv. Can., Open File 303.

Table 46. 1.

Geological Time Symbols – Operation Porcupine

Period	Symbol	Age/Epoch	Symbol	Age/Epoch	Symbol	Age/Epoch	Symbol		
Quaternary	Q	Holocene	Ho						
		Pleistocene	QP						
Tertiary	T	Pliocene	TP1						
		Miocene	TM						
		Oligocene	TO						
		Eocene	TE						
		Paleocene	TPa						
Cretaceous	K	Maastrichtian	KM	Senonian	KSe				
		Campanian	KCa						
		Santonian	KSa						
		Coniacian	KCo						
		Turonian	KT						
		Cenomanian	KCe						
		Albian	KAl						
		Aptian	KAp	Neocomian	KN				
		Barremian	KBa						
		Hauterivian	KH						
		Valanginian	KV						
		Berriasian	KBe						
Jurassic	J	Portlandian	JPo	Tithonian	JTi	Volgian	JV		
		Kimmeridgian	JKi						
		Oxfordian	JO						
		Calloviaian	JC						
		Bathonian	JBt						
		Bajocian	JBj						
		Toarcian	JTo						
		Pliensbachian	JPl						
		Sinemurian	JS						
		Hettangian	JH						
		Triassic	T					Rhaetian	TR
Norian	TRN								
Karnian	TRK								
Ladinian	TRL								
Anisian	TRA								
Spathian	TRSp								
Smithian	TRSm								
Dienerian	TRD								
Griesbachian	TRG								
Permian	P	Dzhulfian	PD	Ochoan	PO				
		Kazanian	PKa	Guadalupian	PG				
		Ufimian	PU						
		Kungurian	PKu						
		Artinskian	PAr	Leonardian	PL				
		Sakmarian	PS	Wolfcampian	PW				
		Asselian	PAs						

Table 46.1 (cont.)

Period	Symbol	Age/Epoch	Symbol	Age/Epoch	Symbol	Age/Epoch	Symbol
Pennsylvanian	Pe	Virgilian	PeV	Orenbergian	CO		
		Missourian	PeMi	Gzhelian	CG		
		Desmoinesian	PeD	Moscovian	CM		
		Atokan	PeA	Bashkirian	CB		
		Morrowan	PeMo	Namurian	CN		
Mississippian	M	Chesteran	MC				
		Meramecian	MM	Visean	CV		
		Osagian	MO				
		Kinderhookian	MK	Tournasian	CT		
Devonian	D	Famennian	DFa				
		Frasnian	DFr				
		Givetian	DGi				
		Eifelian	DEi				
		Emsian	DEm				
		Siegenian	DS				
		Gedinnian	DGe				
Silurian	S	Pridolian	SP				
		Ludlovian	SLu				
		Wenlockian	SW				
		Llandoveryan	SLl				
Ordovician	O	Ashgillian	OAs	Richmondian	OR		
				Maysvillian	OMy	Cincinnatian	OCi
				Edenian	OE		
		Caradocian	OCr	Barneveld	OB		
				Wilderness	OWl	Mohawkian	OMk
				Porterfield	OP		
		Llandeilian	OLd	Ashby	OAb		
		Llanvirnian	OLv	Marmor	OMm	Chazyan	OCh
				Whiterock	OWk		
						Canadian	OCa
Cambrian	-C	Trempealeauan	-CT				
		Franconian	-CF				
		Dresbachian	-CD				
		Albertan	-CAI				
		Waucoban	-CW				

Peter J. Hood and E. Ready
Resource Geophysics and Geochemistry Division

The Past

In 1947, aeromagnetic surveys were commenced by the Canadian Federal Government as an aid to both geological mapping and mineral exploration programs. For a number of years the Geological Survey of Canada operated its own survey aircraft and during the 10-year period 1947-1956 inclusive an average of 40 000 line miles were flown each year (Fig. 47.1). During this period of time the value of the aeromagnetic survey technique as a geological mapping tool was clearly demonstrated; in addition the program received a considerable psychological boost in the early years as a result of the discovery of a 20 million ton iron deposit at Marmora, Ontario, beneath 120 feet of Ordovician limestone. This aeromagnetic survey was flown by Aero Service in 1949 and was jointly-funded by the Survey and the Ontario Department of Mines. Lang (1970) has carried out a cost-benefit analysis of the Marmora discovery and he estimates that the 1949 aeromagnetic survey cost about \$45,000, whereas production and reserves at the Marmoraton property to the end of 1969 amounted to \$198 million. Lang stated that this figure was much more than the total expenditure of the Geological Survey from 1842 to 1969!

In 1960, the need for an accelerated aeromagnetic survey program became increasingly apparent, and led to the present Federal-Provincial aeromagnetic survey plan being formulated. In retrospect it is clear that the timing of the proposal was propitious for the following reasons:

1. The aeromagnetic method had become an established survey technique which could be carried out by contract survey companies for a reasonable price. In addition the survey industry was actively seeking Canadian government work to help provide some stability in their operations, and thus ensure a continuing Canadian airborne geophysical survey capability. It is of some interest that the Canadian airborne geophysical survey industry is presently the largest by far in the world, and that it presently gets much more than its share of overseas contracts.
2. A pilot program had been carried out by the Geological Survey to demonstrate the value of the aeromagnetic survey technique as an aid to geological mapping and to mineral exploration. Thus because the Survey had a cadre of personnel who were themselves technically competent in the technique, it was possible to draw up an objective set of specifications and subsequently ensure that they were adhered to through field and office inspections.
3. It was appreciated that government-funded surveys of the Canadian Shield would provide an orderly, standardized coverage with a common specification in comparison to that which would result if the surveys

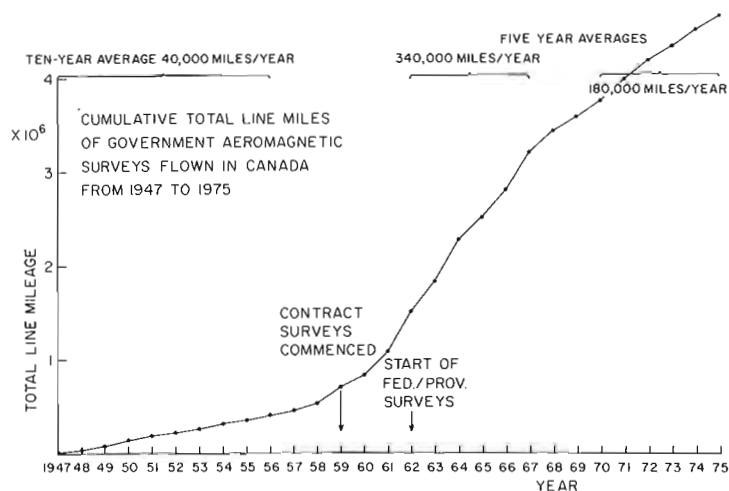


Figure 47.1.

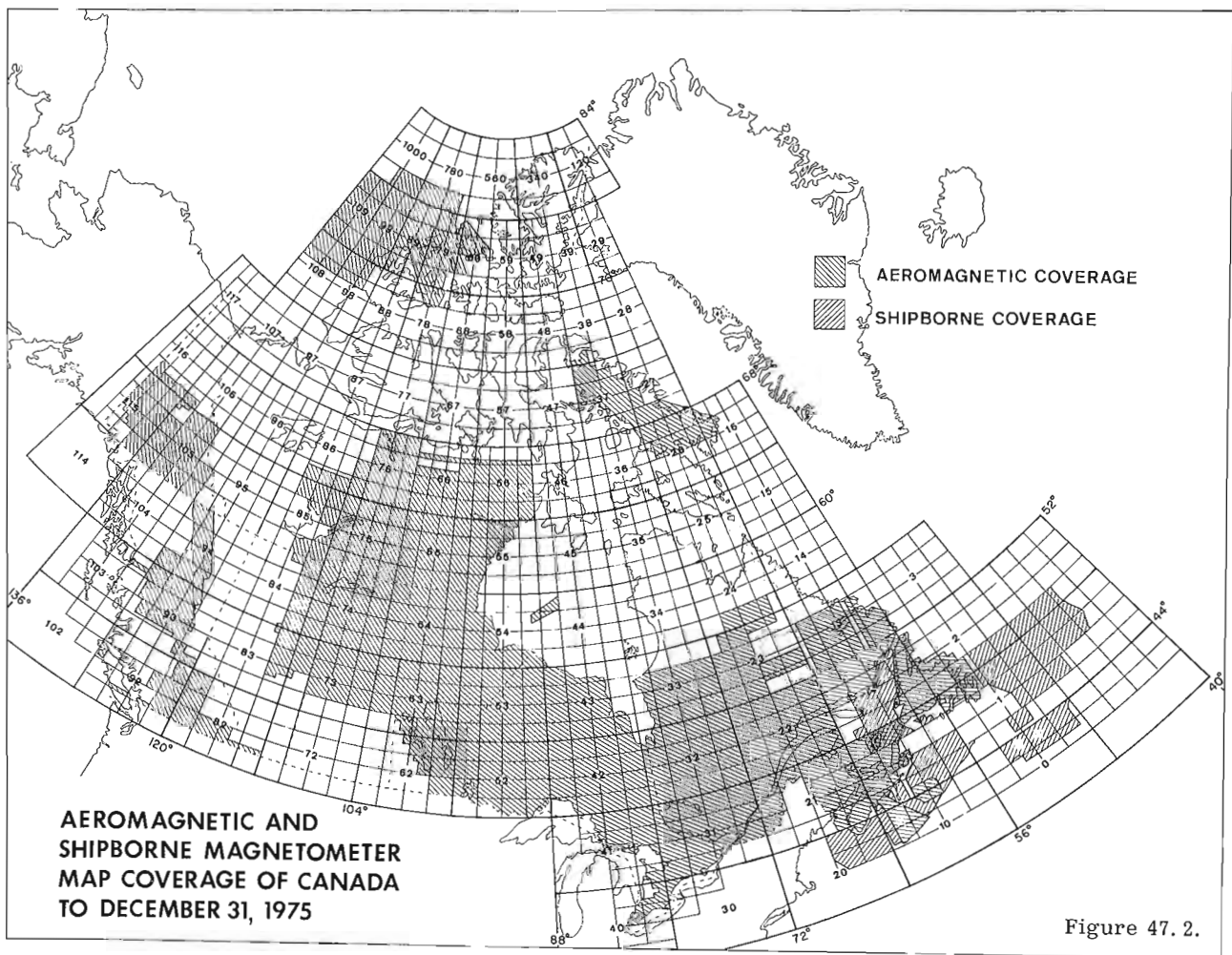
were carried out by various private mining companies; in any case the end products of surveys by private companies would remain proprietary. It was also recognized that orderly coverage would permit large areas to be compiled in order to produce regional aeromagnetic survey maps.

4. Outside agencies both in the private sector and in the provincial governments were enthusiastic about the proposed aeromagnetic survey program. At the 1960 Mines Ministers Conference held in Quebec City the resolution to proceed with the present Federal-Provincial aeromagnetic survey plan was unanimously approved.

The aeromagnetic survey of the Precambrian Shield proceeded as planned, and it can be seen from Figure 47.1 that the rate of coverage jumped 8.5 fold from 40 000 line miles a year to 340 000 line miles per year after the inception of the program.

A number of significant factors have combined to reduce the present average production rate to the lower level of 180 000 line miles per year. These factors include the poorer operating and weather conditions in the north, fewer landing strips which increases the percentage of non-productive flying, the fact that the magnetic diurnal is generally more active in the north, and last but not least that the high rate of inflation which has increased the cost of the surveys because a cost-of-living factor was included in the payment schedule.

The Federal-Provincial aeromagnetic survey program appears to be the most generally approved of any recent government program by the mineral exploration industry being much used in the planning of mineral exploration programs and is credited with a prime role in a number of discoveries in Canada and a lesser role in others. The delineation of iron formation is relatively easy from aeromagnetic surveys and there are many examples which may be quoted; e.g. in Ontario alone -



Agwa, Briarcliffe, Bruce Lake, Kababeca Falls, Lake St. Joseph, and North Spirit Lake. In addition orebodies associated with iron formation such as the Brunswick No. 12 orebody in the Bathurst mining camp were found as a result of an initial aeromagnetic survey. Because pyrrhotite has strong magnetic properties those base metal sulphides which contain significant amounts of pyrrhotite will consequently produce distinct magnetic anomalies and these appear to be more prevalent on aeromagnetic maps than hitherto was thought to be the case.

It should be appreciated that the Canadian Federal-Provincial aeromagnetic survey plan has had a considerable influence in promoting the use of the method overseas. Consequently the so-called Canadian specifications for aeromagnetic surveys have been used in many overseas surveys and this has helped our domestic airborne geophysical survey industry to obtain a considerable amount of overseas work. In addition, CIDA-funded aeromagnetic surveys managed by the Geological Survey of Canada have been carried out in Cameroun, Guyana, Ivory Coast, Niger, and Upper Volta by Canadian companies. It is hoped that such CIDA-funded aeromagnetic surveys will continue to be carried out as a contribution to Canada's overseas aid programs.

The Present

To date a total of 4 654 410 line miles have been flown in Canada and the program has been completed for New Brunswick, Ontario, Manitoba, Saskatchewan, and Alberta (Fig. 47.2). Prince Edward Island and Nova Scotia were surveyed prior to the start of the Federal-Provincial program. In addition, the island of Newfoundland is now entirely surveyed as is approximately 60 per cent of Labrador and 70 per cent of Quebec. At the present time 6262 one-mile, 478 four-mile, and 547 aeromagnetic maps at other scales have been issued.

There has been a gradual upgrading in the survey specification since the Federal-Provincial aeromagnetic program began. The fluxgate magnetometer has been replaced to a considerable extent by proton precession magnetometers. In addition the first digital recording contracts have been let (Quebec and British Columbia) which will facilitate the storage and any subsequent treatment of the data.

Aeromagnetic maps with air photographs are almost indispensable tools for the mapping geologist, especially in areas with a low percentage of outcrop. With some geological knowledge of the area, a preliminary map can usually be deduced using these two aids alone and

such a map can be used to plan the geologists' traverses and indicate where he should concentrate his efforts. Thus in addition to providing a good indication of the geological framework of an area, aeromagnetic maps can also be utilized to improve the efficiency of geological mapping. Certainly a number of the provincial mines departments utilize the aeromagnetic maps for this purpose, to make their geological mapping more cost-effective.

Aeromagnetic maps are the biggest single item distributed by the Geological Survey of Canada (in conjunction with the Provincial agencies). Starting in April 1974, the statistics for aeromagnetic maps have been kept separately by the Geological Information Division of the Geological Survey. About 38 000 aeromagnetic maps are currently being distributed per year. The price is now \$1 per sheet.

Another good indicator of the demand for aeromagnetic maps are the number of map sheets reprinted.

Usually 300 copies of a given map are reprinted and in some cases this may go as high as 500. During the 11-year period 1964-74 inclusive, 5555 aeromagnetic maps were reprinted. The ratio of reprinted to new aeromagnetic maps expressed as a percentage is 32 per cent. Although a number of the reprinted maps will be from the 1752 aeromagnetic maps published prior to 1964, nevertheless it is felt that the time period considered is sufficiently long and the annual draw down rate of 38 000 maps is sufficiently large that it would be reasonable to expect that the reprint rate will be maintained for some years to come at the one-third level or higher. Because Canada is proceeding towards metrication, a decision has been made to change the publication scale of one inch to one mile (1:63 360) to the more compatible scale of 1:50 000. Similarly the one inch to four mile aeromagnetic maps will now be issued at the 1:250 000 scale.

On-going Aeromagnetic Survey Contracts

Four aeromagnetic survey contracts are presently in progress; these are in the Northwest Territories, Labrador, northern British Columbia, and northern Quebec. As the contracts in Quebec and Labrador end, aeromagnetic coverage of these provinces will be completed. A progress report on each of these four surveys follows:

1. Keewatin-Mackenzie Aeromagnetic Survey (Project 690068)

The Keewatin-Mackenzie aeromagnetic survey is a six-year contract which was awarded in 1969 to Kenting Earth Sciences Ltd. of Ottawa. The contractor is required to survey 359 536 line miles in order to produce 543 one-mile and 46 four-mile maps (Fig. 47.3).

By the end of 1974, 322 402 line miles had been flown (Ready and Hood, 1975) and 455 one-mile and 28 four-mile aeromagnetic maps had been published. The 1975 field season resulted in an additional 37 134 line miles of production, and during the past year 28 one-mile aeromagnetic maps were published using a 10-gamma contour interval. In 1975 the flying component of the Keewatin-Mackenzie aeromagnetic contract was completed. One inspection visit was made during the field season by E. J. Derouin to Cambridge Bay during the period August 5-15, 1975.

It is anticipated that the remaining 60 one-mile maps will be delivered by June 1, 1976. All raw analog data, 24 1:250 000 maps and 1:500 000 scale composites will be delivered by August 1, 1976.

Between 66°N and 68°N, two one-mile map-areas are printed together on a single map-sheet (15 minutes of latitude by 1 degree of longitude).

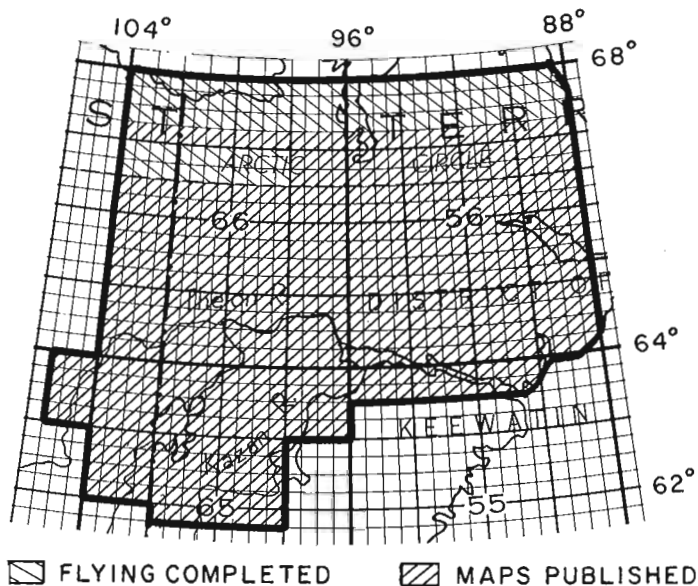


Figure 47.3. Status of Keewatin-Mackenzie aeromagnetic survey on April 1, 1976.

2. Labrador-Melville-Coppermine Aeromagnetic Survey (Project 690072)

The Labrador-Melville-Coppermine aeromagnetic survey was originally a 6-year contract which was awarded in 1969 to a consortium of three companies, consisting of Geotrex Ltd. Ottawa, Lockwood Survey Corporation Ltd., Toronto, and Survair Ltd., Ottawa. In 1975, the contract period was extended to 10 years. The consortium is required to obtain 519 550 line miles of aeromagnetic survey data in three areas: namely Labrador (314 000 line miles), Melville Peninsula (87 500 line miles) and the Coppermine area (118 050 line miles). The resultant aeromagnetic data will be compiled into 801 one-mile and 65 four-mile maps as follows: Labrador - 443 one-mile and 33 four-mile aeromagnetic maps, Melville Peninsula - 122 one-mile and 15 four-mile aeromagnetic maps, Coppermine area - 236 one-mile and 17 four-mile aeromagnetic maps.

At the end of 1974, 201 824 line miles had been flown in Labrador and 47 631 line miles had been flown in the Melville Peninsula for a total of 249 455 line miles for the contract. In addition 152 one-mile and 13 four-mile aeromagnetic maps were published up to the end of 1974 using a 10-gamma contour interval. .

(a) Labrador (Fig. 47.4)

No survey flying was carried out in Labrador during the 1975 field season as the contractor was required to give priority to Melville Peninsula area. Forty four one-mile maps were published during the calendar year for Labrador. To date a total of 201 one-mile sheets have been published out of a total of 443 one-mile sheets. There are 34 complete and/or part four-mile maps of which 3 have been published at the scale of 1: 253 440 and 3 at the scale of 1: 250 000. The 59 one-mile maps now being compiled and/or drafted for Labrador will be published by August 1, 1976.

(b) Melville Peninsula

Priority has been given to flying the Melville Peninsula for the past several years so that the aeromagnetic mapping might precede the geological mapping program in that area as much as possible. Production in the Melville Peninsula has been relatively poor due to adverse weather and diurnal conditions. However by the end of 1974, 47 631 line miles had been flown in the Melville Peninsula.

In the 1975 flying season, 25 000 line miles of production were obtained in the Melville Peninsula utilizing two aircraft, from mid-June to the end of August 1975, under adverse diurnal and weather conditions. This brings the total line mileage flown in the Melville Peninsula to 72 631 line miles (Fig. 47.5).

Twenty five one-mile maps have been compiled and checked north of 67°30'N and east of 81°00'W. These maps will be converted to a scale of 1: 50 000 prior to publication. An additional 36 maps are in various stages of compilation resulting in approximately 60 out of a total of 123 maps being published by April 1, 1976. One inspection visit was made to Repulse Bay, Northwest Territories, by K. Anderson during August 6 to August 16, 1975.

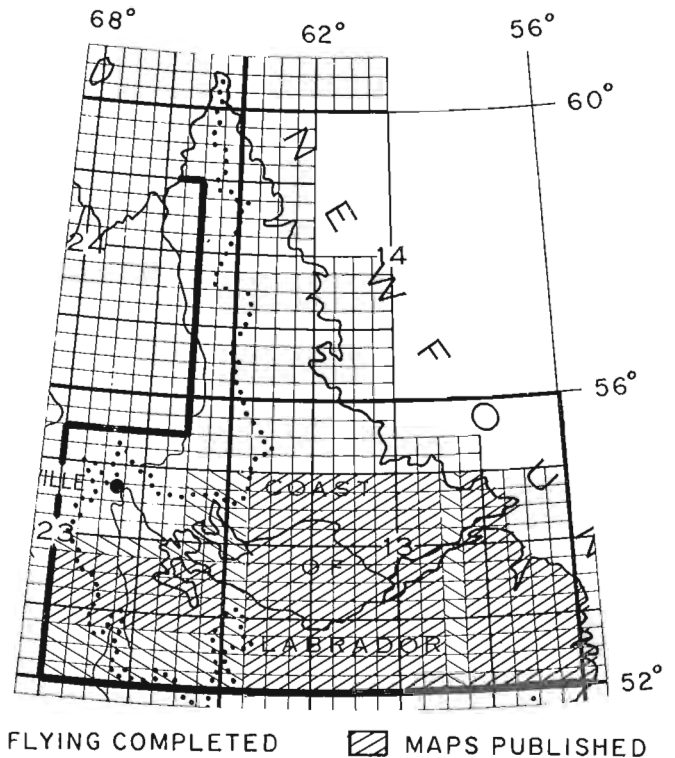


Figure 47.4. Status of Labrador aeromagnetic survey on April 1, 1976.

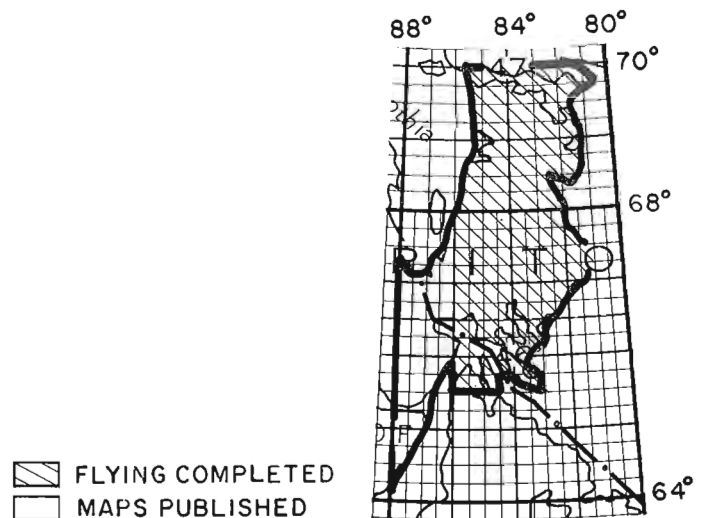


Figure 47.5. Status of aeromagnetic survey of Melville Peninsula, on April 1, 1976.

(c) Coppermine Area

No aeromagnetic survey flying has yet been carried out in this survey area which comprises NTS 76L, part of M, 86E, F, G, H, I, K, L, M, N, and parts of 86 A, B, C, O, P. However the consortium will commence survey operations of map-areas 76L, 86I, J, and K during mid-June 1976 because this area has been given first priority by the Regional and Economic Geology Division.

3. Aeromagnetic Survey of Northern Quebec
(Project 730012)

The aeromagnetic survey of northern Quebec (Fig. 47.6) is being carried out under a six-year contract to obtain 332 912 line miles of aeromagnetic survey data in northern Quebec. The contract was awarded in 1972 to a consortium of companies consisting of Photographic Survey Inc. of Montreal and Geotrex Ltd. of Ottawa. The contractor is responsible for the compilation of the resultant data into 519 one-mile and 40 four-mile maps to be published jointly by the Geological Survey and the Quebec Department of Natural Resources who have shared the costs of the contract equally.

By the end of the 1974 survey season, 136 410 line miles had been flown. During the 1975 season an additional 81 511 line miles were completed (Fig. 47.6) bringing the total to 217 921 line miles which is 65 per cent of the line miles contracted. No maps have been published to date but it is anticipated that several will be released by July 1976.

All survey aircraft are equipped to record the survey data in digital form which is the first such contract requiring digital recording under the Federal-Provincial aeromagnetic survey scheme. In addition, the compilation will be fully automated. The contractor's survey aircraft has been based at Fort Chimo and will probably continue to work from there as well as from Deception Bay, Quebec for the next two field seasons. A Geological Survey inspector, W. Knappers, visited the project during the period of June 9 to June 15, 1975.

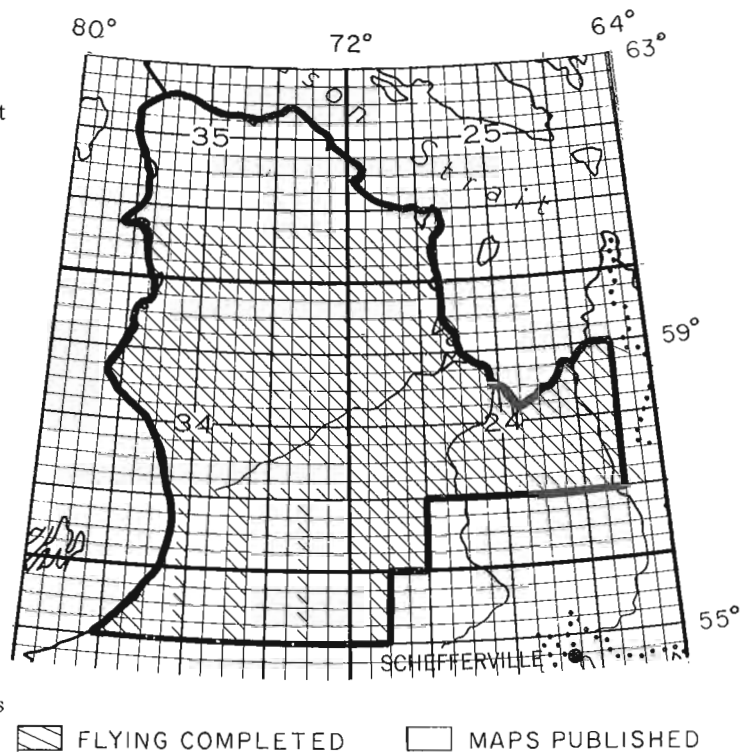
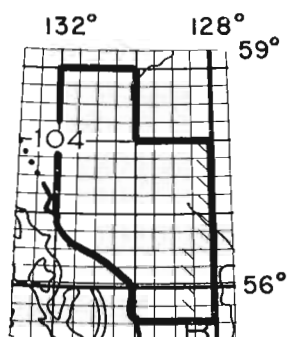


Figure 47.6. Status of aeromagnetic survey of New Quebec on April 1, 1976.





 FLYING COMPLETED
 MAPS PUBLISHED

Figure 47.7. Status of aeromagnetic survey in northern British Columbia on April 1, 1976.

4. Aeromagnetic Survey of Northern British Columbia
(Project 750030)

The aeromagnetic survey of northern British Columbia (Fig. 47.7) is a two-year contract to obtain 33 100 line miles of digital aeromagnetic data in northern British Columbia and to publish the data as 86 1:50 000 and six 1:250 000 total field maps. The contract was awarded to Sander Geophysics Ltd. on July 24, 1975, and the cost of the survey is shared equally between the British Columbia Department of Mines and Petroleum Resources and the Geological Survey of Canada.

The contractor elected to provide a higher performance aircraft than he tendered for, namely a Cessna 402 B instead of a Beech 18, and spent several months installing the necessary magnetometer, navigation, and ancillary equipment on the aircraft and debugging the system. The aircraft, therefore, arrived at Terrace, British Columbia, late in the season. Surveys have been flown through the winter months and to date about 3900 line miles have been completed (Fig. 47.7). A field inspection was made by W. Knappers during the period November 3-9, 1975.

Summary

Since the last report one year ago, a total of 147 545 line miles of aeromagnetic data of previously-unsurveyed areas has been obtained under the Federal-Provincial aeromagnetic survey scheme and in the Northwest Territories by contract surveys. In addition, 86 one-mile maps were published, including 14 maps at the scale of 1: 50 000 covering NTS map-areas 94C/1 to 8 and 94C/10 to 15, purchased jointly by the British Columbia Department of Mines and Petroleum Resources and the Geological Survey of Canada from Northway Survey Corp. Ltd. Nine maps at the scale of 1: 250 000 also were purchased from Northway Survey Corp. Ltd. , and published, covering all or portions of NTS map-areas 93 O, 94 B, C, F, G, K, L, M, N referred to as the Liard Trough Area in British Columbia. Another 1: 250 000 map covering the southern portions of 95 C and D was also acquired and published.

In addition to the foregoing standard sensitivity aeromagnetic maps, 96 high resolution aeromagnetic maps were published by the Geological Survey of Canada. These 1: 250 000 scale maps covered areas in the Bathurst mining camp of New Brunswick and in the Kirkland Lake region of Northern Ontario.

Thus the total number of aeromagnetic maps published during the report year is 192, which brings the total number of aeromagnetic maps published to the end of 1975 by the Geological Survey of Canada in co-operation with the respective Provincial agencies to 7287.

References

- Lang, A. H.
1970: Discovery and benefits of the Marmora iron deposit; *Can. Min. J.*, v. 91, p. 47-49.
- Ready, E. and Hood, P. J.
1975: Contract aeromagnetic surveys; *in* Report of Activities, Part A; *Geol. Surv. Can.*, Paper 75-1A, p. 129-132.

Project 730013

D. M. Jones¹, W. W. Shilts, and R. W. Weir¹
Terrain Sciences DivisionIntroduction

It has long been known that certain plant species may be associated with soils that are characterized by high heavy metal levels. Some plants also preferentially concentrate certain heavy metals. The genus *Astragalus*, for instance, is a good indicator for selenium and uranium in soil. Heavy metal uptake by plants has important implications to mineral prospecting and to animals harvesting the plants.

Little detailed work on heavy metal uptake has been conducted in southern Canada and even less has been done in the subarctic and arctic areas. During the summer of 1975 a pilot study examining the uptake of copper, lead, zinc, cobalt, nickel, silver, cadmium, and uranium by arctic plants was carried out in the central District of Keewatin. The objective of this pilot project was to determine to what extent characteristic arctic species concentrated these metals in their tissues in areas of strongly contrasting geology and soil metal levels.

Of the seven sites chosen for the study (Table 48.1) two were intended to be background areas, two were located on or near known uranium mineralization, one

was located on a nickel-copper-rich gossan (only one species collected), one was located adjacent to zinc-lead mineralization with some copper, and one was located on a glacial indicator train about 2 km down-ice from zinc-lead mineralization.

Methods

At each site collections of the major plant species (Table 48.2) and peat were made within a 100 m-diameter area. Glacial sediments were sampled in detail around all but one area. Tissue from shrubby species consisted of growth from the last two years, which was collected from several individual plants at each site. From other plants that have annual aerial parts, only the annual growth from several individuals was collected. Tissue was cut with shears or a knife and was put into a plastic bag until it could be taken to camp. The tissue then was transferred to a paper bag and dried in a field oven at 60° to 80°C. Peat samples also were collected and dried, as above. In areas of mud boils peat was taken from the rim of a mud boil.

In the laboratory the plant and peat samples were redried and ground to fragments passing through a

Table 48.1

Characteristics of sites sampled

Collection site No.	Geological characteristics	Dominant vegetation
1 Yandle Lake background	mud boils (control)	sedges to <i>Betula</i>
2 Spi Lake gossan	rock outcrop (Cu, Zn, Pb), mud boils on till and gossan, mixed	sedges to <i>Betula</i> , some snowbed species
3 Spi Lake Island	till covered, mud boils, (Zn, Pb, Cu) indicator train on island	heath species
4 15 km southwest of Yandle Lake (dry site)	rock outcrop (U, Cu); thin till over bedrock, only site above marine limit	scattered heath species
4a 15 km southwest of Yandle Lake (wet site)	mud boils (U, Cu)	sedges in wet sites and <i>Betula</i>
5 Pitz Lake background	(control) mud boils, till, marine sediment (sand, silty clay)	wide range of habitat from sedges to <i>Betula</i> -heaths
6 Kazan River uranium showing	(U, Cu) mud boils, frost-heaved bedrock, thin till over bedrock	
7 Ferguson Lake	(Cu, Ni), gossan	only <i>Ledum</i>

¹Department of Biology, University of New Brunswick, Fredericton, New Brunswick

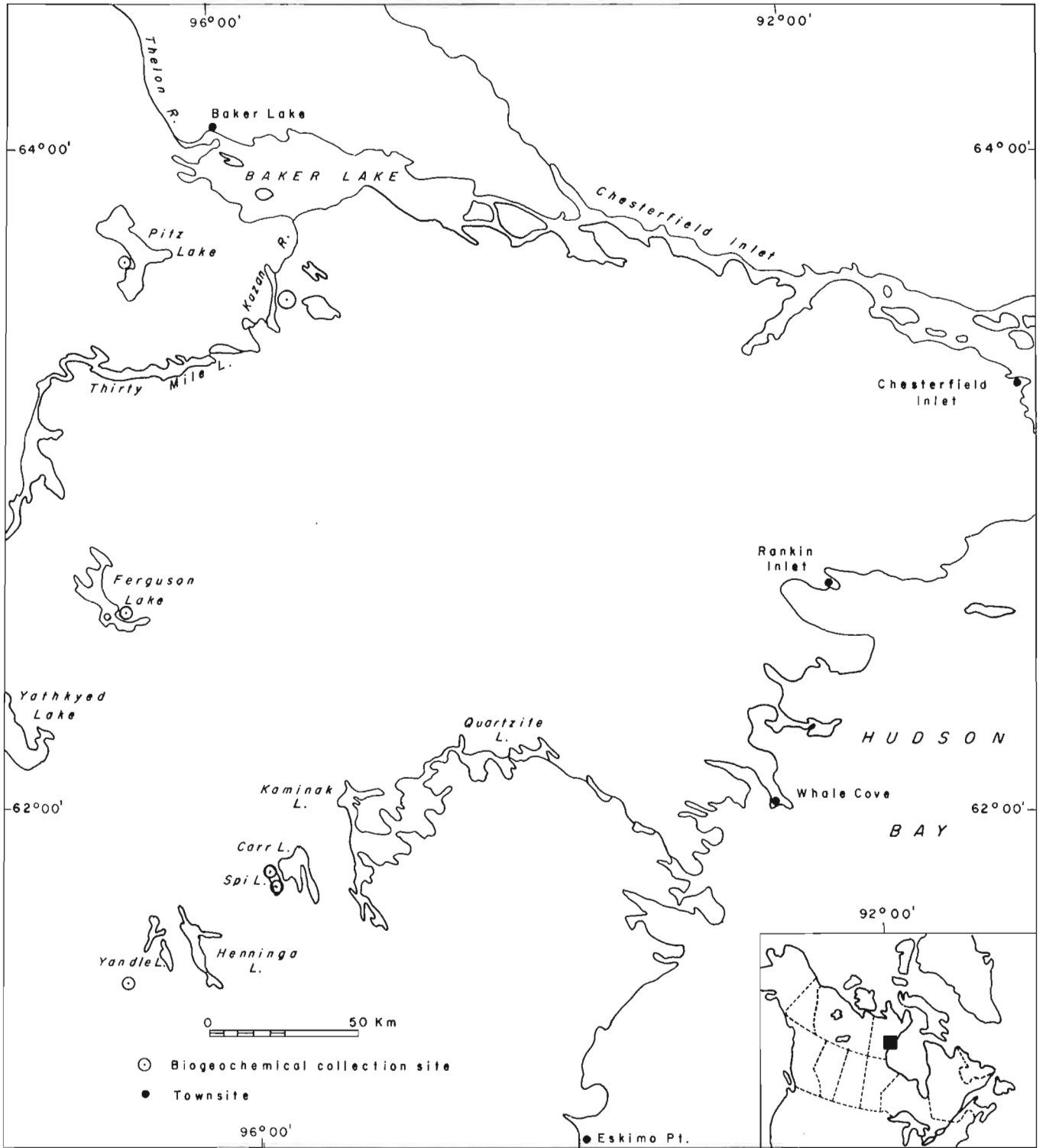


Figure 48.1. Location of sites sampled.

Table 48.2

Summary of samples collected in the pilot study

Sample	Collection site						
	1	2	3	4	4a	5	6 7
Mineral soil	x	x	x	x	x	x	x x
Peat	x	x	x	x	x	x	x
<i>Arctostaphylos alpina</i>	x	x	x	x		x	x
<i>Astragalus alpinus</i>	x						
<i>Betula glandulosa</i>	x	x	x	x		x	x
<i>Calamagrostis canadensis</i>	x	x	x		x	x	x
<i>Carex Bigelowii</i>						x	
<i>Cassiope tetragona</i>		x				x	x
<i>Dryas integrifolia</i>						x	x
<i>Empetrum nigrum</i>	x	x		x		x	x
<i>Eriophorum angustifolium</i>						x	
<i>Eriophorum vaginatum</i>	x		x		x	x	
<i>Hedysarum Mackenzii</i>							x
<i>Ledum palustre</i>	x	x	x	x		x	x x
<i>Oxytropis Maydelliana</i>	x		x				x
<i>Oxytropis Bellii</i>	x						
<i>Rubus Chamaemorus</i>	x	x	x		x	x	
<i>Salix alaxensis</i>		x					
<i>Salix planifolia</i>	x	x	x			x	x
<i>Vaccinium uliginosum</i>	x	x	x	x		x	x
<i>Vaccinium Vitis-idaea</i>	x	x	x	x		x	x

1 mm sieve. The samples were ashed and analyzed by Bondar-Clegg and Co. Ltd. The ash, obtained by slowly increasing temperatures to ignition, was dissolved in aqua regia and analyzed by atomic absorption (Cu, Zn, Pb, Co, Ni, Ag, Cd) and fluorimetric (U) techniques. Results are reported in ppm of the ash.

Previous Research

Mineral Prospecting

Canadian pioneers in the study of heavy metal uptake have been H. V. Warren and his co-workers who have conducted research since 1944 at the University of British Columbia. Their biogeochemical work has included studies on a large number of heavy metals (e. g. , Warren and Delavault, 1948, 1949, 1955a, b; Warren *et al.* , 1955). A progress report on Canadian biogeochemical research has been published recently (Fortescue and Hornbrook, 1967, 1969).

The question of whether arctic plants can assimilate anomalous amounts of metal on sites overlying metal deposits or can act as indicator species has never been resolved adequately. Most of the experimental work has taken place in Russia, and much of this material is relatively unknown in the West. One of the main problems in the Arctic is that permafrost prevents deep root penetration and in some areas may inhibit roots from penetrating into the mineral layer. Malyuga (1964) reported that the penetration of root system is not always limited to the active layer but, for some plants (wood reed, rose, sedge, cloudberry, and horsetail), also extends into the permafrost.

In Alaska, researchers in biogeochemistry have had limited success in mineral prospecting in perennially frozen terrain, possibly because of inhibition of root growth by permafrost. Although no flowering plants were found as indicators, several species of mosses and liverworts were found to be associated with mineralization (Chapman and Shacklette, 1960). Shacklette (1965, 1967) reported that a copper moss (*Mielichhoferia macrocarpa* (Drumm.) Br. & S.) was found to have an obligative relation to Alaskan copper deposits. In the forests of Yukon Territory and Northwest Territories dwarf birch (*Betula glandulosa*), Labrador tea (*Ledum groenlandicum*), and willow (*Salix* sp.) have been found to concentrate zinc and copper from underlying glacial sediment or bedrock (Warren and Delavault, 1955b).

In Finland, workers have found that leaves of *Vaccinium Vitis-idaea* concentrate copper and that *Ledum palustre* assimilates abnormal concentrations of copper and molybdenum over mineral deposits (Marmo, 1953). Despite the fact that this work was conducted in a nonpermafrost area, it has particular significance to the present study because these two species commonly are found in the eastern Canadian Arctic.

Environmental Effects

There is little information in the literature concerning the effects that the uptake of heavy metals by plants may have on the remainder of the biological system. Shacklette (1962) suggested, in a hypothetical model, that heavy metals ingested annually in browsing can have an effect on the distribution of large herbivores.

Results

Metal in the Mineral Soil Substrate

Table 48.3 lists typical metal content values for glacial soils and gossans on or near which the plants were growing at each sample site. Presumably the plants have concentrated metal from soils with these or similar compositions. It should be noted that these are considered to be typical values for the <250-mesh (<64 μ) portion of the soil within each 100 m-diameter collection area but that values can vary radically due to periglacial mixing of gossanous and true glacial soils near the sites of mineralization. Several samples from

Table 48.3
Typical Metal Content, Mineral Soils*

Site	Cu	Pb	Zn	Ni	U
	ppm				
Yandle background (No. 1)	22	8	20	16	0.5
Spi showing (No. 2)	1500	3800	2200	8	1.1
Spi train (No. 3)	24	100	32	6	1.0
Kinga River (No. 4, 4a)	68	11	24	24	3.0
Pitz background (No. 5)	5	11	14	8	1.4
Kazan River (No. 6)	24	10	13	6	5.9
Ferguson Lake (No. 7)	1140	18	8	54	2.5

* (< 250 mesh, -64 μ)

the Spi Lake showing, for instance, have zinc variations from less than 100 ppm to more than 2000 ppm over the space of a few metres.

Background Areas

Most species of plants collected from the background areas have lower concentrations of the metals tested than those from sites where either uranium or base metals have influenced the soil. Yandle Lake samples were collected from an island where a thin mantle of till covers interbeds of Archean felsic to basic metavolcanic bedrock, which contains numerous 1 to 2 m-diameter pods of sulphide (mostly pyrite) mineralization. As at all sites, Yandle Lake *Betula* contains more than 4000 ppm zinc. The single peat sample collected from that site contains abnormal amounts of copper and lead of unknown origin.

At Pitz Lake the vegetation collected was growing on a wet, complex terrain comprising till, marine silty clay, and marine nearshore sand, which form a continuous cover over sandstone, agglomerate, or porphyritic volcanic rocks of the Proterozoic Dubawnt Group. The collection site was at the base of a gentle slope, several kilometres long, which rises above the level of postglacial marine inundation. The samples from this site are slightly elevated in cadmium and uranium; the latter element is an economically important one which has spurred much ongoing exploration in the areas of Dubawnt outcrop. Concentrations of most other metals are relatively low except in two samples of sedges and the willow (*Salix*) sample. Ash from these two sedge samples contains over 13 000 ppm and over 60 000 ppm (6 per cent) copper, with abnormally high concentrations of lead, zinc, nickel, and silver; *Salix* contains over 16 000 ppm zinc and has high cadmium values but moderate to low amounts of other elements. The source of these high concentrations is not known, but the chemical conditions in the generally poorly drained terrain may have caused some sort of deposition

or preferential concentration of certain elements derived from background materials higher up the slope behind the site. However, peat, which forms the substrate on which sedges, in particular, grow, is impoverished in all metals except uranium. Alternatively, these metals may be derived from mineralization in the concealed, underlying bedrock, but such mineralization without associated uranium would be unusual in the Dubawnt Group.

Spi Lake, Zn-Pb-Cu Showing

Samples were collected from mud boils developed on a mixture of till and gossanous material within 200 m downslope from a well known outcrop of massive sphalerite, galena, and minor chalcopryrite on Spi Lake. A related suite of samples was collected from the middle of a small island in Spi Lake, about 2 km down-ice from the above mentioned mineralization. The island is underlain by Archean pyroclastics and volcanic rocks and covered by till with abundant mud boils. The till is enriched in zinc and includes an indicator train with several sphalerite-galena-chalcopryrite-bearing boulders (Shilts, 1974, p. 259).

At both sites several species are enriched in copper, zinc, lead, and cadmium. Birch (*Betula*), willow (*Salix*), blueberry (*Vaccinium*), and bearberry (*Arctostaphylos*) show the greatest values, but the sedges on Spi Island are notably enriched in copper, zinc, and lead. Sedges were not found at the Spi Lake mineralization.

Birch and willow seem to be the best indicators of this type of mineralization, but sedges, where present, also may be a useful group of plants to indicate copper-lead-zinc mineralization.

Uranium Showings

Samples were collected from mud boils and from a marshy area on a till plain above marine limit near Kinga River, 15 km southwest of Padlei. The local bedrock is a basal conglomerate of the Montgomery Lake Sediments (Bell, 1971) in which uranium mineralization occurs. Drift sampling around the collection site reveals locally anomalous copper-uranium concentrations in the soils, and uranium exploration was carried out in the early sixties by drilling at the collection site. Elevated uranium values, relative to nearby sites at Spi Lake and Yandle background, were found in several species at this site. Relatively high copper values were found in peat and willow samples but, unfortunately, no birch was collected here. Sedges show a slight tendency to concentrate copper, but are impoverished in other metals. It is noteworthy that the uranium values, while elevated with respect to other sites near Kinga River, are approximately equivalent to the background values obtained for similar species at Pitz Lake.

The Kazan River site is a commercially attractive site of copper-uranium mineralization in a Dubawnt Group sandstone host rock. Birch, *Dryas*, vetches, and peat have elevated uranium contents compared to

all other sites. Cadmium levels are high in birch and blueberry, and copper is elevated in cranberry and willow. The very high lead concentration in peat may be related to a spill of lead-rich gasoline, for numerous barrels indicate that drilling and aircraft activity has been carried on at the site over a period of several years.

Ferguson Lake Nickel

Not shown in Figure 48.2 are results of sampling at Ferguson Lake, a nickel sulphide prospect that was explored extensively in the early 1960's. Only one species, Labrador tea (*Ledum palustre*), was growing on the extensive gossan associated with the sulphide mineralization. Ash from this sample contained 550 ppm nickel and about 2000 ppm copper on a gossanous soil that contained (-80 mesh) 54 ppm nickel and 1140 ppm copper. Average *Ledum* values for the rest of the sites are 71 ppm nickel (range 36 to 137) and 427 ppm copper (range from 174 to 1075).

Discussion

Threshold Metal Levels

There tended to be stable threshold concentrations of some metals in the plant tissues although the metal content in the soil or peat varied radically from site to site. Thus, in general, metal concentration in the plant tissues was much less variable than metal content in the soil or peat samples. This threshold for species tended to be most pronounced with silver and cobalt (i.e., for silver: *Betula glandulosa*, *Empetrum nigrum* L., *Vaccinium Vitis-idaea*, *V. uliginosum* L., *Cassiope tetragona* (L.), D. Don, the various vetch species, *Arctostaphylos alpina*, and *Calamagrostis* sp.; for cobalt: *Ledum palustre*, *E. nigrum*, *V. uliginosum*, *C. tetragona*, *Rubus Chamaemorus*, the various vetch species, *A. alpina*, and *Calamagrostis* sp.). There also tended to be a threshold level of zinc in *L. palustre*, of cadmium in the various vetch species, and of copper in *R. Chamaemorus*.

The reason for the apparent threshold of heavy-metal concentrations in these plants is open to speculation. It could mean that plants have homeostatic control and absorb the metals up to a certain point (somewhere below the level of toxicity) after which they do not absorb further quantities. Epstein (1972), however, believed that metal tolerance in plants is not necessarily based upon restricting or controlling uptake of large amounts of toxic ions.

The only vascular species found on Ferguson Lake gossan was *Ledum palustre*, accompanied by a lichen species. Possibly the levels of metals in the soils were above the toxicity levels for other plant species. *L. palustre* possibly is an example of a tolerant plant (proposed by Epstein (1972)), which can synthesize chelating compounds that form complexes with the heavy metal ions and thereby render them harmless. There are probably a number of such complexing agents, each more or less specific for a certain toxic metal.

In addition to heavy metals, colonization of other plant species also may be inhibited by the low pH of the gossan (<2.0).

Uranium Accumulator Plants

The four highest uranium concentrations in plant tissue came from the Kazan River site: *Salix planifolia* Pursh, 65.0 ppm; *Dryas integrifolia* M. Vahl, 14.0 ppm; *Oxytropis Maydelliana* Trautv., 10.2 ppm; and *Hedysarium Mackenzii* Richards., 9.5 ppm (Fig. 48.2). The average uranium content in ash from the plants collected from the uranium showing was 10.1 ppm while the average uranium concentration in plants collected from the other six areas was only 1.0 ppm. The vetch species *O. Maydelliana* and *H. Mackenzii* are particularly important as they are closely related to the genus *Astragalus* which is one of the better known examples of an accumulator plant (Cannon, 1960; Epstein, 1972). The concentration of uranium in the tissues of *O. Maydelliana* was 10.2 ppm whereas uranium was not even detectable in the same species from the two other areas where it was collected. Uranium was not detectable in any of the *Calamagrostis* sp. samples except the sample collected from the Kazan River area which showed an uranium concentration of 2.4 ppm.

Peat

There has been some research in biogeochemical peat prospecting (Brooks, 1972). Peat biogeochemical analysis, however, is complex because many factors influence the chelating ability of humic matter, such as pH and the atomic weight and the valence of the element. For instance, humic acid loses its ability to fix metals with decreasing pH to the extent that lead, copper, zinc, nickel, and cobalt are released almost completely from humic matter once the pH is lowered to 1.0 (Chowdhury and Bose, 1971).

Preliminary Conclusions

Mineral Exploration

This preliminary study has demonstrated a number of aspects of trace metal fixation by plants that may warrant further work. In relationship to mineral exploration, the study shows that dwarf birch and dwarf willow species are the most consistent concentrators for the elements studied — at least in close proximity to mineralization. Willow particularly seems to concentrate uranium and cadmium, whereas birch is very rich, even in background areas, in zinc. Both tree species concentrate cobalt to levels of two or more times those of other plants sampled. Sedges show some tendency to reflect copper, lead, and zinc mineralization, but the very high values for copper and zinc in two of the five sedge samples from Pitz Lake background site suggest that caution should be exercised in interpreting sedge values. Also, sedges are more restricted in their occurrence than some of the other species.

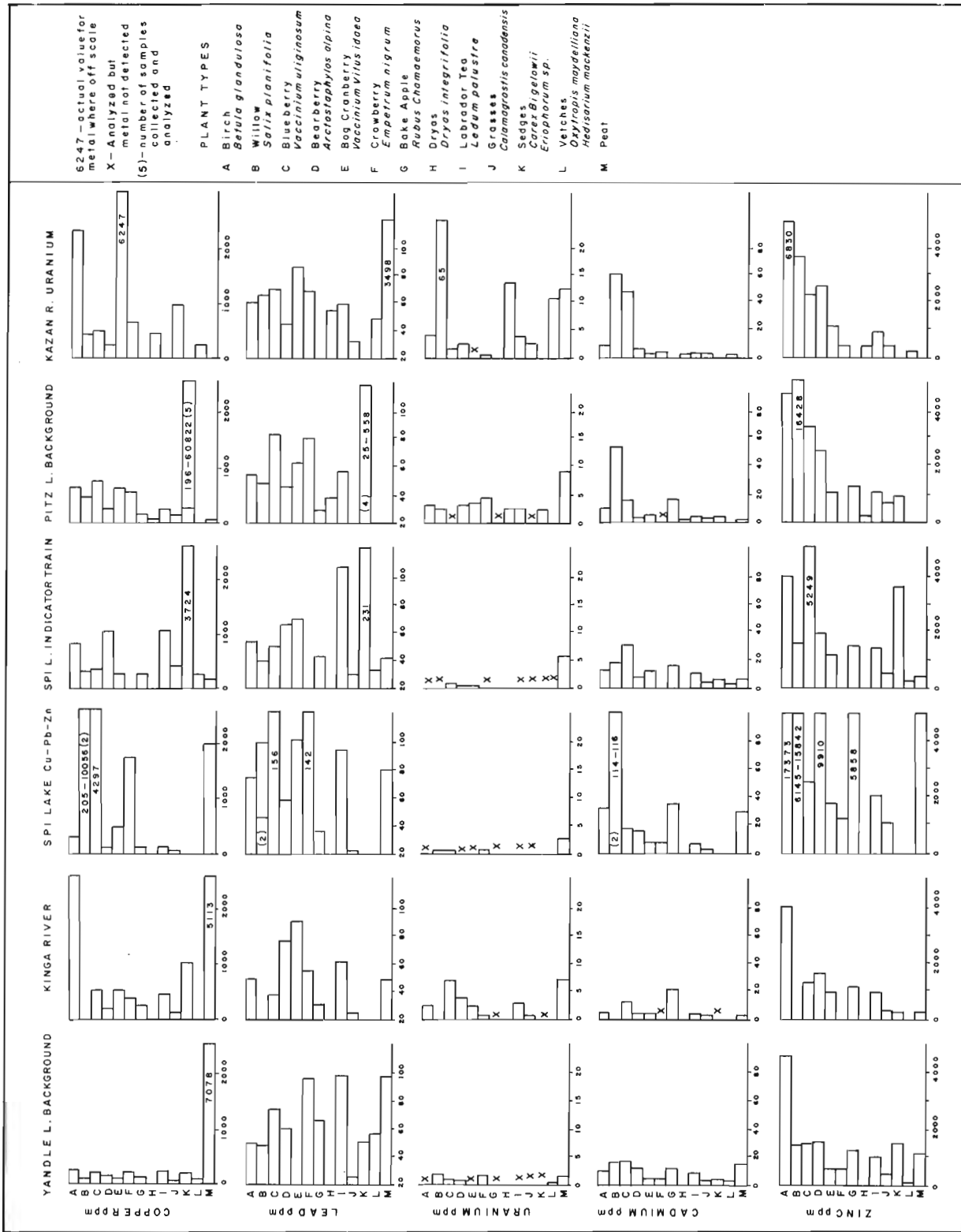


Figure 48.2. Histograms of metal concentrations in ash of various tundra plants.

Vetches and, possibly, *Dryas* might be investigated further for their uranium-concentrating tendencies.

Trace Elements in the Environment

Little can be said about the effects of metal levels in plants from these sites and their relationship to the food chain. The relatively high levels of cadmium in certain species from both background and mineralized sites in the Pitz Lake-Kazan River area might bear further investigation because of their proximity to the settlement of Baker Lake and to areas of intense herbivore browsing activity.

Implications for Lacustrine Sedimentation

The allochthonous organic components of lacustrine sediments tend to be important in this region because of the relatively low productivity of the lakes (Shilts *et al.*, 1976). The chemistry of the organic component of lake sediments certainly will be influenced by whether the allochthonous component is largely derived from woody plants with their generally high metal levels or from grasses, sedges, or other annual plants with their low to variable metal levels. Since significant portions of lake shores or entire lakes tend to be dominated by one or the other type of vegetation, these are important parameters to evaluate when studying variations in lake-sediment chemistry. Because of the concentration of metal in the easily eroded ash left after a tundra fire (Shilts, 1975; Wein and Shilts, 1976), tundra fires could have a significant, albeit temporary, influence on lake-sediment and water chemistry within the drainage basin.

References

- Bell, R. T.
1971: Geology of Henik Lakes (east half) and Ferguson Lake (east half) map-areas, District of Keewatin; Geol. Surv. Can., Paper 70-61, 31 p.
- Brooks, R. R.
1972: Geobotany and Biogeochemistry in Mineral Exploration; Harper and Row, New York, 290 p.
- Cannon, H. L.
1960: Botanical prospecting for ore deposits; Science, v. 132, p. 591-598.
- Chapman, R. M. and Shacklette, H. T.
1960: Geochemical exploration in Alaska; U.S. Geol. Surv., Prof., Paper 400-B, p. 104-107.
- Chowdhury, A. N. and Bose, B. B.
1971: Role of humus matter in the formation of geochemical anomalies; Can. Inst. Min. Met., v. 11, p. 410-413.
- Epstein, E.
1972: Mineral Nutrition of Plants: Principles and Perspectives; John Wiley and Sons Inc., Toronto, 412 p.
- Fortescue, J. A. C. and Hornbrook, E. H. W.
1967: Progress report on biogeochemical research at the Geological Survey of Canada 1963-1966; Geol. Surv. Can., Paper 67-23, Part I, p. 143.
1969: Progress report on biogeochemical research at the Geological Survey of Canada 1963-1966; Geol. Surv. Can., Paper 67-23, Part II, 101 p.
- Malyuga, D. P.
1964: Biogeochemical Methods of Prospecting; Consultants Bureau Enterprises, New York, 205 p.
- Marmo, V.
1953: Biogeochemical investigations in Finland; Econ. Geol., v. 48, p. 211-224.
- Schacklette, H. T.
1962: Biotic implication of Alaskan biogeochemical distribution patterns; Ecology, v. 43, p. 138-139.
1965: Bryophytes associated with mineral deposits and solutions in Alaska; U.S. Geol. Surv., Bull. 1198-C, 18 p.
1967: Copper mosses as indicators of metal concentrations; U.S. Geol. Surv., Bull. 1198-G, 18 p.
- Shilts, W. W.
1974: Drift prospecting in the Ennadai-Rankin Inlet greenstone belt, District of Keewatin; in Report of Activities, Part A; Geol. Surv. Can., Paper 74-1A, p. 259-261.
1975: Tundra fires, southeast District of Keewatin; in Report of Activities, Part B; Geol. Surv. Can., Paper 75-1B, p. 187-195.
- Shilts, W. W., Dean, W. E., and Klassen, R. A.
1976: Physical, chemical, and stratigraphic aspects of sedimentation in lake basins of the eastern Arctic Shield; in Report of Activities, Part A; Geol. Surv. Can., Paper 76-1A, p. 245-254.
- Warren, H. V. and Delavault, R. E.
1948: Biogeochemical investigations in British Columbia; Geophysics, v. 13, p. 609-624.
1949: Further studies in biogeochemistry; Geol. Soc. Am., Bull., v. 60, p. 531-560.
1955a: Some biogeochemical investigations in Eastern Canada, I and II; Can. Min. J., v. 76, p. 49-54 and 58-63.
1955b: Biogeochemical prospecting in northern latitudes; Roy. Soc. Can., Trans., v. 49, p. 111-115.
- Warren, H. V., Delavault, R. E., and Fortescue, J. A. C.
1955: Sampling in biogeochemistry; Geol. Soc. Am., Bull., v. 66, p. 229-238.
- Wein, R. W. and Shilts, W. W.
1976: Tundra fires in the District of Keewatin; in Report of Activities, Part A; Geol. Surv. Can., Paper 76-1A, p. 511-515.

Project 730004

A. K. Sinha

Resource Geophysics and Geochemistry Division

Geophysical techniques utilizing plane wave electromagnetic fields have become popular in recent years (Barringer, 1971). One important difference between radio wave fields and conventional e. m. fields where the receiver is close to the transmitter is that the total energy of the wave is distributed equally between the electric and the magnetic modes in the case of the former. Thus the electric field components may profitably be used for exploration when plane wave radio sources are used.

In the last few years, an airborne technique of measuring the wave tilt of the ground, called the E-Phase has been perfected by Barringer Research Ltd. The system is capable of measuring the wave tilt (rather the quadrature part of the wave tilt) at three widely separated frequencies from the VLF (very low frequency) to the BCB (broadcast band) range which yield three different apparent resistivity values at each position. The sources of the fields vary from VLF communication transmitters (15-25 khz), military transmitters (50-100 khz), navigational transmitters (200-400 khz) to broadcast transmissions (500 khz - 1.5 Mhz). At distances of several wavelengths, the fields are practically plane and consist of a vertical electric field E_z and a horizontal magnetic field H_y , if no resistive material is in the vicinity. The exciting field interacts with any material with finite conductivity including a conducting earth producing a secondary field E_x and the electric field is elliptically polarized. The electrical constants of the ground may be determined by measuring the consequent wave tilt.

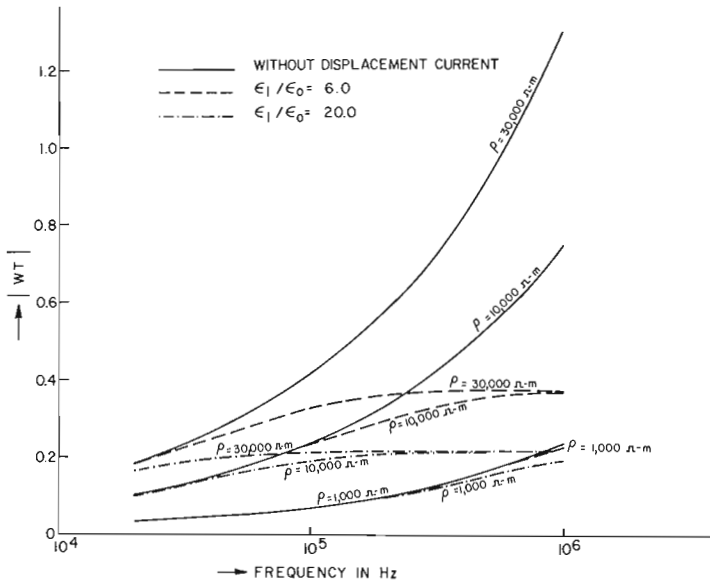


Figure 49.1. Effect of displacement currents on the amplitude of the wave tilt over a homogeneous ground.

In the interpretation of E-Phase results, two assumptions are usually made. First, the quasi-static assumptions (negligible displacement currents) are made at all frequencies and, secondly, the effect of the finite altitude of the aircraft (about 100 m) on the wave tilt is ignored. The second assumption was investigated in a previous study (Sinha, 1975), but the results were given in terms of the tilt and ellipticity of the field. Since wave tilt, and not tilt and ellipticity are measured by the E-Phase system, it is useful to take another look at the effects in terms of the wave tilts, especially with a view to formulating some technique for obtaining the true resistivity of the ground from airborne E-Phase results. Extensive computer modelling has been done on this problem (Sinha, in press).

Electric wave tilt is defined as the ratio of the horizontal to the vertical electric field just above the surface. A similar definition may be used for the magnetic wave tilt also, but in this paper the electric wave tilt only will be considered which is measured by the E-Phase system.

$$\text{Thus Wave Tilt} = WT = E_x/E_z \Big|_{z=0} \quad (1)$$

Assuming a harmonic time dependence $e^{i\omega t}$, the wave tilt at an altitude of h may be written as (Norton, 1937)

$$WT = \frac{v \sqrt{1-v^2}}{1 - \gamma_0 h v \sqrt{1-v^2}} \quad (2)$$

In this expression

$v = \gamma_0/\gamma_1$, h = altitude in metres, $i = \sqrt{-1}$,
 $\gamma_0 = (-\omega^2 \mu \epsilon_0)^{1/2}$ = the propagation constant of air,
 $\gamma_1 = (i\omega \mu \sigma_1 - \omega^2 \mu \epsilon_1)^{1/2}$ = the propagation constant of the medium,
 ϵ_0 = permittivity of air (8.854×10^{-12} F/m),
 ϵ_1 = permittivity of the medium,
 σ_1 = conductivity of the medium,
 μ = permeability of air and the medium.

It is easy to see that

$$\gamma_1^2 / \gamma_0^2 = \epsilon_1 - i\sigma_1 / \omega \epsilon_0 \quad (3)$$

where $\epsilon_1 = \epsilon_1/\epsilon_0$ = dielectric constant of the medium.

Figure 49.1 shows the influence of the displacement currents on the magnitude of the wave tilt in the frequency range of 20 khz to 1 Mhz. Since highly resistive media like the permafrost terrains are especially suitable for surveying with wave tilt measuring techniques because of the high anomalies that may

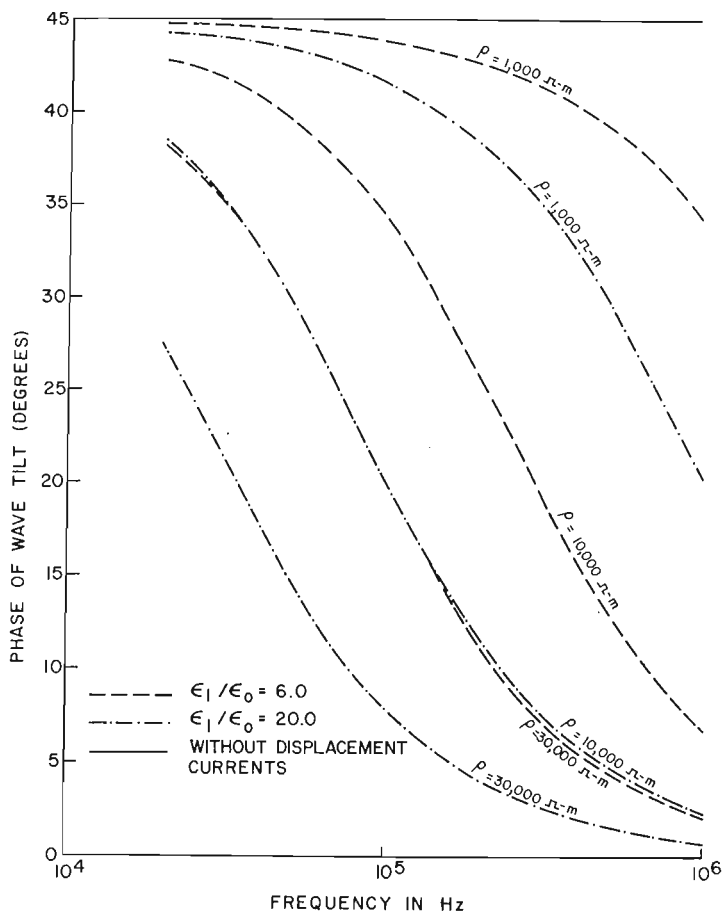


Figure 49.2. Dependence of the phase of the wave tilt on the displacement currents over a homogeneous ground.

be expected over them, three resistivity values from 1000 to 30 000 Ω -m and two dielectric constant values of 6.0 and 20.0 have been considered. It is clear that the net effect of considering displacement currents is to decrease the wave tilts effectively. In the VLF range, the effect is very small and almost unnoticeable. At high frequency and resistivity values, however, the differences in the $|WT|$ values with and without displacement currents are considerable. At very high frequency and resistivity values, the $|WT|$ values are almost independent of resistivity as may be expected for low-loss media. Figure 49.2 shows the variation of the phase of the wave tilt against frequency for the same models. If the displacement currents are ignored, the phase should always be 45 degrees (Sinha, 1975) as shown by the solid line. Phase values, however, vary from close to 45 degrees to almost zero degrees. Phase values, in fact, are more sensitive to displacement currents since the effect is present even in the VLF range. The altitude effect on the wave tilt is similar to the variation of the tilt and ellipticity of the field with height as presented earlier (Sinha, 1975) and will not be repeated here.

If the altitude and displacement current effects are ignored in interpreting E-Phase results, the simplified formula for wave tilt looks like

$$WT = E_x/E_z|_{z=0} = (1+i) \frac{(\omega \epsilon_0 \rho_a)^{\frac{1}{2}}}{2} \quad (4)$$

where ρ_a is the apparent resistivity. Since only the quadrature part of the wave tilt is measured in the E-Phase system, the apparent resistivity is determined from the relation

$$\rho_a = \frac{WT_q^2 \times 10^9}{(\pi \times 8.854 \times f_{\text{kHz}})} \quad (5)$$

where WT_q is the quadrature part of the wave tilt and f_{kHz} is the frequency in kilohertz. Table 49.1 shows the results of our numerical modeling over a homogeneous ground where the altitude of the system was assumed to be 100 m, the dielectric constant to be 10.0 and resistivity values from 1000 to 30 000 Ω -m. The table shows the apparent resistivity values that would be deduced by the E-Phase system according to Equation 5.

It is clear from Table 49.1 that in order to make meaningful interpretation of airborne wave tilt data over a range of frequency, the contribution of the displacement currents and altitude of the aircraft except at VLF range over low resistivity media must be considered. A graphical technique, therefore, has

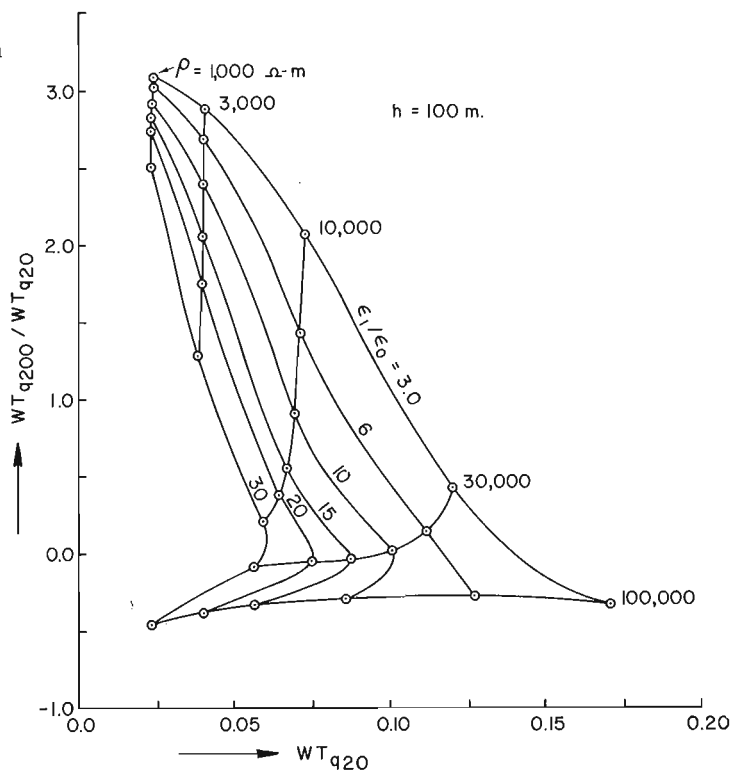


Figure 49.3. Correction diagram for E-Phase results for an altitude value of 100 metres.

Table 49.1

$h = 100 \text{ m}$ and $\epsilon_1/\epsilon_0 = 10.0$
Apparent resistivities in $\Omega\text{-m}$ according to Equation 5

True Resistivity in $\Omega\text{-m}$	f_{kHz}	20	50	100	200	500	1000
1 000		986.0	967.0	933.0	853.0	503.0	3.0
3 000		2885.0	2704.0	2375.0	1649.0	119.0	305.0
10 000		8696.0	6641.0	3647.0	711.0	143.0	570.0
30 000		18 276.0	6469.0	9.0	1.0	384.0	631.0

been tried for obtaining the correct estimate of the ground resistivity from E-Phase surveys. Figure 49.3 shows a typical correction diagram that may be used for this purpose. Here the ratios of the quadrature parts of the wave tilt at two frequencies (200 and 20 khz in this case) are plotted against the quadrature part at the lower frequency for an altitude of 100 m for several resistivity and dielectric constant values. Similar diagrams may be plotted for other frequency and altitude combinations. Therefore if the quadrature parts of the wave tilt are known at two frequencies, then both resistivity and dielectric constant of the ground may be correctly estimated using such a diagram.

This approach of using correction diagrams not only eliminates the errors in resistivity estimates due to altitude and displacement current effect, but also enable us to estimate the dielectric constant of the ground. This additional parameter may give us some idea about the ice content of frozen ground in permafrost terrains.

References

- Barringer, A. R.
1971: Airborne exploration; Min. Mag., v. 124, no. 3, p. 1-6.
- Norton, K. A.
1937: The propagation of radio waves over the surface of the earth and in the upper atmosphere, Part II; Proc. of the Institute of Radio Engineers (IRE), v. 25, no. 9, p. 1203-1236.
- Sinha, A. K.
1975: Altitude dependence of plane wave E.M. fields; in Report of Activities, Part A, Geol. Surv. Can., Paper 75-1A, p. 147-148.
- Influence of altitude and displacement currents on plane wave E.M. field; Geophysics. (in press)

Project 680093

A. E. H. Pedder

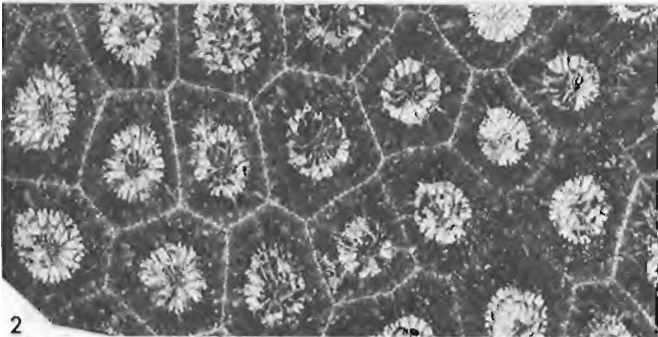
Institute of Sedimentary and Petroleum Geology, Calgary

Little is known of the Late Silurian coral faunas of western Canada. Two well-dated Pridolian species have been described (Pedder, 1971) from Prongs Creek in the Wernecke Mountains, Yukon Territory (coordinates approximately Lat. $65^{\circ}18'N$, Long. $135^{\circ}40'W$) and several genera have been listed (Pedder in Lenz and Pedder, 1972) from the two principal sections in the headwaters area of Royal Creek, which is also in the Wernecke Mountains of Yukon Territory (coordinates approximately Lat. $64^{\circ}46'15''N$, Long. $135^{\circ}13'W$).

Since these publications were prepared, two rather unusual genera, hitherto unrecorded from Canada, have been identified from lesser known sections at Royal Creek. Both are represented by new species but, since only one specimen of each is presently available, formal description is deferred. Their occurrence, however, is being made known because their distinct morphology and the stratigraphic range of the genera in other countries suggest that the new Canadian species have excellent potential as indices of Late Silurian time.



1



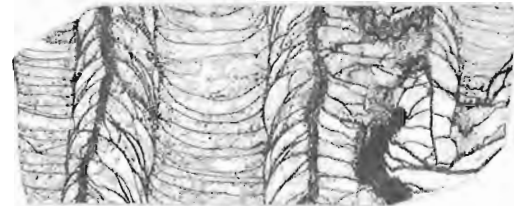
2

Figures 50.1, 50.2.

Niajuphyllum sp. nov., x4, GSC 45901. Ludlow limestone. Royal Creek headwaters, Yukon Territory; Shell Canada Limited DB33, N63, unit 4; approximately Latitude $64^{\circ}47'30''N$, Longitude $135^{\circ}10'W$. Collected by D. Basso, 1963.



3



4



5

Figures 50.3, 50.4, 50.5.

Yassia sp. nov., x2, GSC 45902. Road River Formation; late Pridolian part. Royal Creek headwaters, section 5, Yukon Territory; GSC loc. C-4265; Latitude $64^{\circ}47'N$, Longitude $135^{\circ}12'W$. Collected by A. E. H. Pedder, 1969.

Family CHONOPHYLLIDAE Holmes, 1887
Genus *Niajuphyllum* Strel'nikov, 1973, p. 48

Type species. *N. obsoletum* Strel'nikov, 1973, p. 48, Pl. 5, figs. 2a, b. Ludlow limestone. Engane-Pe Ridge, Niya-Yu River, Polar Urals.

Remarks. The diagnostic features of this genus are: 1) cerioid corallum; 2) long septa that are thickened and contiguous both axially, where they form an axial structure, and peripherally, where they form a prominent dense marginarium; 3) absence of dissepiments or presepiments; and 4) tabulae that slope downward toward the marginarium. The original microstructure is not well preserved in any known material, but appears to have consisted of coarse uniserial monacanth.

Strel'nikov was aware of the morphological similarity between *Niajuphyllum* and *Kodonophyllum*, but was reluctant to place them in the same family because of the massive colonial growth form of *Niajuphyllum*. The present author rejects any diagnostic value of growth form at family level and places *Niajuphyllum* with little hesitation in the Chonophyllidae, which has priority over the name Kodonophyllidae proposed by Wedekind in 1927.

According to dating by paleontologists of Shell Canada Limited, the new Canadian occurrence of *Niajuphyllum*, like the original, is in Ludlow limestone. The Polar Urals and Yukon Territory are at present the only areas from which the genus is known. The specimen from Royal Creek is much smaller, has fewer septa and a much greater diameter of tabularium/diameter of corallite ratio than *N. obsoletum*, and certainly represents a new species.

Family KETOPHYLLIDAE Lecompte, 1952
Genus *Yassia* Jones, 1930, p. 36

Type species. *Spongophyllum enorme* Etheridge, 1913, p. 35-37, Pls. 4-7. Boonoo Ponds Limestone, Upper Silurian. Escarpment northeast of Boonoo Ponds Creek, Hatton's Corner, Yass River, near Yass, New South Wales, Australia. This limestone is now considered equivalent to the Bowspring Limestone, which is correlated with part of the Ludlow Series.

Remarks. Description and synonymies of *Yassia* and its type species have been given most recently by McLean (1974, p. 665-667, Pl. 95, figs. 6-8). The salient features of the genus are: 1) cerioid corallum; 2) weak septa, consisting of low ridges or, less commonly, short discrete spines; 3) coarse presepiments, forming a dissepimentarium of variable width, that tends to have horizontal surfaces at the periphery and steeply sloping surfaces adjacent to the tabularium; and 4) broad, mostly complete and irregularly grouped tabulae that form flat to sagging tabularial surfaces.

Crinophyllum Jones (1932, p. 61) is based on the same type species as *Yassia* and is thus an objective synonym of it. The type species of *Klamathastraea* Merriam (1972, p. 40), which is *K. dilleri*, differs from *Yassia enormis* only in being smaller, having slightly

better developed septa and more numerous and less elongated presepiments. These differences are not considered sufficient to justify a separate genus for *Klamathastraea*. Representatives of *Yassia* have been described from Wenlock strata in the Moyero River Basin of the Siberian Platform and from Ludlow beds in New South Wales and California. An undescribed species also is present in probable Pridolian beds on Cornwallis Island in the Canadian Arctic Archipelago.

The specimen of *Yassia* illustrated here is associated with a late Pridolian *eosteinhornensis* conodont fauna, identified by G. Klapper. It is undoubtedly a new species, differing from others in having more spinose septa and a wall much thickened by multiserially arranged monacanthine spines and sclerenchyme.

References

- Etheridge, R.
1913: A very remarkable species of *Spongophyllum* from the Upper Silurian rocks of New South Wales; Rec. Australian Mus., v. 10, p. 35-37.
- Jones, O. A.
1930: A revision of some Palaeozoic coral genera and species; Abstracts of dissertations approved for the Ph.D., M.Sc. and M.Litt. degrees in the University of Cambridge for the academical year 1928-29, p. 35, 36.
1932: A revision of the Australian species of the coral genera *Spongophyllum* E. & H. and *Endophyllum* E. & H. with a note on *Aphrophyllum* Smith; Roy. Soc. Queensland, Proc., v. 44, p. 50-63.
- Lenz, A. C. and Pedder, A. E. H.
1972: Lower and Middle Paleozoic sediments and paleontology of Royal Creek and Peel River, Yukon, and Powell Creek, N.W.T.; XXIV Intern. Geol. Congr., Guidebook Field Excursion A14.
- McLean, R. A.
1974: Chonophyllinid corals from the Silurian of New South Wales; Palaeontology, v. 17, p. 655-668.
- Merriam, C. W.
1972: Silurian rugose corals of the Klamath Mountains region, California; U.S. Geol. Surv., Prof. Paper 738.
- Pedder, A. E. H.
1971: An Upper Silurian (Pridolian) coral faunule from northern Yukon Territory; Geol. Surv. Can., Bull. 197, p. 13-21.
- Strel'nikov, S. I.
1973: Rugozy iz siluriyskikh otlozheniy podnyatiya Chernova i Polyarnogo Urala; Paleontol. Zhurnal, 1973, no. 2, p. 46-51.

FIRST RECORDS OF FIVE RUGOSE CORAL GENERA
FROM UPPER SILURIAN ROCKS OF THE CANADIAN ARCTIC ISLANDS

Project 500029

A. E. H. Pedder
Institute of Sedimentary and Petroleum Geology, Calgary

Preliminary studies of Late Silurian coral faunas, submitted by field geologists from numerous localities in the Canadian Arctic Islands, reveal that these are among the richest of their age known from anywhere in the world. In many cases, the faunas were collected during reconnaissance work and the quantity of material available is insufficient for formal description of species. It is, however, adequate for recognition of genera.

The purpose of the present report is to establish the occurrence of the genera *Mazaphyllum*, *Rhizophylloides*, *Stylopleura*, *Prohexagonaria* and *Stereoxyloides* (*Nanshanophyllum*) in Pridolian, or probable Pridolian strata of the Canadian Arctic islands. None of these has been identified previously in any of the Silurian or Devonian sequences of Canada, although two, *Stylopleura* and *Prohexagonaria*, were described originally from Nevada, and species of the recently proposed genus *Rhizophylloides* have long been known from Kentucky. Early indications are that species of all five of these genera are short ranging and likely to become useful index fossils.

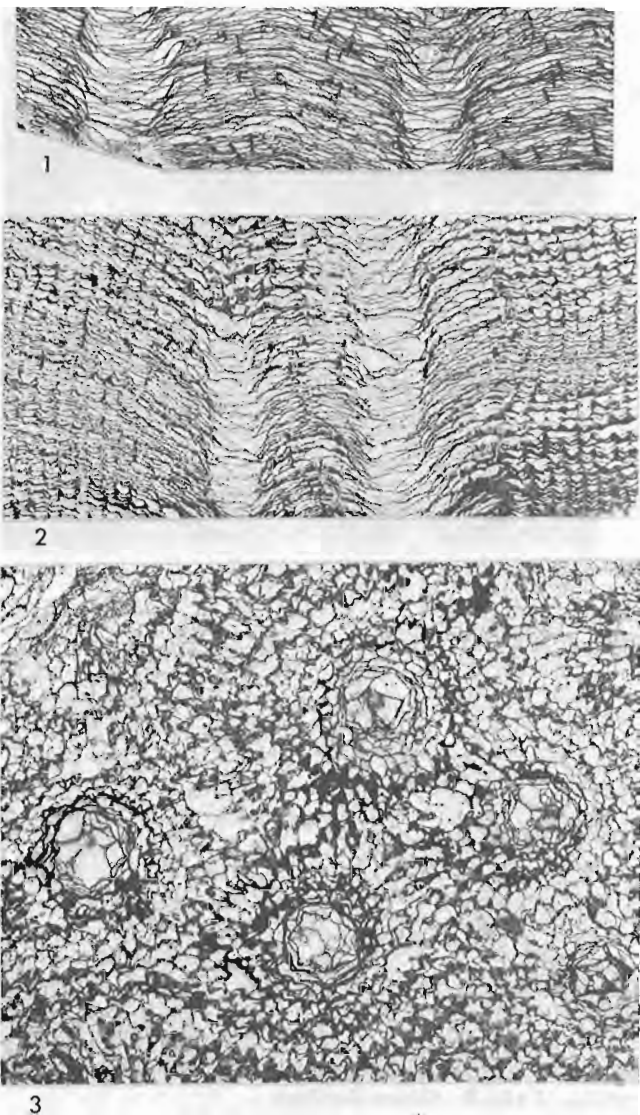
Family CYSTIPHYLLIDAE Edwards and Haime, 1850
Genus *Mazaphyllum* Crook, 1955, p. 1052, 1053

Type species. *Mazaphyllum cortisjonesi* Crook, 1955, p. 1053-1056, Textfig. 2A-3D. Unnamed limestone lens, possibly equivalent to part of the Wenlock Series. Valley of Palmer's Oaky Creek, Portion 60, Parish of Turon, County of Roxburgh, 45 km (28 miles) northeast of Bathurst, New South Wales, Australia.

Remarks. This genus has been discussed recently by McLean (1974, p. 27, 28). It is characterized principally by its plocoid, almost thamnasterioid corallum, septal spines that typically penetrate several dissepimental surfaces and are believed to have been originally rhabdacanthine, and by its shallow, flat to gently sagging tabularia. It is known from several limestones of possible Wenlock and Ludlow ages in Eastern Australia.

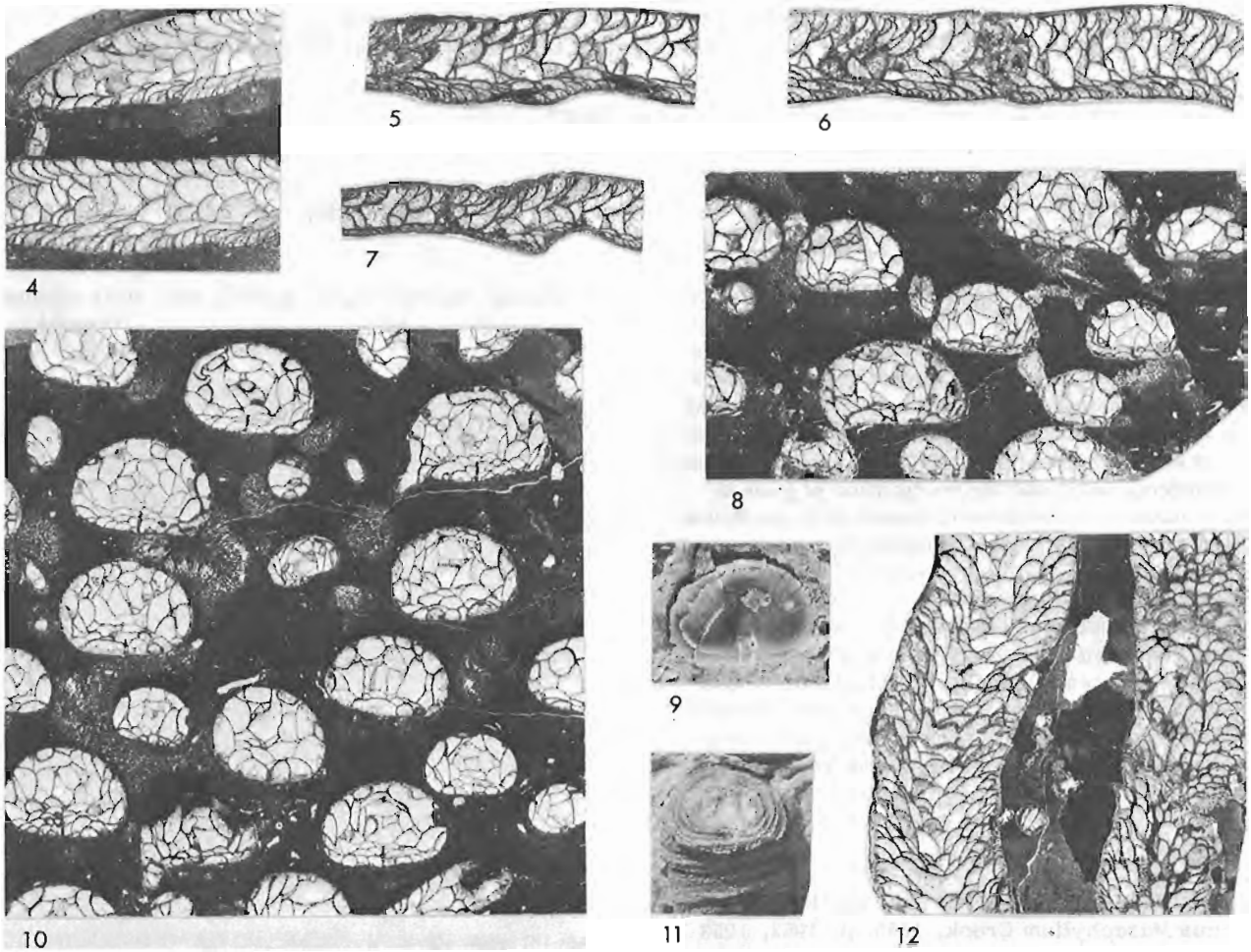
The first specimen of *Mazaphyllum* identified from Canada was collected from at least 58 m (190 ft.), and possibly as much as 120 m (393 ft.), above the base of the Read Bay Formation on northeastern Somerset Island. Since the lower 3.0 to 9.2 m (10-30 ft.) of the formation have yielded late middle Ludlow to early Pridolian conodonts (T. T. Uyeno in Reinson *et al.*, 1976, p. 499), it is reasonable to suppose that the specimen of *Mazaphyllum* is Pridolian. It represents a new species, differing from *M. cortisjonesi* in having smaller tabularia, flatter tabularial surfaces, some complete

tabulae, shorter septal spines, and more profusely developed sclerenchymal tissue on some dissepimental surfaces.



Figures 51.1-51.3

Mazaphyllum sp. nov., x4, GSC 45903. Read Bay Formation, at least 58 m (190 ft.) and possibly as much as 120 m (394 ft.) above base; probably Pridolian. East end of main cliff, southeastern Garnier Bay, Somerset Island; grid reference GZD15XWN2804. Collected by O. A. Dixon, 1975.



Figures 51. 4-51. 12. *Rhizophylloides* sp. nov., x2.5. Figures 51. 4-51. 8, 51. 10, 51. 12, GSC 45904. Read Bay Formation, approximately 123 to 131 m (403-430 ft.) above base, 97 to 105 m (318-344 ft.) below top; probably Pridolian. Unnamed gorge 10 km (6.2 miles) north of Creswell Bay, Somerset Island; grid reference GZD15XVL7586. Collected by S.R. Williams, 1975. Figures 51. 9, 51. 11, GSC 45905. Read Bay Formation, isolated outcrop; probably Pridolian. Fury Beach area, 3.2 km (2 miles) north of river mouth, Somerset Island; grid reference GZD15XWL3583. Collected by O.A. Dixon, 1975.

Family GONIOPHYLLIDAE Dybowski, 1873
 Genus *Rhizophylloides* Spasskiy and Kravtsov
 in Spasskiy *et al.*, 1975, p. 171

Type species. *Rhizophyllum elongatum* Lindström, 1883, p. 32-38, Pl. 1, figs. 9-12, Pl. 2, figs. 1-18, Pl. 3, figs. 13, 15, 16, Pl. 4, figs. 1-6, Pl. 5, figs. 13, 14. Eke Beds, equivalent to the Upper Ludlow Series. Lau, Southern Gotland.

Remarks. This genus may be diagnosed as follows: corallum dendroid to phaceloid; corallites long, slender and calceoloid, produced by parricidal or nonparricidal budding, and characteristically developing long hollow talons, locally partitioned by sinuous plates that are apparently homologous with the dissepiments; septal apparatus consisting of a prominent, although short, more or less continuously developed septum

along the centre of the interior of the flattened side of the corallite, and rare, short septal spines; dissepiments tend to be elongated toward the apex of the corallite, and those on the flattened side of the corallite are distinctly smaller than the others; tabellae are vesicular, incomplete and poorly differentiated from the dissepiments; corallites are provided with a single semicircular, slightly convex operculum; a broad ridge is present on the lower interior surface of operculum.

The genus is distinguished from *Rhizophyllum* by its long slender corallites, profuse talons, and genuinely dendroid growth form.

Calceola attenuata Lyon, 1879 and the synonymous species *C. proteus* Davis, 1887 are representatives of *Rhizophylloides*. They occur in the upper Wenlock to lower Ludlow Louisville Limestone of northern Kentucky and have been figured recently by Stumm (1965, Pl. 5, figs. 5-7). The genus also occurs in probable Pridolian

strata of the Solovikha Suite in the Mountain Altay region of central Asia (Ivaniya *et al.*, 1968, Pl. 8, figs. 35, 36) and in the Ludlow Silverdale Formation of the Yass region of New South Wales (R.A. McLean, pers. comm.). The new Canadian species has been collected from two outcrops of probable Pridolian limestone of the Read Bay Formation on Somerset Island.

Family MUCOPHYLLIDAE Hill, 1940
Genus *Stylopleura* Merriam, 1974, p. 34, 35

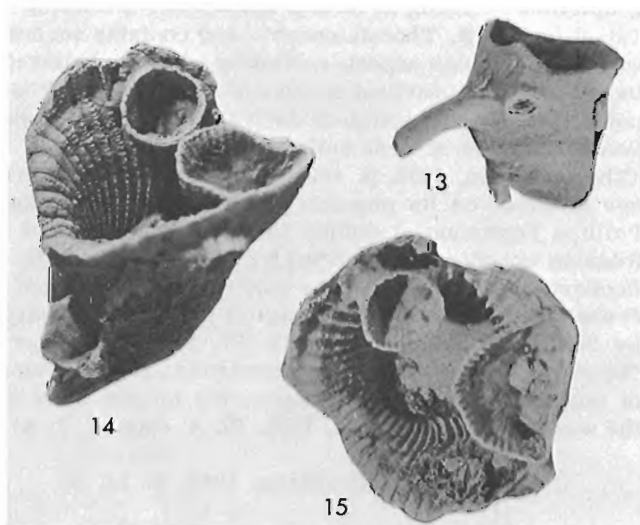
Type species. *Stylopleura berthiaumi* Merriam, 1974, p. 35, Pl. 3, figs. 6-20. Most of the original material, including the holotype, derives from the upper part of unit 3 of the Roberts Mountains Formation at upper Pete Hanson Creek, northwest side of Roberts Creek Mountain, central Nevada. Although Merriam believed the type horizon to be Silurian ("Silurian coral zone D") it now is considered to be early Lochkovian, which is the earliest Devonian stage.

Remarks. The protocorallite in *Stylopleura* is typically ceratoid or subcylindrical. At maturity it develops a flaring trumpet-like calice, around which as many as 11 offsets may develop simultaneously. These offsets may or may not develop sufficiently to form a genuinely fasciculate corallum. Both the protocorallite and offsets typically produce long talons. The septa are extremely short and commonly undifferentiated. In the unexpanded part of the corallite, trabeculae are aligned and usually project somewhat from the distal edge of

the septum. As the calice flares, the trabeculae protrude less and become multiserial, producing low, broad septal ridges. There are no dissepiments. Tabulae are complete and widely spaced. The original fine trabecular structure is unknown due to silicification of the material examined to date.

The calice likens *Stylopleura* to *Mucophyllum*, but it is not thickened or everted as in typical specimens of that genus. Hill (1940, p. 399; 1956, p. 278) believed *Aspasmophyllum* to be a mucophyllid. As such, it would resemble *Stylopleura*. However, R. Birenheide has kindly sent photographs of the unique specimen from the Ahrdorf beds of Germany and these reveal a markedly bilateral arrangement of the septa in two quadrants, suggesting halliid affinities. Other genera that have to be considered before *Stylopleura* is accepted include *Fletcheria* Edwards and Haime, *Pycnostylus* Whiteaves and *Cyathopaedium* Schlüter. All are based on diaphragmatoporous species capable of multiple calicinal budding. Lang *et al.* (1940, p. 112) and others have considered *Fletcheria* to be a senior synonym of *Pycnostylus*, but this opinion was rejected by Hill (1940, p. 390), Duncan (1956, legend to Pl. 25) and Merriam (1974, p. 34). *Fletcheria tuberosa*, the type species of *Fletcheria*, is distinguished from *Stylopleura* by its unflared calice, lack of septa and supporting talons, and by the presence of some incomplete convex tabulae. It may well be a tabulate coral (Stasińska, 1967, p. 101, 102, Pl. 33, figs. 3a-4, Pl. 34, fig. 4). *Pycnostylus* and the Pycnostylidae are not easily interpreted because of the inadequacy of the preservation of *P. guelphensis*, the type species, at the type locality. It certainly differs from *Stylopleura* in lacking a flared calice and supporting talons and is possibly further differentiated by having amplexoid septa (Hill, 1940, p. 391; Stearn, 1956, p. 82). *Cyathopaedium* is based on an inadequately known type species from the Middle Devonian ("Stringocephalenkalk") of Germany. Weissmerl (1939, p. 14, 23) examined the original material of this species and found the septa to be lamellar with spinose inner margins, as in *Stylopleura*, but believed the wall to be formed by accumulation of thin layers of sclerenchyme between the septa. *Cyathopaedium* also differs in lacking a flared calice.

Stylopleura is represented by several species of Late Silurian age in the Canadian Arctic Archipelago and Late Silurian and Early Devonian age in Yukon Territory. *Calophyllum phragmoceras*, described from Seal Island by Salter (1852, p. ccxxx, Pl. 6, figs. 4, 4a) is probably one of these. Unfortunately, enquiries have failed to locate the original material, which will have to be re-examined before its generic position is established with certainty. The specimens figured in this paper were collected 20 m (66 ft.) above the base of the Devon Island Formation at the type section on northwestern Devon Island. From the same collection (GSC loc. C-55407), R. Thorsteinsson isolated brachiopods identified by J.G. Johnson as *Salopina* sp., *Dicaelosia* sp., *Conchidium* spp., *Atrypa* sp., *Reticulatrypa neutra* and *Gracianella cryptumbra*, and conodonts identified by T.T. Uyeno as *Ozarkodina confluens*, *O. remscheidensis remscheidensis*, *O.*



Figures 51. 13-51. 15

Stylopleura sp. nov., cf. *S. berthiaumi* Merriam, x3. Figure 51. 13, GSC 45906. Figures 51. 14, 51. 15, GSC 45907. Both from the type section of the Devon Island Formation, 20 m (66 ft.) above base; late Pridolian. Douro Range, northwestern Devon Island; UTM Zone 15, 505350 m E, 8471500 m N; GSC locality C-55407. Collected by R. Thorsteinsson, 1975.

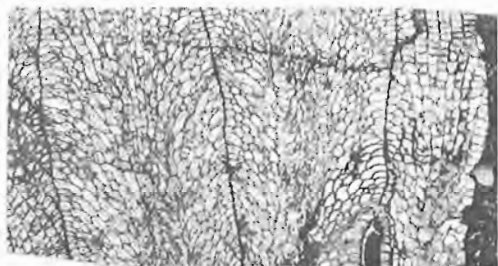
remscheidensis eosteinhornensis and *Pedavis* sp. The age of the assemblage is undoubtedly late Pridolian. In addition to the North American species, *Tryplasma liliformis* Etheridge, 1907 (see Hill, 1940, p. 401, Pl. 11, figs. 18, 19, Pl. 12, figs. 3-6) from the Ludlow Silverdale Formation of the Yass district of New South Wales, and possibly *Amplexus (Coelophyllum) eurycalyx* Weissermel (1894, p. 634-638, Pl. 50, figs. 8, 9, Pl. 51, fig. 1) from glacial drift in northern Germany, are further species of *Stylopleura*. The species figured here is new; nevertheless, it is closely related to *Stylopleura berthiaumi* Merriam.

Family CYATHOPHYLLIDAE Dana, 1846

Subfamily ARACHNOPHYLLINAE Dybowski, 1873

Genus *Prohexagonaria* Merriam, 1974, p. 50

Type species. *Entelophylloides (Prohexagonaria) occidentalis* Merriam, 1974, p. 50, 51, Pl. 9, figs. 1-4. Roberts Mountains Formation, lower beds of unit 3, Silurian coral zone C. Northwest side of Roberts Creek Mountain, Nevada. Merriam correlated his Silurian coral zone C with the Wenlock Series, but rough stratigraphic calculations suggest that the type stratum of *Prohexagonaria occidentalis* is well above the occurrence of *Ozarkodina remscheidensis* in the Roberts



16



17

Figures 51. 16-51. 17

Prohexagonaria sp. nov., x3. GSC 45908. Unnamed Pridolian limestone. Near the mouth of Rookery Creek, northwestern Cornwallis Island; UTM Zone 15, 420250 m E, 8365250 m N; GSC locality C-3094. Collected by J. W. Kerr, 1965.

Mountains (Klapper and Murphy, 1974). This, and the knowledge that Merriam's Silurian coral zone D is Lochkovian, suggest that the type horizon of *Prohexagonaria occidentalis* is Pridolian.

Remarks. The diagnostic features of *Prohexagonaria* are its cerioid corallum; thin walls; thin, weakly to moderately carinate septa, the major of which terminate at or very close to the axis and may be withdrawn locally from the periphery, while the minor terminate near the periphery of the tabularium; dissepimentarium consisting of several rows of mostly small dissepiments, increasing in inward inclination toward the axis; and closely spaced, incomplete tabulae that form axially arched tabularial floors.

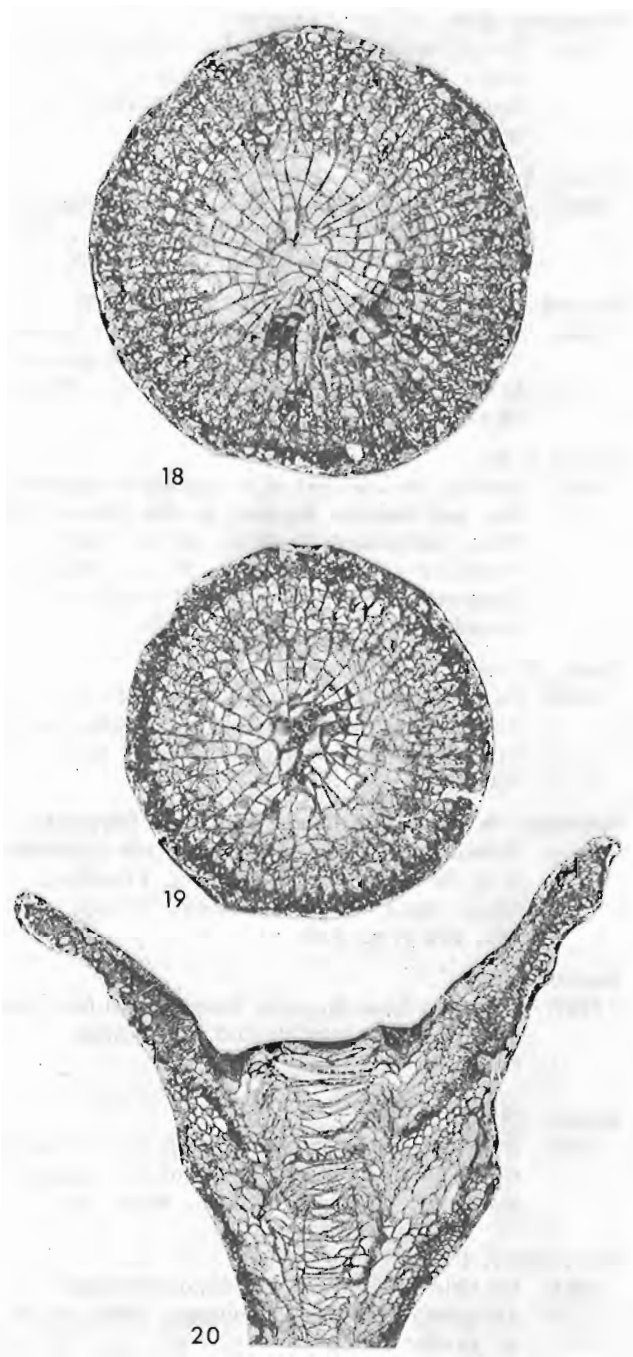
Merriam proposed *Prohexagonaria* as a subgenus of *Entelophylloides* Rukhin, 1938, of which the type species is *Columnaria inequalis* Hall, 1852, from the "coralline limestone at Schoharie", which is the Pridolian Cobleskill Formation of New York. This species is closely related to several species of *Xystriphyllum*, but not to *Prohexagonaria occidentalis*. If *Prohexagonaria* were to be considered a subgenus of any other genus, it should be *Tenuiphyllum* Soshkina, 1937. However, recently published photographs of the type species of *Tenuiphyllum* (Ivanovskiy and Shurygina, 1975, Pl. 9, figs. 1a, b) show it to have significantly expanded septal bases.

The specimen illustrated here is of a new species and comes from unnamed limestone near the mouth of Rookery Creek, northwestern Cornwallis Island. This limestone rests with angular discordance on the Cape Phillips Formation, which in this area has yielded graptolites as young as *Monograptus fritschi linearis* (identified by R. Thorsteinsson), and contains several corals of Devonian aspect, including what are believed to be some of the earliest species of *Radiastraea*. It is not surprising that boulders derived from it on Marshall Peninsula were at first believed to be Devonian (Thorsteinsson, 1958, p. 109). Evidence of its Pridolian age is based on its physical relationship to the Cape Phillips Formation, together with the occurrence of Silurian conodonts, identified by T. T. Uyeno, at the Rookery Creek outcrop. The only other specimens of *Prohexagonaria* known to the writer are one illustrated by Smith and Tremberth (1929, Pl. 8, fig. 1) from "Upper Silurian" strata at Norderstrand, Visby, Island of Gotland, and others from possible Ludlow beds of the western Urals (Sytova, 1952, Pl. 4, figs. 1, 2, 4).

Genus *Stereoxyloides* Wang, 1944, p. 24, 25

Type species. *Cyathophyllum (Heliophyllum) pseudodianthus* Weissermel, 1894, p. 591-594, Pl. 47, figs. 2, 3. Glacial drift. Bludzen near Goldap and Lauth, Germany.

Remarks. Corals of this genus are either dendroid or solitary; peripherally, their septa are dilated and strongly carinate, locally even retiform; major septa are long and may reach the axis, minor septa terminate



Figures 51. 18-51. 20

Stereoxylodes (Nanshanophyllum) sp. nov., x2.5. Figures 51. 18, 51. 19, GSC 45909. Figure 51. 20, GSC 45910. Both from the Devon Island Formation, 45.7 to 50.1 m (150-165 ft.) above base; Pridolian. Muskox Fiord, southern Ellesmere Island; UTM Zone 16, 492800 m E, 8492500 m N; GSC locality C-2688. Collected by R. Thorsteinsson, 1968.

near the inner margin of the dissepimentarium; dissepiments are numerous and the tabulae are normally differentiated into an elevated axial and periaxial series, and a downward-sloping peripheral series.

The type species is probably a colonial form. The name *Nanshanophyllum* is available for solitary forms and is accorded here subgeneric rank. The genus *Carinophyllum* Strel'nikov (1964, p. 59), which is based on *Cyathophyllum confusum* Pořta from the Ludlow Budnany Limestone of Czechoslovakia, is a possible synonym of *Stereoxylodes* (S.), although McLean (1975, p. 62) noted that it may deserve recognition at subgeneric level because of the profuse sclerenchymal thickening of the septa in the type species.

Subgenus *Stereoxylodes (Nanshanophyllum)* Yü, 1956, p. 601, 612, 613

Type species. *Nanshanophyllum typicum* Yü, 1956, p. 601, 602, 613, 614, Pl. 2, figs. 4-6. Chuan-Nau-Kou Series, "Middle Silurian". Chiyinkungtai, Chiuchüan, Kansu Province, China.

Remarks. This subgenus differs from *Stereoxylodes (Stereoxylodes)* in being solitary. Axial terminations of the major septa are expanded slightly in the type species, but this is believed to have no taxonomic significance at either generic or subgeneric level. Despite the binomial nomenclature used by Yü, he clearly indicated that *Nanshanophyllum* was being proposed as a subgenus of *Ptychophyllum*. *Stereoxylodes* differs from *Ptychophyllum* in having strongly carinate and less rotated septa, and typically two series of tabulae.

The genera *Ramulophyllum* Nikolaeva (1964, p. 52, 53) and *Ornatophyllum* Nikolaeva (1964, p. 57, 58) are probably synonymous with *Nanshanophyllum*.

Provided some latitude in the degree and type of carination is allowed in species assigned to *Nanshanophyllum*, their previously recorded distribution may be summarized as: upper Llandovery of New South Wales, Australia (McLean, 1975); "Middle" Silurian of Kansu Province, China; Ludlow of Czechoslovakia (Prantl, 1940), Estonia (Ivanovskiy, 1965) and Vaygach Island in the western Soviet Arctic (Sytova, 1970); and Pridolian of Podolia (Sytova, 1968). In addition, several species have been described from the Aynasuy Suite in the Karaganda Basin of Kazakhstan (Nikolaeva, 1964; Sytova and Ulitina, 1966) but the precise ages of these are not established.

The newly recognized Canadian occurrence of *Stereoxylodes (Nanshanophyllum)* is from 45.7 to 50.1 m (150-165 ft.) above the base of the Devon Island Formation, northwestern Devon Island. Evidence of its Pridolian age comes from its association with *Atrypella phoca* sensu Holtedahl not Salter, identified by J.G. Johnson, and *Hemiarges bigener* Bolton, identified by A.R. Ormiston, and from the occurrences of *Monograptus bohemicus tenuis* Bouček, 2.43 m (8 ft.) above the base of the formation, and *M. sp. aff. M. ultimus* Perner, 19.81 to 34.05 m (65-112 ft.) above the base of the formation. R. Thorsteinsson measured the section, collected the material and identified the graptolites.

The Devon Island specimens do not resemble closely any previously described forms and are best identified as *Stereoxylodes (Nanshanophyllum)* sp. nov.

References

- Crook, K. A. W.
1955: *Mazaphyllum*, a new cystiphyllid coral from the Silurian of New South Wales; *J. Paleontol.*, v. 29, p. 1052-1056.
- Duncan, H.
1956: Ordovician and Silurian coral faunas of western United States; *U. S. Geol. Surv., Bull.* 1021-F.
- Hill, D.
1940: The Silurian Rugosa of the Yass-Bowling district, N. W. S.; *Linn. Soc. New South Wales, Proc.*, v. 65, p. 388-420.
1956: Rugosa in *Treatise on invertebrate paleontology*, R. C. Moore, ed.; *Geol. Soc. Am. and Univ. Kansas Press, Pt. F, Coelenterata*, p. 233-324.
- Ivaniya, V. A., Kosareva, E. G., and Fedorovich, A. I.
1968: Novye materialy po faune devona Gornogo Altaya (rugozy); *Tomsk. Ordena Trud. Krach. Znamenii Gosudarst. Univ. im V. V. Kuybysheva, Trudy*, tom 202 (ser. geol.), p. 83-100.
- Ivanovskiy, A. B.
1965: Drevneyshie rugozy; *Akad. Nauk SSSR, Sib. Otdel., Izdatel. Nauka, Moskva*.
- Ivanovskiy, A. B. and Shurygina, M. V.
1975: Reviziya rugoz Urala; *Inst. Geol. i Geofiz., Akad. Nauk SSSR, Sib. Otdel., Trudy*, vyp. 218.
- Klapper, G. and Murphy, M. A.
1974: Silurian-Lower Devonian conodont sequence in the Roberts Mountains Formation of central Nevada; *Univ. California Publ., Geol. Sci.*, v. 111.
- Lang, W. D., Smith, S., and Thomas, H. D.
1940: Index of Paleozoic coral genera; *Brit. Mus. (Nat. Hist.)*, London.
- Lindström, G.
1883: Om de Palaeozoiska formationernas operkelbärande koraller; *Bihang Till Kongl. Svenska Vetensk.-Akad. Handlingar*, Bd. 7, no. 4, p. 1-112 (1882).
- McLean, R. A.
1974: Cystiphyllidae and Goniophyllidae (Rugosa) from the Lower Silurian of New South Wales; *Palaeontographica, Abt. A, Bd.* 147, p. 1-38.
1975: Lower Silurian rugose corals from central New South Wales; *Roy. Soc. New South Wales, J. and Proc.*, v. 108, p. 54-69.
- Merriam, C. W.
1974: Silurian rugose corals of the central and southwest Great Basin; *U. S. Geol. Surv., Prof. Paper* 777 (1973).
- Nikolaeva, T. V.
1964: Novye rugozy semeystva Ramulophyllidae iz silura tsentral'nogo Kazakhstana; *Vses. Nauchno-Issled. Geol. Inst. (VSEGEI), Trudy*, tom 93, p. 49-70.
- Prantl, F.
1940: Vyskyt rodu *Xylodes* Land & Smith (Rugosa) v ceském siluru; *Rozpravy České Akad.*, Tridy 2, roč. 50, p. 1-30.
- Reinson, G. E., Kerr, J. W., and Stewart, W. D.
1976: Stratigraphic field studies, Somerset Island, District of Franklin (58B to F); in *Report of Activities, Part A; Geol. Surv. Can., Paper* 76-1A, p. 497-499.
- Salter, J. W.
1852: Geology in *Journal of a voyage in Baffin's Bay and Barrow Straits, in the years 1850-1851, performed by H. M. ships "Lady Franklin" and "Sophia"...*, P. C. Sutherland; Longman, Brown, Green and Longmans, London, v. 2, p. ccxvii-ccxxxiii.
- Smith, S. and Tremberth, R.
1929: On the Silurian corals *Madreporites articulatus*, Wahlenberg, and *Madrepora truncata*, Linnaeus; *Ann. Mag. Nat. Hist.*, ser. 10, v. 3, p. 361-376.
- Spasskiy, N. Ya., Kravtsov, A. G., and Tsyganko, V. S.
1975: Kolonial'nye tsistimorfi in Drevnie Cnidaria, B. S. Sokolov, ed.; *Inst. Geol. i Geofiz., Akad. Nauk SSSR, Sib. Otdel, Trudy*, vyp. 201, tom 1, p. 170-172.
- Stasińska, A.
1967: Tabulata from Norway, Sweden and from the erratic boulders of Poland; *Palaeontol. Polonica*, no. 18.
- Stearn, C. W.
1956: Stratigraphy and palaeontology of the Interlake Group and Stonewall Formation of southern Manitoba; *Geol. Surv. Can., Mem.* 281.
- Strel'nikov, S. I.
1964: Ob ob'eme semeystva Kodonophyllidae (Rugosa); *Paleontol. Zhurnal*, 1964, no. 4, p. 49-60.
- Stumm, E. C.
1965: Silurian and Devonian corals of the Falls of the Ohio; *Geol. Soc. Am., Mem.* 93 (1964).
- Sytova, V. A.
1952: Korally semeystva Kyphophyllidae iz verkhnego silura Urala; *Paleontol. Inst., Trudy*, tom 40, p. 127-158.
1968: Tetrakorally skal'skago i borshchovskogo gorizontov Podolii in Siluriysko-devonskaya fauna Podolii, E. G. Balashov, ed.; *Izdatel' Leningrad Univ.*, p. 51-71.

- Sytova, V. A. (cont'd.)
 1970: Tetrakorally grebenskogo gorizonta Vaygacha in Stratigrafiya i fauna siluriyskikh otlozheniy Vaygacha (sbornik statey), S. V. Cherksova, ed.; Nauch.-Issledovatel. Inst. Geol. Arktiki, Leningrad, p. 65-86.
- Sytova, V. A. and Ulitina, L. M.
 1966: Rugozy isen'skoy i biotarskoy svit in Stratigrafiya i fauna siluriyskikh i nizhnede-
 vonskikh otlozheniy nurinskogo sinklinoriya, A. A. Bogdanov, ed.; Materialy po geol. Tsentral. Kazakhstan, Izdatel. Moskovskogo Univ., tom 6, p. 198-253.
- Thorsteinsson, R.
 1958: Cornwallis and Little Cornwallis Islands, District of Franklin, Northwest Territories; Geol. Surv. Can., Mem. 294.
- Wang, H. C.
 1944: The Silurian rugose corals of northern and eastern Yunnan; Geol. Soc. China, Bull., v. 24, p. 21-32.
- Weissermel, W.
 1894: Die Korallen des Silurgeschiebe Ostpreussens und des östlichen Westpreussens; Zeit. Deutsch. Geol. Gesell., Bd. 46, p. 580-674.
 1939: Neue Beiträge zur Kenntnis der Geologie, Palaeontologie und Petrographie der Umgegend von Konstantinopel, 3. Obersilurische und devonische Korallen, Stromatoporiden und Trepostome von der Prinzeninsel Antirovitha und aus Bithynien; Preuss. Geol. Landes., Abh., Neue Folge, Heft 190.
- Yü, C.-M.
 1956: Some Silurian corals from the Chiuchüan Basin, western Kansu; Acta Palaeontol. Sinica, v. 4, p. 599-609 (Chinese), 610-620 (English).

GENERA AND STRATIGRAPHIC DISTRIBUTION OF THE SILURIAN AND DEVONIAN RUGOSE CORAL FAMILY CYSTIPHYLLIDAE EDWARDS AND HAIME

Project 740108

R. A. McLean

Institute of Sedimentary and Petroleum Geology, Calgary

The Cystiphyllidae are important constituents of most of the world's carbonate faunas from Middle Llandovery to Givetian age. Because of the simplicity of their internal morphology and the considerable variability commonly found in a population of a single species, cystiphyllid taxonomy is especially problematical and considerable differences of opinion regarding it have been expressed in previous literature. The

following summary account attempts to stabilize generic identifications of the Cystiphyllidae for current and future publications of the Geological Survey of Canada. Ranges of the genera as presently known are shown in Figure 52.1.

Many of the problems raised in a review of the cystiphyllids are discussed in greater detail in a forthcoming study of the large cystiphyllid fauna of the Eifelian Hume Formation of northwestern Canada (McLean, in press). In the proposed classification, solitary and fasciculate forms with the same internal morphology are placed provisionally in the same genus, although there is no consistency of opinion on this practice. Generally, solitary and fasciculate Silurian cystiphyllids have been split generically, while comparable Devonian forms most commonly have been lumped. However, an extreme splitting classification of solitary and branching cystiphyllids has been proposed recently by Spasskiy *et al.* (1974). It is considered here to be more practical at present to group these forms, since frequently it is extremely difficult to determine whether a species is branching or not and the degree of development of offsets is highly variable.

	SILURIAN				DEVONIAN				
	Llandovery	Wenlock	Ludlow	Pridolian	Lochkovian	Pragian	Late Emsian	Eifelian	Givetian
<i>Cystiphyllum</i>	-----	-----	-----	-----	-----	-----	-----	-----
<i>Cystilasma</i>	-----	-----	-----	-----	-----	-----	-----	-----	-----
<i>Kymocystis</i>	-----	-----	-----	-----	-----	-----	-----	-----
<i>Microplasma</i>	-----	-----	-----	-----	-----	-----	-----	-----
<i>Dentilasma</i>	-----	-----	-----	-----	-----	-----	-----	-----	-----
<i>Hedstroemophyllum</i>	-----	-----	-----	-----	-----	-----	-----	-----	-----
<i>Holmophyllum</i>	-----	-----	-----	-----	-----	-----	-----	-----
<i>Holmophyllia</i>	-----	-----	-----	-----	-----	-----	-----	-----	-----
<i>Gyalophyllum</i>	-----	-----	-----	-----	-----	-----	-----	-----	-----
<i>Spinolasma</i>	-----	-----	-----	-----	-----	-----	-----	-----	-----
<i>Coronaruga</i>	-----	-----	-----	-----	-----	-----	-----	-----	-----
<i>Chavsakia</i>	-----	-----	-----	-----	-----	-----	-----	-----	-----
<i>Angullophyllum</i>	-----	-----	-----	-----	-----	-----	-----	-----	-----
<i>Mazaphyllum</i>	-----	-----	-----	-----	-----	-----	-----	-----
<i>Ningqiangophyllum</i>	-----	-----	-----	-----	-----	-----	-----	-----	-----
<i>Cystiphylloides</i>	-----	-----	-----	-----	-----	-----	-----	-----
<i>Coleophyllum</i>	-----	-----	-----	-----	-----	-----	-----	-----	-----
<i>Edaphophyllum</i>	-----	-----	-----	-----	-----	-----	-----	-----	-----
<i>Zonophyllum</i>	-----	-----	-----	-----	-----	-----	-----	-----	-----
<i>Loboplasma</i>	-----	-----	-----	-----	-----	-----	-----	-----	-----
<i>Mackenziephyllum</i>	-----	-----	-----	-----	-----	-----	-----	-----	-----
<i>Cayugaea</i>	-----	-----	-----	-----	-----	-----	-----	-----	-----
<i>Diplochone</i>	-----	-----	-----	-----	-----	-----	-----	-----	-----
<i>Digonophyllum</i>	-----	-----	-----	-----	-----	-----	-----	-----	-----
<i>Lekanophyllum</i>	-----	-----	-----	-----	-----	-----	-----	-----	-----
<i>Mesophyllum</i>	-----	-----	-----	-----	-----	-----	-----	-----	-----

----- range known;
 ----- range uncertain;
 known range in Canada.

Figure 52.1. Stratigraphic distribution of cystiphyllid genera (*Xiphelasma* is omitted as its range within the Silurian is not known; in addition, a possible Famennian species of *Microplasma* from Poland is recorded by Rozkowska, 1969).

Family CYSTIPHYLLIDAE Edwards and Haime, 1850

Diagnosis. Corallum solitary or compound. Septa consist of spines, either discrete or partially fused, based on either corallite wall, horizontal skeletal elements or both. Dissepiments are usually numerous and tabellae are commonly developed, generally being larger than the dissepiments. Tabulae, if present, are mainly flat or sagging, complete or incomplete.

Remarks. Two subfamilies are recognized here, the Cystiphyllinae M'Coy and Digonophyllinae Wedekind.

Subfamily CYSTIPHYLLINAE M'Coy, 1851

Diagnosis. Cystiphyllidae in which septal spines are either discrete or fused into "crusts", but do not form continuous, radial septal crests.

Remarks. The subfamily is discussed by McLean (in press).

Cystiphyllum Lonsdale, 1839

- Conophyllum* Hall, 1852
- Cysticonophyllum* Zaprudskaya and Ivanovskiy, 1962
- ?*Microconoplasma* Ivanovskiy, 1965

Type species. *Cystiphyllum siluriense* Lonsdale, 1839. Late Wenlock, England.

Diagnosis. Solitary or ?fasciculate corallum characterized by typically globose dissepiments and tabellae (or tabulae) differentiated into separate zones. Septa consist of short, holacanthine spines on the surfaces of the horizontal skeletal elements.

Remarks. The genus *Microconoplasma* Ivanovskiy, 1965 is inadequately known for its affinities to be determined with certainty, but it would appear to represent a phaceloid form of *Cystiphyllum* and is thus considered here to be a probable synonym of that genus.

Cystilasma Zaprudskaya and Ivanovskiy, 1962

Type species. *Cystilasma sibiricum* Zaprudskaya and Ivanovskiy, 1962. Late Llandoverly, Siberian Platform.

Diagnosis. Morphology as in *Cystiphyllum*, except for total lack of septal spines in late growth stages.

Remarks. *Nataliella* Sytova in Sytova and Ulitina, 1966 was originally considered as being closely related to *Cystilasma*, and later to *Chavsakia* Lavrusevich (Ivanovskiy, 1969; McLean, 1974). However, its large, flat, elongate dissepiments and narrow tabularium of sagging tabulae suggest that its affinities may be closer to *Neomphyma* Soshkina, which is either a spongophyllid or ptenophyllid; certainly it is not a cystiphyllid.

Kymocystis Strelnikov, 1968

Type species. *Kymocystis notabilis* Strelnikov, 1968. Late Wenlock, Chernyshev Ridge, western arctic U. S. S. R.

Diagnosis. Morphology as in *Cystiphyllum* except for dissepiments having an irregular, undulatory surface.

Remarks. *Kymocystis* is represented by undescribed material of Pridolian age from Cornwallis Island in the Canadian Arctic.

Microplasma Dybowski, 1874

Pseudomicroplasma Soshkina, 1949
? *Cystiplasma* Taylor, 1951
Nardoplasma Spasskiy and Kravtsov in Spasskiy et al., 1974

Type species. *Microplasma gotlandicum* Dybowski, 1874. Wenlock, Gotland.

Diagnosis. Corallum fasciculate or solitary. Septa, where apparent, represented as sparse, short spines confined to a thin, peripheral stereozone or occasionally developed on peripheral dissepiments. Horizontal skeletal elements as in *Cystiphyllum*.

Remarks. *Microplasma* differs from *Cystiphyllum* in having a predominance of septal spines developed at the corallite wall rather than on the dissepiments. The

genus *Cystiplasma* Taylor, 1951 requires further study but is most likely a synonym of *Microplasma*.

Dentilasma Ivanovskiy, 1962

Type species. *Dentilasma honorabilis* Ivanovskiy, 1962. Late Llandoverly, Siberian Platform.

Diagnosis. Corallum solitary or fasciculate. Septa consist of sparse, short spines on dissepimental surfaces. Horizontal skeletal elements comprise complete and incomplete, flat or slightly sagging tabulae and large dissepiments.

Hedstroemophyllum Wedekind, 1927

Hedstroemoplasma Spasskiy and Kravtsov in Spasskiy et al., 1974

Type species. *Hedstroemophyllum articulatum* Wedekind, 1927. Wenlock, Gotland.

Diagnosis. Corallum solitary or fasciculate. Septa consist of discrete spines piercing several dissepimental layers; their primary microstructure is monacanthine, although this is often modified by recrystallization to holacanthine. Coarse tabellae, less commonly tabulae, usually are developed axially.

Remarks. This genus is reviewed by Jell and Hill (1970) and McLean (1974).

Holmophyllum Wedekind, 1927

Nipponophyllum Sugiyama, 1940
Baeophyllum Hill, 1940
Dendroholmia Spasskiy and Kravtsov in Spasskiy et al., 1974

Type species. *Holmophyllum holmi* Wedekind, 1927. Late Ludlow, Gotland.

Diagnosis. Corallum solitary or fasciculate. Septa comprise long, discrete rhabdacanths (often recrystallized to holacanths) piercing several dissepiments or tabulae. Horizontal skeletal elements include peripheral dissepiments and a generally broad tabularium of flat or concave, complete and incomplete tabulae.

Holmophyllia Sytova, 1970

Type species. *Holmophyllia boreale* Sytova, 1970. Pridolian, Vaygach Island, arctic U. S. S. R.

Diagnosis. Corallum solitary or fasciculate. Septa comprise rhabdacanths partly fused vertically near periphery, becoming discrete toward the axis. Tabulae complete and incomplete, dissepiments very variable in shape and abundance.

Remarks. This genus differs from *Holmophyllum* only in the partial fusion of the trabeculae. It is possible

that *Gukoviphyllum* Sytova, 1968 is a senior synonym but the septal microstructure of that genus requires elucidation.

Gyalophyllum Wedekind, 1927

Type species. *Gyalophyllum angelini* Wedekind, 1927. Early Ludlow, Gotland.

Diagnosis. Corallum solitary. Septa comprise thick, long, tightly packed rhabdacanths, fused both radially and to a large extent vertically to occupy much of the corallite interior. Horizontal skeletal elements, where apparent, are comparable to those of *Cystiphyllum*.

Remarks. This genus shows perhaps greatest similarities to *Holmophyllia* in the fusion of the rhabdacanths, but their abundance and the weakness of the tabularium suggest that its separate status is justified. Jell and Hill (1970) have discussed and re-illustrated the holotype.

Spinolasma Ivanovskiy, 1965

Type species. *Spinolasma crossimarginalis* Ivanovskiy, 1965. Late Llandovery, Siberian Platform.

Diagnosis. Corallum solitary. Septa reduced to short, closely packed spines based largely on corallite wall and to a minor degree on adjacent dissepiments. Dissepiments small, in narrow peripheral zone, enclosing broad tabularium of flat or sagging complete and incomplete tabulae.

Remarks. The septal microstructure of the type species is preserved as holacanths, but from the illustration of Ivanovskiy (1965, p. 125, Fig. 77) they are probably recrystallized. Species previously referred to *Holmophyllum*, but possessing short rhabdacanthine spines at the periphery ("*H.*" *taltiense* Nikolaeva, 1949, sensu Shurygina, 1968, Lavrusevich, 1968, 1971a; "*H.*" *squamosum* Lavrusevich, 1960) appear most likely to be representative of this genus.

Coronoruga Strusz, 1961

Type species. *Coronoruga dripstonense* Strusz, 1961. Late Wenlock or early Ludlow, New South Wales.

Diagnosis. Corallum solitary. Septa represented by short trabeculae embedded in a narrow stereozone separating the tabularium and dissepimentarium, with minor occurrences of short spines on dissepiments and tabulae. Dissepiments generally are developed as in *Cystiphyllum*, tabulae are complete and incomplete, in arched series.

Remarks. The type material was reviewed by McLean (1975). The affinities of *C. paucisclerenchymata* Flügel in Flügel and Saleh, 1970 are unclear, but it appears not to be representative of that genus (Flügel and Saleh, 1970, Pl. 3, fig. 5, Pl. 4, fig. 5).

Chavsakia Lavrusevich, 1959

Type species. *Chavsakia chavsakiensis* Lavrusevich, 1959. ?Early Lochkovian, Tadzhikistan.

Diagnosis. Corallum solitary. Septa reduced to very short, sparse spines in peripheral region. Dissepiments and tabulae horizontally based, very large and irregularly shaped.

Remarks. This genus, known only from the type species, is an aberrant form and apparently endemic to central Asia (Zeravshan-Gissar Range of Tadzhikistan, *Chavsakia* Beds, ?early Lochkovian).

Xiphelasma Smith and Lang, 1931

Type species. *Tubiporites tubulatus* Schlotheim, 1813. Silurian, Gotland.

Diagnosis. Corallum cerioid or subcerioid. Septa occur as spines of moderate length, based mainly on dissepiments and corallite wall. Dissepiments occur in 1 or 2 unevenly developed rows lining corallite walls. Broad tabularium composed of flat or sagging, complete and incomplete tabulae.

Remarks. This genus was considered a synonym of *Storthygophyllum* Weissermel, 1894 by Hill (1956), but this author follows Lang *et al.* (1940) in suggesting that Weissermel's illustrated material probably comprises two species, one being the lectotype of *S. megalocystis* Weissermel and the other conspecific with *X. tubulatum* (Schlotheim). Pending revision of both *Storthygophyllum* and *Xiphelasma*, the latter genus is retained. Hill (*op. cit.*) also referred *Xiphelasma* to the family Tryplasmataidae, but the clear development of dissepiments (Smith and Lang, 1931, Pl. 2, figs. 1-5), suggests it has closer affinities with the cystiphyllids. The stratigraphic distribution of the type species is not known.

Angullophyllum McLean, 1974

Type species. *Angullophyllum warrisi* McLean, 1974. Late Llandovery, New South Wales.

Diagnosis. Corallum cerioid, characterized by broadly conical corallites in lateral contact. Septa consist of short, closely spaced trabeculae wrapped in sclerenchyme and occurring in layers on dissepimental and tabular crests and corallite walls. Tabularium is narrow with mainly complete, arched tabulae, while dissepiments are large and elongate.

Remarks. *Angullophyllum* is distinguished from *Mazaphyllum* by its growth form, shorter trabeculae in layers, development of trabeculae in the tabularium and arched tabulae.

Mazaphyllum Crook, 1955

Type species. *Mazaphyllum cortisjonesi* Crook, 1955.
?Wenlock, New South Wales.

Diagnosis. Corallum thamnasterioid. Septa comprise long, discrete spines piercing many dissepimental layers and generally showing marked radial alignment. Tabularia are narrow, consisting of flat, slightly arched or sagging series of complete and incomplete tabulae.

Remarks. The genus is not uncommon in strata of Wenlock-Ludlow age in Eastern Australia and is represented also in the middle part of the Read Bay Formation (?Pridolian) of Somerset Island in the Canadian Arctic.

Ningqiangophyllum Ke and Yü, 1974

Type species. *Ningqiangophyllum cystosum* Ke and Yü, 1974. Late Wenlock, China.

Diagnosis. Corallum aphroid. Septa apparently developed as short spines in sclerenchyme in layers on dissepiments and tabulae as in *Angulophyllum*. Tabularia are narrow, with flat or sagging, complete tabulae, and dissepiments are large and elongate.

Remarks. The affinities of this genus are not certain but it is likely a cystiphyllid. It shows similarities to *Angulophyllum*, but may be distinguished by its apparent lack of dividing corallite walls and shorter trabeculae which do not appear as the clear, radial rows in transverse section, characteristic of *Angulophyllum* and *Mazaphyllum*. The trabeculae seem to be developed most abundantly near the margin of the dissepimentarium and tabularium, giving a transverse section rather similar to that of the ketophyllid *Yassia* Jones, but the clear septal spines indicate its cystiphyllid affinities (Ke and Yü, 1974, Pl. 78, figs. 7, 8).

Cystiphyllodes Chapman, 1893

?*Bucanophyllum* Ulrich, 1886
Pseudozonophyllum Wedekind, 1924
Lythophyllum Wedekind, 1925
Paralythophyllum Wedekind, 1925
Nardophyllum Wedekind, 1925
Plagiophyllum Wedekind and Vollbrecht, 1931
Skoliophyllum Wedekind, 1937
Wedekindophyllum Stumm, 1949
?*Praenardophyllum* Spasskiy, 1955
?*Cladionophyllum* Stumm, 1961
Comanophyllum Flügel and Flügel, 1961
Patridophyllum Ulitina, 1968

Type species. *Cystiphyllum aggregatum* Billings, 1859. Late Emsian, Ontario.

Diagnosis. Corallum fasciculate or solitary. Septa developed as short, discrete spines and crusts of fused

trabeculae or "fibrous sclerenchyme", based mainly on dissepiments and to a minor degree on corallite wall. Short, discontinuous septal crests may be developed, but they do not form complete, radial septa in transverse section. Horizontal skeletal elements as in *Cystiphyllum*.

Remarks. A neotype of the type species is proposed by McLean (in press). Simpler forms of the genus may be particularly difficult to distinguish from *Cystiphyllum*, but they normally show a tendency toward development of dilated trabeculae not known in *Cystiphyllum*. *Bucanophyllum* Ulrich, 1886 and *Cladionophyllum* Stumm, 1961 are probably synonyms of *Cystiphyllodes*, differing only in rather aberrant growth form. *Praenardophyllum* Spasskiy, 1955 also is likely to be synonymous with *Cystiphyllodes*.

The genus is known from undescribed material of Pridolian age from Cornwallis Island in the Canadian Arctic.

Coleophyllum Hall, 1883

Type species. *Coleophyllum romingeri* Hall, 1883.
?Eifelian, Indiana-Kentucky.

Diagnosis. Like *Cystiphyllodes*, but horizontal skeletal elements reduced, corallite interior being almost entirely filled by closely packed septal crusts.

Remarks. This genus is tentatively separated from *Cystiphyllodes* on the basis of the abundance of septal crusts. However, further study is required to ascertain its variability.

Edaphophyllum Simpson, 1900

Type species. *Cystiphyllum bipartitum* Hall, 1882.
?Eifelian, Indiana-Kentucky.

Diagnosis. Like *Cystiphyllodes*, but having a very pronounced counter septum in the calice.

Remarks. Further study may show this genus to be synonymous with *Cystiphyllodes*. *Edaphophyllum irregularum* Mitchell and Driscoll, 1971 from the lower Arkona Formation (Givetian) of southwestern Ontario shows no significant differences from *Cystiphyllodes* and is referred to that genus (see Mitchell and Driscoll, 1971, Fig. 1).

Zonophyllum Wedekind, 1924

Legnophyllum Wedekind, 1924
Cystiphyllodes Yoh, 1937 (non Chapman, 1893)
Neozonophyllum Ulitina, 1968

Type species. *Zonophyllum duplicatum* Wedekind, 1924.
Early Eifelian, the Eifel, West Germany.

Diagnosis. Corallum solitary. Septal spines generally long, usually fused radially to some degree to form

weak crests, but not to the extent of consistently producing complete, radial septa in transverse section. Some dilation of trabeculae to form crusts may occur but is subordinate to formation of discrete spines and weak crests. Horizontal skeletal elements as in *Cystiphyllum*.

Remarks. The genus is mainly distinguished from *Hedstroemophyllum* by the fusion of the trabeculae and development of septal crusts. It is intermediate in morphology between *Cystiphyllodes* and *Lekanophyllum*. *Cystiphyllodes spinosum* McLaren in McLaren and Norris, 1964 from the Horn Plateau Formation (Givetian) of District of Mackenzie has longer septal spines than is characteristic of that genus and is perhaps better placed in *Zonophyllum* (McLaren and Norris, 1964, Pl. 9, figs. 1b, 2b).

Loboplasma Spasskiy, Kravtsov and Tsyganko, 1974

Type species. *Pseudomicroplasma multilobata* Spasskiy in Bulvanker et al., 1968. "Coblentian", southern Urals.

Diagnosis. Fasciculate or solitary corallum. Septa largely confined to broad peripheral stereozone, composed of dilated trabeculae in contact. Rare trabeculae may be developed on peripheral dissepiments. Horizontal skeletal elements as in *Cystiphyllum*.

Remarks. The genus is reviewed by Pedder and McLean (in prep.). It is distinguished from *Microplasma* by having coarse, dilated trabeculae in contact in the stereozone; it differs from *Cystiphyllodes* in having a pronounced stereozone and general rarity of trabeculae on the dissepiments. It comprises many species previously referred to *Pseudomicroplasma* Soshkina, 1949, the type species of which is most probably a representative of *Microplasma* and not congeneric with *P. multilobata*.

Mackenziephyllum Pedder, 1971

Zonastraea Tsyganko, 1972

Type species. *Mackenziephyllum insolitum* Pedder, 1971. Late Eifelian, Northwest Territories.

Diagnosis. Corallum aphroid, occasionally showing incipient corallite wall development. Septa represented only as sparse, short, discrete or partially fused spines. Radial septal crests not developed. Dissepiments large, globose to elongate, forming arched floors between tabularia. Tabulae similar in shape to dissepiments but generally in flat series.

Remarks. The genus differs from *Mazaphyllum* by having less pronounced tabularia and shorter, sparser spines.

Cayugaea Lambe, 1901

Type species. *Cayugaea whiteavesiana* Lambe, 1901. ?Late Emsian or Eifelian, Ontario.

Diagnosis. Corallum solitary. Septa developed mainly as a stereozone of variable width separating dissepimentarium and tabularium. Individual trabeculae are difficult to distinguish in stereozone but sparse short spines are developed also on dissepimental surfaces. Dissepiments are large, strongly elongate and in steeply inclined layers. Tabularium is occupied by a strongly sagging series of coarse, incomplete tabulae and tabellae.

Remarks. The author has examined the type material of *Cayugaea whiteavesiana* and the septal microstructure is largely obscured by recrystallization. In some places, faint outlines of bundles of fibres normal to dissepimental surfaces in the stereozone may be discerned, comparable to the structure in some specimens of *Cystiphyllodes aggregatum* (see McLean, in press). The genus appears similar to *Coronoruga*, differing in the nature of the tabulae and weaker development of trabeculae in the stereozone of *Cayugaea*. *Cayugaea secunda* Lavrusevich, 1971 from the Kunzhak Horizon (?Pridolian or Lochkovian) of the Northern Zeravshan Range of Tadzhikistan has a tabularium more like that of *Coronoruga* (Lavrusevich, 1971b, Pl. 6, figs. 1-4) and is probably a representative of that genus.

Diplochone Frech, 1886

Type species. *Diplochone striata* Frech, 1886. Givetian, Rhineland, West Germany.

Diagnosis. Corallum solitary. Septa not apparent in interior of corallite in type species. Dissepiments irregularly developed in one or two rows, strongly elongate, lining corallite wall. Tabulae occupy most of corallite interior, complete and incomplete, in strongly sagging series.

Remarks. Doubts have been expressed as to whether *Diplochone* is in fact a cystiphyllid (e.g. Birenheide, 1964, 1974), but its cystiphyllid affinities are indicated by forms such as *D. sachaninensis* Kravtsov, 1966, which develop weak septal crusts (Kravtsov, 1966, Pl. 7, fig. 2). It differs from *Cayugaea* largely in the absence of the stereozone.

Subfamily DIGONOPHYLLINAE Wedekind, 1923

Diagnosis. Cystiphyllidae in which the trabeculae are fused radially and vertically to produce the appearance of largely complete radial septa in transverse section. Horizontal skeletal elements are comparable to those of *Cystiphyllum*.

Remarks. This subfamily seems to be a late Early to Middle Devonian offshoot of the main cystiphyllinid stock. To a large extent, it includes forms referred to the subgenus *Mesophyllum* (*Mesophyllum*) Schlüter by Birenheide (1964, 1974).

Digonophyllum Wedekind, 1923

Type species. *Digonophyllum schulzi* Wedekind, 1923. Early Eifelian, the Eifel, West Germany.

Diagnosis. Corallum solitary. In neanic stage, trabeculae are strongly dilated, fused to a variable degree and frequently fill a large portion of the corallite. In ephebic stage, septal crests are strongly developed, forming largely complete, radial septa with dilation confined to the axial region.

Remarks. Transitional forms to *Cystiphyllodes* and *Lekanophyllum* occur. *Zaphrentis recta* Meek, 1867 and *Cysteophyllum americanum* var. *arcticum* Meek, 1867 from the Hume Formation (late Eifelian) of District of Mackenzie are conspecific representatives of *Digonophyllum*.

Lekanophyllum Wedekind, 1924

Atelophyllum Wedekind, 1925

Dialytophyllum Amanshauser in Wedekind, 1925

Hemicystiphyllum Wedekind, 1925

?*Zonodigonophyllum* Vollbrecht, 1926

?*Pseudodigonophyllum* Spasskiy, 1960

?*Asperophyllum* Spasskiy in Dubatolov and Spasskiy, 1964

?*Aculeatophyllum* Zhavoronkova in Strelnikov and Zhavoronkova, 1972

Scissoplasma Spasskiy and Kravtsov in Spasskiy et al., 1974

Type species. *Lekanophyllum punctatum* Wedekind, 1924. Middle Eifelian, the Eifel, West Germany.

Diagnosis. Solitary or branching coralla. Septal crests commonly well developed throughout, particularly in ephebic stage where they form largely complete, radial septa whose axial trabeculae lack significant dilation. Neanic septal dilation is generally minor or absent.

Remarks. This genus is distinguished from *Digonophyllum* on the basis of the absence or only weak development of neanic septal dilation, together with a general lack of axial septal dilation in the ephebic stage. The type species of *Zonodigonophyllum* Vollbrecht, 1926 (*Z. primum*) is probably a representative of *Lekanophyllum*, although the other species referred to *Zonodigonophyllum* by Vollbrecht belong to *Digonophyllum*. *Asperophyllum* Spasskiy in Dubatolov and Spasskiy, 1964 and *Aculeatophyllum* Zhavoronkova in Strelnikov and Zhavoronkova, 1972 require further study but may be synonyms of *Lekanophyllum*. Forms transitional to *Zonophyllum* occur,

although the latter has consistently weaker and more discontinuous septa than is typical for *Lekanophyllum*.

Of described Canadian species, *Actinocystis variabilis* Whiteaves, 1892 from the Winnipegosis Formation (Early-Middle Givetian) of southwestern Manitoba may belong to *Lekanophyllum*, but the type material is too poorly preserved for accurate determination. However *Lekanophyllum* is represented by undescribed material from the Elm Point Formation (probably early Givetian part) of the same region.

Mesophyllum Schlüter, 1889

?*Cosmophyllum* Vollbrecht, 1922

?*Mochlophyllum* Wedekind, 1923

Arcophyllum Markov, 1926

Hemicosmophyllum Wedekind and Vollbrecht, 1931

?*Pseudocosmophyllum* Wedekind and Vollbrecht, 1931

?*Uralophyllum* Soshkina, 1936

Type species. *Actinocystis defecta* Schlüter, 1882 (= *Cyathophyllum vesiculosum* Goldfuss, 1826; see Birenheide, 1964). Early Givetian, the Eifel, West Germany.

Diagnosis. Solitary or fasciculate corallum. Septal development as in *Lekanophyllum* except for the presence of abundant peripheral discrete carinae.

Remarks. The pronounced development of discrete carinae in the region of presepiments distinguishes this genus from both *Lekanophyllum* and *Digonophyllum*, which at most show only very rare discrete carinae. In the Eifel material described by Birenheide (1964), this feature seems rather variable, but elsewhere it appears to be a useful distinguishing criterion. *Pseudocosmophyllum* Wedekind and Vollbrecht, 1931 and *Cosmophyllum* Vollbrecht, 1922 are probably also synonyms of *Mesophyllum*, while *Mochlophyllum* Wedekind, 1923 and *Uralophyllum* Soshkina, 1936 have some axial septal dilation, but require further study to see if they should be separated from *Mesophyllum*.

Acknowledgments

The author is grateful to A.E.H. Pedder, B.S. Norford, and W.A. Oliver, Jr. for critical review of the manuscript.

References

Birenheide, R.

1964: Die "Cystimorpha" (Rugosa) aus dem Eifeler Devon; Senckenberg. Naturforsch. Ges., Abh. 507.

1974: Zur Herkunft der devonischen cystimorphen Rugosa; Senckenbergiana Lethaea, Bd. 54, p. 453-473.

Flügel, H.W. and Saleh, H.

1970: Die paläozoischen Korallenfaunen Ost-Irans. I. Rugose Korallen der Niur-Formation (Silur.); Jahrb. Geol. Bundesanst., Bd. 113, p. 267-302.

- Hill, D.
1956: *Rugosa* in Treatise on Invertebrate Paleontology, Part F. Coelenterata, R. C. Moore, ed.; Geol. Soc. Am., and Univ. Kansas Press, Lawrence, Kansas, p. F233-F324.
- Ivanovskiy, A. B.
1965: *Drevneyshie rugozy*; "Nauka", Moscow.
1969: *Korally semeystv Tryplasmataidae i Cyathophylloidaidae (rugozy)*; "Nauka", Moscow.
- Jell, J. S. and Hill, D.
1970: The Devonian coral fauna of the Point Hibbs Limestone, Tasmania; R. Soc. Tasmania, Pap. Proc., v. 104, p. 1-16.
- Ke, C. C. and Yü, C. M.
1974: Silurian corals in A handbook of the stratigraphy and paleontology in southwest China, Nanking Institute of Geology and Paleontology, ed.; Science Press, Nanking, p. 165-173 (in Chinese).
- Kravtsov, A. G.
1966: *Rannedevonskie i eifelskie chetyrekhluchevie korally yuzhnogo ostrova Novoy Zemli (valnevskiy gorizont)*; Nauch.-Issled. Inst. Geol. Arktiki, Uch. Zap., Paleontol. Biostratigr., vyp. 16, p. 22-63.
- Lang, W. D., Smith, S., and Thomas, H. D.
1940: Index of Palaeozoic coral genera; Brit. Mus. (Natur. Hist.); London.
- Lavrusevich, A. I.
1968: *Rugozy postludlovskikh otlozheniy r. Zeravshan (Tsentralny Tadzhikistan) in Biostratigrafiya pogranychnykh otlozheniy silura i devona*, B. S. Sokolov and A. B. Ivanovskiy, eds.; "Nauka", Moscow, p. 102-130.
1971a: *Cheshuychatye rugozy tsentralnogo Tadzhikistana in Rugozy i stromatoporoidei paleozoya SSSR*, A. B. Ivanovskiy, ed.; II Vses. simp. izuch. iskopaemykh korallorov SSSR, Tr., vyp. 2, "Nauka", Moscow, p. 32-41.
1971b: *Nekotorye rugozy iz pozdnesiluriyskikh i rannedevonskikh otlozheniy tsentralnogo Tadzhikistana in Paleontologiya i stratigrafiya*, A. I. Lavrusevich, ed.; Uprav. geol. sov. minist. Tadzhik SSR, Tr., vyp. 4, p. 33-52.
- McLaren, D. G. and Norris, A. W.
1964: Fauna of the Devonian Horn Plateau Formation, District of Mackenzie; Geol. Surv. Can., Bull. 114.
- McLean, R. A.
1974: *Cystiphyllidae and Goniophyllidae (Rugosa) from the Lower Silurian of New South Wales*; Palaeontographica, Abt. A, Bd. 147, p. 1-38.
1975: *Silurian rugose corals from the Mumbil area, central New South Wales*; Linn. Soc. N. S. W., Proc., v. 99, p. 181-196.
Middle Devonian cystiphyllid corals from the Hume Formation, northwestern Canada; Geol. Surv. Can., Bull. (in press)
- Mitchell, S. W. and Driscoll, E. G.
1971: *Edaphophyllum irregularum*, a new Middle Devonian digonophyllid coral from the lower Arkona Formation, Ontario, Canada; Ohio J. Sci., v. 71, p. 309-312.
- Pedder, A. E. H. and McLean, R. A.
Lower Devonian cystiphyllid corals from North America and Eastern Australia, with notes on the genus *Utaratuia*. (in prep.)
- Rozkowska, M.
1969: *Famennian tetracoralloid and heterocoralloid fauna from the Holy Cross Mountains (Poland)*; Acta Palaeontol. Pol., v. 14, p. 5-187.
- Shurygina, M. V.
1968: *Pozdnesiluriyskie i rannedevonskie rugozy vostochnogo sklona severnogo i srednogo Urala in Korally pogranychnykh sloev silura i devona Altae - Sayanskoy gornoy oblasti i Urala*, A. B. Ivanovskiy, ed.; "Nauka", Moscow, p. 117-150.
- Smith, S. and Lang, W. D.
1931: *Silurian corals - the genera Xiphelasma, gen. nov. and Acervularia Schweigger*, with special reference to *Tubiporites tubulatus* Schlotheim, and *Diplophyllum caespitosum* Hall; Ann. Mag. Natur. Hist., ser. 10, v. 8, p. 83-94.
- Spasskiy, N. Ya, Kravtsov, A. G., and Tsyganko, V. S.
1974: *Kolonnalnye Tsistimorfy in Drevnie Cnidaria*, Tom I, B. S. Sokolov, ed.; Akad. Nauk SSSR, Sib. Otd., Inst. Geol. Geofiz., Tr., vyp. 201, p. 170-172.

Project 680081

A. Dicaire, T.R. Flint, H.W.C. Knapp, D. Olson, and P. Sawatzky
Resource Geophysics and Geochemistry Division

During the summer of 1975, the Gradiometer system that had been installed in the Queenair was test flown and operated. To make this possible, the aeromagnetic instrumentation group who are located in the Alert Hangar at Ottawa airport had to design and build the necessary systems to operate both of the required high sensitivity magnetometers simultaneously.

The total system was installed and test flown during the winter of 1974-75. The first problem that had to be overcome was the very basic one of compensating the two magnetometers when both were operating. Because there was no precedent, a method had to be devised that would lead to a degree of success. The compensation was initially carried out by first compensating each system separately, and then repeating the procedure with both operating. The basic procedure followed when compensating an airborne magnetometer installation

that is equipped with CAE's nine- or sixteen-term (AN/ASA-65) compensators is as follows:

1. Select an area with relatively little air traffic.
2. The area should be magnetically flat and preferably large so that it is possible to remain on a desired heading for some time.
3. The area should be close to an airport so that as little time as possible is wasted in ferrying.
4. Fly the aircraft at about 10 000 feet to get away from near surface anomalies.
5. Fly the aircraft on the four cardinal headings.
6. While on each of these headings, the pilot should perform the following pure manoeuvres:

(a) Rolls — a back and forth rocking manoeuvre about the longitudinal axis of the aircraft about $\pm 10^\circ$ in magnitude.

(b) Pitches — a nose up and nose down manoeuvre about the Transverse axis of the aircraft about $\pm 10^\circ$ in magnitude.

(c) Yaws — a left to right manoeuvre about the Vertical axis of the aircraft, about $\pm 10^\circ$ in magnitude.

(d) the period of the manoeuvres should be between two and five seconds.

7. While the aircraft is Rolling back and forth, the terms affected are the Vertical and Transverse. These are engaged on the compensator, one at a time, and the results observed on an analogue recorder until the manoeuvre-induced signal has reached a minimum value. The terminology used is to "run in" the compensating value.
8. While the aircraft is Pitching, the terms affected, the Vertical and Longitudinal components are "run in".
9. While the aircraft is Yawed, the terms affected, Transverse and Longitudinal components are "run in". This manoeuvre is generally omitted because the affected terms have already been dealt with.
10. While these manoeuvres are being performed a set of work sheets are filled out, see the attached Figures 53.1, 53.2.

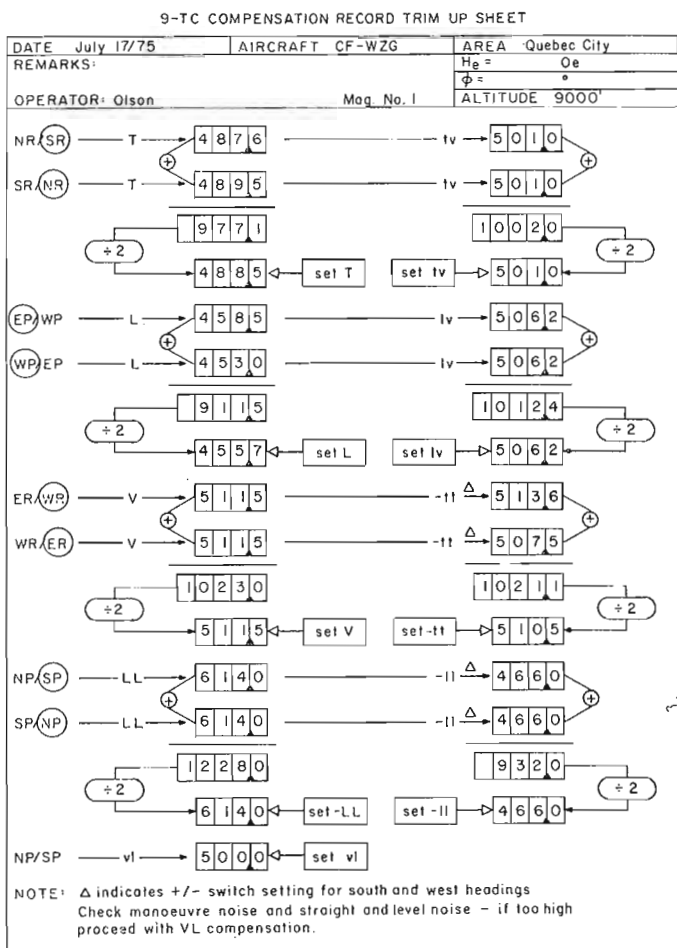


Figure 53.1. Compensator settings for Mag. no. 1.

Obtaining a figure of merit for the system was similar to compensating the system. The procedure used was as follows:

1. Fly the aircraft at about the 10 000-foot altitude over an area that is magnetically flat.
2. Fly the aircraft on the four cardinal headings.
3. Cause the aircraft to perform the three compensating manoeuvres while on each of the cardinal headings.
4. Note the amount of manoeuvre noise caused by each manoeuvre, and enter it on the special work sheet, Figure 53. 3.
5. After completing these manoeuvres there should be 12 entries for each magnetometer. Sum these 24 separate entries to obtain the worst case error signal. This is the combined figure of merit for the system (Fig. 53. 3).

Another method used to obtain the combined figure of merit was to monitor the manoeuvre effect on the Difference output of the combined Gradiometer system (Fig. 53. 4).

The gradiometer system was tested by flying several areas in the vicinity of Ottawa.

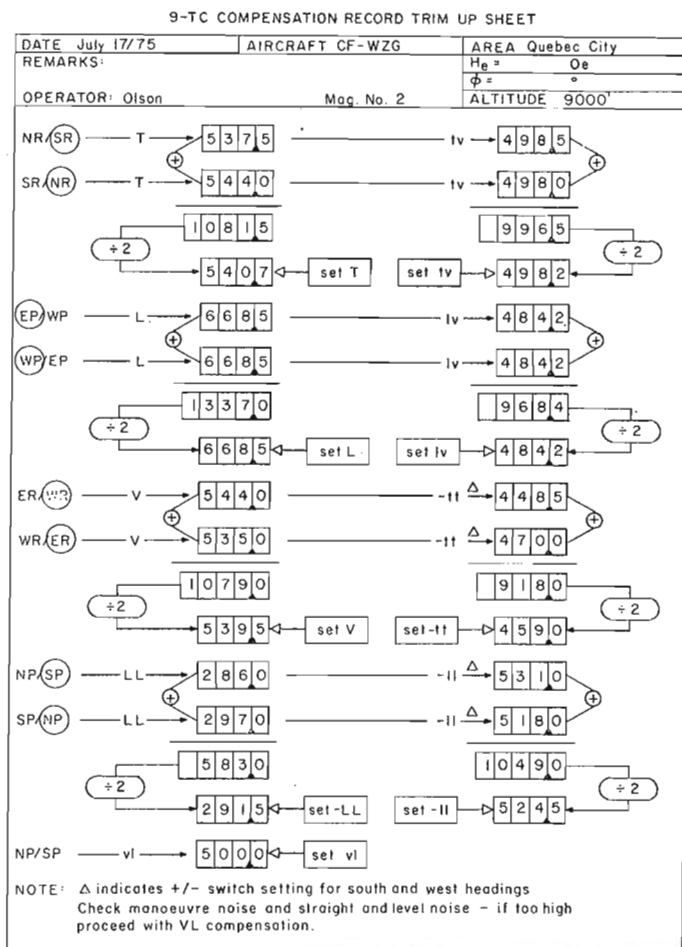


Figure 53.2. Compensator settings for Mag. no. 2.

1. The White Lake area was flown at two altitudes, 500 feet and 1000 feet above terrain. At each altitude the area was flown in two directions, North/South and East/West. The line spacing in each case was 500 feet. This test was to see what altitude would best show up the fine detail known to exist in this area (see Fig. 53.5).
2. The Carleton Place area was flown at an altitude of 500 feet above the terrain, also in both directions.
3. A test area close to Bourget, just east of Ottawa, was surveyed in great detail both horizontally and vertically, by flying the same path over the ground at various altitudes. It is proposed to use the Bourget aeromagnetic calibration range to check the accuracy of air-borne magnetometer systems.

Besides these tests, the high resolution magnetometer system was used to obtain additional data to be used to prepare a composite magnetic map of Canada. For this purpose, loops were flown that crossed older surveys that had been conducted previously by various aerial survey companies. This information should help to bring these surveys to a common base.

MAG. COMPENSATION FLIGHT RECORD - PERM/IND/EDDY COMP. INFORMATION											
DATE: July 17/75											
REMARKS: 9 TERM				AIRCRAFT: CF-WZG				AREA: Quebec City			
		No. 1		No. 2		No. 1		No. 2			
		INITIAL SETTINGS		FIRST TRIM-UP		SECOND TRIM-UP					
PERM	T	498.3	527.5	T	488.5	540.7	T				
	L	463.9	652.4	L	455.2	668.5	L				
	V	504.7	530.4	V	511.5	539.5	V				
INDUCED	-TT			-TT			-TT				
	LT			LT			LT				
	-LL	605.0	308.2	-LL	614.0	291.5	-LL				
	VL			VL			VL				
	TV			TV			TV				
EDDY	-II	509.3	465.9	-II	510.5	459.0	-II				
	II			II			II				
	Iv	497.5	509.5	Iv	501.0	498.2	Iv				
	iv	513.8	478.0	iv	506.2	484.2	iv				
	vi			vi			vi				
	vv			vv			vv				
	±II	468.0	528.5	II	466.0	524.5	II				
vi	500.0	500.0	vi	500.0	500.0	vi					
ESTIMATED STRAIGHT AND LEVEL NOISE .01											
FIGURE OF MERIT Mag No.1						FIGURE OF MERIT Mag No.2					
	N	S	E	W	TOTAL		N	S	E	W	TOTAL
ROLL	.10	.08	.14	.20	.52	ROLL	.08	.15	.12	.08	.43
PITCH	.04	.03	.02	.02	.11	PITCH	.14	.10	.08	.02	.34
YAW	.08	.01	.02	.08	.19	YAW	.08	.06	.08	.06	.28
TOTAL	.22	.12	.18	.30	.82	TOTAL	.30	.31	.28	.16	1.05
COMBINED 1.87											
Signature of operator: OLSON											

Figure 53.3. Work sheet, to obtain figure of merit.

MAG. COMPENSATION FLIGHT RECORD - PERM/IND/EDDY COMP. INFORMATION											
DATE: July 17/75											
REMARKS: 9 TERM			AIRCRAFT: CF-WZG			AREA: Quebec City					
PERM	INITIAL SETTINGS			FIRST TRIM-UP			SECOND TRIM-UP				
	T			T			T				
	L			L			L				
INDUCED	V			V			V				
	-TT			-TT			-TT				
	LT			LT			LT				
	-LL			-LL			-LL				
	VL			VL			VL				
EDDY	TV			TV			TV				
	-II			-II			-II				
	II			II			II				
	Iv			Iv			Iv				
	IV			IV			IV				
	vI			vI			vI				
	VV			VV			VV				
	II			II			II				
	VI			VI			VI				
	ESTIMATED STRAIGHT AND LEVEL NOISE										
FIGURE OF MERIT No.1					FIGURE OF MERIT No.2						
	N	S	E	W	TOTAL		N	S	E	W	TOTAL
ROLL	.12	.08	.12	.12	.44	ROLL					
PITCH	.08	.08	.08	.08	.32	PITCH					
YAW	.08	.08	.08	.08	.32	YAW					
TOTAL	.28	.24	.28	.28	1.08	TOTAL					
Signature of operator: OLSON											

Figure 53.4. Work sheet, to obtain figure of merit using difference output.

During the course of last summer's operation, it was found that there still were some problems in the gradiometer system. These were:

1. Mechanical:

It was found that the vibration of the top boom during periods of high turbulence was considerably greater than had been expected, and was ruining the self-orienting head. This was reduced by not flying during peak periods of turbulence, and by cushioning the sensing head.

2. Electrical:

Operating two high sensitivity magnetometer systems in close proximity created problems that had not been foreseen. These were especially difficult to locate in the servo systems that controlled the orientation of the sensors.

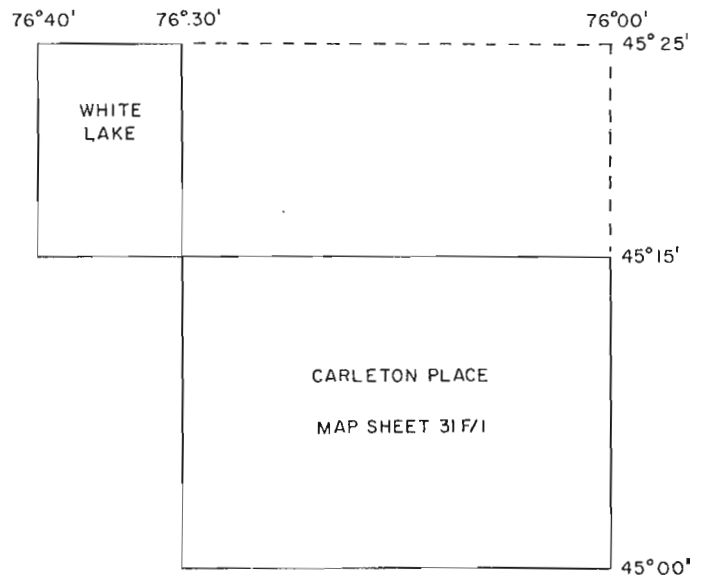


Figure 53.5. Gradiometer test areas.

3. Temperature:

Many of the components that had been used were of the ordinary industrial type. The majority of these just would not operate satisfactorily during the extremes of temperature that were encountered. Attempts were made to cure these last two problems, but not always with the desired degree of success, due to the work load and lack of time. Some of the temperature problems were solved by using military type components that were available on short notice, but for most of these delivery was slow.

Last fall when the aircraft was on its way to Victoria, British Columbia a refueling stop was made in Winnipeg, Manitoba. During the course of the landing, the main undercarriage collapsed. No one was hurt and the damage to the aircraft was not serious in the sense that it was repairable. A contract to accomplish this was let to CAE in Winnipeg, and the aircraft was originally expected to return by January 15, 1976. Due to the slow delivery of parts this has now been delayed to the latter part of March 1976.

After the accident, the survey equipment was all removed from the aircraft and returned to Ottawa for a thorough check out. The faults in the system that were noted above have been tracked down and repaired. In addition the digital data system has been upgraded. This group feels that the time spent on the equipment should result in much better data during the coming summer.

Project 710091

W. S. Hopkins, Jr. and A. R. Sweet
Institute of Sedimentary and Petroleum Geology, CalgaryIntroduction

During September 1975, a day was spent obtaining comparative palynological sample material of late Eocene or early Oligocene age from sections of the Kishenehn Formation from which Russell (1964) had recovered invertebrate and vertebrate remains.

Kishenehn Formation

The Kishenehn Formation is poorly and intermittently exposed in the valley of the Flathead River of south-eastern British Columbia and north-central Montana. According to Jones (1969), this unit is about 4760 m (15 600 ft) thick and is composed of some 2621 m (8600 ft) of fine grained, largely lacustrine deposits overlain by about 2137 m (7000 ft) of conglomerate and breccia. The formation was deposited in a half graben on the west side of the Flathead Fault, and apparently was deposited contemporaneously with the faulting. For further details on the geology of this unit, the reader is referred to Price (1965) and Jones (1969). The latter paper contains a complete bibliography of relevant papers.

Samples

Eight samples of dark grey, grey and greenish grey mudstone collected from the south end of the outcrop at Russell's locality E4 and four samples of mudstone collected immediately downstream from Russell's locality E3 proved to be nearly barren of indigenous palynomorphs. (Some reworked Early Cretaceous or Jurassic miospores and, from one sample, megaspores similar to those found in the Kootenay Formation were recovered.) However, samples from a section whose base conforms approximately to the base of the section at Russell's locality C4, and which extends to encompass the limestone and marl beds of his locality C3, were found to contain a well-preserved and diverse microflora. This section, located on Couldrey Creek at 49°02'45"N, and 114°32'30"W, is only about 61 m (200 ft) thick, but was examined and sampled in detail. The base of the section lies about 896 m (2939 ft) above the base of the Kishenehn Formation and about 3846 (12 609 ft) below the top (see Jones, 1969). Consequently, the following discussion refers to a sampled interval which is only slightly more than one per cent of the total formation thickness.

Palynology

From the above section (GSC locs. C-47888 to C-47899), 12 samples of varying lithologies were processed using standard palynological techniques. The lower 11 m (36 ft) of section were completely exposed and consisted from bottom to top of: 1.5 m (5 ft) of bentonitic mudstone, 1 cm of coal, 2.5 m (8 ft) of grey mudstone, 0.5 m (1.5 ft) of coal — referred to as 1 foot of lignite by Russell (1964) (subbituminous C, pers. comm., P. R. Gunther), 4.5 m (15 ft) of fissile shale and 2 m (6.5 ft) of grey mudstone. The next approximately 50 m (164 ft) of section were mostly covered and appeared to consist of shale and mudstone with intercalated beds of marl. A sample of brown shale from 10 m (32 ft) above the top of the main exposure and a sample of black shale from the top of the section were collected. One limestone and one marl sample were collected also from blocks washed out of the creek bank. Of the above, only the limestone and bentonitic mudstone were barren of miospores whereas only the sample of black shale from the top of the section, the 0.5 m (1.5 ft) coal and the 1 cm coal yielded significant numbers of seeds and megaspores. The following is a combined microfloral list from the entire 61 m (200 ft).

Division LYCOPODOPHYTA

Family LYCOPODIACEAE

Lycopodium sp.

Division PTEROPHYTA

Family POLYPODIACEAE

Laevigatosporites sp.

Family OSMUNDACEAE

Osmunda sp.

Family AZOLLACEAE

Azolla sp. (megaspores only)

Family SALVINIACEAE

Salvinia spp. (megaspores only)

Division GNETOPHYTA

Family EPHEDRACEAE

Ephedra sp.

Division CONIFEROPHYTA

Family TAXODIACEAE

Glyptostrobus sp.

Taxodium sp.
 cf. *Metasequoia* sp.
 Family PINACEAE
 Pinus sp.
 Picea sp.
 Tsuga sp.
 Family PODOCARPACEAE
 cf. *Podocarpus* sp.
 Division ANTHOPYTA
 Class MONACOTYLEDONAE
 Family TYPHACEAE
 Typha spp. (pollen and seeds)
 Family LILIACEAE
 Class DICOTYLEDONAE
 Family ONAGRACEAE
 ? *Boisduvalia* sp.
 Family CARPINACEAE
 Carpinus sp.
 Family CORYLACEAE
 Corylus sp.
 Family BETULACEAE
 Alnus sp.
 Betula sp.
 Family NYSSACEAE
 Nyssa sp.
 Family JUGLANDACEAE
 Carya sp.
 Engelhardtia sp.
 Juglans sp.
 Pterocarya sp.
 Family ACERACEAE
 Acer sp.
 Family FAGACEAE
 Castanea sp.
 Fagus sp.
 Quercus sp.
 Family of LORANTHACEAE
 Family ALTINGIACEAE
 Liquidambar sp.
 Family SALICACEAE
 Salix sp.

Family TILIACEAE
 Tilia sp.
 Family ERICACEAE
 Family ULMACEAE
 Ulmus sp.
 Family NYMPHAECEAE
 cf. *Nuphar* sp.
 Incertae sedis
 Tricolpites sp.
 Triporopollenites sp.
 Sigmopollis sp.

Division CHLOROPHYTA (green algae)
 Pediastrum sp.

Most of the *Typha* seeds agree closely in size and shape with those of *T. latissima* A. Br. known from the Oligocene of England and western Siberia (Dorofeev, 1963a). A few specimens of *Typha elongata* Dorofeev, 1963b, an Oligocene species from Kazakhstan identifiable by its oblong, flask-like shape, also were found. Of the over 500 specimens of *Salvinia* megaspores recovered, the majority are greyish brown, and from 250 μ to 300 μ in diameter. Their surfaces are covered with intersecting corrugations forming a coarse reticulum and the proximal, trilobate extension characteristic of *Salvinia* is subdued. The associated microsporangia are oval in outline and average 216 μ by 186 μ (50 specimens) in size. These specimens appear closely allied with *Salvinia maeotica* Dorofeev, 1968, from the upper Miocene of the Ukraine. Five specimens, slightly larger, white, and ornamented by elongate rugulae, were recovered also. These appear identifiable with *Salvinia turgaica* Dorofeev, 1963b, from the lower and middle Oligocene and possibly Eocene of western Siberia. All the above specimens are referable to *Salvinia* Section *Cerebrata* Dorofeev, 1963a, whose age range extends from the Eocene to the Holocene. Fewer specimens of *Azolla* than of *Salvinia* were recovered. The *Azolla* megaspores appear similar to, but not identical with, the Eocene species *Azolla primaeva* from central British Columbia.

Environment of deposition

The entire measured section appears to be composed of marsh and lacustrine deposits; apparently this is characteristic of the entire lower member (Jones, 1969). The microflora, therefore, largely represents the vegetation which grew along the lake shores and, to a lesser extent, the valley sides and along the streams draining into the lakes. The principal family, based on pollen abundance, would be the Juglandaceae (*Carya*, *Engelhardtia*, *Juglans*, *Pterocarya*). Pollen from these four genera is exceedingly abundant, and presumably indicates that these plants comprised a

major element of the flora. In present-day settings these plants are confined to stream sides, flood plains and, at times, the lower levels of valley slopes. Other families such as the Typhaceae, Taxodiaceae, Ulmaceae, Nymphaeaceae and Osmundaceae, all of which are comparatively abundant in the pollen record, probably also made up a substantial portion of the lowland vegetation. As the occurrence of *Typha* (seeds) and *Salvinia* and *Azolla* megaspores was almost entirely restricted to either carbonaceous shale or coal, these plants probably occupied open marshes bordering the lake. In the lacustrine environment, the algae *Pediastrum* must have been common.

The lowland temperatures must have been warm because the Juglandaceae, Taxodiaceae and Altingiaceae all require at least 18-20°C mean July temperatures (Wolfe and Leopold, 1967; Pabst, 1968). *Englhardtia*, which is represented abundantly in the pollen diagram, is even more specific (Leopold and Macginitie, 1972), requiring a considerable total heat (ET 18-20°C). All of the above groups are warm-temperate to tropical in modern distribution, requiring abundant moisture, and comparatively dry but warm winters.

A second component of the floral assemblage consists of those genera such as *Picea*, *Tsuga*, *Betula* and *Alnus*, which occur at a reduced frequency and require temperate to warm-temperate conditions. As their comparative rarity suggests a distant source, these genera presumably occupied the highlands to the east of the Flathead Fault which were being elevated continuously and acted as a sediment source. *Ephedra*, which also occurs in low frequency, probably was derived from plants growing in dry locations, possibly on the leeward slope of the mountains.

Age

Although the combined fauna obtained by Russell (1964) from the Kishenehn Formation indicated a late Eocene-early Oligocene age, a precise dating of his sections C3 and C4 is less well defined as these contained only a molluscan fauna. However, his stratigraphically higher C2 section, immediately downstream from C3, contains vertebrate remains of the genus *Protadajidamo*, of latest Eocene age (Russell, 1964). Hence, it is probable that this section (C3) is of late Eocene rather than early Oligocene age based on faunal evidence. Even though a boundary between the Eocene and Oligocene has not been agreed upon either in Europe or North America, it is conceded generally that no significant floral change coincides with the interval spanning late Eocene-early Oligocene time. In fact, no significant floral change takes place until the climatic deterioration of the middle Oligocene. Nevertheless, it is reassuring that the miospore, megaspore, seed, and pollen assemblage we describe from the Kishenehn Formation is typical of assemblages previously considered to be representative of late Eocene-early Oligocene time. This is based on our conclusion that the flora is generally subtropical in character and, hence, predates the climatic deterioration of the middle

Oligocene, the record of a possible occurrence of *Boisduvalia* which has not been reported from rocks older than the Oligocene, and the absence of such genera as *Platycarya* and *Pistillipollenites* from the assemblage which are omnipresent in lower and middle Eocene strata of North America.

Conclusions

The large and well-preserved microflora from this short section of the Kishenehn Formation represents a late Eocene or early Oligocene subtropical flora. Possibly both undisputed Eocene and Oligocene floras may be found if further palynological studies are made of the strata below and above the short section described here.

References

- Dorofeev, P. I.
 1963a: Tertiary plants of Kazakhstan; Bot. Shurn., v. 45, p. 171-181.
 1963b: The Tertiary floras of western Siberia; Akad. Nauk. SSSR, Bot. Inst. Komarov.
 1968: Megaspores of *Salvinia*, *Azolla* and *Pitularia* from Neogene deposits of Ukraine; Ukr. bot. Zh., v. 25, p. 63-72.
- Jones, P. B.
 1969: The Tertiary Kishenehn Formation, British Columbia; Bull. Can. Pet. Geol., v. 17, p. 234-246.
- Leopold, E. B. and Macginitie, H. B.
 1972: Development and affinities of Tertiary floras in the Rocky Mountains in Floristics and paleofloristics of Asia and eastern North America, A. Graham, ed.; Elsevier Publ. Co., p. 147-200.
- Pabst, M. B.
 1968: The flora of the Chuckanut Formation of northwestern Washington. The Equisetales, Filicales and Coniferales; Univ. Calif. Pubs. Geol. Sci., v. 76.
- Price, R. A.
 1965: Flathead map-area, British Columbia and Alberta; Geol. Surv. Can., Mem. 336.
- Russell, L. S.
 1964: Kishenehn Formation; Bull. Can. Pet. Geol., v. 12, p. 536-543.
- Wolfe, J. A. and Leopold, E. B.
 1967: Neogene and early Quaternary vegetation of northwestern North America and northeastern Asia in The Bering Land Bridge, D. M. Hopkins, ed.; Stanford Univ. Press, p. 193-206.

Project 710036

D. W. Myhr and R. R. Barefoot
Institute of Sedimentary and Petroleum Geology, CalgaryIntroduction

The purpose of this report is to demonstrate that easily measured geochemical parameters, such as pH, conductivity, and sulphate tests, can be used to differentiate and correlate strata of similar lithology. The samples analyzed are from formations of Early Cretaceous age (Albian shale-siltstone division and Upper Sandstone division equivalent) and Late Cretaceous age (Boundary Creek Formation and overlying Fish River Group).

Test cases and parameters measured

Three test cases (Fig. 55.1) and the parameters measured for each are listed as follows:

- 1) IOE Tuk F-18 borehole (69°17'29"N, 133°04'W)
- 26 samples; pH, conductivity, and sulphate tests, concentration of sodium and calcium
- 47 samples; pH, and sulphate tests
- 2) Gulf Mobil Parsons N-10 borehole (69°00'N, 133°30'W)
- 24 samples; pH, and sulphate tests
- 3) outcrop samples (collected by F. G. Young, I. S. P. G., Calgary)
- 25 samples; pH, conductivity, sulphate tests

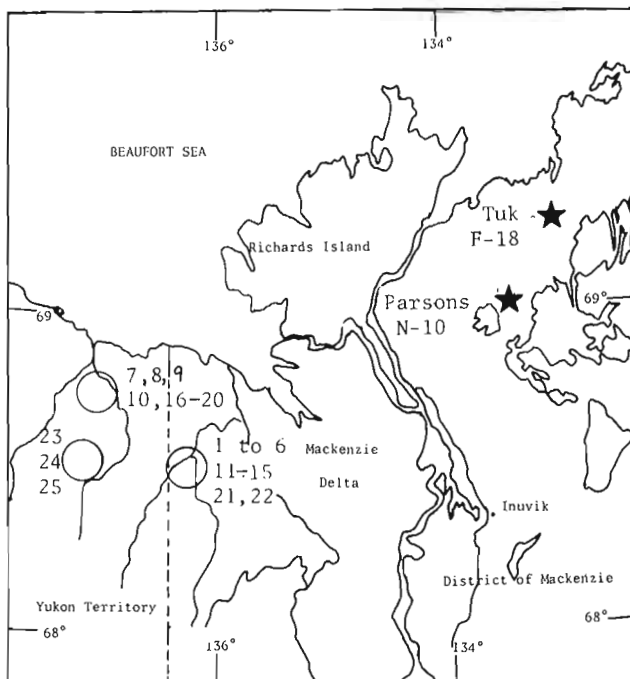


Figure 55.1. Index map, circles represent location of outcrop samples in Figure 55.4.

The IOE Tuk-F-18 borehole was chosen as the "type" test case (Fig. 55.2). Considerably more samples were analyzed and, in addition to the three standard parameters measured, the concentrations of calcium and sodium also were determined.

The following is a brief outline of the tests and the manner in which the data obtained were converted for presentation (Figs. 55.2, 55.3, 55.4). One gram of sample and 3.5 ml of distilled water were added to a clean glass vial. After a 24-hour waiting period, the following tests were conducted on the sample solution:

1. pH was measured with a pH meter. To enable a rapid quantitative assessment, the pH measurement was converted to its equivalent concentration of H^+ or OH^- using the formulae $[H^+] = 10^{-pH}$ or $[OH^-] = 10^{-pOH}$.
2. Conductivity was measured with a conductivity meter in $\mu\text{mhos}/\text{cm}^2$ and divided by 100 to convert to its approximate milli-equivalence per litre (meq/l), in order to express total cation concentration.
3. Cation concentration was measured by fluorometry methods. The concentration of Na^{+1} in ppm of solution was converted to its equivalent in milli-equivalence per litre by dividing by 23 (equivalent weight of Na^{+1}). Similarly, the concentration of Ca^{+2} in ppm was divided by 20 (equivalent weight of Ca^{+2}) to obtain its equivalent in milli-equivalence per litre.
4. A sulphate test was conducted by the addition of 2 drops of 5 per cent $BaCl_2$ to the sample solution. A positive test was indicated by precipitation of a milky, white substance — barium sulphate ($BaSO_4$). The code used for evaluating the visual amounts of precipitate is subjective; 1 (nil to trace of precipitate), 2 (low precipitate), 3 (moderate precipitate), 4 (heavy precipitate).

Results and discussion

In order to test the reliability of the geochemical parameters as a tool for correlation and contact delineation of Upper Cretaceous from Lower Cretaceous strata, the following evidence was ascertained: (a) In the Tuk F-18 well, the contact was determined to be at a depth of 8590 feet (2619 m) on micropaleontological grounds (Chamney, 1973). For the purposes of this report, the contact is chosen at a depth of 8600 feet (2621 m), where there is a change in log and sample characteristics. (b) The contact in the Parsons N-10 well is placed at a depth of 6060 feet (1848 m) on palynological grounds (W. W. Brideaux, pers. comm., 1975). (c) Delineation of outcrop samples into their respective formations on the bases of biostratigraphy and lithostratigraphy (F. G. Young, pers. comm., 1975).

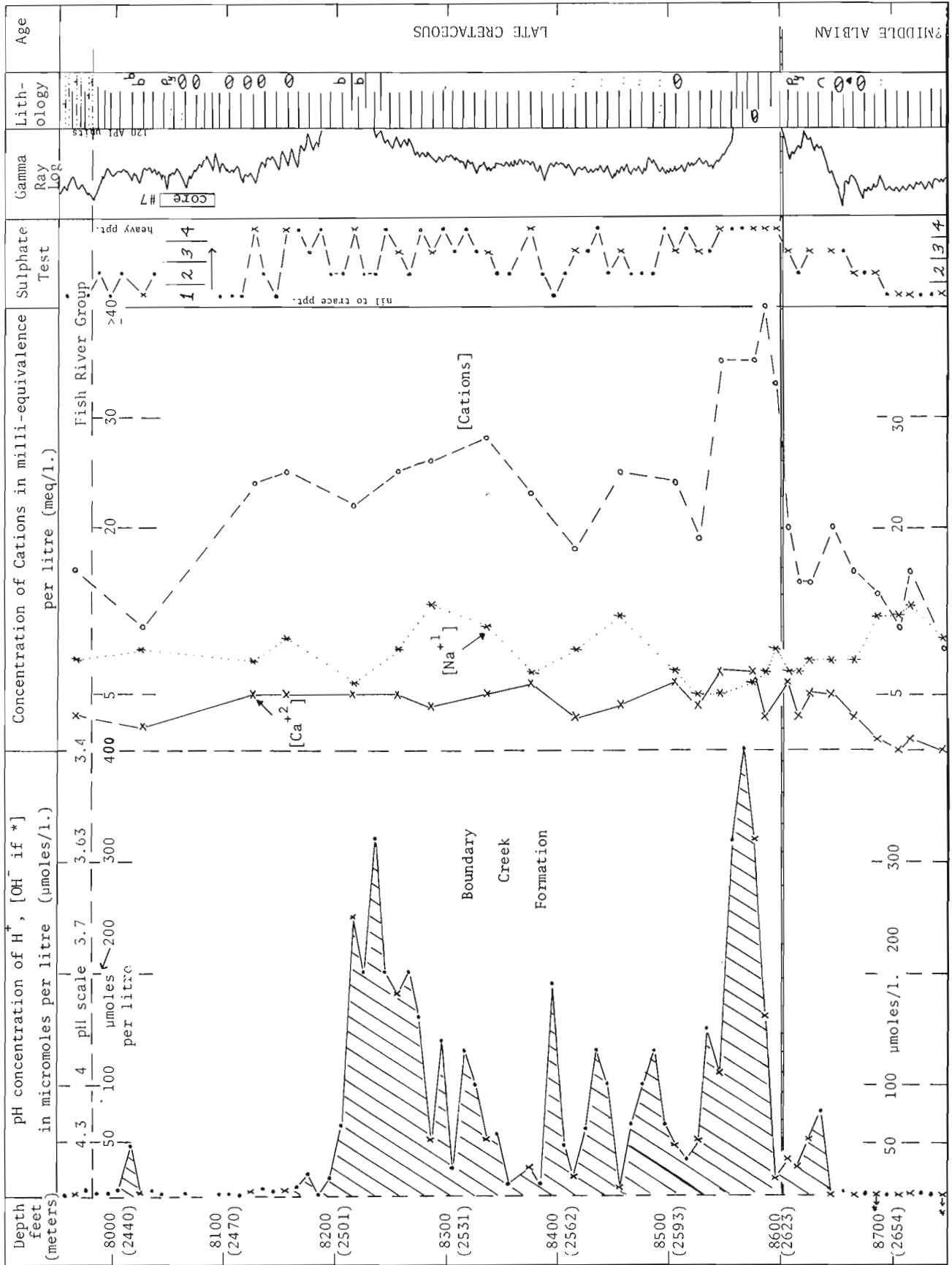


Figure 55.2. Graphic illustration of geochemical parameters, gamma ray and lithology — IOE Tuk F-18 well.

pH test

The results of the pH test are as follows: (a) The Upper Cretaceous Boundary Creek Formation is acidic; hydrogen-ion concentration being largest in the out-crop samples (Fig. 55.4). In the IOE Tuk F-18 bore-hole (Fig. 55.2), the highly radioactive (note gamma ray log), bituminous shales of this formation yield more hydrogen ions compared with adjacent strata (less radioactive and less bituminous). The low pH of the bituminous shales may be due to a greater concentration of finely disseminated iron sulphide (A. E. Foscolos, pers. comm., 1975) and organic compounds in these strata, which are directly related to the restricted, euxinic nature of the depositional environment. (b) Lower Cretaceous (Albian and Aptian) strata are acidic to slightly basic. Hydrogen-ion concentration is less compared with the overlying Boundary Creek Formation (Figs. 55.2, 55.3, 55.4). (c) Hydrogen-ion concentration in the borehole samples was found to decrease with increasing depth across the Upper-Lower Cretaceous contact. (d) Contamination of the Lower Cretaceous samples (determined by visual examination of the lithologies in the sample vials) from caving material of the more acidic Boundary Creek

Formation accounts for the low pH values (high hydrogen-ion concentration) below the contact. In the Parsons N-10 and Tuk F-18 wells, sample contamination is negligible below the depths of 6800 and 8640 feet (2074 and 2635 m), respectively.

Visual examination of the Lower Cretaceous lithologies indicates that these strata are relatively less rich in organic matter (consequently, less radioactive as determined by the gamma ray log), and are interpreted, therefore, to contain lesser amounts of pyrite compared with overlying strata. This may account for the relatively lower hydrogen-ion concentration (high pH).

Conductivity test

The graphs of conductivity data, expressed in terms of total cation concentration, nearly mirror those of the pH test (Figs. 55.2, 55.3, 55.4). Cation concentration in the upper Cretaceous Boundary Creek Formation is greater than in the underlying Lower Cretaceous strata. In the subsurface, cation concentration decreases gradually with increasing depth beneath the unconformity (similar to pH). Higher values in the Lower Cretaceous strata immediately below the contact may be attributed to sample contamination.

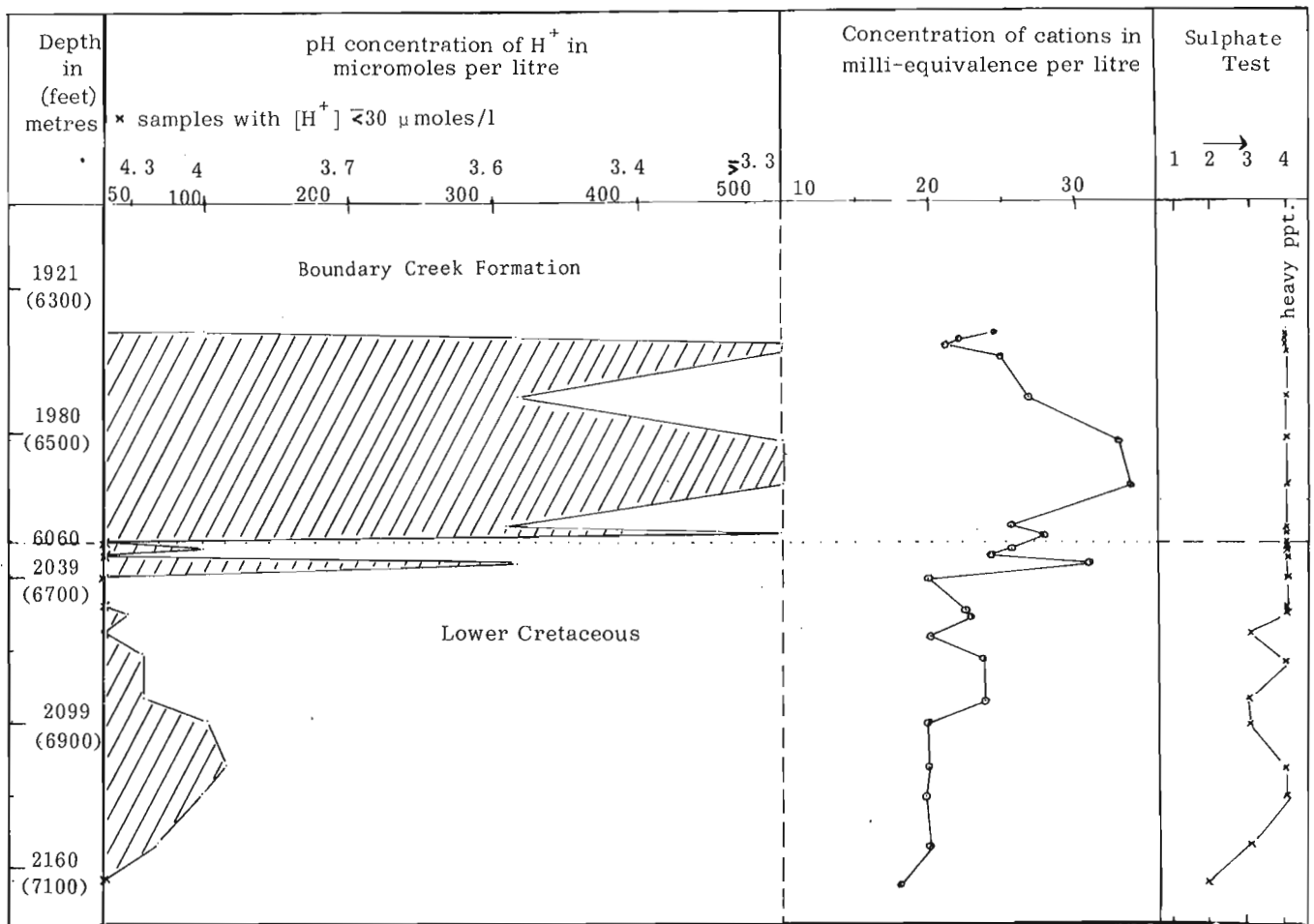


Figure 55.3. Graphic illustration of geochemical parameters, Gulf Mobil Parsons N-10 well.

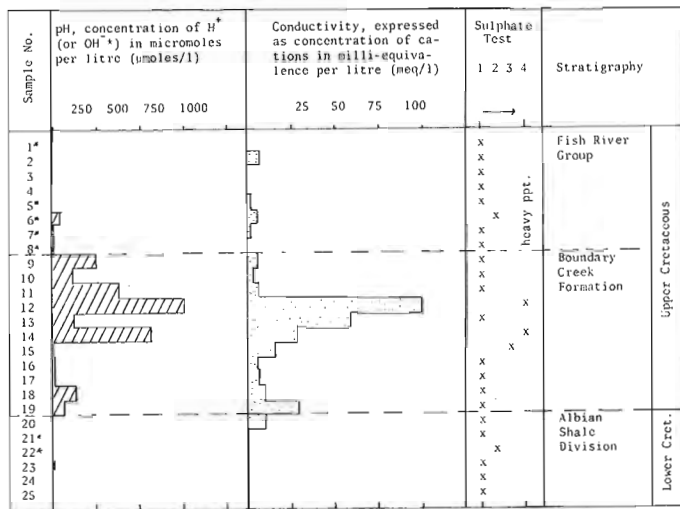


Figure 55. 4. Geochemical and stratigraphic data of outcrop samples. Yukon Coastal Plain (refer to Fig. 55. 1 for general location).

Sulphate test

In the subsurface, the Boundary Creek Formation contains a larger concentration of sulphate compounds relative to underlying strata (Figs. 55. 2, 55. 3). Conversely, from this formation eight out of eleven outcrop samples yielded only trace amounts (Fig. 55. 4). These results are low, probably because of the removal of the soluble sulphates by ground waters and by bacterial action which could dramatically alter the sulphate (i.e. FeSO₄ to gypsum) and ferruginous compounds. This may explain the common occurrence of both selenitic and ferruginous encrustations on outcroppings of the Boundary Creek Formation (Young, 1975).

Calcium-sodium cation test

This test was made only on the Tuk F-18 sample solutions (Fig. 55. 2). Both cations are present in Upper Cretaceous strata, sodium cation concentration being dominant in all but two samples within the highly radioactive, bituminous shale zone. Of interest is the fact that these cations show dissimilar trends beneath

the unconformity in that [Ca⁺²] decreases to zero with increasing depth, whereas [Na⁺¹] increases moderately such that [Na⁺¹] nearly equals total cation concentration.

Conclusions

The results of the tests show that changes in easily measured geochemical parameters (pH, conductivity, and a sulphate test) can be used to differentiate strata in which there are only minor variations in lithologic characteristics. These parameters reflect the mineralogy and compositional variations within the strata, a function of diagenesis, fluid migration movements, and the depositional environment.

These geochemical parameters may be used as a correlation tool in conjunction with other criteria (geophysical logs, biostratigraphy, lithology). Each parameter measured varied slightly for each test case. What one must look for is any type of abrupt or gradational change in one or more of the parameters measured, not necessarily a specific change in only one parameter.

The Upper Cretaceous Boundary Creek Formation yields more hydrogen ions relative to underlying Lower Cretaceous strata, a factor which may be related to a greater concentration of iron sulphide and organic matter. Total cation concentration also is relatively greater which, in turn, is dependent on hydrogen-ion concentration. In the subsurface test cases, it was found that sulphate anions are more dominant in the Boundary Creek Formation than in the Lower Cretaceous strata, and are concentrated in the organic-rich shale units of the Boundary Creek Formation.

References

Chamney, T. P.
 1973: Tuktoyaktuk Peninsula Tertiary and Mesozoic biostratigraphic correlation; in Report of Activities, Pt. B; Geol. Surv. Can., 73-1B, p. 171-178.

Young, F. G.
 1975: Upper Cretaceous stratigraphy, Yukon Coastal Plain and northern Mackenzie Delta; Geol. Surv. Can., Bull. 249.

Project 670068

D. G. Cook and J. D. Aitken
Institute of Sedimentary and Petroleum Geology, CalgaryIntroduction

In the northern Franklin Mountains, the oldest rocks exposed in folds and reverse faults (involving horizontal shortening) belong to the Saline River Formation. Consequently, the writers have suggested that structures there probably developed above a detachment zone in evaporites and shale of the Saline River (Cook and Aitken, 1971, 1973), even though they recognized that older strata were involved in the McConnell Range to the southeast. Colville Hills structures are geometrically similar to those of the northern Franklin Mountains and, as far as can be determined from surface mapping, involve the same formations; accordingly, the writers (*ibid.*) suggested that Colville Hills structures probably also developed above a Saline River detachment.

On the basis of drilling and geophysical surveys by industry, it appears now that Colville Hills structures

cannot be attributed to detachment in the Saline River (P. de Groot, pers. comm., 1975; J. Davis, pers. comm., 1975). If we accept involvement of pre-Saline River rocks in the Colville Hills, then the argument of geometric similarity obviously can be turned back to suggest that northern Franklin Mountains structures also may involve older strata.

Two cross-sections across specific structures (Fig. 56.1) bear on the question. The first, across Carcajou Ridge (Fig. 56.2), has excellent subsurface control and is best interpreted using a model of Saline River detachment. The second, across the Norman Range (Fig. 56.3), is much more conjectural (two interpretations are shown), but seems to imply that sub-Saline River beds are involved in the structure. The second cross-section also implies that the thickness (2782 ft; 835 m) of the Saline River Formation encountered in the Imperial Vermilion Ridge No. 1 well is a stratigraphic rather than a tectonically increased thickness.

Subsurface Data

Formation tops for the wells used in the Carcajou Ridge cross-section were provided by D. C. Pugh. Formation tops for the Vermilion Ridge No. 1 well were taken from Tassonyi (1969). The wells and the tops used in each are listed below.

Mesa Murphy GCOA Hanna R. J-05

65°44'30"N; 128°15'30"W

KB el. 127 m (415')

Tops picked by D. C. Pugh

<u>Formation or unit</u>	<u>Depth from K. B.</u>	<u>Comments</u>
Cretaceous	surface	
Ramparts Formation	251 m (824')	
Hare Indian Formation	359 m (1178')	
Hume Formation	490 m (1606')	
Gossage limestone	585 m (1918')	included in Bear Rock in cross-section A-A'
Gossage dolomite	596 m (1955')	included in Bear Rock in cross-section A-A'
Bear Rock evaporite	663 m (2174')	
Delorme/Mount Kindle Fm.	825 m (2706')	Mechanical log only, no samples
Total Depth	985 m (3230')	

Amoco et al. Carcajou K-68

65°37'42"N; 128°12'23"W

KB el. 219 m (717')

Tops picked by D.C. Pugh

<u>Formation or unit</u>	<u>Depth from KB</u>	<u>Comments</u>
Hare Indian Formation	0 m 0	
Hume Formation	14 m (45')	
Gossage limestone	99 m (325')	included in Bear Rock in cross-section A-A'
Gossage dolomite	113 m (370')	included in Bear Rock in cross-section A-A'
FAULT		
Hume Formation	163 m (535')	
Gossage limestone	209 m (684')	included in Bear Rock in cross-section A-A'
Gossage dolomite	220 m (720')	included in Bear Rock in cross-section A-A'
Bear Rock evaporite	271 m (889')	
Delorme(?) Formation	500 m (1638')	included in Bear Rock in cross-section A-A'
Mount Kindle Formation	504 m (1654')	
Franklin Mountain cherty unit	620 m (2032')	
FAULT		
Bear Rock evaporite	773 m (2533')	This fault slice is too thin to show in cross- section A-A'
Mount Kindle Formation	791 m (2592')	
FAULT		
Hume Formation	816 m (2676')	
Gossage limestone	828 m (2716')	included in Bear Rock in cross-section A-A'
Gossage dolomite	840 m (2755')	included in Bear Rock in cross-section A-A'
Bear Rock evaporite	894 m (2932')	
Mount Kindle Formation	1126 m (3691')	
Franklin Mountain cherty unit	1258 m (4126')	
Total Depth	1377 m (4515')	

McD. Can GCO Maida F-57

65°35'26"N; 128°10'17"W

KB el. 120 m (395')

Tops picked by D.C. Pugh

<u>Formation or unit</u>	<u>Depth from KB</u>	<u>Comments</u>
Cretaceous	surface	
Imperial Formation	282 m (924')	

<u>Formation or unit</u>	<u>Depth from KB</u>	<u>Comments</u>
Canol Formation	454 m (1490')	
Ramparts Formation	463 m (1518')	
Hare Indian Formation	661 m (2166')	
Hume Formation	741 m (2431')	
Gossage limestone	828 m (2714')	included in Bear Rock in cross-section A-A'
Gossage dolomite	837 m (2744')	included in Bear Rock in cross-section A-A'
Bear Rock Evaporite	881 m (2888')	
Delorme(?) Formation	1068 m (3503')	included in Bear Rock in cross-section A-A'
Mount Kindle Formation	1081 m (3544')	
Franklin Mountain cherty unit	1184 m (3881')	
Total Depth	1483 m (4863')	

McD. Can GCO S. Maida G-56

65°35'36"N; 128°12'23"W

KB 118 m (388')

Tops picked by D. C. Pugh

<u>Formation or unit</u>	<u>Depth from KB</u>	<u>Comments</u>
Cretaceous	surface?	no samples, no logs above 27 m (90')
Imperial Formation	278 m (913')	
Canol Formation	512 m (1680')	
Ramparts Formation	530 m (1737')	
Total Depth	642 m (2105')	

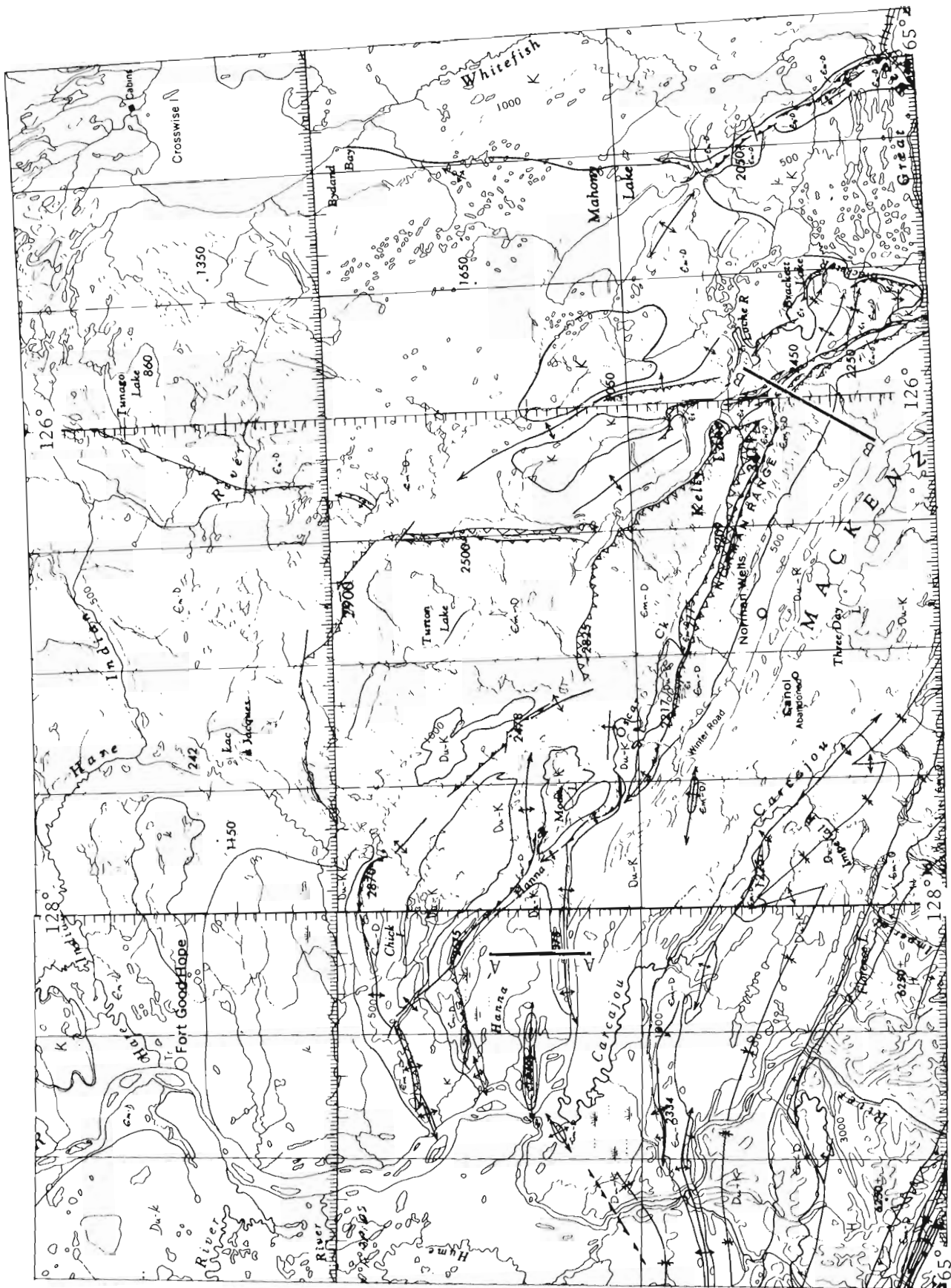
Imperial Vermilion Ridge No. 1

65°07'51"N; 126°05'00"W

KB 282 m (925')

Tops from Tassonyi (1969)

<u>Formation or unit</u>	<u>Depth from KB</u>	<u>Comments</u>
Canol Formation	0 m	
Hare Indian Formation	113 m (370')	
Hume Formation	143 m (470')	
Gossage Formation	258 m (845')	included in Bear Rock in cross-section B-B'
Bear Rock Formation	284 m (930')	
Ronning Formation	569 m (1865')	Franklin Mountain Formation
Saline River shale member	853 m (2798')	
Saline River salt member	1024 m (3360')	
Mount Cap Formation	1701 m (5580')	
Total Depth	1821 m (5972')	



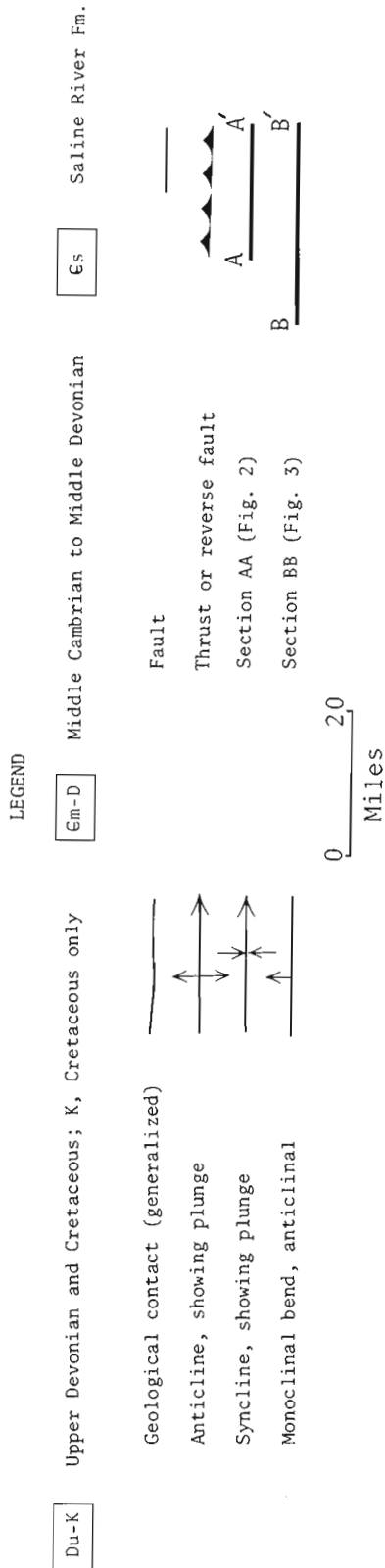


Figure 56.1. Generalized geological map of part of the northern Franklin Mountains and adjacent areas.

Carcajou Ridge

Cross-section A-A' (Fig. 56.2) was drawn perpendicular to the trend of Carcajou Ridge and through the Amoco et al. Carcajou K-68 well. Two wells south and one well north of the ridge are close enough to the line of section to permit projecting them directly into the cross-section. The wells combined with surface exposure on the ridge provide the best control available for any uplifted structure in the northern Franklin Mountains.

Surface mapping indicates that Carcajou Ridge is an asymmetric anticline, whereas the K-68 well reveals repetitions of stratigraphic units at three faults. One small fault slice cannot be shown at the scale of the cross-section; if it is ignored, the greatest fault effectively places Franklin Mountain cherty unit on Hume Formation and is clearly a thrust fault. The cross-section (Fig. 56.2) shows the surface asymmetric anticline to be a drag fold on the leading edge of the largest thrust fault. The cross-section is balanced so that shortening represented by faulting at deeper levels is represented by faulting and folding at higher levels. Every through-going formation is shortened by about three-quarters of a mile.

If the "regional" concept of petroleum geologists is applied, formation tops in the footwall of the major thrust in the Carcajou K-68 well lie approximately "on regional". That is, those formation tops lie close to the elevations they would be assigned by interpolation between Maida F-57 and Hanna R. J-05 wells. This emphasizes the fact that the Carcajou Ridge Anticline exists at shallow depths only.

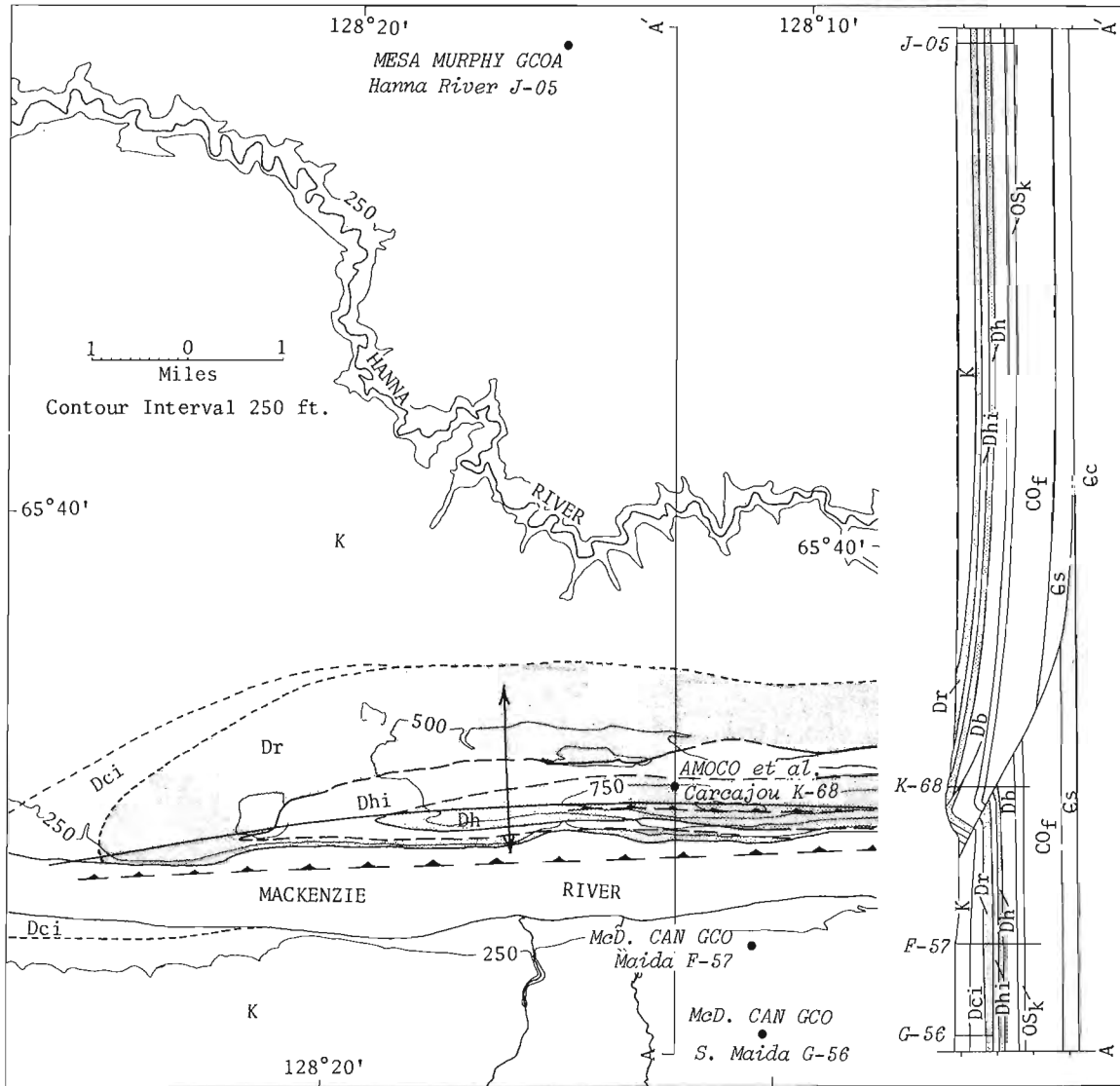
The structure is most easily rationalized as being due to a splay from a detachment zone in the Saline River Formation, although the available data do not preclude the fault extending into deeper strata. The data do preclude the possibility that Carcajou Anticline is a drape structure above a vertically uplifted basement block.

Carcajou Ridge, because of the subsurface control, provides a model for interpreting other structures in the northern Franklin Mountains. Probably all narrow, asymmetric anticlines mark the existence of an underlying thrust fault.

Norman Range

Cross-section B-B' (Fig. 56.3) is part of a section selected for regional considerations. It is more or less perpendicular to the strike of geological contacts on the west side of the ridge but, consequently, is not perpendicular to the strike of thrust faults on the east side. Formation tops in Imperial Vermilion Ridge No. 1 well have been projected along strike into the line of cross-section. Of a variety of possible structural interpretations, two are shown (Fig. 56.3).

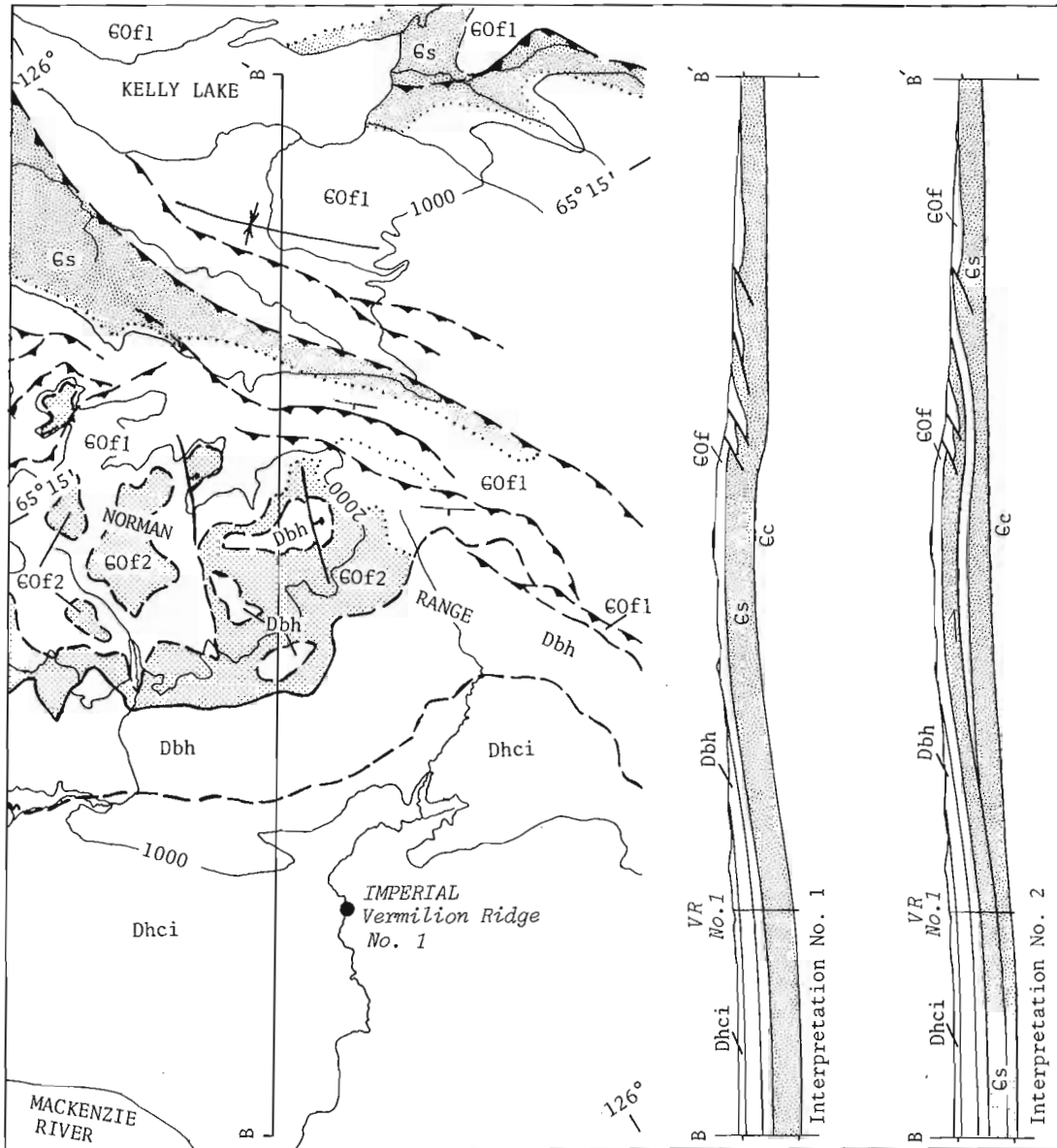
Interpretation (1) implies that sub-Saline River strata are structurally high beneath the Norman Range. In interpretation (2), structural relief on the base of



LEGEND

CRETACEOUS		CAMBRIAN AND ORDOVICIAN	
K	Cretaceous undivided	CO_f	FRANKLIN MOUNTAIN FORMATION
DEVONIAN		G_s	SALINE RIVER FORMATION
D_{ci}	CANOL AND IMPERIAL FORMATIONS	CAMBRIAN AND OLDER	
D_r	RAMPARTS FORMATION	E_c	MOUNT CAP FORMATION AND OLDER
D_{hi}	HARE INDIAN FORMATION	Geological boundary (defined, approximate, assumed)	
D_h	HUME FORMATION	Thrust fault (approximate)	
D_b	BEAR ROCK FORMATION	Asymmetric Anticline (short arrow indicates steeper limb)	
ORDOVICIAN AND SILURIAN			
OS_k	MOUNT KINDLE FORMATION		

Figure 56.2. Cross-section and geological map of Carcajou Ridge.



LEGEND

DEVONIAN

Dhc i HARE INDIAN, CANOL AND IMPERIAL FMS.

Dbh BEAR ROCK AND HUME FMS.

CAMBRIAN AND ORDOVICIAN

Gof2 CHERTY UNIT

Gof1 RHYTHMIC AND CYCLIC UNITS

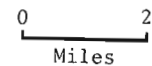
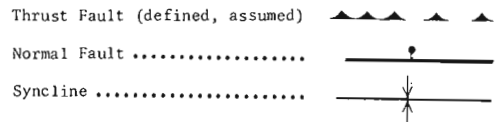
Gof FRANKLIN MTN. FM. UNDIVIDED

CAMBRIAN

Gs SALINE RIVER FM.

CAMBRIAN AND OLDER

Gc MOUNT CAP FM. AND OLDER



Contour Interval 1000 ft

Figure 56.3. Cross-section and geological map of part of the Norman Range.

the Saline River Formation is eliminated by introducing a footwall wedge of Franklin Mountain Formation.

Interpretation (1) seems more likely because it is consistent with the high-angle, short displacement reverse faults that have been observed in the northern Franklins to date. Interpretation (1) implies that the thickness of salt in the Vermilion Ridge well represents the stratigraphic thickness because the well is low on the west flank of the structure where there is no apparent structural reason for the thick salt. Because this is the thickest known Saline River section in the region, the Saline River Formation is drawn as thinning eastward.

Interpretation (1) is drawn to illustrate the possibility that an earlier structure related to the pre-Upper Cretaceous Keele Arch (Cook, 1975) has localized the Laramide structure. Conversely, the entire deformation may be Laramide, as in the McConnell Range to the southeast, where sub-Saline River strata are involved in Laramide structure.

Interpretation (2) implies approximately 13 km (8 miles) of translation on a flat thrust underlying the Norman Range. Although this model provides a structural explanation for the thick salt in Vermilion Ridge No. 1 well, it is not consistent with the high-angle reverse faults observed in the northern Franklin Mountains to date.

Conclusions

Despite the assertion by others that Colville Hills structures are not simply detached above the Saline River Formation, the detachment model works very well for Carcajou Ridge, the only structure in the northern Franklin Mountains with excellent surface and subsurface control. If Carcajou Ridge is taken as a model, other narrow ranges in the northwestern Franklin Mountains can be interpreted similarly. Conversely, higher and broader structures such as the Norman Range probably involve older strata. The Saline-River-detachment model is still viable for parts of the Franklin Mountains, but is applicable readily to a smaller region than was originally considered. The thick salt section in the Vermilion Ridge No. 1 well probably represents, more or less, the stratigraphic thickness because it is not explained readily as due to tectonic thickening.

Recent oil and gas exploration in the Colville Hills appears to have been directed toward evaluation of the basal Cambrian sandstone (Mount Clark or Old Fort Island Formation). Ashland Oil's gas discovery at Tedji Lake, about 225 km (140 miles) northeast of Carcajou Ridge, was from a Cambrian sandstone (Oilweek, 1974). This potential reservoir unit has not been tested in any structure in the northern Franklin Mountains. If Carcajou Ridge is representative of other narrow structures in the northeastern part of the Franklins, then no favourable structure can be expected at the level of the Mount Clark sandstone. Conversely, broad high relief structures such as the Norman Range (Fig. 56.3) and the unnamed range east of the Norman Range appear to involve sub-Saline River strata (i. e. Mt. Clark Formation) and may provide substantial structural traps. The possibility that these are older structures that have localized the Laramide deformation greatly enhances their potential as petroleum traps.

References

- Cook, D. G.
1975: The Keele Arch — a pre-Devonian and pre-Late Cretaceous paleo-upland in the northern Franklin Mountains and Colville Hills; in Report of Activities, Part C, Geol. Surv. Can., Paper 75-1C, p. 243-246.
- Cook, D. G. and Aitken, J. D.
1971: Geology, Colville Lake-map-area and part of Coppermine map-area, Northwest Territories; Geol. Surv. Can., Paper 70-12.
1973: Tectonics of northern Franklin Mountains and Colville Hills, District of Mackenzie, Canada in Arctic Geology; Am. Assoc. Pet. Geol., Mem. 19, p. 13-22.
- Oilweek
1974: Ashland strikes gas in N.W.T.; Oilweek, v. 25, no. 9, p. 19.
- Tassonyi, E. J.
1969: Subsurface geology, Lower Mackenzie River and Anderson River area, District of Mackenzie; Geol. Surv. Can., Paper 68-25.

J. R. McLean

Institute of Sedimentary and Petroleum Geology, Calgary

Pre-Cadomin paleogeography

It is well established (Stott, 1968; Norris, 1964) that the Lower Cretaceous Cadomin Formation (Table 57.1) lies unconformably on Jurassic Kootenay, Nikanassin, Minnes, and Fernie beds in the Foothills and Front Ranges of the Rocky Mountains. These units underlying the Cadomin reflect a basic change in the paleogeography and paleodrainage in western Canada. Easterly sources supplied coarse clastic detritus, including chert pebble conglomerate, to the Fernie Group. Marine conditions, with deposition of dark shales, prevailed in the west. Tipper (1959, p. 48) suggested that a major land area existed in central British Columbia during the Middle Jurassic, but its influence does not appear in the present outcrops of most of the Fernie Group (Frebold, 1957, p. 37-41). However, the Passage Beds at the top of the Fernie Group represent the first influx to the Rocky Mountain region of detritus from the west, in approximately mid-Oxfordian time (Frebold, 1957, Fig. 4). Thus, there was a converging of two drainage systems, and some part of the Kootenay-Nikanassin beds was undoubtedly derived from the east. Stott (1967, p. 33) indicates that some of the Monteith Formation (of the Minnes Group) also may have been derived from this direction.

Uplift in the west, or a lowering of base level, terminated deposition, and a period of erosion of unknown duration, but probably spanning several million years, removed hundreds of metres of sediment (Norris, 1964, p. 528; Stott, 1968, p. 13) from the present Foothills area prior to deposition of the Cadomin Formation. To the west, the Cadomin rests on progressively younger beds and, far to the west, may be conformable with the Kootenay. However, to the east, erosion removed a vast amount of sediment which, it is suggested, was transported to the north as part of an extensive drainage pattern covering much of the Western Interior of the United States and Canada (McGookney, 1972, p. 196, Fig. 14; Christopher, 1974, p. 107; Williams and Stelck, 1975, p. 4).

Eastern limit

An erosional feature (Figs. 57.1, 57.2) in the Jurassic subcrop, shown by Springer *et al.* (1964, p. 145, Fig. 10-6) but not elaborated upon, is believed to represent a major channel transporting sediment northward into the Peace River Basin. This basin, connected to the Pacific Ocean on the west, is described by Jeletzky (1971, p. 36). The channel is herein named the Spirit River Channel after the town in township

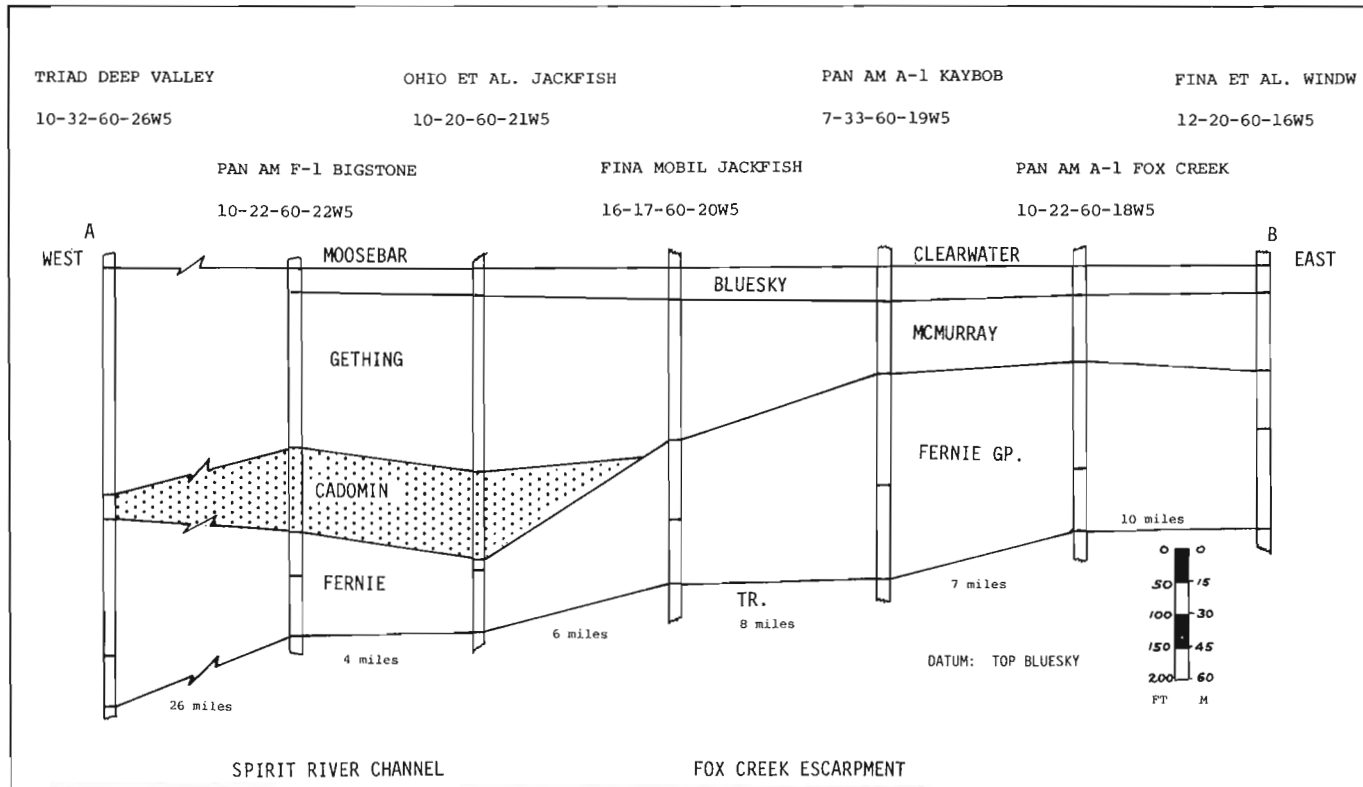


Figure 57.1. Stratigraphic cross-section illustrating eastern limit of Cadomin Formation.

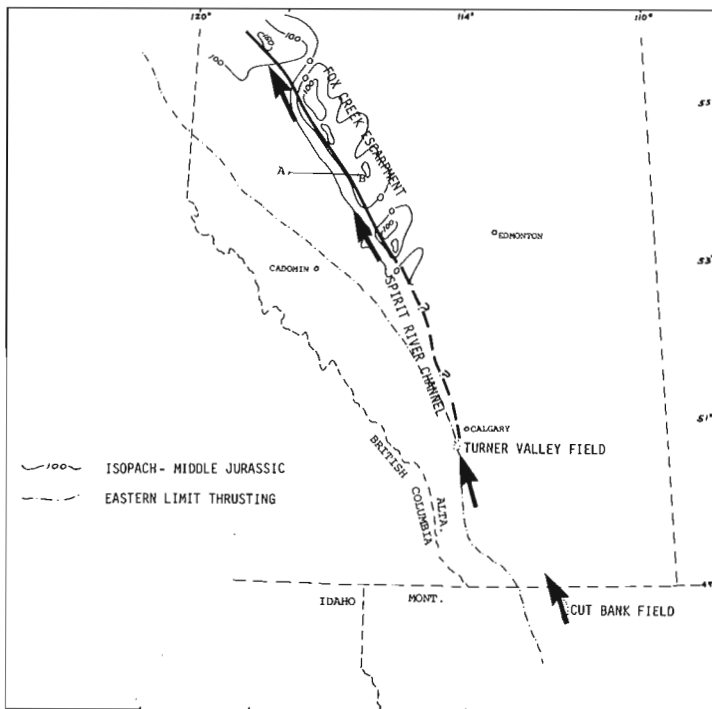


Figure 57.2. Location of Fox Creek Escarpment and Spirit River Channel.

78-6W6. The eastern edge of this channel is a prominent 76-m (250 ft) high escarpment (Fig. 57.1) herein called the Fox Creek Escarpment (township 62-19W5), which provided an effective barrier to eastward transport of chert-rich, distinctly Cadomin sediment. The western margin of the channel is less distinct, indicating a marked asymmetry to the valley.

Mellon (1967, p. 139), in relating the lower part of the Blairmore Group in the Foothills to the same interval in the Mannville Group of the Plains, observed,

"To the east in the Plains, Gladstone strata grade into or interfinger with the quartzose sandstones and siltstones of the McMurray Formation. . . ."

"Exactly where and how this lateral change in sandstone composition takes place is uncertain owing to lack of control in the western Plains. . . ."

It is suggested here that the Fox Creek Escarpment forms the eastern margin of the Cadomin Formation and Mellon's Gladstone Formation. It cannot be stated definitely that none of the Cadomin penetrated east beyond the escarpment because there appear to be gaps in it. These may have permitted some transport farther east or, alternatively, may have allowed easterly derived detritus to be added to the channel.

The Cadomin Formation is believed to be of fluvial origin. The change in sandstone composition from west to east suggests that there was not a large influx of Cadomin sediment east of the escarpment. Therefore, eastward-flowing streams must have merged into the northward-flowing river system which persisted during deposition of the Cadomin. Alluvium derived from the

Table 57.1.
Stratigraphic Chart

SOUTHERN FOOTHILLS		PLAINS		NORTHERN FOOTHILLS	
BLAIRMORE GROUP		COLORADO GP.		HASLER FM.	
		MILL CREEK		VIKING FM. JOLI FOU	
BLAIRMORE GROUP		BEAVER MINES FM.		COMMOTION FM.	
		FORT AUGUSTUS FM.		MOOSEBAR FM.	
BLAIRMORE GROUP		CALCAREOUS MBR.		WABISKAW MBR. CALCAREOUS MBR.	
		GLADSTONE FM.		BLUESKY MBR.	
BLAIRMORE GROUP		CADOMIN		GETHING FM.	
		KOOTENAY FM.		CADOMIN FM.	
BLAIRMORE GROUP		JURA-MISS.		MINNES GP.	
BLAIRMORE GROUP		FERNIE			

west intertongued with, and in part was incorporated into, detritus from farther south as it was transported northward along the channel.

The Spirit River Channel and Fox Creek Escarpment illustrated in Figure 57.2 are readily identified between latitudes 56° and 53° North. South of this, the escarpment is not distinct but the channel probably continues southward along the eastern edge of the Jurassic subcrop (Springer *et al.*, 1964, Figs. 10-6 and 10-7), possibly connecting with the Dalhousie Sand in the Turner Valley Field and the Cut Bank Sand in the Cut Bank Field of northern Montana. The Cut Bank Sand is described by Shelton (1966, p. 5, 6) as a succession of point bar deposits formed in a northward-flowing stream. There also, the eastern margin is an escarpment, 46 m (150 ft) high, cut in Jurassic sediments. D.K. Norris (pers. comm.) measured crossbedding in the Cadomin Formation in the region of the Crowsnest Re-entrant, just north of latitude 49°30'N, and found that paleocurrent flow was in a north to northwesterly direction.

Depositional environment

The environment of deposition of the Cadomin has long been the subject of speculation. The most recent discussions are by Stott (1968), Schultheis (1970), and Schultheis and Mountjoy (1971). Stott (1968, p. 109) considered a piedmont alluvial plain environment most likely. Schultheis (1970, p. 82) and Schultheis and Mountjoy (1971), suggested a lacustrine beach

environment for the Cadomin Formation in the Foothills between the Athabasca and North Saskatchewan rivers, and a fluvial origin farther south.

It is suggested that all of the Cadomin throughout its length of occurrence is of fluvial origin with the possibility of alluvial fan deposits at the western limit of the formation. The following discussion is restricted to the area between latitudes 52° and 54° North. The model is a low sinuosity stream depositing sheet-like units of coarse sediment during periodic flood stages.

Several characteristics of the Cadomin Formation are pertinent to this interpretation:

1. Pebbles and larger clasts are usually rounded.
2. There is a distinct bimodality with good sorting in each mode (Schultheis, 1970, p. 79). The first mode is the framework of pebbles; the second, the sand matrix.
3. The base is unconformable but usually not conspicuously channelled into underlying sediments.
4. The coarsest clasts usually occur at the base, but have been observed in other parts of the formation.
5. Larger, elongate clasts often show good preferred orientation, and imbrication is sometimes observed.
6. Stratification is poor. A vague horizontal to low-angle stratification is observed in places. High-angle cross-stratification is uncommon in the conglomerate, although it is observed in some localities. Lenses of sand within the conglomerate are often crossbedded.
7. Normal graded bedding is common.

The size of clasts in the Cadomin (75 to 100 mm is common, with some 300 – 450 mm boulders) indicates strong current flow. Such currents were probably periodic, with the coarse detritus being transported only during flood stage, or perhaps only during exceptionally high floods, with all fine material taken into suspension. Deposits during this stage are essentially structureless.

Rust (1972, p. 232) observed that the coarse, heterogeneous bedload (clasts up to 128 mm) of the Donjek River in the Yukon formed a deposit with no internal structure or only poorly defined horizontal bedding. This was interpreted as transportation in planar sheets, a condition which would be expected in the very high energy flow required to move such coarse material. The coarsest material was believed to be moved only during exceptional floods. Similar observations were made by Smith (1974, p. 221) for the gravel facies of a braided outwash deposit and by Eynon and Walker (1974, p. 57) for their bar core gravel model. These gravels were characterized by crude horizontal stratification, imbricate pebbles, and a noticeable lack of cross-stratification. Both observed a bimodal grain size distribution – pebbles and cobbles being moved as bedload, with infilling sand moved mainly in suspension and gradually filtering into interstitial spaces during periods of low flow.

The lack of clay and silt in the Cadomin Formation suggests that currents were sufficiently strong to

retain this material in suspension at all times. Many gravel bars have a very coarse lag gravel at the base, only a few pebble diameters in thickness, which represents the coarsest bedload and moves only at highest discharges (Walker, 1975, p. 150). This would explain the coarsest pebbles often found at the base of the Cadomin. After the lag gravel had ceased to move, the bar builds upward by addition of finer material still in transport, so that there is a net upward fining resulting in normal grading (Walker, 1975, p. 152).

It is clear that, during deposition of the Cadomin Formation, relief was sufficient to produce high-energy streams which could move pebbles, cobbles, and boulders as well as sand, and which were of sufficient strength that sand bedforms were rarely preserved and finer sediment was not deposited. A multitude of streams draining the newly elevated source areas, with lateral migration over a long period of time, led to the wide-spread occurrence of coarse clastic detritus along the sub-Cadomin unconformity. Scours into the underlying bedrock undoubtedly are present but on a magnitude that is not observable on the usual limited exposure of a single outcrop. For example, Norris (1958, p. 18) observed that the stratigraphic interval between the Cadomin and an underlying coal seam in the Kootenay decreased from 24 to 4 m (78 to 12 ft) over a distance of 6.4 km (4 miles). It is commonly believed that the Cadomin is sheet-like and laterally continuous. However, the thickness of the conglomerate near Luscar Creek [6.4 km (4 miles) northwest of Cadomin townsite] was observed to vary from 10 m (33 ft) to zero in less than 30 m (100 ft), and there are many areas in which the Cadomin does not outcrop where it cannot be assumed to be present.

The rounded nature of most of the coarser gravel clasts is attributed to mechanical and chemical weathering in the source terrane prior to the tectonic event which introduced them into the Cadomin depositional regime. Fossiliferous chert pebbles have been traced to Carboniferous and Permian carbonates, and quartzite pebbles are believed to be from the Lower Cambrian Gog Group (Schultheis and Mountjoy, 1971). Chemical weathering and rapid mechanical breakdown removed most of the softer carbonate fragments, although Stott (1968, p. 19) reported some in northeastern British Columbia. The maximum clast size in north-eastern British Columbia suggests that the region was closer to the source area than were any of the exposures observed farther south in the Foothills. Chert and quartzite pebbles were concentrated in valleys or local basins during earlier erosion of the source areas and were not moved eastward until the Cadomin tectonic event which increased gradients and allowed this coarse sediment to be swept out into the foredeep. This accumulated gravel, once removed, was not replenished, so that the Cadomin is the product of a single 'wave' of coarse detritus in many areas. Where new areas of gravel concentration were tapped by the drainage networks, new waves of coarse detritus were moved eastward to form the stratigraphically higher conglomeratic beds in the Blairmore Group.

There is a marked decrease in clast size eastward and conglomerate units extend only a short distance east of the Foothills. The sand and finer sediment bypassed the area of gravel deposition and was carried eastward and then northward along the Spirit River Channel to be deposited in lower energy environments. Some pebbles are found in the Cadomin along the Fox Creek Escarpment but concentrations are confined to the base, and elsewhere occur as pebbly sandstones.

Beds overlying the Cadomin are usually distinctly finer grained and lie abruptly on the Cadomin. They represent deposition under much more tranquil conditions and suggest a lowering of gradients probably associated with the transgression of the Boreal Sea in Early Albian time (Jeletzky, 1971, p. 42, 43). Stott (1968, p. 39) reports several marine tongues in the Gething Formation in northeastern British Columbia. At least one tongue has been identified in the Gething as far south as the Smoky River (J.H. Wall, pers. comm.).

Oil and gas

Both oil and gas are produced from the Cut Bank Sand in the Cut Bank Field (Blixt, 1941). Some gas and naphtha have been produced from beds equivalent to the Cadomin in the Turner Valley Field (White, 1960, p. 209). To the north, no production is known from the Cadomin or laterally equivalent formations, but there are reported oil shows in several wells. Potential fields, similar to Cut Bank, may be present along the Fox Creek Escarpment.

References

- Blixt, J. E.
1941: Cut Bank Oil and Gas Field, Glacier County, Montana in *Stratigraphic type oil fields*, A.I. Levorsen, ed.; Am. Assoc. Pet. Geol., p. 327-381.
- Christopher, J. E.
1974: The Upper Jurassic Vanguard and Lower Cretaceous Mannville Groups of southwestern Saskatchewan; Sask. Dep. Mineral Resour., Rep. 151.
- Eynon, G. and Walker, R. G.
1974: Facies relationships in Pleistocene outwash gravels, southern Ontario: a model for bar growth in braided rivers; *Sedimentology*, v. 21, p. 43-70.
- Frebold, H.
1957: The Jurassic Fernie Group in the Canadian Rocky Mountains and Foothills; *Geol. Surv. Can., Mem.* 287.
- Jeletzky, J. A.
1971: Marine Cretaceous biotic provinces and paleogeography of Western and Arctic Canada: illustrated by a detailed study of ammonites; *Geol. Surv. Can., Paper* 70-22.
- McGookney, D. P.
1972: Cretaceous System in *Geologic Atlas of the Rocky Mountain region*, U.S.A., W.W. Mallory, ed.; *Rocky Mountain Assoc. Geol.*, p. 190-228.
- Mellon, G. B.
1967: Stratigraphy and petrology of the Lower Cretaceous Blairmore and Mannville Groups, Alberta Foothills and Plains; *Res. Council Alberta, Bull.* 21.
- Norris, D. K.
1958: Structural conditions in Canadian coal mines; *Geol. Surv. Can., Bull.* 44.
1964: The Lower Cretaceous of the south-eastern Canadian Cordillera; *Bull. Can. Pet. Geol., Special guidebook issue - Flathead Valley*, v. 12, p. 512-535.
- Rust, B. R.
1972: Structure and process in a braided river; *Sedimentology*, v. 18, p. 221-245.
- Schultheis, N. H.
1970: Petrography, source and origin of the Cadomin Conglomerate between the North Saskatchewan and Athabasca Rivers, Alberta; unpubl. M.Sc. thesis, McGill Univ.
- Schultheis, N. H. and Mountjoy, E. W.
1971: Cadomin Conglomerate of Alberta - derived from Main Range Thrust sheets uplifted during Early Cretaceous time (Abs.); *Geol. Soc. Am., Rocky Mtn. Sect., 24th Ann. Mtg. (Calgary)*.
- Shelton, J. W.
1966: Stratigraphic models and general criteria for recognition of alluvial, barrier-bar, and Turbidity-current deposits; *Billings Geol. Soc., 17th Ann. Field Conf. Guidebook*, p. 1-17.
- Smith, N. D.
1974: Sedimentology and bar formation in the Upper Kicking Horse River, a braided outwash stream; *J. Geol.*, v. 82, p. 205-223.
- Springer, G. D., MacDonald, W. D. and Crockford, M. B. B.
1964: Jurassic; in *Geological History of Western Canada*, R. G. McCrossan and R. P. Glaister, eds.; p. 137-155.
- Stott, D. F.
1967: Fernie and Minnes strata north of Peace River, Foothills of northeastern British Columbia; *Geol. Surv. Can., Paper* 67-19.
1968: Lower Cretaceous Bullhead and Fort St. John Groups, between Smoky and Peace Rivers, Rocky Mountain Foothills, Alberta and British Columbia; *Geol. Surv. Can., Bull.* 152.

Tipper, H. W.

1959: Revision of the Hazelton and Takla Groups of central British Columbia; Geol. Surv. Can., Bull. 47.

Walker, R. G.

1975: Conglomerate: sedimentary structures and facies models; *in* Depositional environments as interpreted from primary sedimentary structures and stratification sequences; Soc. Econ. Mineralogists and Paleontologists, Short Course No. 2, Dallas, p. 133-161.

White, R. J. (ed.)

1960: Oil Fields of Alberta; Alberta Soc. Petrol. Geologists

Williams, G. D. and Stelck, C. R.

1975: Speculations on the Cretaceous palaeogeography of North America; *in* The Cretaceous System in the Western Interior of North America, W. G. E. Caldwell, ed.; Geol. Assoc. Can., Spec. Paper 13, p. 1-20.

Projects 710003 and 680068

H. R. Balkwill and W. S. Hopkins, Jr.
Institute of Sedimentary and Petroleum Geology, CalgaryIntroduction

A section of Cretaceous strata along the eastern flank of Hoodoo Dome (Lat. 78°12'N, Long. 99°45'W), southeastern Ellef Ringnes Island (Fig. 58. 1a, b) is summarized and interpreted in this report. The section was measured and sampled in 1973, during geological mapping in the central part of the Sverdrup Basin (Balkwill, 1974a). Hopkins studied palynomorphs from the samples in 1976. Data from those studies, combined with earlier macrofossil determinations and age assignments by J. A. Jeletzky (pers. comm., 1973, 1974), are significant for correlation within Sverdrup Basin and beyond its limits.

Hoodoo Dome is a doubly-plunging anticline, cored and pierced locally by a diapir composed of halite and other evaporitic rocks of Carboniferous age (Stott, 1969; Davies, 1975). Strata along the eastern flank of the dome dip eastward at low to moderate angles and are fairly well exposed (Fig. 58. 1b). Nonmarine Lower Cretaceous sandstones of the Isachsen Formation are in diapiric fault contact with Carboniferous rocks in the core of the dome; Eureka Sound sandstones of Maastrichtian age are the youngest beds in the concordant succession.

DescriptionChristopher Formation

About 850 m (2800 ft.) of pelite-dominated Christopher Formation strata lie conformably on Isachsen Formation sandstone at Hoodoo Dome (Fig. 58.2). The Christopher Formation can be divided there, as in neighbouring parts of Sverdrup Basin (Balkwill, 1974a), into two informal members: a lower member, about 395 m (1300 ft.) thick, consisting of dark greenish grey, moderately to very silty shale, with sparse, poorly preserved macrofossils, some buff calcareous mudstone nodules, and, at the top, an interval about 60 m (200 ft.) thick of fine grained glauconitic sandstone; and an upper member, about 455 m (1500 ft.) thick, of dark grey, slightly silty, partly fossiliferous shale, with small red-brown ironstone nodules. Glauconitic sandstones near the top of the lower informal member have well developed, low-angle cross-strata comparing closely with structures recently termed hummocky cross-strata (Harms *et al.*, 1975, p. 87).

Uppermost beds of the Christopher Formation grade to overlying Hassel Formation sandstone. Carbonate mounds, of the type described by Nassichuk and Roy (1975) and present in the Christopher Formation on the western flank of Hoodoo Dome, were not observed in the strata on the eastern flank.

Hassel Formation

Hopkins and Balkwill (1973) previously described the lithology and palynology of the Hassel Formation at Hoodoo Dome, and estimated the thickness of the formation there to be about 180 m (600 ft.). That estimate is too low: a section was measured using surveying instruments, and found to be about 270 m (900 ft.) thick. The lower 45 m (150 ft.) of this succession consists of yellow-brown to green-grey, fine grained, glauconitic sandstone. Those beds are overlain by very light buff, coarse- to fine-grained, fining-upward cycles of partly carbonaceous sandstone, with some tabular cross-strata. The Hassel Formation is conformably and abruptly overlain by Kanguk Formation shale. Distinction between intra-Hassel lithologies is obvious in most outcrops, somewhat less obvious from low-flying aircraft, but very difficult to detect on aerial photographs, and consequently the intraformational contact is not easily mappable. Nonetheless, distinction of these contrasting lithologies may help in regional correlation of the Hassel Formation.

Kanguk Formation

The Kanguk Formation on the eastern flank of Hoodoo Dome is about 450 m (1500 ft.) thick. Throughout southern Ellef Ringnes Island, the formation can be divided into two informal members. The lower member is about 240 m (800 ft.) thick and consists of black, slightly silty, soft, pyritic shale, with abundant very thin beds and laminations of yellow-grey-weathering jarositic clay. At Hoodoo Dome, lower beds of this interval locally have brick-red surface colours because of oxidation of iron-sulphate minerals. No macrofossils were observed in any part of this interval on Ellef Ringnes Island; however, beds about 45 m (150 ft.) above the base of the formation on nearby Amund Ringnes Island (Fig. 1a) contain well-preserved early Turonian faunas (*Watinoceras* and *Inoceramus labiatus* zone; J. A. Jeletzky, pers. comm., 1973; and see Jeletzky, 1968), permitting the assumption that part of the lower member at Hoodoo Dome is of about the same age (Fig. 58.2). Samples of lower Kanguk strata, analyzed by A. E. Foscolos, had a mean pH of about 3.5 in aqueous suspension. This extreme acidity may cause significant leaching, and may explain the paucity of calcareous foraminifers in the lower part of the Kanguk Formation (J. H. Wall, pers. comm., 1975).

The upper informal part of the Kanguk Formation consists of dark brown-grey shaly siltstone and silty shale, containing small red-brown ironstone nodules and relatively few jarositic clay beds. This succession is about 210 m (700 ft.) thick at Hoodoo Dome. The

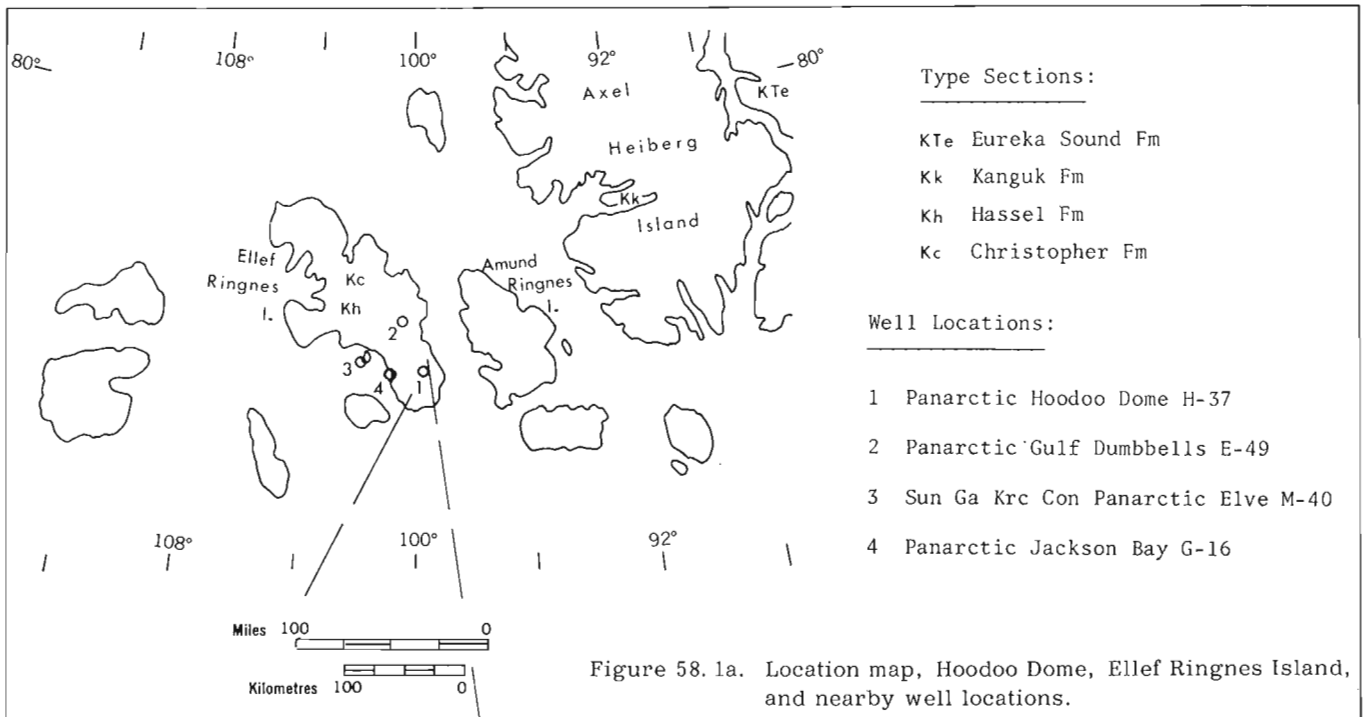


Figure 58. 1a. Location map, Hoodoo Dome, Ellef Ringnes Island, and nearby well locations.

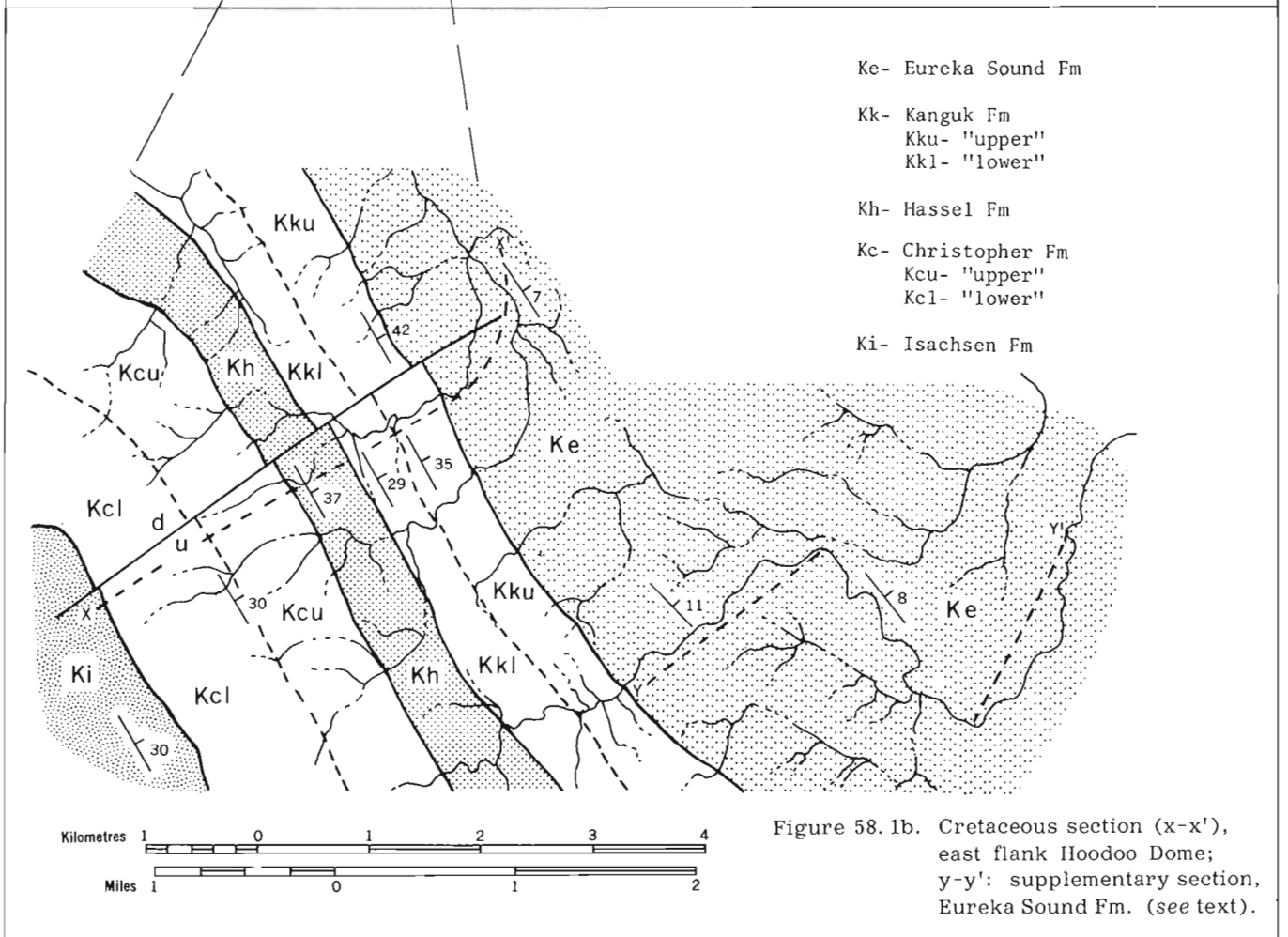


Figure 58. 1b. Cretaceous section (x-x'), east flank Hoodoo Dome; y-y': supplementary section, Eureka Sound Fm. (see text).

approximate base of the silt-dominated sequence is marked throughout southern Ellef Ringnes Island by a low but prominent escarpment. Strata composing the upper Kanguk succession contain well-preserved molluscs. A collection from about 5 m (15 ft.) above the base, dated by Jeletzky (pers. comm., 1974) as late early or early late Santonian, contains the oldest macrofaunas obtained from this informal unit.

Eureka Sound Formation

Kanguk pelites are conformably and transitionally overlain by sandstone-dominated strata of the Eureka Sound Formation (Fig. 58.2). About 300 m (1000 ft.) of Eureka Sound beds are exposed on the eastern flank of Hoodoo Dome; the upper surface of the formation forms the axis of a syncline that parallels the eastern coast of the island. Lower Eureka Sound beds are partly green-grey, glauconitic sandstones, and partly dark grey, shaly mudstones, containing marine foraminifers. The remainder of the succession is mainly light buff sandstone with very thin lignite beds and carbonized logs and plant debris. All of the Eureka Sound beds at Hoodoo Dome are Late Cretaceous in age.

Palynology

The accompanying stratigraphic range chart (Fig. 58.2) is abbreviated greatly because of space limitations. Only those genera significant for age or ecological considerations are itemized, and numerous species of long-ranging genera are not listed. Because of this abbreviation, it seems appropriate to discuss briefly the microflora of the upper part of the Kanguk and lower part of the Eureka Sound formations. Our interpretations rely greatly on the published work of Brattseva (1965), Chlonova (1961, 1967), Felix and Burbridge (1973), McIntyre (1974), Tschudy and Leopold (1970), and others, as well as several unpublished sections by W. S. Hopkins.

In addition to the section described here, another section of upper Kanguk-lower Eureka Sound strata, located several miles to the southwest (Fig. 58.1b), was sampled. For discussion, the results of sample study of both sections are combined. In the upper Kanguk, the following angiosperm species make their first appearance: *Azonia pulchella*, *Expressipollis ocliferius*, *Aquilapollenites reticulatus*, *Aquilapollenites* cf. *A. turbidus*, as well as several other unidentified species of *Aquilapollenites*. Although not abundant, all of these species apparently make their first appearance in the Campanian. In the lower Eureka Sound, a great multiplicity of age-diagnostic angiosperm species make their first appearance and comprise a substantial proportion of the microflora. Although not a complete list, the following forms appear rather abruptly: *Aquilapollenites attenuatus*, *A. spinulosus*, *A. quadrilobus* and other species of *Aquilapollenites*; *Fibulapollis mirificus*, *Integricorpus* sp., *Expressipollis accuratus*, *E. sibiricus*, *E. barbatus*, *Azonia ovata*, *Wodehouseia spinata*, *W. jacutense*, *Orbiculapollis globosus* and, somewhat higher in the section, *Paraalnipollenites confusus*. The

earlier named species, from the upper Kanguk, also are found here.

The species listed as first occurring in the Kanguk are generally regarded as making their first appearance in the middle to late Campanian. Of those listed as first occurring in the lower Eureka Sound, at least five first appear in the Campanian, whereas the others are considered to be restricted to the Maastrichtian. *Paraalnipollenites confusus* apparently appears first in the early or middle Maastrichtian and in the sections at Hoodoo Dome was found only in the uppermost samples.

There is no clearly defined and unequivocal microfloral boundary between the Campanian and Maastrichtian stages. It seems, however, that the boundary at Hoodoo Dome lies very close to the contact between the Kanguk and Eureka Sound formations. It is possible (in fact probable) that the Campanian-Maastrichtian boundary lies in the lower part of the Eureka Sound Formation, so that the basal beds of that unit are locally as old as Campanian. Further, it appears that there are no rocks younger than middle Maastrichtian in the sections at Hoodoo Dome.

Interpretation

Greenish grey sandstones are present in the middle part of the Christopher Formation on Ellesmere and Axel Heiberg islands (Thorsteinsson and Tozer, 1970, p. 583) and, perhaps, are approximately coeval and correlative with glauconitic sandstones at the top of the lower informal member of the Christopher Formation at Hoodoo Dome. Hummocky cross-stratification, of the type common in those sandstones, has been interpreted (Harms *et al.*, 1975) as a product of strong wave action (possibly from storm-wave surges) in moderately shallow offshore environments. If the sandstone succession is as widespread as it seems to be, its presence may indicate early Middle Albian or slightly older shallowing of Sverdrup Basin and accelerated contribution of sand to the basin, possibly as a response to regional uplift distant from the basin.

Fine grained glauconitic sandstones of the lower part of the Hassel Formation are likely marine shoreface deposits. Miall (1975) reported Upper Albian, glauconitic, marine shoreface sandstones, lying on Christopher Formation pelites, at Banks and Eglinton islands. He tentatively assigned the rocks there to the Hassel Formation, but indicated his intention to re-name the succession at a later time. The Cenomanian Stage does not seem to be represented at Banks Island and other areas peripheral to Sverdrup Basin; however, the nonmarine middle and upper parts of the Hassel Formation at Hoodoo Dome and environs may be partly Cenomanian. The abundance of tabular cross-strata, and lack of pelitic beds, may be taken to indicate (Smith, 1970) that Hassel arenites were deposited by a braided stream system on a deltaic or alluvial plain and, likely, are not the products of a large meandering river.

Cenomanian Kanguk strata have been reported in the Sverdrup Basin (Thorsteinsson and Tozer, 1970, p. 583). Basal Kanguk beds at Hoodoo Dome are not

dated but, reasonably, may be as old as Cenomanian (Fig. 58.2), considering that there are proven lower Turonian beds within 45 m (150 ft.) of the base of the formation on nearby Amund Ringnes Island. The Hassel/Kanguk succession may represent more or less continuous deposition from late Early to early Late Cretaceous, in contrast with other parts of the Canadian Arctic where there is commonly a hiatus at the series boundary (Jeletzky, 1971, p. 47-49).

Regional volcanism had a profound influence on the lithologic character of the lower Kanguk shales, not only in contributing the distinctive clays of the succession, but also by imparting its extreme acidity and high iron content. Preservation of very thin tuffaceous clay beds in the lower part of the formation implies that low-energy conditions of accumulation prevailed until approximately late early or early late Santonian, the age of the oldest dated beds in the silt-dominated upper Kanguk succession (Fig. 58.2). Most of the Upper Cretaceous strata in areas adjacent to Sverdrup Basin, as on Banks Island (Miall, 1975), are Santonian or younger, and are separated from underlying rocks by a hiatus.

Fricker (1963, p. 119) divided the Kanguk Formation on western Axel Heiberg Island into an informal lower shale member and an informal upper siltstone member; his descriptions of those units are similar to the lithologies of informal members observed at Hoodoo Dome (Fig. 58.2). These contrasts in lithology may represent a widespread intra-basin response to Arctic regional epeirogenesis and changed depositional regimes. With additional mapping and biostratigraphic data, it may be feasible to separate the distinctive successions on a formal basis.

Campanian and Maastrichtian Eureka Sound strata are the youngest part of the conformable succession in this part of the Sverdrup Basin. [There is a thicker, about 800 m (2400 ft.), section of Eureka Sound beds at Malloch Dome, western Ellef Ringnes Island, but the uppermost beds there are Upper Cretaceous also.] In contrast, nearly horizontal, Paleocene/Eocene, non-marine sandstones lie unconformably on folded Mesozoic rocks on Amund Ringnes and Cornwall islands (Balkwill, 1974b). Therefore, folding, major uplift, and erosion in the Ringnes Islands seem mainly to have ranged from late Maastrichtian to about late Paleocene. These events are approximately contemporaneous with initial broad uplift of Princess Margaret Arch in central Axel Heiberg Island, but are older than the middle Eocene/Oligocene phase of compressive tectonism that affected the type region of the Eureka Sound Formation in eastern Axel Heiberg Island and western Ellesmere Island (Balkwill *et al.*, 1975).

References

- Balkwill, H. R.
 1974a: Structure and stratigraphy, Ringnes Islands and nearby smaller islands, District of Franklin; in Report of Activities, Pt. A; Geol. Surv. Can., Paper 74-1A, p. 287-289.
- Balkwill, H. R. (cont'd.)
 1974b: Structure and tectonics of Cornwall Arch, Amund Ringnes and Cornwall Islands, Arctic Archipelago; in Proc. Vol., 1973 Symposium on the Geology of the Canadian Arctic, J.D. Aitken and D.J. Glass, eds.; Geol. Assoc. Can./Can. Soc. Petrol. Geologists, p. 39-62.
- Balkwill, H. R., Bustin, R.M., and Hopkins, W.S., Jr.
 1975: Eureka Sound Formation at Flat Sound, Axel Heiberg Island, and chronology of the Eureka Orogeny; in Report of Activities, Pt. B; Geol. Surv. Can., Paper 75-1B, p. 205-207.
- Brattseva, G.M.
 1965: Pollen and spores of the Maastrichtian deposits of the Far East; Akad. Nauk SSSR, Geol. Inst., Tr., no. 129.
- Chlonova, A.F.
 1961: Spores and pollen of the upper half of the Upper Cretaceous in the eastern part of the western Siberian Lowland; Akad. Nauk SSSR, Geol. Geofiz. Inst. Sib. Otd., Tr., v. 7.
 1967: Possible botanical relationships of the pollen of the morphological type "Oculata"; Rev. Paleobot. Palynol., v. 5, p. 217-226.
- Davies, G.R.
 1975: Hoodoo L-41: diapiric halite facies of the Otto Fiord Formation in the Sverdrup Basin, Arctic Archipelago; in Report of Activities, Pt. C; Geol. Surv. Can., Paper 75-1C, p. 23-29.
- Felix, C.J. and Burbridge, P.P.
 1973: A Maastrichtian age microflora from Arctic Canada; Geoscience and Man, v. 7, p. 1-29.
- Fricker, P.E.
 1963: Geology of the Expedition area, west-central Axel Heiberg Island, Canadian Arctic Archipelago; McGill Univ., Axel Heiberg Island Research Reports, no. 1.
- Harms, J.C., Southard, J.B., Spearing, D.R., and Walker, R.G.
 1975: Depositional environments as interpreted from primary sedimentary structures and stratification sequences; Soc. Econ. Paleontol. Mineral., Lecture Notes, Short Course No. 2 (Dallas, Texas), Tulsa, Okla.
- Hopkins, W.S., Jr. and Balkwill, H.R.
 1973: Description, palynology and paleoecology of the Hassel Formation (Cretaceous) on eastern Ellef Ringnes Island, District of Franklin; Geol. Surv. Can., Paper 72-37.

Jeletzky, J. A.

1968: Macrofossil zones of the marine Cretaceous of the Western Interior of Canada and their correlation with the zones and stages of Europe and the Western Interior of the United States; Geol. Surv. Can., Paper 67-72.

1971: Marine Cretaceous biotic provinces and paleogeography of western and Arctic Canada: illustrated by a detailed study of ammonites; Geol. Surv. Can., Paper 70-22.

McIntyre, D. J.

1974: Palynology of an Upper Cretaceous section, Horton River, District of Mackenzie, N. W. T.; Geol. Surv. Can., Paper 74-14.

Miall, A. D.

1975: Post-Paleozoic geology of Banks, Prince Patrick and Eglinton Islands, Arctic Canada in Canada's continental margins and offshore petroleum exploration, C. J. Yorath, E. R. Parker and D. J. Glass, eds.; Can. Soc. Petrol. Geologists, Mem. 4, p. 557-587.

Nassichuk, W. W. and Roy, K. J.

1975: Mound-like carbonate rocks of Early Cretaceous (Albian) age adjacent to Hoodoo Dome, Ellef Ringnes Island, District of Franklin; in Report of Activities, Pt. A; Geol. Surv. Can., Paper 75-1A, p. 565-569.

Smith, N. D.

1970: The braided stream depositional environment: comparison of the Platte River with some Silurian clastic rocks, north-central Appalachians; Bull. Geol. Soc. Am., v. 81, p. 2993-3014.

Stott, D. F.

1969: Ellef Ringnes Island, Canadian Arctic Archipelago; Geol. Surv. Can., Paper 68-16.

Thorsteinsson, R. and Tozer, E. T.

1970: Geology of the Arctic Archipelago; in Geology and Economic Minerals of Canada, R. J. W. Douglas, ed.; Geol. Surv. Can., Econ. Geol. Rept. 1, p. 548-590.

Tschudy, D. D. and Leopold, E. B.

1970: *Aquilapollenites* (Rouse) Funkhouser -- selected Rocky Mountain taxa and their stratigraphic ranges; Geol. Soc. Am., Spec. Paper 127, p. 113-167.

Project 700041

J. L. Jambor¹ and W. J. McMillan²
Regional and Economic Geology DivisionIntroduction

Gypsum and anhydrite have been reported to occur in several porphyry copper deposits in the United States (Meyer, 1965; Lowell, 1968; Sheppard and Taylor, 1974; Phillips *et al.*, 1974; Corn, 1975), in Puerto Rico (Cox *et al.*, 1973), in Chile (Howell and Molloy, 1960; Sillitoe, 1973), in the Philippines (Bryner, 1969), and in Canada (e.g., Barr, 1966; Carson and Jambor, 1974). Occurrences of anhydrite seem to be much more common than those of gypsum, and where mention is made of either mineral, the association seems to be most commonly with the zone of potassic alteration in porphyry deposits. In the compilation by Lowell and Guilbert (1970), anhydrite appears only in the "Inner Zone" of hydrothermal alteration at one deposit, and in the "Innermost Zone" at eight deposits. Although the mineral has not been found in the outer zones of alteration, detailed studies of the El Salvador (Chile) orebody by Gustafson and Hunt (1975) have shown that the sulphate zone overlaps several of the major hydrothermal alteration zones.

To the writers' knowledge, the distribution of sulphates in porphyry deposits has not been studied in detail except at El Salvador. This paper presents the results of a study of gypsum distribution in the Valley Copper porphyry deposit, Highland Valley, British Columbia. The deposit is about 55 km southwest of Kamloops and is entirely in Bethsaida quartz monzonite of the Triassic Guichon Creek batholith. Reserves in the deposit are approximately 850 million tons grading 0.48 per cent copper to a depth of 1450 feet. The largest part of the copper zone is in Valley Copper proper, which is controlled by Cominco Ltd., but part extends into claims held by Bethlehem Copper Corporation (Fig. 59.1). Bethlehem has named its part of the deposit the Lake Zone. No date has been set for bringing the Valley Copper deposit into production.

Gypsum at Valley Copper

Although gypsum in porphyry deposits of the Highland Valley was recognized several years earlier, the spatial distribution of the mineral was first published by McMillan (1971). In two vertical cross-sections through the Valley Copper deposit, McMillan demonstrated that the initial appearance of gypsum down the drillholes is not erratic but occurs at a fairly

constant topographic elevation that can be projected from hole to hole to form a "gypsum line". Below this "line" gypsum is common. Subsequently, J. L. Jambor logged all the drillholes in the Cominco part of the deposit in order to define more precisely the distribution of gypsum both in the copper zone and peripheral to it. Drill core from the Lake Zone was sampled, but the L-series holes (Bethlehem Copper) were not logged. Therefore, the vertical distribution of gypsum in L-holes is based on laboratory samples and is not accurate.

Recently, Jones (1975) established the position of the gypsum line in the deposit in 12 surface drillholes not logged by McMillan (1971). These independently determined results are generally in excellent agreement with the more extensive data reported here.

Description of Sulphates

Most gypsum is white to orange and fibrous, but plates up to 5 mm long are present locally. The principal occurrence is in veinlets from less than 1 mm to about 5 mm thick. The maximum width is 8 cm (Jones, 1975), but veinlets more than 1 cm wide are rare. Veinlet abundances are variable, but several occurrences per foot are common in some drill-holes. The veinlets extend at least 2500 feet below surface, but the general impression is that widths decrease near the bottoms of the deepest holes. Gypsum veinlets cut all hydrothermal alteration types, and all quartz and sulphide-bearing veinlets in the deposit.

In addition to its presence as veinlets, gypsum also occurs as patches disseminated in potassic-altered rocks and is present in minor amounts as interstitial grains in both mineralized quartz and K-feldspar-quartz veins. No gypsum has been found near the surface of the deposit, and its distribution is not related to the oxidation zone which is only locally developed and rarely more than 50 m deep.

Anhydrite is common as microscopic grains associated with K-feldspar and sericite in rocks which have intense potassic-alteration but no significant argillic alteration. Rare megascopic anhydrite grains are pale purple and have been noted in masses up to 2 by 2 cm. Although anhydrite veinlets have not been observed, Jones (1975) reported that anhydrite is present in gypsum from moderately argillized rock, and in sulphide-bearing quartz and quartz-sericite veins. According to Jones, virtually all the anhydrite is below the 3400-foot level.

¹J. L. Jambor, CANMET, 555 Booth Street, Ottawa, K1A 0G1

²W. J. McMillan, British Columbia Department of Mines and Petroleum Resources, Victoria, B. C.

of late-stage, barren quartz veins and associated silicification. The most intensely veined and silicified part of this zone forms an elongate dome which extends from the Lornex fault toward the core of the deposit. Rocks within the dome commonly consist of up to 50 per cent barren quartz. The contacts of the dome are gradational. The highest grade part of the copper zone (> 0.5 per cent copper) is centrally located in the deposit and is wrapped around the northwestern part of the quartz-rich dome.

The three-dimensional shape of the copper zone is not precisely known. However, near the Lornex fault (Section 9, Fig. 59.1), the copper zone appears to have a steep or vertical dip whereas the western side of the deposit dips inward at a moderate angle.

In plan, the drill-intersected gypsum line conforms fairly closely with the copper zone. Cross-sections of the deposit (Fig. 59.2) show that the gypsum line has the following features:

1. At the southeastern end of the deposit, gypsum is absent in Sections 9 and 10 and comprises only a thin band in Section 11 in diamond drill holes 68-14 (Fig. 59.2). Gypsum-bearing samples in holes L-7 and L-12, which are southeast of the section, are approximately 250 feet lower. Because the holes were not logged in detail it is not certain whether the gypsum line is almost horizontal, is offset by faulting between holes 68-14 and L-12, or plunges steeply southeastward.
2. The gypsum zone broadens and thickens northward. The elevation of the top of the gypsum line rises from about 3200 feet in Section 11 to 3500 feet in Section 12, beyond which its elevation remains fairly constant to Section 17. Gypsum in this extensive central area of the deposit persists to the bottoms of the deepest drillholes.
3. In Section 17, the elevation of the gypsum line southwest of the reference line decreases to about 3100 feet elevation, and in Section 18 the gypsum zone pinches out to the southwest.

Relationship to Hydrothermal Alteration

Hydrothermal alteration at Valley Copper has been described by McMillan (1971), Jones (1975), and in less detail by several others. Additional studies by J. L. Jambor are still in progress, but some generalizations with respect to gypsum and hydrothermal alteration can be made.

The copper zone at Valley Copper is roughly centrally located within a zone of potassic alteration, the outer limits of which are marked by the disappearance of hydrothermal biotite. In the core of the deposit, K-feldspar is abundant and at depth the potassic assemblage is K-feldspar-sericite-biotite-anhydrite. Within the copper zone, argillic alteration is locally extremely intense to the point where large masses of rock in the deposit are cream coloured and chalky in appearance; in such material the feldspars are largely obliterated, and primary and hydrothermal

biotite commonly is completely replaced, though sericite and quartz are not visibly affected. Areas in which intense argillic alteration of this type predominate are shown in several cross-sections (Fig. 59.2). Such areas are not laterally continuous outside the copper zone and are rare outside it. Significantly, these intense argillic zones decrease with depth; the change is seen best in Sections 16 and 17 (Fig. 59.2) because this area is distant from the zone of late-stage silicification. These sections show a downward change from intense argillic to potassic alteration at depth. Within the deep core of the deposit, pink K-feldspar is a conspicuous megascopic constituent, sericite is coarse but not demarcated as well-defined selvages, and sharply-bounded discrete quartz veins are rare. In the potassic zone peripheral to the K-feldspar-rich core, hydrothermal biotite predominates and relatively linear quartz-poor sericitic veinlets occur. These veinlets clearly cut the pervasively biotitized rock.

The so-called transition zone (Section 16 and 17) consists largely of the K-feldspar-rich potassic assemblage, but contains minor zones of argillic alteration. Below the lower boundary of this transition zone, pervasive argillic alteration is negligible. Rare argillized sections of core, which are not demonstrably related to faults, show that the clay alteration has been superimposed on the gross pattern of potassic alteration. This trend is also evident throughout the deposit because vestiges of potassic alteration are locally preserved in the upper argillic zone.

The distribution of hydrothermal alteration assemblages and gypsum show a clear spatial relationship. Intense argillization and gypsum veining are generally antithetic whereas gypsum and "deep" K-feldspar-rich potassic zones are sympathetic. There are indications that the gypsum zone deepens and pinches out at the periphery of the copper zone, and this too is correlative with the decline in overall intensity of potassic alteration.

Origin of the Gypsum Line

A hypogene origin is accepted for the Valley Copper sulphate zone. The top of the zone is a gently undulating surface below which primary anhydrite is present. A similar sulphate distribution also appears to be present in the porphyry deposit at El Salvador, Chile. Because of the presence of tiny relict grains of anhydrite preserved in quartz, Gustafson and Hunt (1975) concluded that the original sulphate zone at El Salvador probably extended at least several hundred feet above its present level. Although sulphates have not been noted above the gypsum line at Valley Copper, the studies to date have not been sufficiently detailed to exclude their presence. The microscopical studies, however, do indicate that some disseminated interstitial anhydrite has been partly hydrated to gypsum, and that disseminated gypsum increases at the expense of anhydrite near the gypsum line.

The interpretation of the origin of the gypsum distribution is inextricably related to the interpretation

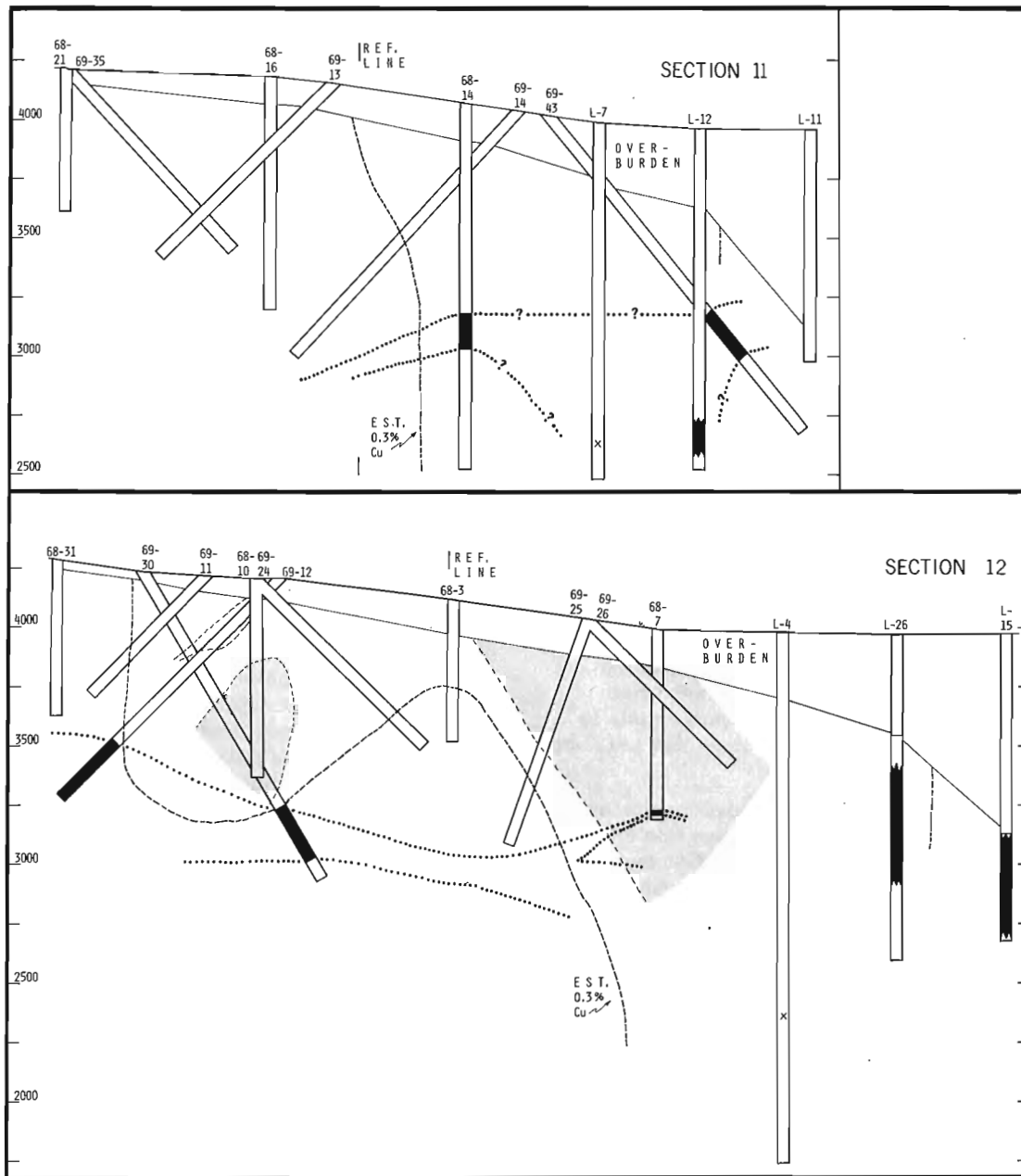
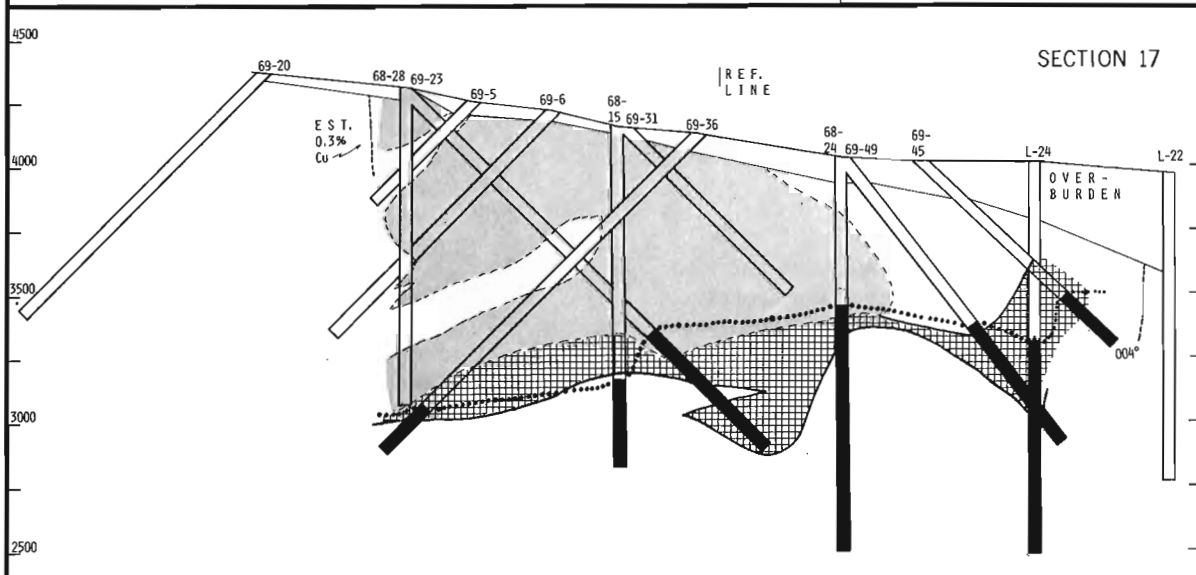
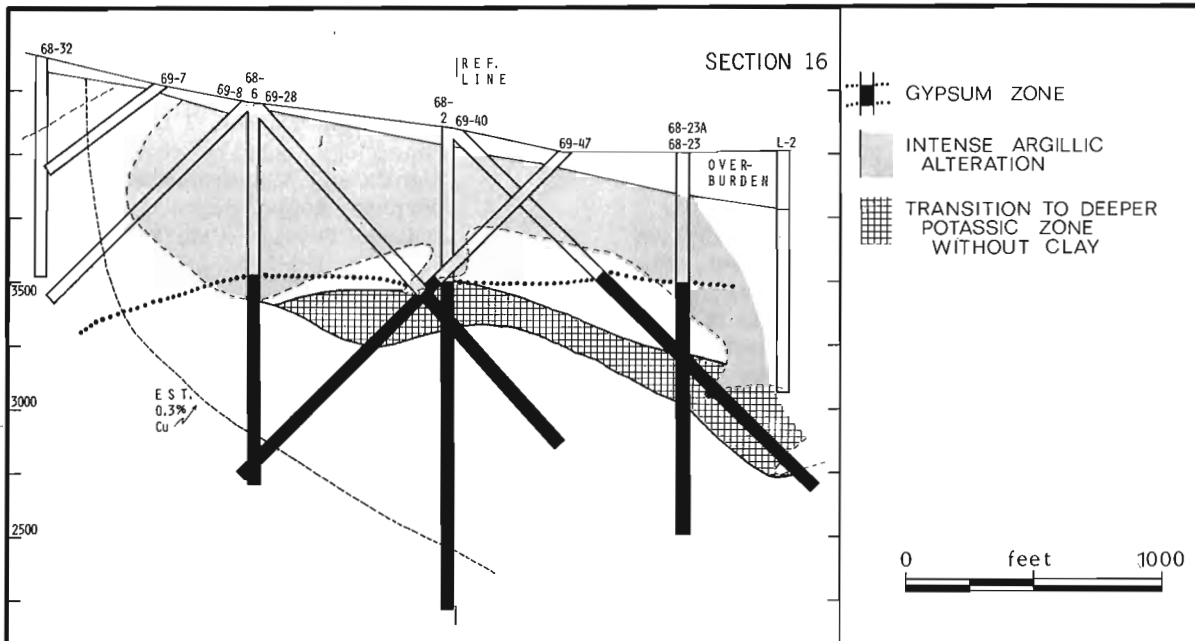
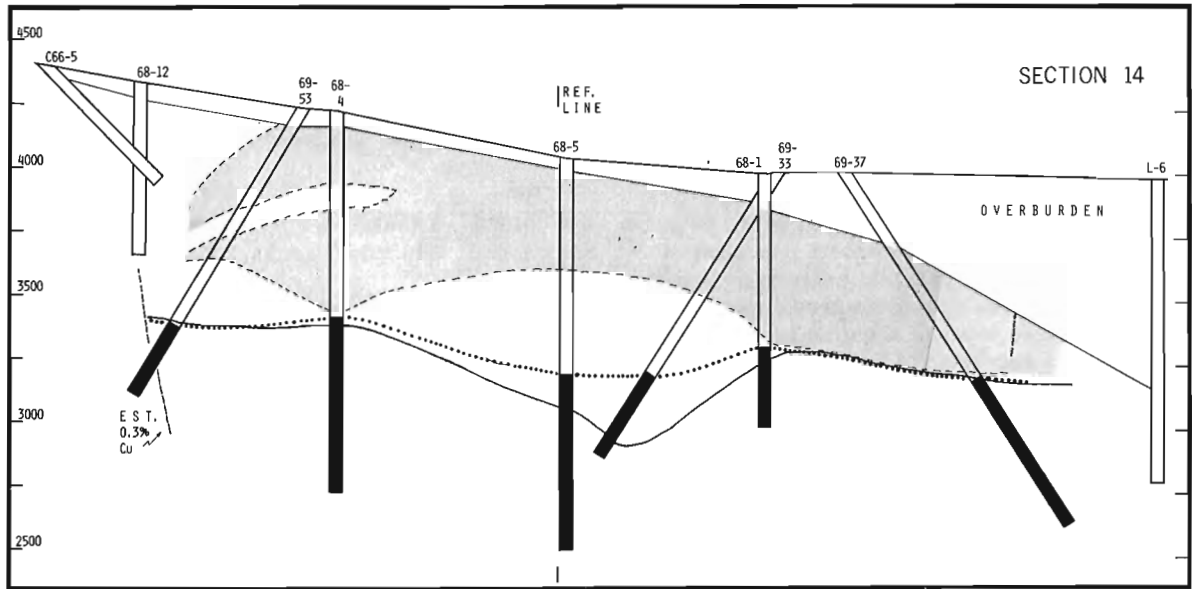


Figure 59.2. Vertical cross-sections of the Valley Copper deposit. Horizontal and vertical scales are identical in all sections. Section lines are shown in Figure 59.1.

- Section 11: gypsum zone is shown in solid black; limits of the zone in hole L-12 are not known, and the single occurrence in hole L-7 is designated by an X. Only local, intense argillic alteration is present in the section.
- Section 12: argillic alteration, designated by shaded pattern, is more intense in the area on the right side of the diagram than on the left. Strong K-feldspar alteration is not present in sections 11 or 12.
- Section 14: solid line beneath the area of intense argillic alteration marks the upper limit of the potassic zone in which only local, minor argillic alteration is present. Moderate K-feldspar alteration occurs between D.D.H. 68-4 and D.D.H. 68-1. The alteration down D.D.H. 68-5 is from intense argillic at the top, through a transition zone in which numerous, discontinuous argillic zones are present in a K-feldspar-bearing potassic zone, and to a deep potassic zone in which argillization is quantitatively insignificant.
- Section 16, 17: argillic alteration is weaker on the extreme left sides of the diagrams than on the right.
- (opposite) Moderate K-feldspar alteration noted in section 14 is continuous to section 16 and declines substantially by section 17. Gypsum in section 18 (not shown) is absent to the left of the reference line.



of the sequence of formation of the major hydrothermal alteration facies. In contrast to the generally prograde sequence advocated by Jones (1975) and Osatenko and Jones (in prep.), the present writers conclude that, although there was considerable overlap, the potassic zone was formed in the initial stage of the development of the deposit and was followed by sericitic (phyllic) and argillic alterations. Although much of the potassic zone in the upper part of the deposit has been obliterated, the innermost residual parts seem to differ only in that they lack the anhydrite present at depth. Thus, the pronounced vertical zonation in the Valley Copper deposit is interpreted to be largely the result of superimposed alteration.

The trend of superimposition appears to have followed the sequence: phyllic → argillic → late-stage silicification → gypsum veining. Although the last two do not have an intimate spatial relationship, a close genetic association between argillic alteration and gypsum veining probably exists. Pervasive argillization and phyllic alteration would release large amounts of calcium to the late-stage hydrothermal system; however, because sulphides do not seem to have been affected, an alternative source or sulphur must be found. Jones (1975) has established from isotopic data that the percentage of ocean water in the Valley Copper hydrothermal system reached its maximum at the time of gypsum deposition. It could be assumed that the residual sulphate-rich magmatic fluids were rapidly cooled by the influx of oceanic water, causing gypsum deposition from the hydrothermal mix. However, this model requires that the residual solution be unreasonably sulphate-rich. The alternative favoured here is that the late-stage influx of ocean water accelerated the temperature decline in the partly cooled hydrothermal system which was already rich in calcium and sulphate derived by leaching of the upper part of the potassic zone during argillic alteration. The assumption that anhydrite initially extended above its present position is supported by the apparent abruptness of the change into anhydrite-bearing rock and the lack of comparable vertical zonation in other minerals of the potassic assemblage. Thus, the top of the gypsum zone is considered to represent the horizon at which significant hydrothermal activity ceased. Although lateral migration of the late fluids could distort the model, the gypsum zone at Valley Copper should ideally pinch out at the extreme periphery of the potassic zone because this area lacked anhydrite and was cooler during the last stages of hydrothermal alteration.

Acknowledgments

The writers are grateful to J. M. Allen and the management of Cominco Ltd. for granting access to the Valley Copper drill core, and to R. Anderson and the management of Bethlehem Copper Corporation for permission to sample Lake Zone drill core.

References

- Allen, J. M.
1969: Engineer's Report; Statement of material facts; Vancouver Stock Exchange.
- Barr, D. A.
1966: The Galore Creek copper deposits; Can. Inst. Min. Met. Trans., v. 64, p. 251-263.
- Bethlehem Copper Corporation Ltd.
1968: Special report on exploration in highland Valley; August 19, 1968.
- 1968-
1969: Report to the shareholders; December 1968-February 1969.
- 1969: Report to the shareholders; March-April-May 1969.
- Bryner, L.
1969: Ore deposits of the Philippines — an introduction to their geology; Econ. Geol., v. 64, p. 644-666.
- Carson, D. J. T. and Jambor, J. L.
1974: Mineralogy, zonal relationships and economic significance of hydrothermal alteration at porphyry copper deposits, Babine Lake area, British Columbia; Can. Min. Metall., Bull.; v. 67, p. 110-133.
- Corn, R. M.
1975: Alteration-mineralization zoning, Red Mountain, Arizona; Econ. Geol., v. 70, p. 1437-1447.
- Cox, D. P., Larson, R. R., and Tripp, R. B.
1973: Hydrothermal alteration in Puerto Rican porphyry copper deposits; Econ. Geol., v. 68, p. 1329-1334.
- Gustafson, L. B. and Hunt, J. P.
1975: The porphyry copper deposit at El Salvador, Chile; Econ. Geol., v. 70, p. 857-912.
- Howell, F. H. and Molloy, J. S.
1960: Geology of the Braden orebody, Chile, South America; Econ. Geol., v. 55, p. 863-905.
- Jones, M. B.
1975: Hydrothermal alteration and mineralization of the Valley Copper deposit, Highland Valley, British Columbia; Ph.D. Thesis, Oregon State University.
- Lowell, J. D.
1968: Geology of the Kalamazoo orebody, San Manuel District, Arizona; Econ. Geol., v. 63, p. 645-654.

- Lowell, J. D. and Guilbert, J. M.
1970: Lateral and vertical alteration-mineralization zoning in porphyry ore deposits; *Econ. Geol.*, v. 65, p. 373-408.
- McMillan, W. J.
1971: Valley Copper; *B. C. Dep. Mines Pet. Ressour., Geol. Explor. Min.*, 1970, p. 354-369.
- Meyer, C.
1965: An early potassic type of wall-rock alteration at Butte, Montana; *Amer. Mineral.*, v. 50, p. 1717-1722.
- Osatenko, M. J. and Jones, M. B.
Valley Copper; Cordilleran Porphyry Copper Deposits; *Can. Inst. Min. Met., Spec. Vol. 15*, in prep.
- Phillips, C. H., Gambell, N. A., and Fountain, D. S.
1974: Hydrothermal alteration, mineralization, and zoning in the Ray deposit; *Econ. Geol.*, v. 69, p. 1237-1250.
- Sheppard, S. M. F. and Taylor, H. P., Jr.
1974: Hydrogen and oxygen isotope evidence for the origins of water in the Boulder Batholith and the Butte ore deposits, Montana; *Econ. Geol.*, v. 69, p. 926-946.
- Sillitoe, R. H.
1973: Geology of the Los Pelambres porphyry copper deposit, Chile; *Econ. Geol.*, v. 68, p. 1-10.

E. M. R. Research Agreement 1135-013-4-181/75

R. M. MacKay¹ and M. Zentilli¹
Regional and Economic Geology Division

Radioactive specimens from the dumps at the Black Brook prospect, a copper-uranium occurrence in Pennsylvanian red beds of Colchester County, Nova Scotia, were collected in April 1975. This paper presents the results of a preliminary examination of small uraniferous, calcareous nodules within the specimens.

Black Brook flows into Waugh River about 5.6 km southeast of Tatamagouche. The prospect is 2.4 km upstream from this junction on the north side of the brook. The mineral occurrence was worked during 1907 and 1908 by the Sterling Mining Company and produced 890 tons of ore, about half of which is still on the dumps. A shipment to the United States in 1908 averaged 5.25 per cent copper, and selected samples from drilling by Kennco indicated values of 0.005 per cent U_3O_8 equivalent (Brummer, 1958). The radioactivity was found to be associated mainly "with a black, carbonaceous, coal-like material" (Steady, 1955, in Brummer 1958), but no radioactive minerals were identified.

The geology of the area has been described by Shumway (1951) and Brummer (1958) and the prospect has been evaluated since by different companies (files, N.S. Department of Mines). The mineralization occurs in grey-green conglomerates, grits, and arkoses with coaly material that fill stream channels in continental red beds of the Pictou Formation of Pennsylvanian age (Brummer, 1958).

Radioactive specimens of greenish grey colour, when split, disclosed calcareous nodules of 1 to 2 cm in diameter composed of brownish red fine grained matrix rich in calcite with black streaks of disseminated sulphides and a uranium-rich mineral. Polished section study of the nodules indicates the presence of chalcocite, covellite, bornite, chalcopyrite, pitchblende, and minor galena (Fig. 60.1). The sulphide minerals occur in small anhedral grains (few microns to several millimetres) and in irregular or laminar aggregates. Chalcocite is the most abundant sulphide, is associated with covellite, and commonly shows wood-cell structures replacing coaly material. Bornite displays exsolution lamellae of chalcopyrite.

The pitchblende occurs as colloform aggregates and lenticular stringers 10 to 50 μ in length and has shrinkage cracks; it surrounds copper sulphide aggregates suggesting that it was deposited relatively late, or occurs independently in the matrix, but is generally speckled with very small (1-2 μ) inclusions of sulphides. Reflectivity of the pitchblende is low (11.63 ± 0.02 % at 546 nm) and the intimate intermixing of discrete sulphide



Figure 60.1. Photomicrograph (reflected light, air, X1000) Pitchblende(?), grey(p) with numerous sulphide inclusions. Light area is bornite (bo) surrounded by chalcocite(cc) and covellite(cv); galena (white) occurs as small crystals throughout the sample. The undefined matrix is mainly calcium carbonate.



Figure 60.2. Distribution of uranium - $U M\alpha$, X-ray picture of area covered in Figure 60.1 (X1000).

¹Department of Geology, Dalhousie University,
Halifax, Nova Scotia, B3H 3J5

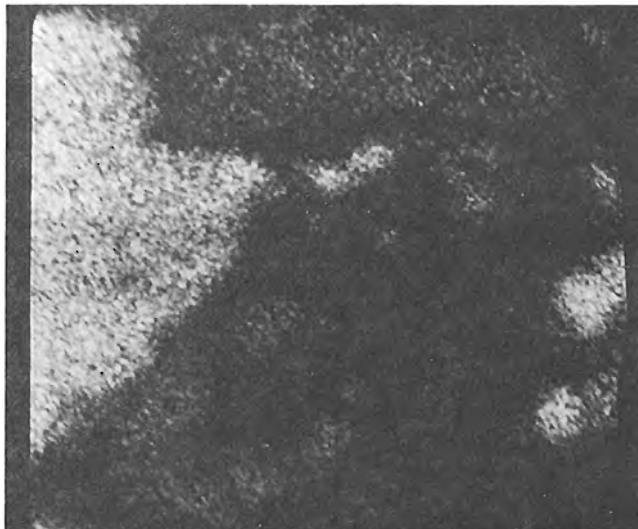


Figure 60.3. Distribution of copper-Cu K α X-ray picture of area covered in Figure 60.1 (X1000).



Figure 60.4. Distribution of iron. Fe K α X-ray picture of area covered in Figure 60.1 (X1000).

inclusions of copper-iron sulphides makes an analysis difficult. Electron probe scans of 15 grains, using pure U₃O₈ as a standard, indicates that the material is composed of 85 to 95 per cent U₃O₈. Other elements indicated in the energy spectrometer and X-ray pictures are copper, iron (Figs. 60.2, 60.3, 60.4), sulphur, and traces of silica, but it is not clear whether these impurities are picked only from the sulphide inclusions or if they are part of the pitchblende groundmass.

Brummer (1958) concluded that the minerals bornite and chalcopyrite are syngenetic with the Carboniferous sediments, but considered that chalcocite, covellite and the uranium mineralization are supergene in origin, probably concentrated during the Pleistocene to Recent time. This interpretation was contested by McCauley (1958), who compared the above occurrences with similar deposits known in Pennsylvania, and ascribed their mineralization to epigenetic hot solutions. The presence in the latter deposits of exsolution lamellae in bornite, he contended, is evidence for higher temperatures of formation than those expected in sedimentary or supergene environments (McCauley, 1958). As mentioned above, bornite from the Black Brook occurrence also shows chalcopyrite exsolution lamellae, but the uranium mineralization may in fact be younger than the bornite. More work is required to evaluate the supergene hypothesis of Brummer (1958), which would limit the potential of many Nova Scotia uranium

concentrations to the present near-surface environments. However, older weathering surfaces under regional unconformities like that under Triassic formations, etc., may deserve equal attention.

References

- Brummer, J. J.
1958: Supergene copper-uranium deposits in northern Nova Scotia; *Econ. Geol.* v. 53, p. 309-324.
- McCauley, J. F.
1958: Supergene copper uranium deposits, Nova Scotia (A Discussion); *Econ. Geol.*, v. 53, p. 1038-1049.
- Shumway, G.
1951: Sedimentary copper, Tatamagouche area, Nova Scotia; Unpublished M. Sc. thesis, M. I. T.
- Steacy, H. R.
1955: Letter to J. J. Brummer, 1st December, 1955, reporting results of investigation on samples submitted to the Radioactivity Laboratory, Mineral Deposits Division, G. S. C.; in *Supergene copper-uranium deposits in northern Nova Scotia*, by J. J. Brummer (1958); *Econ. Geol.*, v. 53, p. 319.

61. MAJOR FEATURES OF THE LOWER AND MIDDLE JURASSIC STRATIGRAPHY OF NORTHERN RICHARDSON MOUNTAINS, NORTHEASTERN YUKON TERRITORY, AND NORTHWESTERN DISTRICT OF MACKENZIE.

Project 750067

T. P. Poulton¹ and J. H. Callomon²

Introduction and acknowledgments

A summary is presented in this report of the pre-Upper Oxfordian Jurassic stratigraphy that is represented in approximately east-west cross-sections of the northern Richardson Mountains in the vicinity of Latitude 68° North (Fig. 60. 1). It is based on the results of four weeks of field work by the writers in 1975, and incorporates interpretations of available previous studies within the area considered.

Most information has been obtained since 1955 by officers of the Geological Survey, primarily J. A. Jeletzky, D. K. Norris, F. G. Young, and E. W. Mountjoy, and considerable data have been provided by the geologists engaged by oil companies. The regional stratigraphic and structural framework has been given by Gabrielse (1957), Martin (1959, 1961, 1963), Norris *et al.* (1963), Moorhouse (1966), Norris (1970, 1973, 1974), Miall (1973), Young (1973, 1975), Jeletzky (1962, 1975), Yorath and Norris (1975), and Yorath *et al.* (1975). Detailed aspects of the Jurassic stratigraphy and paleontology are described by Jeletzky (1967, 1971, 1972a, b, 1974), Frebold (1960, 1961, 1964, 1975), and Frebold *et al.* (1967); these authors include valuable descriptions of stratigraphic sections not reproduced here.

F. G. Young provided the writers with logistical facilities and with free discussion of the Jurassic stratigraphy and sedimentology. J. A. Jeletzky supplied invaluable information and advice, and recommended stratigraphic sections for study. D. K. Norris introduced the senior author to the geological framework of the area and discussed aspects of the Jurassic stratigraphy. The ammonite identifications are by H. Frebold, and J. H. Callomon. J. H. Callomon acknowledges with gratitude travel grants made by the Royal Society of London and the London University Central Research Fund.

Stratigraphy

The pre-Upper Oxfordian Jurassic rocks of northern Yukon and adjacent areas (Figs. 60. 1 - 60. 3) consist of the dominantly sandstone and siltstone Bug Creek Formation (Jeletzky, 1967) to the east and the mainly shale, mudstone and siltstone equivalents of part of the Kingak Formation (Leffingwell, 1919) to the west.

Throughout the area studied, the Jurassic rocks lie on different units of Permian or older Paleozoic

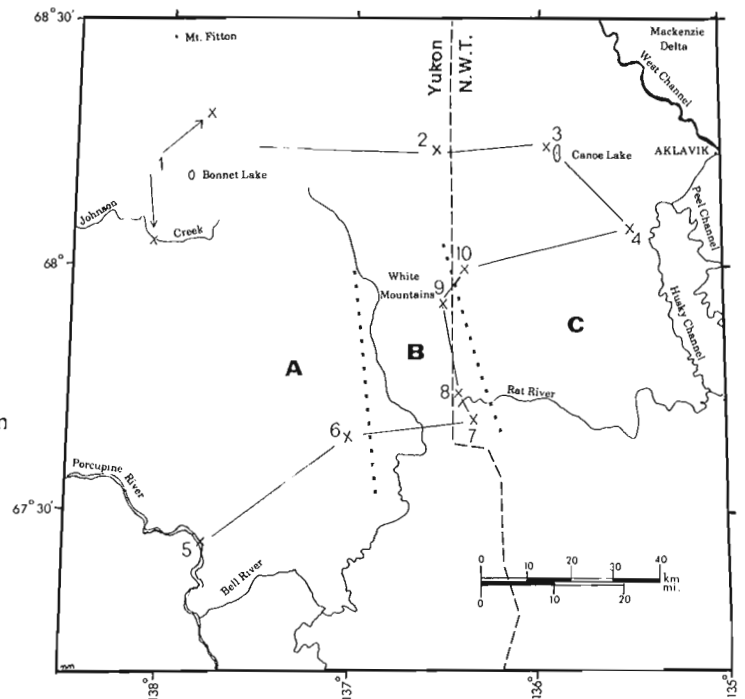


Figure 61. 1. Index map, northern Richardson Mountains. Lettered regions A, B and C correspond with those of text and Figure 61. 2; locations of sections are those of Figures 61. 2 and 61. 3.

rocks (see Bamber and Waterhouse, 1971; Young, 1975) with apparent structural conformity or with gently to strongly angular regional unconformity. The basal contact of the Jurassic, however, is rarely well exposed. In most of the area, the Husky (shale) Formation (Late Oxfordian and younger) overlies the Bug Creek Formation. To the southwest, however, an equivalent, unnamed Upper Jurassic sandstone unit overlies the older Jurassic rocks (Jeletzky, 1975).

The lithologies of the Jurassic rocks are monotonous and most individual units do not appear to be continuous over large areas. The determinations of ammonites, therefore, are of paramount importance in understanding the stratigraphy. Brief accounts of the zonation have been given by Jeletzky (1967, p. 10-12) and Frebold *et al.* (1957, p. 10-11). Where ammonites are absent, certain other fossils, primarily bivalves, are useful for recognition of gross biostratigraphic units. Pending more detailed taxonomic work, the following generalizations concerning the biostratigraphic distribution of non-ammonoid fossils are of interest to field geologists.

¹Institute of Sedimentary and Petroleum Geology, Ottawa.

²University College London, London, England.

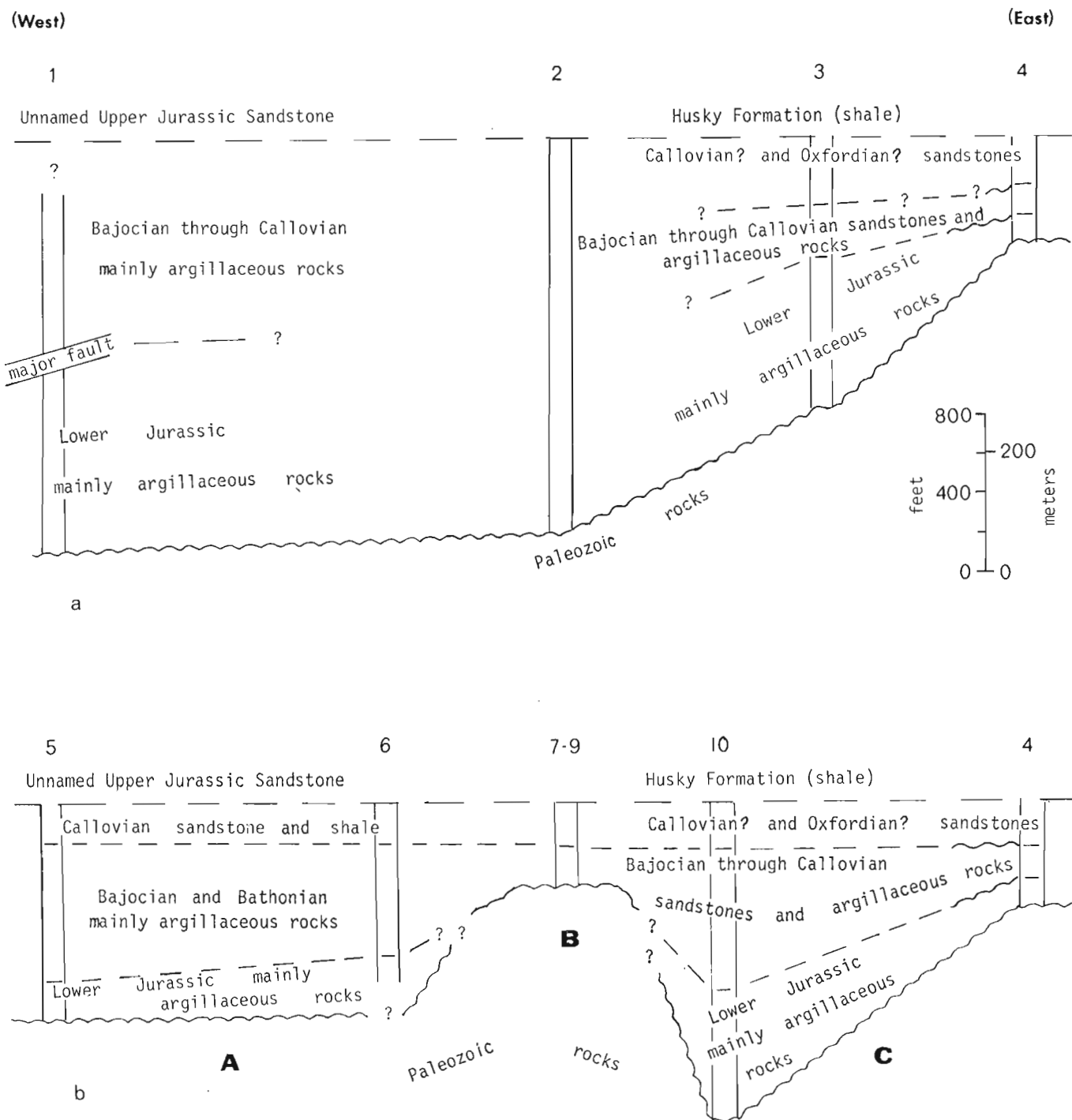


Figure 61.2. Generalized stratigraphic profiles of Jurassic rocks of pre-Late Oxfordian age in northern Richardson Mountains. Locations of sections are shown in Figure 61.1. Section 1 is taken in part from Jeletzky (1971, 1975); the thickness of Section 2 is from Mountjoy and Procter (1969, Sec. 117A5, units 3-8 inclusive). Section 6 is generalized from Jeletzky (1975, Fig. 6, Sec. E2). F. G. Young (pers. comm.) considers the succession 16 km (10 miles) northwest of Section 2 to be considerably thicker than that represented on this diagram.

1. Belemnites have not been found in the pre-Toarcian Jurassic rocks (Jeletzky, 1967, p. 12), but they are common locally in younger beds.

2. Abundant gastropod-brachiopod-bivalve associations characterize the Lower Jurassic strata.

3. *Gryphaea* is a common bivalve in Pliensbachian beds and in a poorly dated, possibly Sinemurian, interval which occurs above Hettangian beds and below reliably dated Pliensbachian beds. Species of *Gryphaea* apparently are absent higher in the column.

4. *Inoceramus* (*Pseudomytiloides*) aff. *I. substriata* (von Münster) is the oldest (Toarcian) species of *Inoceramus* present. *Inoceramus* (*Retroceramus*) species characterize the Middle Jurassic.

Three approximately north-south-trending tectono-stratigraphic facies belts are recognized in Lower and Middle Jurassic strata at approximately Latitude 68° North in the northern Richardson Mountains (Figs. 61.1, 61.2b). The central belt (B), with a relatively thin Middle Jurassic sandstone succession separates the western and eastern belts (A and C, respectively) which exhibit, in addition to thicker Middle Jurassic units, thick Lower Jurassic argillaceous successions. The rocks of the three facies belts merge southward with those on the northern flank of the Aklavik Arch described by previous authors (Jeletzky, 1975; Young, 1975; Yorath *et al.*, 1975). Evaluation of the varying interpretations of these authors regarding the relationships of the Lower to Middle Jurassic rocks of northern Yukon with the Aklavik Arch or with its individual elements is beyond the scope of this paper. The east-west three-fold regional subdivision discussed here apparently is not well represented to the north, where only a general southeasterly thinning is evident (Fig. 2a; Jeletzky, 1967, p. 19; 1975). A general northward thickening and increase in the proportion of argillaceous rocks appears to take place in all three facies belts. Jeletzky (1975, p. 18) considers much of the shale to the north to be representative of outer neritic to (?) upper bathyal depths. The lateral variations in thickness may be due, in part, to differential erosion of rocks below the overlying unnamed Upper Jurassic sandstone (Norris, 1976, p. 460, 461).

The central facies belt (B), with its relatively thin, Middle Jurassic arenaceous succession, conforms both geographically and in the reduced record preserved with the White Uplift and Cache Creek Uplift of previous authors. Jeletzky (1975, p. 31, Fig. 12) described the stratigraphic record of the uplift in its Valanginian manifestation, and Yorath *et al.* (1975, p. 6, Fig. 5) recognized that these uplifts had an effect on the Bug Creek Formation. The nature of the boundaries of the central facies belt remain unknown, and the possibility that these boundaries conform with north-south-trending strike-slip faults with vertical components of displacement (Yorath and Norris, 1975) cannot be dismissed.

In its general character, the western belt (A) of this paper is inferred to be an Early to Middle Jurassic generation of the Porcupine Plains-Richardson Mountains

Trough of Jeletzky (1975, Fig. 9). However, the writers are not able to comment on the somewhat differing interpretations of this depositional basin that have been offered by Young (1975) and Yorath *et al.* (1975). The eastern belt (C) appears to be the Early to Middle Jurassic generation of the Canoe Depression of Cretaceous time (Norris, 1972; Jeletzky, 1975) that has been called the Kugmallit Trough by Yorath *et al.* (1975, p. 6).

It is probable that the region of the Cache Creek Uplift was depressed and filled with sediment in Early Jurassic time (Jeletzky, 1967, p. 18; 1975; Norris, 1976, p. 461), the sediments having been removed by Middle Jurassic or pre-Middle Jurassic erosion. This hypothesis is based on the general similarity of lithologies, faunas, and succession of the Lower Jurassic rocks to the east and west of the central facies belt. This interpretation is supported further by the failure to recognize, in Lower Jurassic rocks just 5 km (3.1 miles) east of the uplift (compare Secs. 9, 10, Fig. 61.3), evidence of submarine slope, lateral facies patterns, paleocurrents, or distinctive detritus that would suggest the presence of a nearby contemporaneous uplift.

A. Western belt

The pre-Upper Oxfordian Jurassic rocks of the western facies belt are predominantly shales and mudstones which were referred to the Kingak Formation of northeastern Alaska (Leffingwell, 1919) by Jeletzky (1971, 1975), Miall (1973), Norris (1972, 1973, 1974), Young (1973) and others. In the Bonnet Lake area (area 1 of Fig. 61.1), the composite section consists of a basal Hettangian sandstone overlain by black shale of Pliensbachian through Callovian ages. The ammonites mentioned by Jeletzky (1962; 1975, Fig. 8) that were identified as *Arcto-asteroceras?* and tentatively dated as Sinemurian by H. Frebold, are known now to be Hettangian; the immediately underlying coal-bearing beds originally believed to be Rhaetian (Jeletzky, 1962, p. 78, 79) are now known to be Paleozoic on paleobotanical evidence (see Jeletzky, 1971, p. 205).

To the south, the thin basal coquina and sandstone at the major bend of the Porcupine River (Section 5, Figs. 61.1, 61.2, 61.3) has not yielded diagnostic ammonites. Overlying shales contain Sinemurian *Echioceras* cf. *E. arcticum* Frebold (1975). Succeeding beds of Late Bajocian through at least Early Callovian ages are mainly argillaceous but contain considerable numbers of sandstone interbeds which Jeletzky (1975, p. 10, 11) considered to be westerly derived, and independent of coeval sandstones to the east discussed below. The main concentrations of sand are in Upper Bajocian, Middle Bathonian, and Lower Callovian strata.

The thicknesses of the western succession shown in Figure 61.2 are minimal estimates; Jeletzky (1975, Fig. 7, Secs. F2, F3) reported approximately 1320 m (4000 ft.) of pre-Upper Oxfordian Jurassic rocks west of White Mountains, and F. G. Young (pers. comm.) recorded approximately 760 m (2500 ft.) in the same general area.

B. Central belt

Permian rocks of the central belt are overlain with regional unconformity by a relatively thin, mainly sandstone succession of Late Bajocian, Bathonian, and possibly Callovian ages. A thin, poorly exposed argillaceous unit, occurring locally at the base, may represent the Lower Jurassic argillaceous unit which occurs to the east and west. The lowest sandstone units are rich locally in belemnites and *Inoceramus* sp. and contain, in places, specimens of *Cranocephalites* spp. This unit, therefore, may be correlated with the upper part of the Intermediate Sandstone Member of the Bug Creek Formation at its type section (Sec. 4, Fig. 61.3; Jeletzky, 1967) and with analogous sandstones in section 5 (Fig. 61.3) on Porcupine River.

The succession is topped by a bluff-forming, commonly crossbedded or massive, orthoquartzite, the upper age limit of which is not known exactly. Poorly preserved ammonites identified as *?Arcticoceras* or *?Cadoceras* sp. and large *Inoceramus* (*Retroceramus*) sp., found by the writers near the top of this unit suggest a Late Bathonian or Callovian age for the beds which contain them (Sec. 7, Fig. 61.3). Although its thickness is difficult to estimate because it commonly forms long dip slopes, this widespread quartzite unit exhibits considerable variation in thickness from place to place. Possibly the variation in thickness of this unit, its high degree of induration, and the apparent lack of ammonites definitely identified as Callovian in age such as those present to the east in the type area of the Bug Creek Formation (Jeletzky, 1967, p. 17) and in equivalent rocks to the west (Sec. 5, Fig. 61.3), are related to pre-Late Oxfordian erosion.

Graphic illustrations of stratigraphic sections studied by the writers, and proposed correlations are shown in Figure 61.3. Locations are shown in Figure 61.1. Section 5 was previously described briefly by Jeletzky (in Frebold, 1961, p. 6; Jeletzky, 1974, p. 4; 1975, Fig. 6). Section 4, the type section of the Bug Creek Formation, was described previously by Jeletzky (1967, p. 86-92). Section 10 was reproduced previously by Jeletzky (1967, p. 166-171; 1975, Fig. 7) based on a description by geologists of British American Oil, but this description cannot be satisfactorily reconciled with that of the present writers. H. Frebold (pers. comm.) indicates that the specimen of *Arietites* sp. sensu lato (Frebold, 1960, p. 13, Pl. I; 1975, p. 16; Jeletzky, 1967, p. 169) obtained by those geologists and identified by him, and *?Echioceras* sp. collected by the present writers but identified by him, may be the same form, both collections being poorly preserved. Besides the difficulty of determining the exact stratigraphic occurrence of the earlier collection, other uncertainties in the section reproduced in Jeletzky (1967) are the unusual and, therefore, probably erroneous, citation of belemnites and *Inoceramus* below the above-mentioned ammonite. The same section also was described by E. W. Mountjoy (in Mountjoy and Proctor, 1969, Sec. 116P6), whose description conforms in general with ours. *Arkelloceras elegans* Frebold (Frebold et al., 1967, p. 17, Pl. III, Fig. 8) was collected by Mountjoy

from a level near the beds that yielded *Cranocephalites* spp. recorded here, but the exact occurrences of these ammonites relative to each other is not yet known.

Only diagnostic ammonite occurrences are shown. The thickness of the upper sandstone unit of some sections cannot be determined precisely.

C. Eastern belt

Interbedded sandstone and shale-siltstone units characterize the Bug Creek Formation which comprises the Lower and Middle Jurassic succession of the eastern belt. The oldest ammonites are Late Sinemurian forms, which occur in the basal unit of the type section (Sec. 8, Fig. 61.3). The youngest ammonites are Early Callovian forms (see below).

The most informative section for the lower part of the succession occurs just northeast of White Mountains (Sec. 10, Fig. 61.3). A lower, poorly exposed argillaceous unit, pebbly at the base and containing *?Echioceras* sp., is overlain by bluff-forming sandstone that is glauconitic in part; this unit is overlain by another argillaceous unit in which *Dactylioceras* sp. and *?Pseudolioceras* sp. were collected. A similar succession is inferred to be present in the poorly exposed section just west of Canoe Lake (Sec. 3, Figs. 61.2, 61.3), although few ammonites have been found there; the correlation is based on general lithologic succession and the rich glauconite content of the characteristically greenish sandstone units near the middle of the section.

The basal, pebble-bearing sandstone of the type section of the Bug Creek Formation (Sec. 4, Figs. 61.2, 61.3) is thinner than recorded by Jeletzky (1967, p. 91, 92), who appears to have measured repeatedly the same 3 m (10 ft.) thick unit in outcrops partially obscured and repeated by slumping. The lower part of the Intermediate Sandstone Member of this section is correlated tentatively with the previously mentioned glauconitic sandstone to the west. Besides the prevalence of glauconite and its general position in the stratigraphic succession, the correlation of these units is supported by the presence of fossiliferous pockets rich in *Meleagrinnella* sp. and *Oxytoma* sp., but lacking belemnites. Such a correlation requires an unconformity in the middle of the Intermediate Sandstone Member, and this is placed below a thin, abundantly pyritic, recessive interval above which the sandstone beds are rich in belemnites. Jeletzky (1967, 1975) proposed an unconformity to account for the absence of Pliensbachian through Early Bajocian faunas in this area but placed it lower than do the present writers, at the base of the Intermediate Sandstone.

The Middle Jurassic part of the succession in the eastern belt is like that of the central belt, with a sandstone rich in *Cranocephalites* spp., belemnites, and *Inoceramus* (*Retroceramus*) sp. near the base, and with beds higher in the section yielding Callovian *Cadoceras* spp. (Jeletzky, 1967), *Kepplerites* sp., and *C. (Pseudocadoceras)* sp. This part of the succession is overlain by a hard, bluff-forming orthoquartzite that has not yielded diagnostic fossils. The differing ages

of ammonites found at different places below this orthoquartzite unit (compare Secs. 3 and 4, Fig. 61.3) may indicate an erosional hiatus below it. As in the central belt, the thickness of the upper orthoquartzite unit is difficult to estimate because it forms broad dip slopes that may conceal a considerable amount of section below the *Buchia*-bearing shales of the Husky Formation.

It is too early to judge whether the lenticular nature of most arenaceous deposits of the central and eastern belts is due entirely to primary sedimentologic causes such as development of local shoals or bars, or whether such features were cannibalistic, being reworked from only slightly older adjacent clastic material, the result being erosional hiatuses adjacent to, and equivalent to, each clastic wedge. The sandstone units have the aspect of migrating shoals and bars (Young, 1973). There is no clear evidence, however, that any of them formed subaerial barrier islands as Young (*ibid.*) suggested.

The pre-Upper Oxfordian Jurassic rocks of the eastern facies belt thin south-eastward and the sandstone content increases (see Yorath *et al.*, 1975, p. 8, Figs. 4, 5, 9). These general facies trends have been inferred to extend north-northeasterly across the Mackenzie Delta region (Yorath *et al.*, 1975, Fig. 9). Details of southerly thickness and facies changes representative of this pattern were described in the Richardson Mountains by Jeletzky (1967, 1975). The correlations proposed in Figures 61.2 and 61.3 suggest that the pre-Late Bajocian and pre-Late Oxfordian erosional episodes (and possibly more) may have removed Jurassic rocks originally deposited to the southeast. These erosional episodes would correspond to those of the central facies belt, as already suggested by Jeletzky (1975, Fig. 10) for the region to the south. Alternatively, the general regional southeasterly thinning, shallowing, and coarsening trends may indicate the presence of a Lower and Middle Jurassic landmass in that direction. There is no direct evidence within the presently described area for either a source direction or for a deltaic or other mode of introduction of the clastic sediments into the area. Jeletzky (1974; 1975, p. 5), however, has proposed easterly, southeasterly and, temporarily at least, southerly sources for sediments in the southern and central Richardson Mountains, and he identified non-marine facies of the Bug Creek Formation in those areas. Many of the Jurassic sandstone units, judging by their relatively mature textural and mineralogical aspects, probably were derived in large part from pre-existing clastic rocks. During the Jurassic, they may have been shifted repeatedly such that the geographical position of their introduction into the depositional basin is totally obscured.

References

- Bamber, E. W. and Waterhouse, J. B.
1971: Carboniferous and Permian stratigraphy and paleontology, northern Yukon Territory, Canada; *Bull. Can. Pet. Geol.*, v. 19, p. 29-250.
- Frebold, H.
1960: The Jurassic faunas of the Canadian Arctic. Lower Jurassic and lowermost Middle Jurassic ammonites; *Geol. Surv. Can., Bull.* 59.
1961: The Jurassic faunas of the Canadian Arctic. Middle and Upper Jurassic ammonites; *Geol. Surv. Can., Bull.* 74.
1964: The Jurassic faunas of the Canadian Arctic. Cadoceratinae; *Geol. Surv. Can., Bull.* 119.
1975: The Jurassic faunas of the Canadian Arctic. Lower Jurassic ammonites, biostratigraphy and correlations; *Geol. Surv. Can., Bull.* 243.
- Frebold, H., Mountjoy, E. W. and Templeman-Kluit, D. J.
1967: New occurrences of Jurassic rocks and fossils in central and northern Yukon Territory; *Geol. Surv. Can., Paper* 67-12.
- Gabrielse, H.
1957: Geological reconnaissance in the northern Richardson Mountains, Yukon and Northwest Territories; *Geol. Surv. Can., Paper* 56-6.
- Jeletzky, J. A.
1962: Pre-Cretaceous Richardson Mountains Trough, its place in the tectonic framework of Arctic Canada and its bearing on some geosynclinal concepts; *R. Soc. Can., Trans.*, v. LVI, p. 55-84.
1967: Jurassic and (?) Triassic rocks of the eastern slope of Richardson Mountains, northwest District of Mackenzie, 106M and 107B (parts of); *Geol. Surv. Can., Paper* 66-50.
1971: Stratigraphy, facies and paleogeography of Mesozoic rocks of northern and west-central Yukon; in *Report of Activities, Part A*; *Geol. Surv. Can., Paper* 71-1A, p. 203-221.
1972a: Stratigraphy, facies and paleogeography of Mesozoic and Tertiary rocks of northern Yukon and northwest District of Mackenzie [NTS 107B, 106M, 117A, 116O (N1/2)]; in *Report of Activities, Part A*; *Geol. Surv. Can., Paper* 72-1A, p. 212-215.
1972b: Stratigraphy, facies and paleogeography of Mesozoic and Tertiary rocks of northern Yukon and northwest District of Mackenzie, N. W. T. [NTS 107B, 106M, 117A, 116O (N1/2), 116I, 116H, 116J, 116K (E1/2)]; *Geol. Surv. Can., Open File* 82.
1974: Contribution to the Jurassic and Cretaceous geology of northern Yukon Territory and District of Mackenzie, N. W. T. (NTS 116I, 116J, 116L, 116O, 116P, 117A); *Geol. Surv. Can., Paper* 74-10.

- Jeletzky, J.A. (cont.)
 1975: Jurassic and Lower Cretaceous paleogeography and depositional tectonics of Porcupine Plateau, adjacent areas of northern Yukon and those of Mackenzie District, N.W.T.; *Geol. Surv. Can.*, Paper 74-16.
- Leffingwell, E. de K.
 1919: The Canning River region, northern Alaska; *U.S. Geol. Surv.*, Prof. Paper 109.
- Martin, L.J.
 1959: Stratigraphy and depositional tectonics of North Yukon-lower Mackenzie area, Canada; *Am. Assoc. Pet. Geol. Bull.*, v. 43, p. 2399-2455.
 1961: Tectonic framework of northern Canada in *Geology of the Arctic*, G.O. Raasch, ed.; Univ. of Toronto Press, v. 1, p. 442-457.
 1963: Tectonics of northern Cordillera in Canada in *Backbone of the Americas*, O.E. Childs and B.W. Beebe, eds.; *Am. Assoc. Pet. Geol.*, Mem. 2, p. 243-251.
- Miall, A.D.
 1973: Regional geology of northern Yukon; *Can. Pet. Geol.*, Bull., v. 21, p. 81-116.
- Moorhouse, M.D.
 1966: Eagle Plain Basin of Yukon Territory (abstr.); *Am. Assoc. Pet. Geol.*, Bull., v. 50, p. 628.
- Mountjoy, E.W. and Procter, R.M.
 1969: Eleven field descriptions of some Jurassic and Cretaceous rocks in Arctic Plateau and Arctic Coastal Plain; *Geol. Surv. Can.*, Open File 16.
- Norris, D.K.
 1970: Structural and stratigraphic studies, Blow River area, Yukon Territory and western District of Mackenzie; in *Report of Activities, Part A*; *Geol. Surv. Can.*, Paper 70-1A, p. 230-235.
- Norris, D.K. (cont.)
 1972: Structural and stratigraphic studies in the tectonic complex of northern Yukon Territory, north of Porcupine River; in *Report of Activities, Part B*; *Geol. Surv. Can.*, Paper 72-1B, p. 91-99.
 1973: Tectonic styles of northern Yukon Territory and northwestern District of Mackenzie, Canada in *Proc. 2nd Intern. Symp. on Arctic Geology*, San Francisco, 1971, M.G. Pitcher, ed.; *Am. Assoc. Pet. Geol.*, Mem. 19, p. 23-40.
 1974: Structural geometry and geological history of the northern Canadian Cordillera in *Proc. 1973 National Convention*, A.E. Wren and R.B. Cruz, eds.; *Can. Soc. Explor. Geophys.*, p. 18-45.
 1976: Structural and stratigraphic studies in the northern Canadian Cordillera; in *Report of Activities, Part A*; *Geol. Surv. Can.*, Paper 76-1A, p. 457-466.
- Norris, D.K., Price, R.A. and Mountjoy, E.W.
 1963: Geology, northern Yukon Territory and northwestern District of Mackenzie; *Geol. Surv. Can.*, Map 10-1963.
- Yorath, C.J., Myhr, D.W. and Young, F.G.
 1975: The geology of the Beaufort-Mackenzie Basin; *Geol. Surv. Can.*, Open File 251.
- Yorath, C.J. and Norris, D.K.
 1975: The tectonic development of the southern Beaufort Sea and its relationship to the origin of the Arctic Ocean Basin in *Canada's continental margins and offshore petroleum exploration*, C.J. Yorath *et al.*, eds.; *Can. Soc. Pet. Geol.*, Mem. 4, p. 589-612.
- Young, F.G.
 1973: Mesozoic epicontinental, flyschoid, and molassoid depositional phases of Yukon's north slope in *Symp. on the geology of the Canadian Arctic*, Univ. Saskatchewan, May 1973; *Can. Soc. Pet. Geol.*, p. 181-202.
 1975: Stratigraphic and sedimentologic studies in northeastern Eagle Plain, Yukon Territory; in *Report of Activities, Part B*, *Geol. Surv. Can.*, Paper 75-1B, p. 309-319.

Projects 550101, 620308, 680023

H. G. Ansell, G. J. Pringle, and A. C. Roberts
Central Laboratories and Administrative Services DivisionIntroduction

One responsibility of the Geological Survey of Canada is the development of a comprehensive reference file of mineral species, many of which are necessarily obtained from foreign localities. In 1974, several specimens of a mineral labelled lanthanite from Curitiba, Parana, Brazil, were purchased for the National Mineral Collection of Canada, and assigned catalogue numbers 12213, 12214, and 12215. This occurrence was first described by Coutinho (1955), who identified the mineral in question as lanthanite from its physical characteristics. A routine X-ray powder diffraction pattern obtained from the mineral did not match the lanthanite pattern (14-190) in the Powder Diffraction File¹, taken from a report by Sabina and Traill (1960).

A preliminary electron microprobe investigation of the Brazilian mineral showed that neodymium and lanthanum are the major cations, present in nearly equal proportion, with no detectable cerium. This is at variance with the accepted chemical composition of lanthanite, reported by Palache *et al.* (1951) to be $(La, Ce)_2(CO_3)_3 \cdot 8H_2O$. This report gives our preliminary data; further work is planned pending receipt of suitable specimen material from other localities.

General Appearance and Physical Properties

The Curitiba mineral occurs as platy to thick tabular orthorhombic crystals, pink in colour with a pearly to vitreous lustre, in a buff-coloured earthy matrix of quartz, carbonate, and clay minerals, with

Table 62.1

X-ray powder diffraction pattern of Hydrated Neodymium-Lanthanum Carbonate, Curitiba, Parana, Brazil (114.6 mm camera, Cu K α radiation ($v = 1.54178 \text{ \AA}$), visual intensities)

I/I_0	d obs. \AA	d calc. \AA	hkl	I/I_0	d obs. \AA	d calc. \AA	hkl
10	8.45	8.451	020	<1	2.278	2.280	420
3	4.74	4.735	200	<1	2.232	2.232	004
3	4.46	4.465	002	<1	2.204	2.200	342
3	4.23	4.226	040	1	2.162	2.158	024
3	4.13	4.131	220	<1	2.126	2.113	080
3	3.95	3.948	022	<1	2.091	2.092	402
		3.859	140			2.065	440
<1b	3.84	3.819	041	<1b	2.061	2.062	180
4	3.25	3.248	202			2.056	081
<1	3.15	3.153	240	1	2.029	2.030	422
<1	3.07	3.069	042	<1b	2.010	2.019	204
4	3.03	3.032	222	1	1.968	1.974	044
<1	3.001	2.999	151	<1	1.931	1.929	280
<1	2.924	2.919	142	1	1.872	1.875	442
1	2.814	2.817	060	<1	1.820	1.822	244
1	2.689	2.687	061	+ numerous, very weak, broad lines			
2	2.576	2.575	242				
<<1b	2.426	2.421	260				

b = broad line

¹ published by the Joint Committee on Powder Diffraction Standards (JCPDS), Swarthmore, Pennsylvania, U. S. A.

Table 62.2
Cell Parameters and Densities,
Lanthanum-Bearing Hydrated Carbonates

	1	2	3	4
a (Å)	9.470(7)	9.52	9.580(4)	9.58
b (Å)	16.902(7)	17.1	17.00(1)	17.22
c (Å)	8.929(6)	9.02	8.984(4)	9.00
Density meas. (g/cm ³)	2.81(3)	2.69-2.74	2.72(2)	
calc.	2.82*		2.732	

1. Curitiba, Brazil; this study
2. Lanthanite; Bethlehem, Penn., USA; Palache *et al.* (1951)
3. La₂(CO₃)₃ · 8H₂O; synthetic; Shinn and Eick (1968)
4. La₂(CO₃)₃ · 8H₂O; synthetic; Nagashima *et al.* (1973)

*calculated for NdLa(CO₃)₃ · 8H₂O

thin crusts of a black amorphous material. The crystals exhibit a well developed platy {010} cleavage with lineations probably caused by twinning parallel to the {101} plane, as described by Coutinho (1955). The mineral has an estimated hardness of 2.5-3, and effervesces vigorously in dilute hydrochloric acid.

Five determinations of density on each of three grains, using a Berman balance with toluene, yielded an average of 2.81 g/cm³ with a standard deviation of 0.03. Assuming a chemical formula of NdLa(CO₃)₃ · 8H₂O, a calculated density of 2.82 was obtained.

X-ray Data

Precession photographs of single crystals were obtained using zirconium-filtered Mo K α and nickel-filtered Cu K α radiations. Measured cell parameters of a = 9.47 Å, b = 16.91 Å, and c = 8.93 Å were refined by the least squares method using the PARAM program of Stewart *et al.* (1972) to yield a = 9.470(7)² Å, b = 16.902(7) Å, and c = 8.929(6) Å. Systematic extinctions were uniquely satisfied by space group Pbnb. Parameters obtained are comparable to those reported for lanthanite in Palache *et al.* (1951) and, after transformation³, to those given for synthetic La₂(CO₃)₃ · 8H₂O by Shinn and Eick (1968) and by Nagashima *et al.* (1973) (Table 62.1). The X-ray powder diffraction pattern presented in Table 62.2 corresponds to the pattern of Neumann and Bryn (1958) for lanthanite from Bastnäs, Sweden. The purported lanthanite pattern, number 14-190, published in the

² standard deviations in the third decimal place are in parentheses.

³ in this study, the c<a<b orientation recommended by the JCPDS is used. Transformation of indices from the a<b<c orientation used by Shinn and Eick (1968), Nagashima *et al.* (1973) and Coutinho (1955) is accomplished by employing the matrix 010/001/100.

Powder Diffraction File of the Joint Committee on Powder Diffraction Standards from Sabina and Traill (1960), proves to be that of talc.

Electron Microprobe Analysis

Preliminary examination of two grains using both energy dispersive and wavelength dispersive spectrometers showed that neodymium and lanthanum are the major elements present as cations. Also found were minor amounts of praseodymium, samarium, gadolinium, and europium, with a trace of dysprosium. Cerium is completely absent.

Quantitative analysis for the six most abundant rare earth elements was attempted on three locations in a single grain. Since the sample deteriorated visibly under the electron beam and the count rate increased significantly with counting times greater than 10 seconds, the sample was moved between successive 10 second counting periods for a total counting time of 100 seconds at each location. Intensity data were corrected using the computer program of Rucklidge and Gasparrini (1969). The average composition obtained is listed in Table 62.3.

Assuming a stoichiometric amount of CO₂, and the balance of the analysis to 100 per cent to be water, the calculated formula would be (RE)₂(CO₃)₃ · 2.7H₂O. This indicates a drastic loss of water from the 8H₂O expected from density calculations and the comparison of cell parameters with other rare earth carbonate octahydrates (Table 62.1). Some water loss may be expected during analysis due to sample deterioration

Table 62.3

Electron Microprobe analysis for Rare Earth Elements

		Weight per cent
La	La ₂ O ₃	23.63
	Pr ₂ O ₃	4.18
	Nd ₂ O ₃	26.57
	Sm ₂ O ₃	5.95
	Eu ₂ O ₃	0.90
	Gd ₂ O ₃	3.72
	CO ₂	(25.61)
		90.56

- Notes:
1. CO₂ assumed to be stoichiometric. A partial chemical analysis on an unaltered sample containing minor impurities gave 24.5 per cent CO₂
 2. balance to 100 per cent assumed to be H₂O
 3. analysis with an MAC electron microprobe, 20 KV, .03 microamperes sample current, approx. 10 micrometers beam diameter

in the electron beam, but it appears that the major loss occurs in sample preparation, where grains are set in epoxy resin and cured at 80°C for one hour before polishing. X-ray powder diffraction patterns obtained from the two microprobe mounts and a separate fragment heated at 80°C for one hour showed marked differences from patterns for the original material. These patterns indicate a mixture of a small amount of the original material with a second phase yielding a pattern unlike that of any other rare earth carbonate given in the Powder Diffraction File.

Because of this water loss, the analysis in Table 62.3 serves only as an indicator of the relative amounts of the rare earth elements present in the original mineral. Further work is in progress on this material.

References

- Coutinho, J. M. V.
1955: Lantanita de Curitiba, Parana (Brazil); Univ. Sao Paulo, Fac. filosof., cienc. e letras, Bol. no. 186, Mineralog. no. 13, p. 119-126.
- Nagashima, K., Wakita, H., and Mochizuki, A.
1973: The synthesis of crystalline rare earth carbonates; Bull. Chem. Soc. Japan, v. 46, p. 152-156.
- Neumann, H. and Bryn, K. O.
1958: X-ray powder patterns for mineral identification. IV. Carbonates; Vid.-Akad. Avh. I Mat.-Naturv. kl. 1958, No. 1, Oslo, 6 p.
- Palache, C., Berman, H., and Frondel, C.
1951: The system of mineralogy, 7th ed., v. II; John Wiley and Sons, Inc., New York, p. 241-243.
- Rucklidge, J. C. and Gasparrini, E. L.
1969: Electron microprobe analytical data reduction. EMPARDR VII; Dep. Geol. Univ. Toronto.
- Sabina, A. P. and Traill, R. J.
1960: Catalogue of X-ray diffraction patterns and specimen mounts on file at the Geological Survey of Canada; Geol. Surv. Can., Paper 60-4, p. 57.
- Shinn, D. B. and Eick, H. A.
1968: The crystal structure of lanthanum carbonate octahydrate; Inorg. Chem., v. 7, p. 1340-1345.
- Stewart, J. M., Kruger, G. L., Ammon, H. L., Dickinson, C., and Hall, S. R.
1972: The X-ray system of crystallographic programs; Univ. Maryland Tech. Rept. TR-192.

Project 550101

J. L. Jambor¹, A. G. Plant² and H. R. Steacy²

A carbonate-rich sill of unique mineralogical composition and petrological significance intrudes flat-lying Ordovician limestone at St. Michel, Montreal Island, Quebec. The uniqueness of the sill is that its principal carbonate mineral is dawsonite, $\text{NaAl}(\text{CO}_3)(\text{OH})_2$, rather than calcite or dolomite. Because of the primary (autohydrothermal) nature of the dawsonite, the intrusion is considered to be a carbonatite-type rock within the definition of Heinrich (1966), viz: "a carbonatite is ... a carbonate-rich rock of apparent magmatic derivation or descent". However, to recognize the higher proportion of silicates — chiefly feldspar — and the silicate-carbonate association, the intrusion is referred to here as a silicocarbonatite.

This preliminary study of the sill was prompted initially by the identification of weloganite $(\text{Sr}, \text{Ca})_3\text{ZrNa}_2(\text{CO}_3)_6 \cdot 3\text{H}_2\text{O}$ (Sabina *et al.*, 1968) and the subsequent detection in the sill of higher-than-normal abundances of zirconium and niobium (Steacy and Jambor, 1969). The sill has since gained prominence both as the sole collecting site for weloganite and as a source of other rare minerals, including dresserite $\text{Ba}_2\text{Al}_4(\text{CO}_3)_4(\text{OH})_8 \cdot 3\text{H}_2\text{O}$ (Jambor *et al.*, 1969).

Although sodium-bearing carbonates do occur in carbonatites (e.g. nyerereite $\text{Na}_2\text{Ca}(\text{CO}_3)_2$, Fleischer, 1975) dawsonite in such rocks is known, so far, only in the Montreal area.

General Features of the Sill

The sill is intersected by the limestone quarry of Francon Limitée and is exposed on the four quarry walls, thereby permitting ready access and sampling. On the basis of quarry development and related drillhole data, the sill is a two-metre thick sheet which intruded limestone of the Ordovician Montreal Formation over a known area of approximately 1100 by 450 m, with the continuation open in all directions. The sill is light grey, except in the southeastern part of the quarry where it is light green. Chill zones, 4 to 5 cm thick at the upper and lower limestone contacts, are noticeably darker. The selvages are predominantly greenish grey but in many places are dark green and some are distinctly brownish. Portions of the sill are mottled near the contacts; extreme examples of this phenomenon are shown in Figures 63.1 and 63.2.

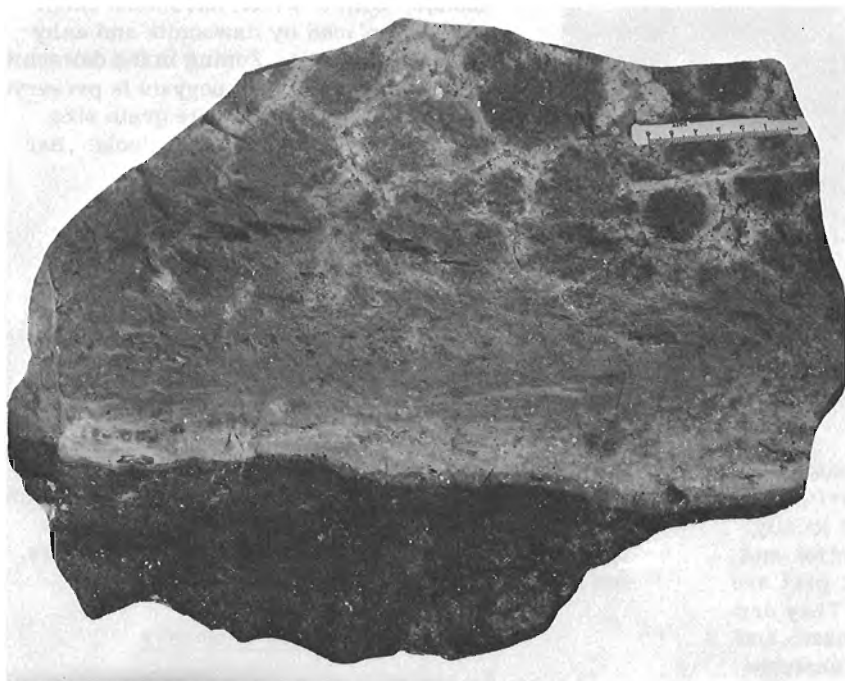


Figure 63.1

Specimen showing the mottled texture of the sill near its contact with limestone (dark, bottom). White spots in the chilled selvage are dawsonite pseudomorphs after phenocrysts. (scale in centimetres)

¹J. L. Jambor, Regional and Economic Geology Division; present address: CANMET, 555 Booth Street, Ottawa, K1A 0G1.

²A. G. Plant and H. R. Steacy, Central Laboratories and Administrative Services Division.

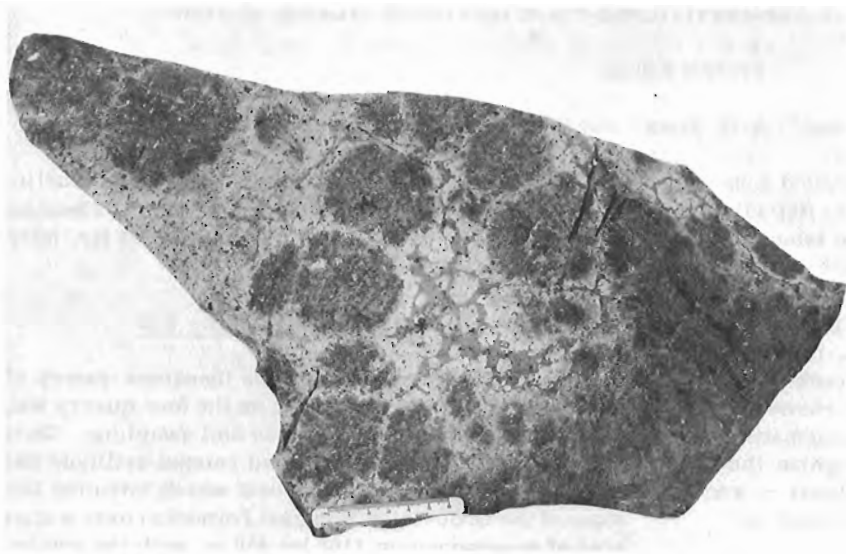


Figure 63.2

Specimen from mottled portion of the sill. The dark grey circular portions are richest in carbonates; the medium grey "interstitial" areas encompassed in white in the central part of the specimen are richest in feldspar and poorest in carbonates. (scale in centimetres)

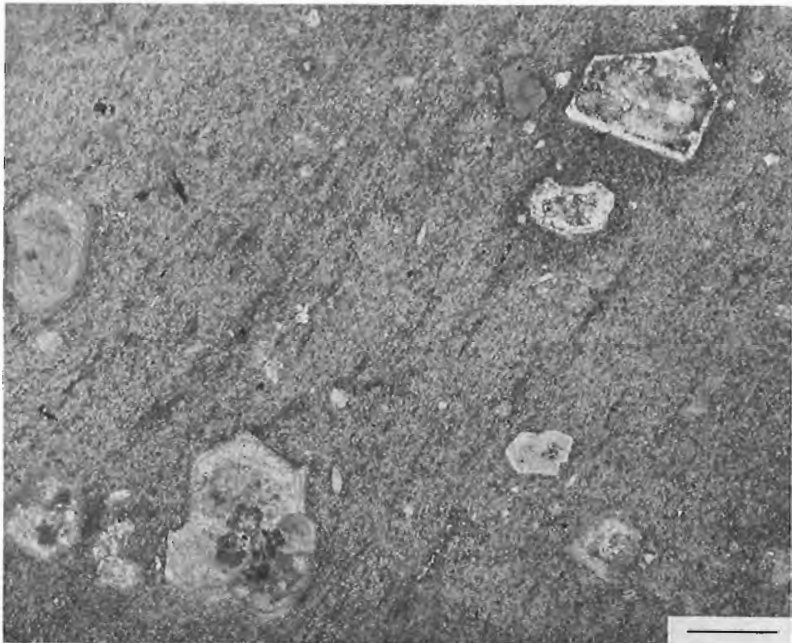


Figure 63.3

Photomicrograph of chill zone showing large phenocrysts and a fine grained matrix, both of which have been extensively replaced by dawsonite and anhydrous carbonates. Zoning in the dawsonite pseudomorphs of phenocrysts is preserved by variations in dawsonite grain size. Transmitted light, crossed nicols. Bar scale is 1.0 mm.

The sill is vesicular; voids probably constitute several per cent of the total volume, with cavities up to several centimetres in diameter present locally. The vesicles are most abundant in the central and upper quarter of the sill and for the most part are elongate parallel to the intrusion contacts. They are normally lined with quartz, calcite, plagioclase, and dawsonite, and contain variable amounts of analcime, strontianite, weloganite, dresserite, pyrite, and marcasite. Minute amounts of many additional minerals, including several as yet unnamed and undescribed species, are also present (Sabina, 1976).

The intrusion of the sill has produced a slight brecciation and recrystallization of the limestone, and locally a yellowish discoloration, but has had little other effect in the specimens examined; fossil outlines

and fine sedimentary laminae in local carbonaceous beds are clearly recognizable at the contacts. Angular inclusions of limestone of a few centimetres in size occur within the sill, particularly near the contacts, but are not unusually abundant.

Petrography and Chemistry

Specimens of the chilled selvages and central portions of the sill were examined in this study. The identifications of the minerals were confirmed by X-ray diffraction patterns and, in some cases, by electron microprobe examination.

The chilled selvages are essentially a microcrystalline intergrowth of dawsonite and feldspar. Phenocrysts occupy five to ten per cent of the rock. The bulk of

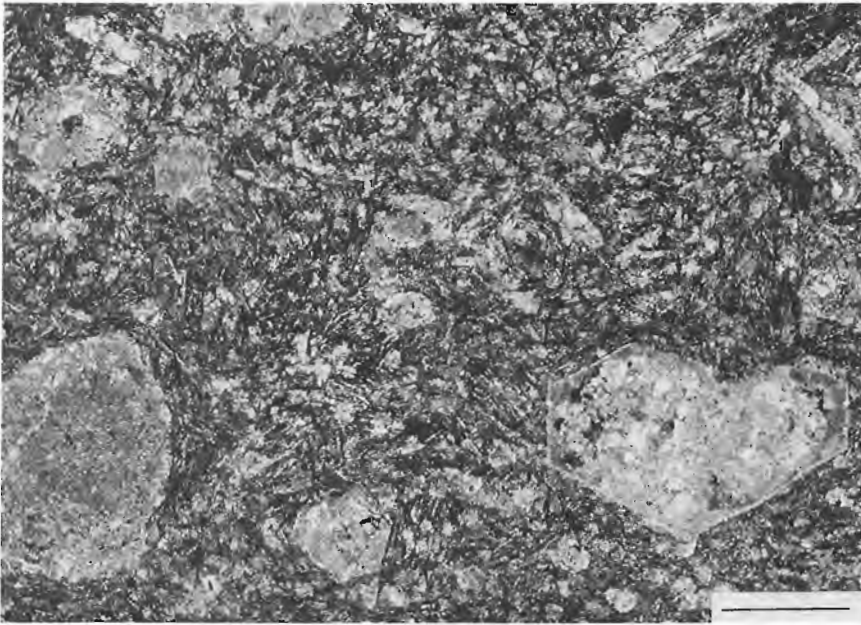


Figure 63. 4

Photomicrograph of the central portion of the sill showing altered phenocrysts in a matrix of dawsonite, fine laths of K-feldspar, and anhydrous carbonates. A few coarse albite laths are visible at the upper right. Note the flow texture of the feldspar laths around the altered phenocrysts. Transmitted light, crossed nicols. Bar scale is 1.0 mm.

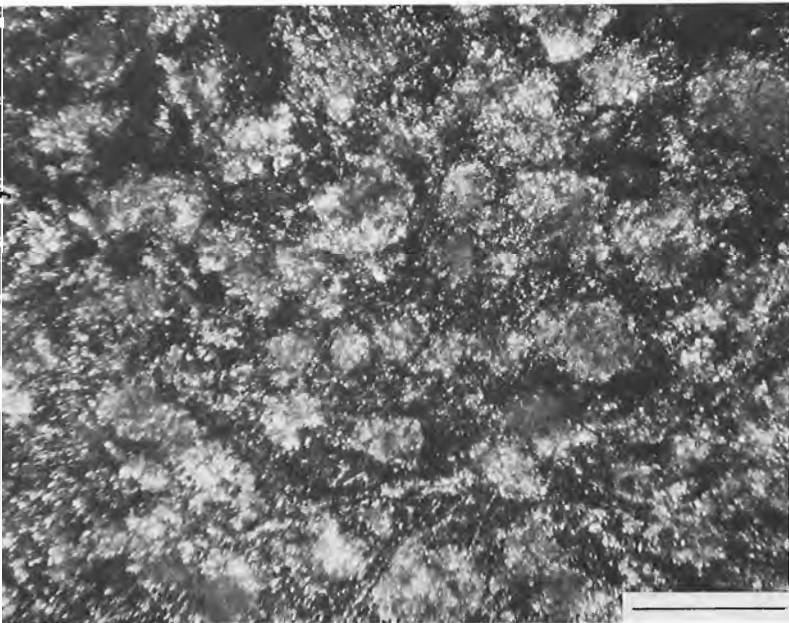


Figure 63. 5

Photomicrograph of a sample from the northern end of the quarry, showing the fine grained nature of the matrix carbonates, most of which are dawsonite and greyish, turbid areas of siderite. Note the rudimentary globular form of the carbonate aggregates. Transmitted light, crossed nicols. Bar scale is 0.2 mm.

these are dawsonite pseudomorphs; their precursor is unknown but probably was analcime as suggested by the outlines preserved by fine grained dawsonite (Figs. 63.3 and 63.4). A minor proportion of the phenocrysts are unaltered albite laths up to 2.5 mm in length.

The central portions of the sill are fine grained and generally turbid in thin sections. The aforementioned pseudomorphs are present here as well, indicating their persistence throughout the sill. The fine grained matrix consists of generally well defined K-feldspar laths and less distinct dawsonite (Fig. 63.4). The proportions of the matrix minerals vary from place to place, with the megascopically darker grey parts of

the intrusion being relatively enriched in dawsonite and other carbonates, and the lighter grey portions being relatively enriched in K-feldspar. In some thin sections, dolomite and siderite are disseminated throughout the matrix and locally are the principal carbonates. Calcite is disseminated throughout the rocks but occurs in vesicles and coarse patches rather than being a component of the fine grained matrix. Dolomite, siderite and dawsonite are similar in grain size and commonly occur in aggregates with somewhat rounded outlines (Fig. 63.5).

In the southeastern part of the quarry dawsonite is less abundant in the sill but aegerine-augite, in needles averaging less than 0.1 mm in length, is an

additional constituent of the matrix and imparts a greenish colour to the rock. Analcime is also common in this area. In addition to its presence as phenocrysts, analcime occurs in small fractures and vugs, and in places partly replaced albite phenocrysts. Much of the analcime is anomalously birefringent and has sharply demarcated lamellar twin units. The phenocrysts are of a similar size and shape as the dawsonite pseudomorphs referred to previously (Figs. 63.3 and 63.4). This similarity, together with the fact that analcime from this southeastern area also shows various stages of replacement by dawsonite, strongly suggests that the dawsonite pseudomorphs were originally analcime. In its simplest terms, part of the pseudomorphic alteration may have followed the reaction: $\text{NaAlSi}_2\text{O}_6 \cdot 6\text{H}_2\text{O}$ (analcime) + $\text{CO}_2 \rightarrow \text{NaAl}(\text{CO}_3)(\text{OH})_2$ (dawsonite) + 2 SiO_2 (quartz).

Table 63.1

Chemical analyses of samples of dawsonite-bearing sill from Montreal Island (in weight per cent)

	F-9	F-21W	F-21D	F-32	F-39
SiO ₂	45.5	49.8	44.7	47.9	48.9
Al ₂ O ₃	19.7	20.1	18.6	20.2	21.7
Fe ₂ O ₃	0.2	0.1	0.8	1.0	1.1
FeO	2.0	2.4	1.6	1.3	1.0
MgO	0.8	1.0	1.2	0.7	0.9
MnO	0.25	0.26	0.24	0.25	0.27
CaO	2.5	2.4	2.1	2.1	2.0
SrO	0.05	0.21	0.26	0.17	0.16
BaO	0.18	0.20	0.21	0.19	0.20
Na ₂ O	8.6	8.6	8.4	8.9	9.8
K ₂ O	4.2	3.9	4.1	4.5	3.5
TiO ₂	0.27	0.35	0.29	0.36	0.26
ZrO ₂	0.06	0.14	0.16 ^c	0.10	0.17
Nb ₂ O ₅	0.12	0.13	0.09	0.14	0.15
P ₂ O ₅	0.12	0.14	0.11	0.11	0.10
CO ₂	11.0	7.8	12.7	6.3	2.9
H ₂ O	<u>3.5</u> 99.05	<u>2.0</u> 99.53	<u>3.6</u> 99.16	<u>4.7</u> 98.92	<u>5.3</u> 98.41

Analysis by Rapid Methods group, Analytical Chemistry Section, Geological Survey of Canada. BaO by optical spectroscopy; Sr, Zr, Nb by X-ray spectroscopy. F-9: normal grey central part of sill, southern part of quarry; F-21W and F-21D: light and dark parts of mottled material near contact, northeastern part of quarry; F-32 and F-39: eastern and southeastern part of quarry, greenish aegirine-augite-bearing part of sill.

Chemical analyses of five samples of the sill are given in Table 63.1. Their specific locations are shown in the plan of the quarry given by Steacy and Jambor (1969). Samples F-21W and F-21D are the light and dark portions, respectively, of the mottled material shown in Figures 63.1 and 63.2. Thin section studies indicate that the darker portions of mottled material are generally enriched in dawsonite and other carbonates, the lighter portions have less total carbonate, of which a large proportion is siderite, and the interstitial areas have the least amounts of all carbonates. The combination of these variations may account for the higher SiO₂ and lower CO₂ values in the lighter F-21W sample (Table 63.1). In all five analyses, silica can be attributed to K-feldspar and quartz, the latter being found both in vesicles and finely dispersed in the analcime pseudomorphs. The matrix feldspar, which accounts for the bulk of the silicon, is orthoclase.

Diffraction scans for feldspar were carried out on five samples pre-concentrated by dissolving the associated carbonates with dilute HCl. The scans yielded similar results for the potash feldspar, but the proportion of albite (present as phenocrysts) was quite variable. The unit-cell dimensions of the K-feldspar in the purest sample (F-39) were calculated from diffraction data using Cu K α_1 radiation and synthetic spinel as an internal standard. From the 201, 130, 112, 002, 131, 041, 132, 060, 241, and 204 reflections, $a = 8.54$, $b = 13.00$, $c = 7.20$ Å, $\beta = 115.96^\circ$. Both the cell dimensions and the 2θ values for 060 and 204 (41.66° and 50.68° respectively) place the K-feldspar in the orthoclase series of Wright (1968) and Wright and Stewart (1968).

Iron in the bulk of the intrusion occurs principally as siderite and as disseminated grains and dust-sized particles of magnetite. The magnetite is difficult to identify in thin sections because of its fine grain size and because of the turbid appearance of many of the slides. However, superpanner concentrates and hand-magnetic fractions from the pulverized rocks show it to be a common constituent of the sill. Pyrite, marcasite, and rare relict phenocrysts of biotite-phlogopite have been identified in the sill, but their occurrence is not quantitatively important. Although the chemical analyses show little variation on total iron, the Fe₂O₃/FeO weight ratio ranges from about 2:1 to 1:1. The two rocks having the latter ratio contain aegirine-augite, but have a significantly lower proportion of magnetite. The total iron budget is thus not appreciably changed as part of it occurs in the ferric state in pyroxene.

Strontium and barium reported in the analyses (Tables 63.1 and 63.2) can be largely or wholly attributed to minerals occurring in vesicles; strontium occurs as strontianite and weloganite, and barium as barite. Niobium is present as tan-coloured octahedra of pyrochlore disseminated throughout the rock matrix. Zirconium is present as weloganite and as zircon; the latter is disseminated in the matrix as euhedral to subhedral grains up to 1 mm in length and 0.3 mm in cross-section. A few euhedral to anhedral grains of apatite averaging about 0.04 mm in basal section also

occur in the matrix; some of these have a sieve texture arising from numerous minute inclusions. Both apatite and zircon have been noted as phenocrysts in the chilled selvages. Dawsonite, as mentioned previously, is very abundant in chilled material, and makes up several per cent of the main part of the sill. However, the intrusion may have less carbonate in the southeastern part of the quarry. For example, sample F39 is carbonate-poor and has a composition and mineralogy approaching that of an alkali syenite. Fluorite and cryolite are minor constituents of the sill. Chemical analyses of four samples listed in Steacy and Jambor (1969) gave the following results in weight per cent for fluorine and chlorine respectively: F-9: 0.25, 0.02; F-21: 0.28, 0.02; F-32: 0.28, 0.03; F-39: 0.45, 0.05.

Table 63. 2

Comparison (in weight per cent) of some element abundances in carbonatites with those of other igneous rocks (after Heinrich, 1966)

	All igneous rocks	Carbonatites and silico-carbonatites	Dawsonite silicocarbonatite
BaO	0.03	0.5-10	0.20
SrO	0.03	0.5- 2	0.14*
Nb ₂ O ₅	0.0005	0.001-0.5	0.11*
ZrO ₂	0.03	0.001	0.09*
TiO ₂	0.8	0.1- 3	0.31
P ₂ O ₅	0.3	0.1- 6	0.12

*Average from 39 samples (Steacy and Jambor, 1969); remainder averaged from Table 63. 1.

Conclusion

The dawsonite-bearing sill is in the Montereian alkalic petrologic province and probably is genetically related to the plutonic intrusions which form the core of Mount Royal, about 7 km south of the quarry. The sill is unlike any rock described previously. The closest similarity is a dawsonite-bearing feldspathic dyke, also at Montreal, which has been described by Stevenson and Stevenson (1965, 1975).

Cooper and Gittins (1974) have suggested that dry alkali carbonatite magmas are probably common, but in wet magmas the alkalis not bound as silicates are lost in the hydrous fluid phase. In the sill described here, the initial magmatic material would appear to have consisted largely of phenocrysts of albite and analcime in a potassium-rich melt highly charged with sodium, carbonate, and water. On cooling, at least part of the volatiles was trapped and reacted with the silicates. Thus, dawsonite was deposited in abundance and is considered to be a primary autohydrothermal mineral in that it was apparently precipitated from the residual volatile constituents of the intrusion.

The quarry is currently operating on a lower bench which has intersected another vesicular sill about four feet thick. This sill is similar to the one described in this study; it is fine grained and dawsonite-rich, and vesicles carry analcime, weloganite and other minerals encountered in the upper sill. The two sills are unquestionably related, and likely derived from a common feeder.

Acknowledgments

The permission of Francon Limitée to collect samples is gratefully acknowledged. Chemical analyses were carried out by the Analytical Chemistry Section and mineral identifications, by X-ray diffraction, by the Mineralogy Section. Mrs. A.P. Stenson kindly provided specimens of the sill from the lower bench.

References

- Cooper, A. F. and Gittins, J.
1974: The system Na₂CO₃-K₂CO₃-CaCO₃ at 1 kb and its significance in carbonatite petrogenesis; *Can. Mineral.*, v. 12, p. 430.
- Fleischer, M.
1975: New mineral names: Nyerereite and Natro-fairchildite; *Am. Mineral.*, v. 60, p. 487-488.
- Heinrich, E. W.
1966: The geology of carbonatites; Chicago, Rand-McNally.
- Jambor, J. L., Fong, D. C., and Sabina, Ann P.
1969: Dresserite, the new barium analogue of dundasite; *Can. Mineral.*, v. 10, p. 84-89.
- Sabina, A. P.
1976: The Francon Quarry, a mineral locality; *in* Report of Activities, Part B, Geol. Surv. Can., Paper 76-1B, report 5.
- Sabina, A. P., Jambor, J. L., and Plant, A. G.
1968: Weloganite, a new strontium zirconium carbonate from Montreal Island, Canada; *Can. Mineral.*, v. 9, p. 468-477.
- Steacy, H. R. and Jambor, J. L.
1969: Nature, distribution and content of zirconium and niobium in a silico-carbonatite sill at St. Michel, Montreal Island, Canada; *Geol. Surv. Can.*, Paper 69-20, 7 p.
- Stevenson, J. S. and Stevenson, L. S.
1965: The petrology of dawsonite at the type locality, Montreal; *Can. Mineral.*, v. 8, p. 249-252.
1975: Fluorite-dawsonite relationships at a new Montreal locality; *Can. Mineral.*, v. 13, p. 313.

Wright, T. L.

1968: X-ray and optical study of alkali feldspar: II.
An X-ray method for determining the composition
and structural state from measurement of 2θ
values for three reflections; Am. Mineral.,
v. 53, p. 88-104.

Wright, T. L. and Stewart, D. B.

1968: X-ray and optical study of alkali feldspar: I.
Determination of composition and structural
state from refined unit-cell parameters and
 $2V$; Am. Mineral., v. 53, p. 38-87.

Project 700056

D. R. Grant
Terrain Sciences Division

Introduction

A few days of field work was done in late March, 1976, along the Bay of Fundy-St. Mary's Bay coast (Fig. 64.1) to examine and photograph sections of Quaternary unconsolidated deposits exposed as a result of a severe day-long storm on February 3, 1976, with winds of 100 to 150 km per hour, and to make incidental observations of the resulting damage, particularly the extent of erosion compared to 'normal' coastal recession under average conditions. In general it was found that the 100-km segment of coast, which is largely composed of relatively compact deposits with weak intercalated members, was cut back several metres and oversteepened while apparently frozen. The multi-layer sequence was exposed as never before in the past ten years, except where it was locally obscured by thaw-induced flow of mud down gullies. Bare cliffs visible in the 1960's that had become completely vegetated in the 1970's nearly everywhere were re-exhumed, and many new exposures were created.

The exposures exhibit various combinations of seven main extensive members, plus others of more local development. Three of these were observed several years ago (Grant, 1967, 1968), although first mention apparently was made in a soils report of Digby County by Hilchey *et al.* (1962, p. 12). A correlation scheme was presented after further brief observations (Grant, 1971), and the marine molluscan paleocology was interpreted by Clarke *et al.* (1972). Their relation to Late Quaternary deposits and events in the Atlantic Provinces as a whole was shown by Grant (1975b). This report modifies earlier interpretations by the addition of new members to the sequence and by the recognition of features bearing upon the age and succession of events.

The deposits are unparalleled in the Atlantic Provinces in terms of their extent, thickness, and time span, and appear analogous to the Pleistocene sequences around Toronto and Lake Erie. Moreover, they underlie a coastal belt along which is localized a ribbon development of Acadian French settlements. A knowledge of the horizontal and vertical variations of texture and composition could be used to capitalize on favourable conditions and avoid inherent problems. Examples include sources of aggregate at surface and at depth and the special considerations of water supply and waste disposal posed by perched water tables, buried aquifers, and iron-charged layers. Continued erosion of this sensitive shoreline has an economic impact in terms of lost land and the revenue therefrom, damaged coastal structures, and remedial measures. Since claims can be expected for special assistance to offset losses

due to 'freak' events, baseline studies are needed to quantify the long-term normal or average coastal response.

Description of Units

Unit 1, Basal rock bench

At a number of localities the sedimentary members rest on a subhorizontal bedrock surface 2 to 3 m above present high tide level, which is smoothed and potholed exactly like the modern intertidal platform. Although the feature may be followed as segments hundreds of metres long at the foot of drift cliffs, only on rocky promontories is its inland margin revealed as a genuine wave-cut notch, hence it need not be confused with glacial pavements. Considering the overlying marine gravel (unit 2, *see below*), it originated as a surface of marine abrasion when sea level was higher. It is tentatively referred to the last interglacial because of the number and age of the overlying tills. If so, it probably correlates with a similar bench around Cape Breton Island (Grant, 1975a) and on Avalon Peninsula, Newfoundland (Henderson, 1972, p. 38).

Unit 1a, Conglomerate

Southeast of Cape St. Mary and at Double Island patches of a distinctive conglomerate can be found resting unconformably on the local greywacke and schist bedrock of Ordovician age (Fig. 64.2). The clasts are subrounded discs of local lithology cemented by iron oxide in a sand matrix. The underlying rock surface is smooth but not striated. Masses of the conglomerate are found in the overlying tills. Although the cemented nature contrasts with the other gravels of similar texture, it may simply be a completely cemented portion of unit 2 (though its relationship to the bench is unclear) or it could be an outlier of the middle or early Wisconsin Bridgewater Conglomerate (Prest *et al.*, 1972, p. 8) known only from the Atlantic Coast. The possibility remains that this conglomerate predates the rock bench and thus is completely unrelated to the overlying sediments.

Unit 2, Older marine sand and gravel

In direct contact with the underlying rock bench and always below the lower red and grey drifts (units 3 and 4) is a veneer of sandy pebble or shingle gravel, rarely more than one metre thick, that is locally iron cemented at top and bottom contacts. The clasts are well rounded and the highly siliceous ones have percussion marks. The bedding is planar, parallel,

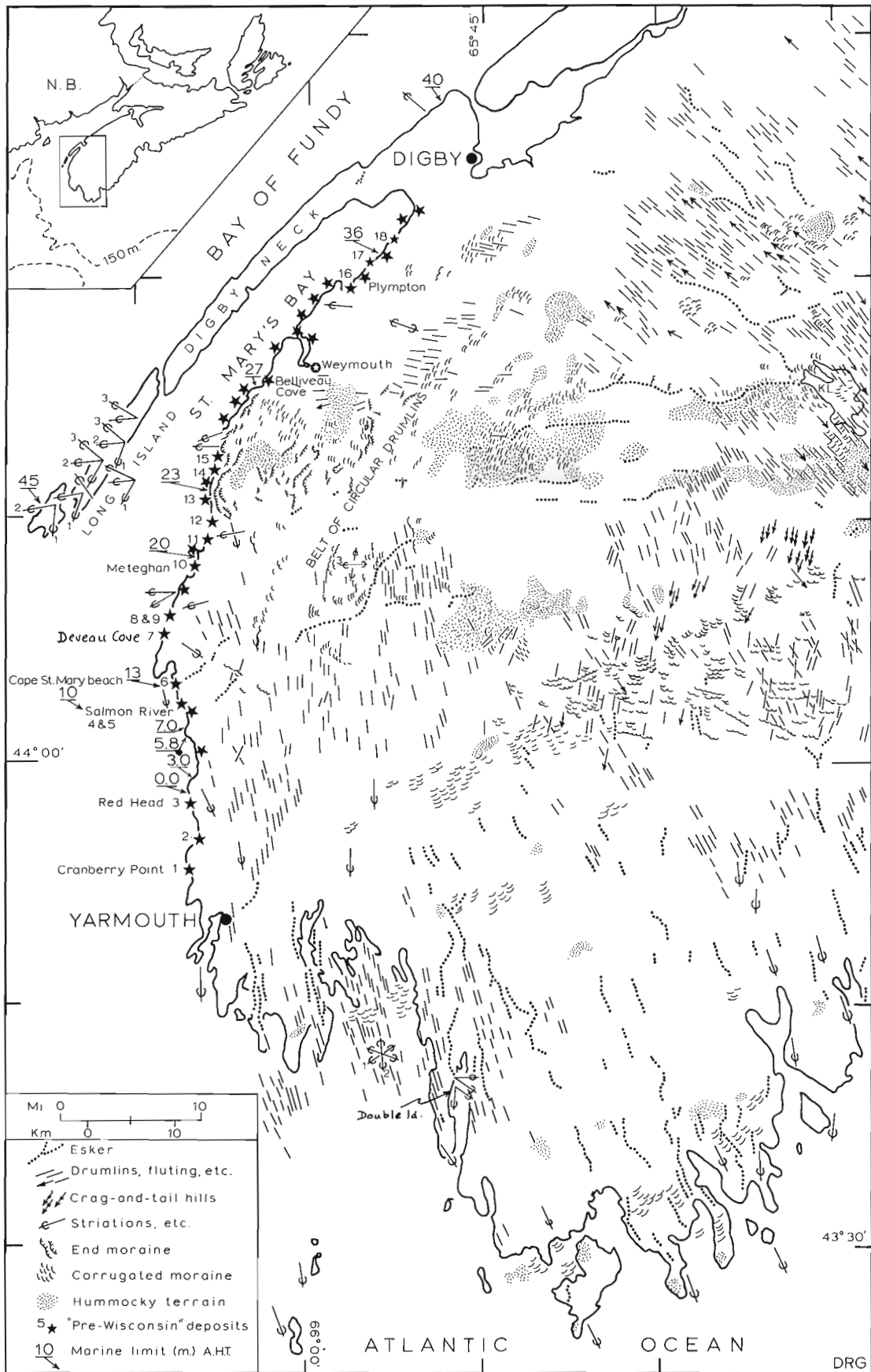


Figure 64. 1. Relation of late Wisconsinan features to older glacial and nonglacial deposits in southwestern Nova Scotia (numbered localities refer to correlation chart in Grant, 1971).

gently dipping seaward, with imbrication of clasts indicating water flow inland. Its lithology may match that of the underlying greywacke or schist, but locally it has a significant component from distant sources such as the North Mountain Triassic amygdaloidal basalt and the diorites and pink granites from southern New Brunswick. Texturally it is regarded as a littoral deposit, essentially coeval with the wave-cut bench, but obviously includes material from pre-existing tills of northern provenance.

Unit 3, Lower grey drift

At about half the fifty or so shoreline segments cut in drift, a hard, sandy, grey material, relatively poor in clasts and containing sparse but disseminated shell fragments, is found below or juxtaposed at the same level as a more extensive reddish drift. The minor content of stones of northern provenance, together with the shell fragments (for which a date is clearly needed), suggests it could be an early basal phase of the till emplaced by ice flowing from New Brunswick as it first impinged on the Nova Scotia coast after crossing marine sediments in Bay of Fundy. Alternatively, its grey colour and dominantly local provenance could be viewed as a basis for regarding it as a till laid down by ice expanding from an upland centre in Nova Scotia. In either case, the time of deposition is bracketed as early Wisconsinan, by the inferred Sangamon age of the underlying bench and the measured mid-Wisconsin age of unit 5 above.

Unit 3a, Solifluction(?) debris

At the Cape St. Mary beach section a lenticular mass, 0 to 5 m thick, of phyllite fragments overlies the basal conglomerate and is plastered on a steeply inclined seaward-facing bedrock surface. It has every appearance of slope debris, liberated by frost action, that acquired a strong imbrication as it accumulated on and at the base of the slope. Although the material is very local and the contact relations unclear, it appears to occupy the same stratigraphic interval as the lower grey drift and may be a local manifestation of the periglacial environment that just preceded the initial glacial cover, inferred as early Wisconsinan.

Unit 4, Lower red shell-bearing till

The core and larger proportion of nearly every undulation produced by variations in the thickness of drift over bedrock are composed of a brick-red to reddish brown, compact, silty drift containing many fragments of marine shells which were dated at more than 38 000 years (GSC-695) at Cape St. Mary. (Most of the 10 to 30 m of local relief over bedrock appears attributable to Wisconsinan glacial deposits that predate the last main glacier expansion. Near Salmon River till and gravel units outcrop on the slopes of south-southeast trending drumlinoid hills as if much of the present topography was carved by glacier flow across pre-existing deposits.) In the stonier phases of this till, the clasts are aligned and have an imbrication

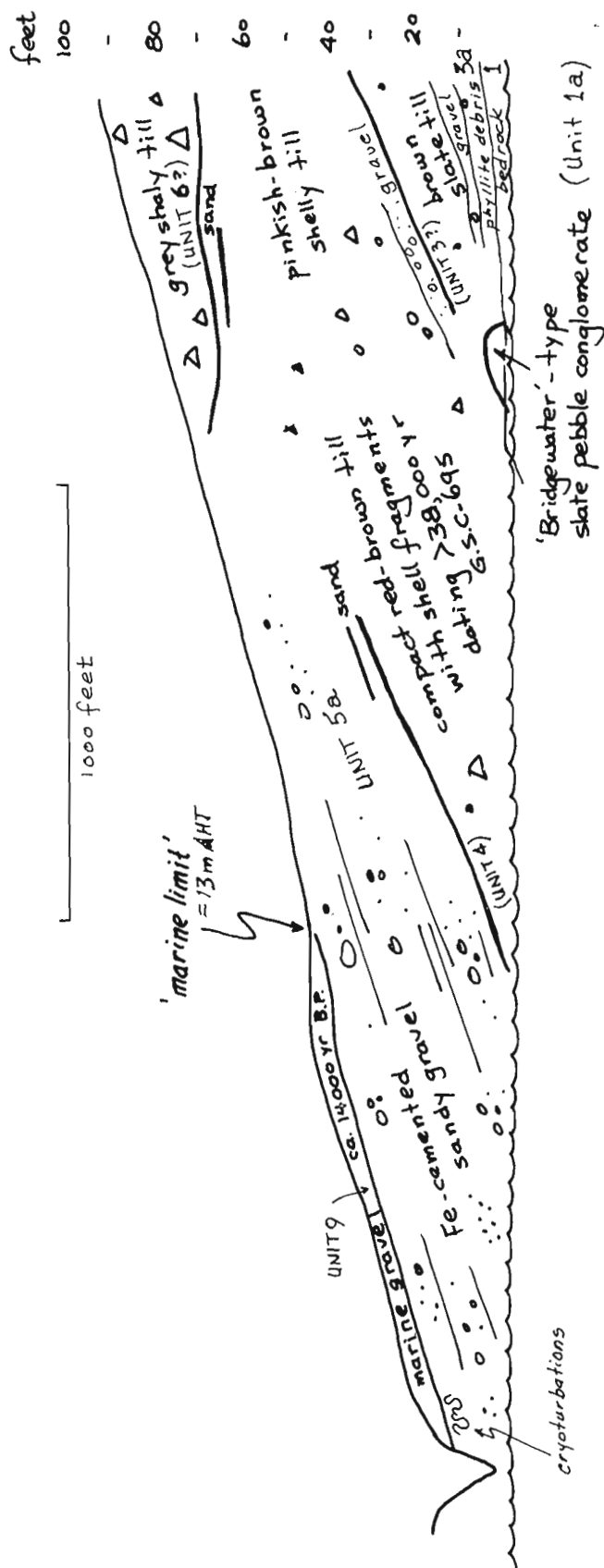


Figure 64.2. Sketch of deposits exposed in sea cliff southeast of Cape St. Mary, Nova Scotia.

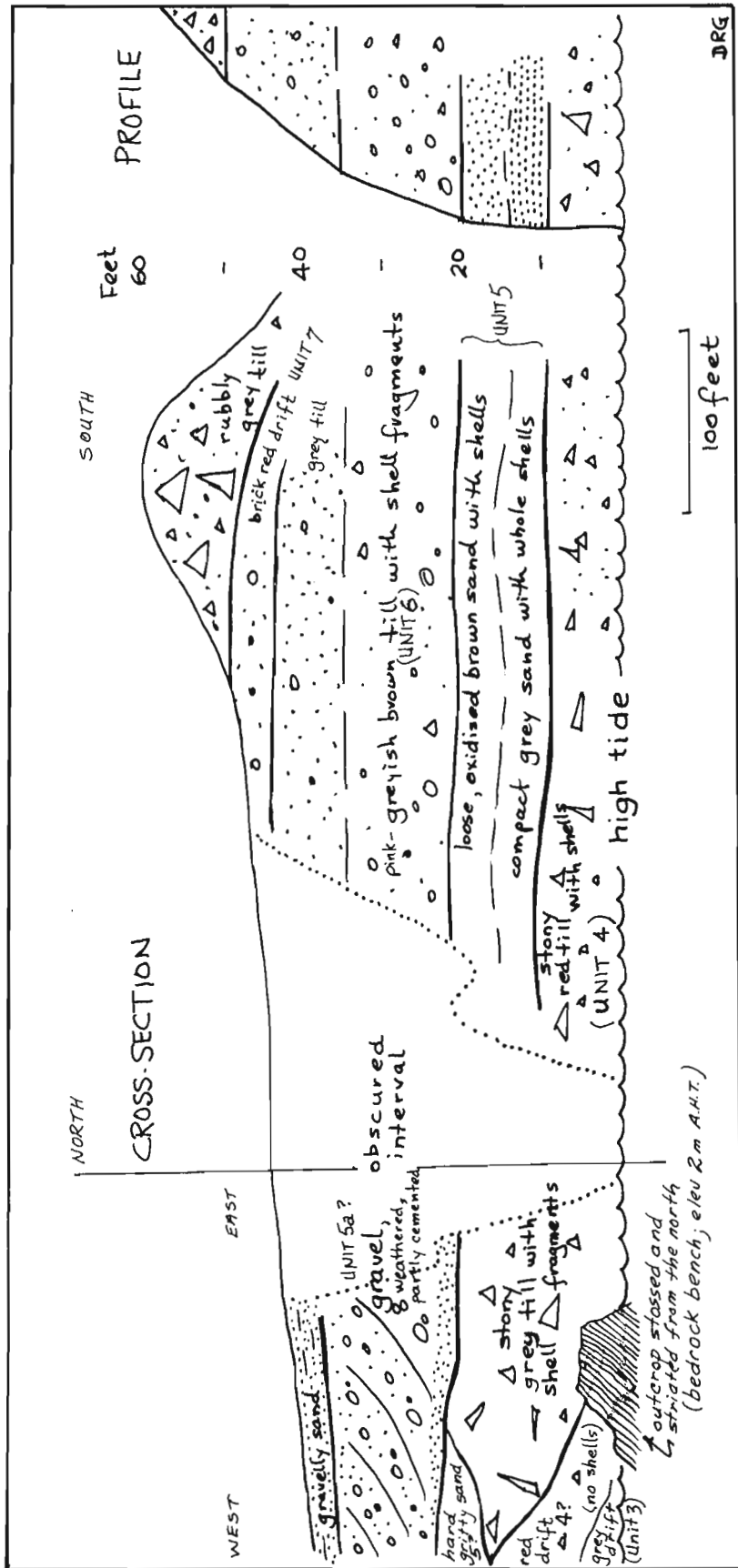


Figure 64.3. Sketch of deposits exposed in sea cliff north of the mouth of Salmon River, Nova Scotia.

trending southerly parallel to striations where this deposit has been emplaced over bedrock as at Salmon River, Red Head, and Cranberry Point. Virtually all the shells are fragmented except for a few of the small, relatively thick species like *Venericardia borealis* and robust specimens (10 to 20 mm) of *Mercenaria mercenaria*. Despite the ubiquitous shells, the marine origin (inferred by Hilchey *et al.*, 1962) should be discounted in favour of subglacial emplacement, especially in view of the glacial tectonics of the underlying sediment and bedrock which can be observed along a 1 km-long exposure at Red Head. There, the top 1 to 2 m of phyllite bedrock, which dips 60°S, has been rotated, dragged, overturned, and entrained into the sole of the covering red till. Wisps of the coherent but deformed mass have been sheared up into the till and thrust over the basal marine gravel (unit 2) overlying the bench. Drag folds and thrust faults extend several metres into otherwise coherent rock. This reddish till has a conspicuous component of distinctive igneous stones of northern provenance from New Brunswick and North Mountain. Although some may have been entrained from the underlying gravel (unit 2), the red matrix can be so conveniently derived from Triassic red beds, which outcrop to the north on the floor of St. Mary's Bay and Bay of Fundy, that the erratics also are regarded at first generation and not recycled. This unit likely was deposited during the maximal phase of a pervasive early pulse of the Wisconsinan stage when ice flooded unidirectionally across Nova Scotia from sources to the north. The thousands of drumlins, also composed of a dense red clay till with northern indicator stones that are scattered throughout the Atlantic upland of Nova Scotia, are a natural correlative. The early glaciation, which preceded the mid-Wisconsinan recession, must have extended well beyond the Atlantic coastline, perhaps to the Scotian Shelf end moraine complex mapped by King *et al.* (1972).

Unit 5, 'Salmon River Sand'

Just north of Salmon River (Fig. 64.3) the lower red till is overlain conformably, and with an abrupt contact, by an unique deposit of very hard, nearly massive, grey, silty sand about 3 m thick; this sand contains few pebbles and mainly unbroken and some paired bivalves, including one extinct species of the gastropod *Atractodon stonei* which gave a ¹⁴C age of 38 600 ± 1300 years B.P. (GSC-1440) and an U/Th age of 33 000 to 40 000 years (L-1348a). Clarke *et al.* (1972) considered the radiocarbon age to be minimal and because of the 'warm' water molluscan assemblage, he referred the bed to the last full interglacial. A subsequent uranium-thorium age determination, however, lends much credibility to the original dating, and because Nielsen (1974) reported evidence of glacio-marine conditions during and following its deposition, Grant (1975b) revised the age to mid-Wisconsinan. (Gustavson, 1976, p. 7, refers a sand bed on Long Island, New York, containing a similar molluscan assemblage, to the early Wisconsinan.) Nonetheless, the Salmon River Sand is considered to represent a

period of marine inundation that intervened after the main early ice flood had calved back landward and before the remnant ice cap on upland Nova Scotia readvanced during the late Wisconsinan stage. Perhaps during this recessional interval the ice front was located along or just inland of the present coast and formed the apparent end moraine feature, composed of red shelly drift, that extends 25 km along the coast from Meteghan to Belliveau Cove. Its seaward slope is gentle, subdued, and veneered with gravel in beach ridges; the landward proximal slope has a scalloped, ice-contact aspect with a subaerial angle of repose, and gravel, where present, occurs only in glaciofluvial bodies. Yet, while the body of the feature is composed of the older shelly deposits, it is overlain by a patchy veneer of rubbly till (unit 8) that has been related to the late Wisconsinan readvance.

Unit 5a, Intermediate, weathered, semi-consolidated gravel

A thick member is found in several places, notably Cape St. Mary beach and Salmon River; it conformably overlies the red shelly till and thus is apparently stratigraphically equivalent to or just above the Salmon River Sand. The unit is inclined northwestward and consists of rounded cobble gravel with sandy matrix; stratification is generally planar or lenticular with imbrication and cross-bedding indicating northward water flow. Also noted were cut-and-fill structures and, significantly, involutions as if from cryoturbation. The two main accumulations, coincidentally perhaps, lie at the seaward end of large eskers which extend radially inland.

Although these eskers are late Wisconsinan, perhaps there were earlier counterparts that debouched the gravel as glaciofluvial fans. This later period of fluvial deposition followed the marine phase of the interstadial by which time glacio-isostatic rebound had caused a withdrawal of the sea.

This hypothesis permits an opportunity for periglacial modification of the gravel, as well as oxidation, weathering, and partial cementing, that is also a feature of the upper part of the Salmon River Sand. Such alteration might also be explained by the confined aquifer role of these pervious beds.

Unit 6, Upper pinkish grey drift (till?)

Commonly the red shelly drift (unit 4) abruptly or gradually grades upwards through a sandy sub-stratified interval to an overlying pinkish or brownish grey, sand, till-like material that may have sparse small shell fragments. In places it appears to be a true till, with fabric and striated stones, yet in others sub-stratified sorted zones are present which indicate water-suspended deposition. Moreover, at Salmon River the marine, *Atractodon*-bearing sand (unit 5) grades up into this unit, and at Savary Provincial Park near Plympton it contains large fragments of oysters, some still attached to rocks. (Some *in situ* crushing and flattening of otherwise complete valves is attributed to glacial loading during deposition of later tills.)

A till and a glaciomarine drift of similar character have been incorrectly correlated because of apparently equivalent stratigraphic position. The difference may be explained by supposing that a glacial readvance, moving out from the Nova Scotia upland presumably during (later?) mid-Wisconsinan time, locally, in marine embayments, deposited a drift that is compositionally equivalent to the adjacent terrestrial till but differs in texture and molluscan content. Presumably the brown or pink tint is related to, if not actually inherited from, the underlying dense red drift.

Unit 7, Upper brick-red sediment

Within the upper few metres of most sections is found a thin but distinctive layer of brick-red sandy silt with pebble-size clasts and weak, if any stratification. Although its elevation ranges from high tide to +20 m, it provides a useful marker bed that separates the lower complex of marine and glacial sediments of inferred early and middle Wisconsin age from the surface till of the last glaciation and the associated gravel veneer of the final marine phase. Although no macrofossils were found in the red drift, its uniformly thin development (usually less than 1 m and commonly 0.25 to 0.5 m thick) regardless of elevation or slope strongly suggests an origin by deposition in water. Glacial, glaciomarine, and marine origins are all reasonable for the various occurrences of this layer.

Unit 8, Rubbly surface till of late Wisconsinan age

Most sequences are veneered with a few metres of rubble light grey till, with yellow or olive tints, composed almost entirely of local sedimentary rocks. Rare stones of northern provenance can be accounted for by reworking from underlying deposits. Granitic rocks from the interior in places are included, and these, together with an east-west fabric and westward-pointing striations were bedrock underlies the till, indicate that the ice flowed radially coastward during this phase. The trend of eskers is consistent. Judging by bevelled facets and crossed striations on Long Island, the late ice expanded at least 10 to 20 km across St. Mary's Bay. The clasts are angular and the matrix is a minor component, signifying an immature product of minimal transport. Small rubbly moraines appear to mark terminal or recessional positions of this late ice. In the vicinity of Cape St. Mary and to the south towards Yarmouth, westerly pointing striations are absent, and the higher bedrock hills at the coast are skirted by these moraines. At the Cape St. Mary section and at Deveau Cove, for example, the older red drifts (unit 4) lack of cover of the young rubbly drift as if the late Wisconsin ice failed to re-expand as far as the present coast in that region. In these areas the older gravel (unit 5a) shows leaching and cementation as if because of longer subaerial exposure. The postulated limited inland retreat of mid-Wisconsin ice and a modest late Wisconsin re-expansion to and beyond the present coast also could apply along the Atlantic Coast of Nova Scotia where the older red drumlins are overlain sporadically by a locally derived till in a belt within 10 to 20 km of the coast.

Unit 9, Postglacial emerged marine gravel

At all points north of Red Head, deposits may be thinly mantled with 1 to 2 m of rounded, well sorted, planar bedded, sandy cobble gravel which is loose and unweathered and reaches progressively greater elevations towards the north (Fig. 64.1). From a sand and clay member underlying the gravel at Gilbert Cove (thought to represent the coeval deep-water facies), littoral seaweed detritus yielded a date of $14\,100 \pm 200$ years (GSC-1459). The elevation of marine overlap is easily seen and measured in cliff sections where the marine derivative flanks drift hills and wedges out upslope against unmodified till. As at Cape St. Mary, for example, where the younger marine gravel has developed *in situ* by reworking of underlying older gravel (unit 5a), it can be distinguished because it is thinner, uncemented, fresher, better sorted, and planar bedded. At Salmon River and Cape St. Mary, marine limit abuts against small moraines of the last glaciation, and there is a regular decrease in elevation from there south to the zero isobase. To the north, however, the variation of marine limit is irregular and partly confused by a prominent lower shoreline feature as if two marine limits were involved – a lower, younger one with isobases parallel to the coast as might be expected if the late Wisconsin ice load was centred on the Nova Scotia upland, and an older, higher marine limit dating from the mid-Wisconsin recession when glaciomarine sedimentation reached demonstrably higher elevations. A careful review of available measurements in relation to elevations of various sediments and ice-marginal features is needed before this possible confusion can be resolved. Beyond the young moraines at Cape St. Mary, small broad-floored valleys terminate at the marine terrace and continue to sea level with markedly reduced width, as if the upper portions functioned for a relatively longer time. This could suggest that they lie in an area beyond the late Wisconsinan ice margin and consequently that the two segments are of different ages. Alternatively, the inferred older upper portions may be broader because they were cut in a periglacial environment when solifluction was an added factor. A useful but as yet untried approach to this and other chronological problems of relative age and interval is the measurement of weathering rinds on clasts and bedrock surfaces, particularly those with striations.

A Newly Discovered Archeological Site

In the vicinity of Yarmouth an accumulation of shells (*Mya truncata* and *Mya pseudoarenaria*) was noted as a lens up to 30 cm thick, extending 15 m just above the modern beach, and buried by 30 to 50 cm of turf. The deposit is almost certainly a midden, probably several thousand years old, as it also contains a few bones, argillite shards, and flakes and blocks of quartz. The feature is backed by a flat area, extending 10 m inland, and pinches out against steeper till slopes to either side.

References

- Clarke, A. H., Grant, D. R., and Macpherson, E.
1972: The relationship of *Atractodon stonei* to the Pleistocene stratigraphy and paleoecology of southwestern Nova Scotia; *Can. J. Earth Sci.*, v. 9, p. 1030-1038.
- Grant, D. R.
1967: Reconnaissance of submergence phenomena; in *Report of Activities, Part A*; *Geol. Surv. Can.*, Paper 67-1A, p. 173-174.
1968: Recent submergence in Nova Scotia and Prince Edward Island; in *Report of Activities, Part A*; *Geol. Surv. Can.*, Paper 68-1A, p. 162-164.
1971: Glacial deposits, sea level changes and pre-Wisconsinan deposits in southwest Nova Scotia; in *Report of Activities, Part B*; *Geol. Surv. Can.*, Paper 71-1B, p. 110-113.
1975a: Surficial geology of northern Cape Breton Island; in *Report of Activities, Part A*; *Geol. Surv. Can.*, Paper 75-1A, p. 407-408.
1975b: Glacial style and the Quaternary stratigraphic record in the Atlantic Provinces, Canada; in *Report of Activities, Part B*; *Geol. Surv. Can.*, Paper 75-1B, p. 109-110.
- Gustavson, T. C.
1976: Paleotemperature analysis of the marine Pleistocene of Long Island, New York, and Nantucket Island, Massachusetts; *Geol. Soc. Am.*, *Bull.* 87, p. 1-8.
- Henderson, E. P.
1972: Surficial geology of Avalon Peninsula, Newfoundland; *Geol. Surv. Can.*, *Mem.* 368, 121 p.
- Hilchey, J. D., Cann, D. B., and MacDougall, J. I.
1962: Soil survey of Digby County, Nova Scotia; *N. S. Soil Survey, Rep.* 11.
- King, L. H., MacLean B., and Drapeau, G.
1972: The Scotian Shelf submarine end-moraine complex; *24th Int. Geol. Congr. Sect. 8*, p. 237-249.
- Nielsen, E.
1974: A mid-Wisconsinan glacio-marine deposit from Nova Scotia; *Int. Symp. Quat. Environments, York Univ.*, May 25, 1974 (abstract).
- Prest, V. K., Grant, D. R., Borns, H. W., Brookes, I. A., MacNeill, R. H., and Ogden, J. G.
1972: Quaternary geology, geomorphology and hydrogeology of the Atlantic Provinces; *24th Int. Geol. Congr., Guide., Excursion A61-C61*, 79 p.

DSS Contract OSU4-0026

R. N. Yong¹ and P. B. Fransham
Terrain Sciences Division

Introduction

The Champlain Sea sediments of eastern Canada constitute important deposits from a geotechnical engineering point of view. In this context it is necessary to provide proper prediction of the performance of these soils as bearing materials and in natural or cut-slopes if rational design procedures and land utilization programs are to be implemented. The sensitivity of these deposits under certain stress conditions and disturbance is well known and has resulted in many cases of unpredicted instability with catastrophic results. There is evidence that instability can occur in sensitive clays when they are subjected to dynamic loads of various types. Dynamic loads can result from natural phenomena such as earthquakes or from man-made disturbances such as vehicle traffic, blasting, etc. To date only a few studies have tried to evaluate the role of vibrations in the stability of slopes. In order to further our understanding of the potential for slope instability in the Ottawa Valley, a research program was undertaken jointly by McGill University and Terrain Sciences Division. This report on the laboratory results and a companion report (in preparation) on the

field tests are based on the Annual Report 1975 submitted to Terrain Sciences Division by the senior author.

Experimental Procedure

Field soils are subject to a wide spectrum of dynamic or transient stress systems including variable stress magnitudes, frequency of application, duration of application, and number of load applications. The change in stability of soils from Saint-Jean-Vianney under known dynamic load systems has been analyzed. These tests consisted of specimens subjected initially to identical triaxial consolidation conditions; following this they were subjected to an axial stress, without drainage, representing one of several predetermined percentages of the axial stress needed to cause failure of the specimen under standard test procedures. A small oscillating axial stress was superimposed on the major axial stress and allowed to cycle for a predetermined number of applications (1 to 10 000) at a frequency of 40 cycles per minute. The axial stress was then removed and the sample brought to failure by the standard constant deformation rate method in order to evaluate changes in strength associated with the

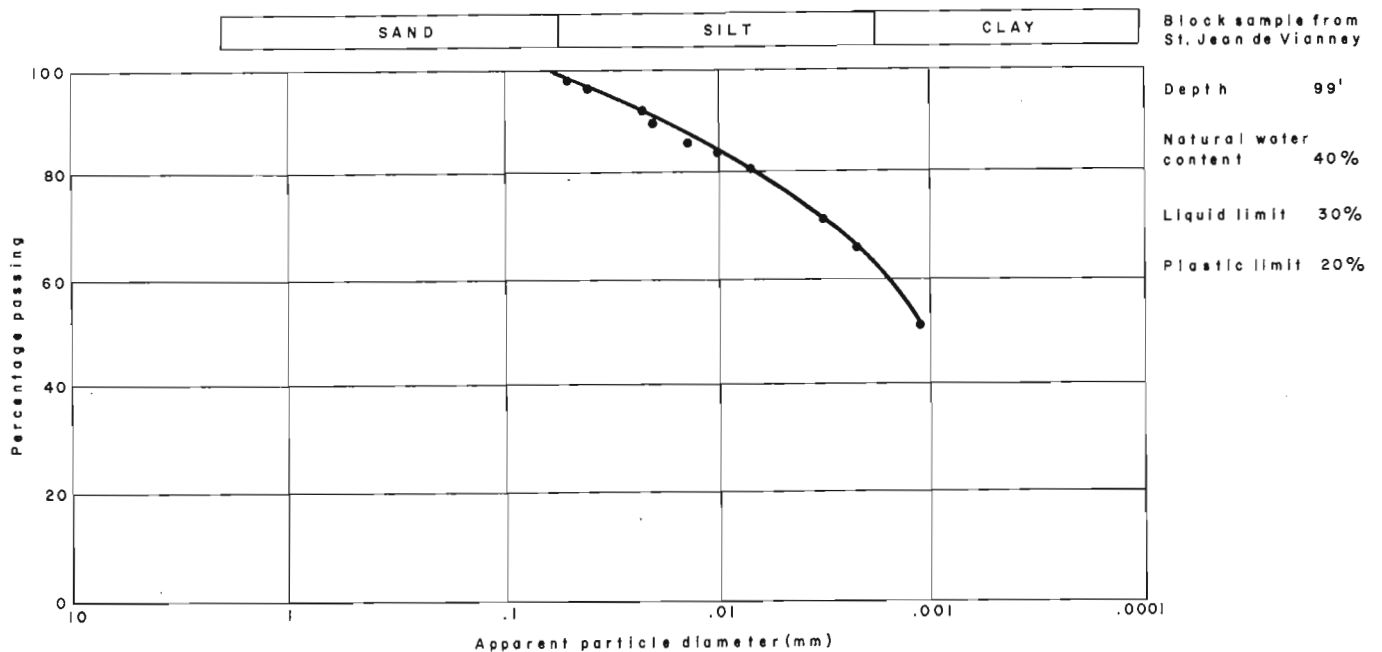


Figure 65.1. Basic soil identification properties - typical values.

¹William Scott Professor of Civil Engineering and Applied Mechanics, Director, Soil Mechanics Research Laboratory, McGill University, Montreal.

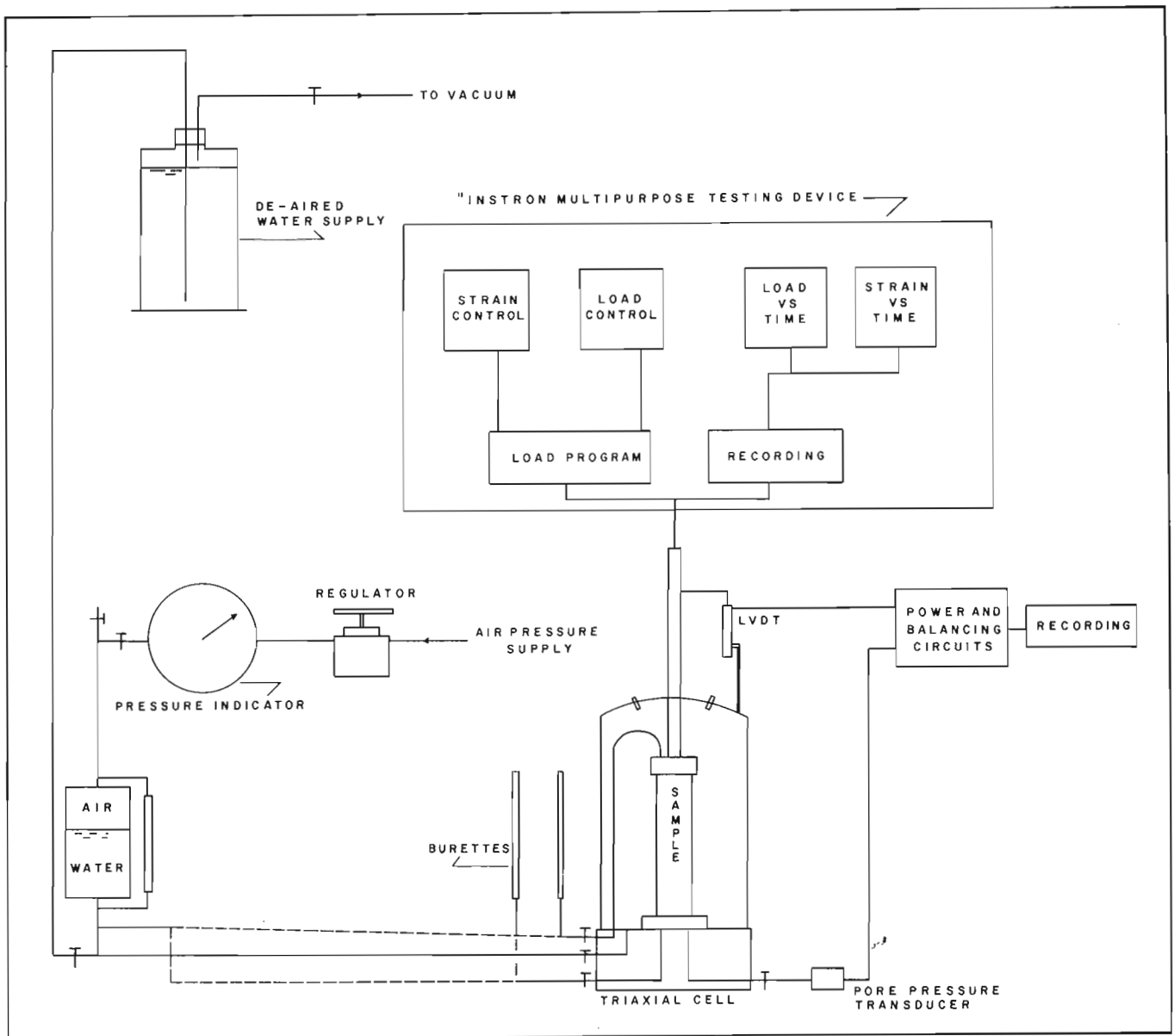


Figure 65. 2. Test arrangement for preliminary testing.

previously programmed application of the repetitive cyclic stress. Typical values of basic soil properties and the experimental set-up are shown in Figures 65. 1 and 65. 2 respectively.

Experimental Program

Figure 65. 3 outlines the testing program which attempts to isolate the effects of each input variable. The possible combination of tests is large, and a systematic examination of the individual and combined effects needs to be properly implemented.

Most slide failure surfaces in the field can be approximated by the arc of a circle, and therefore the orientation of the failure plane with respect to soil bedding can vary between 0 and 90 degrees. Thus,

reference tests were carried out on both horizontal and vertical specimens. To clarify this last statement, "reference" applies to specimens which were not subject to cyclic loading; "vertical" refers to the direction of the specimen with the longest axis normal to the surface of the ground, whereas "horizontal" refers to the specimen with its longest axis parallel to the surface of the ground.

Repeated tests were carried out on both horizontal and vertical specimens using the closed-loop loading system (Instron). These tests were performed along the lines of research outlined in Figure 65. 4. For example, under the main heading of cyclic load and the subheading of vertical (1), the variables studied in this series of tests are: mean stress, pulse stress,

number of cycles, and deformation rate. The objectives of the tests were:

- a) to study the effect of the number of cycles on the strength of the sensitive clay while keeping constant the mean cyclic stress and pulse cyclic stress (cf. Fig. 65.5) at various combinations of mean to pulse cyclic stresses, and
- b) to study the effect of variable mean cyclic stress on the strength of the clay while keeping constant the number of cycles and pulse cyclic stress.

A third type of test, defined as a constant load test, was undertaken and may be regarded as a special case of the dynamic test where the number of cycles is equivalent to unity. The main purpose of this test was to compare the effect of the strength of a noncyclically loaded specimen with that of a repeated cyclically

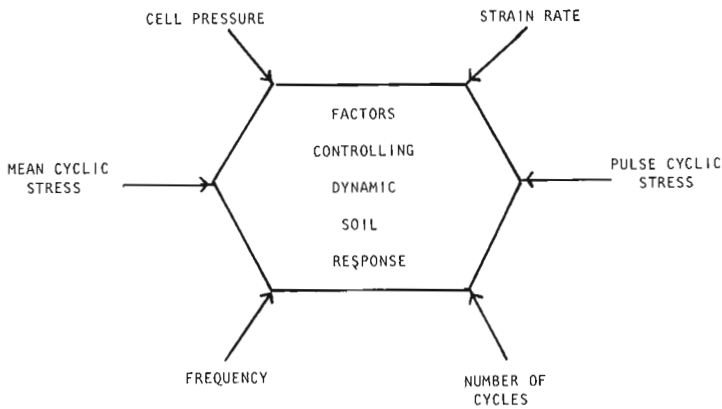


Figure 65.3. Parametric variables.

loaded specimen where time and mean stress were the same for both cases. This, in effect, will show the effect of the pulse stress.

Figure 65.4 outlines the extent of the experimental program completed to date.

Test Results

Strain Rate Effects

Both horizontal and vertical specimens were failed over a range of axial deformation rates of between 0.0005 in./min. to 0.5 in./min. The objectives of these reference noncyclic tests were:

- a) to determine the effect of deformation rate on the strength at failure;
- b) to select the best possible deformation rate, within the limitations of the Instron, for obtaining the most information from both dynamic and constant load tests;
- c) to appraise any possible anisotropic effect on the strength between horizontal and vertical tests; and
- d) to provide strength data for specimens that were not subjected to cyclic loading which would provide a base line for comparison with specimens subjected to cyclic loading.

Analysis of the strength data was performed using the maximum deviator stress ($\sigma_1 - \sigma_3$) and the effective stress ratio (σ_1' / σ_3') failure criteria. For vertical samples application of these two criteria for analysis of test measurements shows a general trend indicating a decrease in strength with an increase in deformation rate ($\dot{\epsilon}$) (Fig. 65.6). For horizontal specimens the results are interesting with respect to the type of failure

TYPES OF TESTS

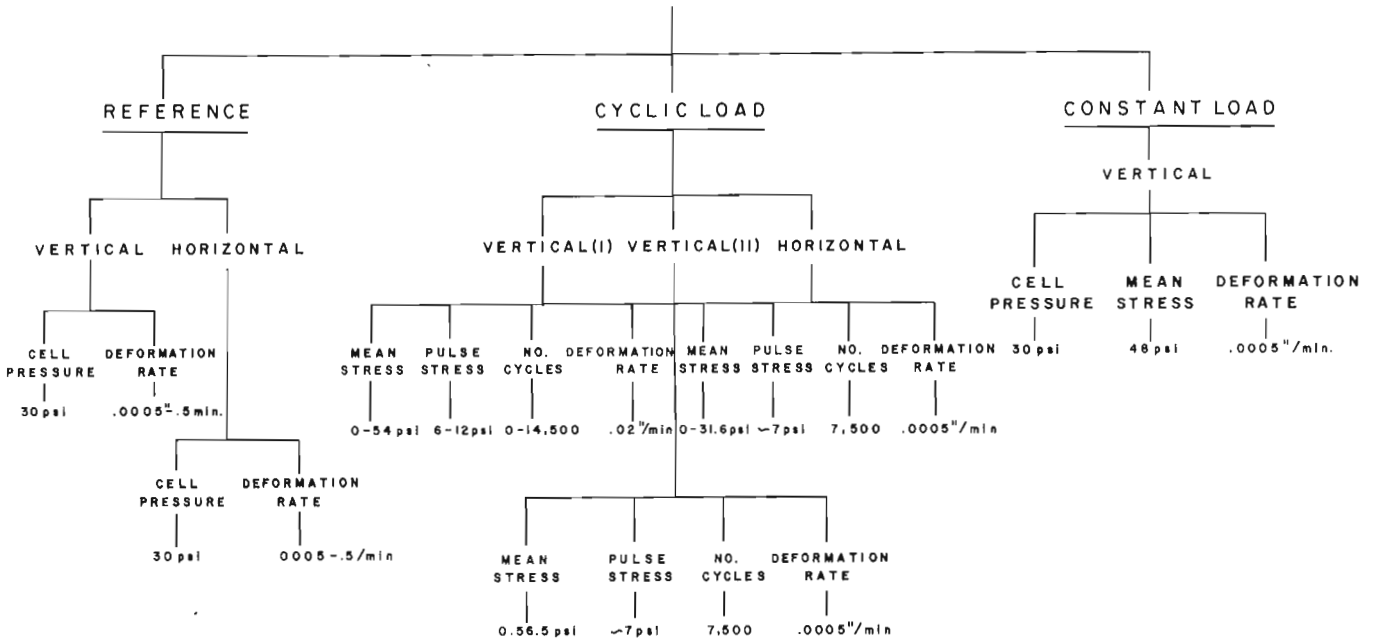


Figure 65.4. Experimental program for cyclic load triaxial tests.

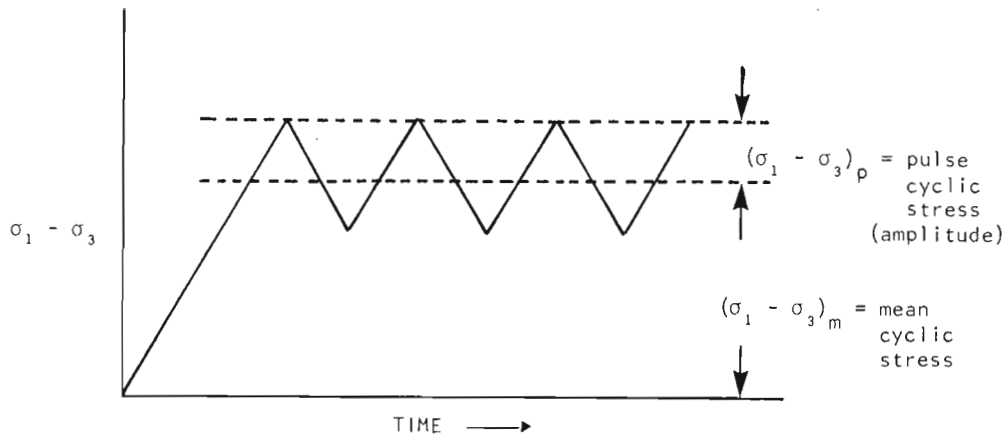


Figure 65.5. Mean stress vs. time.

criteria used for strength tests. The results of $(\sigma_1 - \sigma_3)$ vs. (axial strain) and (σ_1'/σ_3') vs. (axial strain) for horizontal tests (Fig. 65.7) indicate different trends with the application of the two different failure criteria.

Figure 65.7 shows that the values of the deviator stress at failure increase with increasing deformation rate, which is contrary to that found with vertical samples. The values of the effective stress ratio, however, decrease with increase in deformation rate; the values are comparable to those obtained for vertical specimens. The overall trend for both vertical and horizontal specimens indicates a reduction in strength of the specimens with increase in deformation rate. This trend is contrary to previously reported results – especially with respect to nonsensitive clays.

Although the strain-rate effect might indicate that increasing strain rate ($\dot{\epsilon}$) produces lower maximum strengths, it is necessary to bear in mind the range of $\dot{\epsilon}$ investigated and also the problem of breakage of soil bonds. Expectations with respect to strength increase due to increasing $\dot{\epsilon}$ are well founded in so far as nonbonded and nonsensitive clays are concerned – especially in the higher ranges of $\dot{\epsilon}$ where inertia terms contribute to material performance. The ranges of $\dot{\epsilon}$ investigated here fall well below the lower limit where inertia may be considered significant (Yong and Japp, 1968). The prime reason for these observed decreases in strength may be the rate of bond breakage.

With respect to development of pore water pressure for tests on horizontal samples during loading to failure, generally more pore pressure developed with a decrease in the deformation rate. Irrespective of the deformation rate, the vertical specimens appear to generate similar pore pressures.

Repeated Loading - Number of Cycles

For the purpose of these tests three combinations of the ratio mean cyclic stress to pulse stress were investigated:

- mean stress = 54 psi; pulse stress = 6 psi
- mean stress = 48 psi; pulse stress = 6 psi
- mean stress = 18 psi; pulse stress = 12 psi

The number of cycles used for series (a) was 100, 1000, and 14 500; for (b) 100, 1000 and 10 000; and for (c) 10, 100, 680 and 10 000.

In general for each case of the mean cyclic stress to pulse cyclic stress used there was an increase in the value of deviator stress $(\sigma_1 - \sigma_3)$ and effective stress ratio (σ_1'/σ_3') at failure with respect to the reference test. Figures 65.8 and 65.9 show the values of $\sigma_1 - \sigma_3$ and σ_1'/σ_3' as a function of the number of cycles; scatter is within the range of ± 5 per cent.

The strains at failure appear to vary from one mean cyclic stress to pulse cyclic stress test to another. In general, the overall trend was for decrease of strain at failure with increase in the ratio of mean cyclic stress to pulse cyclic stress. No trend was evident, however, between number of cycles and strain at failure within each particular series of mean cyclic stress to pulse cyclic stress. In the case of pore pressure development during loading to failure, no trends were found with respect to the number of cycles imposed. The nonconclusive behaviour patterns observed are likely due to the limited number of test variables completed within the available time period. A sufficiently encompassing view of material performance would require more detailed testing under a variety of conditions.

Repeated Loading - Effect of Mean Cyclic Stress

Three different sets of tests were performed to evaluate the effect of the mean cyclic stress on the soil strength after pulsing. The test groupings are shown in Table 65.1.

The results shown in Figures 65.10 and 65.11 indicate a linear increase in strength, in terms of $\sigma_1 - \sigma_3$ criterion, with an increase in mean cyclic stress. The slope of the lines from the results of $(\sigma_1 - \sigma_3)$ vs. (mean cyclic stress) are similar for 0.02 in./min. and 0.005 in./min. The vertical test results indicate strain hardening with increased cyclic loading at low frequency; this increase in strength is approximately 10 per cent. This trend is not as obvious with the horizontal specimens in view of the large amount of

variation in the value of the reference test. Nevertheless, the plots of σ_1'/σ_3' against mean cyclic stress show a general increase in strength with both vertical and horizontal tests as seen in Figure 65. 11. Although an apparent trend exists towards work hardening, it is important to note that there appears to be a threshold value above which strength degradation occurs.

Comparison of Results from Horizontal and Vertical Tests

In order to evaluate any anisotropic effects, a comparison of results obtained from horizontal and vertical tests is necessary. The following observations have been made previously.

1) Based upon $\sigma_1-\sigma_3$ failure criterion, horizontal specimens appear to increase in strength with strain whereas for vertical specimens the reverse is true. A typical value of $\sigma_1-\sigma_3$ at failure for a deformation rate of 0. 005 in. /min. was 70 psi for the vertical specimen and approximately 30 psi for the corresponding horizontal specimen. At 0. 5 in. /min. , however, the two were approximately equal in strength – approximately 5. 4 psi.

2) The value of σ_1'/σ_3' at failure were the same for both the horizontal and vertical specimens and showed the same trend of decreasing strength with increasing deformation rate.

3) Under cyclic loading, both horizontal and vertical specimens strain hardened or showed an increase in strength upon application of the σ_1'/σ_3' and $\sigma_1-\sigma_3$ failure criteria.

4) Failure under cyclic loading occurred at different mean stress levels of approximately 55 psi for vertical test samples and approximately 25 psi for horizontal test samples.

5) The apparent preconsolidation pressure was 86 psi for horizontal specimens and 130 psi for vertical specimens (e - log P curves are not included in this report).

6) The soil samples exhibited a tendency to fracture in a horizontal plane.

The purpose of this particular section is not to make direct conclusions but to draw attention to the differences found between horizontal and vertical test results. A strength difference exists between horizontal and vertical samples which is dependent on deformation rate. Nevertheless, consolidation tests show that the preconsolidation pressures are different for horizontal and vertical samples and, as such, the overconsolidation values at which the tests were completed are larger for the vertical than horizontal tests. In fact, the overconsolidation ratios are 2. 9 and 4. 3 for horizontal and vertical tests, respectively. The effect of different overconsolidation ratios on the strength parameters of this particular sensitive clay was not evaluated.

Analysis using σ_1'/σ_3' failure criterion shows no strength differences between the horizontal and vertical specimens, irrespective of deformation rate. The mean stress under cyclic conditions for failure is much

less for the horizontal specimens than for the vertical specimens.

Constant Load Test

As previously defined, the constant load test has the number of cycles equal to unity. The test completed was loaded at 48 psi; test results are shown in Figure 65. 12 together with the stress = strain curves for a cyclically loaded test with the mean cyclic load at 48 psi.

The value of $\sigma_1-\sigma_3$ at failure is 70 psi for the constant load test compared to the higher value of 80. 5 psi for the cyclically loaded sample. The σ_1'/σ_3' values at failure are also much smaller for the constant load test (4. 3) than for the cyclically loaded specimen (approximately 6. 0). As the constant load test is actually a one-cycle test, using Figures 65. 8 and 65. 9 which plot the $\sigma_1-\sigma_3$ and σ_1'/σ_3' values at failure divided by the number of cycles for a sample cycled at 48 psi, there would only be an increase of 2 psi in $\sigma_1-\sigma_3$ (above that of the reference test value). Thus there is actually little difference between results from the constant load test and those from a comparable one-cycle test.

Repeated Loading - Failure Mechanism

As previously reported the test results for the Saint-Jean-Vianney clay indicate apparent strain hardening of the order of about 10 per cent as analyzed in terms of $\sigma_1-\sigma_3$ for mean cyclic stress of between 0 and 54 psi for vertical tests and 0 to 25 psi for horizontal tests. With respect to σ_1'/σ_3' evaluation, the increases in strength over the mean cyclic stress range were considerably higher than the reference strength. For all tests this increase in strength occurred up to a mean stress of 80 per cent of the reference deviator stress at failure.

Contrary to initial expectations, there was no sign or indication of any strain weakening and hence no gradual deterioration of strength for the level of mean stress applied. This does not mean however that repeated loading did not create detrimental or deteriorative effects. When failure occurred it was of a brittle or catastrophic nature. If the level of mean stress is increased, application of cyclic loads probably would produce a strain softening effect in view of progressive soil bond breakage.

Table 65. 1
Experimental Program for
Effect of the Mean Cyclic Stress

Sample Orientation	No. of cycles	Pulse stress	Deformation rate to failure
Vertical	7 500	6 psi	0. 0005 in/min
Vertical	10 000	6-12 psi	0. 02 in/min
Horizontal	7 500	6 psi	0. 005 in/min

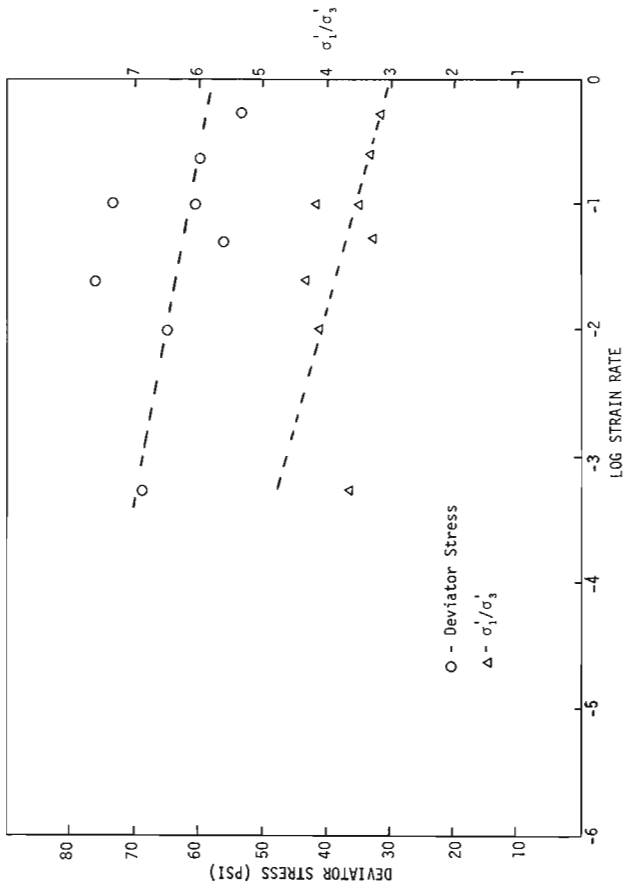


Figure 65.6. Deviator stress (psi) vs. log strain rate and σ_1'/σ_3' vs. log strain rate for vertical reference samples.

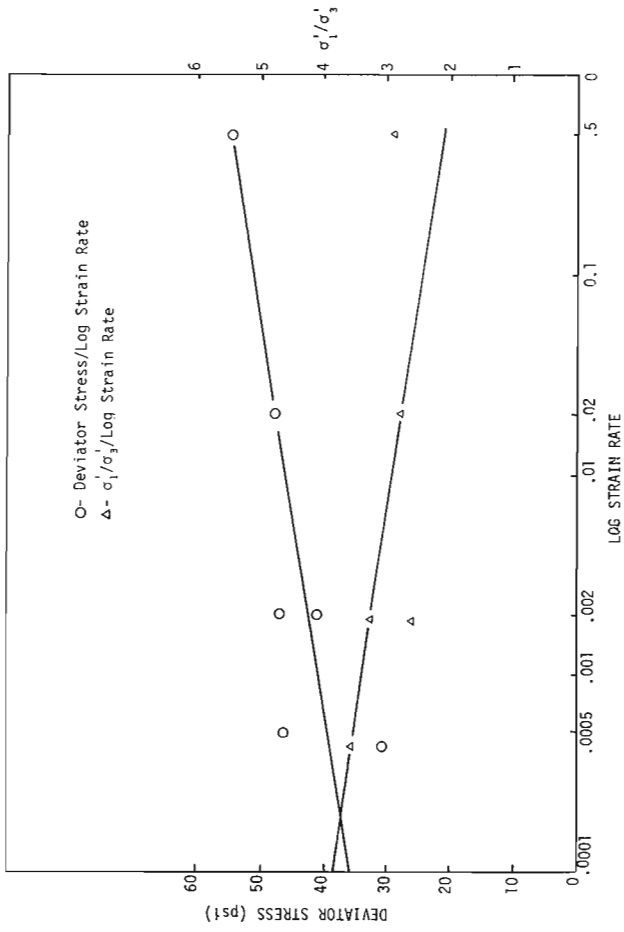


Figure 65.7. Deviator stress and σ_1'/σ_3' at failure (psi) vs. log strain rate for horizontal tests.

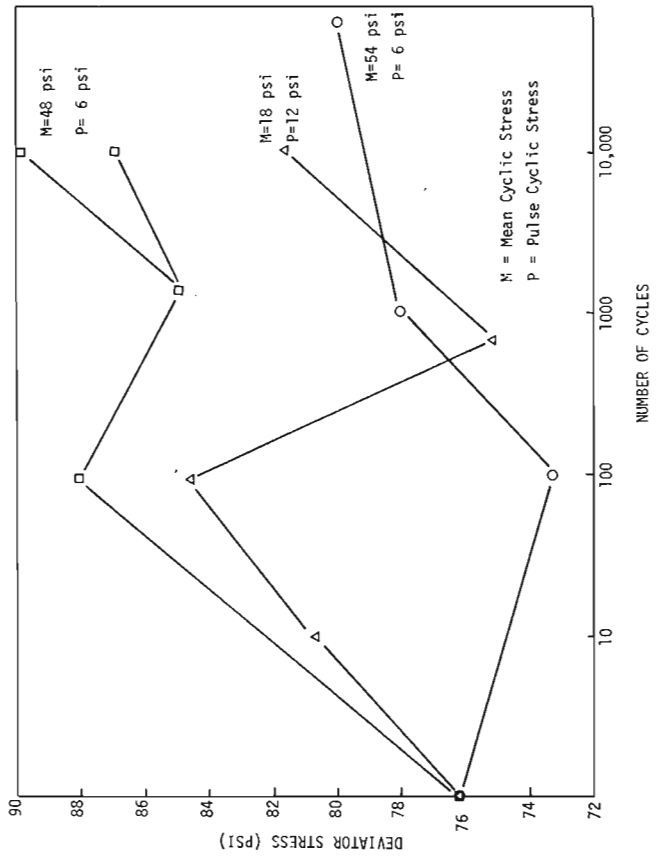


Figure 65.8. Deviator stress (psi) at failure vs. number of cycles.

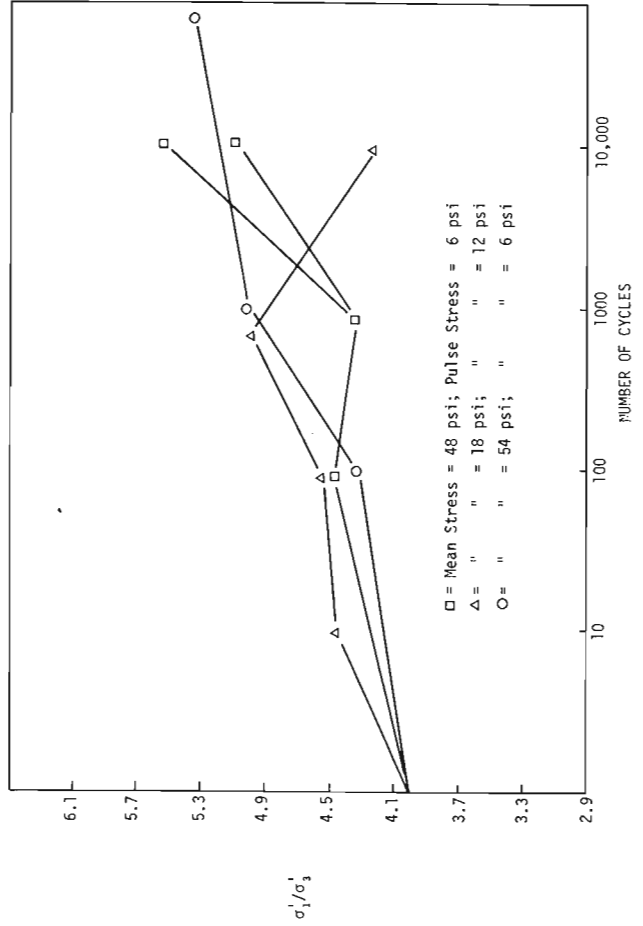


Figure 65.9. Values of σ_1'/σ_3' at failure vs. number of cycles.

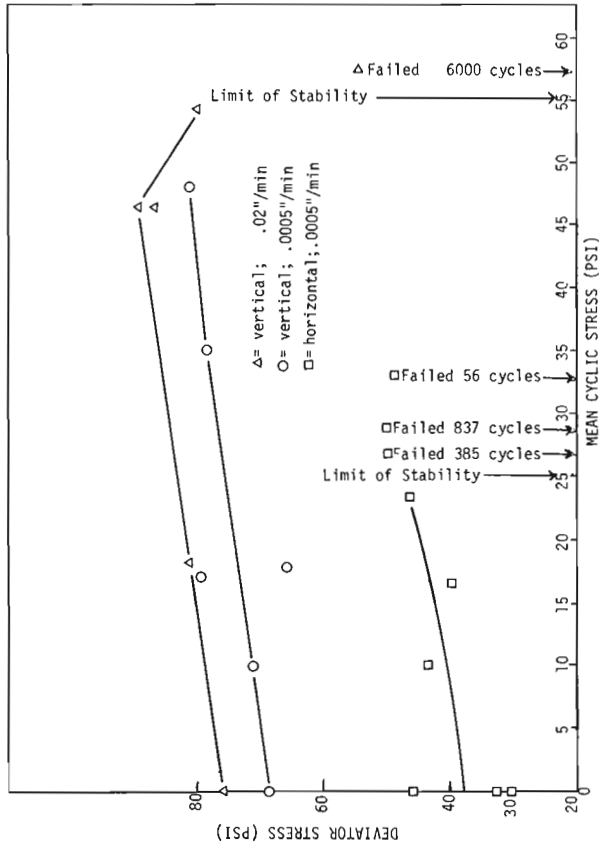


Figure 65.10. Deviator stress (psi) at failure vs. mean cyclic stress (psi) for both horizontal and vertical tests.

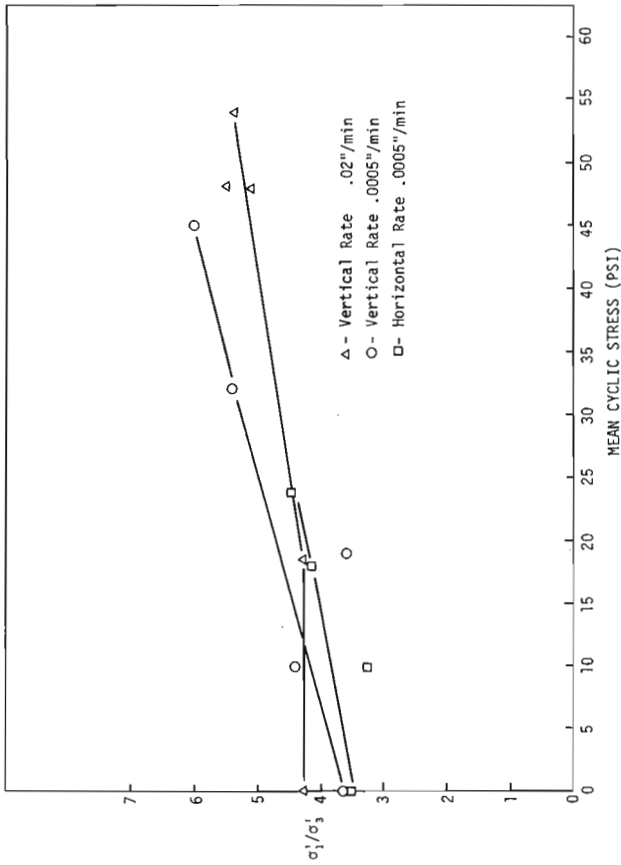


Figure 65.11. σ_1/σ_3 at failure vs. mean cyclic stress (psi) for both horizontal and vertical tests.

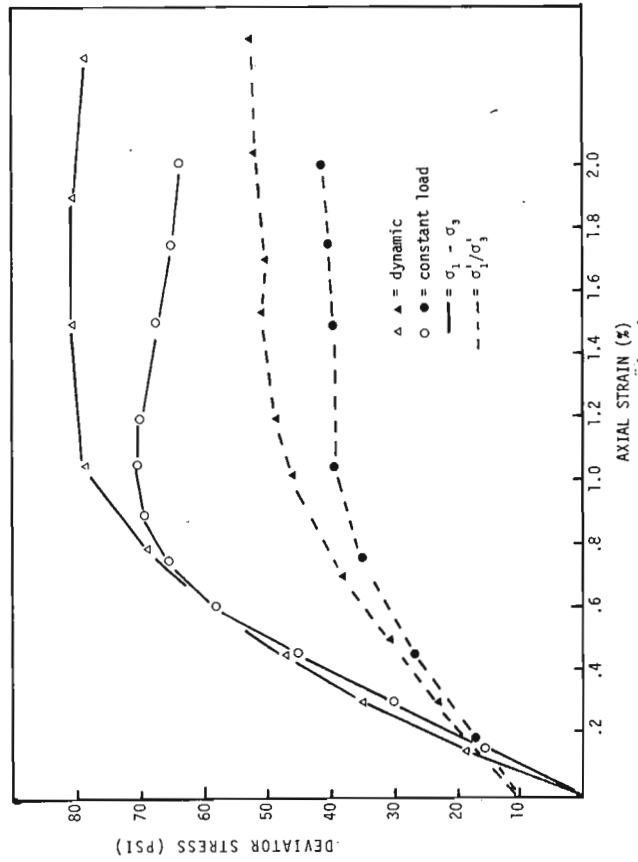


Figure 65.12. Deviator stress (psi) and σ_1/σ_3 vs. axial strain (%) during strain to failure of cycled test and constant load test both at mean stress of 48 psi.

The failure mechanism in Saint-Jean-Vianney appears to centre around the strain level of repeated load provocation. The highly overconsolidated nature of the soil is reflected in terms of bond performance and resultant brittle fracture. Past experiments on sensitive clays have shown that dynamic loading tends to strain weaken by irreversible breakage of weak organic or inorganic cementing bonds. The observations may be correct if the soils studied are not too highly overconsolidated and also are not strongly bonded. The brittle or catastrophic failure observation reinforces initial expectations of fatigue modelling. Until threshold stress is exceeded – through combinations of amplitude, frequency, mean stress level, and number of cycles – abrupt fatigue failure will not occur. When this level is reached, as shown by some samples, failure occurs.

A critical factor in the failure mechanism is that this particular clay has a thixotropic nature in that disturbance of the soil produces a very wet and fluid mixture which stiffens on standing. Assuming that

once a sufficient rate of strain has been achieved, this would initiate a plastic-liquid change and thus make failure inevitable. At low levels of mean cyclic stresses the strains were insufficient to produce a continual disturbance of the sample.

Permanent strains are produced as a result of the cyclic loading. Regardless of the number of cycles, stress level, duration, and magnitude, the strength of the samples decreases in reference to the noncyclic sample in the relationship to the residual or permanent strains occurring during cycling. The greater the strain generated as a result of cycling, the lower is the strength of the material.

Reference

- Yong, R. N. and Japp, R. D.
1968: Stability of clays in dynamic compression; in Vibration effects of earthquakes on soils and foundations, ASTM Spec. Tech. Publ. 450, p. 233-262.

AUTHOR INDEX

	Page		Page
Abbey, Sydney (4)	13	Hardy, I. A. (8)	31
Aitken, J. D. (56)	315	Hicock, S. R. (38)	197
Anderson, J. C. (37)	187	Hills, L. V. (13)	61
Ansell, H. G. (62)	353	Hood, P. J. (47)	267
Armstrong, J. E. (38)	197	Hopkins, W. S., Jr. (54)	307
Ayres, L. D. (10)	39	(58)	329
Barefoot, R. R. (55)	311	Jambor, J. L. (14)	65
Barss, M. S. (26)	131	(59)	335
Blake, W., Jr. (39)	201	(63)	357
Balkwill, H. R. (58)	329	Jansa, L. F. (22)	99
Bouvier, J.-L. (4)	13	Jonasson, I. R. (15)	71
Brideaux, W. W. (43)	235	Jones, D. M. (48)	273
(44)	251		
Brown, P. (30)	147	Katsube, T. J. (42)	229
Bustin, R. M. (13)	61	Knapp, H. W. C. (53)	303
Callomon, J. H. (61)	345	Lau, J. S. O. (34)	161
Champ, W. H. (3)	11	Lawrence, D. E. (34)	161
Christie, R. L. (45)	259	Lichti-Federovich, S. (27)	133
Clague, J. J. (33)	157	Luternauer, J. L. (35)	169
Cook, D. G. (56)	315		
Copeland, M. J. (18)	83	Mackay, J. Ross (12)	59
Crilley, B. (26)	131	MacKay, R. M. (60)	343
Currie, R. G. (20)	95	Matthews, John V., Jr. (41)	217
(21)	97	McLean, J. R. (57)	323
Day, T. J. (36)	173	McLean, R. A. (52)	295
(37)	187	McMillan, W. J. (59)	335
Dicaire, A. (53)	303	Meeds, C. F. (3)	11
Dimroth, Erich (23)	107	Muller, J. E. (21)	97
Dubois, J.-M. (19)	89	Myhr, D. W. (43)	235
Dugal, J. (30)	147	(55)	311
Dyke, A. S. (40)	209		
Fahrig, W. F. (32)	153	Norris, D. K. (46)	263
Fermor, P. R. (2)	7	Olson, D. (53)	303
Findlay, D. J. (10)	39	Patton, George (7)	25
Flint, T. R. (53)	303	Pedder, A. E. H. (50)	285
Ford, D. C. (31)	151	(51)	287
Fransham, P. B. (65)	371	Plant, A. G. (63)	357
Frydecky, I. (20)	95	Poole, W. H. (24)	113
Gale, J. E. (30)	147	Poulton, T. P. (61)	345
Gale, R. J. (36)	173	Price, R. A. (2)	7
Glover, J. K. (6)	21	(6)	21
Gordey, S. P. (1)	1	Pringle, G. J. (62)	353
Grant, D. R. (64)	363	Raven, K. (30)	147
Grasty, R. L. (16)	77	Ready, E. (47)	267
(17)	81	Roberts, A. C. (62)	353
		Ruzicka, V. (25)	127

	Page		Page
Sabina, Ann P. (5)	15	Umpleby, D. C. (8)	31
Sawatzky, P. (53)	303		
Schwarcz, H. P. (31)	151	Weir, R. W. (48)	273
Schwarz, E. J. (9)	37	Woo, V. (29)	143
Shilts, W. W. (48)	273		
Sinha, A. K. (49)	281	Yong, R. N. (65)	371
Steacy, H. R. (63)	357		
Swan, D. (20)	95	Zentilli, M. (60)	343
Sweet, A. R. (54)	307	Zoltai, S. C. (29)	143
Tarnocai, C. (28)	137		
Taylor, R. B. (11)	43		
Tempelman-Kluit, D. J. (1)	1		

